Department of Civil & Structural Engineering
University of Sheffield

Probability-Based Estimation of Vibration for Pedestrian Structures due to Walking

by

Stana Živanović

A thesis submitted for the Degree of Doctor of Philosophy in Engineering

February 2006

To my brave mother Ivanka Živanović

and

in loving memory of my father Vidoje Živanović

Abstract

Modern civil engineering structures exposed to human-induced dynamic loading due to walking, such as footbridges and long-span floors, are becoming increasingly slender and therefore more prone to vibrations generated by people. As a consequence, the vibration serviceability of these structures is becoming their governing design criterion. Currently, the design procedures for the vibration serviceability check used in practice are mainly of a deterministic nature. This means that the walking force is modelled via a unique set of parameters, such as walking frequency, step length and force amplitude assumed to be representative for all pedestrians. Therefore, the natural inter-subject variability that exists in these parameters generated by different people is neglected. Moreover, these parameters vary with each step even in the force time history of a single person (intra-subject variability). This implies that the walking force is a narrow-band random process rather than a deterministic force. As a result of these shortcomings, current design procedures based on deterministic forces do not predict reliably the vibration responses to single person walking across as-built slender structures.

To improve design procedures, it is necessary to take into account the both inter- and intra-subject variabilities in the walking force. This implies that a probability-based approach, whereby the probability of occurrence of various walking parameters can be taken into account, might be more appropriate to model the walking excitation.

In this thesis, a *probability-based framework* for a vibration serviceability check due to a *single person walking* is developed. For this, the probability density functions for walking frequencies, step lengths, magnitude of walking force and imperfections in human walking are proposed. They are used as building blocks to develop a design procedure that can estimate the probability of occurrence of a certain level of vibration response. Based on this result, a probability that the vibration response will not exceed certain predefined limiting values can be found. Moreover, a methodology for finding a reasonable limiting vibration level, based on the assumption that some human-structure dynamic interaction takes place when walking across perceptibly moving bridge, is suggested. A provisional value of $0.35\,\mathrm{m/s^2}$ is identified for two footbridges investigated.

The probability-based design procedure developed in this thesis can be used for vibration serviceability check of footbridges responding in one or more vibration modes to excitation induced by a single walker. The method has potential to be used for vibration serviceability check of other slender structures.

Acknowledgements

The work described in this thesis was conducted in the Department of Civil & Structural Engineering at the University of Sheffield starting from October 2002, with a three month break during 2003/2004. During these 37 months of full-time research I was a member of the Vibration Engineering Section. I owe my thanks to all current and former members of the section for their help and everyday company throughout the work on this thesis. Special thanks go to my supervisor Professor Aleksandar Pavic for his patience, advice, continuous encouragement and inspiring discussions. The help and advice of Dr Paul Reynolds, especially regarding vibration testing matters, is gratefully acknowledged, as are the valuable discussions with Professor James M. W. Brownjohn. The assistance of Dr Pero Vujović and his team from the University of Montenegro in Podgorica during field testing is very much appreciated. I would also like to thank the National Institute of Education in Singapore and Professor Brownjohn for their permission to use the measured force time histories in the analysis conducted. Thanks also go to Dr Tianjian Ji of the University of Manchester for supplying data presented in Figure 6.2b.

I was lucky to have the constant support of many friends and colleagues during my research. These include Marija Nefovska-Danilović, Vladimir Novak, Jelena and Fredi Dobrić, Chee-Ming Chan, Gordana Vasić, Nino Pešić and Zoran Mišković. Also, life would not be the same without everyday discussions with my housemates on world problems, music, arts, engineering and other topics highly relevant for each of us. Thanks to Marco Ajovalasit, Nicola Tassini, Indra Tumur and Caroline Turner. Finally, necessary is to mention the invaluable support of my family. Without their understanding during my ups and downs of the last several years and the sincere friendship of Ivana Spasojević and Dr Mihail Petkovski everything would have been much more difficult. Also, thanks go to Mihail for our numerous and challenging discussions.

Finally, I would like to acknowledge the financial support which came from the Universities UK Overseas Research Student Award Scheme (reference ORS/2002036023) and from the UK Engineering and Physical Sciences Research Council (EPSRC) for the grant reference GR/S14924/01 ("Investigation of the As-Built Vibration Performance of System Built Floors") as well as for the grant reference GR/T03000/01 ("Stochastic Approach to Human-Structure Dynamic Interaction") provided to Professor Pavic.

Memorandum

The accompanying thesis entitled "Probability-Based Estimation of Vibration for Pedestrian Structures due to Walking" is submitted for the degree of Doctor of Philosophy in the Faculty of Engineering at the University of Sheffield. The thesis is based entirely on the independent work carried out by the author in the University of Sheffield between October 2002 and February 2006 (with a three months long leave of absence during 2003/2004) under the supervision of Professor Aleksandar Pavic and Dr Paul Reynolds. All the work and ideas recorded are original except where acknowledged in the text or by reference. The work contained in the thesis has not previously been submitted for a degree or diploma at this, or any other, University or Examining Body.

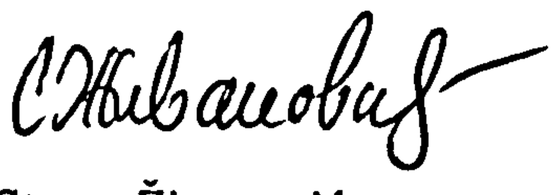

Stana Živanović
February 2006

Contents

List of Figures

List of Tables

Notation

Vectors and Matrices

$[\ ]$	Matrix
$\{\ \}$	Vector
$[\ ]^T$	Transpose of a matrix
$[\ ]^{-1}$	Inverse of a matrix
$\{\ \}^T$	Transpose of a vector
$[\mathbf{A}]$	Discrete state matrix
$[\mathbf{C}]$	Discrete output matrix
$[\mathbf{C}_P]$	Diagonal matrix of weighting coefficients for parameters
$[\mathbf{C}_R]$	Diagonal matrix of weighting coefficients for target responses
$[\mathbf{G}]$	Matrix connecting vectors of changes in target responses and updating parameters
$\{\mathbf{P}_0\}$	Initial vector of updating parameters
$\{\mathbf{P}_u\}$	Vector of updated parameters
$\{\mathbf{R}_0\}$	Initial vector of target responses
$\{\mathbf{R}_e\}$	Experimentally obtained vector of responses
$\{\Delta\mathbf{R}\}$	Vector of response differences in analytical and experimental models
$\{\Delta\mathbf{P}\}$	Vector of parameter differences in two successive iterations
$[\mathbf{S}]$	Sensitivity matrix
$\{\mathbf{v}_k\}$	Measurement noise vector at time instant k
$\{\mathbf{w}_k\}$	Process noise vector at time instant k
$\{\mathbf{x}_k\}$	State vector at time instant k
$\{\mathbf{y}_k\}$	Response vector at time instant k

Small Letters

a	Acceleration response
a, b	Parameters describing a gamma distribution
$a_c(t)$	Modal acceleration due to a narrow band force
$a_{i,k}, b_{i,k}, c_{i,k}$	Fitting parameters for i^{th} harmonic $(k = 1, 2, 3)$

$a^s_{i,k}, b^s_{i,k}, c^s_{i,k}$	Fitting parameters for i^{th} subharmonic ($k = 1, 2$)
a_{lim}	Limiting value of peak acceleration
$a_{sin}(t)$	Modal acceleration due to a sinusoidal force
$a(t)$	Time varying modal acceleration
c	Correction coefficient
$d(t)$	Time varying modal displacement
er	Error function
f_0	Fundamental natural frequency
f_a	Natural frequency from an analytical model
f_e	Natural frequency obtained experimentally
$\bar{f}_j$	Frequency ratio between the current frequency line in a spectrum around a harmonic and the step frequency
$\bar{f}^s_j$	Frequency ratio between the current frequency line in a spectrum around a subharmonic and the step frequency
f_n, f	Natural frequency of a footbridge
f_s	Walking frequency
$f(x)$	Probability density functions of random variable x
h	Thickness
i	Current (sub)harmonic number
i, j	Imaginary unit, $\sqrt{-1}$
k	Spring stiffness
l_s	Step length
m	Modal mass; Number of target responses
n	Number of updating parameters
p_c	Probability density function of correction coefficient c
$p(f_s/f_n)$	Probability density function for variable f_s/f_n
$p(f_s/f_n, N)$	Joint probability density for variables f_s/f_n and N
$p(f_s/f_n, N, c)$	Joint probability density for variables f_s/f_n, N and c
r	Current mode number
n	Model order
t	Time
v_p	Walking speed
$v(t)$	Time varying modal velocity
x	Longitudinal axis of a footbridge; Random variable

Capital Letters

A_c	Peak modal acceleration due to a narrow band walking force (without taking into account variability of the dynamic loading factor)
A_r, B_r	Modal constants of the r^{th} mode of vibration

$A_{sin}(t)$	Peak modal acceleration due to a sinusoidal force
DLF_i	Dynamic loading factor for i^{th} harmonic
DLF_i^s	Dynamic loading factor for i^{th} subharmonic
$\overline{DLF_i}(\bar{f}_j)$	Normalised amplitude in spectrum around i^{th} harmonic
$\overline{DLF_i^s}(\bar{f}_j^s)$	Normalised amplitude in spectrum around i^{th} subharmonic
E	Error function; Dynamic modulus of elasticity
F	Force amplitude
F_d	Dampening force
F_h	Modal harmonic force
$F_i(t)$	Time varying force having energy that corresponds to i^{th} harmonic
$F_i^s(t)$	Time varying force having energy that corresponds to i^{th} subharmonic
$F_{sin}(t)$	Time varying harmonic force
$F(t)$	Time varying force induced by walking
$F(t,x)$	Time and space varying modal force induced by walking
L	Length of a footbridge; Number of test points
MF	Multiplication factor
N	Number of steps required to cross a footbridge; Number of vibration modes
$P_{A_{c,k}:A_{c,k+1}}$	Probability of $A_{c,k} < A_c \leq A_{c,k+1}$
P_c	Probability of occurrence of a certain peak acceleration A_c
P_j	j^{th} updating parameter
$P_{x=x_i}$	Probability of having random variable x equal to x_i
R_i	i^{th} target response
S_{ij}	Sensitivity of i^{th} response to a change in j^{th} parameter
$S_{n,ij}$	Normalised sensitivity of i^{th} response to a change in j^{th} parameter
T	Data acquisition time length
T_c	Time needed to cross a footbridge
W	Weight of a pedestrian

Greek Letters

$\alpha(\omega)$	Receptance
α, α^*	Mathematically modelled receptance and its complex conjugate
$\hat{\alpha}, \hat{\alpha}^*$	Measured receptance and its complex conjugate
α_0	Complex constant
δ	Variation
μ_x	Mean value of variable x
ϕ	Rotational shift in the Nyquist plane
ω	Forcing frequency
ω_r	Natural frequency of the r^{th} mode of vibration

ρ	Density
σ_x	Standard deviation of variable x
$\theta(\bar{f}_j)$	Phase for current frequency line around a harmonic
$\theta(\bar{f}_j^s)$	Phase for current frequency line around a subharmonic
ζ	Modal damping ratio
$\zeta_p(t)$	Time varying additional damping
ζ_r	Damping ratio of the r^{th} mode of vibration
Δc	Discrete step of correction coefficient
Δf	Frequency resolution
$\Delta(f_s/f_n)$	Discrete step of walking to natural frequency ratio
ΔN	Discrete step of number of steps
ΔP_j	Change in parameter P_j
ΔR_i	Change in response R_i
Δx	Discrete step for random variable x
Φ_i	Mode shape of the i^{th} mode of vibration
$\Phi_n(x)$	Space varying amplitude of a mode shape
$\Phi(t)$	Mode shape expressed as a function of time

Abbreviations

3D	Three-dimensional
AVS	Ambient Vibration Survey
BS	British Standard
COMAC	Coordinate Modal Assurance Criterion
CVA	Canonic Variate Analysis
DLF	Dynamic Loading Factor
DOF	Degree Of Freedom
FE	Finite Element
FEM	Finite Element Model
FRF	Frequency Response Function
HA	Horizontal Anti-symmetric (mode of vibration)
HS	Horizontal Symmetric (mode of vibration)
ISO	International Standardization Organization
MAC	Modal Assurance Criterion
MDOF	Multi Degree Of Freedom
RMS	Root Mean Square
SDOF	Single Degree Of Freedom
TP	Test Point
UK	United Kingdom
VES	Vibration Engineering Section
VA	Vertical Anti-symmetric (mode of vibration)
VS	Vertical Symmetric (mode of vibration)

Chapter 1

Introduction

Modern civil engineering structures exposed to human-induced dynamic loading, such as footbridges, long-span floors and staircases, have been becoming increasingly slender. As a consequence, the vibration serviceability of these structures is becoming their governing design criterion. The research reported in this thesis is concerned with vibration performance of slender pedestrian structures (footbridges, walkways, etc.) under dynamic loading induced by walking. However, the procedures developed in this thesis can also be readily adapted for checking the vibration performance of other slender structures exposed to walking excitation.

The rationale for the research and the thesis outline are described in this introductory chapter.

1.1 Research Problem

Excessive vibrations of slender pedestrian structures, such as footbridges, long-span floors and staircases, have occurred more frequently in the last 20 years than in the past. There are several reasons for this, such as:

- improved mechanical properties of structural materials leading to reduced structural mass,
- increased length of structural spans leading to increased slenderness, and
- aesthetic design requirements for eye-catching 'transparent' structural forms.

The factors mentioned above usually lead to very light structures that are also lightly damped. For example, a modal damping ratio as low as 0.5% has become a very frequent characteristic of modern footbridges, especially those that are made of steel, while the modal damping for composite long-span floors can be as low as 1%. In addition, these structures tend to have natural frequencies of the fundamental and often higher modes of vibration that are in the range of normal walking frequencies (1.5-2.5 Hz) or the first few of their integer multiples.

All this makes pedestrian structures prone to vibration due to human-induced dynamic loading, such as walking, jumping, running, swaying and bouncing. Examples of lively structures are numerous (Bachmann & Ammann, 1987; Bishop et al., 1993; Pimentel, 1997). Among them are the structures made from different materials and using different structural systems, indicating that the vibration serviceability problem is not exclusive to certain types of materials and structural forms. The problem is omnipresent and should be addressed comprehensively, starting from first principles.

1.1.1 Vibration Assessment due to Walking Excitation

Among the various types of human-induced dynamic excitation, walking is often the most frequent type for many structures. Therefore, it is necessary to model it mathematically to enable prediction of structural vibration behaviour under this load, which is often critical for design.

Walking, as are all types of human activities, is an extremely complex activity to model. This is because people generally walk in different styles making different numbers of steps for the same amount of time, having different step lengths and inducing different time-varying dynamic forces into the surfaces they walk on. Not only are these forces different for different people, but also a single person walks differently in different circumstances, depending on their mood, weather they are hurrying, if they are in a group and so on. As an additional illustration of the complexity of the walking process finally comes the fact that a single person during walking makes successive steps that differ slightly in terms of their length, duration and intensity of the force induced. Because of this, the walking force is not periodic, as assumed in most current design codes and guidelines, but it is a narrow-band random process (Brownjohn et al., 2004b). Therefore, the study of forces induced by people during walking requires research into their inter- and intra-subject variability (Rainer et al., 1988; Ebrahimpour et al., 1996; Kerr, 1998; Brownjohn et al., 2004b). The term inter-subject variability implies that different pedestrians generate different dynamic forces, and intra-subject variability means that even a single pedestrian induces a walking force that differs with each step. This study should be done by making use of statistics and probability theory as done in other engineering disciplines dealing with random loading, such as wind engineering.

A good general framework for handling vibration serviceability is developed in the ISO 10137 guideline (ISO, 1992). This guideline deals with serviceability of buildings and walkways and defines the vibration source, path and receiver as three key, but separate, issues which require consideration when dealing with the vibration serviceability of any structure. Although this rationalisation of the vibration serviceability problem into the characterisation of the three separate parts seems straightforward, it is actually a very difficult task. This becomes clear when trying to make use of existing design provisions available for vibration serviceability assessment. Namely, they often fail to predict level of vibration occurring in practice either

by overestimating or underestimating it. This overestimation or underestimation can be quite significant, depending on the loading scenarios considered.

In the case of footbridges, the current design practice worldwide usually addresses the vibration serviceability problem in an oversimplified way. For example, the current British guideline for footbridge design (BSI, 1978) treats human-induced loading as that produced by an average person who walks at constant frequency to cause resonance of the footbridge structure. The response of the footbridge to this loading is calculated and then used for vibration serviceability assessment. Therefore this performance-based code provision (when response is calculated and assessed) uses a typical deterministic approach to model the walking force. Moreover, the walking force is essentially random in nature, so a deterministic approach may not be appropriate. Similar code provisions exist in Canadian design guidelines (OHBDC, 1983; CSA, 2000) as well as in American (AASTHO, 1997), European (ENV, 1997) and Hong Kong (HD, 2002) design guidelines. On the other hand, some design guidelines, such as those in Switzerland (SIA, 1989) and Japan (Yoshida et al., 2002) avoid performance-based assessment of vibrations altogether by restricting the range of natural frequencies that are allowed for footbridge structures. Their criteria for avoiding certain frequency ranges are often too restrictive for design (Pimentel, 1997) since the structural natural frequency is not the only relevant parameter that governs vibration behaviour of the footbridge. If actual mass, stiffness and/or damping are high enough, the actual dynamic response may be low enough so that a footbridge having any natural frequency may have satisfactory vibration performance under pedestrian-induced excitation.

Some new and interesting concepts have recently been employed in guidance for vibration serviceability assessment of post-tensioned concrete floors in buildings. Namely, to account for inter-subject variability, the UK Concrete Society has introduced a new design procedure (Pavic & Willford, 2005) that indirectly makes use of a probability-based approach to vibration serviceability assessment. In this approach, a deterministic sinusoidal force, that has 25% of probability of exceedance, is suggested as a model for human walking in design. Although this criterion might be on the safe side when doing vibration assessment for everyday loading scenarios, it is valuable as it is a pioneering attempt to introduce a probability approach into design practice dealing with human-induced dynamic loads.

This thesis concentrates on improvement of the design strategy for a *single* person walking primarily across footbridges. Among the three key aspects of the design against excessive vibrations according to ISO 10137 (vibration source, path and receiver) most attention in this thesis is devoted to the modelling of the vibration source, that is the walking force induced by a single walker. The modelling of the force generated by a single pedestrian is a necessary building block for group- and crowd-induced walking excitations of footbridges and other structures. These loadings due to group and crowd of pedestrians are beyond the scope of this thesis. Since the walking across footbridges and similar structures is analysed in this thesis, the current practice in vibration serviceability assessment of footbridge structures under human-induced load will be considered in more detail in the next section.

1.1.2 Vibration Assessment in Footbridges

To prevent problems with excessive footbridge vibrations, in the late 1970s the pioneering design code BS 5400 appeared in the UK to deal with the effects of human-induced excitation (BS, 1978). At that time it was known that, while walking, pedestrians induce a dynamic force that has components in all three directions: vertical, horizontal-lateral and horizontal-longitudinal (Harper, 1962). However, the design code considered the vertical component only. This was done because this component was the largest of the three and believed to be the only one capable of causing excessive vibrations.

The code gives a procedure for checking the vibration serviceability of footbridges due to a single person walking with a constant speed and with a frequency equal to the fundamental natural frequency of the footbridge investigated. This harmonic force was considered as the worst case scenario. The code itself was the first footbridge design code treating the vibration serviceability problem and it is, after almost 30 years, among the most advanced in the world. Similar code provisions appeared after 1978 in some other countries such as Canada (OHBDC, 1983) and Hong Kong (HD, 2002).

Since 1978, considerable research has emerged highlighting shortcomings of the BS 5400 and similar design codes used for vibration serviceability checks around the world. The infamous problem with excessive lateral vibration of the London Millennium Bridge in 2000, prompted the UK Highways Agency to include provisions for lateral vibrations in their Design Manual for Roads and Bridges (HA, 2001). However, the procedure for checking vibration serviceability in the vertical direction, although almost 30 years old, stayed the same as in the BS 5400.

The following issues which do not feature in BS 5400 have emerged as its main shortcomings:

1. Human-induced force is dependent on the walking frequency (Rainer et al., 1988).
2. There is inter-subject variability in human-induced forces such as variability in their amplitudes (Rainer et al., 1988; Kerr, 1998), frequencies (Matsumoto et al., 1978) as well as duration of the load indicating the time required to cross the bridge (Rainer et al., 1988; Young, 2001).
3. There is intra-subject variability in human induced walking forces, that is a pedestrian cannot make two exactly the same steps (Ebrahimpour et al., 1996) and as a consequence these forces are narrow band random processes in their nature (Brownjohn et al., 2004b) rather than deterministic periodic forces.
4. Not only is the first harmonic of the walking force important, but also higher harmonics might be relevant (Pimentel, 1997).
5. The binary pass-fail criterion based on a single value for limiting acceleration response, currently featuring BS 5400, might not be appropriate for the vibration serviceability

check. Bearing in mind inter-subject variability in vibration perception for different people, it might be more appropriate to define a probability based vibration limit (Kajikawa & Kobori, 1977). Also, the BS vibration limit defined as a single value is a compromise based on laboratory-based research work conducted in the late 1960s (Leonard, 1966; Smith, 1969). Because of this, there is a need to check the appropriateness of this vibration scale on as-built footbridges in open space environments. It might be useful to take into account some additional factors during this check, such as location of the footbridge, frequency of pedestrian traffic and whether people standing on the bridge might be expected. The current BS perception limit is actually a compromise between the limits for a standing and a walking person and it is not explicitly defined for which of these two options the bridge should be designed.

As a consequence of these shortcomings, there is a strong body of evidence of unsatisfactory code provision when either predicting structural vibration response or people's reaction to it, or both. Some examples illustrating this are reported by Bachmann & Ammann (1987) and Pimentel (1997).

1.2 Need for Research

It is interesting that, despite the BS 5400 shortcomings, not much has been done to improve its design procedure. A possible reason for this is that it is difficult to formulate a new procedural framework that is broad enough to cover force variability and, at the same time, simple enough to be used in practice. For example, Ebrahimpour et al. (1996) suggested a probability approach for taking into account all randomness in human-induced forces. However, they did not manage to make a comprehensive force model and make greater impact on design practice.

It is generally accepted nowadays that vibrations induced by pedestrians are in most cases a serviceability, rather than a safety (i.e. strength-related) issue. This is because these vibrations mainly have the potential to cause discomfort for users of the structure without compromising structural integrity. This is one more reason why the procedures for vibration serviceability check are not well developed. Historically, in the past priority was given to researching ultimate limit states of structures since their better understanding and handling in design would reduce the probability of structural collapse with catastrophic consequences.

When the high profile problem with excessive lateral vibration of the London Millennium Bridge occurred on its opening day in June 2000, research communities worldwide concentrated their efforts in researching this relatively new phenomenon. This, to some extent, masked the emerging problem with vibrations in the vertical direction, and might be a reason why not much work has been done on improvement of design codes in this sense. Interestingly, the author of this thesis herself was attracted by the area of vibration serviceability of footbridges after experiencing strong, unexpected and, from personal point of view, quite

disturbing lateral vibrations of a massive road bridge over Sava River in Belgrade, occupied only by a walking crowd of people during a mass civic protest in 1996.

However, it should be said that some good quality research took place after the 1978 edition of BS 5400. Although not codified, this research pointed in the right direction and inspired other researchers worldwide. For example, inter-subject variability in the walking frequency was documented by Matsumoto et al. (1978) while variability in the force magnitude was reported by Rainer et al. (1988) and 10 years later by Kerr (1998) in a more detailed investigation. Imperfections in the walking force induced by an individual were explained by Brownjohn et al. (2004b) and further studied by Sahnaci & Kasperski (2005). Most of these works are explained in detail in the literature review presented in Chapter 2. Here, they are mentioned as important building blocks in understanding key aspects of modelling of the walking force. This understanding has enabled a development of a comprehensive design procedural framework in this thesis that can take into account stochasticity of all relevant parameters describing walking excitation.

Following the ISO (1992) proposal for the rationalisation of vibration serviceability problem into three separate parts (source, path and receiver), the main questions, still unanswered, can be sumarised as follows:

- Human-induced walking excitation: How to model it in a way to take into account both inter- and intra-subject variability? Which loading scenarios are relevant for design (single person excitation, stream of pedestrians, crowd load, etc.)?
- Path: How to get reliable modal properties of the bridge, especially in the design phase?
- Human as a receiver: Who is the receiver: walking or/and standing person? What are the appropriate vibration perception scales for vibrations in both the vertical and horizontal directions?

The latest draft of the revised ISO 10137 (ISO, 2005) deals with some of these questions. For example, it suggests that in the vibration serviceability design of footbridges, four loading scenarios could be considered. These are: a single person, small groups, a stream of pedestrians and occasional festive events. In addition, this draft suggests checking of vibration perception for both a standing and a walking person. This is a significant step forward having in mind that most design codes consider only a single person walking scenario and define the vibration limit as a single number, for which it is not clear if it applies to a walking or a standing person.

1.3 Proposed Solution and Scope

This thesis combines the experimental and analytical approach to create a new and improved framework for the vibration serviceability check of footbridges. The main aim is to investigate, propose and verify a probability-based design procedure that can replace the existing

deterministic one for a *single* person walking. In this way not only can the most important factors describing inter- and intra-subject variability be taken into account, but also the probability of a certain vibration level not to be exceeded can be calculated. This enables development of a new probability-based vibration serviceability design philosophy.

The reason for considering a single person is that it is necessary to describe individual loading reliably before extending the procedure to more complicated and realistic loading scenarios involving groups of people. As previously mentioned, group loading is beyond the scope of this thesis.

As a side product in this thesis, a procedure for finding unacceptable vibration limits for moving (walking) people has been developed. This is based on an assumption that some human-structure interaction in the vertical direction takes place during walking.

Therefore, this thesis concentrates on research into modelling of the vibration source, which is the walking force, and it also gives some insight into the modelling of the vibration path and human perception of footbridge vibration. An assumption used when developing a design procedure is that modal properties of the structure are known in advance. It should be said that this thesis has no ambition of resolving all questions quoted in Section 1.2, but rather aims to give a contribution towards updating the existing design procedures primarily through improving the walking force modelling.

To reduce uncertainty in the structural modal properties required when doing vibration serviceability assessment, as well as to demonstrate a reliable way of their estimation, an as-built lively footbridge was tested and its modal properties were estimated. By doing this and by measuring vibration response to single person excitation, this bridge became available as a test-bed structure for the verification of the force model in addition to two other footbridges for which data were collected by other members of the Vibration Engineering Section in the past. An additional motive for modal testing of the as-built footbridge during the work on this thesis was to equip the author with knowledge and skills relevant for vibration serviceability assessment of existing structures (such as modal testing, data acquisition, signal processing and parameter estimation). This gave confidence when using and analysing the data collected in the past, helped understanding the way the data were collected and difficulties that can be encountered during experimental measurements in laboratory and field conditions.

1.4 Thesis Outline

The work in this thesis was conducted over 37 months of full-time research. It is organised in the form of six papers with the aim to publish them in peer-reviewed scientific journals. Chapters 2-7 contain these papers, three of which are already in print. The remaining three papers have been submitted for publication. Since the journal papers were written to stand alone, each chapter-paper is briefly introduced in a preface. The aim of this is to describe the importance of the chapter and its relationship with the rest of the thesis. Also, the chapters-

papers are slightly amended in comparison with the submitted papers to avoid repetition wherever possible and to convey information in a form appropriate to thesis format.

The research work reported in this thesis is presented in nine chapters. Chapter 1 is this introductory chapter explaining the problem being researched in the thesis, the scope of work as well as the organisation of the thesis. A literature review giving background in vibration serviceability problems in footbridges is outlined in Chapter 2. Chapter 3 deals with modal testing and experimental estimation of dynamic properties of a test-bed footbridge as well as its finite element modelling and manual correlation with experimental results. To further improve the correlation between the manually tuned finite element and the experimental models, an automatic updating procedure was used as explained in Chapter 4. This combination of analytical and experimental approach enabled a reliable estimation of modal properties of the footbridge analysed. These properties, together with modal properties of two other as-built footbridges for which data were already available, were then used for studying the human-structure dynamic interaction during a footbridge crossing (Chapter 5). Also, in Chapter 5 the effect of the human-structure interaction on development of the structural vibration response was investigated. Based on this analysis, a methodology for establishing limiting vibration level for a pedestrian crossing a footbridge is suggested. Chapters 6 and 7 are the main body of the thesis and are concerned with mathematical modelling of the dynamic force induced by walking as well as the estimation of the structural vibration response. More precisely, Chapter 6 describes a probability-based analytical framework for vibration serviceability check of footbridges responding in a single vibration mode. Chapter 7 then extends this model to allow for estimating the multi-mode response of a footbridge structure. A discussion of the research and its findings is given in Chapter 8, whereas Chapter 9 contains a summary of its conclusions and recommendations for future work.

Preface to Chapter 2

Chapter 2 contains a literature review addressing the vibration serviceability of footbridges under human-induced dynamic excitation. The review is written as a comprehensive paper reviewing and discussing all important aspects of the topic such as:

- human-induced dynamic force,
- dynamic properties of footbridge structures,
- pedestrians as receivers of footbridge vibrations,
- design aspects regarding vibration serviceability and
- measures for suppressing excessive vibrations in as-built lively footbridges.

Chapter 2

Literature Review

This chapter, in a slightly amended form, has been published under the following reference:

Živanović, S., Pavic, A. and Reynolds, P. (2005) Vibration Serviceability of Footbridges under Human-Induced Excitation: a Literature Review, Journal of Sound and Vibration, 279 (1-2), 1-74.

Abstract

Increasing strength of new structural materials and longer spans of new footbridges, accompanied with aesthetic requirements for greater slenderness, are resulting in more lively footbridge structures. In the past few years this issue attracted great public attention. The excessive lateral sway motion caused by crowd walking across the infamous Millennium Bridge in London is the prime example of the vibration serviceability problem of footbridges. In principle, consideration of footbridge vibration serviceability requires a characterisation of the vibration source, path and receiver. This review is the most comprehensive review published to date of about 200 references which deal with these three key issues.

The literature survey identified humans as the most important source of vibration for footbridges. However, modelling of the crowd-induced dynamic force is not clearly defined yet, despite some serious attempts to tackle this issue in the last few years.

The vibration path is the mass, damping and stiffness of the footbridge. Of these, damping is the most uncertain but extremely important parameter as the resonant behaviour tends to govern vibration serviceability of footbridges.

A typical receiver of footbridge vibrations is a pedestrian who is quite often the source of vibrations as well. Many scales for rating the human perception of vibrations have been found in the published literature. However, few are applicable to footbridges because a receiver is not stationary but is actually moving across the vibrating structure.

During footbridge vibration, especially under crowd load, it seems that some form of human-structure interaction occurs. The problem of influence of walking people on footbridge vibration properties, such as the natural frequency and damping is not well understood, let alone quantified.

Finally, there is not a single national or international design guidance which covers all aspects of the problem comprehensively and some form of their combination with other published information is prudent when designing major footbridge structures. The overdue update of the current codes to reflect the recent research achievements is a great challenge for the next 5-10 years.

2.1 Introduction

In recent decades there has been a trend towards improved mechanical characteristics of materials used in footbridge construction. It has enabled engineers to design lighter, more slender and more aesthetic structures. A considerable variety of modern footbridge structural forms can be seen, for example, in recent articles by Biliszczuk et al. (2002), Block & Schlaich (2002), Eyre (2002), Firth (2002), Iso & Masubuchi (2002), Mimram (2002), Schlaich (2002), Strasky (2002), Takenouchi & Ito (2002) and Wörner & Schlaich (2002). As a result of these construction trends, many footbridges have become more susceptible to vibrations when subjected to dynamic loads.

This review is focused on human-induced dynamic loading of footbridges. This is a frequently occurring and often dominant load for footbridges as it stems from the very purpose of a footbridge - to convey pedestrians. It was noted very early that this type of dynamic excitation could cause excessive vibrations and in extreme cases even a collapse of the structure. It is known that in 1154 a timber footbridge collapsed under a crowd that wanted to greet the Archbishop William (Wolmuth & Surtees, 2003). However, details related to the exact crowd behaviour are not known. Probably the oldest case of footbridge failure due to dynamic human-induced load reported in detail was the one which occurred in 1831 in Broughton, UK while 60 soldiers were marching across a bridge. It was this event that prompted the placement of the famous notices on a considerable number of bridges with a warning to troops to break step when crossing (Tilly et al., 1984). One of the notices displayed on a railway suspension bridge at Niagara Falls, USA reads as follows (Taylor, 2002):

> A fine of $50 to $100 will be imposed for marching over this bridge in rank and file or to music, or by keeping regular step. Bodies of men or troops must be kept out of step when passing over this bridge. No musical band will be allowed to play while crossing except when seated in wagons or carriages.

Although there have been many reported cases of lively footbridges in the past (Bachmann & Ammann, 1987; Bachmann, 1988; 1992a; 1992b; Fujino et al., 1993), this problem attracted considerably greater public and professional attention after the infamous swaying of the new and attractive Millennium Bridge in London during its opening day on 10 June 2000 (Dallard et al., 2001a). The Millennium Bridge problem attracted more than 1000 press articles and over 150 broadcasts in the media around the world. In this and almost all other previously reported problems related to footbridge vibrations, the excessive vibrations were caused by a near resonance of one or more modes of vibration. The reason for this is that the range of footbridge natural (vertical or lateral) frequencies often coincides with the dominant frequencies of the human-induced load (Leonard, 1966). It is important to note that the problems have occurred on a range of different structural types, such as cable-stayed, suspension and girder bridges, as well as on footbridges made of different materials (e.g. timber, composite steel-concrete, steel, reinforced and prestressed concrete). The problem of

footbridge vibrations is becoming so alarming that a major international conference, entitled Footbridge 2002, was recently held in Paris and was almost completely devoted to this issue. Among many articles given at the conference, three presented the current state-of-the-art in footbridge vibration serviceability design, especially with regard to human-induced dynamic load (Bachmann, 2002; Schlaich, 2002; Willford, 2002).

Nowadays, it is generally accepted that vibration produced by human-induced loads is usually a serviceability rather than a safety (i.e. strength-related) problem (Wood, 1948; Jones et al., 1981; Bachmann & Ammann, 1987; Pimentel et al., 1999). This is because human beings are very sensitive to vibration levels as low as 0.001 mm (Pretlove & Rainer, 1995). This high sensitivity usually triggers the vibration serviceability problem much before the vibration levels are even remotely sufficient to cause damage of the structure itself.

The ISO 10137 guidelines (ISO, 1992) define the vibration source, path and receiver as three key, but separate, issues which require consideration when dealing with the vibration serviceability of any structure. Following the notion of such an analytical framework, this chapter reviews these three issues for footbridges separately.

The literature review contains six parts. In the first three, the materials related to the vibration source, path and receiver are presented. The fourth part outlines the human-structure dynamic interaction phenomenon while in the fifth some important design procedures/recommendations are reviewed. In this chapter, the term 'design procedure' or 'design recommendation' stands for design checking methods offered by different authors which are not formally codified, while for codified procedures the terms 'design guidelines/codes (of practice)' are used. Naturally, some of the design recommendations tend to be adopted in key design codes of practice which deal with footbridge vibration serviceability. These codes are also presented. The last part reviews typical remedial measures which can be undertaken to lessen the excessive vibrations of footbridges.

2.2 Humans as Vibration Source for Footbridges

During walking, a pedestrian produces a dynamic time varying force which has components in all three directions: vertical, horizontal-lateral and horizontal-longitudinal (Bachmann & Ammann, 1987). This single pedestrian walking force, which is due to accelerating and decelerating of the mass of their body, has been studied for many years. In particular, the vertical component of the force has been most investigated. It is regarded as the most important of the three forces because it has the highest magnitude. Other types of human-induced forces important for footbridges are due to running and some forms of deliberate vandal loading (jumping, bouncing or horizontal body swaying). Some of these types of human-induced forces have been studied not only for a single person, but also for small groups of people. However, large groups of pedestrians have seldom been formally investigated.

2.2.1 Early Works

Probably the oldest report of noticeable vibrations in footbridges was made by Stevenson in 1821. In addition to this, the same author reported severe vibrations due to a marching regiment crossing over a bridge, indicating very early a need to consider human-induced dynamic loads in bridge design. It is interesting that 10 years after Stevenson's observations, as previously mentioned, a bridge collapse in Broughton was caused by marching soldiers.

Tilden (1913) wrote an excellent article for that time primarily devoted to the crowd load. However, he also reported some experiments in which, although not having precise measurement devices, he tried to quantify the dynamic effect of a force generated by a single person due to different activities.

2.2.2 Single Person Force Measurements

One of the first measurements of pedestrian-induced forces was conducted by Harper et al. (1961; Harper, 1962) with the aim to investigate the friction and slipperiness of a floor surface. They measured horizontal and vertical force from a single footstep using a force plate (Cross, 1999). The shape of the vertical force with two peaks and a trough of the kind shown in Figure 2.1a was recorded. This general shape of the force time history was confirmed by other researchers such as Galbraith & Barton (1970), Blanchard et al. (1977), Ohlsson (1982), Kerr (1998) and many others.

A lot of research into walking forces has been done in the field of biomechanics, usually with the aim to investigate differences in the step patterns between patients who are healthy and those with abnormalities. In one of these investigations, Andriacchi et al. (1977) measured, similar to Harper et al. (1961), single step walking forces in all three directions by means of a force plate. Typical shapes are presented in Figure 2.1. They also reported that increasing walking velocity led to increasing step length and peak force magnitude. In other words, the dynamic effect of the forces was changing with the walking speed. This demonstrates the complex nature of human-induced dynamic forces and their dependence on many parameters. For example, tests with control of only one of the parameters, such as the pacing frequency, speed or step length, each produce different relationships between the walking speed and the pacing frequency (Bertram & Ruina, 2001). Also, with increasing walking speed, the variability in vertical and lateral forces over successive steps increases, whereas the longitudinal force has the minimum variability at a normal walking speed (Masani et al., 2002).

Galbraith & Barton (1970) measured a single step vertical force on an aluminium plate, ranging from slow walking to running. They reported that the shape of running force differed from the walking force in having only one peak (Figure 2.2). Subject weight and step frequency were identified as important parameters which increase led to higher peak amplitudes of the force. On the other hand, the force was not dependent on the type of footwear and walking surface. By combining individual foot forces, which are assumed to be identical, a continu-

ous walking or running force can be obtained artificially (Figure 2.2). During walking there are some short time periods when both feet are on the ground which gives an overlapping between the left and right leg in the walking time history (Figure 2.2 - right). On the other hand, during running there are periods when both feet are off the ground leading to zero force recorded (Figure 2.2 - left).

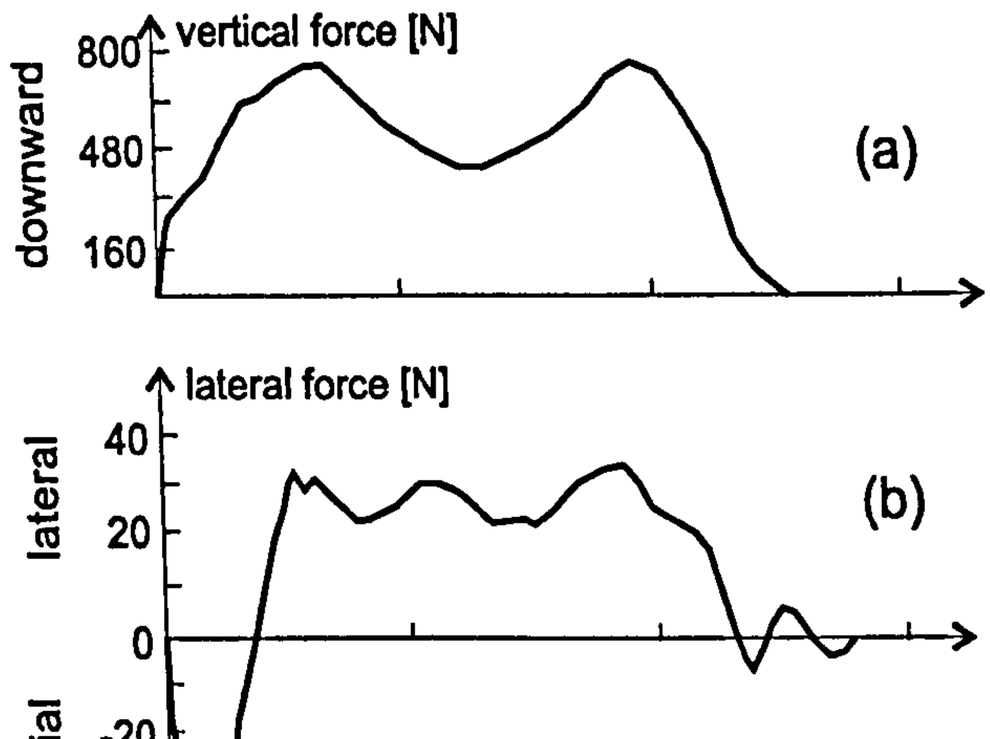

Figure 2.1: Typical shapes of walking force in a) vertical, b) lateral and c) longitudinal direction (after Andriacchi et al., 1977).

A very comprehensive research into human forces relevant to footbridge dynamic excitation was conducted by Wheeler (1980; 1982) who systematised the work of other researchers related to different modes of human moving from slow walking to running (Figure 2.3). He also presented dependence of many walking parameters, such as step length, moving velocity, peak force and contact time (the time while one foot is in the contact with the ground) as a function of the pacing frequency (Figure 2.4). It was noted that all these parameters are different for different persons, but some general conclusions can be drawn. For example, that with increasing step frequency the peak amplitude, stride length and velocity increase while contact time decreases.

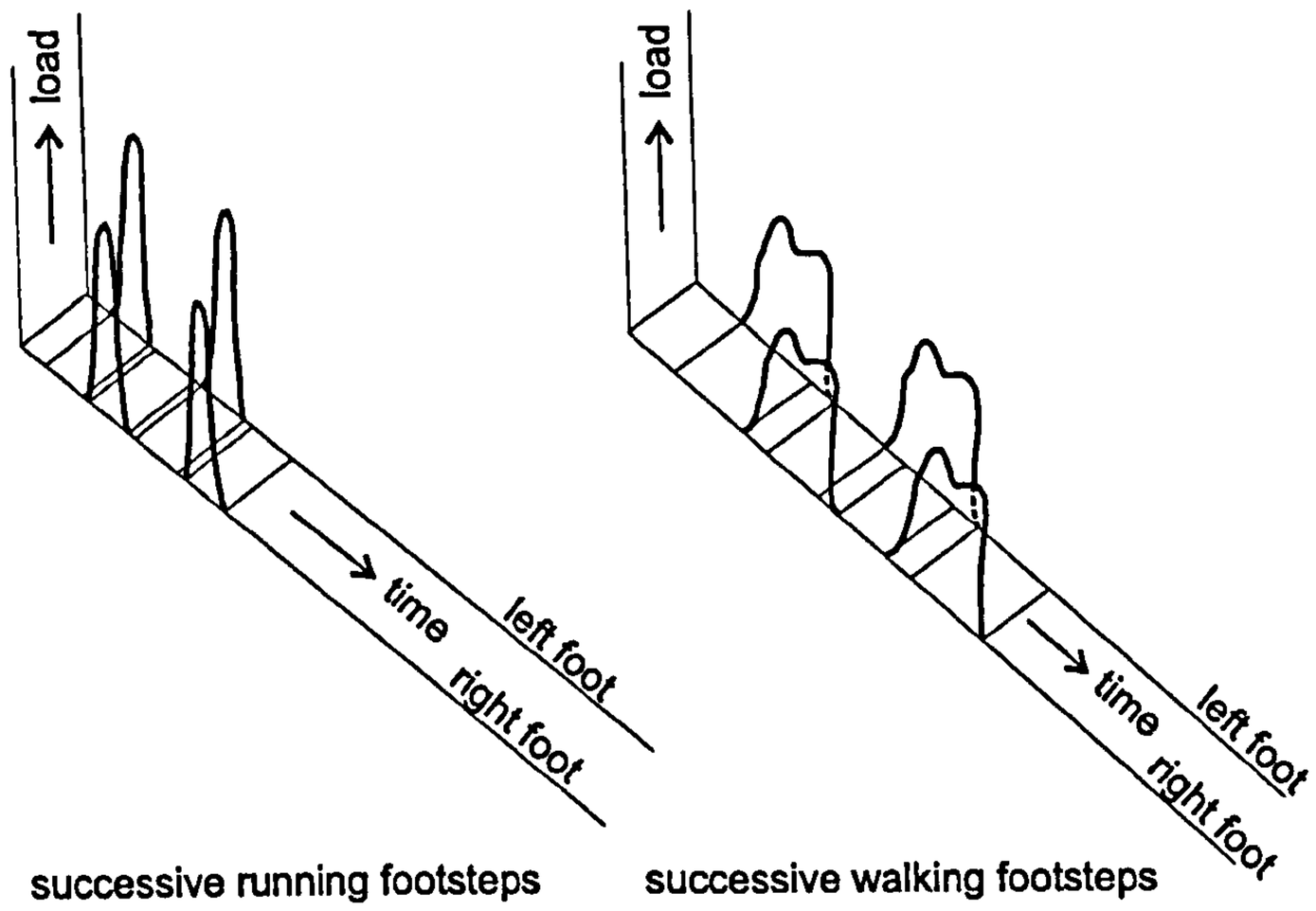

Figure 2.2: Typical pattern of running and walking forces (after Galbraith & Barton, 1970).

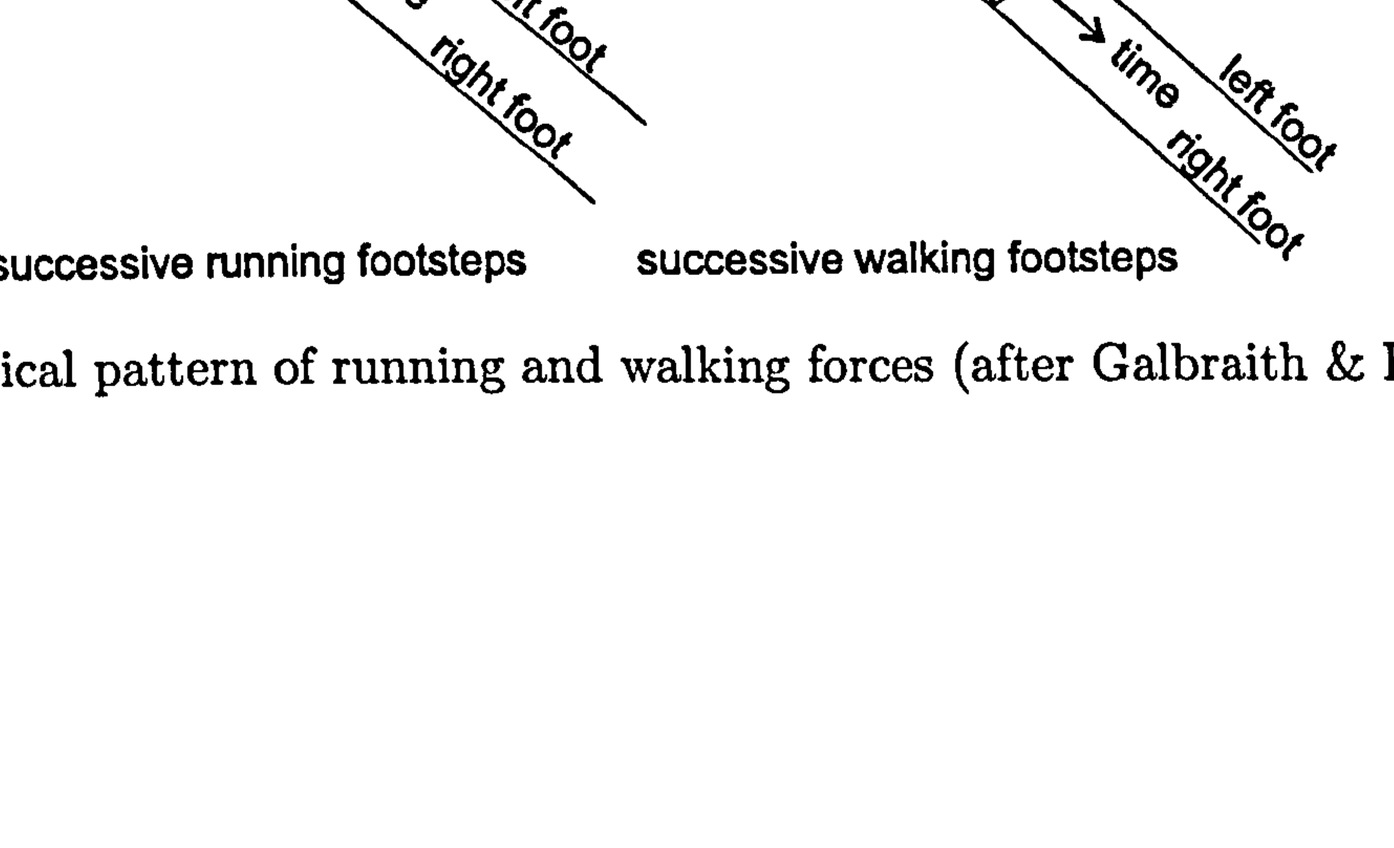

Figure 2.3: Typical vertical force patterns for different types of human activities (after Wheeler, 1982).

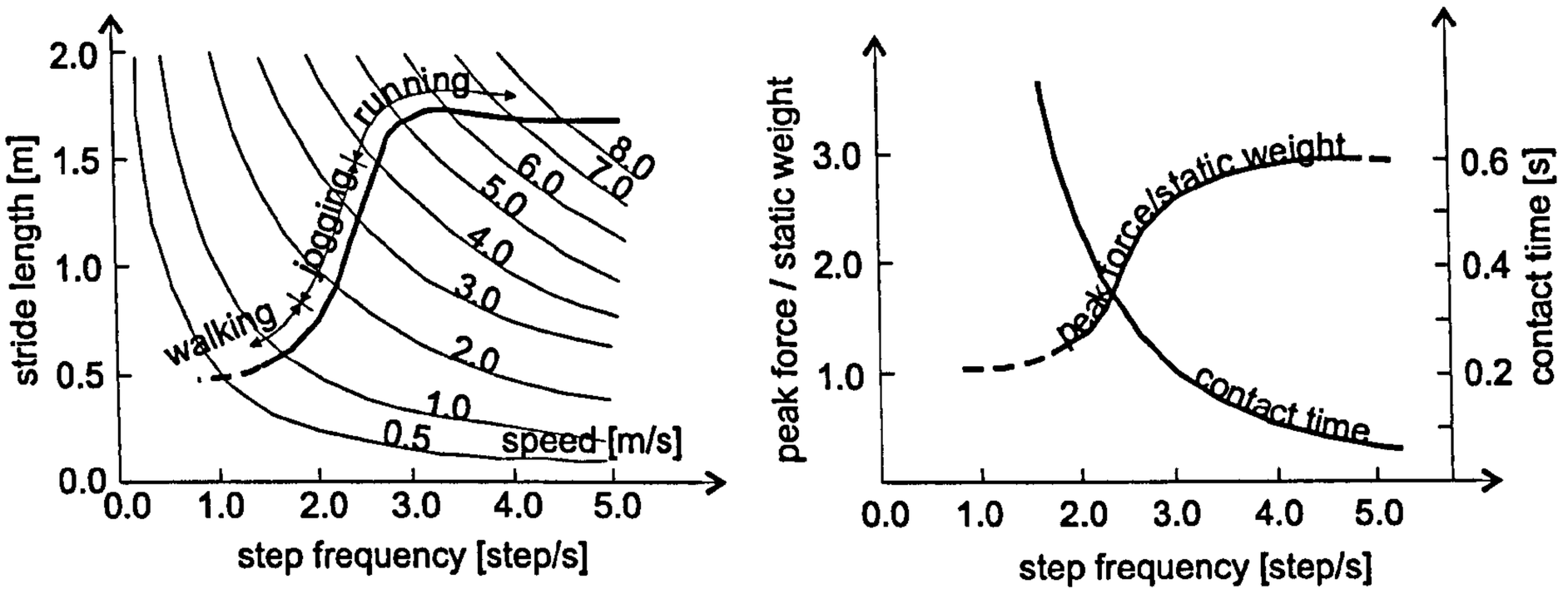

Figure 2.4: Dependence of stride length, velocity, peak force and contact time on different pacing rates (after Wheeler, 1982).

Measurements of individual step forces were followed by the more advanced and informative measurements of continuous walking time histories comprising several steps. For this purpose Blanchard et al. (1977) used a gait machine described by Skorecki (1966), Rainer et al. (1988) used a floor strip, whereas Ebrahimpour et al. (1994; 1996) used a platform instrumented with several force plates. The measured time histories were obviously near periodic with the (average) period equal to reciprocal value of the (average) step frequency. Unfortunately, in all these works the attention was paid only to vertical forces. However, based on measurements by Andriacchi et al. (1977) and taking into account that the fundamental frequency of the lateral walking-induced force is two times lower than its counterpart relevant to the vertical and longitudinal forces (Bachmann & Amman, 1987), general shapes for continuous forces in all three directions can be constructed if their perfect periodicity is assumed (Figure 2.5).

A reliable statistical description of normal walking frequencies was first given by Matsumoto et al. (1972; 1978) who investigated a sample of 505 persons. They concluded that the frequencies followed a normal distribution with a mean pacing rate of 2.0 Hz and standard deviation of 0.173 Hz (Figure 2.6). Kerr & Bishop (2001) obtained a mean frequency of 1.9 Hz but from an investigation of only 40 subjects. It is also interesting that Leonard in 1966 concluded that the normal walking frequency range is 1.7-2.3 Hz, which is in broad agreement with what Matsumoto et al. (1978) and successive researchers have found. Similar comprehensive statistically based investigations, such as the one given by Matsumoto et al. (1978) for walking, do not exist for other types of human-induced forces. However, there are some proposals as to the typical frequency ranges for different human activities (running, jumping, bouncing, etc.). For example, Bachmann et al. (1995b) defined typical frequency ranges of 1.6-2.4 Hz for walking, 2.0-3.5 Hz for running, 1.8-3.4 Hz for jumping, 1.5-3.0 Hz for bouncing and 0.4-0.7 Hz for horizontal body swaying while stationary.

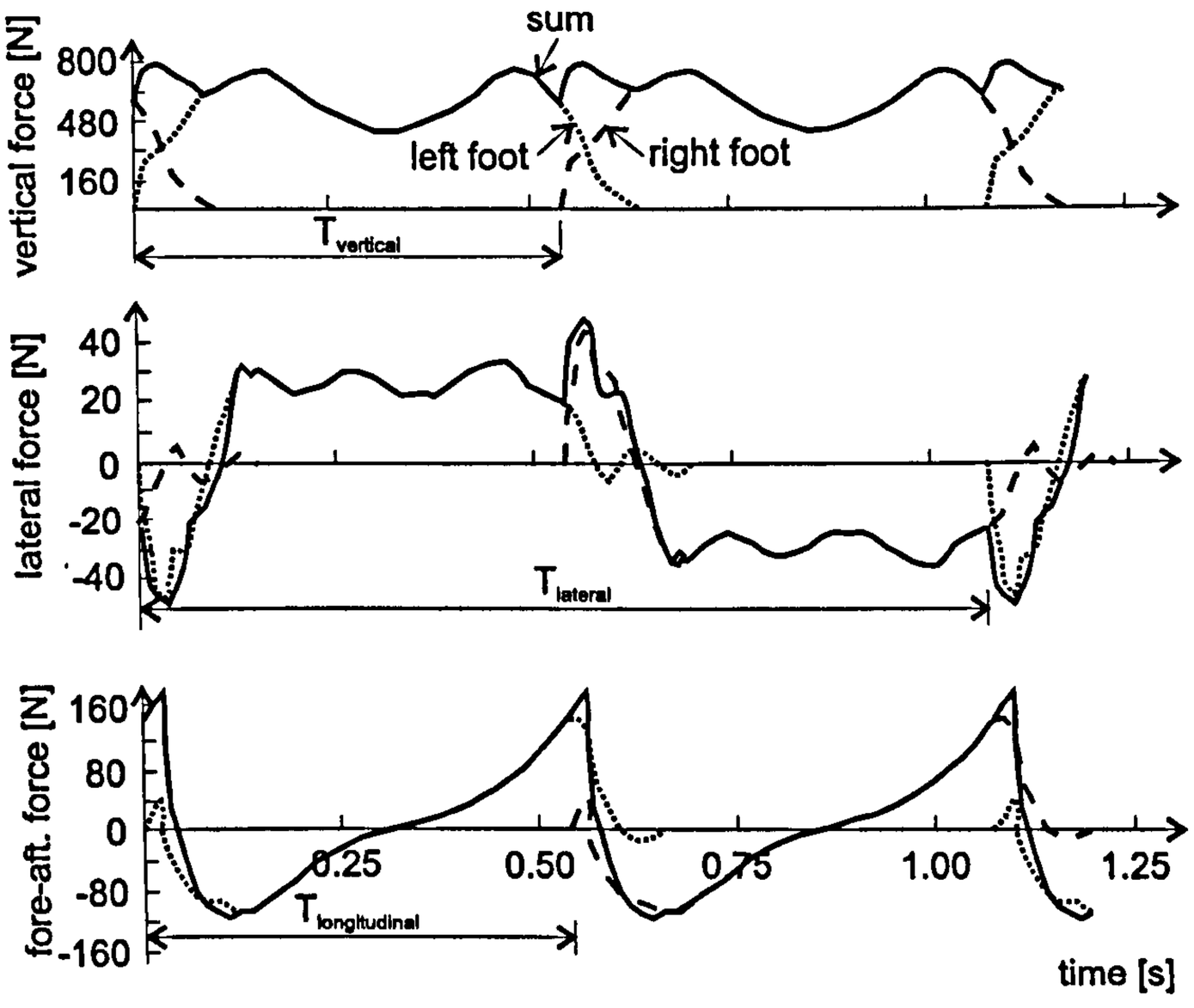

Figure 2.5: Periodic walking time histories in vertical, lateral and longitudinal directions.

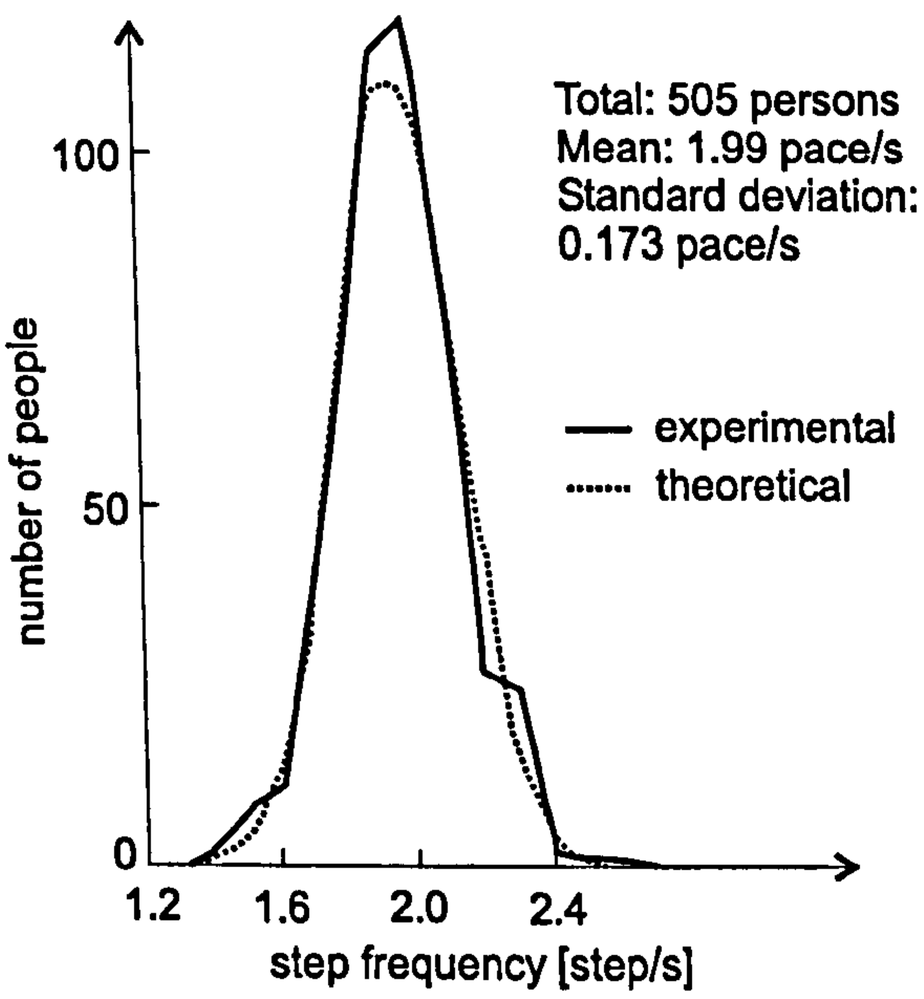

Figure 2.6: Normal distribution of pacing frequencies for normal walking (after Matsumoto et al., 1972).

Taking an alternative approach to the problem, Ohlsson (1982) was interested more in the energy and frequency content than in the exact time history of the vertical force. He concluded that a single step force had most of its energy in the frequency range from 0 to 6 Hz. His successor Eriksson (1994) investigated this issue more closely. He measured a continuous walking force indirectly, concluded that it was a narrow-band random process and, quite conveniently, presented it in terms of its auto (or power) spectral density (Figure 2.7).

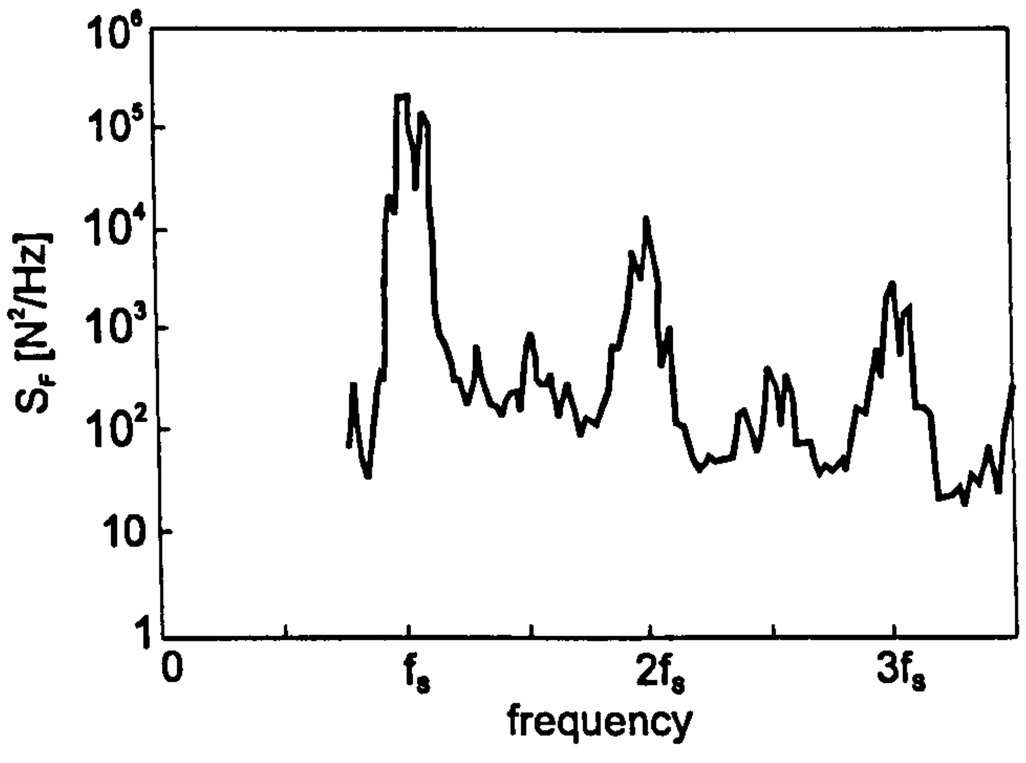

Figure 2.7: Auto spectral density of a walking force (after Eriksson, 1994).

With regard to all this, it is prudent to stress that practically all mentioned measurements of the walking forces were conducted on various forms of rigid surface, such as a force plate on stiff ground, gait machine or high-frequency structure (for indirect measurements of the kind performed by Rainer et al. in 1988 and Eriksson in 1994). This leaves the possibility that the reported forces could be different from the ones that actually occur on low frequency footbridge structures that move perceptibly.

Regarding vandal loading, some researchers have presented jumping forces from individuals (Ebrahimpour, 1987; Ellis & Ji, 1994; Bachmann et al., 1995b, Yao et al., 2002; 2003). During jumping, the peak forces have been found to be several times higher then the jumper's weight. Moreover, very recently gathered experimental evidence has shown that horizontal forces due to vertical jumping also exist (Pavic et al., 2002c), where the front-to-back force was considerably larger than its side-to-side counterpart. Also, time histories of the bouncing force were recently presented by Yao et al. (2002) who, quite differently from other researchers, measured these forces on a flexible and perceptibly moving instrumented platform.

It should be noted that the majority of past investigations have been into forces due to activities of a single person. However, some limited measurements of forces produced by groups of people do exist and will be mentioned later.

2.2.3 Force Modelling

To successfully apply the measured dynamic forces in design it is necessary to model them analytically. Two types of such models can be found in the literature: time domain and frequency domain models. Although the former is much more common than the latter, in both cases mathematical modelling of human-induced dynamic forces is a complicated task. This is because:

1. there are many different types of human-induced forces and some of them change not only in time but also in space (e.g. walking and running);
2. forces are dependent on many parameters as demonstrated in the preceding text;
3. dynamic force generated by a single person is essentially a narrow-band random process which is not well understood and therefore difficult to mathematically model;
4. the influence of the number of persons as well as their degree of synchronisation (correlation) is difficult to generalise; and
5. there are strong indications that the forces are different in cases of perceptibly and not so perceptibly moving footbridges because of different behaviour of people in these two situations.

However, force models do exist and are used in contemporary design. They are based on some more or less justifiable assumptions which will be presented.

2.2.3.1 Time Domain Force Models

Generally, two types of time domain models have been found in the literature: deterministic and probabilistic. The first type intends to establish one general force model for each type of human activity, while the other takes into account the fact that some parameters which influence human force, such as the previously mentioned activity frequency, person's weight and so on, are random variables whose statistical nature should be considered in terms of their probability distribution functions.

In any case, time-domain models for walking and running are based on an assumption that both human feet produce exactly the same force and that the force is periodic. The assumption of perfect repetition is also frequently used in modelling of vandal loading generated by a single person and small groups.

Deterministic Force Models

It is well-known that each periodic force $F_p(t)$ with a period T can be represented by a Fourier series (Bachmann et al., 1995b):

$$F_p(t) = G + \sum_{i=1}^{n} G\alpha_i \sin(2\pi i f_p t - \phi_i), \tag{2.1}$$

where G is the person's weight [N], α_i the Fourier's coefficient of the i^{th} harmonic i.e. dynamic loading factor (DLF), f_p the activity rate [Hz], ϕ_i the phase shift of the i^{th} harmonic, i the order number of the harmonic and n the total number of contributing harmonics.

Based on Fourier decomposition, many researchers have tried to quantify DLFs which are the basis for this most common model of perfectly periodic human-induced force. Blanchard et al. (1977) proposed a simple walking force model based on resonance due only to the first harmonic with the DLF equal to 0.257 and pedestrian weight $G = 700\,\text{N}$. This was given for footbridges with a vertical fundamental frequency of up to 4 Hz. For fundamental frequencies between 4 and 5 Hz some reduction factors were applied to account for the lower amplitude of the second harmonic because this frequency range could not be excited by the first harmonic of walking. On the other hand, Bachmann & Ammann (1987) reported the first five harmonics for vertical walking force and also harmonics for the lateral and longitudinal direction. They reported that the 1^{st} and 3^{rd} harmonics of the lateral and the 1^{st} and 2^{nd} harmonics of the longitudinal force are dominant (Figure 2.8). It is interesting that in the latter case some sub-harmonics also appeared. Bachmann & Ammann (1987) explained it as a consequence of "more pronounced footfall on one side". The same authors suggested DLF values for the first harmonic of the vertical force between 0.4 (at frequency 2.0 Hz) and 0.5 (at 2.4 Hz), with linear interpolation for other frequencies inside the 2.0-2.4 Hz range. For the second and third harmonic they suggested identical DLFs equal to 0.1 for step frequencies near to 2 Hz.

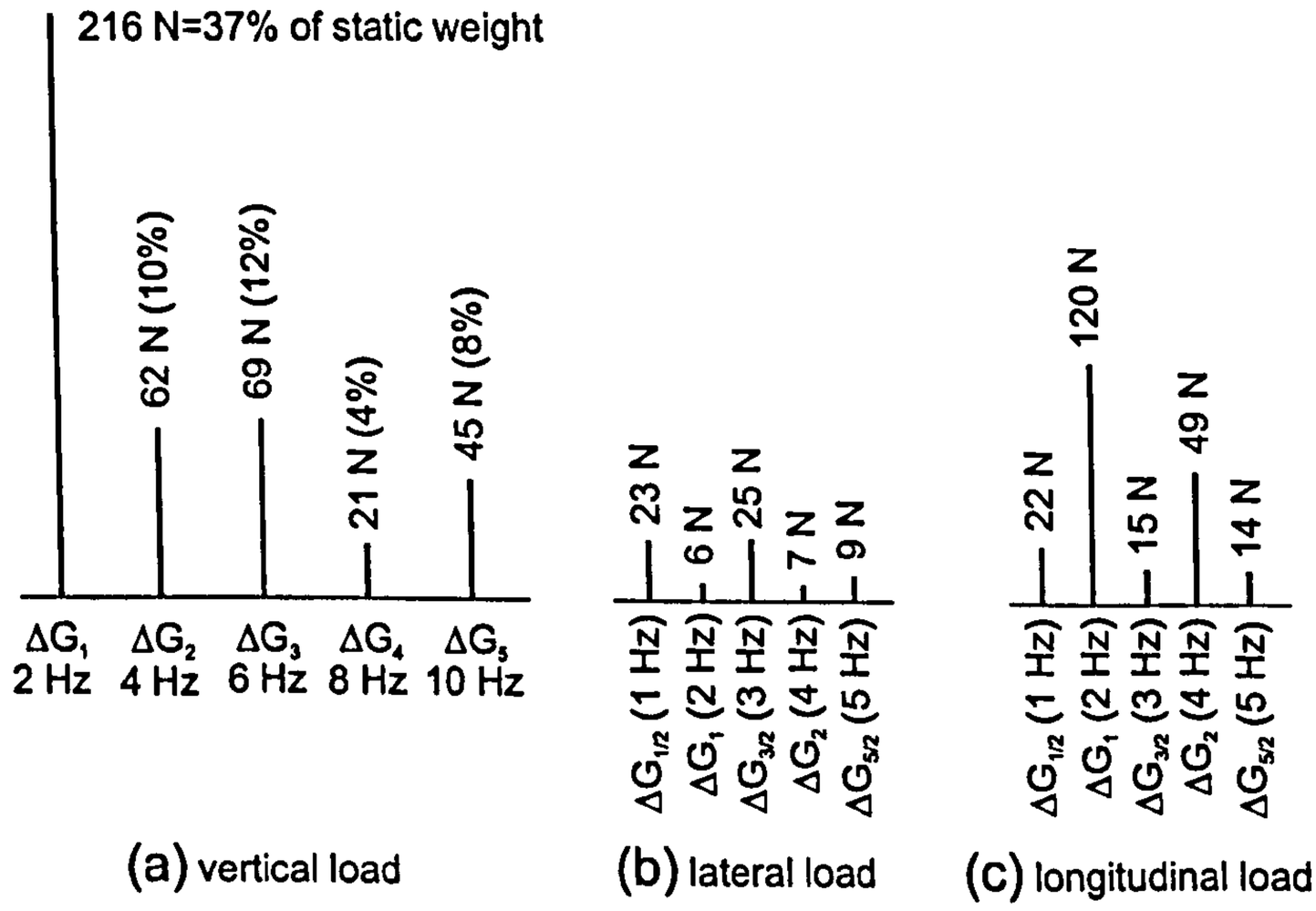

Figure 2.8: Harmonic components of the walking force in (a) vertical, (b) lateral and (c) longitudinal directions (after Bachmann & Ammann, 1987).

In 1982, Kajikawa formulated "correction coefficients" (i.e. DLFs) for walking and running as a function of step frequency (Yoneda, 2002). This function, together with person's velocity is given in Figure 2.9. A significant boost to the field was provided in the late 1980s by an excellent work of Rainer et al. (1988). They measured continuous single person force not only from walking but also from running and jumping. It was confirmed that DLFs strongly depended on the frequency of the activity. Values of the first four DLFs were presented (Figure 2.10). The only shortcoming of this work was that measurements had been done with only three human test subjects and therefore lacked statistical reliability. Much more extensive work, but only for the walking force, was presented by Kerr (1998) in his PhD thesis. His 40 subjects produced about 1,000 force records covering walking rates ranging from unnaturally slow 1 Hz to equally unnaturally fast 3 Hz. Kerr reported large scatter in the DLF values. However, the first harmonic had a clear trend to increase with increasing pace frequency and these results were similar to those reported by Rainer et al. (1988). However, DLFs of the higher harmonics in Kerr's work were very scattered, so they have been characterised statistically by mean values and coefficient of variation (Figure 2.11).

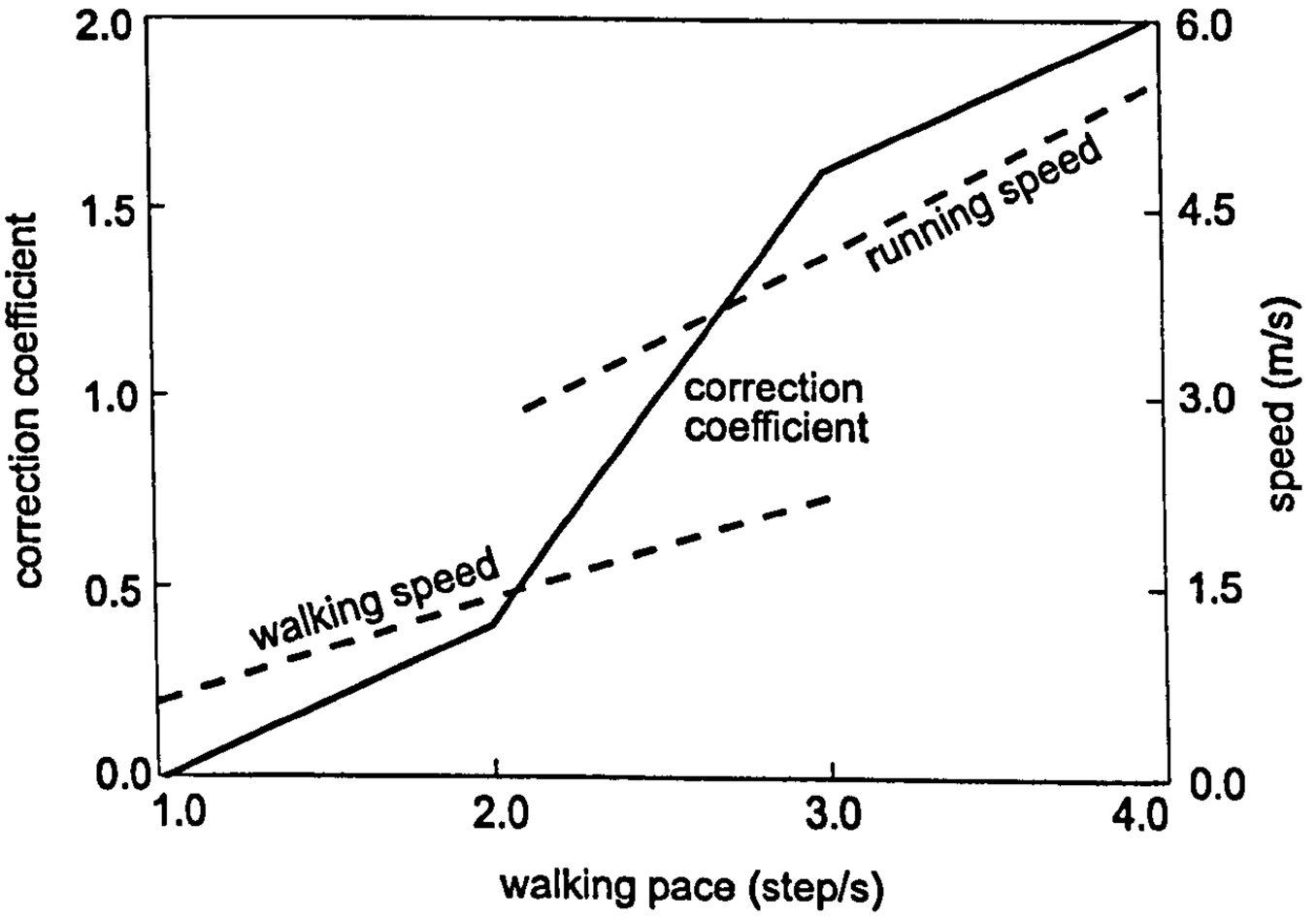

Figure 2.9: DLFs and pedestrian velocity as a function of step frequency (after Yoneda, 2002).

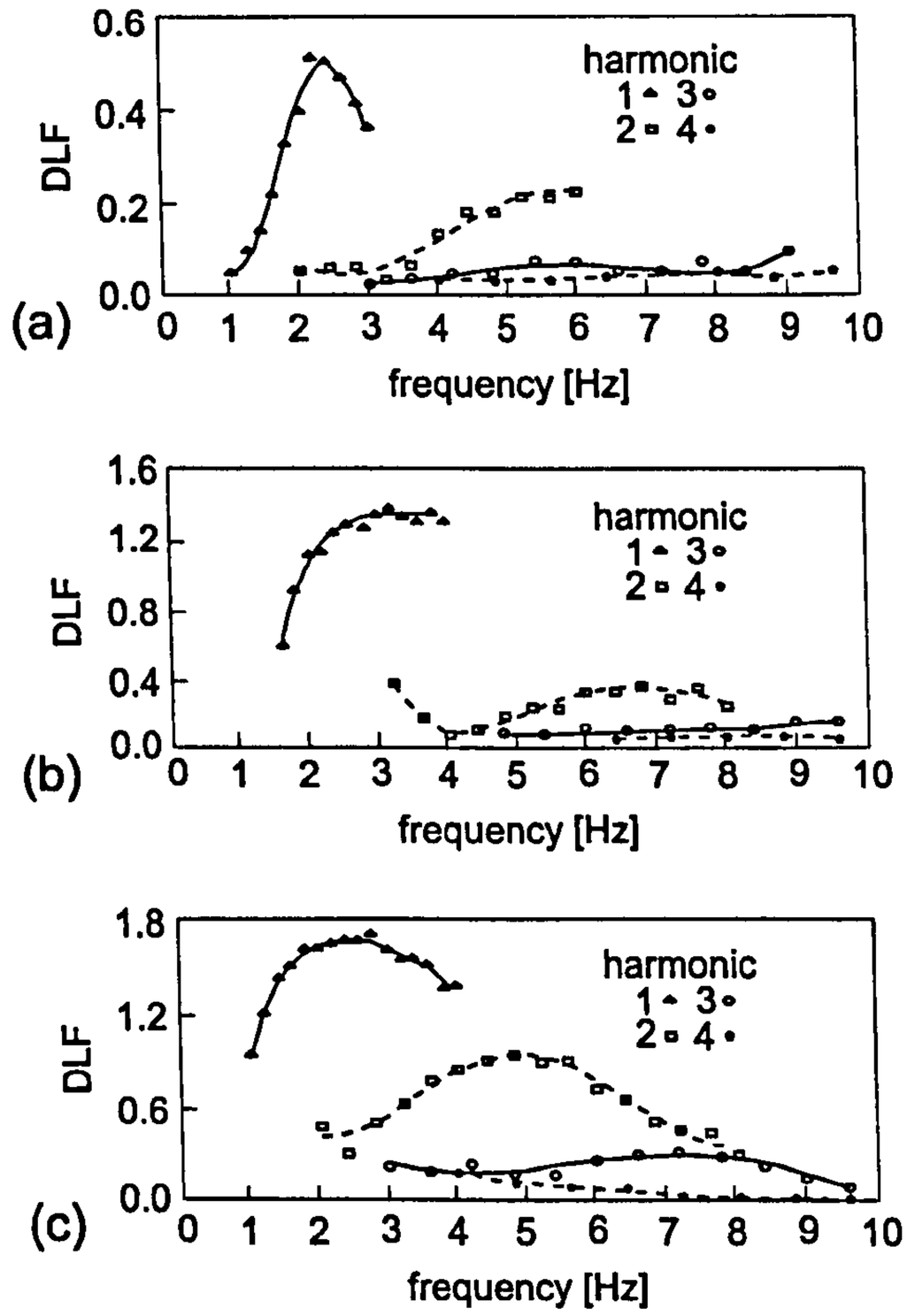

Figure 2.10: DLFs for the first four harmonics for (a) walking, (b) running and (c) jumping force (after Rainer et al., 1988).

Young (2001) presented the work of Kerr and others (Figure 2.12) and outlined basic principles which are used by Arup Consulting Engineers when modelling walking forces and the corresponding structural responses. He proposed DLFs for the first four harmonics as a function of the walking frequency assumed to be in the range from 1.0 to 2.8 Hz. The design values of DLFs presented as

$$\begin{aligned} \alpha_1 &= 0.41(f-0.95) \leq 0.56 \text{ if } f = 1.0-2.8\,\text{Hz} \\ \alpha_2 &= 0.069+0.0056f \text{ if } f = 2.0-5.6\,\text{Hz} \\ \alpha_3 &= 0.033+0.0064f \text{ if } f = 3.0-8.4\,\text{Hz} \\ \alpha_4 &= 0.013+0.0065f \text{ if } f = 4.0-11.2\,\text{Hz}, \end{aligned} \tag{2.2}$$

where f is the frequency of an appropriate harmonic, had 25% chance of being exceeded. This is the first attempt known to the author of this review to take into account the stochastic nature of human walking in day-to-day design. Statistical mean values of DLFs defined by Young (2001) are given in Table 2.1.

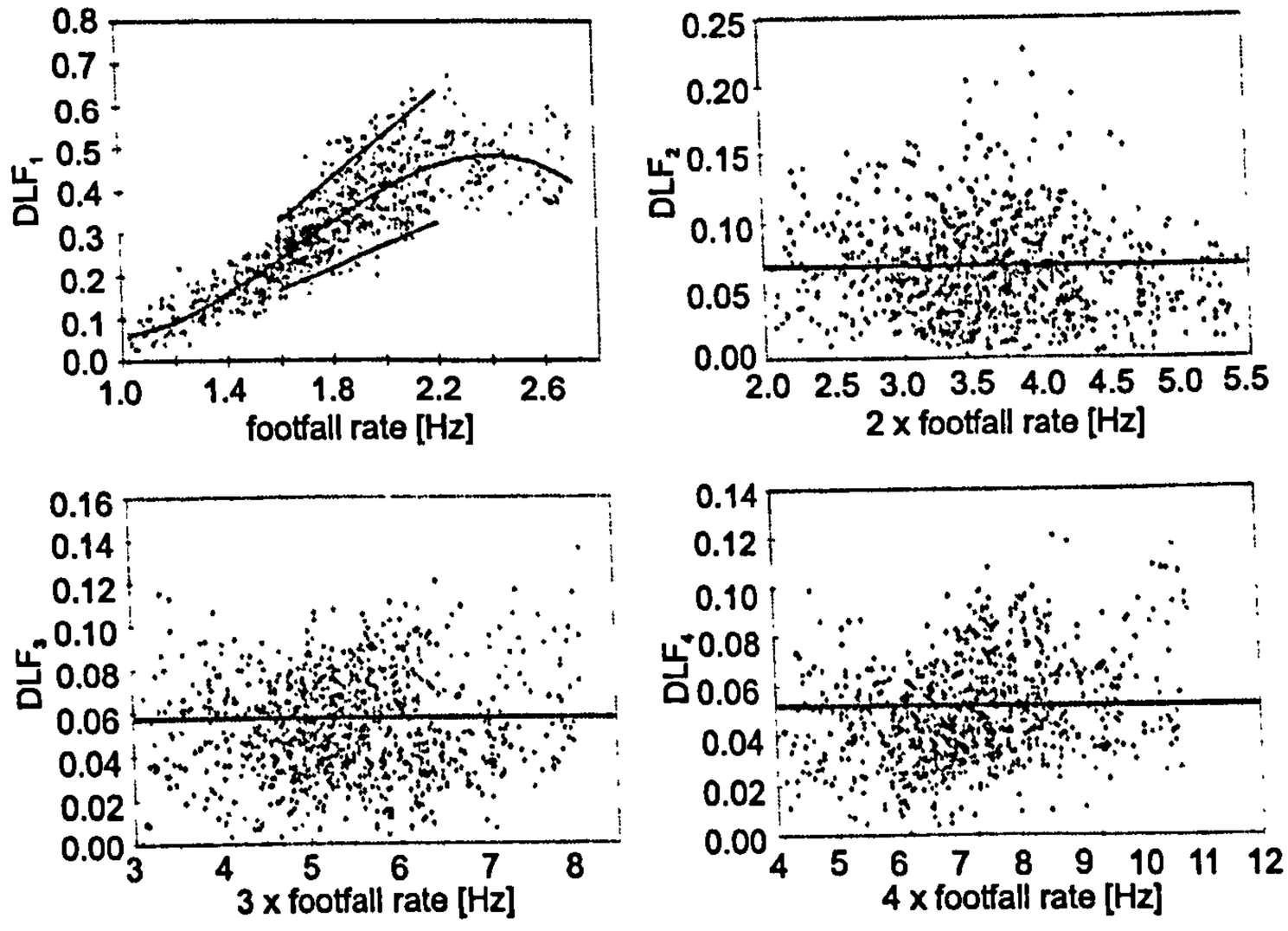

Figure 2.11: DLFs of walking force for the first four harmonics (after Kerr, 1998).

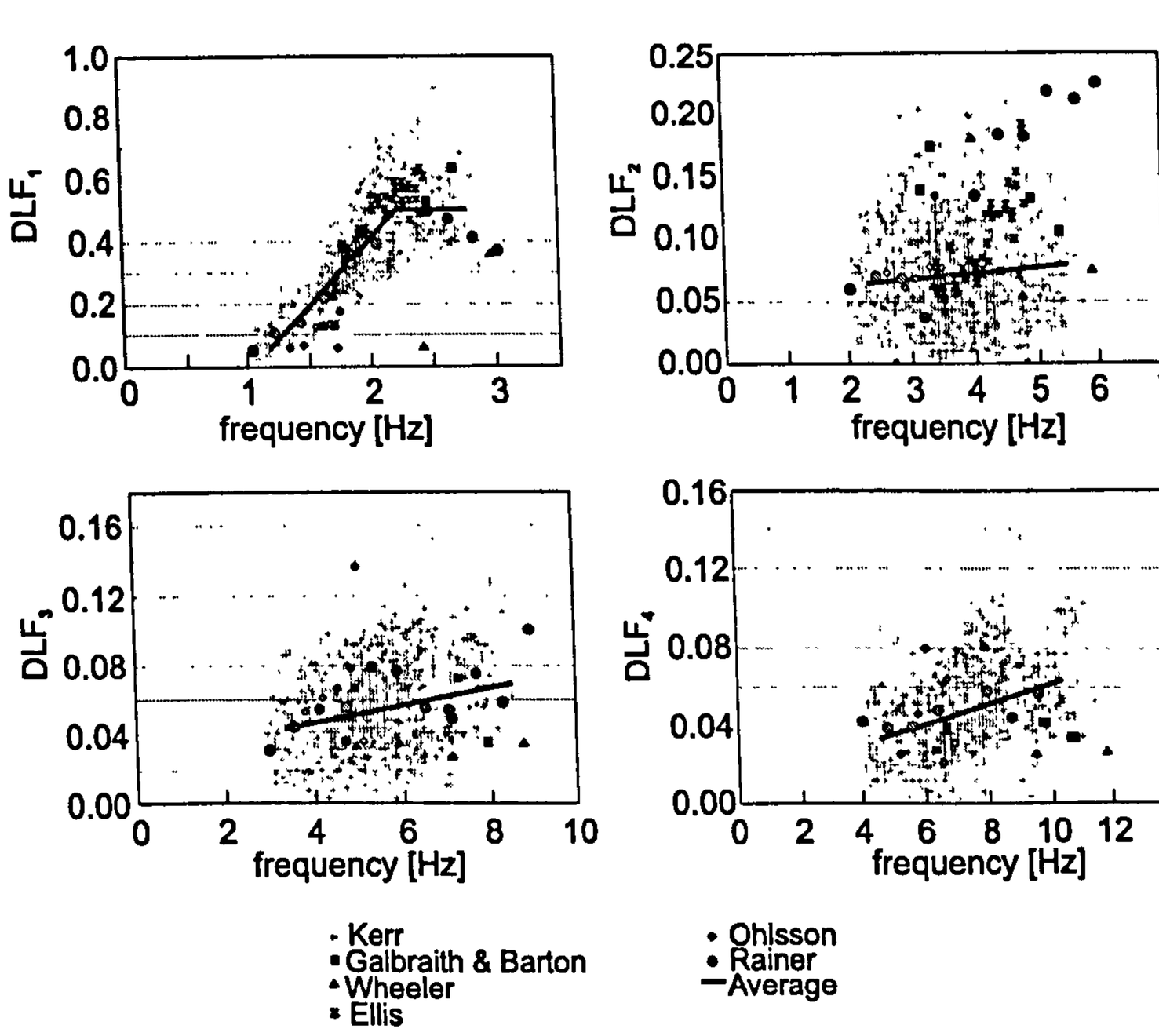

Figure 2.12: Review of DLFs for the first four harmonics after different authors (after Young, 2001).

It should be stressed again that in the described investigations, the DLFs were obtained by direct or indirect force measurements on rigid surfaces. However, Pimentel (1997) found that, for two full-scale footbridges investigated both analytically and experimentally, DLFs for resonant vertical harmonics (the 1^{st} and 2^{nd} harmonics) were considerably lower than those reported in literature. It seemed that the human-induced force differed from that measured on a rigid surface probably due to an interaction which exists between humans and low-frequency structures like footbridges. Yao et al. (2002; 2003) found this to be the case when jumping on a perceptibly moving structure, but similar direct measurements of the walking force are yet to be made.

Table 2.1: DLFs for single person force models after different authors. V, L and LO stand for vertical, lateral and longitudinal directions, respectively.

Author(s)	**DLFs for considered harmonics**	**Comment**	**Activity and its direction**
Blanchard et al. (1977)	$\alpha_1 = 0.257$	DLF is lessen for freq. from 4 to 5 Hz	Walking - V
Bachmann & Ammann (1987)	$\alpha_1 = 0.4 - 0.5$ $\alpha_2 = \alpha_3 = 0.1$	Between 2.0 and 2.4 Hz At approximately 2.0 Hz	Walking - V
Schulze (after Bachmann & Ammann, 1987)	$\alpha_1 = 0.37$, $\alpha_2 = 0.10$, $\alpha_3 = 0.12$, $\alpha_4 = 0.04$, $\alpha_5 = 0.08$	At 2.0Hz	Walking - V
	$\alpha_1 = 0.039$, $\alpha_2 = 0.01$, $\alpha_3 = 0.043$, $\alpha_4 = 0.012$, $\alpha_5 = 0.015$	At 2.0 Hz	Walking - L
	$\alpha_{1/2} = 0.037$, $\alpha_1 = 0.204$, $\alpha_{3/2} = 0.026$, $\alpha_2 = 0.083$, $\alpha_{5/2} = 0.024$	At 2.0 Hz	Walking - LO
Rainer et al. (1988)	α_1, α_2, α_3, α_4	DLFs are frequency dependent (Fig. 2.10)	Walking, run, jumping - V
Bachmann et al. (1995b)	$\alpha_1 = 0.4/0.5$, $\alpha_2 = \alpha_3 = 0.1/-$	At 2.0/2.4 Hz	Walking - V
	$\alpha_1 = \alpha_3 = 0.1$	At 2.0 Hz	Walking - L
	$\alpha_{1/2} = 0.1$, $\alpha_1 = 0.2$, $\alpha_2 = 0.1$	At 2.0 Hz	Walking - LO
	$\alpha_1 = 1.6$, $\alpha_2 = 0.7$, $\alpha_3 = 0.2$	At 2.0-3.0 Hz	Running - V
Kerr (1998)	α_1, $\alpha_2 = 0.07$, $\alpha_3 \approx 0.06$	α_1 is frequency dependent (Fig. 2.11)	Walking -V
Young (2001)	$\alpha_1 = 0.37(f - 0.95) \leq 0.5$ $\alpha_2 = 0.054 + 0.0044f$ $\alpha_3 = 0.026 + 0.0050f$ $\alpha_4 = 0.010 + 0.0051f$	Mean values for DLFs	Walking - V
Bachmann et al. (1995b)	$\alpha_1 = 1.8/1.7$, $\alpha_2 = 1.3/1.1$, $\alpha_3 = 0.7/0.5$	Normal jump at 2.0/3.0 Hz	Jumping -V
	$\alpha_1 = 1.9/1.8$, $\alpha_2 = 1.6/1.3$, $\alpha_3 = 1.1/0.8$	High jump at 2.0/3.0 Hz	Jumping - V
	$\alpha_1 = 0.17/0.38$, $\alpha_2 = 0.10/0.12$, $\alpha_3 = 0.04/0.02$	At 1.6/2.4 Hz	Bouncing - V
	$\alpha_1 = 0.5$	At 0.6 Hz	Swaying - L
Yao et al. (2002)	$\alpha_1 = 0.7, \alpha_2 = 0.25$	Free bouncing on a flexible platform with natural freq. of 2.0 Hz	Bouncing - V

A jumping force can be modelled in a similar way using the Fourier series. The shape of the time history of this force is qualitatively similar to that one from running (Figure 2.3) with the difference that jumping force is not moving across the structure. During one jumping cycle, a period of time, also known as the contact time, is spent in contact with the jumping surface and the rest of the jumping cycle is when the jumper is flying and not touching the surface. Bachmann & Ammann (1987) described a half-sine jumping force model and presented dependence of the first four harmonics on the ratio of the contact time to the duration of the jumping cycle, which is known as the contact ratio. Earlier, Wheeler (1980; 1982) suggested modelling all walking, running and jumping forces using the "half-sine" model defined by a set of parameters which vary for different activities.

Bachmann et al. (1995b) divided jumping into two categories: normal and high jump. For the latter case they reported the jumping DLFs for the first three harmonics as high as 1.9, 1.6 and 1.1, respectively at the jumping frequency of 2 Hz. Compared with the walking force, it can be noticed that more harmonics are needed to accurately describe the jumping force. The same authors reported DLF values for vertical bouncing with hand clapping (0.38 and 0.12 for the first two harmonics corresponding to the 2.4 Hz rate of the activity) and for horizontal in-place body swaying (0.5 for the first harmonic). However, Yao et al. (2002) measured the first two DLFs of 0.7 and 0.25 during bouncing. This was done in a test when the test subject was asked to bounce freely and in a way so as to produce maximum physically possible response of a flexible and perceptibly moving structure having fundamental frequency of 2 Hz.

The overview of DLFs for single person force reported by different authors is given in Table 2.1.

Some work on jumping forces from groups of people, usually at controlled frequencies, has also been carried out. For example, Rainer et al. (1988) reported that individuals jumping in groups of two, four and eight people produced on average lower DLFs than when jumping alone. This holds particularly well for higher harmonics, but not for the fundamental harmonic which DLF exhibits values approximately the same as when a single person is jumping. Pernica (1990) added that the average vertical DLFs per person tend to decrease with increasing number of people (in all walking, running and jumping activities). This clearly suggests that larger groups have reduced synchronisation between jumping people.

Investigations, specifically related to low frequency footbridges, on forces due to activities performed by groups of people are very limited. Because of this, it is interesting to mention some work related to floors. For example, Allen (1990) indirectly measured the force from 10-25 people jumping on a floor and proposed individual averaged DLFs of 1.5, 0.6 and 0.1 for the first three harmonics, respectively. He reported that synchronisation above 2.75 Hz was very difficult. Willford (2001) confirmed that several people jumping cannot achieve perfect synchronisation. Using the half-sine model and Ebrahimpour's (1987) proposal for statistical distribution of time delays between jumping people, Willford used a Monte Carlo approach and simulated the group effects. He independently confirmed Allen's proposal for

reduced, in comparison with a single person, group DLFs. In another investigation related to walking across a floor, a large group of 32 people was involved in experiments related to uncontrolled and controlled walking on a high frequency floor (Ellis, 2000; 2003). In both cases the response of the high-frequency floor was similar to the one due to a single person walking in such a way that one of the higher harmonics matched a natural frequency of the floor. However, it should not be forgotten that walking patterns in floors and footbridges are different, particularly because bridges are usually much narrower and longer structures having only one dominant dimension (length).

Probabilistic Force Models

A more detailed probabilistic approach to the walking force model is based on the fact that a person will never produce exactly the same force-time history during repeated experiments. In the case of two persons it is even more so (Saul et al., 1985). For a single person force, which is still assumed to be periodic, randomness can be taken into account by probability distributions of person's weight, pacing rate and so on. For several people, the probability distribution of time delay between people who perform a particular activity can be added. The main idea of this philosophy is to get a reliable estimate of the force from a group of people by combining forces from individuals. Naturally, for a reliable statistical description of human forces, a large database of measurements with a single person should be provided. Some work on this was done by Tuan & Saul (1985) who measured forces from many different activities mainly typical for grandstands, among which was jumping.

In his PhD thesis, Ebrahimpour (1987) continued the work of Tuan and Saul and conducted measurements of different types of forces using a specially constructed force platform. Among many types of forces typical for activities on grandstand structures, a single jump and periodic jumping with controlled frequencies at 2, 3 and 4 Hz were investigated. For a statistical description of continuous jumping force time histories from individuals, Ebrahimpour chose the first three harmonics of the Fourier series and the force repeating period. Then, by comparing the measured force from two people simultaneously with computer simulations obtained by a combination of forces from individuals, he identified the time delay distribution between two people who were trying to perform synchronised jumping. The idea was to use this time delay distribution together with statistically described individual time histories to enable the calculation of the resulting force from any number of people. The procedure was experimentally verified for only four people. Further Monte Carlo computer simulations revealed that the force peak amplitude per person decreased with increasing the number of people, which was in line with the already mentioned findings of Pernica (1990) related to DLFs. However, this model was hardly applicable in practice because of the fact that peak force amplitude is not enough to describe that force. A very good digested version of whole procedure is given by Ebrahimpour & Sack (1989).

In a subsequent experimental work Ebrahimpour et al. (1989) found that the previously used computer program gave good estimates of the peak jumping forces for groups of up to

40 people. Three years later, Ebrahimpour & Sack (1992) tried to improve Ebrahimpour's previous design suggestion by proposing design curves for the first three harmonics of jumping load as a function of the group size, which was a much more practical proposal.

An identical procedure was applied on walking loads by Ebrahimpour et al. (1996). A vertical dynamic load by a group of pedestrians was investigated. As a result, a design proposal for only the fundamental DLF was given as a function of a number of people (Figure 2.13). The reason was probably the fact that the spectrum of measured uncorrelated force for four people revealed that only the first harmonic is important. It is even more so in case of a larger number of people. However, this design proposal, although it includes up to 100 people, does not take into account the fact that people in such large crowds sometimes adjust their step according to the movement of others. The authors stressed that this effect, which is dependent on the crowd density, should be added but did not explain how. The DLFs given in Figure 2.13 are lower in comparison with the results of Pernica (1990).

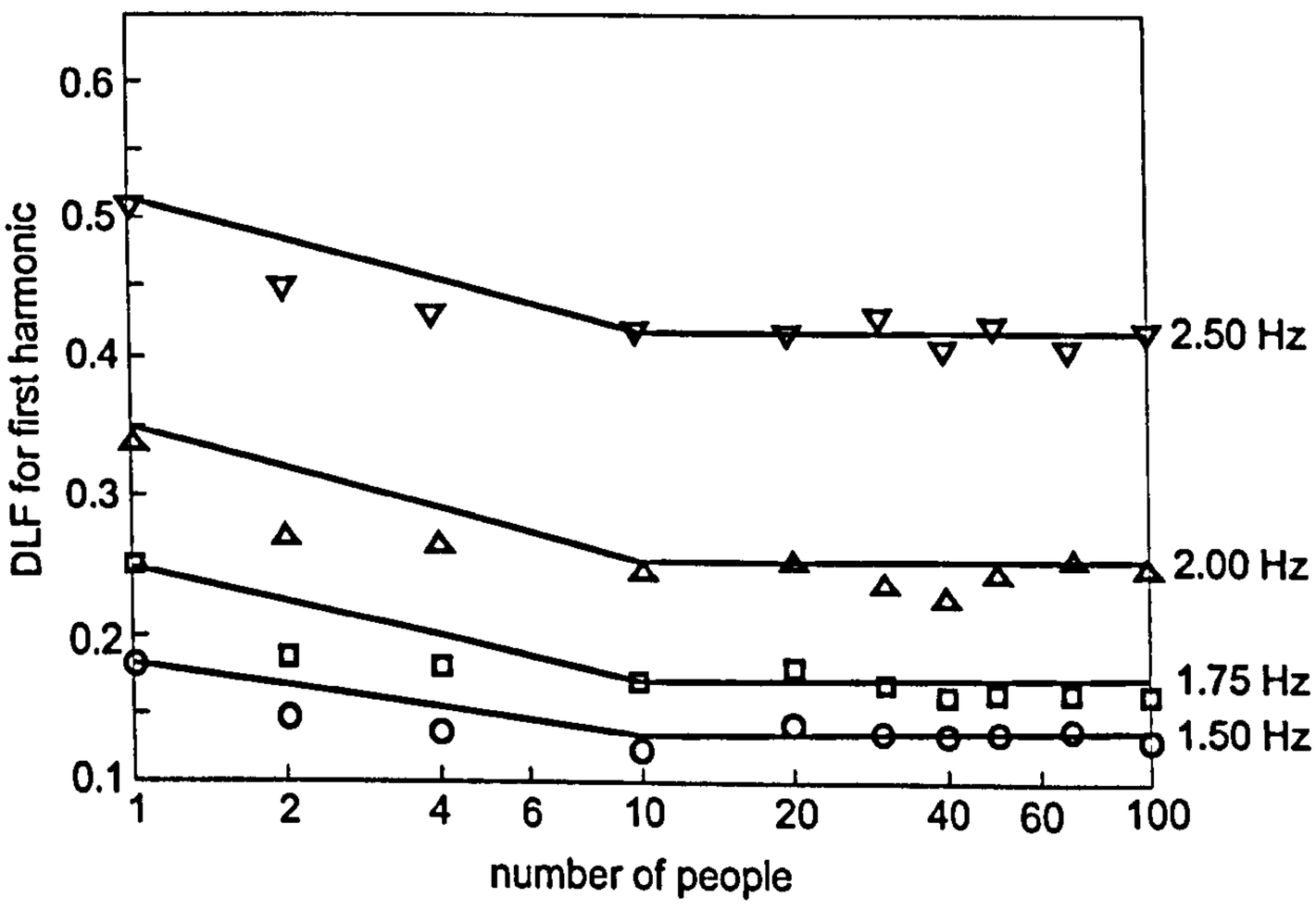

Figure 2.13: DLF for the first harmonic of the walking force as a function of number of people and walking frequency (after Ebrahimpour et al., 1996).

2.2.3.2 Frequency Domain Force Models

In his PhD thesis, Ohlsson (1982) introduced at that time a rather new concept for mathematical modelling of the human-induced force. Namely, as previously mentioned in Section 2.2.2, he measured a single step force and then produced continuous walking force assuming artificial force periodicity. Then, he determined the auto spectral density (ASD) of the force treating it as a transient signal where identical steps were repeated perfectly but for a limited number of times. Ohlsson studied only the high frequency content of the ASD between 6 and 50 Hz because he was investigating behaviour of high-frequency building floors made of timber. This approach was further developed over the next 10-15 years and extended

to low-frequency floors. As a result, in his PhD thesis Eriksson (1994), who was Ohlsson's student, focused on low-frequency floors and made use of the ASD frequency range below 6 Hz. Figure 2.7 presents this part of the spectrum of a measured continuous force lasting about 100 s. Eriksson explained that the fact that each peak has some width in this spectrum means that human walking cannot be perfectly periodic and therefore cannot be accurately described by DLFs. This whole procedure is based on the assumption that human-induced force can be treated as a stationary random process. This model, and several others based on the frequency-domain approach, will be explained in more detail in Section 2.6, because they tend to be 'packaged' with the structural modelling and/or assessment.

2.2.3.3 Vandal Loading

This type of load was not researched very much in the past. Although recognised as an issue in the literature (Stevenson, 1821; Blanchard et al., 1977; Wheeler, 1980; 1982; Tilly et al., 1984; Eyre & Cullington, 1985; Bachmann & Ammann, 1987; Grundmann & Schneider, 1991; Grundmann et al., 1993), vandal loading is not precisely defined in terms of which type of human activity, besides jumping, could be considered as it. Probably, deliberate horizontal body swaying can be added (Bachmann & Ammann, 1987) as well as deliberate bouncing. The earliest record of vandal loading and its consequences dates from 1821 when Stevenson reported very strong vibrations on a bridge for "foot passengers and led horses" when three or four persons were "amused" by noticeable vibration on the bridge and tried to increase it deliberately. The result was that one of the supporting bridge chains broke. Although we do not know exactly how this action was performed, it demonstrated very early the potential and consequences of deliberate synchronised human action. Also, Tilden (1913) reported that "jouncing" (i.e. bouncing) has a "high kinetic intensity". He did not explain more precisely this term, but it could be deduced from his paper that it was quite possible that this type of load was capable of producing a high level of response.

Vandal loading has been much more debated in terms of whether it is relevant for a particular type of a structure than in terms of how it could be modelled. For example Blanchard et al. (1977) only confirmed that the data about this load type are very scarce, while Wheeler (1982) rather boldly concluded that synchronisation of people had not been a real possibility. This was based on a measurement of the response to jumping in unison of two and three people which proved to be similar to the response in a single person case. As previously mentioned, Rainer et al. (1988) reported a similar case when investigating correlated jumping of two, four and eight persons. However, Bachmann (2002) stated that synchronisation of a small number of people seems possible at least when considering the first loading harmonic. In that case, he proposed to simply multiply single person influence by the number of persons involved, meaning perfect synchronisation. Grundmann et al. (1993) suggested to link the dynamic amplitude due to rhythmical knee-banding with the displacement of the centre of gravity for a single person. However, the dependence between this amplitude and the frequency of this excitation was not stated. Also, the synchronisation factor for the case of several people

was not suggested. Finally, Pimentel & Fernandes (2002) claimed that there were no known cases of footbridge damage from vandals, probably not being aware of the case mentioned by Stevenson in 1821.

In summary, it may be said that vandal load does not occur often in practice but it certainly deserves greater attention. This is especially so nowadays when footbridges are very light structures which can be excited relatively easily. Also, it should be remembered (Leonard, 1966) that this type of load should probably be related to and treated as a social problem. The BS 5400 bridge design code (BSI, 1978) only requires robust construction of bearings and some reserve in reinforcement for prestressed bridges as measures against vandal loading. BS 5400 does not contain any more explicit design procedure related to vandal loading and/or applicable for bridges of different materials.

2.3 Footbridge Structures as Vibration Path

The vibration path which transmits vibrations from the source to the receiver is the footbridge structure itself. Knowing mass, damping and stiffness properties of a footbridge, together with the previously defined force model, is necessary to calculate its dynamic response according to the well-known equation of motion of a multiple-degree-of-freedom (MDOF) system (Clough & Penzien, 1993):

$$\mathbf{M}\ddot{\mathbf{x}}(t) + \mathbf{C}\dot{\mathbf{x}}(t) + \mathbf{K}\mathbf{x}(t) = \mathbf{f}(t) \tag{2.3}$$

where $\mathbf{M}$, $\mathbf{C}$ and $\mathbf{K}$ are the mass, damping and stiffness matrices respectively, each of order $n \times n$ where n is the number of degrees of freedom. In addition, $\ddot{\mathbf{x}}(t)$, $\dot{\mathbf{x}}(t)$, $\mathbf{x}(t)$ and $\mathbf{f}(t)$ are $n \times 1$ vectors of acceleration, velocity, displacement and external force. Mass and stiffness matrices depend on the geometry of the footbridge and material properties. They are usually determined by the finite element (FE) concept. This implies a discretisation of the real structure having an infinite number of DOFs into an ensemble of finite elements which are interconnected at a limited number of points (nodes) and which possess a finite number of DOFs. These elements and their corresponding DOFs form the basis for further calculations. Namely, for each element type, mass and stiffness element matrices are defined and by their combination the mass and stiffness matrices for whole structure can be determined. In practice, however, the damping matrix cannot be evaluated in the same way. In footbridge vibrations, it is usually expressed via modal damping ratios ζ_n which are experimentally determined.

Assuming that the system is linear and proportionally damped, which is a fair assumption for most footbridges, the given system of n coupled equations with n unknown variables can be uncoupled into the n equations each featuring only one variable, that is, to n single-degree-of-freedom (SDOF) systems which standard form is (Clough & Penzien, 1993):

$$\ddot{Y}_n(t) + 2\zeta_n\omega_n\dot{Y}_n(t) + \omega_n^2 Y_n(t) = \frac{P_n(t)}{M_n}. \tag{2.4}$$

Here, $\ddot{Y}_n(t)$, $\dot{Y}_n(t)$ and $Y_n(t)$ are modal (or generalised) acceleration, velocity and displacement, ζ_n and ω_n are the damping ratio and natural circular (or angular) frequency for the n^{th} mode of vibration, while $P_n(t)$ and M_n are the modal force and mass for the same mode. Then, the total displacement vector $\mathbf{x}(t)$ can be presented as a linear combination of mode shape vectors $\mathbf{\Phi_n}$, where coefficients of that combination vary with time and are generalised displacements $Y_i(t)$, $i = 1, 2, \ldots, n$:

$$\mathbf{x}(t) = \mathbf{\Phi_1} Y_1(t) + \mathbf{\Phi_2} Y_2(t) + \ldots + \mathbf{\Phi_n} Y_n(t). \tag{2.5}$$

Generally, the most popular method for establishing and solving Equation 2.3 is the finite element (FE) method (Clough & Penzien, 1993). However, when one mode dominates, which often happens in footbridges, the response can be estimated sufficiently accurately using an SDOF modal equation (Equation 2.4) for the appropriate mode. This is very often implemented in practice when checking footbridge vibration serviceability (see design procedures outlined in Section 2.6).

Therefore, for a reliable estimate of the structural response, it is necessary to determine dynamic properties of the footbridge which feature in Equations 2.3 and 2.4 as accurately as possible. In the next two sections issues related to the accurate determination of the mass, stiffness and damping in footbridges will be considered. The most convenient way to present these properties is in their modal form.

2.3.1 Mass and Stiffness

Knowing the characteristics of structural materials and geometry, an FE model of a bridge can be developed. After an eigenvalue extraction, performed using the established mass and stiffness properties, footbridge natural frequencies and mode shapes, can be determined. However, sometimes the obtained results can contain large errors due to uncertainties in the FE modelling process. For example, Deger et al. (1996) reported an error in the first natural frequency of 37% when compared with the test of a full-scale structure mainly due to inadequate modelling of footbridge boundary conditions. In circumstances when both analytical and experimental results exist, the FE model can be updated by their comparison assuming that the experimental results are correct. This approach helps future modelling of bridges with similar layouts. However, it should be noted that an FE model updating cannot be successful without good quality of experimental data (Cantieni, 1996; Pavic et al., 1998). The most uncertain and sensitive parameters considered in the updating of footbridges are boundary conditions, material properties and modelling of certain aspects of the key structural and non-structural elements (such as decks, cables, handrails) which have the potential to influence significantly the footbridge dynamic behaviour. However, it should

also be noticed that changes in the temperature can cause changes in dynamic properties. For example, increasing in temperature from 21.4°C to 42.1°C was accompanied by a decrease of the fundamental frequency of a pedestrian walkway of 7.1% (Ventura et al., 2002).

General procedures for FE model updating are given in the now classical textbook by Friswell & Mottershead (1995). However, this technology, widely used in the mechanical and aerospace engineering disciplines, requires special considerations when applied to civil structural engineering problems (Pavic et al., 1998; Brownjohn & Xia, 2000). Generally, FE model updating can be done manually, by trial and error, or automatically by using software developed for that purpose, where the latter is much faster than the former (Pavic et al., 1998; Hartley et al., 1999). However, it is recommended to conduct manual updating first to develop an FE model which features meaningful starting parameters for the automatic procedure where the choice of these parameters is very important (Pavic et al., 1998; Brownjohn & Xia, 2000). Usually, the most uncertain parameters are the stiffness of some nonstructural elements, dynamic modulus of elasticity for concrete, stiffness of cracked concrete and stiffness of the supports. They should be parametrically investigated until a good agreement with experimental data, usually with frequencies only or frequencies and mode shapes, is obtained. The level of matching is typically checked by calculating the Modal Assurance Criterion (MAC) and/or the Coordinate Modal Assurance Criterion (COMAC) which represent degree of correlation between the analytical and experimental modes of vibration (Friswell & Mottershead, 1995). Ideally, due to orthogonality of mode shapes, MAC should be equal to 1 when the same modes are compared, and 0 in other cases (Ewins, 2000). However, MAC values, for the same modes, as low as 0.7 are acceptable in civil engineering applications due to imperfect measurements typically made in noisy environments. Similar considerations apply to COMAC values which should also be between 1 and 0. Prior to updating, it is very important to conduct a sensitivity analysis to determine which parameters have the biggest influence on the target values of natural frequencies, MAC and COMAC (Brownjohn & Xia, 2000). Some practical observations as to the modelling of footbridges are given in the remainder of this sub-section.

For the cases when there are significant axial forces in structural elements, second order effects should be taken into account. However, this does not apply to internally prestressed concrete elements were second order effects do not develop. When required, the geometric stiffness should be considered together with the elastic stiffness (Przemieniecki, 1968), having in mind that compression force reduces and tension force increases the stiffness. This geometric nonlinearity effect is present in cable stayed bridges. It can change the overall stiffness of the structure and, consequently, influence mode shapes and frequencies. Large axial forces are typical not only for cables but also for girders and towers in these structures (Gardner-Morse, 1990). In an investigation of a cable stayed footbridge, the geometric stiffness was taken into account only for cables, while it was neglected for other bridge elements because their axial compression forces were small compared with the buckling forces (Gardner-Morse, 1990; Gardner-Morse & Huston, 1993). The cable behaviour was very dif-

ficult to model having in mind big differences (up to 40%) in the measured and calculated cable forces and the sensitivity of results to the cable modulus of elasticity. Similarly, in the FE modelling of a suspension footbridge, Brownjohn et al. (1994) modelled the whole bridge using 3D beam elements adding the geometric nonlinearity effect for tower pylons, cables and hangers. However, Pimentel (1997) found that, for a fibre reinforced cable-stayed footbridge investigated, taking into account the geometric stiffness induced only small differences in the obtained natural frequencies in comparison with the model where nonlinear effects were neglected. Khalifa et al. (1996) modelled cables as truss elements and took into account geometric nonlinearities but their influence on the dynamic performance of a fibre reinforced plastic cable-stayed footbridge was not given.

For a cable-stayed footbridge, modelling the footbridge timber deck as a plate element gave much better agreement between experimentally and analytically obtained modal properties (Gardner-Morse, 1990; Gardner-Morse & Huston, 1993) than treating the deck only as a mass as in some previous case studies for the same bridge (Lintermann, 1986; Huston et al., 1988). Moreover, Brownjohn et al. (1994) found that prestressed, precast, concrete panels of which the deck of a suspension footbridge was made, had potential to influence strongly the horizontal lateral frequencies and should be modelled in an FE model as plate elements. However, in suspended bridges lateral and torsional deck stiffnesses have little influence on vertical modes, which means that the structure can be modelled as a 2D model with the deck presented as a beam element when modelling vertical oscillations (Brownjohn, 1997).

Brownjohn et al. (1994) reported differences of up to 10% in the footbridge natural frequencies obtained analytically and experimentally. The authors quoted uncertainties in the dynamic Young's modulus for concrete and the exclusion of the stiffness of railings and asphalt surfacing from the FE model as likely reasons for this discrepancy. To illustrate the variability of the dynamic modulus for concrete it should be mentioned that the values of 30.8 and 42.5 GPa were obtained by Pimentel (1997) in the updating process of two tested footbridges. The same author reported nearly 300 times greater horizontal stiffness of the elastomeric bearings for a composite bridge than the manufacturer's design static value. He also found that handrails in a stressed ribbon footbridge increased the fundamental frequency by about 20%. Obata et al. (1999) found that 50% of handrail stiffness was effective in investigated footbridges.

In conclusion, in all examples mentioned, the footbridge FE models were either developed using only beam elements or the deck was additionally modelled using plate elements. The FE model can be useful in detecting closely spaced modes of vibration or modes with combined lateral and torsional motion. The latter is typical when the mass and the shear centre of the footbridge section do not coincide (Gardner-Morse, 1990; Gardner-Morse & Huston, 1993). Finally, there is sufficient evidence that footbridge handrails can increase, sometimes significantly, frequencies of vertical modes of vibration.

2.3.2 Damping

Damping represents energy dissipation in a vibrating structure (Tilly, 1977). Each structure inherently possesses some capability to dissipate energy. That capability is very beneficial because it reduces structural response to a dynamic excitation near resonance. The near-resonant condition is the governing condition when considering footbridge vibration serviceability due to human-induced load. Therefore, it is very important to model damping as accurately as possible.

In general, there are several dissipation mechanisms within a structure, the individual contributions of which are extremely difficult to assess. They can be divided into two groups: 'dissipation' mechanisms which dissipate energy within the boundaries of the structure and 'dispersion' or 'radiation' mechanisms which propagate energy away from the structure. The overall damping in the structure which comprises both mechanisms is often called 'effective damping' and it is this damping which is actually measured as modal damping in practice (Pavic, 1999).

However, it is very hard to model mathematically these damping mechanisms. There are several damping models (Wyatt, 1977; Weber, 2002) but the most often used is the viscous one. Although this model does not describe the real behaviour of the structure, it is very convenient because of its simplicity. The usual way to express viscous damping is in its modal form i.e. by using the damping ratios defined for each mode separately. In the case of footbridges, this is very convenient both for the FE modelling and the experimental measurements.

As previously mentioned, damping is very important if the structure vibrates at or near a resonant frequency, when the stiffness and inertial forces tend to cancel each other (ISO, 1992). However, it is hard to predict it. To get better idea about damping, it is necessary to conduct testing. In testing it is very important to make the right choice of excitation which will generate resonant excitation for a mode investigated (Tilly, 1977). Therefore, frequency content for the excitation force should be chosen carefully.

Modern construction technologies have brought a reduction of damping in structures because of a significant decrease in the amount of friction which was present in old structures. For example, Wyatt (1977) stated that until 1960 there had been a widespread belief that logarithmic decrement in bridges could not be below 0.05 (i.e. viscous damping ratio 0.8%). In the mid-1940s the minimum value had even been 0.1 (1.6%), whereas nowadays, modern steel bridges regularly exhibit damping of 0.5% or less.

In the following sections, the damping measurements using some rather old and nowadays obsolete procedures are presented. Then, some relatively new procedures gaining popularity in footbridge testing are outlined. Although in all tests natural frequencies and mode shapes were determined too, emphasis is given on damping measurements because of their relative uncertainty. It suffices to mention here that natural frequencies are usually determined from spectral plots of response frequency vs. amplitude while mode shapes, due to their

spatial nature, are determined by response measurements made at different locations on the structure.

2.3.2.1 Research Work in the 1970s

In one of the earliest attempts to measure damping, people who were jumping in unison with a frequency near the structural resonant frequency were used to excite the bridge on which they were jumping (Selberg, 1950). In another attempt in 1966, an impulsive force in the centre of the span of a road bridge was applied by means of cables attached to the bridge and pulled from a boat (Borges et al., 1968). Although this attempt was not successful, which is to be expected on a bridge with a central span as long as 1013 m, it is interesting to mention it considering the development of vibration measurement techniques. A short review of dynamic testing on full-scale civil engineering structures in general is given by Hudson (1977) and Severn et al. (1988). Rainer (1979) wrote an excellent paper full of practical advice related to vibration measurements on civil engineering structures. It deals with the planning of tests, instrumentation, way of collecting data and data analysis and interpretation of results. In absence of more data related to footbridges, some findings obtained for road bridges are presented in this sub-section too.

In the 1970s, many investigations of bridge damping were conducted by the UK Transport and Road Research Laboratory. In those experiments, resonance tests were usually conducted. This was done using a single electro-hydraulic exciter, or a pedestrian whose pacing was adjusted to match resonance by means of a metronome (Leonard, 1974). However, tests with the electro-hydraulic exciter were regarded as more reliable to estimate experimentally not only footbridge damping, but also its natural frequencies and mode shapes because of the ability to control the excitation (and consequently response) frequencies. These were in essence stepped-sine tests in which, when a steady-state resonant response was established, the harmonic excitation was cut and damping was obtained from the free decay trace. Usually, acceleration response was measured because it was established as the best parameter for describing people's reaction to vibrations and, also, it was easy to measure it using widely available accelerometers. Test procedures used at that time not only for footbridges, but also for highway bridges are described in detail by Leonard (1974).

Leonard & Eyre (1975) investigated eight bridges with steel box girder and concrete deck, among them one footbridge. However, measured logarithmic decrement in the first bending mode showed considerable variability - from 0.023 (0.37%) for the footbridge up to 0.18 (2.86%) for road bridges. Therefore, it was obvious that a single value cannot be proposed for future design for this type of structure (steel box girders with concrete deck). The authors rightly concluded that supports and end conditions have great influence on the (radiation part of) damping. Also, they found that with increasing vibration amplitude damping also increases, which suggests that damping mechanism was amplitude dependent. However, Eyre (1976) could not confirm this finding during testing of a road bridge made completely of steel.

It was a bridge with very low first natural frequency of 0.53 Hz where maximum achieved amplitude was 13 mm which was possibly too low to activate extra damping mechanisms.

Eyre & Tilly (1977) did measurements on 23 steel and composite bridges, many of which were footbridges. All structures were steel box girder or steel plate girder bridges, with different number of spans (one to six) and span length (17-57 m, plus one road bridge with the main span of 213 m). The authors reported that damping was dependent of number of spans (single span bridges had higher damping then multi span ones) and vibration mode considered (higher modes generally had higher damping). Typically, logarithmic decrement for footbridges was between 0.02 and 0.03 (0.32% and 0.48%). The authors also confirmed Leonard & Eyre's (1975) finding that damping is dependent on response amplitude. Furthermore, using all available data, Tilly et al. (1984) concluded that it was wrong to generalise that damping increases in higher modes or that it is dependent on the stiffness and span length. However, it appears to be certainly dependant on type of material - steel bridges exhibit the lowest and classically reinforced concrete bridges the highest level of damping. They also suggested that, because of amplitude dependence, it is always necessary to quote measured damping together with the level of response amplitude. This sound suggestion is, unfortunately, very often omitted in the published literature.

All these results are mainly related to damping in the vertical modes, although some measurements were done in torsional modes too.

2.3.2.2 New Measurement Techniques

Towards the end of the 1970s, new and more reliable techniques were introduced to experimentally determine the dynamic properties of bridges. These techniques made use of improved signal analysis techniques and were based on impulsive (hammer), forced and ambient vibration excitation. There are numerous examples of these methods, such as those presented by Rainer & Van Selst (1976) and Buckland et al. (1979) on ambient testing and vehicle impact, Abdel-Ghaffar (1978) and Brownjohn et al. (1987) on ambient testing, and Rainer & Pernica (1979) on ambient testing and harmonic forced vibrations.

In general, damping can be obtained using different methods. Related to civil engineering structures Rainer (1979) mentioned the time-domain free decay method after the excitation (impulsive or harmonic) stops, the frequency-domain half power bandwidth method (for the ambient and forced tests) and the time-domain based random decrement method (for the ambient vibration surveys). All of them can produce slightly different results as a consequence of different theoretical assumptions which usually cannot be completely satisfied in practice. Also, the frequency response function (FRF) curve (mainly circle) fitting method in the frequency domain is used very often (see Table 2.2) and the principle of that method can be found, together with many other methods, in standard textbooks dealing with modal identification procedures (Maia et al., 1997; Ewins, 2000).

Table 2.2: Measured damping ratios (for vertical ζ_v, horizontal ζ_h and torsional ζ_t modes) for some footbridges.

Author(s)	Bridge type	Main span [m]	Girders	Deck	ζ_v [%]	ζ_h [%]	ζ_t [%]	Estimation method
Gardner-Morse & Huston (1993)	Cable-stayed	54.9	Steel	Laminated wood	0.53/0.22	-	0.46/0.36	Curve fitting
Brownjohn et al. (1994)	Suspended	50	Steel	Concrete panels	2.68/0.50	1.00/0.70	0.84[a]/0.50	Curve fitting
Brownjohn (1997)	Suspended	35	Steel	Timber	1.0/1.0	High[b]	2.4[b]/1.4[b]	Free-decay after jumping
Cantieni & Pietrzko (1993)	Continuous space truss	54	Wood	-	1.4/1.3	2.9/2.1[c]	1.4	Curve fitting
Pimentel (1997)	Pre-cambered beam	19.9	Steel	Concrete	0.73 & (0.40) [0.53]/0.65	-	-	Curve fitting & free-decay after (walking)[jumping]
Pimentel (1997)	Stressed ribbon	34	-	Prestressed concrete	0.56 (0.65) / 0.64 (1.02)	-	-	Free-decay after walking (jumping)
Pimentel (1997)	Cable-stayed	63	-	Glass-reinforced plastic	0.84/0.94	-	-	Free-decay after bouncing
Pavic & Reynolds (2002)	Stressed ribbon	34	-	Pre-stressed concrete	0.53/0.65	-	0.50/0.60	Curve fitting
Pavic et al. (2002b)	Suspended	144	Steel	Aluminium	-	0.76/1.30	-	Curve fitting
Hamm (2002)	Framework	68	Wood & steel	-	1.2 (0.80-1.35)	-	-	Half power bandwidth (free-decay)
Caetano & Chuna (2002)	Stressed ribbon	30	-	Concrete	1.7/3.6[d]	-	-	Free-decay after skipping
Fletcher & Parker (2003)	Cable-stayed	53	-	Reinforced concrete	0.40 (0.51)/	0.44[b]	-	Free-decay (curve fitting)

Note: In case of more than one damping value measured, the average value is given.

[a]Half power bandwidth.

[b]Estimation methods are not stated.

[c]Coupled with vertical movement.

[d]Not clear the way of identification having in mind that two closely spaced modes appeared.

Interpretation of measurement results should be conducted very carefully. For example, the SDOF half-power bandwidth method using ambient testing response data tends to produce higher damping because of the averaging during data processing and the impossibility to have ideally stationary input necessary for ambient testing (Brownjohn et al., 1987). Also it can neither produce good damping estimate for closely spaced modes nor give insight into the amplitude dependence phenomenon. Problems with closely spaced modes can happen in the time-domain based free vibration decay method too (Rainer & Van Selst, 1976).

The choice of the most appropriate excitation method for each bridge is very important. In almost all articles relevant to footbridges some examples of merits and demerits of one or more methods are given. It is known that for large structures, which are difficult to be excited artificially because of low frequencies, ambient testing is the most appropriate choice. Also, it is cheaper than forced testing and does not disrupt the normal service of the bridge. This testing is often used as preliminary investigation for other methods to give a quick and rough indication of bridge natural frequencies. However, damping values from these measurements can be unreliable as previously noted, especially when closely spaced modes exist.

For short bridges featuring higher natural frequencies and modest testing budgets, hammer testing leading to FRFs may be more appropriate. It gives relatively reliable values of damping and it is very easy to conduct such a test if a bridge can be closed. However, inevitable ambient extraneous excitation can easily make analysis more complicated.

Finally, excitation by a controlled force produced by an electrodynamic or hydraulic shaker is believed to be most reliable method suitable for bridges of medium size. In principle, it requires shorter time for data acquisition than ambient tests. Also, electrodynamic and hydraulic shakers can produce different types of excitation which give flexibility in the measurement procedure. However, this method tends to be the most expensive. Also, it is hard to excite low frequencies, especially below 1.0 Hz.

Table 2.2 contains key published results related to damping measurements on footbridges. Damping ratios ζ_v, ζ_h and ζ_t for the first two vertical, horizontal and torsional modes are given whenever data were available.

Gardner-Morse & Huston (1993) investigated a small cable-stayed pedestrian bridge using an impact hammer. They successfully extracted the first 14 modes. Although the deck was wooden, measured damping ratios were very low - up to only 0.75%, except for the fourth vertical mode. Brownjohn et al. (1994) investigated a suspension footbridge, also using hammer testing. Besides results presented in Table 2.2, Brownjohn (1988) obtained very different damping estimates using the half-power bandwidth method. However, it should be said that these investigations were conducted just as a preparation exercise for measurements on a long suspended road bridge. Again by using an instrumented hammer (7.25 kg), Brownjohn (1997) successfully identified two closely spaced modes at frequency near 2 Hz on a suspended bridge. Cantieni & Pietrzko (1993) identified the first 12 modes on a wooden bridge using a vibration generator driven by a burst random signal (0.5-25 Hz). In his PhD thesis, Pi-

mentel (1997) tested two footbridges (pre-cambered beam and stressed ribbon) by means of the hammer testing. However, damping values were determined mainly using jumping and walking free-decay tests where the value obtained by jumping was higher due to presence of the test subject on the bridge. Pavic & Reynolds (2002) used a electrodynamic shaker with chirp excitation (1-30 Hz) to investigate the same catenary (i.e. stressed ribbon) footbridge and found almost the same damping values as in Pimentel's (1997) walking tests. Pimentel (1997) also investigated a cable stayed bridge by ambient vibrations.

Pavic et al. (2002a) successfully tested the London Millennium Bridge using two different shakers to excite horizontal lateral and vertical modes, respectively. The lowest lateral frequency was 0.5 Hz, which required the construction of a special hydraulic shaker which would be able to excite such a low frequency mode - an inertial shaker with moving mass of 1000 kg (Figure 2.14). It is interesting to compare it with the first attempts of using mechanical exciters in dynamic investigations of bridges such as that reported by Chasteau (1973) where an eccentric mass of 3.75 kg was used, or that reported by Eyre & Tilly (1977) where a hydraulic actuator could not excite a vertical mode with frequency at 0.53 Hz. The damping of the Millenium Bridge was measured for different configurations while some viscous dampers and/or a tuned mass damper were in operation. These results were published by Pavic et al. (2002b), while in Table 2.2 results for the first two lateral modes of the central span without any additional damping devices are given.

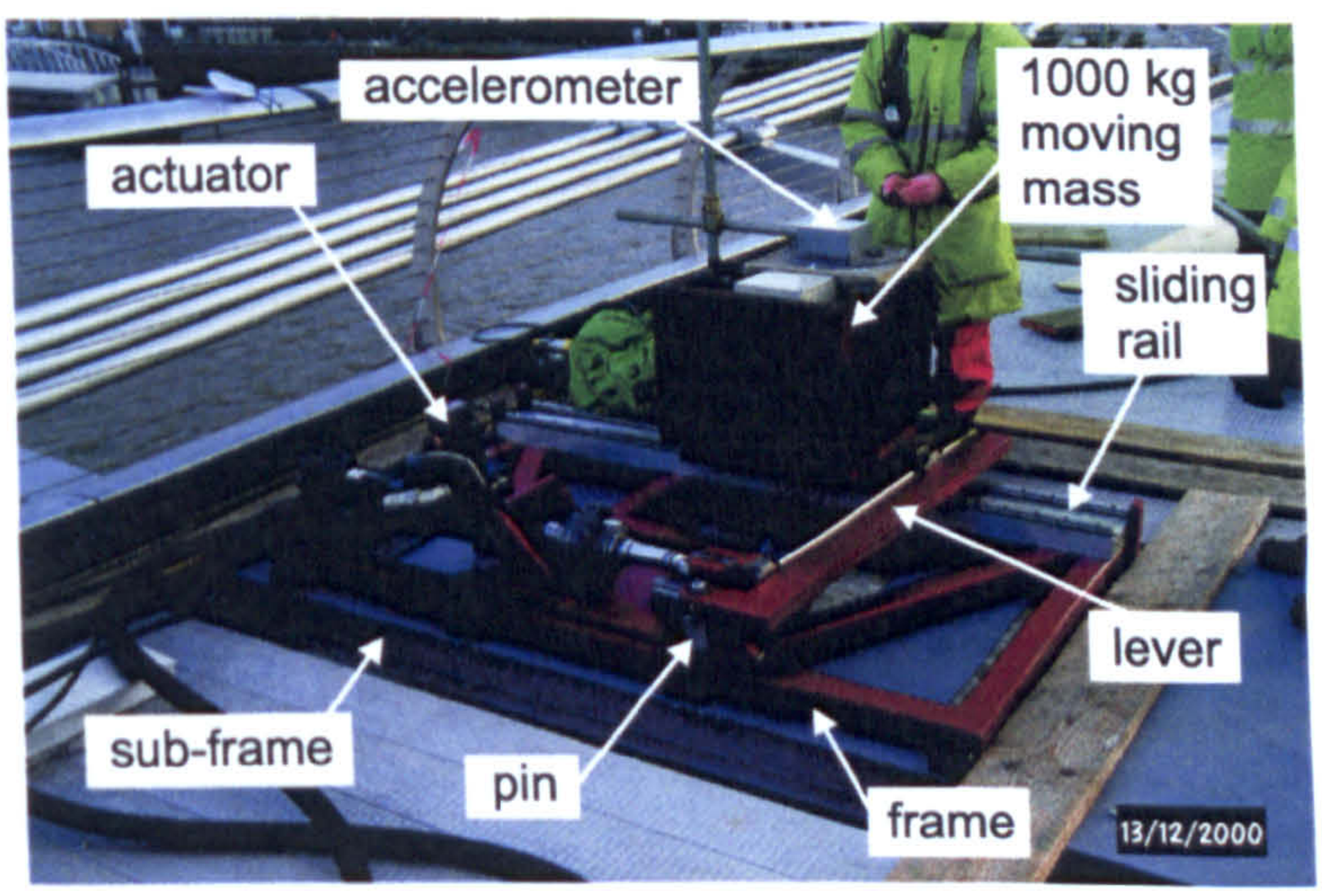

Figure 2.14: Horizontal shaker used for testing of the Millennium Bridge (after Pavic et al., 2002a).

A timber footbridge was investigated by Hamm (2002) whose result confirmed Eurocode 5 (ENV, 1997) proposal for damping of this type of pedestrian bridges of 1.0% and 1.5% depending on the construction type. Unfortunately, only the first vertical mode was investigated.

Based on everything stated so far, it is obvious that it is not possible to define unique value(s) for footbridge damping. To overcome this, Bachmann et al. (1995a) suggested in 1995 using Table 2.3 as a guidance based on data collected on 43 footbridges in the 1980's (Cantieni

et al., 1986). Based on the new data since published, these recommendations still look very reasonable.

Table 2.3: Provisional values of damping ratio in footbridges (after Bachmann et al., 1995a).

	Damping ratio [%]		
Construction type	**Minimum**	**Mean**	**Maximum**
Reinforced concrete	0.8	1.3	2.0
Prestressed concrete	0.5	1.0	1.7
Composite	0.3	0.6	-
Steel	0.2	0.4	-

2.4 Receiver of Footbridge Vibrations

The main receivers of vibrations on pedestrian bridges, who govern their vibration serviceability, are walking people. Although Walley (1959) reported that "a pedestrian at rest on the bridge might 'feel' the passage of other pedestrians and be disturbed", Leonard (1966) claimed that it was economically unjustifiable to design footbridges where standing people would feel no vibrations.

The reaction of human beings to vibrations is a very complex issue having in mind that humans are "the greatest variables with which anyone may deal" (Jacklin, 1936). According to Lippert (1947), not only different people react differently to the same vibration conditions, but also an individual exposed to the same vibrations on different days will likely react differently. This is known as the inter- and intra-subject variability of humans and their reactions to vibrations (Griffin, 1996). Knowing that human sensitivity to vibrations is very high (Wood, 1948), it is clear that this issue is of paramount importance for footbridge vibration serviceability.

2.4.1 Early Works

Probably one of the first laboratory works and certainly the most often referenced in the future studies was conducted by Reiher and Meister in 1931 (Wright & Green, 1959). They investigated the effect of harmonic vibrations on ten people having different postures (laying, sitting, standing) on a test platform driven by different amplitudes, frequencies and direction of vibrations. As a result they classified the human perception into six categories and as a function of vibration amplitude and frequency (Figure 2.15).

In the 1940s, some very valuable systematisations of the work until that time were published by Postlethwaite (1944) and Goldman (1948). Postlethwaite (1944) tried to construct perception curves by combining experimental results of different authors and by the use of "some imagination where experimental results were lacking". The acceleration perception

threshold in the low frequency region of up to 1 Hz was 0.01 ft/s^2 (0.03%g). Mallock, who investigated unpleasant vibrations at 10-15 Hz in some London houses due to traffic, found that the vibration displacement amplitude was very low (0.001 in i.e. 0.025 mm) but the corresponding acceleration level (up to 2.3%g) caused the problem. As a result, he proposed 1%g and 5%g as noticeable and nuisance values, respectively (Postlethwaite, 1944). This example shows the importance of the vibration descriptor in which vibration amplitude is expressed (displacements, velocities or accelerations). Goldman (1948) used all known work regardless of the vibration direction, subject's posture and type of vibration to define three categories of human reaction to vibrations: perception, discomfort and maximum tolerable levels. According to this study, the minimum discomfort level was about 4.6%g while the perception value was only 0.25%g. This minimum occurred around the frequency of 5 Hz which was the main resonant frequency of the human body (Dieckmann, 1958). Dieckmann also separated sensitivity to vibrations in the horizontal and vertical direction where for frequencies below about 4 Hz sensitivity was higher for horizontal vibrations.

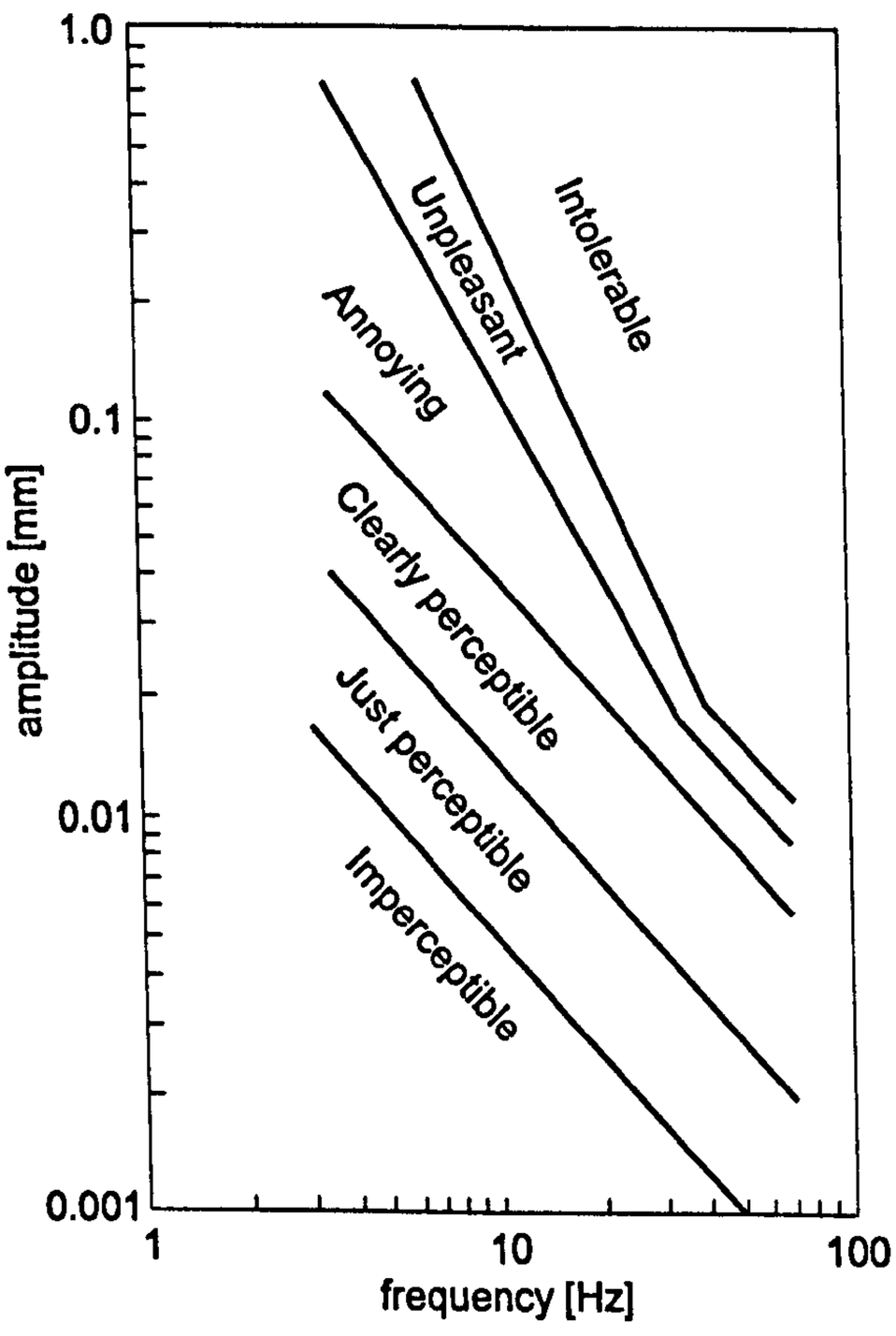

Figure 2.15: Reiher and Meister's scale of human perception (after Smith, 1988).

Although these few examples of early findings are not directly related to footbridges, they present the first steps in human vibration perception research which triggered and became a basis for subsequent investigations. They also give insight into large variations of vibration threshold limits caused typically by different test conditions and illustrate the need to research this issue separately for each type of structure of interest.

2.4.2 Perception of Vertical Vibrations on Bridges

Trying to investigate the human perception of vibration on highway bridges, Wright & Green (1959) noticed that real vibrations on bridges are much more complex than the harmonic vibrations usually used in past investigations of human perception. Also, research was conducted in laboratory conditions and therefore its applicability to footbridges is questionable. Finally, many parameters specific to bridge vibrations were not considered such as the fact that the receiver is not stationary but is moving, the transient nature of footfall excitation and the limited duration of exposure to vibrations. As a confirmation of the desperate situation regarding the knowledge of human perception of bridge vibrations the Committee on Deflection Limitations of Bridges (CDLB, 1958) reported that there was no scale at that time which was appropriate for bridge applications.

In a large investigation Wright & Green (1963) measured the peak oscillations on 52 highway bridges under normal traffic and found they were "unpleasant" or even in 25% cases "intolerable" according to their isosensors scale based on a refinement of Goldman's (1948) work. Similar results were obtained using Reiher and Meister scale. They concluded that these, and similar, scales based on long time vibrations might not be appropriate for bridge vibrations where peak vibrations usually lasted only for a short period of time. The duration of vibrations depends to some extent on the bridge damping which is considered as the most important factor in the human perception in Lenzen's (1966) work, but related to floors.

Motivated by the lack of research related to walking and standing people under vibrations with limited duration, Leonard (1966) conducted a laboratory experiment on a 10.7 m long beam driven by sinusoidal excitation at different amplitudes (up to 0.2" i.e. 5.08 mm) and frequencies (1-14 Hz). Forty walking and standing persons helped in these tests to define the boundary between acceptable and unacceptable vibrations in individual tests lasting up to one minute during which vibration amplitude was held on a constant level. Results clearly indicated that a standing person is more sensitive to vibrations than a walking one (Figure 2.16). Similarly to Wright & Green (1963), it was shown that the Reiher and Meister scale is fairly inappropriate for application to bridges. Leonard further suggested using the curve applicable to stationary standing people for vibration perceptibility in the case of large numbers of pedestrians because of a prolonged duration of the vibration level. A similar recommendation was made regarding the perception of vibration in the horizontal direction because of the greater human sensitivity in this direction.

Smith (1969) conducted an experiment using a single walking pedestrian excitation on a flexible aluminium alloy plank. He pointed out that a pedestrian, even in the case of sustained sinusoidal bridge vibrations, felt the maximum amplitude only near the midspan (Figure 2.17). Twenty-six subjects were asked to walk several times across the plank and to classify vibration level into three groups: acceptable, unpleasant and intolerable. During tests the frequency of the plank was adjusted to be as close as possible to the walking frequency. Because of the inter-subject variability and overlapping of the three vibration levels rated by different

test subjects, Smith decided only to define regions of acceptable and unacceptable vibrations (Figure 2.16). His threshold curve was much higher than the Leonard's. As a possible reason Smith mentioned possibility that Leonard chose to draw a lower limit curve rather than a mean curve. However, it could be that the length of the plank of only 4.88 m had influence too. It is interesting that in some of Smith's tests, when the resonant build up of vibration was achieved, some subjects were afraid.

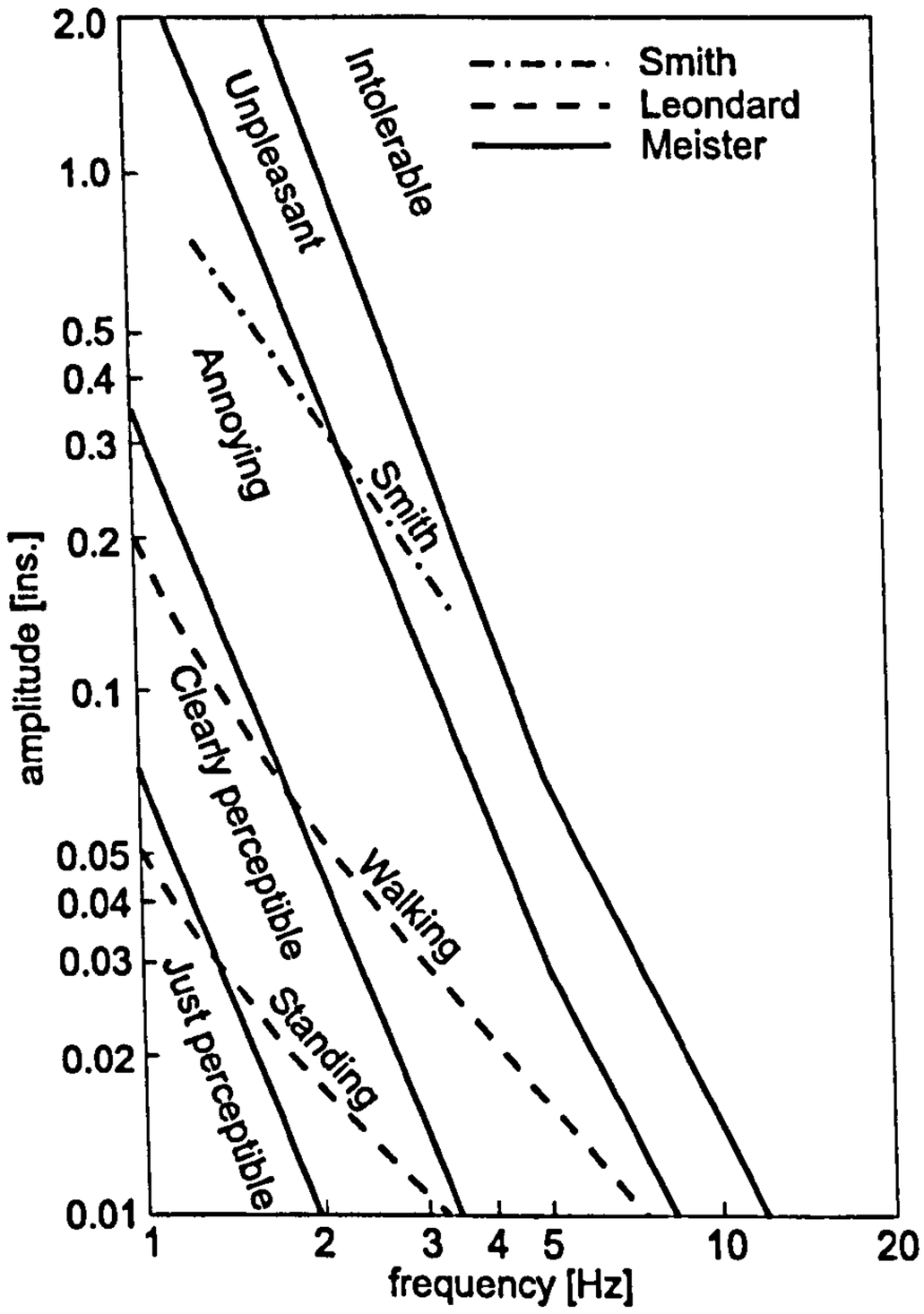

Figure 2.16: Leonards and Smiths scales of human perception (after Smith, 1969).

Kobori & Kajikawa (1974) conducted experiments similar to Leonard's tests, with 11 walking subjects on a vertically vibrating shaking platform driven by a sinusoidal force in the frequency range 1-10 Hz. It was found that the vibration velocity is the main parameter which influenced the human perception. The two authors formulated analytically the relationship between the vibration perception and the vibration velocity and reported a comparison between responses to: a sinusoidal vibration, vibration having two harmonic components and random vibration. They concluded that the sensitivity is the same if the "effective value of both stimuli" is the same. However, it is not quite clear what this statement precisely means and how the results are processed. The same authors investigated the possibility that a footbridge will be unserviceable under a number of pedestrians (Kajikawa & Kobori, 1977). Using probability theory and assuming a Poisson distribution of pedestrian arrivals as well as a normal distribution of human response, they found the probability that serviceability of a footbridge will not be satisfied, in terms of a percentage of pedestrians who will feel an unac-

ceptable level of vibrations. Unserviceability curves for a pedestrian bridge, as a function of arriving number of pedestrians per second and the bridge damping are given in Figure 2.18. Unfortunately, none of these two articles (Kobori & Kajikawa, 1974 and Kajikawa & Kobori, 1977) contains a list of pertinent references which could help to understand better the approach proposed. It should be noted that velocity is adopted as the parameter for evaluation of footbridge serviceability in Japan (Yoneda, 2002).

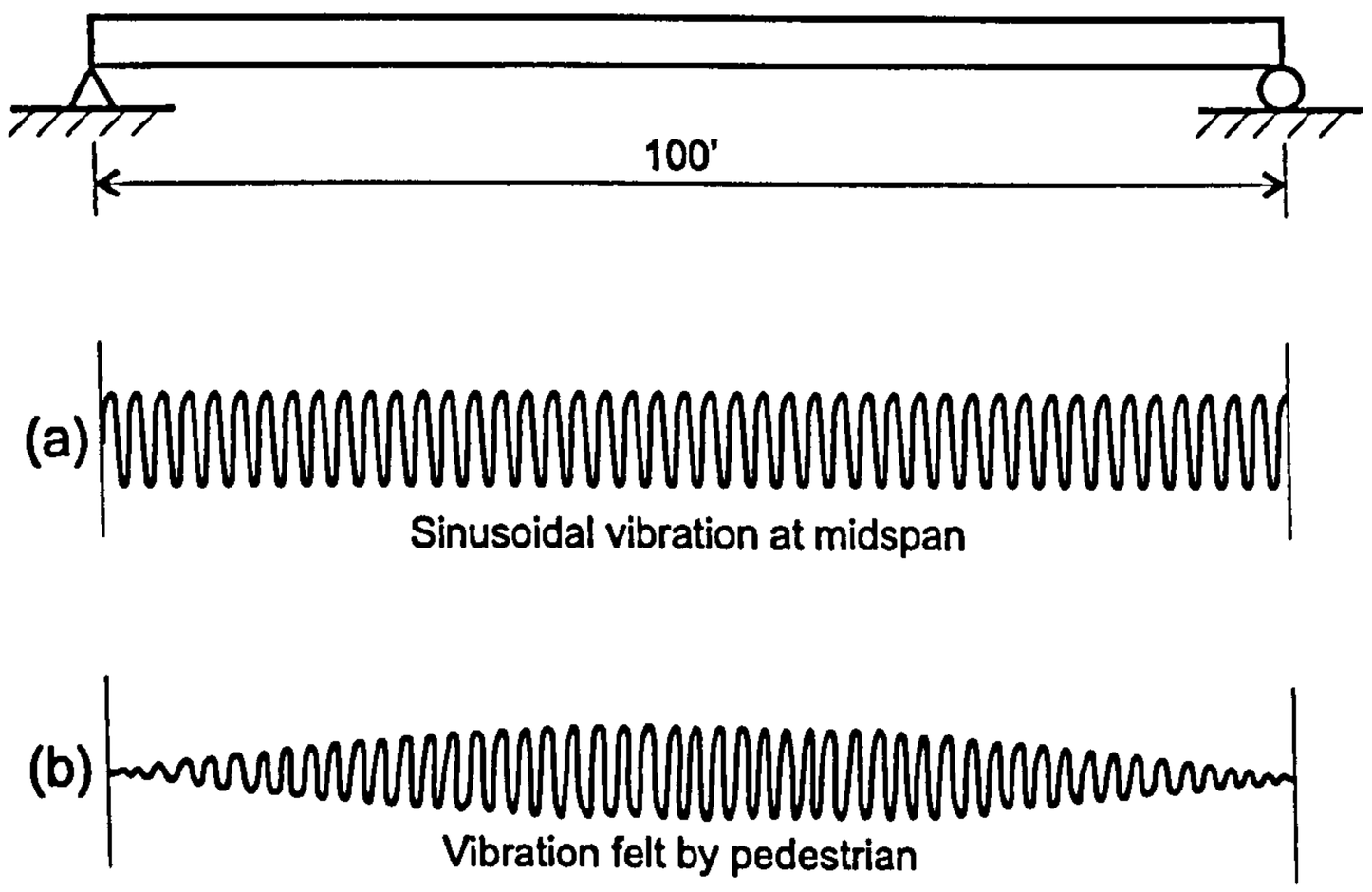

Figure 2.17: (a) Sinusoidal vibrations in the middle of the span. (b) Vibrations felt by a walking pedestrian (after Smith, 1969).

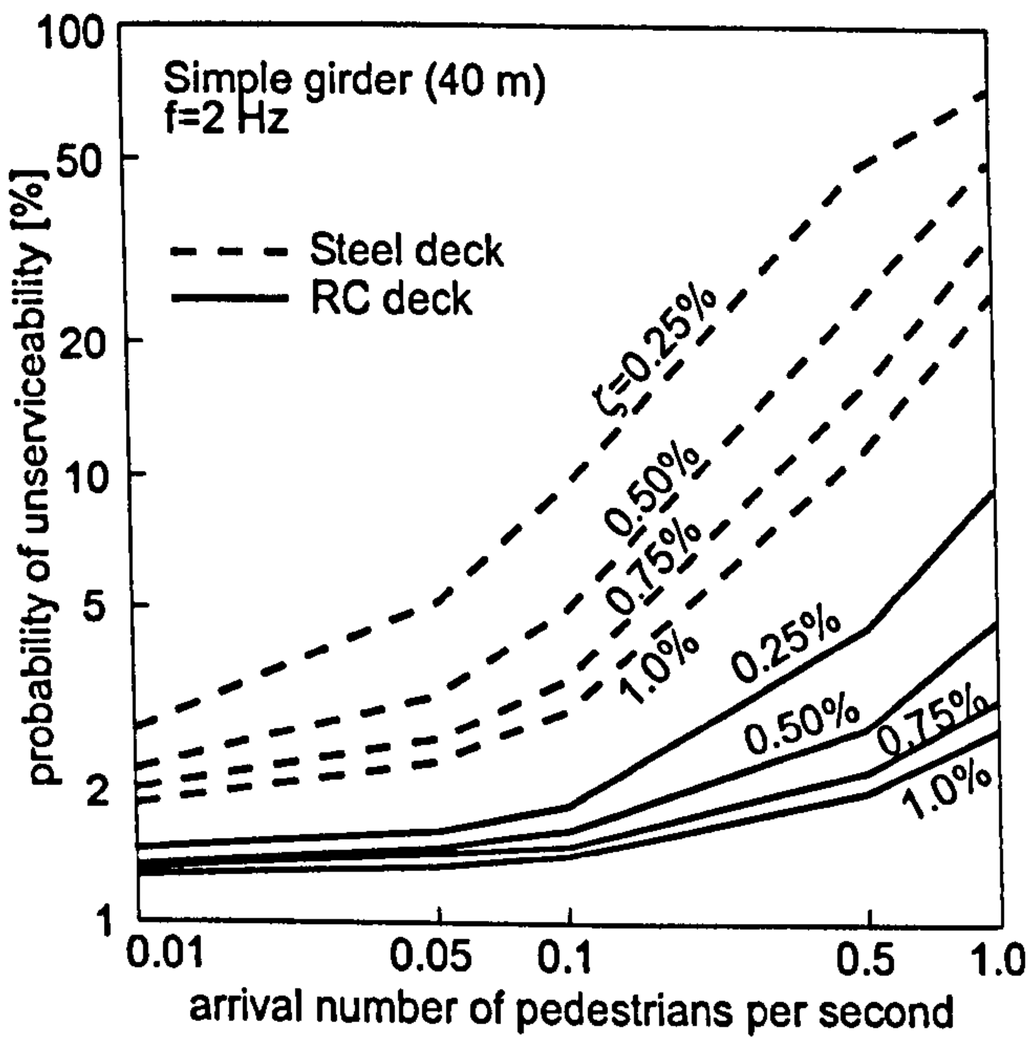

Figure 2.18: Probability of footbridge unserviceability (after Kajikawa & Kobori, 1977).

In their design proposal for footbridges, Blanchard et al. (1977) used the mean value of Leonard's and Smith's results to define a level of acceptable acceleration a_{limit}, expressed as:

$$a_{limit} = 0.5\sqrt{f}, [\mathrm{m/s^2}] \tag{2.6}$$

where f [Hz] is the footbridge fundamental frequency. This value is adopted in the current British standard for assessing vibration serviceability of footbridges BS 5400 (BSI, 1978). However, Tilly et al. (1984) mentioned the possibility that the limit of $\sqrt{f}$ might be more appropriate outside the frequency range 1.7-2.2 Hz, but without detailed elaboration of this recommendation.

Irwin (1978) collected data about human response to vibration from different sources based on both laboratory and tests on full-scale structures. He constructed either the perception or maximum allowable magnitude curves for different types of structures and different type of vibrations. Among them, the limits for root-mean-square (RMS) accelerations for bridges are given, separately for everyday usage and storm conditions (Figure 2.19). The maximum sensitivity for everyday curve for vertical vibrations was between 1 and 2 Hz, and was 0.07 $\mathrm{m/s^2}$ when expressed as an equivalent harmonic peak value. This frequency range is far lower than the 4-8 Hz range in ISO 2631-2 (ISO, 1989) applicable to floor vibrations. The curve for storms is obtained by multiplying the base (everyday) curve by the factor 6. However, the horizontal motion is considered only for storm conditions, while for everyday usage it is neglected as rare. This work was founded on the base curve principle, which means that curves for different purposes can be obtained from the base curve by multiplying by some factor. All perceptibility curves were expressed, contrary to a lot of previous research based on peak values, via the RMS accelerations. This quantity is the square root of the mean value of the square acceleration during time record (Griffin, 1996):

$$\mathrm{RMS} = \sqrt{\frac{\int_{t_1}^{t_2} \ddot{x}(t)^2 dt}{t_2 - t_1}} \tag{2.7}$$

where $\ddot{x}(t)$ is the acceleration time history, and t_1 and t_2 define the beginning and end of the time interval considered. However, the choice of RMS accelerations as the vibration perception descriptor, which became common in many guidelines related to human perception of vibrations, was based primarily on the fact that it is relatively easy to measure accelerations and the corresponding RMS values, using both analog and digital methods (Griffin, 1996).

One of the recommendations for acceptable footbridge vibrations, which is based on RMS acceleration limits, is given in the ISO 10137 guidelines for serviceability in buildings (ISO, 1992). It suggests using the base curves for vibrations in both vertical and horizontal directions given in ISO 2631-2 (1989) multiplied by the factor of 60 (Figures 2.20 and 2.21). However, this recommendation is, to the best of author's knowledge, not based on published research pertinent to footbridge vibrations.

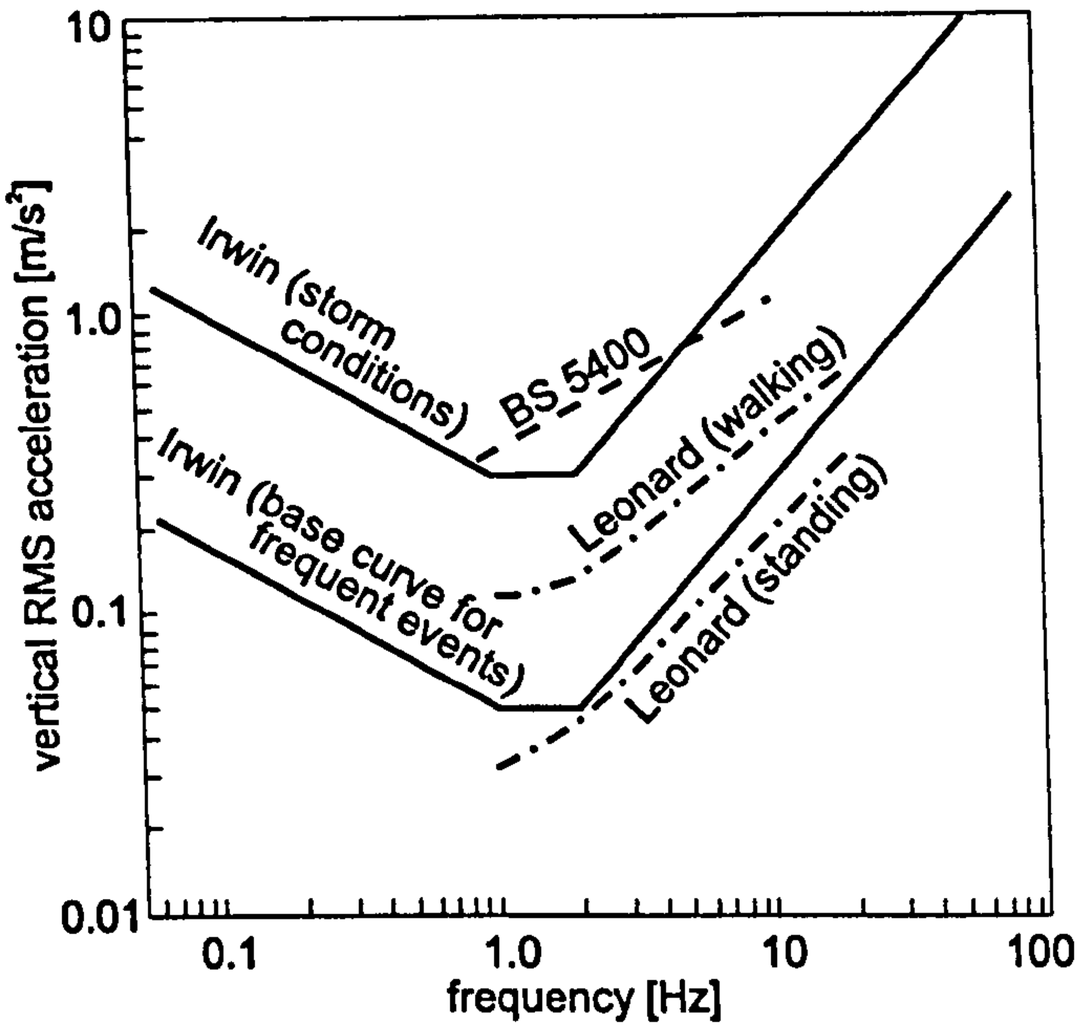

Figure 2.19: Acceptability of vibrations on footbridges after different scales (after Smith, 1988).

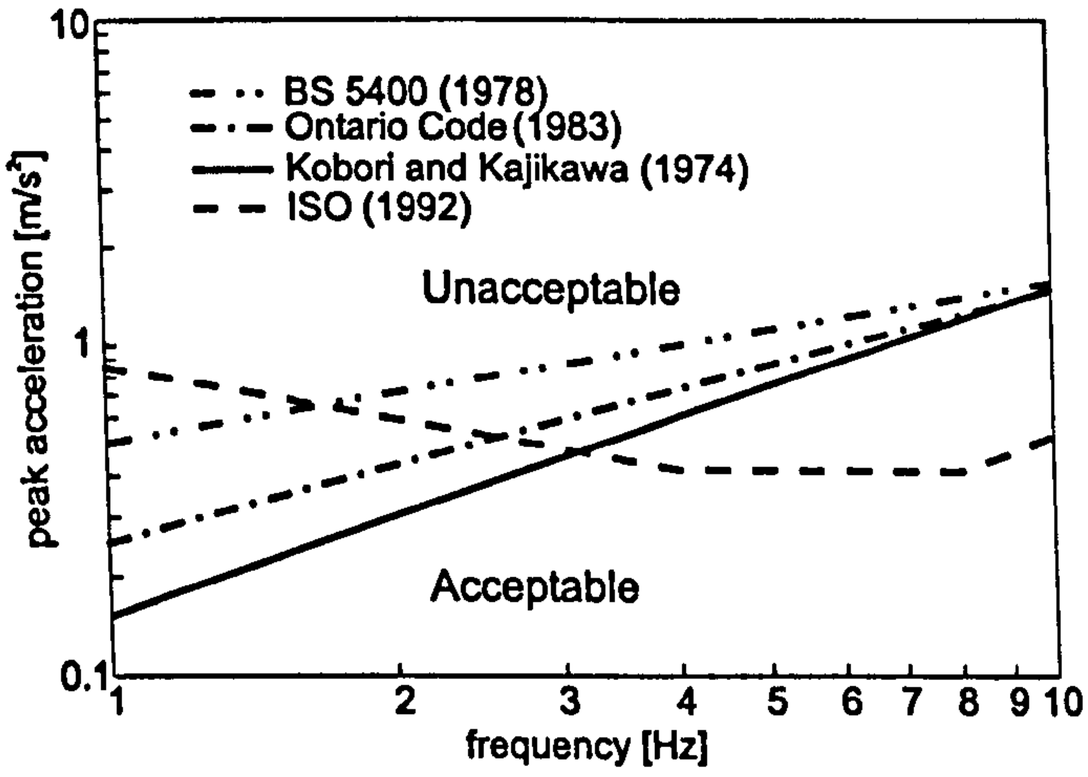

Figure 2.20: Acceptability of vertical vibrations in footbridges after different scales (after Pimentel, 1997).

Pimentel (1997) compared vibration limits given in BS 5400 (BSI, 1978), Ontario Code (OHBDC, 1983), Kobori & Kajikawa (1974) and ISO 10137 (ISO, 1992) related to footbridges. They are presented in Figure 2.20, while Figure 2.19 compares limits according to BS 5400, Leonard (1966) and Irwin (1978). A comparison of these limits shows that, for example, BS 5400 allows the highest level of vibrations over a typical range of footbridge response frequencies. On the other hand, Bachmann et al. (1995a) proposed a constant acceleration acceptance level of $0.5\,\mathrm{m/s^2}$. All these limits form a database of results related to footbridges. It should be noticed that the ISO (1992) curve given in Figure 2.20 was obtained by converting the RMS acceleration to the peak value by multiplying by the factor $\sqrt{2}$.

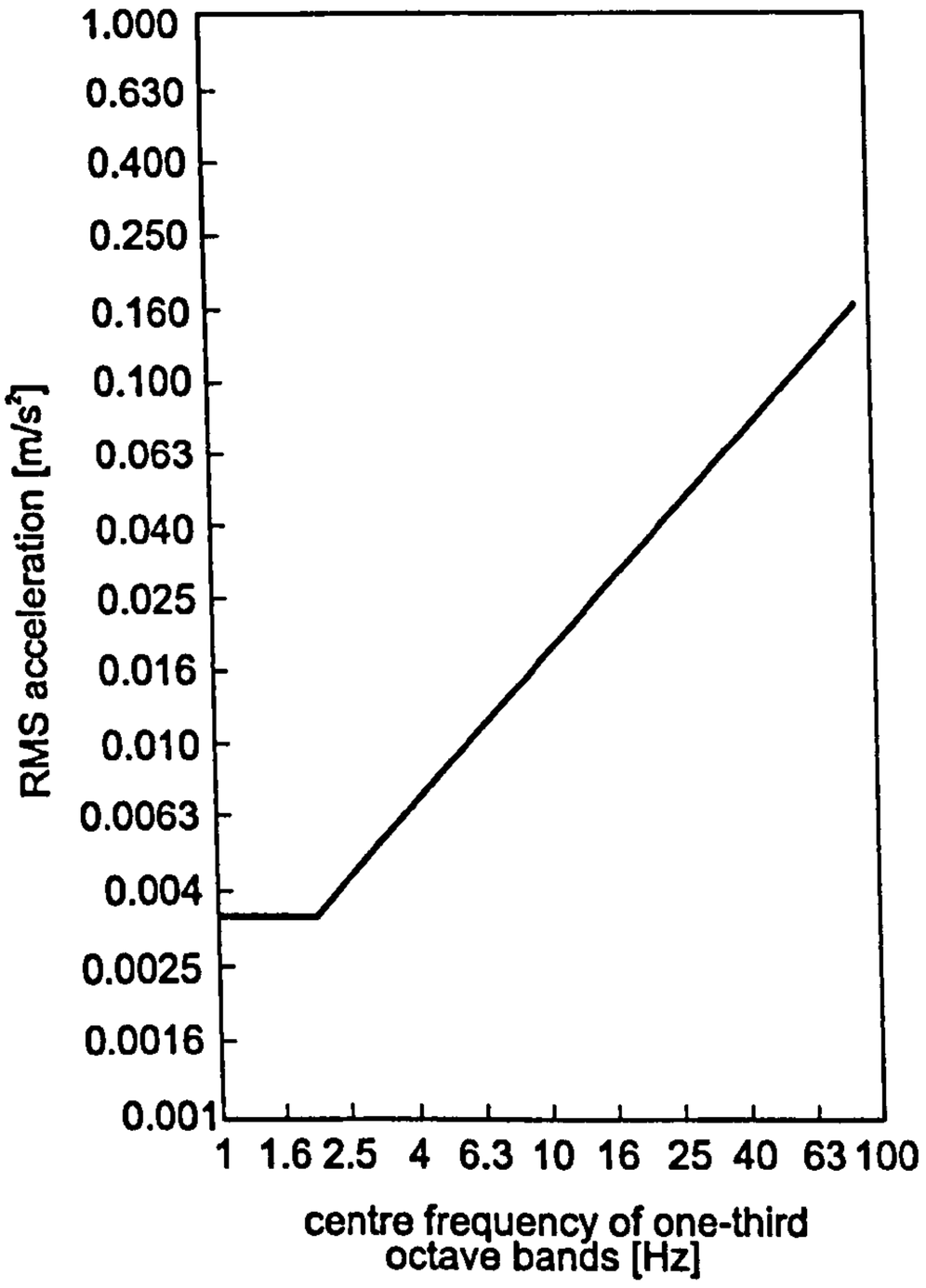

Figure 2.21: Acceptability of vibrations in horizontal direction. This base curve should be multiplied by the factor 60 (after ISO, 1992).

To account for different reactions between different people, Obata et al. (1995) presented, for each of four defined perception levels (lightly perceptible, definitely perceptible, lightly unpleasant and greatly unpleasant), curves of 25, 40, 50, 60 and 75% probability where the reactions to vibrations will happen. They suggested that footbridge serviceability will not be compromised for a peak velocity of 1 cm/s, while it is rare that vibrations are unpleasant up to the peak 1.4 cm/s. For a footbridge with, for example, a natural frequency of 2 Hz, converting these velocity peak values to corresponding peak accelerations gives 0.13 and 0.18 m/s^2 respectively, where these limits are far lower than those in Figure 2.20.

2.4.3 Horizontal Vibration and Its Perception within a Crowd

Data on human perception of horizontal vibration of bridges are very scarce. However, there are many works related to human perception of horizontal vibrations in buildings. For example Chen & Robertson (1972) investigated the human perception threshold to horizontal sinusoidal vibrations with frequencies between 0.067 Hz and 0.20 Hz, which are characteristic of tall building response due to wind. Although this frequency range is unlikely to be relevant for footbridges, this work is interesting because it identified the most important factors typical for this issue: the frequency of vibrations, body movement, expectancy of motion and body posture. The authors found that, also in this low frequency region, the vibration perception

threshold of walking people is higher than for a stationary person and that the perception threshold is lower when the person expects the movement. However, it should be noticed that the tolerance level (as opposed to the perception level) is higher if one expects vibrations, regardless of its direction (Smith, 1988). Another interesting experiment was conducted by Nakata et al. (1993). Forty test subjects were exposed to horizontal sinusoidal vibrations at frequencies 1-6 Hz. The amplitude of vibrations was gradually increased and the perception value when the test subject felt vibration was recorded. It was concluded that the fore-aft perception threshold was higher than the side-to-side threshold in the range 1-3 Hz, while in the range 3-6 Hz the opposite was true. However, only the sitting posture was considered.

Wheeler (1982) noticed that the human perception of vibration in a walking crowd on footbridges is different than for a single isolated person. An additional proof that different perception scales are necessary for circumstances involving different numbers of people was provided by Ellis & Ji (2002). They reported that during an experiment with a jumping crowd, jumpers were not concerned although the measured acceleration was 0.55g. It is not clear if the noise, the presence of other people or something else contributed to the fact that such high accelerations were considered as tolerable.

As mentioned earlier, the only guideline which recommends a horizontal vibration limit for footbridges is ISO 10137 (ISO, 1992). The perception curve is presented in Figure 2.21. The highest sensitivity to this type of vibration is in the frequency region up to 2 Hz and is at about 3.1%g peak acceleration.

Probably most valuable information about the tolerance level to footbridge lateral vibrations due to crowd loading is given by Nakamura (2003). Based on pedestrian experience of vibrations on full-scale footbridges, he concluded that the amplitude of deck displacement of 45 mm (corresponding to an acceleration of $1.35\,m/s^2$) is a reasonable serviceability limit. At the same time he noticed that a deck displacement amplitude of 10 mm (corresponding to acceleration level of $0.3\,m/s^2$) was tolerable by most pedestrians, while a displacement of 70 mm ($2.1\,m/s^2$) would make people to feel unsafe and prevent them from walking.

2.4.4 Concluding Remarks

In the majority of tests conducted it has been generally accepted that acceleration is the vibration parameter which should be used to describe the problem. One of the key reasons is that acceleration is convenient to be measured even though there are situations when the vibration effect can be explained better by other quantities such as velocity (Griffin, 1996). It is now widely accepted that the vibration tolerance for moving pedestrians on bridges is higher than for people in buildings, and that pedestrians can accept certain (initially unacceptable) level of vibrations when they accustom themselves to it (Smith, 1988). Therefore, the expectation of vibrations plays a very important role in footbridge vibration serviceability. However, hard numbers which would quantify these observations are scarce.

Further work in this area for footbridges is necessary, especially with regard to the perception

of vibration in the horizontal lateral direction. This should be done by simulating real conditions as much as possible and by verifying results on full-scale structures. Finally, there is some limited evidence of some probability-based approaches to vibration perception on footbridges. Considering the large inter- and intra-subject variability, probability based methods are likely to be the best way forward when assessing the effects of footbridge vibrations.

2.5 Human-Structure Dynamic Interaction in Footbridges

It is now widely accepted that during footbridge vibration some kind of human-structure interaction almost inevitably occurs. Often, this interaction can be neglected, but it is becoming more common that it cannot. In general, there are two aspects of this issue. The first considers changes in dynamic properties of the footbridge, mainly in damping and natural frequency, due to human presence. The second aspect concerns a degree of synchronisation of movement between the pedestrians themselves as well as between the pedestrians and the structure whose motion is perceived. Both phenomena are currently not well understood and research related to them has been intensified in recent years.

2.5.1 Dynamic Properties of Footbridges under Moving People

It is well-known that the presence of a stationary (standing or sitting) person changes the dynamic properties of a structure they occupy. The most important effect is the increase in damping in the joint human-structure dynamic system compared with the damping of the empty structure (Ellis & Ji, 1994; Sachse, 2002). The effect is greater if more people are present (Ellis & Ji, 1997; Sachse, 2002). Therefore, it can be concluded that the human body behaves like a damped dynamic system attached to the main structural system. Such a system can be described by biodynamics methods, structural dynamics methods or by their combination (Ji, 2000). The human body is in effect a complex non-linear MDOF system with its parts responding in different ways to structural movement (Williams et al., 1999). In a simplified study of human body-structure interaction, the human body can be approximated by a linear SDOF system (Ji, 2000). One of very few reported attempts to carry out system identification of the dynamic properties of a standing person, applicable to civil engineering, was done recently by Zheng & Brownjohn (2001). Their SDOF human body model had a damping ratio of 39% and natural frequency of 5.24 Hz. However, the simplified SDOF human body system has been shown to be dependent on structural frequency and cannot be always represented by the same set of mass, stiffness and damping parameters (Sachse, 2002; Sachse et al., 2002).

The problem is even less researched in the case of moving people, which is usual for footbridges. Ellis & Ji (1994) found that a person running and jumping on the spot cannot change dynamic characteristics of the structure and, therefore, should be treated only as load. However, this investigation was conducted using a simply supported beam having a

high fundamental frequency of 18.68 Hz compared with typical footbridge natural frequencies. Nevertheless a similar conclusion was reached by the same researchers regarding the effects of a moving crowd on grandstands (Ellis & Ji, 1997).

2.5.2 Dynamic Forces on Flexible Footbridges

Ohlsson (1982) reported that the spectrum of a force measured on a rigid surface differed from that measured on a flexible timber floor. The spectrum experienced a drop around the natural frequency of the structure where the motion was the highest. This could be a consequence of the interaction phenomenon and is in agreement with previously mentioned Pimentel's (1997) findings of lower dynamic loading factors (DLFs) on real and moving footbridges in comparison with those measured on rigid surfaces. Ohlsson also claimed that a moving pedestrian increased the mass and the damping of the structure. However, it should be stressed again that he investigated only light timber floors where human-structure dynamic interaction is more likely due to large ratios of the mass of the humans and the empty structure. However, Willford (2002) also mentioned a result of data analysis from pedestrian tests on the Millennium Bridge which indicated that walking crowd had increased the damping of the structure in the vertical direction.

That jumping and bouncing can change dynamic properties of a flexible structure was reported by Yao et al. (2002). They found that jumping forces are lower on a more flexible structure, but it should be noted that in their investigation the subject to structure mass ratio was very high (0.41). Further, Pavic et al. (2002c) compared horizontal jumping forces directly measured on a force plate and indirectly measured on a concrete beam. They found that the force on the structure was about two times lower than that one on the force plate. This could also be a consequence of a human-structure interaction effect but no conclusive evidence for it was presented.

All these reported observations give only an indication that human-structure interaction really occurs without a more precise quantification of the phenomenon. Furthermore, with the exception of a paper by Pavic et al. (2002c), all reviewed research is related to vibrations in the vertical direction. Information on possible effects of moving people on the dynamic characteristics of footbridges in the horizontal direction is very scarce.

It is clear that research into human-structure interaction involves various human activities (e.g. waking, jumping, sitting, standing) on different types of structure. In case of footbridges, although some previous findings are quite useful, the most relevant interaction scenario appears to be a walking crowd. Considering the extremely scarce published data, this is an area that clearly requires further investigation.

2.5.3 Synchronisation of People Walking in Groups and Crowds

Ninety years ago Tilden (1913) posed a question which is still unanswered:

> Against what loads, horizontal and vertical, should an engineer design a structure which is likely to have to carry a dense crowd of human beings?

In an attempt to consider this question, he noted that none of the following two extreme cases are real. Neither is an increase in load directly proportional to the number of people involved, in comparison with a single pedestrian force (i.e. the case of perfect synchronisation), nor should only the static weight of the crowd be taken into account (i.e. dynamic effects be neglected). Subsequent research has shown that the solution is somewhere between these two scenarios.

The first attempts to define the load induced by several pedestrians were in terms of multiplication of the load induced by a single pedestrian. One of the first proposals was given by Matsumoto et al. (1978). Assuming that pedestrians arrived on the bridge following a Poisson distribution, they stochastically superimposed individual responses and found that the total response can be obtained by multiplying a single pedestrian response by the multiplication factor $\sqrt{\lambda T_0}$, where λ is the mean arrival rate expressed as the number of pedestrians per second per width of the bridge and T_0 [s] is the time needed to cross over the bridge. Therefore, $\sqrt{\lambda T_0}$ is equal to $\sqrt{n}$, where n is the number of pedestrians on the bridge at any time instant. According to random vibration theory (Newland, 1993), if the response due to n equal and randomly distributed inputs is $\sqrt{n}$ times higher than the response due to a single input, it means that inputs (in this case pedestrians) are absolutely uncorrelated (unsynchronised).

Similar to Matsumoto et al. (1978), Wheeler (1982) stochastically combined individual forces (defined deterministically using the half-sine model) assuming random arrival rate, normal distribution of step frequencies and a distribution of people's weights obtained for the Australian population. However, his simulations revealed that group loads were not a more onerous design case than a single pedestrian load, at least for footbridges with fundamental natural frequency away from approximately 2 Hz. Namely, the group load on bridges with the fundamental frequency away from the normal walking frequency range can be regarded as a non-resonant load which probably generates lower response than the one induced by a single pedestrian walking at the resonant frequency. However, the question still is if this can be applied in case of non-random walking of groups of pedestrians when some degree of synchronisation between people can be established.

In any case, Matsumoto et al.'s proposal was regarded as appropriate at least for footbridges with natural frequencies in the range of walking frequencies (1.8-2.2 Hz), while for bridges with natural frequencies in the ranges 1.6-1.8 Hz and 2.2-2.4 Hz a linear reduction of Matsumoto et al.'s multiplication factor $\sqrt{\lambda T_0}$ was suggested with its minimum value of 2 at the ends of these intervals in the case of more than four people present on the bridge at the same

time (Bachmann & Ammann, 1987). Mouring (1993) simulated a vertical force from walking groups in a way similar to Wheeler (1982). However, she described a single pedestrian force more precisely using the first 10 coefficients of the Fourier series instead of the half-sine model. As a result, she found that the effect of group loads should be considered even in case of footbridges with fundamental frequency outside the normal walking frequency range (1.8-2.2 Hz). The response obtained agreed with Matsumoto et al.'s findings. However, Pimentel (1997) measured the response under three uncorrelated people on two footbridges and confirmed the inapplicability of the proposed multiplication factor for bridges with frequencies outside the normal walking frequency range, as claimed by Bachmann & Ammann (1987). It appears that group loading becomes more important precisely in the normal walking frequency range, and in that case it should be considered. Also, Matsumoto et al.'s proposal did not consider the possibility of synchronisation between people in a dense crowd, a phenomenon which has attracted a great deal of attention from researchers since the Millennium Bridge problem in London occurred in 2000.

In 1985, Eyre & Cullington noticed that the vertical acceleration recorded on a footbridge in a controlled resonance test with a single pedestrian was 1.7 times lower than the one measured in normal usage which included two or more pedestrians who were not formally synchronised in any way. They explained it as a possible consequence of the occasional and by chance synchronisation between two people. Ebrahimpour & Fitts (1996) reported that the optical sense plays an important role in the synchronisation of people's movement. Namely, two jumping persons who could see each other synchronized their movement better than when they were looking in opposite directions. In both cases the jumping frequencies were controlled by an audio signal. Eriksson (1994) claimed that the first walking harmonic could be almost perfectly synchronised for highly correlated people within a group, while the higher harmonics should be treated as completely uncorrelated. Not surprisingly, Ebrahimpour et al. (1996) therefore focussed only on the first harmonic (Figure 2.13) claiming that higher harmonics cannot produce significant response for a walking crowd.

It is now widely accepted that people walking in a crowd, because of the limited space on the bridge deck and the possibility that they can see each other, would subconsciously synchronise their steps. This becomes more likely if the crowd is dense. Bachmann & Ammann (1987) reported that the maximum physically possible crowd density can be 1.6-1.8 persons per square metre of the footbridge deck. However, they concluded that a value of 1 person/m^2 is more probable. During the opening day of the Millennium Bridge in London, the maximum density was 1.3-1.5 people/m^2 (Dallard et al., 2001a). The crowd density on the T-bridge in Japan (also prone to lateral movement) was between 1 and 1.5 people/m^2 (Nakamura & Fujino, 2002). In any case, crowd density influences the walking speed (Figure 2.22), the degree of synchronisation between people and, consequently, the intensity of the human-induced force.

Grundmann et al. (1993) proposed three models corresponding to different pedestrian configurations on a footbridge which should be considered separately:

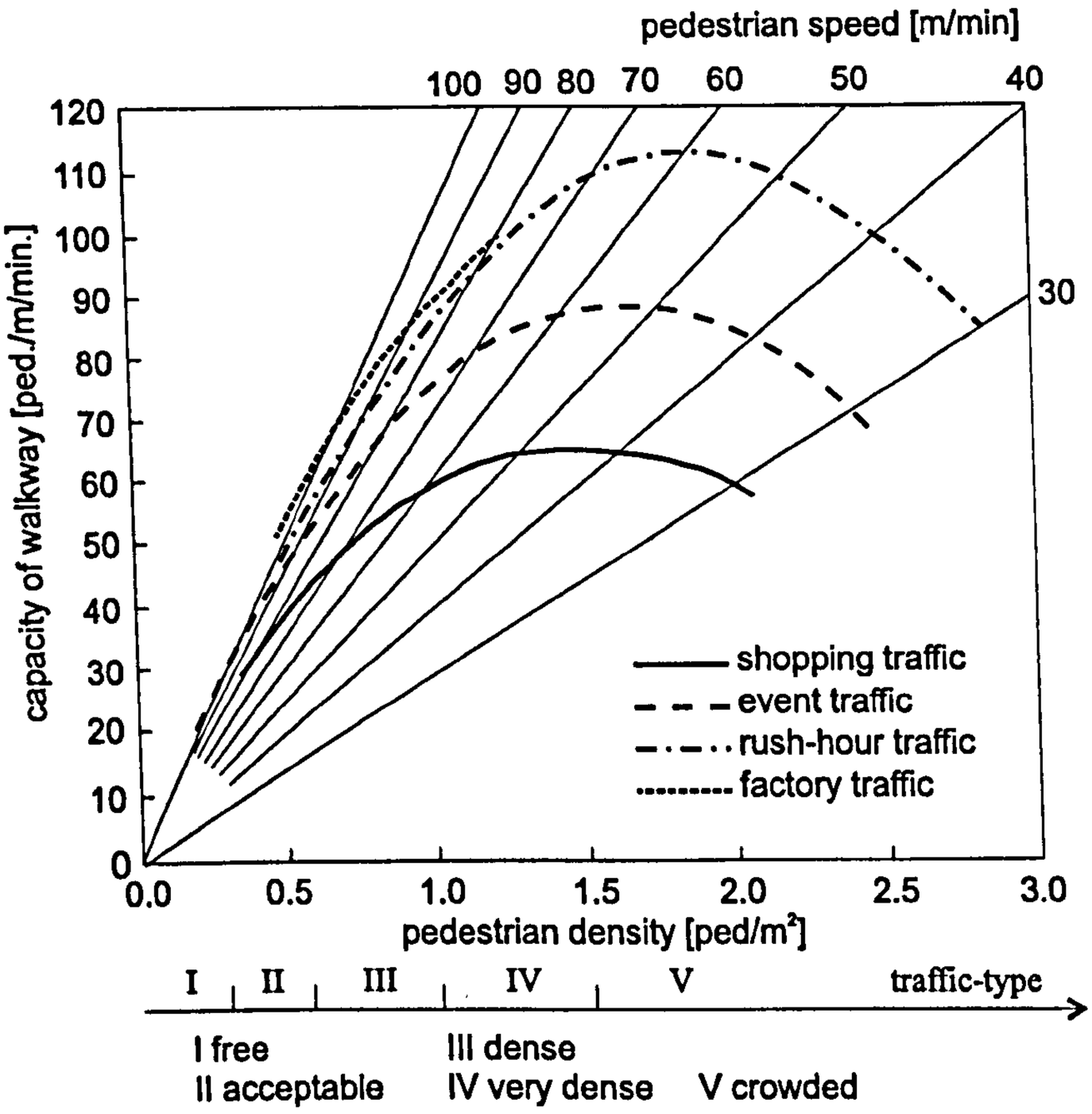

Figure 2.22: Relationship between the bridge capacity, pedestrian density and their velocity (after Schlaich, 2002).

1. When people walk in small groups it is probable that they will walk with the same speed v_s, and slightly different step frequencies f_s and step length l_s according to the equation:

$$v_s = f_s l_s. \tag{2.8}$$

   In such cases, some synchronisation between these people is expected, but only when the bridge frequency is within the normal walking frequency range.

2. On bridges with a light stream of pedestrians where people can move freely and their walking frequencies are randomly distributed. The maximum density of 0.3 pedestrians per square metre was suggested as an upper limit for unconstrained free walking. This type of walking (i.e. free walking) was considered in the previously mentioned proposal by Matsumoto et al.'s (1978).

3. If footbridges are exposed to pedestrian traffic of 0.6-1.0 pedestrians/m^2 then free unconstrained movement is practically impossible. In such circumstances, pedestrians are forced to adjust to some extent their step length and speed to the motion of other pedestrians. The previously mentioned swaying problems of the Millennium Bridge

and the Japanese T-Bridge belong to this group, despite the fact that their pedestrian densities were higher than proposed by Grundmann et al.

As for the third model, it should be added that the case of crowd walking on a perceptibly moving bridge deck is related not only to synchronisation between people but also to synchronisation between people and the structure.

Before considering the research into the human-structure synchronisation phenomenon, two terms widely used in this review will be defined. The term 'group' of walking pedestrians is used for several people walking at the same speed as defined in *Model 1* above, while the term 'crowd' is related to densely packed walking people who have to adjust their step to suit the space available, as explained in *Model 3*.

2.5.3.1 Lateral Synchronisation

The phenomenon when people change their step to adapt it to the vibrations of the bridge, is - for the same level of vibrations - much more probable in the horizontal than in the vertical direction. This is because of the nature of human walking and desire to maintain the body balance on a laterally moving surface. When it occurs, this is known as the synchronisation phenomenon (Bachmann & Ammann, 1987) or lock-in effect (Dallard et al., 2001a). As a consequence of the adjusted step when people tend to walk with more spread legs, the motion of the upper torso becomes greater and the pedestrian-induced force becomes larger. This in turn increases the bridge response and, finally, results in structural dynamic instability (Inman, 2001). In such circumstances, only reducing the number of people on the footbridge or disrupting/stopping their movement can solve the problem (Dallard et al., 2001a; 2001b; 2001c; Fitzpatrick and Ridsdill-Smith, 2001; Fitzpatrick et al., 2001). It is interesting, however, that in a laboratory experiment (McRobie et al., 2003) with a single pedestrian walking across a laterally moving platform, not every pedestrian walked in a way to boost the lateral vibrations. Some of them even managed to damp vibrations out. This fact complicates further study of pedestrian behaviour within a crowd, but also points out the need to define and investigate a factor which will describe the degree of synchronisation between people.

Typically, the excessive swaying occurs on bridges with lateral natural frequencies near 1 Hz which is the predominant frequency of the first harmonic of the pedestrian lateral force (Figure 2.8). Fujino et al. (1993) reported such a case on the previously mentioned T-bridge in Japan. During very crowded times, significant lateral movement occurred in the first lateral mode with frequency of 0.9 Hz. The procedure proposed by Matsumoto et al. (1978) underestimated the actual bridge response. By video recording and observing the movement of people's heads in the crowd, and by measuring the lateral response, Fujino et al. concluded that 20% of the people in the crowd perfectly synchronised their walking. Fujino et al.'s assumption was also that the individual forces produced by the rest of pedestrians cancelled each other, so that their net effect was zero. Later, using image processing technique for tracking people's movement on the same bridge, Yoshida et al. (2002) estimated the overall

lateral force in the crowd of 1500 pedestrians at 5016 N, which gives an average of only 3.34 N per pedestrian.

During the opening day of the Millennium Bridge in London, lateral acceleration of 0.20-0.25g was recorded. This corresponded with lateral displacement amplitudes of up to 7 cm. Dallard et al. (2001a; 2001c) tried to define the problem analytically on the basis of observations made during tests with a gradually increasing number of people on the bridge (up to 275 people). Assuming that everybody contributed equally, they identified the amplitude of the modal lateral force per person (Figure 2.23a) and the dependence of the lateral force on the footbridge velocity (Figure 2.23b). This force was considerably higher than the one reported by Yoshida et al. (2002). Based on results in Figure 2.23b, Dallard et al. concluded that people, after synchronising their movement with the movement of the structure, produced a dynamic force $F(t)$ which was proportional to the deck lateral velocity $v(t)$:

$$F(t) = kv(t). \tag{2.9}$$

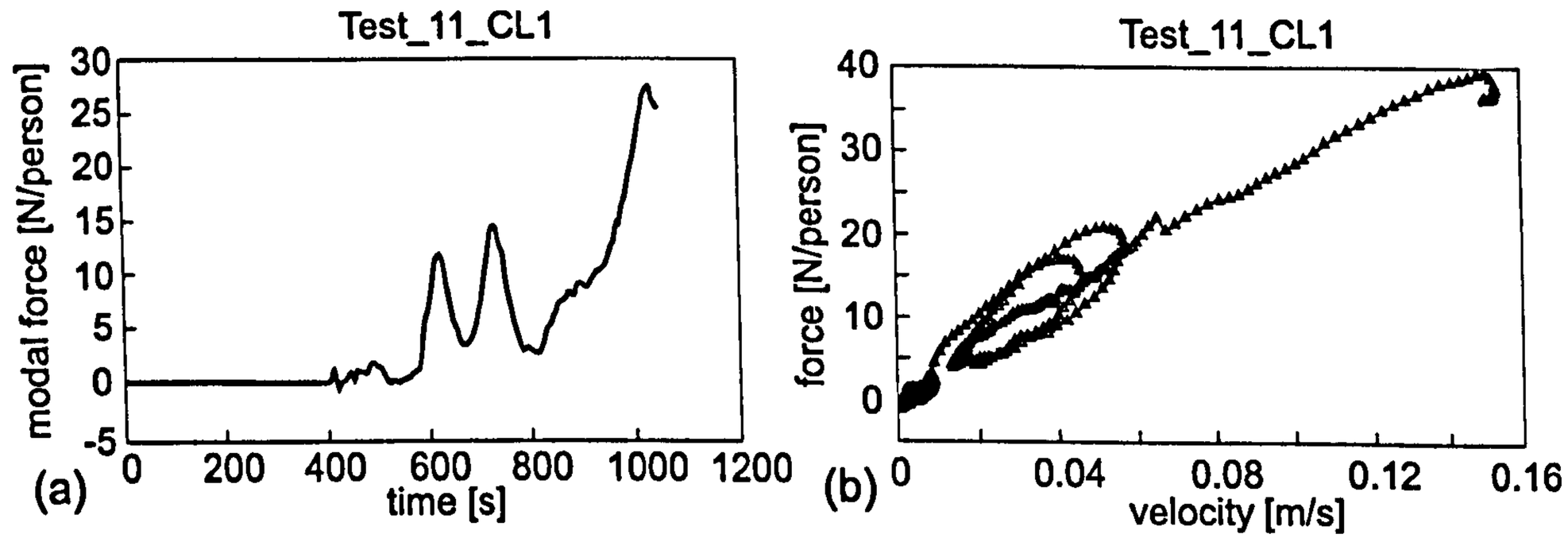

Figure 2.23: (a) Peak amplitude of the lateral modal force per person per vibration cycle. (b) Lateral force per person per vibration cycle versus deck velocity (after Dallard et al., 2001a).

This means that moving pedestrians act as negative dampers (i.e. amplifiers) increasing the response of the structure until walking becomes so difficult, due to body balancing problems, that they have to stop. This clearly indicates the need to model differently the human-induced load before and after the synchronisation occurs. Also, it seems more relevant to investigate bridge behaviour before (and not after) the lock-in occurs, in order to predict and prevent the problem in the future. Bearing in mind several other known examples of excessive lateral vibrations of crowded bridges, Dallard et al. (2001a; 2001b; 2001c) further concluded that the same problem can happen on every bridge with a lateral frequency below 1.3 Hz and with sufficient number of people crossing the bridge. That triggering (critical) number of people N_L was defined as:

$$N_L = \frac{8\pi cfM}{k} \tag{2.10}$$

where c is the modal damping ratio, f is the lateral frequency of the bridge, M is the corresponding modal mass and k [Ns/m] is the lateral walking force coefficient introduced in Equation 2.9. For the case of the Millennium Bridge it was found by back analysis that k=300 Ns/m in the lateral frequency range 0.5-1.0 Hz. However, it would be interesting to find this factor for other bridges with the lateral swaying problem to compare with this value. Also, the shape of the force time history in Figure 2.23a revealed that the lock-in started at about 900 s. However, it seems that the lock-in was unsuccessfully triggered two times between 600 s and 800 s. The factors which prevented these two lock-ins are still not identified and it would be extremely beneficial to know what they are. Also, it should be emphasized that, although the predominant lateral load frequency is about 1 Hz, during the bridge opening day the first lateral mode at about 0.5 Hz was also excited. This can be caused by the reduced frequency of the lateral walking force in a crowd (down to 0.6 Hz) and by some 'meandering' patterns in human walking on moving bridge deck surfaces, as observed by Dallard et al. (2001c).

Research described in three papers by Dallard et al. stressed the need to investigate the dependence between the probability of synchronisation between people and the amount of bridge movement in the lateral direction. In that sense, Willford (2002) reported tests with a single walking person on a platform moving laterally. The results showed that the lateral pedestrian force was increasing when the lateral movement increased. Also, he found that in the case of structural movement at 1 Hz with an amplitude of 5 mm, the probability of people adapting their step to the bridge movement is 40%. These relationships are nonlinear and dependent on frequencies of the bridge movement, even for a single person (Figure 2.24). These observations were made for individuals and their applicability to people walking in a crowd is still unknown.

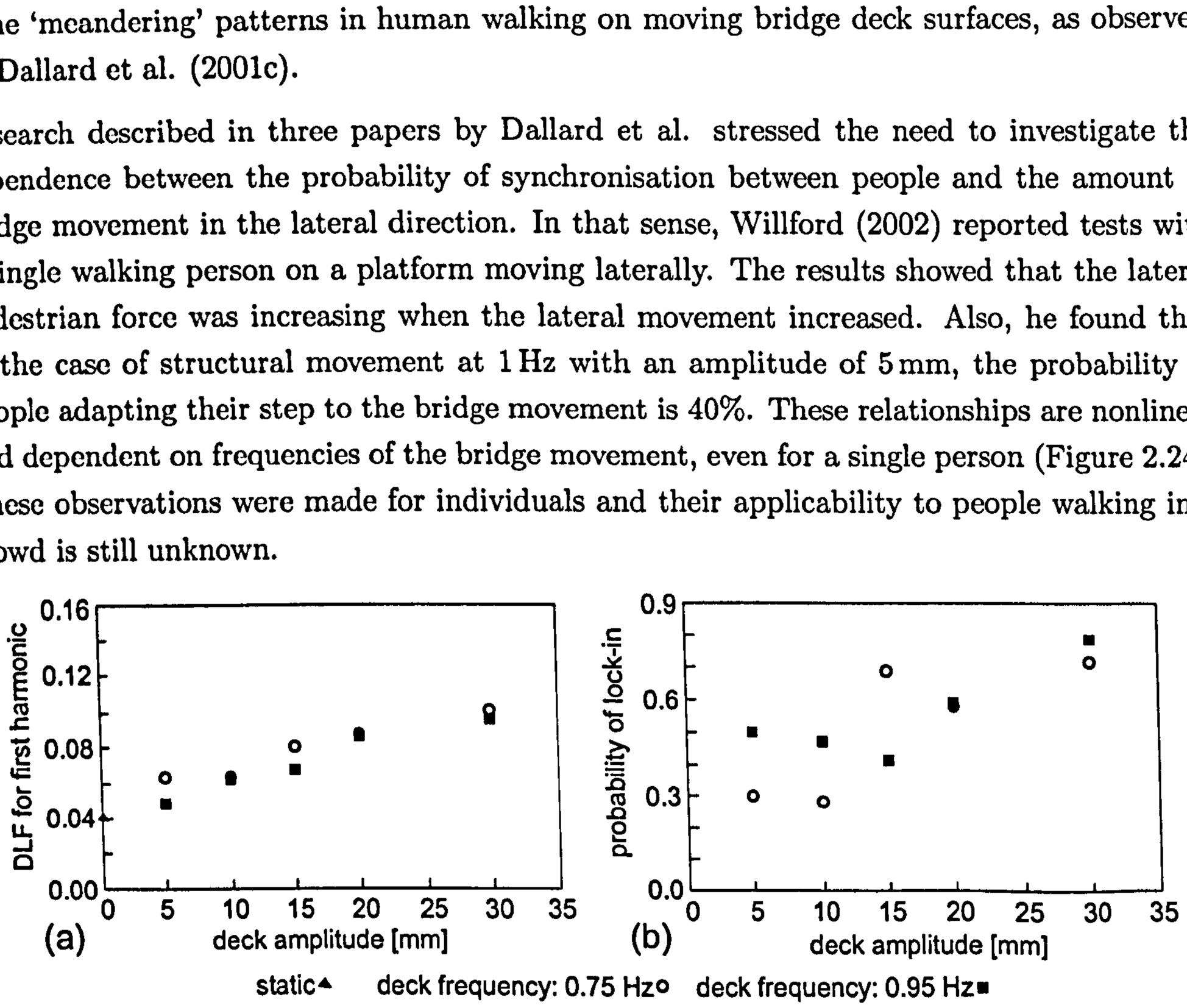

Figure 2.24: (a) DLF and (b) probability of lock-in for a single person as a function of the moving platform amplitude and frequency (after Dallard et al., 2001a).

An interesting study on a lively footbridge (M-bridge) in Japan revealed that a pedestrian, walking within a crowd on a perceptibly moving deck, synchronised their movement with the bridge vibrations (Nakamura, 2003). A phase from 120° to 160° between girder and pedestrian motion was identified. This synchronisation was only spoiled at maximum measured deck

amplitude of 45 mm, when it became much harder to walk. It is interesting that excessive lateral vibrations on this footbridge occurred at two different response frequencies (0.88 Hz and 1.02 Hz) depending on the crowd density. These two frequencies corresponded to two modes as high as the sixth and seventh lateral mode of vibrations. A very low damping ratio of 0.5% and also very low bridge mass of 400 kg/m^2 certainly contributed to developing of such large vibrations. Nakamura (2003) also reported that the bridge mass was lower than the mass on other two well-known lively (in lateral direction) footbridges: Millennium Bridge (about 500 kg/m^2) and T-bridge (800 kg/m^2).

Nowadays, increasing efforts are made to quantify the vibrations due to crowds using the basis of wind engineering theory. In one such attempt, Stoyanoff et al. (2002) suggested a correlation factor $c_R(N)$ in a moderate crowd of N people when the density is below 1 pedestrian/m^2 similar to one from vortex-shedding theory:

$$c_R(N) = e^{-\gamma N}, \tag{2.11}$$

where the factor γ could be obtained from a condition that $c_R(N) = 0.2$ (20%) for the maximum congested footbridge as it was in the work by Fujino et al. (1993). However, Fujino et al.'s methodology could not predict the structural response during the Millennium Bridge tests (Dallard et al., 2001c). On the other hand, Yoneda (2002) stressed that several factors influenced the synchronisation factor: the lateral natural frequency, damping, length between node points in the resonant mode, walking speed and bridge length on which synchronisation occurs. This observation was not experimentally verified on full scale structures but it deserves attention because of its generality.

Interestingly enough, an entirely different theory to the one considered so far in this section which is based mainly on observations made on the Millennium Bridge, was given by Barker (2002). He claimed that the response to crowd movement may increase without any synchronisation between people. Further, Dinmore (2002) suggested treating the human induced force as a wave which propagates through the structure. As a way to control bridge response and avoid synchronisation, he recommended to vary the dynamic stiffness through the structure using different materials which will provide energy loss due to wave reflection and refraction on their contact.

2.5.3.2 Vertical Synchronisation

An attempt to quantify the probability of synchronisation in the vertical direction was made by Grundmann et al. (1993). They defined the probability of synchronisation $P_S(a_g)$ as a function of the acceleration amplitude of the structure a_g (Figure 2.25). They proposed that the response to N people on a structure should be calculated from the following formula:

$$a_g = P_S(a_g) N_r a_{1rz} \tag{2.12}$$

where a_{1rz} is the response to a single pedestrian and $N_r = NK$ is the number of people reduced by the factor $K < 1$ which takes into account that the load changes position along the structure. For a single span $K = 0.6$ was proposed. For a bridge with fundamental frequency of 2 Hz the probability of synchronisation was suggested as 0.225. Therefore, for these parameters the multiplication factor $P_S(a_g)N_r$ for the single pedestrian response a_{1rz} becomes:

$$P_S(a_g)N_r = 0.225 \cdot 0.6 \cdot N = 0.135N. \tag{2.13}$$

This is lower then the value $\sqrt{N}$ given by Matsumoto et al. (1978) for N up to 55 people, despite the fact that Grundmann et al. took into account the synchronisation possibility, and that $\sqrt{N}$ implies N completely uncorrelated people. Grundmann et al. (1993) finally suggested that for groups of up to 10 people, the multiplication factor can be taken as presented in Figure 2.26, with maximum value of 3 for vertical natural frequencies between 1.5 and 2.5 Hz. The same factor was proposed for the lateral direction but corresponding to two times lower natural frequencies. It should be said that synchronisation with bridge movement in the vertical direction is much less likely, although Bachmann & Ammann (1987) reported that it could happen when the vertical amplitude becomes at least 10 mm.

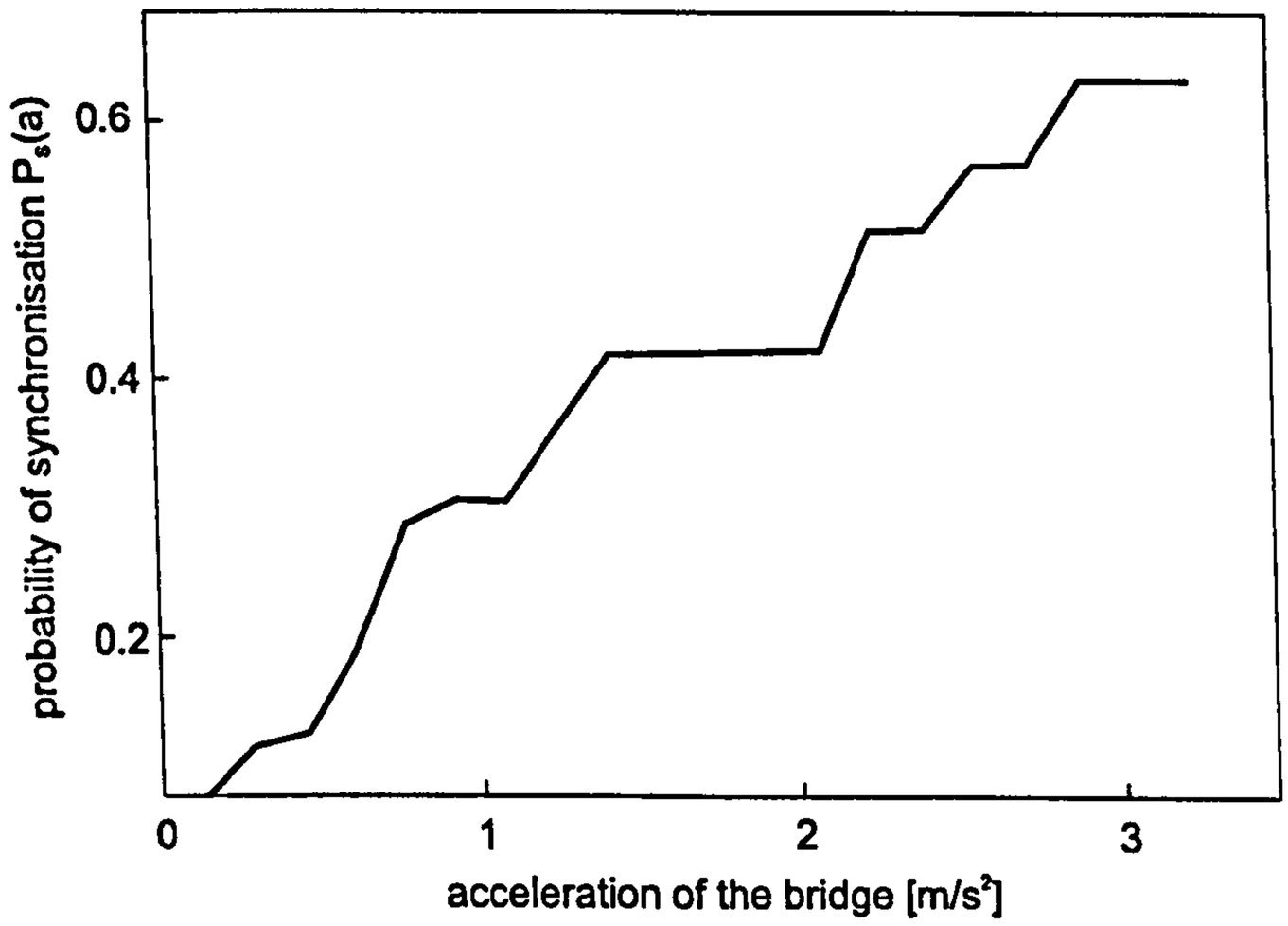

Figure 2.25: Probability of synchronisation as a function of the acceleration of the bridge (after Grundmann et al., 1993).

Dallard et al. (2001a) suggested using random vibration theory to predict the bridge vertical response due to crowd. The mean square acceleration response $E(a^2)$ due to N pedestrians with normally distributed pacing rates was given as:

$$E(a^2) \approx \frac{\pi N}{16c}\frac{\omega_n}{\sigma}p\left(\frac{\omega_n - \mu}{\sigma}\right)\left(\frac{F_{\omega_N}}{M}\right)^2 \tag{2.14}$$

where c, ω_n and M are the modal damping ratio, natural frequency and modal mass, F_{ω_n} is the amplitude of the harmonic human force while p is the probability density function for normally distributed pacing frequencies with mean value μ and standard deviation σ. However, this formula was conservative even in the Millennium Bridge case. Its assumption that people were uniformly distributed across the structure and that the mode shape was a sinusoid could induce errors and should be corrected according the real conditions on the bridge considered (Moutinho et al., 2002). Also, the distribution of step frequencies within a crowd is unknown. Finally, Mouring (1993) and Brownjohn et al. (2004) identified that a quantification of the degree of correlation between people in a crowd is a primarily task for future research. Brownjohn et al. (2004) went further and suggested a mathematical model for calculation of the bridge response under crowd of pedestrians based on theory of a turbulent wind on linear structures (Simiu & Scanlan, 1996). They proposed that the auto spectral density (ASD) of the response in a single mode $S_z(f)$ in a degree of freedom (DOF) specified by the coordinate z should be calculated as:

$$S_z(f) = \Psi_z^2 \left|H(f)\right|^2 S_{P,1}(f) \int_0^L \int_0^L \Psi_{z1}\Psi_{z2}\mathrm{coh}(f, z_1, z_2)\mathrm{d}z_1\mathrm{d}z_2 \tag{2.15}$$

where Ψ_z is the mode shape ordinate in the same DOF, $H(f)$ is the frequency response function (FRF) for acceleration response, $S_{P,1}(f)$ is the ASD of the pedestrian loads per unit length while Ψ_{z_1} and Ψ_{z_2} are mode shape ordinates related to the location of each two pedestrians on the bridge described by coordinates z_1 and z_2. Moreover, $\mathrm{coh}(f, z_1, z_2)$ is the correlation factor, between 0 and 1, which should be further researched, as mentioned earlier. This method gave a good estimate of the response for the footbridge investigated, but needs wider verification.

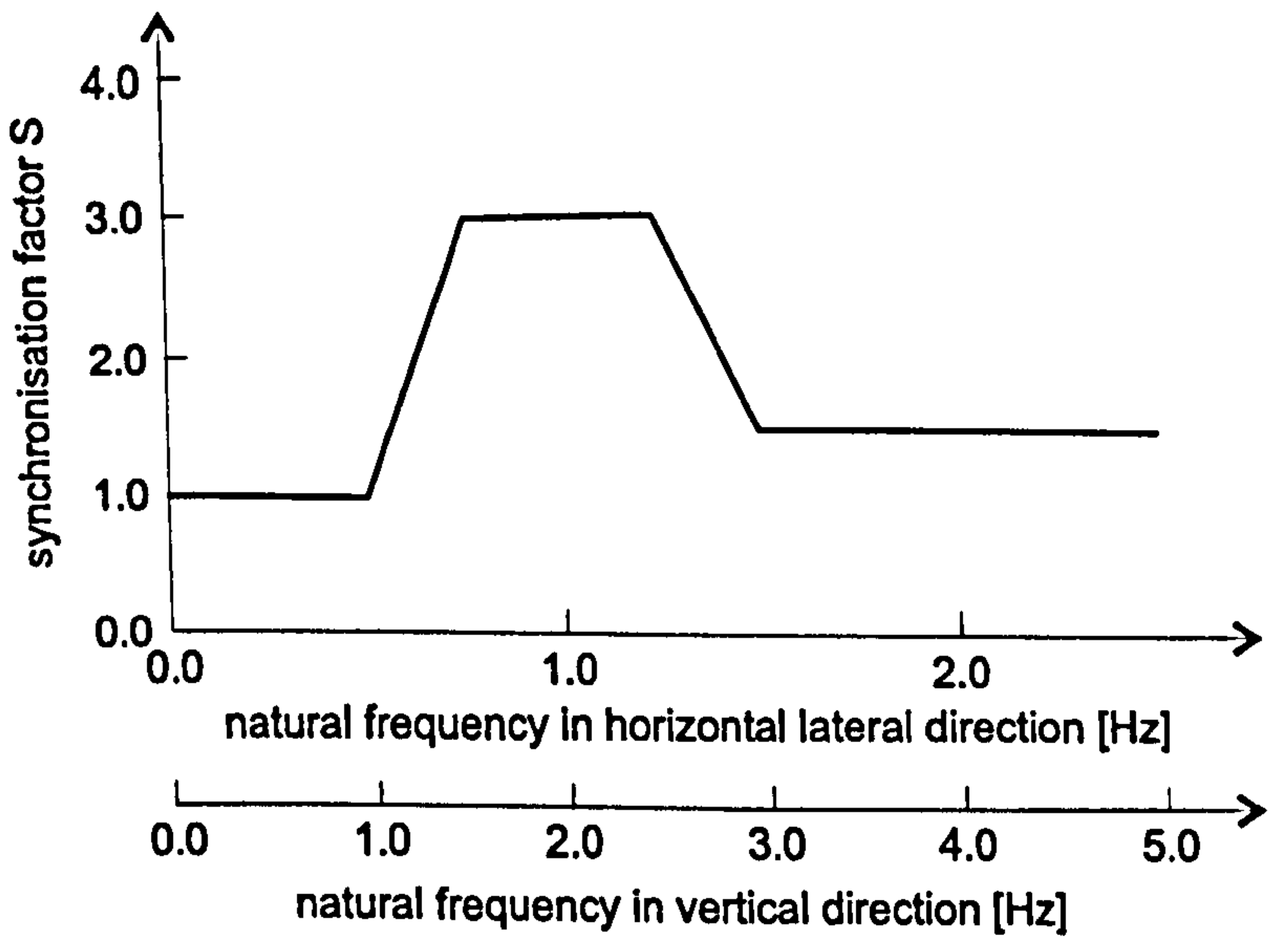

Figure 2.26: Multiplication factor for groups of up to 10 pedestrians (after Grundmann et al., 1993).

An interesting suggestion for the assessment of liveliness of footbridges in the vertical direction under large crowd load, also based on the wind engineering theory (Simiu & Scanlan, 1996), was given by McRobie & Morgenthal (2002) and McRobie et al. (2003). It was proposed that the acceptability of vertical vibrations can be assessed by comparing the pedestrian Scruton number $vPSN$ which is achieved with the one required for a particular footbridge. This number is defined as:

$$vPSN = k_1 k_2 m \tag{2.16}$$

where factors $k_1 = \frac{\zeta}{0.005}$ and $k_2 = \frac{0.6}{n}$ take into account the damping ratio of the empty footbridge ζ (relative to the typical damping ratio of 0.5%) and the possibility that crowd density n could be different from a typical value of 0.6 persons/m^2, respectively. In Equation 2.16 m represents the mass per unit deck area for an equivalent simply supported beam having constant cross section. To have structure which will meet vibration serviceability requirements, a larger pedestrian Scruton number (i.e. larger damping and mass and lower pedestrian densities) is preferred. Data about acceptable Scruton numbers as a function of footbridge frequency should be provided by collecting data from existing footbridges known to be lively in the vertical direction. However, this task is hampered by the fact that not many footbridges have experienced large vertical vibrations under crowd load.

In conclusion, it can be said that although the two considered types of synchronisation (among people, and between the people and the structure) are different in their nature, they usually happen simultaneously and lead to the same result - an increase in the response of the structure. In order to understand better the interaction between the moving crowd and the structure it is necessary to identify (Dallard et al., 2001c):

1. the relationships between the crowd density, walking speed, walking frequency and probability of synchronisation, and
2. the probability of lock-in and effective force per person in a crowd as a function of the amplitude and frequency of the bridge motion.

2.6 Design Procedures and Guidelines

Having a simple and accurate model of the human-induced force, knowing the footbridge dynamic properties and having defined the tolerance level of human perception of vibrations are all required for checking the vibration serviceability of a footbridge. However, this is easier said than done. Based on previous sections, it is clear that researchers and practitioners have been working for many years on the formulation of footbridge vibration serviceability design procedures. As a result, some design guidelines have been adopted (BSI, 1978; OHBDC, 1983). In general, it is important that these design procedures satisfy two somewhat contradictory requirements: to be simple and to be as accurate as possible. In this part of the

review, key design procedures reported in scientific literature and design guidelines which are parts of formal national and international codes of practice are outlined.

2.6.1 Design Procedures Reported in Literature

The aim of most of the design procedures, defined either in the time or the frequency domain, is to determine the peak or the root-mean-square (RMS) response of a footbridge in order to assess its vibration serviceability.

2.6.1.1 Time-Domain Design Procedures

Chronologically the first and largest group of design procedures is based on an assumption that human-induced forces are perfectly periodic and can be therefore decomposed into harmonics by means of Fourier decomposition as given in Equation 2.1. Then, only a single force harmonic which can, theoretically, excite footbridge resonance related to the fundamental mode shape, should be considered. This means that the structure can be regarded as a SDOF system in modal space as explained in Section 2.3. Usually, the first three or four excitation harmonics are considered as potentially resonant. All models presented in this sub-section are applicable to vertical forces only, if not stated otherwise. In general, the biggest problem in the modelling process is to simulate a pedestrian moving across a footbridge and the corresponding time limitation of such an excitation.

Blanchard et al. (1977) proposed that serviceability should be checked in footbridges with fundamental natural frequencies f up to 5 Hz. As a serviceability criterion, they proposed that the acceleration response [m/s^2] due to one pedestrian should not exceed a limit of $0.5\sqrt{f}$, where f is expressed in Hz. Blanchard et al. proposed a walking force model which was a resonant sinusoid moving across the bridge with velocity v of $0.9f$ (Figure 2.27a). Modal force per modal mass from the righthand side of Equation 2.4 for the fundamental vibration mode was given as:

$$\frac{P_1(t)}{M_1} = \frac{P}{M_1}\phi(0.9ft)\sin(2\pi ft) \tag{2.17}$$

where P and M_1 are the force amplitude of 180 N (which corresponds to the DLF of 0.257 given in Section 2.2.3.1) and the generalised mass for the fundamental mode, respectively. $\phi(0.9ft)$ is the location-dependent ordinate of the first mode shape which is dependent on the position $x = 0.9ft$ of the pedestrian at time t after the beginning of walking. However, for simple bridge configurations (one, two or three spans), the procedure was simplified to a direct calculation of maximum acceleration response a using the formula:

$$a = \omega_1^2 y_s K\psi \tag{2.18}$$

where $\omega_1 = 2\pi f$ is the fundamental circular frequency of the bridge, y_s is the static deflection at the midspan due to the weight of one pedestrian, K is a configuration factor which depends on the number of spans and ψ is a dynamic response factor which takes into account the span length and footbridge damping. The last two parameters were obtained by numerical simulations on footbridges having up to three spans due to the general pedestrian load presented in Figure 2.27b. This work was probably the first attempt to define a design procedure for checking human-induced vibrations of footbridges and as such it is very valuable. However, the DLF equal to 0.257 used in Equation 2.17 is not representative of the whole frequency range of up to 5 Hz. In the 1970s, when Blanchard et al. (1977) published this groundbreaking paper, the concept of higher harmonics of human-induced dynamic loading was still not developed, so it is not surprising that the main criticism of their approach stems from this fact. Namely, for bridge frequencies in the range 1.6-2.4 Hz the influence of the first harmonic depends strongly on the walking frequency (Figure 2.10) and should not be represented by one value which is constant for all frequencies. At higher frequencies the response could be overestimated because the first harmonic is not relevant there. Also, this design procedure is only concentrated on the fundamental mode of vibration. However, if this mode had low natural frequency (up to 1.4 Hz), it hardly can be relevant for bridge response under human-induced force. In such a situation, a mode having frequency in the normal walking frequency range becomes more important.

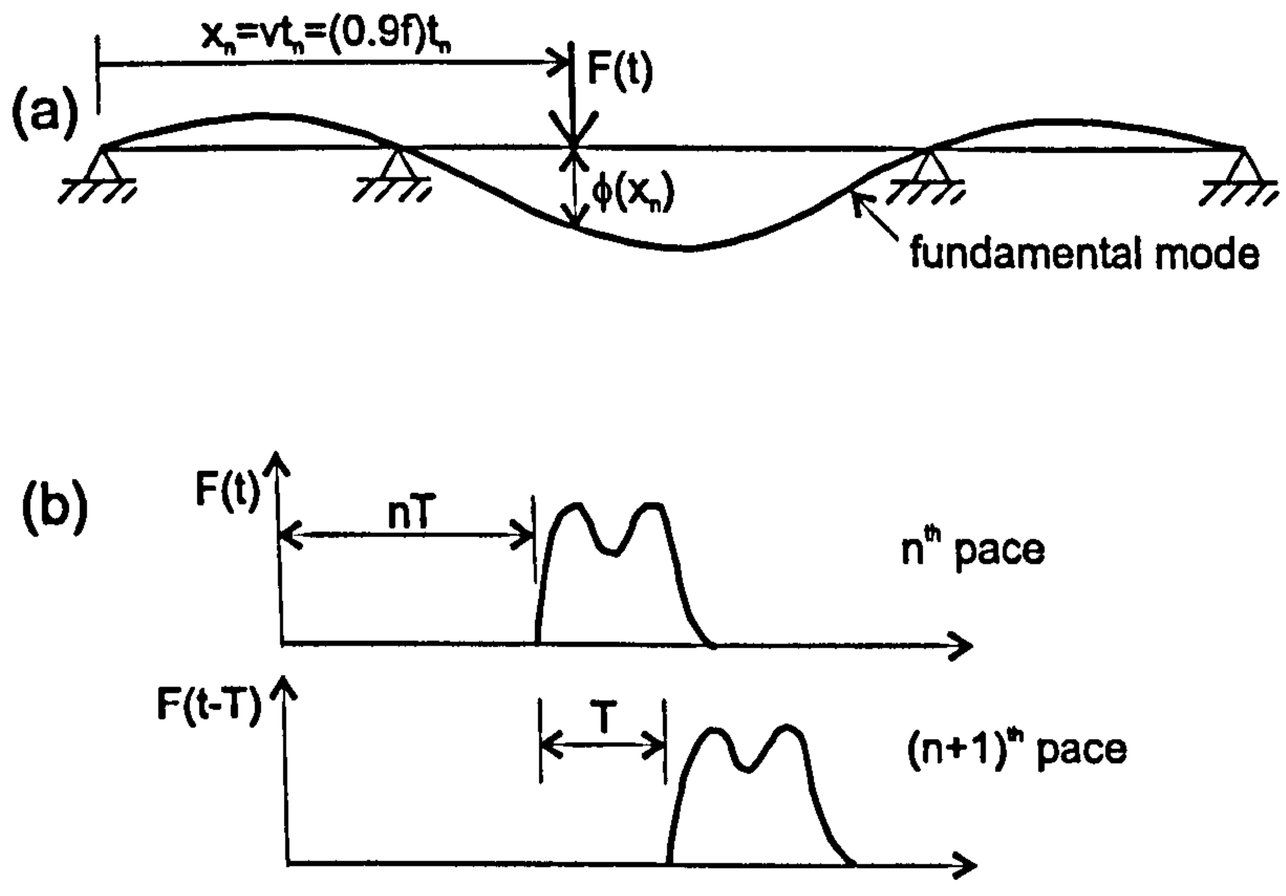

Figure 2.27: (a) Moving force model and (b) forcing function for a pedestrian load (after Blanchard et al., 1977).

Implementing the half-sine force model, Wheeler (1980; 1982) simulated response due to a single pedestrian walking at different frequencies on 21 footbridges. He used a computer program written for that purpose. He compared maximum displacements at each frequency with those obtained experimentally on each bridge. The differences in the results are explained as a consequence of many uncertainties encountered during the dynamic modelling process. Some of them, quoted in Wheeler's article from 1980, were nonlinear cable behaviour in cable-

stayed bridges, column supports modelled as pin joints, difficulties in predicting structural damping, neglecting of the mass of non-structural elements such as handrails, surfacing and so on.

A considerable improvement of Blanchard et al.'s procedure was achieved with a model which took into account that the walking (or running) force had DLFs dependent on step frequency and harmonic considered (Figure 2.10), the force was moving and its duration was time limited by the length of the bridge (Rainer et al., 1988). The representative SDOF model is presented in Figure 2.28, where m, c and k refer to the modal mass, damping and stiffness respectively. A dynamic amplification factor Φ was introduced to account for the force moving and its limited duration, which was dependent on the structural damping and number of force cycles needed to cross the bridge. The modal peak acceleration response was then given as:

$$a = \frac{\alpha P}{m}\Phi \tag{2.19}$$

where m is the modal mass, P is the pedestrian weight and α is the appropriate DLF according to Figure 2.10. This procedure demonstrated good agreement with an experimental study. Unfortunately, this design proposal was related only to single span footbridges. In the same article, it was proposed that the response to a jumping force could be calculated using an appropriate DLF for jumping (Figure 2.10) and the well-known formula for steady state response knowing that this force does not move along the bridge. Therefore, theoretically it could produce steady-state response although the practical duration of such an excitation is in question.

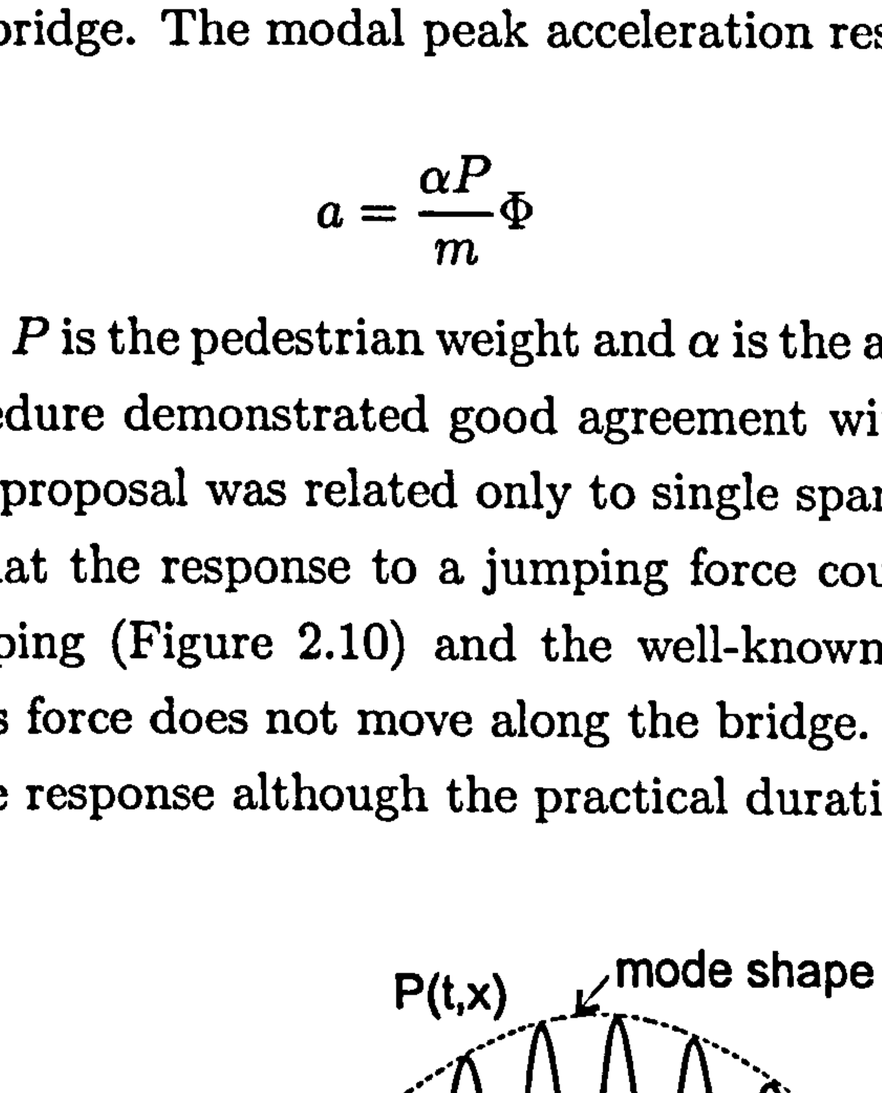

Figure 2.28: Pedestrian modal force model based on the design procedure by Rainer et al. (1988).

After this proposal, several attempts to simplify or extend it were made. For instance, Allen and Murray (1993) simplified the procedure by replacing the walking force with a stationary

sinusoid acting at the centre of the span which amplitude and frequency depended on the relevant harmonic. In such conditions, the steady-state response was obtained and then a unique reduction factor R was introduced to take into account the exact nature of the force, that is the fact that it is moving and is of limited duration. The non-dimensional ratio between the harmonic peak response and gravity acceleration was then given by:

$$\frac{a}{g} = \frac{R\alpha_i P}{\beta W}\cos(2\pi i f t) \tag{2.20}$$

where α_i is a DLF, P is the pedestrian weight, β is the damping ratio, W is the bridge total weight while R is a reduction factor which is adopted as 0.7 for footbridges. However, this constant factor could not involve all possible situations produced by different span lengths and therefore different time needed to cross the bridge. Also, constant values for DLFs for each harmonic were adopted here as the maximum values given in Figure 2.10 ($\alpha_1 = 0.5$, $\alpha_2 = 0.2$, $\alpha_3 = 0.1$ and $\alpha_4 = 0.05$) which can give overconservative results. After some manipulations and taking into account the acceleration limits based on ISO (1992), Equation 2.20 was converted into a condition for minimum natural frequency of the bridge:

$$f_0 \geq 2.86 \ln \frac{K}{\beta W} \tag{2.21}$$

where K is a constant equal to 8 kN. The recommended damping ratio was $\beta = 0.01$.

Further, Kerr (1998) converted Rainer et al.'s (1988) procedure into an analytical form to avoid using the graphs for DLFs and the factor Φ. Also, he used his own expression for DLF as a function of step frequency (Figure 2.11) instead of the one proposed by Rainer et al.

Finally, Pimentel & Fernandes (2002) extended the procedure proposed by Rainer et al. to footbridges with two spans introducing a factor k_a. The peak modal acceleration was given in the form:

$$a_{max} = \omega_0^2 y_s \alpha_i \Omega_d k_a \tag{2.22}$$

where ω_0 is the fundamental circular bridge frequency, y_s is the static deflection due to the weight of a pedestrian, α_i is the DLF of the resonant i^{th} harmonic, Ω_d is the dynamic amplification factor and k_a is a numerically obtained factor which takes into account bridges with two spans in addition to single span structures.

Grundman et al. (1993) used full theoretical expression (with transient and steady-state parts and assuming zero initial conditions) to calculate the resonant response due to a single pedestrian harmonic force. Acceleration response was given as:

$$a_{1rz} = 0.6\frac{0.4G}{M}\frac{\pi}{\delta}(1 - e^{-n\delta}) \tag{2.23}$$

where the factor 0.4 is adopted as DLF for the first harmonic, G is the weight of a pedestrian, M is the modal mass of the structure, δ is the logarithmic decrement and n is the number of steps needed to cross the bridge. Introducing n means that a real duration of the moving force (i.e. the possibility that steady-state response is not achieved) has been taken into account. The factor 0.6 was included to involve moving of the pedestrian force i.e. the variation of the mode shape amplitude along the walking path. However, it is difficult to devise a formula representative of all footbridge span lengths and all simplifications of this kind will necessarily increase the errors in the response estimates. Grundmann et al. also proposed a similar approach for response calculation in the horizontal lateral direction but with DLF equals to one fourth of the DLF for the vertical harmonic.

Probably the biggest shortcoming of all these procedures is their limitation to girder footbridges with only a few spans, usually one. Nowadays, when new footbridges have unusual structural form, it is necessary to formulate a more general design approach based on first principles.

Young (2001) made an attempt to develop a design procedure independent of footbridge type. His procedure was based on the full theoretical expression for a steady-state acceleration response a_n in a single vibration mode n (with the modal mass M, damping ratio ζ_n and natural frequency f_n) to a harmonic force with amplitude P and frequency f:

$$a_n = \mu_i \mu_j \left(\frac{f}{f_n}\right)^2 \frac{P}{M} DMF, \tag{2.24}$$

where μ_i and μ_j are mode shape ordinates at the walking point and response point, respectively, while DMF is the dynamic magnification factor:

$$DMF = \frac{1}{1 - \left(\frac{f}{f_n}\right)^2 + i\left(2\zeta_n \frac{f}{f_n}\right)}. \tag{2.25}$$

At resonance, only the imaginary part of DMF remains. Young proposed a reduction factor r for this part to account for a limited duration of the pedestrian force and its moving across the structure:

$$r = 1 - e^{-2\pi\zeta_n N} \tag{2.26}$$

where N depends on the number of cycles needed for the relevant n^{th} harmonic to cross the bridge:

$$N \approx 0.55 n \frac{L}{l}. \tag{2.27}$$

L and l represent the span and step lengths, respectively.

In addition to controlling the vibration serviceability under single person excitation, the response of the footbridge under a stream of pedestrians, groups and a crowd of people has been also considered by some authors, as previously described in Section 2.5.3.

2.6.1.2 Frequency Domain Design Procedures

Although design procedures presented in this section are not necessarily related to footbridges, they can be used as the basis for further investigations of these structures. The idea to assess the vibration serviceability of structures by using the theory of stationary random processes appeared in the early eighties (Ohlsson, 1982). It is known that for such a process, the auto spectral density (ASD) of the response $S_y(\omega)$ can be calculated by the following relation (Newland, 1993):

$$S_y(\omega) = \mid H(\omega) \mid^2 S_x(\omega) \tag{2.28}$$

where $H(\omega)$ is the frequency response function of the structure and $S_x(\omega)$ is the ASD of the force. The mean square value of the response $E[y^2]$ can then be calculated as an area under the spectral density curve of the response (Newland, 1993):

$$E[y^2] = \int_{-\infty}^{+\infty} S_y(\omega) d\omega \tag{2.29}$$

and, further, the value of the root-mean-square (RMS) or peak acceleration, on which human perception criteria are often based, can be obtained. To obtain peak accelerations crest factors are usually used.

As mentioned in Section 2.2.3.2, Eriksson (1994) paid great attention to force modelling in the frequency range up to 6-7 Hz, which was the typical range for fundamental frequency of the low-frequency floors he investigated. He assumed that a floor structure responded predominantly in one ("weakest") mode and therefore could be modelled in the modal space as a SDOF system. Based on measurements of acceleration responses due to a single person (walking, running and jumping) and groups of 7 and 11 walking people and using the relationship between spectral densities of the force and the response of the kind given in Equation 2.28, Eriksson proposed a force mean square design model with constant mean square in the range of the first harmonic frequencies and frequency dependent for higher harmonics (Table 2.4) where F_{rms} presents the root-mean-square function of the walking force while $K_{np}(n_p)$ is a multiplication factor for a single person RMS force as a function of the number of people in the group n_p. He therefore found that group of people moving in step can be considered as almost perfectly correlated in considering its first harmonic. For that case it was proposed to multiply single force mean square by the factor of $n_p^{0.9}$ while for higher harmonics that factor was $n_p^{0.5}$ which is typical for uncorrelated people, where n_p is the number of people.

Table 2.4: Design force model after Eriksson (1994).

Activity	Frequency interval [Hz]	F_{rms} [N]	$K_{np}(n_p)$
Walking	0 - 2.5	220	$n_p^{0.9}$ [a]
	2.5 - 10.0	$180(f_0/f)$	$n_p^{0.5}$
Running	0 - 3.0	690	$n_p^{0.9}$ [a,b]
	3.0 - 10.0	$4300(f_0/f)^2$	$n_p^{0.5}$ [b]
Jumping	0 - 3.5	1000	$n_p^{0.9}$
	3.5 - 10.0	$13000(f_0/f)^2$	$n_p^{0.5}$ [b]

$f_0 = 1.0\,\text{Hz}$

[a] Proposed factor is applicable for well correlated group. In case of normal traffic, the factor $n_p^{0.5}$ should be applied.

[b] Factors given inter-alia in absence of sufficient data.

Mouring (1993) and Mouring & Ellingwood (1994) modelled the auto spectral density of a modal force due to crowd dynamic loading as a product of number of people and the auto spectral density of an individual force. This is equivalent to the condition that time-domain acceleration response due to a group of n uncorrelated people is $\sqrt{n}$ times higher than the acceleration due to a single person, as obtained by Matsumoto et al. (1978).

Hansen & Sørensen (2002) defined jumping crowd load in terms of its harmonics, each of which was based on the appropriate harmonic due to a single person. Crowd effect and lack of synchronisation between people were taken into account by a crowd reduction factor. This factor was obtained for each harmonic separately as the ratio between the magnitude of deflection spectrum for a group to the magnitude of a single person spectrum. It seems that the calibration of the crowd reduction factor was based on measurements of the jumping response only at 2 Hz.

Brownjohn et al. (2004) paid attention to imperfections in individual human walking patterns which spread excitation energy into adjacent spectral lines in comparison with the perfectly periodic force where the whole energy is concentrated at a single harmonic frequency. The spread of energy effect was shown to be more emphasized for higher harmonics. Based on direct measurements of the vertical force time histories for three test subjects walking on a treadmill, they proposed a model which described a forcing function for the first six harmonics. Namely, the ratio between Fourier amplitudes for real and periodic forces G'_n was given as a function of frequency f:

$$G'_n\left(\frac{f}{\bar{f}}\right) = A + Be^{\frac{-\left|\frac{f}{n\bar{f}}-1\right|^C}{D}} \tag{2.30}$$

where $\bar{f}$ is the fundamental frequency of the appropriate perfect periodic force, n is the order number of harmonic while A, B, C and D are constants dependent on the harmonic considered. Knowing the ASD of the force harmonic $S_{F,n}(f)$:

$$S_{F,n}(f) = \left[WG_n(\bar{f}_i)\right]^2 S_{G'_n}\left(\frac{f}{\bar{f}}\right) \tag{2.31}$$

where W, G_n and $S_{G'_n}\left(\frac{f}{\bar{f}}\right)$ are the pedestrian weight, the DLF for the appropriate harmonic of the perfectly periodic walking force and the ASD of the previously defined function G'_n, respectively, the ASD of the response due to a single pedestrian can be obtained by applying Equation 2.28. On the other hand, for groups of people walking, it is suggested to evaluate the ASD of the response in terms of turbulent wind theory, as explained in Section 2.5.3.2. In principle, Brownjohn et al.'s model can take into account all relevant modes of the structure, including closely spaced modes.

2.6.1.3 Other Suggestions

Attempts to use the genetic algorithm optimisation procedure in modelling the serviceability problems are given by Obata et al. (1999) and Miyamori et al. (2001). Optimisation was carried out after the force and "human model" parameters, respectively. These parameters were used in calculation of the response with the aim to match it with the experimental response due to a pedestrian. However, it seems that optimisation parameters were different for different bridges which makes it difficult to generalise the model.

2.6.2 Design Guidelines

An early formal attempt to cope with the problem of vibrations perceptible by pedestrians on highway bridges was codified by the American Association of State Highway Officials (CDLB, 1958). For many years they limited the deflection due to live load to span-length ratio and the depth to span length ratio. However, Leonard (1966) reported that day-to-day design practice showed that such an approach had not led to bridges with acceptable level of vibrations. A different approach, related to composite highway bridges, was suggested by Mason & Duncan (1962). They proposed to limit the minimum bridge natural frequency to 4 Hz and the maximum level of vertical acceleration to $0.15\,\mathrm{m/s^2}$ (1.5%g).

Nowadays, there are two concepts which are present in design guidelines for footbridge vibration serviceability. The first requires a calculation of the actual dynamic response of the bridge and checking if it is within the acceptable limits for the bridge users. The second approach is based on the request to avoid footbridge natural frequencies which are in ranges coinciding with frequencies typical for human-induced dynamic excitation.

A key example of the first approach is BS 5400: Part 2 (BSI, 1978). Historically, this is the first design code which dealt explicitly with the footbridge vibration serviceability issue. In its Appendix C a procedure for checking vertical vibrations due to a single pedestrian was defined for footbridges having the natural frequency of the fundamental vertical mode of vibration of up to 5 Hz. This was based on the previously described work by Blanchard et al. (1977). Many

years later, based on experience with lateral vibrations of the London Millennium Bridge, the UK Highway Agency started requiring checking the vibration serviceability also in the lateral direction in their Design Manual for Roads and Bridges (HA, 2001). For all footbridges with fundamental lateral frequencies lower than 1.5 Hz a detailed dynamic analysis is now required. However, the procedure for that is not given. Also, no improvement of the design procedure for vertical forces has been made in this provision. The vibration checking procedure is still based on Blanchard et al.'s (1977) work despite the fact that many shortcomings of that work have been identified in the last 25 years; some of them were explained in Section 2.6.1 of this chapter. Also, although it is understandable that the natural frequency of a footbridge with up to three spans is estimated by a simplified calculation in 1977 when Blanchard et al. published their work, it is not justifiable nowadays. Modern trends in current footbridge design practice rely on finite element modelling. This and the fact that new footbridges usually have more complicated and unusual structural forms should be taken into account by proposing a methodology which is based on first principles and does not necessarily rely on simple formulae, which are very much discredited.

The Ontario Highway Bridge Design Code (OHBDC, 1983) requires a calculation of the dynamic response of a bridge due to a footfall force simulated, similar to BS 5400, by a moving sinusoidal force with amplitude 180 N and frequency equal to the fundamental frequency or 4 Hz, whichever is lower. Alternatively, if this full dynamic analysis is not done, then the simplified procedure based on Blanchard et al.'s (1977) paper should be conducted. The resulting peak acceleration response should be less than an acceleration limit defined graphically. This limit acceleration is lower than in BS 5400 (BSI, 1978; HA, 2001) given in Equation 2.6. Therefore, this code, like BS 5400, is based on a consideration of a single pedestrian force model. To avoid the problem of coupling between horizontal and vertical modes under wind loading, the Code also requires that lateral and longitudinal frequencies of the superstructures should not be less than the smaller of 4 Hz and $1.5f$ where f is the fundamental natural frequency for vertical modes. For a footbridge with the natural vertical frequency of, say, 2 Hz this means that the lateral frequency should not be below 3 Hz. In principle, it would enable avoiding the first 2-3 harmonics of the lateral pedestrian force. However, having in mind Figure 2.29, this criterion can be prohibitively restrictive for footbridges with long spans. The same provisions for footbridges are given in Canadian Highway Bridge Design Code (CSA, 2000).

A lot of research has been conducted to check applicability of the previous two guidelines. For example, Grundamnn et al. (1993) pointed to some problems with the applicability of BS 5400 to footbridges with natural frequencies around 2 Hz which are exposed to groups of pedestrians. Also, some work criticised the DLF given in the BS and OHBDC codes which is not representative of forces in the normal walking frequency range (Pimentel & Waldron, 1996; 1997; Pimentel, 1997; Pimentel et al., 2001).

Eurocode 5 (ENV, 1997) contains some interesting information relevant to design of timber bridges. It requires the calculation of the acceleration response of a bridge due to small groups

and streams of pedestrians in both the vertical and lateral directions, with the proposed frequency independent acceleration limits of $0.7\,\mathrm{m/s^2}$ and $0.2\,\mathrm{m/s^2}$ in these two directions, respectively. These limits should be checked for bridges with natural frequencies lower than 5 Hz for the vertical modes and below 2.5 Hz for the horizontal modes.

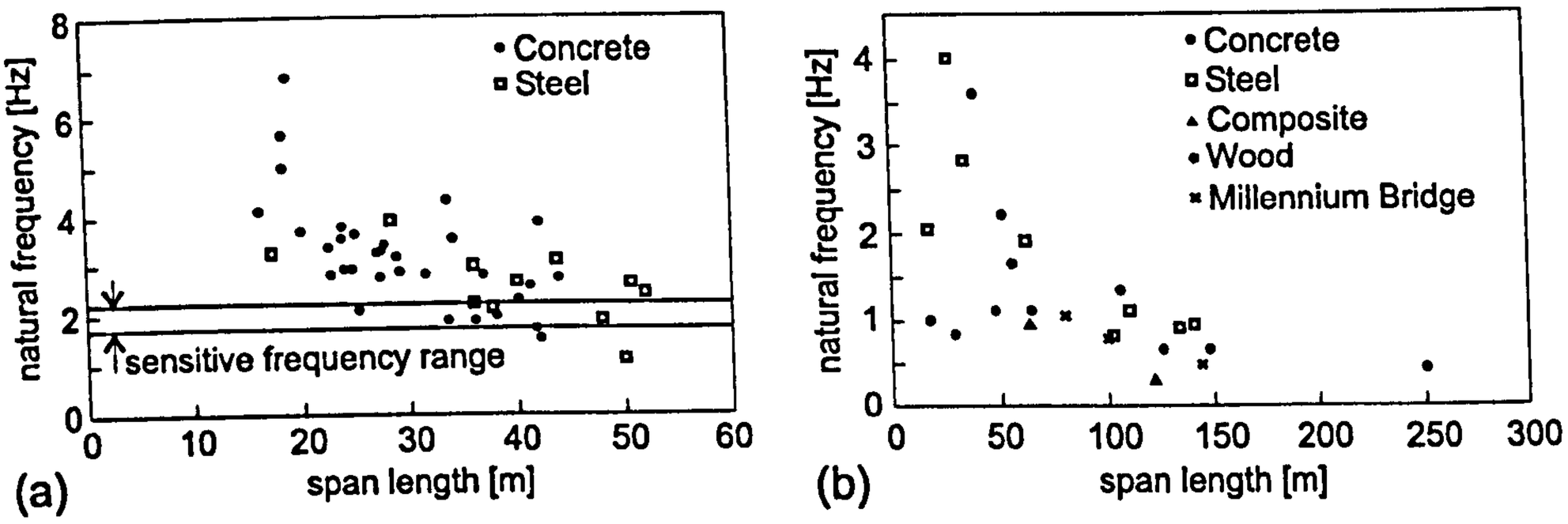

Figure 2.29: Dependence of the fundamental natural frequency on span of the bridge for (a) vertical modes (after Tilly et al., 1984) and (b) lateral modes (after Dallard et al., 2001c).

The procedure for the calculation of the vertical acceleration response for bridges with one, two or three spans is based on obtaining $a_{vert,a}$:

$$a_{vert,a} = 165 k_a \frac{1 - e^{-2\pi n\zeta}}{M\zeta}, \tag{2.32}$$

which can be regarded as a response in a single mode and due to a single pedestrian excitation. Here, k_a is a configuration factor based on Blanchard et al. (1977), while n, ζ and M are the number of cycles necessary to cross the bridge with step length of 0.9 m, damping ratio and the total mass of the bridge, respectively. This formula originates from a full theoretical expression for resonant response due to a harmonic force, where the force amplitude is 165 N. This amplitude includes the DLF as well as the fact that the force moves across the bridge (Hamm, 2002). For the case of a footbridge which has a more general structural configuration, the acceleration response should be calculated for the force $F_{vert}(t)$ which is moving across the bridge with velocity of $0.9 f_{vert}$:

$$F_{vert}(t) = 0.28 \sin(2\pi f_{vert} t) \ \ [\mathrm{kN}], \tag{2.33}$$

where f_{vert} [Hz] is the fundamental natural frequency in the vertical direction. This force amplitude of 0.28 kN is higher than in BS 5400 (BSI, 1978) and the Ontario design code (OHBDC, 1983), and corresponds to a DLF of 0.4 for an average pedestrian weighing 700 N. More detailed background of this formula and some possible modifications can be found in Hamm (2002).

The response due to small group of pedestrians can be obtained by multiplying the calculated $a_{vert,1}$ by a factor $k_{vert,f}$ which is dependent on the footbridge fundamental natural

frequency. Its maximum value of 3 is predicted for the range of common step frequencies 1.5-2.5 Hz, as given by Grundmann et al. (1993) for groups of up to 10 people (Figure 2.26). However, if the bridge has a deck area greater than 37 m^2, then this group response should be increased further by a factor which is dependent on the area, probably to take into account the possibility of synchronisation of a crowd of pedestrians in the vertical direction. The same procedure should be followed when calculating the lateral acceleration response by replacing the quantities related to the vertical direction with the lateral direction ones. There are also differences in the force amplitudes in Equations 2.32 and 2.33 which are 40 N and 0.07 kN instead of 165 N and 0.28 kN, respectively and in the expression for the pedestrian velocity which becomes $1.8 f_{hor}$ [m/s] where f_{hor} [Hz] is the fundamental natural frequency in the lateral direction. The factor $k_{hor,f}$ has, as $k_{vert,f}$, the maximum value of 3, but in the frequency range typical for lateral force induced by pedestrians: 0.75-1.25 Hz. However, deriving this lateral response based on the procedure for the vertical one and without any experimental data could be problematic and erroneous as noted by Dallard et al. (2001c) and Briseghella et al. (2002). Therefore, as in previous guidelines, this proposal is also based on assumptions of the resonance condition and a single DLF value over a range of walking frequencies. However, the proposal considers a group of pedestrians which is a rather new and advanced approach in design codes.

There are few data about the applicability of this guideline. On some bridges it has successfully predicted liveliness of structures, although more detailed explanation as to the level of agreement between the calculated and measured response was not given (Pedrazzi & Beltrami, 2002). On the other hand, an attempt to apply this procedure to the Millennium Bridge for the case of high density of people produced significantly lower response in the lateral direction than the measured one (Dallard et al., 2001c).

The Hong Kong Structures Design Manual for Highways and Railways (HD, 2002) requires controlling the acceleration response due to a pedestrian in accordance with BS 5400. Also, it limits the lateral acceleration to 0.15 m/s^2. Moreover, it requires additionally a check of the acceleration response due to a stream of pedestrians. The assumption is that the stream is a continuous load moving with velocity 3 m/s over a simple beam. However, sufficient detail as to how to perform the load simulation was not given in the Hong Kong manual.

Swiss standard SIA 160 (1989) belongs to the second group of guidelines which utilises the frequency checking and tuning approach. It requires avoiding footbridge natural frequencies in the range of the first (1.6-2.4 Hz) and the second walking harmonics (3.5-4.5 Hz) with the addition of frequencies 2.4-3.5 Hz if joggers/runners can appear on the structure. If these requirements are not fulfilled then the vibration response of the structure should be checked. Identical provisions as for the frequency ranges which should be avoided are given in the Design Code issued by Comité Euro-International du Béton (CEB, 1993).

The American Guide Specification (AASHTO, 1997) also proposed to avoid fundamental footbridge frequencies in the vertical direction, but below 3 Hz. However, in the case of low stiffness, damping and mass, and when running and jumping on the footbridge are possible, all

frequencies below 5 Hz should be avoided to neutralise the influence of the second harmonic. However, it is not stated what the lower limits for these low dynamic properties are. If the frequency conditions are not satisfied, then the minimum natural frequency given by Allen & Murray (1993) in Equation 2.21 should be a target for the structure to satisfy serviceability requirements. As a possible measure to improve poor dynamic performance of bridges, installation of vibration absorbers and dampers is suggested. Finally, Yoshida et al. (2002) reported that Japanese design code for footbridges requires avoiding frequencies between 1.5-2.3 Hz for the vertical modes.

Regarding the second group of guidelines, Pimentel et al. (2001) found that the frequency tuning approach can be restrictive because there are footbridges which are serviceable although they have frequencies in the range recommended for avoidance.

A list of existing codes and their division between those which specify acceleration limits and those with frequency limits was given by Schlaich (2002). Unfortunately, the author omitted their exact references which leaves uncertainties as to the exact code titles and editions.

As has been shown in this section, some codes recommend avoiding the resonant frequency range typical for the first or second force harmonic, the others give a more or less complex design procedure to calculate the response of the bridge and check if it is acceptable. None of the codes consider all aspects of vibrations induced by humans i.e. vibrations in both horizontal lateral and vertical direction and vibrations not only due to a single person but also due to groups and crowds. Therefore, there is a clear need to revise and update design guidelines featuring obsolete or missing information.

2.7 Measures against Excessive Vibrations of Footbridges

With the occurrence of the first problems related to the liveliness of footbridges, some early design recommendations, such as the one by Walley (1959), proposed that the fundamental vertical natural frequency of a structure below 2.7 Hz should be avoided. It is interesting to note that this corresponds to the upper limit of the range of the first walking harmonic, although at that time little was known about the actual nature of the walking force as no widely reported measurements of it existed. Leonard (1966), on the other hand, claimed that there was no need to avoid any frequency range if an appropriate damping and stiffness had been provided. For example, some footbridges are serviceable although their natural frequencies are inside the problematic ranges (Pimentel et al., 2001) or the damping ratio is as low as 0.4% (Parker et al., 2003). However, with modern trends towards slenderness in footbridge design, it happens that footbridges more and more frequently do not perform well in service as far as their vibration behaviour is concerned. A list of examples of such problematic footbridges was compiled by Pimentel (1997).

There are several measures which can be used to predict, prevent and resolve the problems of liveliness in footbridges (Bachmann & Ammann, 1987; Bachmann, 1992a):

1. *Frequency tuning*: As previously mentioned, this measure means avoiding the critical frequency ranges for the fundamental modes. For vertical mode these are the frequencies of the first (1.6-2.4 Hz) and, for bridges with low damping, the second walking harmonic (3.5-4.5 Hz). Although Bachmann & Ammann proposed the same provision for the lateral modes (namely, 0.8-1.2 Hz for the first and possibly 1.6-2.4 Hz for the second harmonic), it should be added that lower frequencies could be excited too, according to observations made on the Millennium Bridge, London where the frequency of the lowest mode excited was only 0.5 Hz (Dallard et al., 2001a). For the longitudinal direction, the first sub-harmonic and the first harmonic, with frequencies 0.8-1.2 Hz and 1.6-2.4 Hz, respectively, should be avoided. Excessive vibrations in this direction are very rare, but one case was reported by Bachmann (2002). It should be stressed that the designer can influence frequencies of the footbridge by choosing an appropriate layout of the structure and by studying different options for distributing its stiffness and mass. Figure 2.29 gives a rough guidance of the possible fundamental frequencies as a function of the bridge span for vertical (Tilly et al., 1984) and lateral modes (Dallard et al., 2001c).

   Structural frequency can, for example, be changed by stiffening the structure (installing stiffer handrails or adding tie-down cables); Tilly et al. (1984) found that footbridges with stiffness in the middle of the main span which is lower than 8 kN/mm are likely to be prone to vibrations in the vertical direction.

2. *Detailed Vibration Response Assessment*: This is a measure which is the basis of many contemporary design procedures (Section 2.6). However, it is underpinned by many uncertain modelling assumptions and its reliability is often questionable.

3. *Measures to Reduce Vibration*: These measures are:

   - Restricting the use of the bridge (for example, ban marching over the bridge);
   - Increasing the damping (e.g. by adding extra damping devices such as viscous dampers or tuned mass dampers).

It can be added here that warning and/or educating people to expect vibrations can help them to tolerate higher vibration levels than they would without an explanation that their safety is not in question. This is not surprising as safety is the main concern of the bridge users in case of excessive vibrations (Leonard, 1966).

The remainder of this section will consider the use of damping devices that are often used in practice.

2.7.1 Tuned Mass Dampers: Theory

Tuned mass dampers (TMDs) are spring-mass or spring-mass-damper systems which can be added to a structure to reduce its vibration response. Contrary to active vibration suppression systems, which directly monitor the structural response and accordingly adjust their dynamic

behaviour to reduce response over a wide frequency range, tuned mass dampers are passive devices which are effective only in a narrow frequency range (Hunt, 1979).

Ormondroyd & Den Hartog theoretically formulated principles of TMDs in 1928. They found that adding a spring-mass system to an undamped SDOF structure, which was excited by a resonant sinusoidal force, would form a new 2DOF system in which the structural response would be completely eliminated in the case when the natural frequency of the absorber was the same as the one of the primary system. Adding damping to the absorber's spring-mass system made it efficient not only at a single frequency but also over a frequency range. The absorber damping was more effective in reducing the response of the main SDOF system than the damping already present in the main system. This was the reason to neglect structural damping in many numerical simulations of TMDs reported in the literature. Although Ormondroyd & Den Hartog (1928) concluded that there was an absorber damping value (the optimum damping) which would give the maximum attenuation of the structural response, they could not find it analytically. This paper was and still is an excellent base for further research in this area.

In his textbook, which had five editions between 1934 and 1985, Den Hartog found the absorber frequency and damping which will minimise the steady-state displacement response of a structure under sinusoidal force, both as functions of a chosen ratio μ of the absorber and SDOF system masses. These optimum (tuning) parameters are (Den Hartog, 1985):

$$f = \frac{1}{1+\mu}, \tag{2.34}$$

$$\left(\frac{c}{c_{cr}}\right)^2 = \frac{3\mu}{8(1+\mu)^3}, \tag{2.35}$$

where f is the ratio of the absorber and structural natural frequencies, while $\frac{c}{c_{cr}}$ is the absorber damping ratio.

Footbridges with well-separated modes which are perceived as lively respond mainly in one mode of vibration. This mode is usually lightly damped. Therefore, by using appropriate modal mass and stiffness, the excited mode can be represented as a SDOF system, and the optimum TMD parameters can be calculated using Equations 2.34 and 2.35. In that case the parameter μ becomes ratio of the absorber mass and modal (generalised) mass of the SDOF system. For a simple beam structure, the assumption that the relevant pedestrian harmonic does not move produces only small differences in the tuning parameters in comparison with a moving force. The effectiveness of the absorber is nevertheless lesser for the moving force case (Jones & Pretlove, 1979).

Generally, an optimisation of absorber parameters (f and $\frac{c}{c_{cr}}$) could be done for different types of excitation and considering different response parameters. A lot of work has been devoted to this issue. For example, Warburton (1982) analysed an undamped SDOF system under harmonic excitation but optimised response against displacement, velocity and acceleration of

the main mass, and also against the force transmitted to the base. He also did optimisation analysis for white noise excitation and harmonic base acceleration. Rana & Soong (1998) analysed numerically the optimisation for a damped system due to harmonic main mass excitation and harmonic base excitation. They also pointed out the possibility to control the response in more than one structural mode by installation one TMD for each mode considered. Several TMDs can also be used for controlling SDOF system response due to wide-band random excitation (Xu & Igusa, 1992; Rana & Soong, 1998).

In the case of footbridges, a single TMD for a dominant mode is usually considered. It is most effective to put the TMD at the point with maximum structural response, that is at the antinode (Jones & Pretlove, 1979).

2.7.2 Tuned Mass Dampers: Practice

Matsumoto et al. (1972) reported one of the first cases of installation of a spring-mass absorber to suppress excessive vibration of a footbridge. An explanation of that exercise, as well as of an installation of two additional absorbers in another pedestrian bridge was given by Matsumoto et al. in 1978. Also, Brown (1977) reported briefly on another installation of a TMD on a bridge.

Chasteau (1973) described the successful installation of two TMDs on a three span footbridge susceptible to wind dynamic excitation. The two TMDs were a new technology at that time which was probably the reason for clients to ask for these devices to be maintenance-free. Because of that, the author decided to use air instead of fluid damping, although it was hard to fabricate that sort of a solution. Finally, the absorbers increased the bridge damping by about five times, but their mass ratios were 0.043 and 0.065 which is quite high. As reported by Eyre & Cullington (1985), this state of affairs probably discouraged engineers at that time to use TMDs more frequently to solve the liveliness problem in footbridges.

Jones & Pretlove (1979) investigated effectiveness of a TMD on a 30 m long beam. It was demonstrated that a TMD of 70 kg having the mass ratio of only 0.006, can be quite effective. However, this was expected, having in mind very low damping ratio in the structure of only 0.13%. Jones & Pretlove also showed that Den Hartog's formulae for optimum TMD design given in Equations 2.34 and 2.35 can be used if the damping of the structure is below 1% and that the effectiveness of the TMD can be reduced because of the internal friction in the absorber. Figure 2.30 shows the difference between theoretical and measured displacement amplitude of the beam for a range of harmonic excitation frequencies.

Bachmann & Weber (1995) wrote an excellent and comprehensive article about the design and effectiveness of vibration absorbers. They showed that Equations 2.34 and 2.35 can be used for all lightly damped structures, especially if the damping is below 2% (Figure 2.31). It was also demonstrated that the effectiveness of the absorber was much more sensitive to the error in the tuning of the TMD frequency than in the tuning of its damping. The procedure for the absorber design was outlined with a particular emphasis on the choice of

the appropriate mass ratio. Namely, an absorber with, for example, mass ratio of 0.02 seems to be a solution which both successfully attenuates the structural response and also keeps the absorber mass movement within reasonable limits (Figure 2.32).

With regard to the usage of TMDs, it is now common practice to design them upfront, but actually manufacture and install them after the footbridge is constructed if problems of excessive vibrations are noted. Also, it is interesting that 26 pairs of TMDs were installed on the Millennium Bridge, London to prevent possible excessive movement in the vertical direction which was not noticed during the conducted tests (Dallard et al., 2001a). Some examples of TMDs installed in footbridges can also be found in articles presented at Footbridge 2002 conference in Paris (Breukelman et al., 2002; Collette, 2002; Hatanaka & Kwon, 2002).

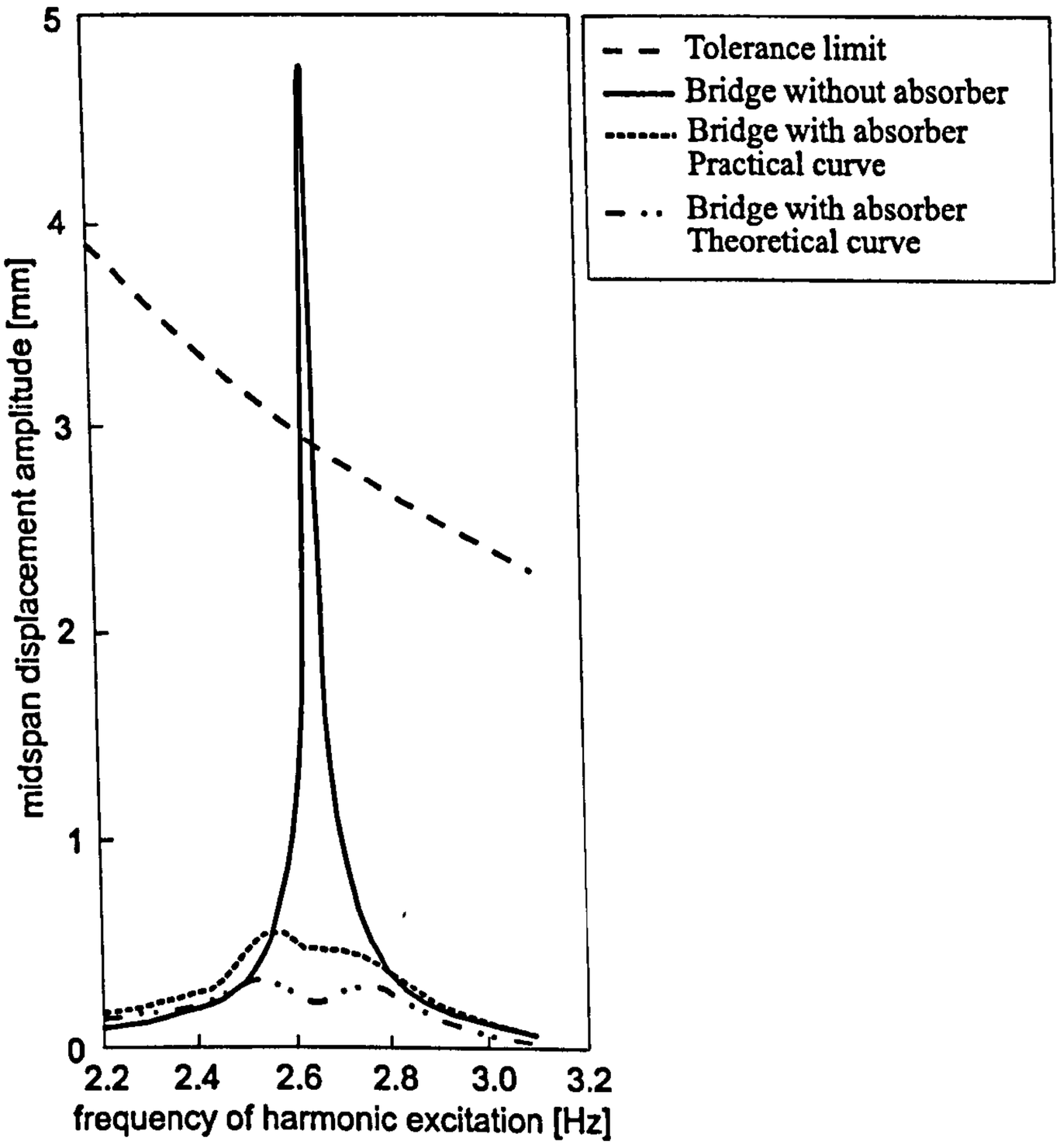

Figure 2.30: Influence of the absorber friction on its effectiveness (after Jones et al., 1981).

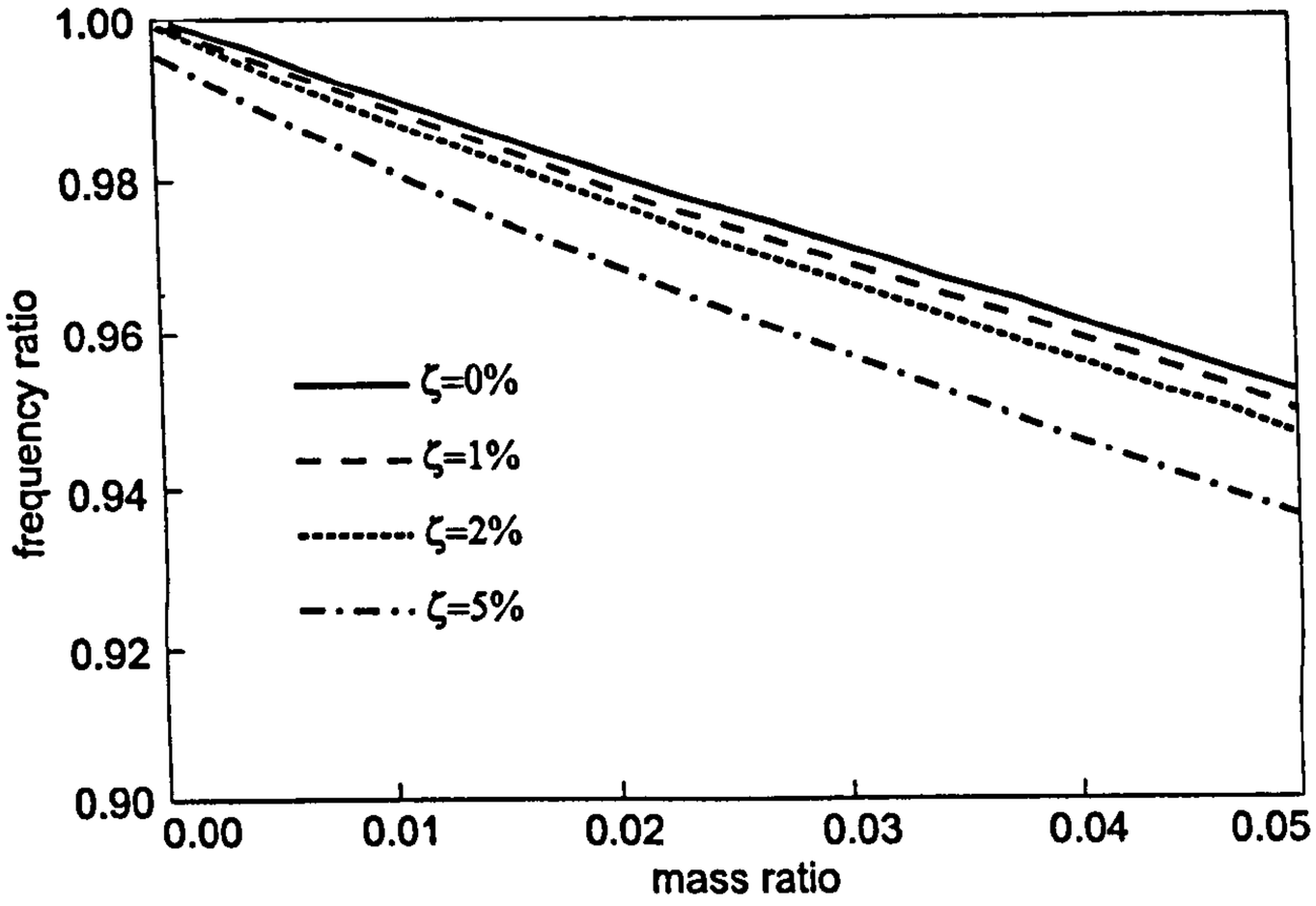

Figure 2.31: Frequency tuning as a function of the mass ratio and the bridge damping (after Bachmann & Weber, 1995).

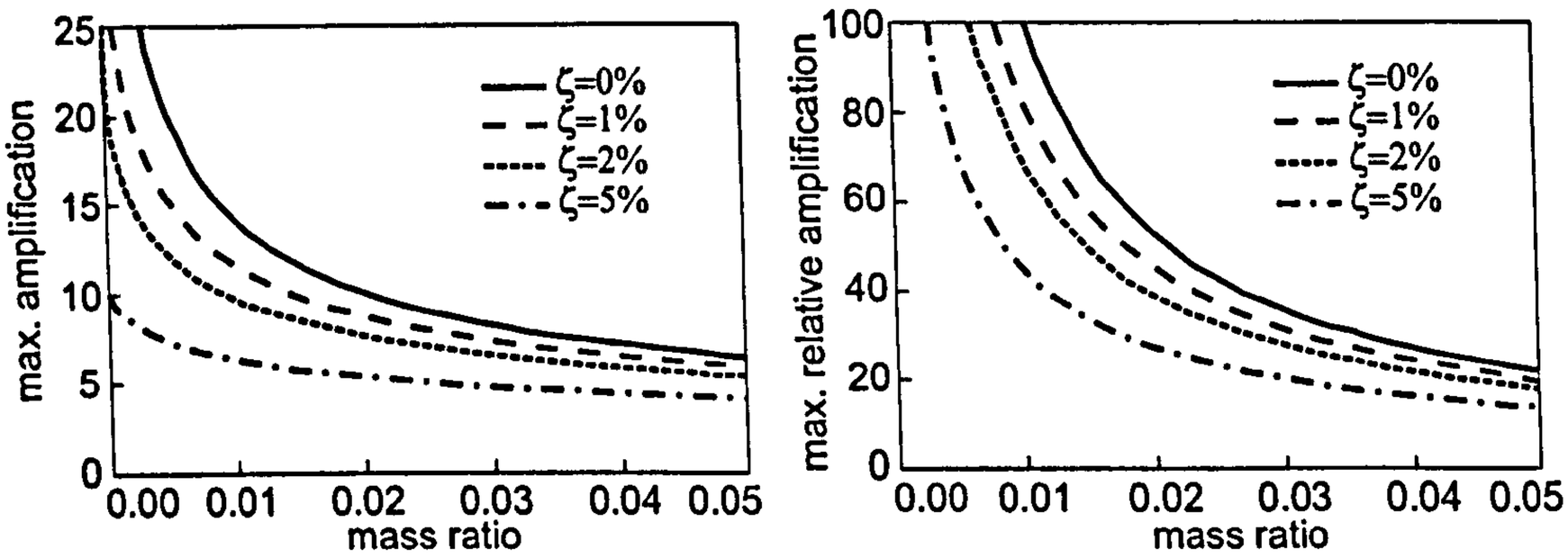

Figure 2.32: Dynamic amplification of the structural and relative structure-TMD response as a function of the mass ratio (after Bachmann & Weber, 1995).

TMDs can suppress either vertical or horizontal movement. TMDs working in the vertical direction usually consist of a mass, helical springs and viscous-fluid damper while the horizontal ones are typically constructed as pendulums (Weber, 2002). Vertical TMDs are more common and they are usually attached to main girders, beneath the deck or above the deck in the plane of the handrails. They are usually low-cost and easy to maintain. However, with time the effectiveness of absorbers can be reduced because of disappearance of viscous oil (Eyre & Cullington, 1985), changing of dynamic properties of the structure (Bachmann & Weber, 1995) and changed nature of the live pedestrian load for which the footbridge was originally designed. In all these cases de-tuning of the TMDs occurs. The last two reasons initiated a quest in the research community for a better solution for vibration suppression. One of the options is replacing the passive with a semi-active damper in the TMDs. Without getting into details of this relatively new technology here, reference will be made to analyses conducted by Occhiuzzi et al. (2002) and Seiler et al. (2002). They described semi active

devices which, owing to their rheological properties, can adjust their stiffness and damping according to changes in the main structure. However, these devices require additional equipment for measurements and control and it may be some time before they become economically viable.

Also, because of the variability of the human pacing rate, the multiple tuned mass dampers (MTMD) can be a more effective solution than a single TMD. Poovarodom et al. (2001; 2002; 2003) reported the installation of six TMDs to reduce the vertical vibration of a footbridge. Although their weight was only 1% of the structural weight, they decreased acceleration by about three times.

2.7.3 Other Damping Devices

Although TMDs are most popular, other devices for suppressing bridge vibration response can also be used. For example, a very simple friction device composed of two springs was installed in the handrails of a footbridge (Brown, 1977). Furthermore, 37 fluid viscous dampers were installed on the Millennium Bridge in London mostly to suppress excessive vibrations in the lateral direction. As a result, the damping ratio increased from 0.5% to 20% and near-resonant accelerations were reduced by about 40 times (Dallard et al., 2001a; Taylor, 2002). Also, tuned liquid sloshing dampers can be used for the same purpose. In this system liquid is contained in a shallow tank which is placed on the structure. The required height of the liquid is established by nonlinear shallow-water wave theory. The motion and viscosity of the liquid generate the required damping. This tuned liquid damper (TLD) is cost-effective, easy to install and maintain and requires a very low vibration level to which it will respond, which is sometimes a problem with standard mechanical TMDs (Fujino et al., 1992). Nakamura & Fujino (2002) reported that 600 plastic tanks with 34 mm of water were employed to suppress lateral vibrations of a cable-stayed footbridge. The TLDs were placed inside the box girder. The mass ratio was only 0.007. It was shown that these TLDs were very effective at the time of installation. However, it was also reported that after 10 years without any maintenance, their effectiveness reduced considerably, mainly because the water evaporated. On the same bridge, secondary wires were used to connect stay cables and decrease their in-plane vertical oscillation which in fact is an example of stiffening rather than dampening of the structure. As a way forward, multiple TLDs with different level of liquids can be used to suppress motion over a range of frequencies (Fujino & Sun, 1993).

2.8 Summary

This chapter has reviewed about 200 references dealing with different aspects of vibration serviceability of footbridges under human-induced load. It is found that the whole issue is very complex and under-researched. However, rationalisation of the problem into its three key aspects: the vibration source, path and receiver (ISO, 1992) is adopted nowadays when

dealing with vibration performance of footbridges.

Among different types of human-induced loads on footbridges, walking force due to a single pedestrian was established in the past as the most important load type because of its most frequent occurrence. Also, almost all existing force models for this type of load (defined either in the time or frequency domain) are developed from the assumption of perfect periodicity of the force and are based on force measurements conducted on rigid (i.e. high frequency) surfaces. However, footbridges which exhibit vibration serviceability problems are low frequency flexible structures with natural frequencies within the normal walking frequency range. In such a situation, walking at a near resonant frequency is expected to generate the highest level of response as considered in the published literature. However, the walking force is not perfectly periodic (Saul et al., 1985; Eriksson, 1994; Brownjohn et al., 2004) and it could be attenuated due to interaction between the pedestrian and the structure (Ohlsson, 1982; Yao et al., 2002; 2003). These two facts deserve more attention in future force modelling.

Apart from a single person walking, a group of pedestrians walking at the same speed to maintain the group consistency are a very frequent load type on footbridges in urban areas. This type of dynamic load was not researched much in the past, especially in relation to pedestrian bridges. Wheeler (1982) and Grundmann et al. (1993) were among a handful of researchers who investigated this issue. They found that, under this type of load, footbridges with a natural frequency of around 2 Hz are prone to experience vibrations at a higher level than those induced by a single pedestrian because of synchronisation of walking steps between people in the group. However, there is no group force model which is generally accepted. The fact that Eurocode 5 (ENV, 1997) recently tried to include this type of load as a compulsory consideration demonstrates a need to codify it more widely.

As this literature survey found, the problem of excessive lateral swaying of the Millennium Bridge in London in June 2000 triggered a lot of urgently needed research into crowd loads on footbridges. Attention was paid to forces induced not only in the lateral but also in the vertical direction. It was found that some degree of synchronisation between people within the crowd exists as a result of not only a limited space available when walking in a crowd but also of pacing adjusted to the bridge movement. Qualitative observations revealed that the degree of synchronisation is dependent on several factors: the natural frequency of the bridge excited by crowd walking, amplitude of the footbridge response, number of people involved, density and velocity of people and so on. However, more research is needed to quantify the influence of all these parameters on the level of synchronisation.

This review also found that forces induced by joggers, runners and vandals have not been researched much in the past. However, there is an increasing awareness that the application of vandal loading, in particular to very slender light structures with low damping, can generate a significant response of the structure and should be treated adequately. It is found that jumping, bouncing and horizontal body swaying are usually considered as possible vandal loads. However, contradictory proposals about the modelling of this type of loads exist. These range from the one that vandals in small groups can be perfectly synchronised (Bachmann,

2002) to the one that vandals can produce only slightly higher response than a single person performing the same activity (Wheeler, 1982). Therefore, a clarification of the exact definition of the vandal loading, regarding its duration, type of load and number of people involved, as well as its force modelling is a task for further investigation.

For a reliable estimate of vibration serviceability performance of footbridges, an appropriate modelling of its dynamic properties (mass, stiffness and damping) is very important. This review showed that, using finite element packages, mass and stiffness can be modelled most successfully using previous experiences when modelling similar structures. In that way, good estimates of natural frequencies and mode shapes can be obtained. However, the only reliable way to determine structural damping is to conduct the testing of the full-scale structure after it is built.

As for evaluation of human-induced vibrations on footbridges i.e. their acceptability to human receiver, it is accepted that in the case of normal footbridges, the vibration level should be evaluated for a walking and not standing person. Issues such as the transient nature of footfall excitation, limited time of exposure to vibrations and the fact that the receiver is not stationary but is moving were identified as important ones. Leonard (1966) and Smith (1969) investigated the acceptability of vertical vibrations to walking test subjects, having in mind the mentioned issues. As a result, they constructed scales of acceptable vibrations as function of their dominant frequency. The average value of these results has been adopted as a design rule in BS 5400 (BSI, 1978; HA, 2001) and it is widely used in design practice. There is no similar widely accepted scale related to acceptability of vibrations in the lateral direction, although some recommendations related to perception within a crowd have recently been published. Also, research into differences in human acceptance of the vibrations when walking alone, in small groups or a large crowd is very scarce.

Finally, it can be said that the most advanced design guidelines, such as BS 5400 (BSI, 1978) and Canadian Highway Bridge Design Code (CSA, 2000), which served as the basis for most of other guidelines, are founded on research data collected in the 1970s. As a consequence, they still imply some parameters which are nowadays proven as inadequate (such as a constant DLF regardless of the pacing frequency and force harmonic considered). Also, although some formal national guidelines require consideration of lateral forces induced by pedestrians, exact procedures as to how to consider them are usually not given or are proven to be inadequate. Based on these facts, the existing guidelines should be used carefully, with plenty of lateral thinking and along with some recently published research which could be relevant for a design case considered.

Preface to Chapter 3

The work on modal testing and finite element (FE) modelling of a lively footbridge in Podgorica (capital of Montenegro) is presented in Chapter 3. In addition, correlation between the experimental results and the FE model is studied to identify any major inaccuracies in the FE model. This work is the first phase in a process of estimating more reliable dynamic properties of the footbridge. The second phase of automatic model updating is presented in Chapter 4.

The rationale for the work in Chapter 3 was to:

- estimate dynamic properties of a footbridge structure that later will be required for verification of a force model, and
- gain necessary experience in dealing with data acquisition, signal processing and parameter estimation that is required for vibration serviceability assessment of footbridges. This proved to be a particularly useful exercise having in mind that data collected by other Vibration Engineering Section members in the past were planned to be used at a certain point of the research. Therefore, understanding of their format and way of collecting was required.

During the work presented in Chapter 3 the author became familiar with data acquisition for both FRF- and ambient-based modal testing, parameter estimation by using ICATS and ARTeMIS software as well as with FE modelling in ANSYS.

Chapter 3

Modal Testing and Finite Element Model Tuning of Podgorica Footbridge

This chapter, in a slightly amended form, has been published under the following reference:

Živanović, S., Pavic, A. and Reynolds, P. (2006) Modal Testing and Finite Element Model Tuning of a Lively Footbridge Structure, Engineering Structures, 28 (6), 857-868.

Abstract

Despite huge advances in numerical modelling in recent decades, finite element models for footbridges should be used with caution when evaluating vibration properties of these structures. This is due to some unavoidable modelling uncertainties such as modelling of boundary conditions, material properties and effects of non-structural elements. These are difficult to deal with at the design stage. A common method to rectify this problem is vibration testing of these structures after construction. As footbridges are unique prototype structures testing in this late stage does not help the design of the actual structure. However, combining testing and analysis improves understanding of vibration behaviour, helps future designs of similar structures and provides key information for the design of remedial measures, if required.

This chapter describes a lively full-scale footbridge, its numerical modelling and dynamic testing. This was done using state-of-the-art procedures available nowadays for finite element modelling and frequency response function based modal testing. The time efficiency of the testing and parameter estimation procedures carried out without formally closing the footbridge is demonstrated as well as good quality of results achieved. The identified vibration parameters compare well with those from an ambient vibration survey where only the bridge responses were measured. Also, it was demonstrated that properly planned testing can be performed successfully even with some limited facilities, such as only two accelerometers available. The correlation between a very detailed finite element model and experimental results is then studied. For this particular structural system, stiffness of girder end supports in the longitudinal direction and bending stiffness of inclined columns were identified as the modelling parameters which influenced most strongly the vertical and the horizontal modes of vibration, respectively.

3.1 Introduction

Finite element (FE) modelling of footbridges is now common in a normal footbridge design process. With advances in numerical modelling, it is often expected that FE models based on technical design data and best engineering judgement can reliably and equally well simulate both the static and dynamic behaviour of the bridge. However, because of modelling uncertainties (such as stiffness of supports and some non-structural elements, material properties and so on) as well as inevitable differences between the designed and as-built structure, these FE models cannot often predict the natural frequencies and mode shapes with the required level of accuracy. This raises the need for verification of the FE models of footbridges after their construction. This is especially so when they are required to further study the structural behaviour, for example when designing vibration suppression measures (e.g. tuned mass dampers). Moreover, the modal damping, a very important dynamic parameter which governs the footbridge dynamic response near resonance, varies from structure to structure and can only be determined experimentally after the particular structure is built.

A common approach nowadays for establishing a feedback between the real structural performance and design FE models is to employ some form of modal testing (Maia et al., 1997) on footbridges in service. The aim of modal testing is to determine as-built natural frequencies, mode shapes and damping ratios. Currently, the dynamic testing and experimental verification of FE models are not part of a normal design procedure in civil structural engineering. This is contrary to mechanical and aerospace engineering disciplines where studying of the prototype models of the structure and its correlation with a corresponding FE model has become a part of everyday design practice (Friswell & Mottershead, 1995). This is often justified by the fact that mechanical and aerospace engineering deal with large production of identical units as opposed to civil structural engineering where almost every structure is actually a unique prototype.

As dynamic testing is not a part of the normal design process in civil structural engineering and it can also be expensive, it is common not to do it. Additionally, there are serious legal and cultural issues related to it, such as a fear of legal liability, possibly leading to additional expense, if the testing proves that the structure does not perform as predicted during design. As a result, there is currently a serious lack of information about the as-built dynamic performance of civil engineering structures, leading also to a lack of information about the reliability of FE modelling in civil structural engineering design. In other words, by avoiding testing as-built structures and correlating the measured data with the numerical models, we do not know how good the created dynamic FE models are even if best engineering judgement and practice is employed in the modelling.

On the other hand, there are multiple benefits of dynamic testing. In the case of footbridges it adds to the body of knowledge about their as-built performance. As mentioned above, this knowledge is currently very limited, which is not satisfactory considering that vibration serviceability is becoming the governing design criterion for footbridges. Also testing enables

retrofitting measures, such as installation of tuned mass dampers. Moreover, it helps future design of structures of similar configurations. Finally, the dynamic testing is nowadays an important part of research into vibration serviceability of footbridges. Namely, good quality experimental data are required for both manual (model tuning) and automatic updating of the design FE model (Fritswell & Mottershead, 1995; Maia et al., 1997). These models are crucial for studying vibration serviceability state of as-built footbridges.

Bearing all this in mind, this chapter presents a case study related to FE modelling, modal testing and manual FE model tuning of a lively footbridge in Podgorica, Montenegro. It demonstrates the reliability of a very detailed design FE model which was firstly developed by employing best engineering judgement and available design data. Then, the lowest modes of vibration in both the vertical and horizontal lateral directions were identified using a state-of-the-art frequency response function (FRF) based testing procedure, using shaker excitation with in-situ data processing and analysis. Also, to verify the shaker test results, an ambient vibration survey (AVS) was conducted to examine the (lively) vertical direction only. Based on the experimental results, the design FE model was then revised and manually tuned to match the actual natural frequencies of the footbridge more closely. Manual tuning is required when developing an FE model suitable for later implementation of the automatic updating procedure (Brownjohn & Xia, 2000). Otherwise, automatic updating may not work as the starting model is too far away from the measured targets. Using the manually tuned FE model, a sensitivity-based automatic updating was also conducted successfully and is presented in Chapter 4.

The first part of this chapter reviews briefly the existing literature concerning the numerical and experimental investigations of dynamic performance of footbridges. Then, the steel box-girder footbridge investigated is described followed by a description of a design FE model and the main assumptions made during its development. Then an FRF-based modal testing of the bridge is described, together with an AVS testing exercise. After this, the as-built modal properties of the footbridge are identified and compared with the numerical results. Finally, the FE model is manually tuned and key results of this interesting exercise are discussed.

3.2 Background Review

There are only a few articles dealing with both vibration testing and FE modelling specifically related to footbridges. Probably the first extensive work related to vibration testing of footbridges was conducted by the UK Transport and Road Research Laboratory in 1970s (Leonard, 1974; Leonard & Eyre, 1975; Eyre & Tilly, 1977). Their work was concentrated on presenting and discussing the experimentally identified modal properties (Leonard & Eyre, 1975; Eyre & Tilly, 1977). The testing equipment used was described separately in a paper by Leonard (1974) and from today's point of view it was quite limited. This is particularly so regarding the type of exciters used, very limited excitation frequency range, the slow data collection and limited vibration parameter estimation techniques. A common shortcoming

related to the 1970s reporting of tests was that the digital data acquisition parameters (sampling rate, type of filtering, etc.) were regularly omitted from written reports. Knowing these parameters is very important to judge the quality of the experimental data collected and, consequently, the quality of the vibration parameter estimation.

In the last 10-15 years, a number of authors started to pay more attention to providing complete data acquisition parameters in their work (Cantieni & Pietrzko, 1993; Pavic & Reynolds, 2002). Together with this trend some work discussing correlation between modal testing and FE model results has also emerged (Gardner-Morse & Huston, 1993; Brownjohn et al., 1994; Deger et al., 1996; Brownjohn, 1997; Pimentel, 1997). The reported discrepancies between the initial model predictions and experimental results were usually highly significant, typically due to inaccurate modelling of boundary conditions, neglecting influence of non-structural elements, such as deck and handrails, and uncertain material properties. This has led to improved structural idealisation (boundary conditions, non-structural elements, etc.) and revised estimates of numerical modelling parameters to be used in creation of the FE models (Pavic et al., 1998; Brownjohn & Xia, 2000).

The modal testing procedures used in all these papers were either FRF-based testing (with either instrumented shaker or hammer excitation) or ambient vibration survey. In the former both the input force and output response are measured. In the latter only the response is measured while the input force due to environmental excitation (wind, traffic, etc.) is assumed to be a stationary random process (that is white noise excitation having approximately flat frequency spectrum within the frequency range of interest). A brief but well presented review of modal testing methods for bridges explaining their advantages and limitations was presented by Salawu & Williams (1995).

3.3 Description of Test Footbridge

The investigated footbridge spans 104 m over the Morača River in Podgorica, capital of Montenegro (Figure 3.1).

The structural system of the Podgorica footbridge is a steel box girder with inclined supports (Figure 3.2). The structure's main span between inclined columns is 78 m and it has two side spans of 13 m each. The top flange of the main girder forms a 3 m wide deck. The depth of the girder varies from 1.4 m in the middle of the central span to 2.8 m at the points where the inclined columns connect to the main box girder (Figure 3.2). Along its whole length the box girder is stiffened by longitudinal and transverse stiffeners, as shown in Figure 3.2. The connection between the inclined columns and box girder is strengthened by vertical stiffeners visible in Figure 3.1. Water supply and drainage pipes pass through the steel box section and they are suspended from the top flange of the main girder (Figure 3.2).

In the early 1970s, when the footbridge was designed and constructed, design guidelines for vibration serviceability of footbridges did not exist in the former Yugoslavia. This is

not surprising considering that the first modern footbridge vibration serviceability guidelines appeared in BS 5400 in the UK in 1978 (BSI, 1978).

Figure 3.1: Photograph of the Podgorica footbridge.

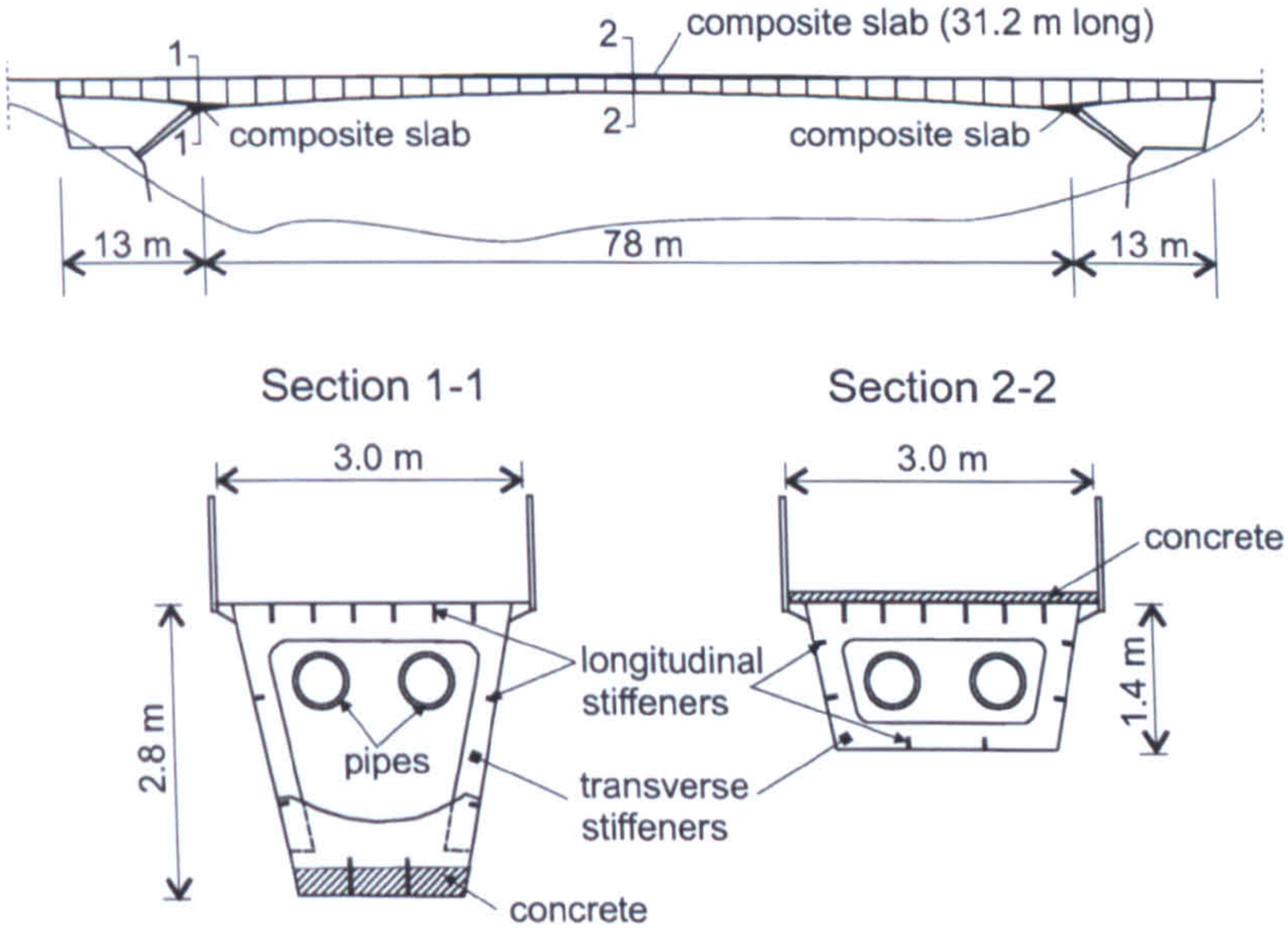

Figure 3.2: General arrangement drawing (not to scale) of Podgorica footbridge.

Since its construction, under pedestrian walking excitation, the footbridge has been very lively in the vertical direction. Also, a review of its design calculations found that a particular design load combination induces stresses close to allowable limits in some of its cross sections. This was the reason for designers to try to strengthen the structure to increase its carrying capacity. The plan for this strengthening was to also stiffen the structure and shift its natural frequencies above the frequency region of normal human walking which is 1.6-2.4 Hz (Bachmann et al., 1995b). The steel box girder was strengthened by a concrete slab cast over the bottom steel flange in the region around columns (Figure 3.2). The aim was to enhance this part of the box section so that it can resist large column reactions and compression due to hogging moments. A similar steel-concrete composite slab was cast around the mid-span of

the footbridge, but this time over the top flange of the box girder (Figure 3.2). However, this added not only stiffness but also some mass to the dynamic system. Consequently the natural frequencies did not change very much and the footbridge remained very lively. Sometimes, perceptible vibrations are excited by just a single pedestrian crossing over the bridge. The vibrations are perceptible to the person generating them and also to other pedestrians, either stationary or walking, who are present on the footbridge deck. At the first sight this is somewhat surprising considering how massive the 260-tonne structure is (Figures 3.1 and 3.2).

This liveliness, together with the fact that information about vibration behaviour of the described structural layout can seldom be found in the published literature, makes the Podgorica footbridge interesting for investigation of its as-built dynamic characteristics.

3.4 Pre-Test Finite Element Modelling

A good practice for modal testing of an as-built structure requires a development of reasonably detailed FE model before the testing (Maia et al., 1997). This first insight into dynamic behaviour of the footbridge helps the test planning and preparation.

A 3D FE model for the Podgorica footbridge was developed (Figure 3.3) using the ANSYS FE code (SAS, 1994). The aim was to construct a detailed model which would be able to simulate the dynamic behaviour of the structure as well as possible. This was based on the limited technical data available and best engineering judgement.

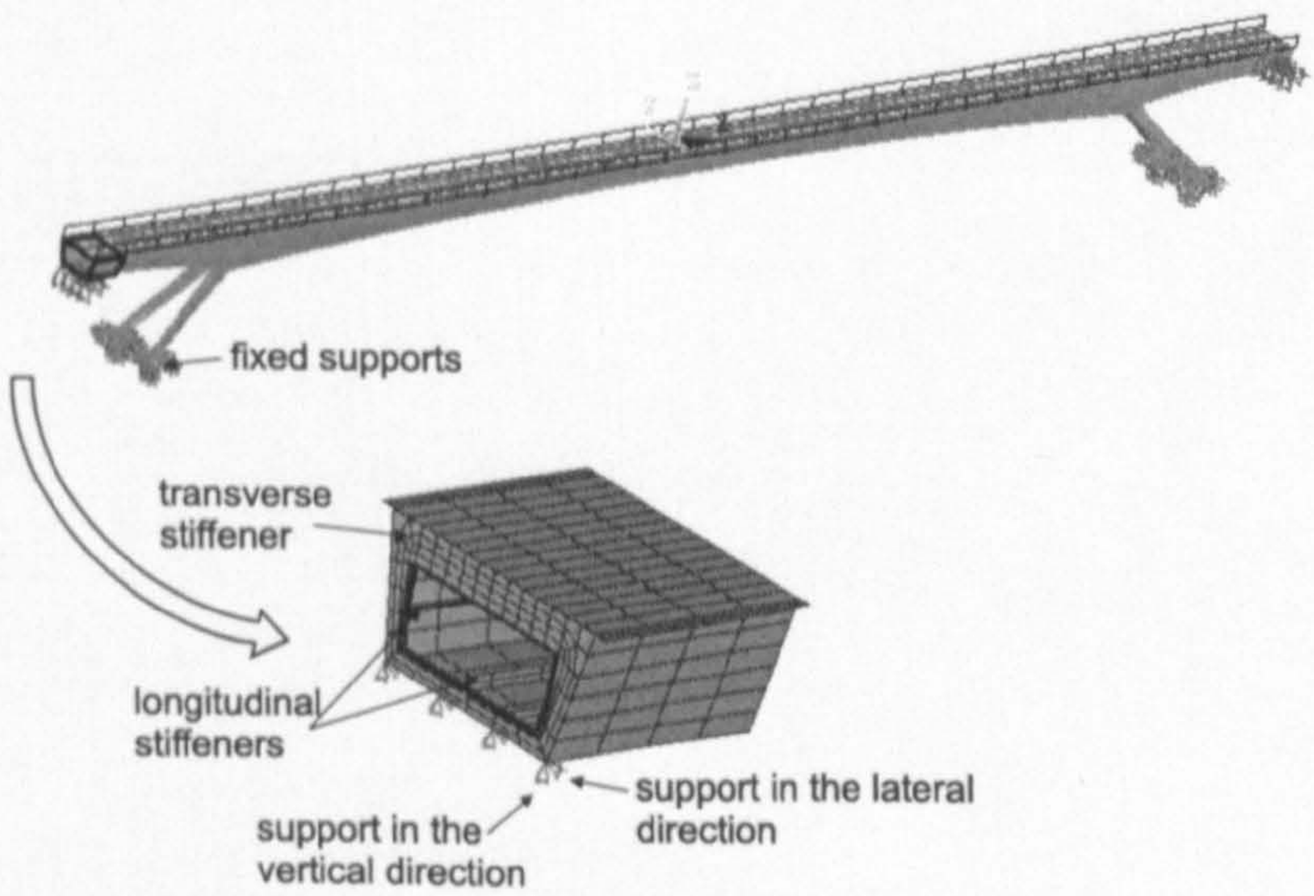

Figure 3.3: Design FE model.

The key modelling assumptions were as follows:

- The main steel box girder and its longitudinal and transverse stiffeners and box section columns were modelled using orthotropic SHELL63 elements assuming isotropic

properties. These elements are capable of transferring both in-plane and out-of-plane loads.

- The composite steel-concrete slabs (Figure 3.2) were modelled using an equivalent steel thickness and, again, SHELL63 elements with isotropic property.
- The handrails were modelled using 3D BEAM4 elements.
- Water and drainage pipes were modelled as distributed mass along the lines connecting points at which the pipes were suspended from the bridge deck. The mass was calculated by assuming that water filled a half of the pipes' volume.
- Inclined column supports were modelled as fully fixed considering solid rock foundations.
- Supports at both ends of the main girder were modelled as pinned, but with a possibility to slide free in the longitudinal direction i.e. along the bridge longitudinal axis (Figure 3.3).

The seven lowest modes of vibration calculated using this model are shown in Figure 3.4. Labels H and V stand for the horizontal and vertical modes, respectively. Similarly, S and A stand for the symmetric and anti-symmetric modes, respectively.

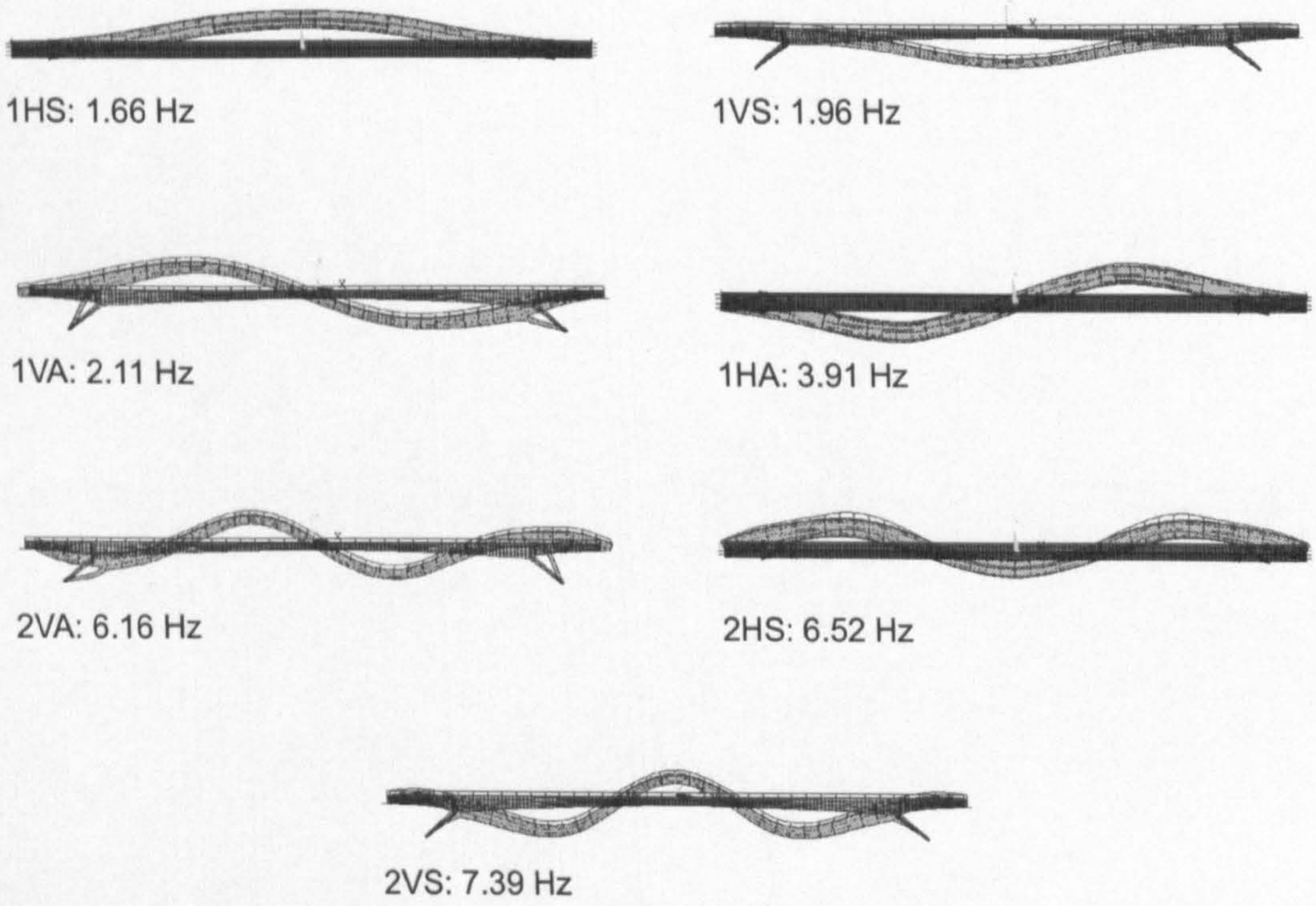

Figure 3.4: The first seven modes of vibration as obtained in the design FE model based on best engineering judgement.

3.5 Testing

The primary aim of the modal testing was to identify the lowest modes of vibration in both the vertical and horizontal lateral directions. For this purpose an FRF-based testing procedure (Maia et al., 1997) was employed. The second aim was to conduct an ambient vibration survey and compare results with the FRF-based modal testing, to check their consistency. Both types of test required the footbridge to be empty, which means closed and without any pedestrians present during measurements. Due to the importance of this footbridge located in the city centre, the only time when the tests could be conducted was during the night when pedestrian traffic was reduced, although still present. The tests were scheduled to last up to five hours during two nights in October 2004, starting at midnight.

3.5.1 FRF-Based Modal Testing

Based on mode shapes identified in the FE model (Figure 3.4) and the fact that only two accelerometers were available for measurements, it was decided to conduct testing at 14 measurement points, as shown in Figure 3.5. This was done to avoid problem with spatial aliasing of mode shapes (Maia et al., 1997) and enable the identification of the lowest few modes of vibration presented in Figure 3.4. The test was first conducted to identify the vertical modes and then repeated for the horizontal lateral modes.

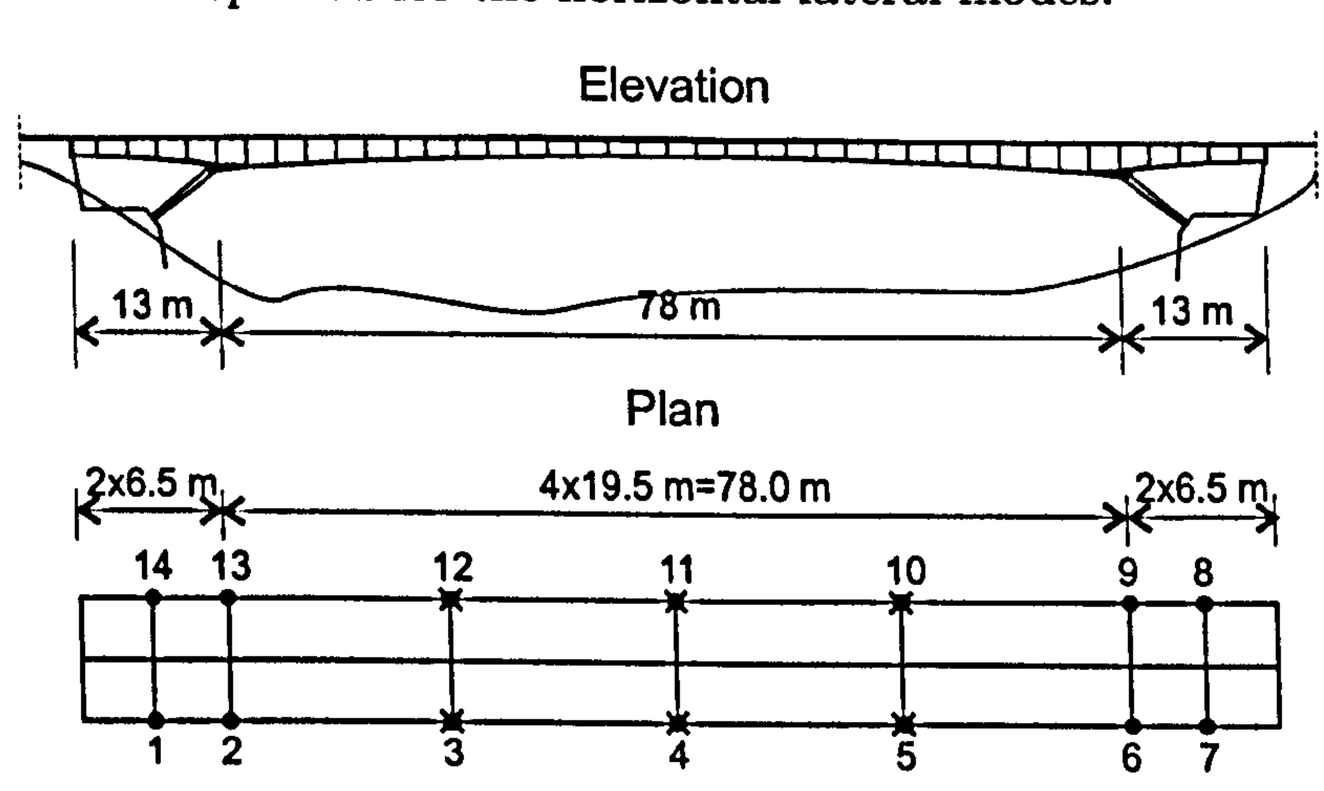

Figure 3.5: Measurement grid for modal testing. Plan drawn not to scale.

The excitation source for the FRF-based testing was an APS Model 113 electrodynamic shaker. The dynamic force induced by the shaker was measured by an accelerometer attached to its armature. The same type of transducer was used for the structural response measurements. Both transducers used were Endevco 7754-1000 piezoelectric accelerometers, having nominal sensitivity 1000 mV/g. They are suitable for low frequency measurements down to less than 1 Hz. The shaker operating in the vertical direction is shown in Figure 3.6a

and the setup used for it in the horizontal direction is shown in Figure 3.6b.

Test point 3 (TP3), at the quarter of the main span (Figure 3.5), was chosen as an excitation point for both directions. For the vertical measurements the vertical response was measured at all 14 points while for the horizontal lateral modes only first seven points were used to measure the horizontal response.

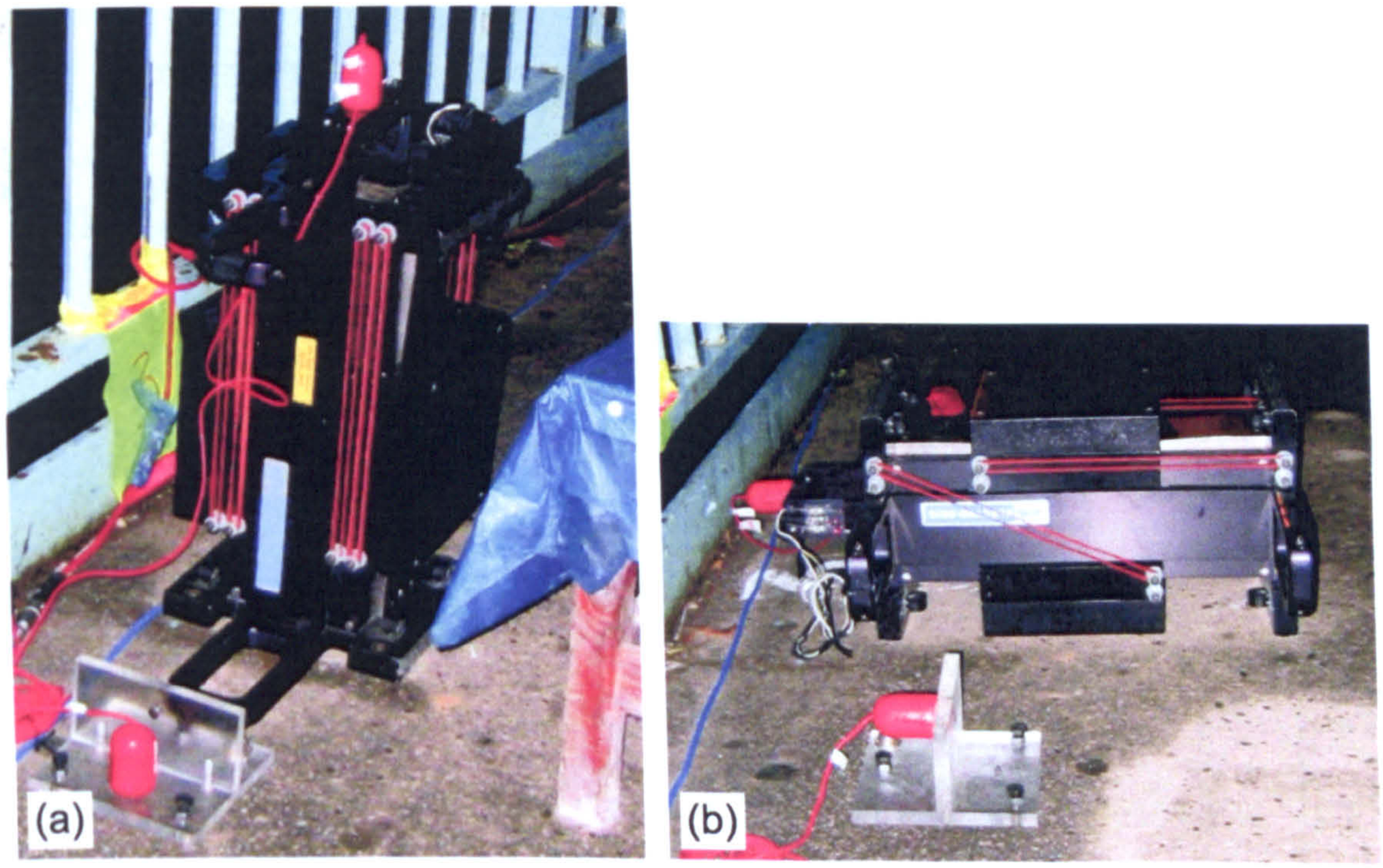

Figure 3.6: The electrodynamic shaker operating in: (a) vertical mode and (b) horizontal mode.

A dual-channel Data Physics SignalCalc ACE dynamic signal analyser was used to acquire the time domain acceleration data and process them leading to a set of FRFs between the excitation and response points. Based on some very limited previous measurements decribed in Appendix A, a damping ratio ζ_1 as low as 0.3% was expected in the vertical fundamental mode of vibration having frequency f_1 of 2.0 Hz. A suggested frequency resolution Δf for data acquisition is therefore approximately (DTA, 1995):

$$\Delta f = \frac{2\zeta_1 f_1}{6} = \frac{2 \cdot 0.003 \cdot 2.0}{6} = 0.002\,\text{Hz}\,. \tag{3.1}$$

This, in turn, required time-domain data blocks lasting at least 500 s, as calculated in Equation 3.2:

$$T = \frac{1}{\Delta f} = 500\,\text{s}\,. \tag{3.2}$$

With this in mind, and considering the limited time available for keeping the bridge closed during the testing, a compromise had to be made. A 327.68 s data block was chosen using

available options in the signal analyser provided that the FRFs were analysed immediately during testing to ensure that the experimental FRF-data can lead to a good and believable curve-fit. The next step was to decide about the type of force signal capable of exciting the 260-tonne bridge so that its response is measurable in all relevant modes of vibration. A typical time history of a chirp excitation signal at TP3 together with the response measurement at the same point, as well as their spectra are shown in Figure 3.7.

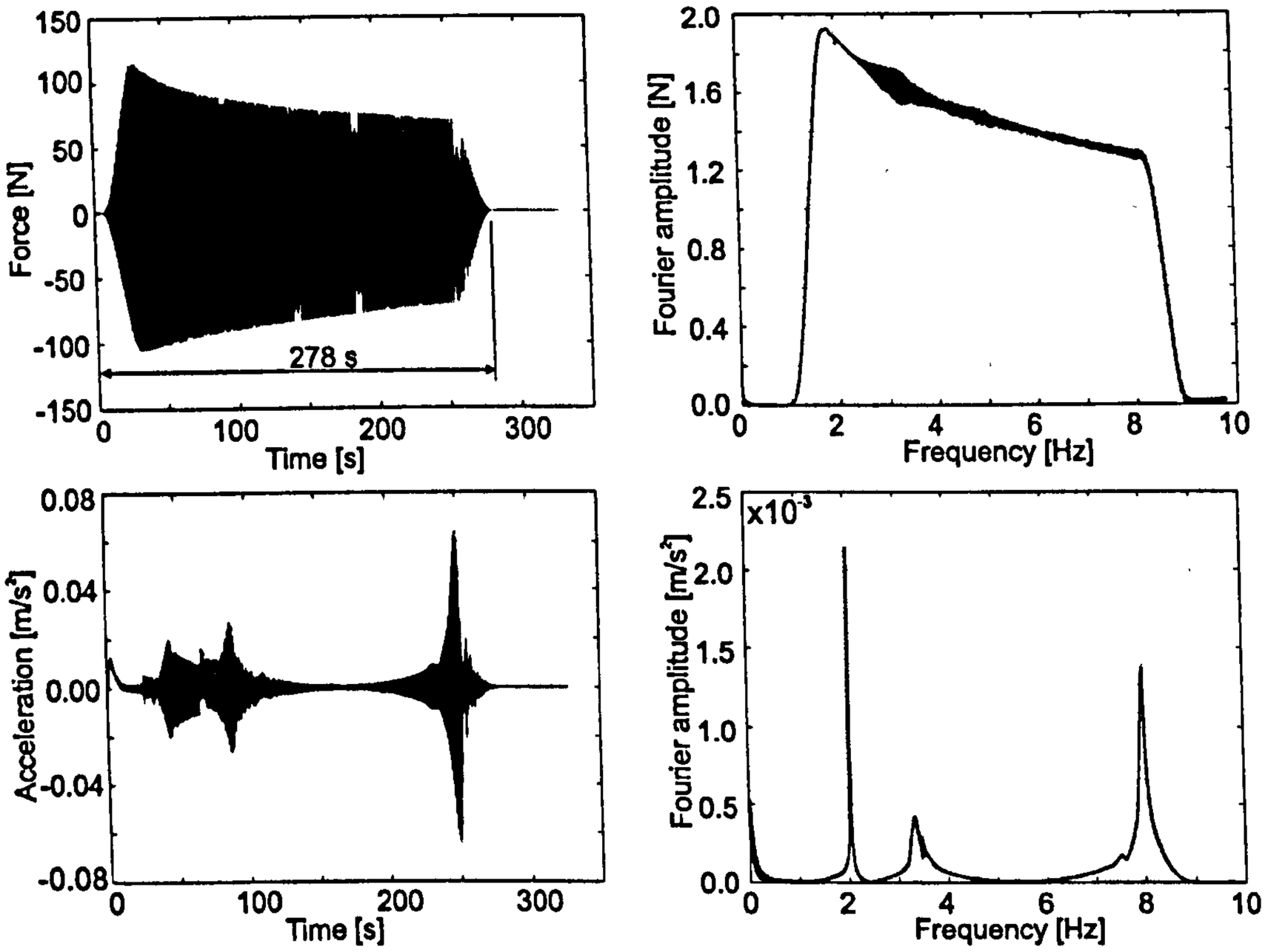

Figure 3.7: Typical chirp excitation and corresponding acceleration response signals at TP3 in the time and frequency domains.

The resulting point accelerance obtained firstly with three averages and then with no average (i.e. using just one block of data) are shown in Figure 3.8. Quite surprisingly the FRF data quality was almost the same. Because it was difficult to close the bridge even for 10 minutes at a time, an FRF estimation without averaging was adopted as it approximately halved the time required for testing. Also, this choice was supported by good quality of the FRF that was not averaged as a consequence of high signal to noise ratio. This ratio was high owing to both the good excitation technique and quiet night with almost no wind. Also, the fact that some modes of vibration had very low damping ratio and therefore were easily excitable, contributed to obtaining high quality FRF data without any averaging. This feature is not often seen when testing full-scale civil engineering structures residing in open-space environments. These are naturally quite noisy a therefore create a considerable level of extraneous unmeasured excitation of the test structure. If uncorrelated with the measured excitation the only way to remove the effects of this excitation is by averaging. However, and quite interestingly, on this particular occasion this was not necessary.

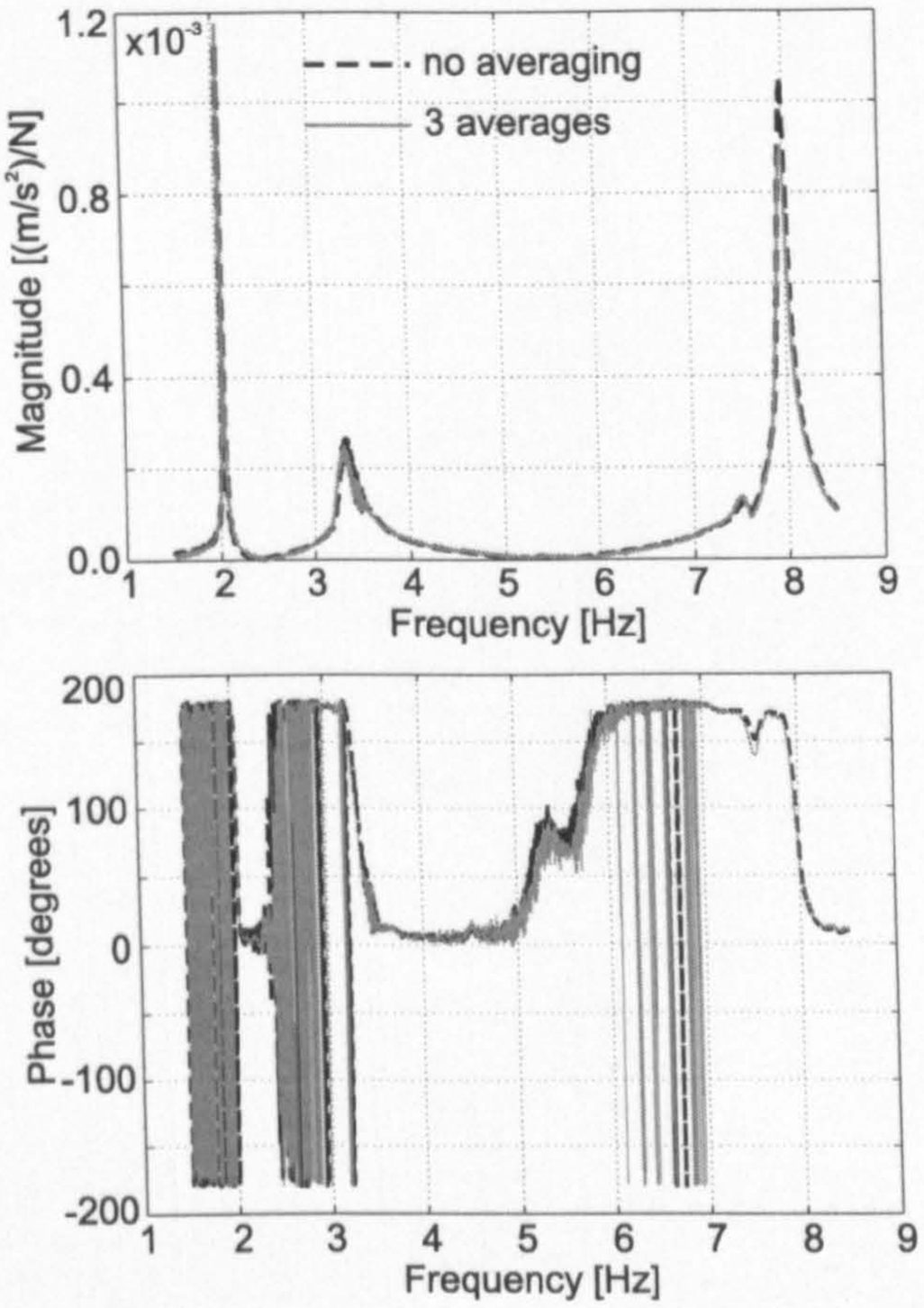

Figure 3.8: Comparison between point accelerance at TP3 with one (black-dashed line) and three averages (grey line) under the chirp excitation.

The adopted data acquisition parameters are shown in Table 3.1. However, having in mind that the modal mass is the least reliable parameter in a parameter estimation process, and that it is very sensitive to response magnitude, it was decided to conduct a single point accelerance measurement due to random excitation with 10 averages, each lasting 327.68 s, just to estimate the modal mass. Hanning window with 75% overlapping was used for this purpose. The whole exercise took about 15 minutes. This measurement was used to estimate modal mass of the second mode of vibration (i.e. first vertical mode denoted as 1VS in Figure 3.4) which dominated footbridge response under normal pedestrian traffic.

For modal testing in the horizontal lateral direction, the shaker as well as the response accelerometer were rotated by 90 degrees (Figure 3.6b). All other parameters remained unchanged.

The test in the vertical direction was completed during the first night. The whole exercise, together with (un)packing the equipment and trials took about five hours, as planned. Although the time required for the data acquisition was less than six minutes per point, the setting up time between two consecutive measurements was about 10 minutes. This long time was primarily required to allow occasional pedestrians to cross the footbridge. Having in mind low damping of the structure, the time needed for it to damp out vibrations after

these crossings was very long. Sometimes this was as long as two minutes, depending on the level of vibration induced by pedestrians. The testing in the horizontal lateral direction was conducted during the second night together with ambient measurements.

Table 3.1: Data acquisition parameters used for FRF-based testing.

Parameter	Value
Acquisition time [s]	327.68
Frequency resolution [Hz]	0.00305
Time step [s]	0.04
Sampling frequency [Hz]	25
Excitation type	linear chirp
Frequency range of excitation [Hz]	1-9
Window type	rectangular
Number of FRF averages	1
Excitation duration [s]	278

3.5.2 Ambient Vibration Survey

The ambient vibration survey was conducted after the FRF-based testing. The shaker was removed and only vertical response measurements due to ambient excitation on the empty bridge were made. The aim was to verify the results obtained by FRF-based testing, having in mind its unusual data acquisition approach (i.e. without averaging). TP3 was again chosen as the location for the reference accelerometer while the traveller accelerometer was placed only at points 4, 5, 10, 11 and 12 (Figure 3.5). This reduced measurement grid (in comparison with the FRF-based testing) was adopted due to short testing time available and difficulties in footbridge closures lasting 10 minutes at a time, as needed for AVS. For this reason the AVS work was focused on the vertical direction only as it was more critical for vibration serviceability.

The data acquisition parameters adopted in these tests are given in Table 3.2 while typical measured time history at the reference point is shown in Figure 3.9.

Table 3.2: Data acquisition parameters used for ambient vibration survey in the vertical direction.

Parameter	Value
Acquisition time [s]	600
Time step [s]	0.04
Sampling frequency [Hz]	25

The complete vertical AVS together with FRF-based testing in the horizontal direction lasted less than 4.5 hours during the second night of testing. For reference, it should be said that tests during both nights were conducted under very pleasant weather with average

temperature being around 18°C.

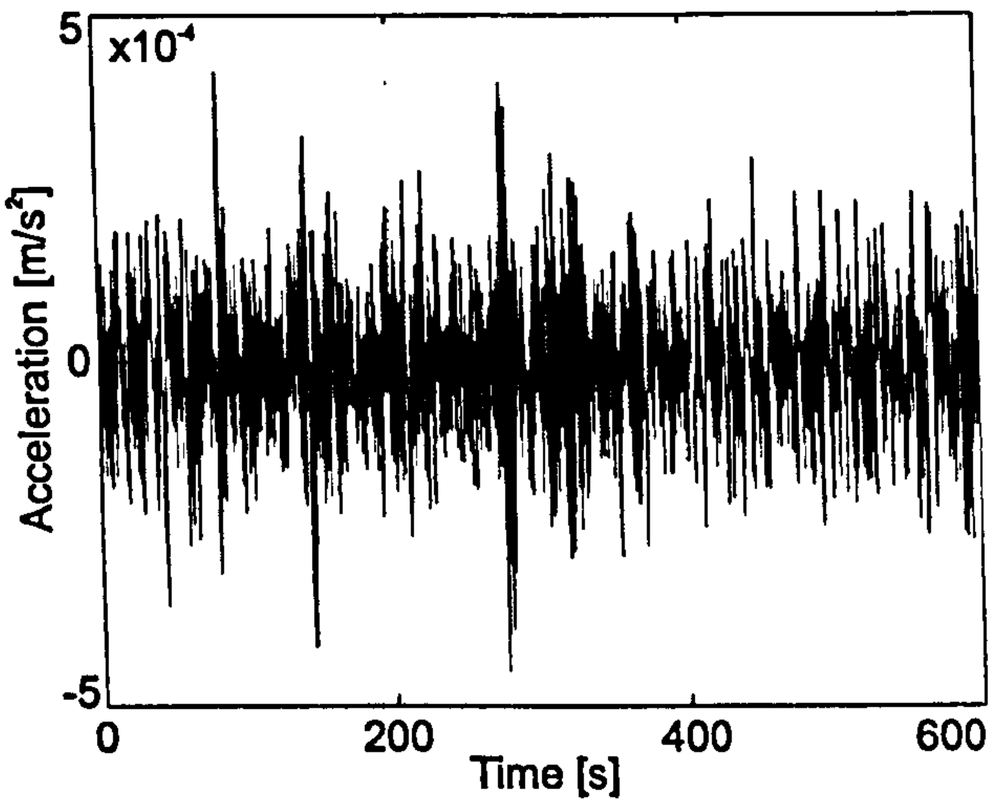

Figure 3.9: Typical acceleration signal @TP3 during AVS.

3.6 Vibration Parameter Estimation

Modal parameter estimation was performed on site for both FRF-based modal testing and AVS.

3.6.1 FRF-Based Estimates

The FRF data collected were analysed using an MDOF parameter estimation procedure available in the ICATS software (IC, 2000) under the usual assumption of linear behaviour of the footbridge for the vibration levels measured. In particular, the Non-Linear Least-Squares (NLLS1-M) method (Gaukroger et al., 1973) was applied. This method produced slightly better fits (judging them visually) than the Rational Fraction Polynomials method (Richardson & Formenti, 1982), called GRF-M in ICATS and the Global Method (Fillod et al., 1985), called GLOBAL-M. The method used is also considered as one of the most accurate single-input multiple-output FRF fitting methods (Gaukroger et al., 1973; DTA, 1995). However, it should be said that the vibration parameter estimates (natural frequencies, mode shapes and modal damping ratios) were similar across the different estimation methods, with the only exception of the damping ratio for mode 1VA which varied most. This is because this mode was quite damped (in comparison with the others) and therefore was difficult to excite.

Basically, the NLLS1-M method fits every receptance function $\alpha(\omega)$ by summing N modes as follows (Gaukroger et al., 1973; DTA, 1995):

$$\alpha(\omega) = \alpha_0 + \left[\sum_{r=1}^{N} \frac{A_r + i\omega B_r}{\omega_r^2 - \omega^2 + i2\omega\omega_r\zeta_r}\right] e^{j\phi} \tag{3.3}$$

with the aim to minimise an error function er, given in the form:

$$er = \sum_{i=1}^{L} (\hat{\alpha}_i^* - \alpha_i^*)(\hat{\alpha}_i - \alpha_i) \tag{3.4}$$

over L measured data points, each corresponding to a different discrete (forcing) frequency ω within the frequency range of interest. In Equations 3.3 and 3.4, α_i and $\hat{\alpha}_i$ represent receptance as mathematically modelled using Equation 3.3 and measured, respectively, while α_i^* and $\hat{\alpha}_i^*$ are their complex conjugates. ω_r and ζ_r are the natural frequency and damping ratio for mode r, respectively, while A_r and B_r are constants containing information about the modal mass and mode shape amplitudes related to mode r. ω is the forcing frequency within the frequency range of interest while α_0 and ϕ are introduced to compensate for measurement errors. α_0 is a complex (constant) number which covers errors due to translation of the true origin for presenting $\alpha(\omega)$ in the Nyquist plane relative to the measurement origin, while angle ϕ compensates for rotational shifts in the same Nyquist plane. One example of the Nyquist plane fitting of an isolated mode of vibration in the horizontal direction is given in Figure 3.10.

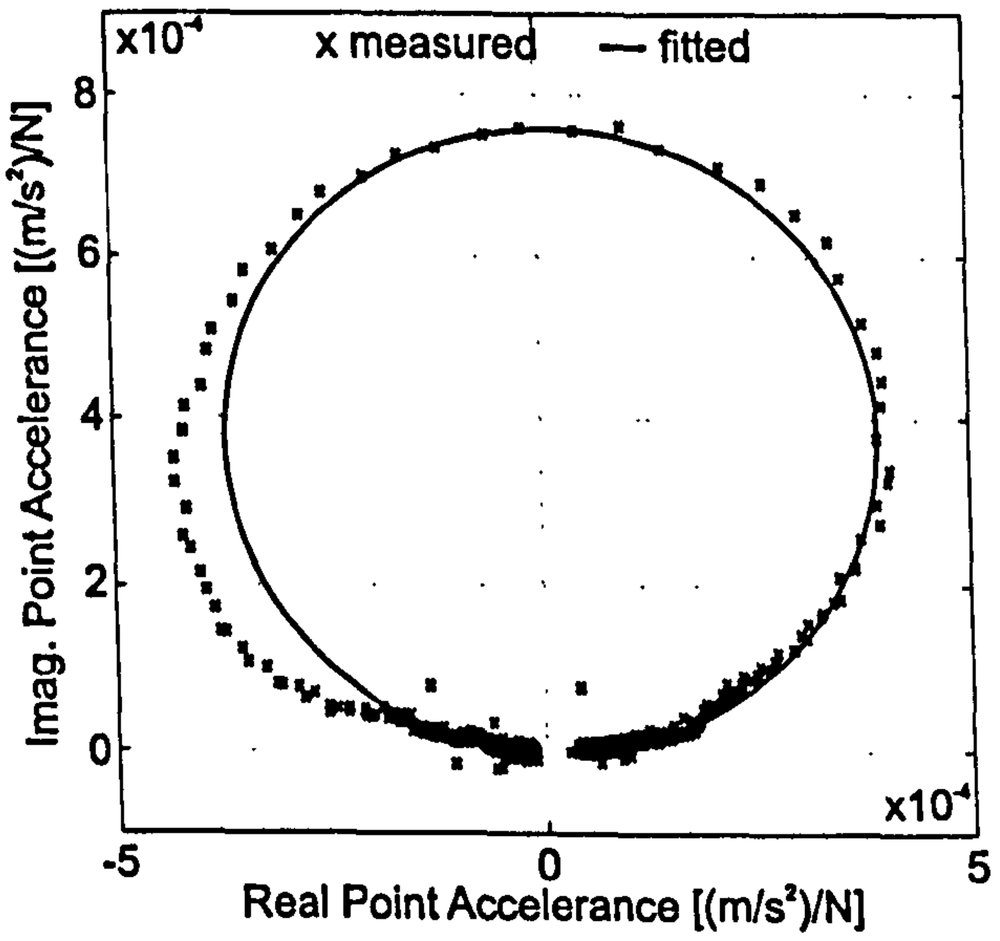

Figure 3.10: Comparison between fitted model and measured data for point accelerance in the horizontal direction in the form of a Nyquist plot. Frequency range [3.5-4.5Hz] relevant for mode 1HA is only presented.

By curve fitting modal frequencies ω_r, damping ratios ζ_r and mode shapes were identified. The seven modes identified are shown in Table 3.3 and Figure 3.11 (black dashed line).

A comparison between the measured and synthesised (via the experimentally estimated modal properties) point accelerance for the vertical direction at TP3 is shown in Figure 3.12. It suggests that the estimated modal properties did represent the measured structural behaviour very well. The mismatching of the measured and curve-fitted FRF phase around 5-6 Hz happened due to presence of a weak mode which was not identified. This is a common problem

which clearly does not affect the accuracy of the curve-fitting around strongly excited modes. The same applies to the obtained quality of analytical model representing horizontal modes which is not elaborated here further.

Table 3.3: Natural frequencies and damping ratios according to different models.

Mode	Design FEM	FRF based		AVS		Model 2	Tuned FEM
#	f [Hz]	f [Hz]	ζ [%]	f [Hz]	ζ [%]	f [Hz]	f [Hz]
1	1.66 (1HS)	1.83 (1HS)	0.26	-	-	1.82 (1HS)	1.82 (1HS)
2	1.96 (1VS)	2.04 (1VS)	0.22	2.05 (1VS)	0.29	2.02 (1VS)	2.02 (1VS)
3	2.11 (1VA)	3.36 (1VA)	1.86	3.42 (1VA)	1.04	2.36 (2VA)	3.47 (1VA)
4	3.91 (1HA)	4.54 (1HA)	0.98	-	-	4.35 (1HA)	4.36 (1HA)
5	6.16 (2VA)	7.35 (2HS)	2.68	-	-	6.52 (2VA)	7.15 (2HS)
6	6.52 (2HS)	7.56 (2VA)	0.76	7.55 (2VA)	0.76	7.13 (2HS)	7.34 (2VA)
7	7.39 (2VS)	7.98 (2VS)	0.60	8.00 (2VS)	0.44	7.56 (2VS)	7.74 (2VS)

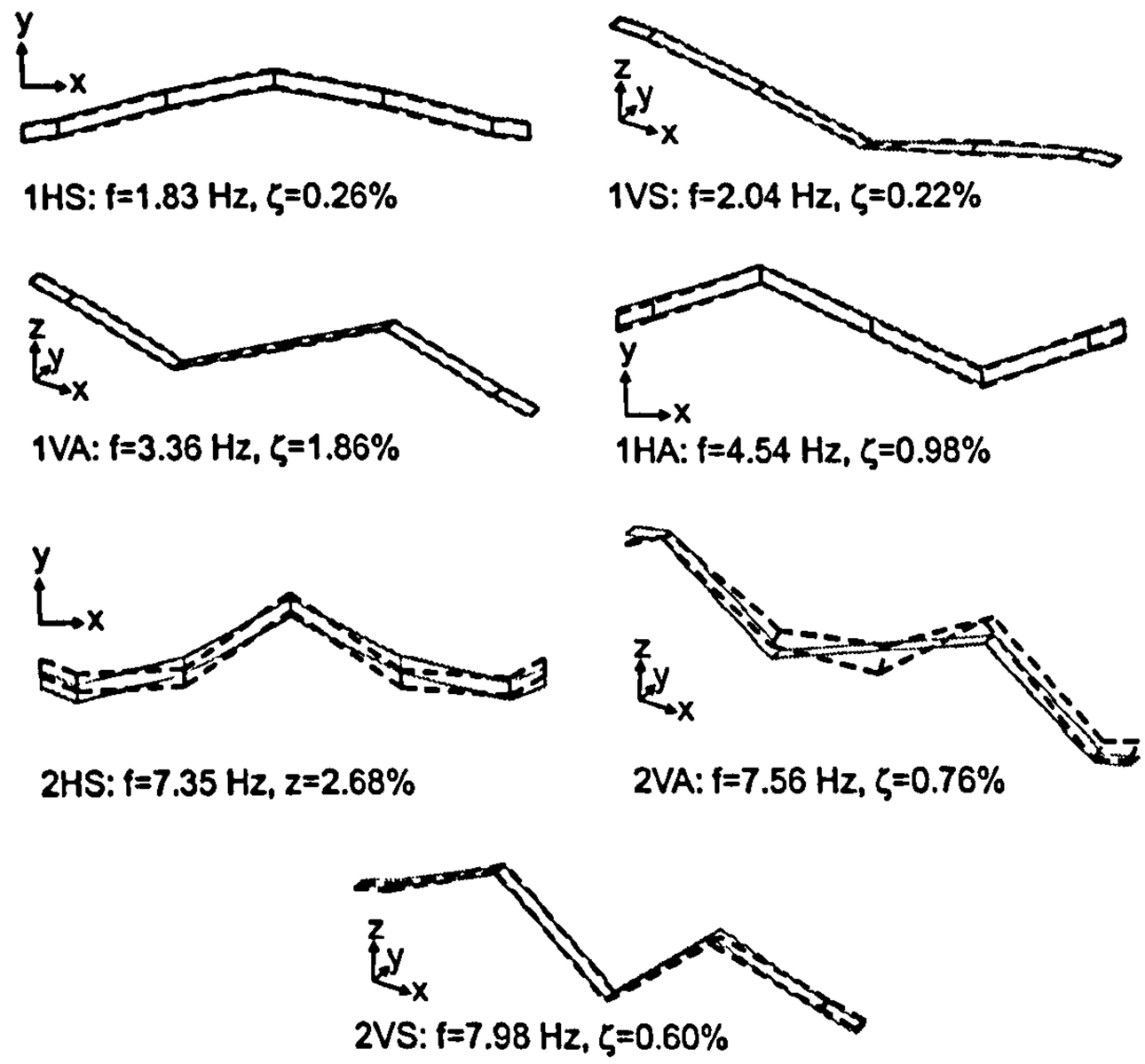

Figure 3.11: Modes identified in the FRF-based testing (black dashed line). Mode shapes obtained from tuned FE model are presented in grey (see Section 3.7).

At the end of parameter estimation process, the modal mass of the first mode of vibration in the vertical direction was calculated. This was done based on the magnitude of acceleration response measured under random excitation. The point accelerance is shown in Figure 3.13 (black dashed line), with the magnitude of 0.001036 m/s^2 under 1 N unit harmonic force. This measurement was conducted at TP3 which is an important detail considering that modal mass is usually defined with regard to the modal amplitude corresponding to an antinode (i.e. maximum amplitude in absolute sense) of a particular mode. In this case the antinode of the 1VS mode was at TP4. Therefore, the ratio between amplitudes at TP3 and TP4,

obtained from experimental mode shapes shown in Figure 3.11, was used as a scaling factor for both the force and response magnitude at TP4. In this way the modal mass m_{1VS} can be calculated from the formula for steady state response under sine resonant excitation (Clough & Penzien, 1993):

$$m_{1VS} = \frac{F_4}{2\zeta_{1VS}a_4} = \frac{\frac{\phi_{3,1VS}}{\phi_{4,1VS}}F_3}{2\zeta_{1VS}(\frac{\phi_{4,1VS}}{\phi_{3,1VS}}a_3)} = \frac{\frac{0.002492}{0.005061}\cdot 1.0}{2\cdot 0.003\cdot(\frac{0.005061}{0.002492}\cdot 0.001036)} = 53,188\,\mathrm{kg}\,. \quad (3.5)$$

Here, $\phi_{3,1VS}$ and $\phi_{4,1VS}$ are mode shape ordinates for mode 1VS at TP3 and 4, respectively, as obtained from curve fitting, F_3 and F_4 are resonant sine force amplitudes at points 3 and 4, while a_3 and a_4 are corresponding measured acceleration amplitudes. ζ_{1VS} is the estimated damping ratio for mode shape 1VS.

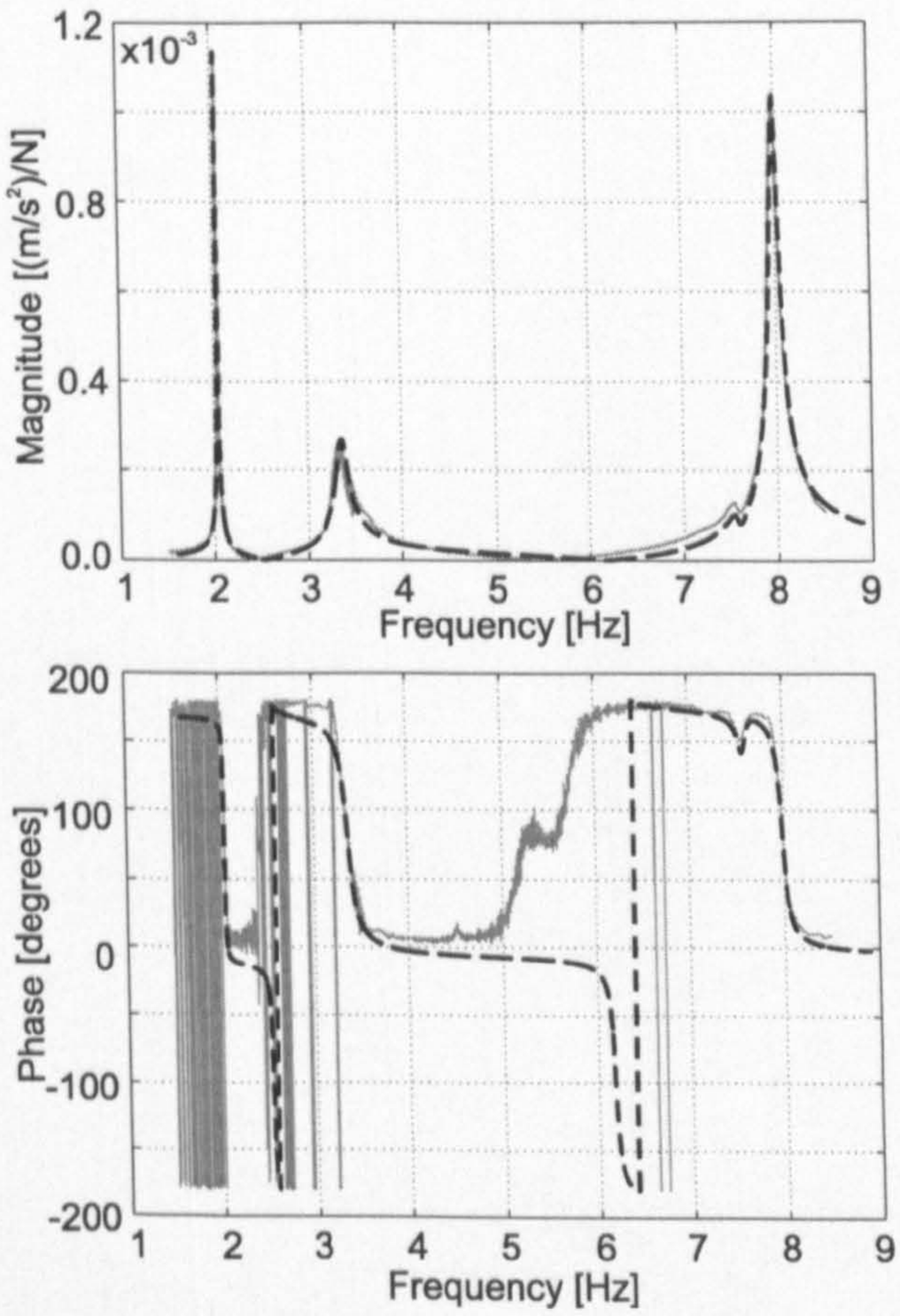

Figure 3.12: Comparison between the point accelerance for the vertical direction as measured (grey line) and as modelled (black dashed line).

If the modal mass is estimated in the same way, but using the point accelerance FRF obtained via the unaveraged chirp excitation (grey line in Figure 3.13), then a mass of 48,763 kg is obtained. This indicates the high level of sensitivity of the estimate of modal mass.

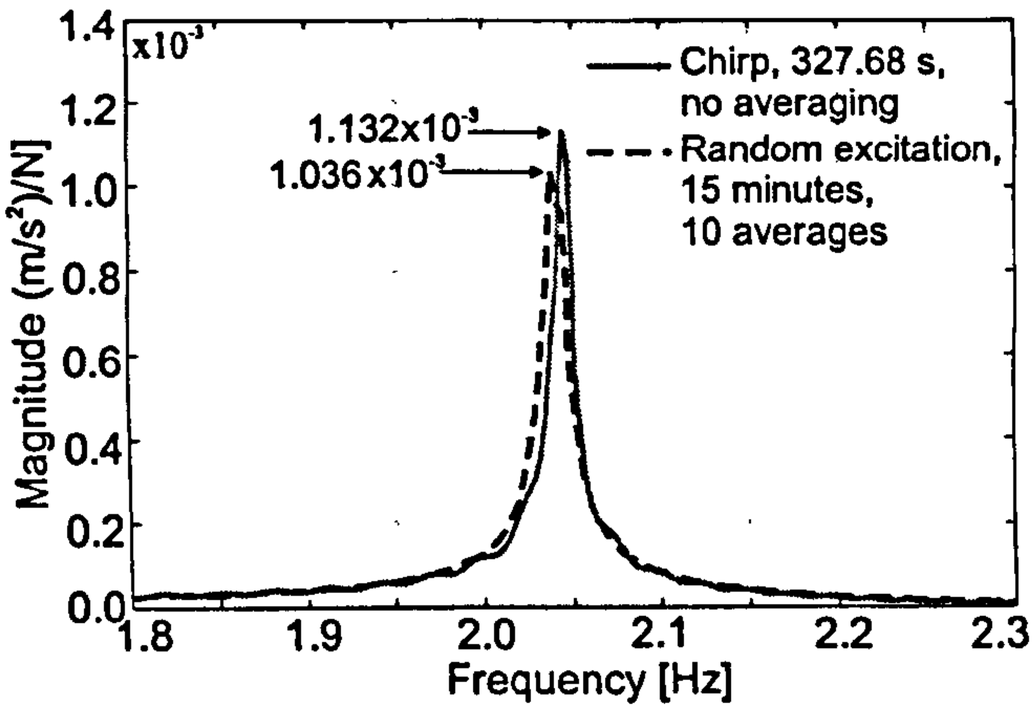

Figure 3.13: Magnitude of accelerance in the first vertical mode of vibration due to two different types of excitation.

3.6.2 AVS-Based Estimates

For parameter estimation using the AVS data, the ARTeMIS software (SVS, 2004) was used. The Canonical Variate Analysis (CVA) identification method (Peeters, 2000), which is a time-domain parameter estimation technique, was chosen. This is one of the so called 'data-driven' stochastic subspace identification methods. This means that the method fits the raw measured time-domain data directly, instead of fitting the covariances (Peeters, 2000) produced using data from different test points. The starting point in the method is to present the dynamics of a structure under unknown environmental excitation in the discrete-time state-space form, assuming structural linearity and time-invariability, as follows (Peeters, 2000):

$$\{\mathbf{x}_{k+1}\}_{n\times 1} = [\mathbf{A}]_{n\times n}\{\mathbf{x}_k\}_{n\times 1} + \{\mathbf{w}_k\}_{n\times 1} \tag{3.6}$$

$$\{\mathbf{y}_k\}_{p\times 1} = [\mathbf{C}]_{p\times n}\{\mathbf{x}_k\}_{n\times 1} + \{\mathbf{v}_k\}_{p\times 1} \tag{3.7}$$

where Equation 3.6 is typically called the state equation while Equation 3.7 is called the observation/output equation. The state equation is sufficient to describe dynamics of the system (instead of using the well-known equation of motion) with $\frac{n}{2}$ degrees of freedom, where n is called the model order. Here, $\{\mathbf{x}_k\} = \{\mathbf{x}(k\Delta t)\}$ is the discrete time state vector containing $\frac{n}{2}$ displacements and $\frac{n}{2}$ velocities describing the *state* of the system at time instant $t_k = t(k\Delta t)$, $\{\mathbf{x}_{k+1}\}$ is the same vector defined at time $t_{k+1} = (k+1)\Delta t$, $[\mathbf{A}]$ is the discrete state matrix dependent on the mass, stiffness and damping properties of the structure, while $\{\mathbf{w}_k\}$ represents the inevitable but unmeasured noise input as well as the noise present due to modelling inaccuracies at time t_k. The observation equation calculates the response of the structure $\{\mathbf{y}_k\}$ at p measurement locations at time t_k via the state vector $\{\mathbf{x}_k\}$. Here, $[\mathbf{C}]$ is the discrete output matrix whose main purpose is to map the state vector into the measured

output, while $\{\mathbf{v}_k\}$ represents the noise due to measurements and unmeasured noise input at time t_k.

It can be shown that modal properties (natural frequencies, mode shapes and damping ratios) of a structure under white-noise excitation can be identified by relying only on the measured output responses $\{\mathbf{y}_k\}$ (Peeters, 2000). However, models of different order will typically produce more or less different estimates. This is the reason to consider several models of different order and to choose the one with the lowest level of error obtained when comparing the measured and analytically predicted outputs. This is how the optimum models were selected for data sets at all five test points while analysing the Podgorica footbridge ambient responses. An example of this process is shown in Figure 3.14 which shows that there are four stable modes identified in all five measurement sets corresponding to the five test points (connected by lines in Figure 3.14).

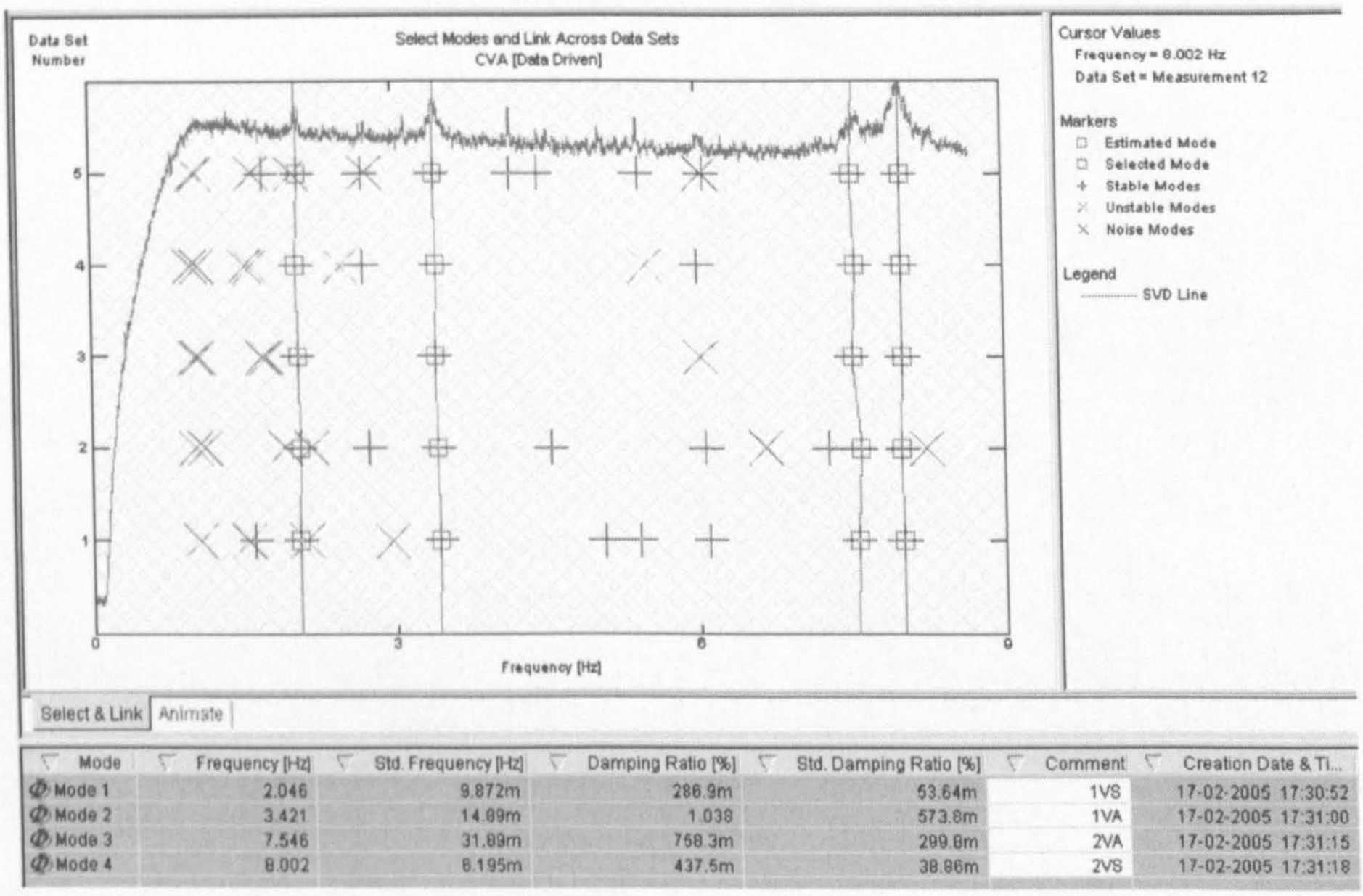

Mode	Frequency [Hz]	Std. Frequency [Hz]	Damping Ratio [%]	Std. Damping Ratio [%]	Comment	Creation Date & Ti...
Mode 1	2.046	9.872m	286.9m	53.64m	1VS	17-02-2005 17:30:52
Mode 2	3.421	14.89m	1.038	573.8m	1VA	17-02-2005 17:31:00
Mode 3	7.546	31.89m	758.3m	299.8m	2VA	17-02-2005 17:31:15
Mode 4	8.002	6.195m	437.5m	38.86m	2VS	17-02-2005 17:31:18

Figure 3.14: Stable modes identified in AVS. Natural frequencies and damping ratios are listed below the diagram and in Table 3.3.

These identified modes are listed in Table 3.3. The identified natural frequencies compared well with those from the FRF-based modal testing procedure. Regarding damping ratios, the largest difference was for mode 1VA. However, the reliability of this damping ratio as identified by AVS is not very high as the scattering across the data sets, expressed as the standard deviation, is as high as 0.57% in comparison with the average (i.e. identified) damping ratio of 1.04% (Figure 3.14). As mentioned earlier the estimation of the damping ratio for this mode was least reliable in the FRF based-testing too. The agreement between the mode shapes in the two methods was good as checked by visual inspection. The signal processing parameters used as input in the ARTeMIS software are given in Table 3.4.

Table 3.4: Signal processing setup as adopted in data analysis in ARTeMIS.

Parameter	**Value**
Acquisition time per point [s]	600
Time step [s]	0.04
Filter type	high-pass Butterworth
Filter order	8
Filter cut-off frequency [Hz]	1

Also, it should be said that differences in damping ratios in the two experimental methods may be due to amplitude dependent damping as the level of vibration during the AVS was up to two orders of magnitude lower than during the FRF measurements. However, it was interesting to additionally check the damping value for a lively mode 1VS, since this value is particularly important for vibration serviceability assessment of the footbridge. For this, the vertical acceleration response to a pedestrian crossing the bridge with controlled step frequency at approximately 2.04 Hz (metronome set at 122 beats per minute), was measured at the middle of the bridge. After the pedestrian crossed the bridge, the free decay of the response was also recorded. The measured response (bandpass filtered with centre frequency of 2.04 Hz) is shown in Figure 3.15a.

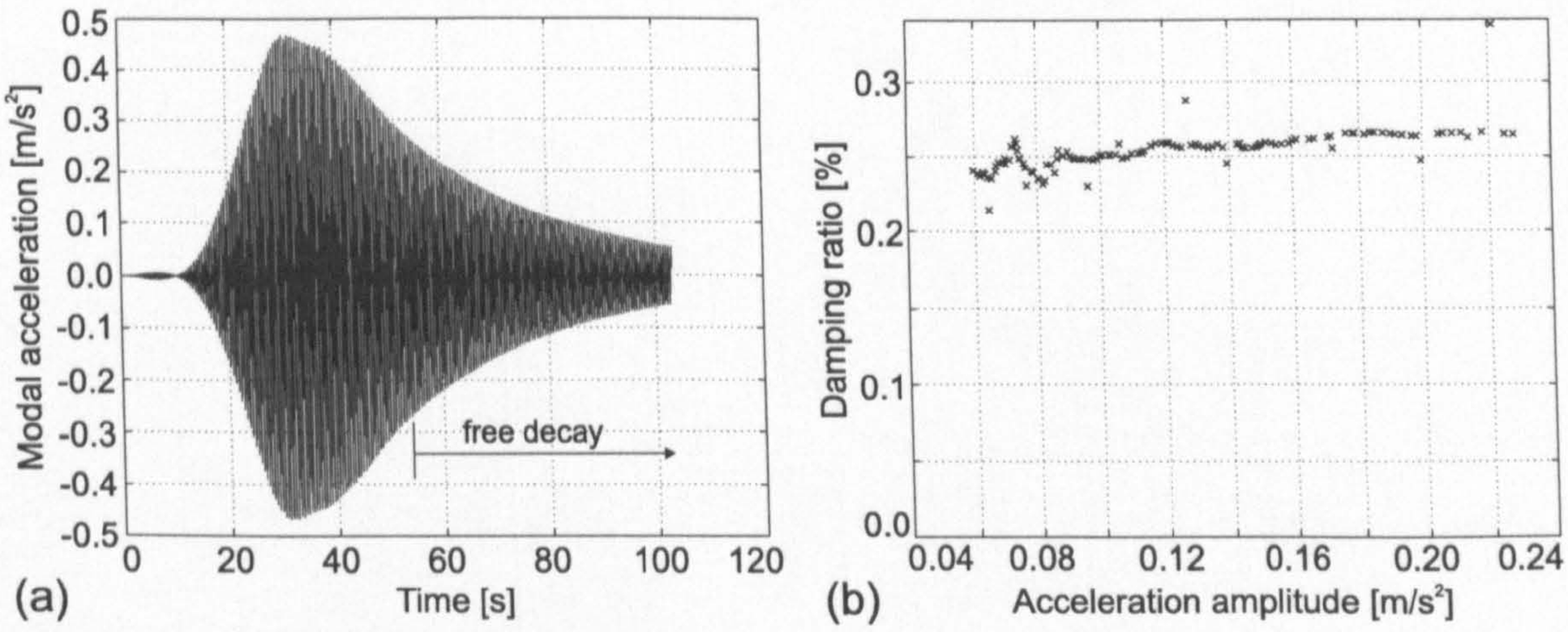

Figure 3.15: (a) Acceleration response due to a pedestrian crossing at step frequency of 2.04 Hz. (b) Damping estimate from the free decay.

Using the logarithmic decrement method (Maia et al., 1997), the damping ratio was estimated for a number of data blocks, each containing eight subsequent cycles of decaying vibration. For this, the MATLAB-based MODAL software developed by Prof. James Brownjohn of Sheffield University, was utilised. Each of these blocks corresponds to slightly different amplitude of the middle cycle and can be used to estimate damping as a function of this amplitude (Figure 3.15b). It can be seen that the damping was weakly dependent on the vibration amplitude, but its average value of 0.26% agreed well with those measured during modal testing.

3.7 FEM Tuning

A comparison between vibration modes obtained experimentally and analytically revealed that all seven mode shapes measured (Figure 3.11) had their counterparts in the design FE model (Figure 3.4). However, the sequence of 2VA and 2HS FE modes was reversed compared with their experimental counterparts (Table 3.3). Also, the FE model underestimated frequencies for all vibration modes, the maximum difference being 37% for mode 1VA. On the other hand, the correlation between mode shapes was good with the modal assurance criterion (MAC) values (Maia et al., 1997) higher than 0.90, except for modes 2HS (0.82) and 2VA (0.84). This implied that there was a problem with inadequate modelling which underestimated the stiffness consistently throughout the whole footbridge. This was despite the fact that the FE model was as detailed as possible using all available design information and based on best engineering judgement.

Some of the differences in the numerical and experimental natural frequencies were significant and somewhat surprising. They prompted the author to do an additional search for information about the properties of the as-built bridge. It was discovered that during the previously described strengthening of the footbridge, the plates which constitute the box cross section of the inclined columns were also strengthened (Djuranović, 2002). These data were missing from the design documentation available for developing the design FE model. As a consequence, the design FE model could not simulate the real behaviour of the footbridge accurately. It should be said that this situation with missing technical information is quite typical when retrofitting structures that are relatively old.

Apart from the fact that the strengthening took place no precise information was available about the actual thickness of the additional plates. Therefore, it was assumed that they were two times thicker than in the design FE model (6.0 and 4.0 cm instead of 3.0 and 2.0 cm, respectively). This improved considerably the correlation between the FE model and experimental results, especially for horizontal modes ('Model 2' in Table 3.3). However, the differences in some of the vertical modes were still quite high. This especially applies for the vertical anti-symmetric modes (1VA and 2VA). Since the movement of the columns was very strong in these modes an attempt to better correlate the FE model with the experimental data was made through further increase of the column stiffness. However, this required a physically unacceptable column thickness of about 25 cm. Because of this, the sensitivity of the vertical anti-symmetric modes to some other uncertain FE modelling parameters was considered. These were: the thickness of the composite slabs, their dynamic modulus of elasticity, mass of the water pipes with water in them and stiffness of additional elastic supports at both ends of the bridge girder in the longitudinal direction (horizontal springs instead of free edge, see Figure 3.16). It was found that the stiffness of the horizontal support springs in the longitudinal direction was the only parameter which increased the frequencies of vertical modes as required. Elastic springs (ANSYS COMBIN14 element), having stiffness of 10^8 N/m per metre length of the width of the bridge deck, were adopted. The physical

explanation of this is the restraint condition caused by the expansion joint between the bridge deck and the walking path used to approach the bridge. For low-level vibration this expansion joint was very much 'stuck' introducing additional support condition. In addition, it might be that for low-level vibration the friction in the longitudinal direction in bearings at the ends of the box girder could not be overcome.

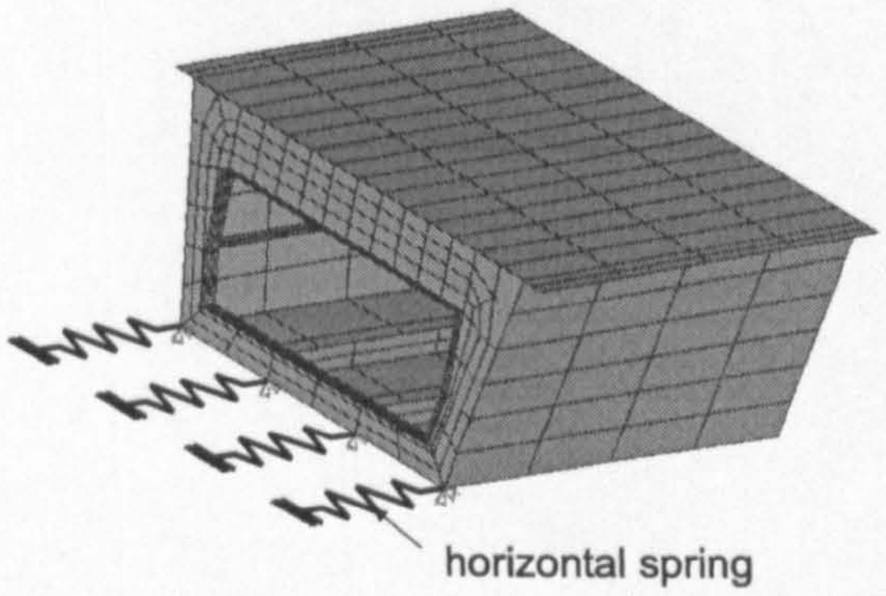

Figure 3.16: The horizontal springs at the girder ends added to the design FE model.

In this way the correlation with the experimental data was significantly improved, with the sequence of modes now being the same as obtained experimentally ('Tuned FEM' in Table 3.3). The maximum difference in natural frequencies was reduced to a reasonable 4% for mode 1HA. The MAC values increased for all modes except for 2HS, which was now 0.81 - still quite acceptable. All FE mode shapes are presented as a grey line in Figure 3.11. Clearly, this tuned FE model simulated the footbridge vibration much better than the design FE model. It was subsequently possible to update automatically this manually tuned FE model, contrary to the design FE model. The design FE model had modes that were simply too far away from their measured counterparts for the automatic updating to be successful. This is another key benefit of the manual tuning, apart from learning about the actual as-built structural behaviour. The results of automatic updating of this FE model are described in the next chapter.

3.8 Conclusions

An FRF-based modal testing conducted to identify dynamic properties of a lively steel box girder footbridge successfully identified the seven lowest modes of vibration in both the vertical and horizontal-lateral directions. The testing procedure, based on chirp excitation by an electrodynamic shaker, was efficient and sufficiently accurate, even though only two channels were used during the FRF measurements and the traditional signal averaging was not performed. These results compared well with those obtained in an ambient vibration survey conducted in the vertical direction only. It was found that the footbridge had very low damping ratio associated with the lowest horizontal-lateral and vertical modes of vibration of only about 0.26% for both modes. This low damping, together with the natural frequency

of 2.04 Hz for the vertical mode, being in the frequency range of normal human walking, contributed to the footbridge liveliness.

A detailed design FE model, which was developed based on the design data available and best engineering judgement, significantly underestimated some of the measured natural frequencies of the structure. This was somewhat surprising and the experimental results proved to be crucial in identifying drawbacks in the FE modelling. It was found that missing design information about the strengthening of the columns was responsible for the general underestimation of natural frequencies, mainly for the horizontal-lateral modes. Moreover, the stiffness of additional horizontal spring supports (in the direction along the footbridge) at the ends of the girder had a significant influence on the vertical modes of vibration. The effect and presence of this stiffness was not anticipated during development of the design FE model which assumed that the expansion joints introduced no stiffness in the longitudinal direction. This type of modelling error is hard to avoid due to difficulties in simulating the real boundary conditions. Manual tuning by trial and error of these two modelling parameters improved significantly the FE model and its correlation with the experimental model, reducing the maximum difference in the natural frequencies from 37% to only 4%. Without this tuning it was impossible to perform automatic updating due to large differences between the measured and analytically predicted natural frequencies using the design FE model. After the tuning, automatic updating was successfully carried out and is presented in Chapter 4. In conclusion, if required after construction, FE models used in design should be critically evaluated, parametrically studied and, if possible, manually updated based on experimental data.

Preface to Chapter 4

Chapter 4 describes the second phase in establishing reliable vibration properties of the Podgorica footbridge introduced in Chapter 3. This phase deals with the automatic updating of the finite element (FE) model described in the previous chapter, by using the specialised FEMtools software. The aim of this work was to experiment with the advanced FE model updating technology and to improve further the correlation between the experimental results and FE model. In this way, modal properties of the footbridge (mode shapes, natural frequencies, modal masses and damping ratios) could be estimated and used for its vibration serviceability assessment.

Since the chapter is written in form of a paper to stand alone, it was necessary to briefly review some information from the previous chapter regarding the FE model development and its manual tuning, before implementing the automatic updating procedure itself. Moreover, in order to avoid confusion, it should be said here that the starting model for the analysis in Chapter 4 was the one that includes more recently found information about column strengthening that was not available when developing the very first model (called 'Design model') in Chapter 3. Therefore, the 'Initial model' described in Chapter 4 is actually the same as 'Model 2' from Chapter 3.

Chapter 4

Finite Element Modelling and Updating of Podgorica Footbridge

This chapter, in an amended form, has been provisionally accepted for publication under the following reference:

Živanović, S., Pavic, A. and Reynolds, P. Finite Element Modelling and Updating of a Lively Footbridge: The Complete Process, Journal of Sound and Vibration.

Abstract

The finite element (FE) model updating technology was originally developed in the aerospace and mechanical engineering disciplines to automatically update numerical models of structures to match their experimentally measured counterparts. The process of updating identifies the drawbacks in the FE modelling and the updated FE model could be used to produce more reliable results in further dynamic analysis. In the last decade the updating technology has been introduced into civil structural engineering. It can serve as an advanced tool for getting reliable modal properties of large structures. The updating process has four key phases: initial FE modelling, modal testing, manual model tuning and automatic updating (conducted using specialist software). However the published literature does not connect well these phases, although this is crucial when implementing the updating technology. This chapter therefore aims to clarify the importance of this linking and to describe the complete model updating process as applicable in civil structural engineering. The complete process consisting of the four phases is outlined and brief theory is presented as appropriate. Then, the procedure is implemented on a lively steel box girder footbridge. It was found that even a very detailed initial FE model underestimated the natural frequencies of all seven experimentally identified modes of vibration, with the maximum error being almost 30%. Manual FE model tuning by trial and error found that flexible supports in the longitudinal direction should be introduced at the girder ends to improve correlation between the measured and FE-calculated modes. This significantly reduced the maximum frequency error to only 4%. It was demonstrated that only then could the FE model be automatically updated in a meaningful way. The automatic updating was successfully conducted by updating 22 uncertain structural parameters. Finally, a physical interpretation of all parameter changes is discussed. This interpretation is often missing in the published literature. It was found that the composite slabs were less stiff than originally assumed and that the asphalt layer contributed to the deck stiffness.

4.1 Introduction

As civil engineering structures, and in particular footbridges, are becoming increasingly slender due to improvements in construction materials and technology, they are also becoming lighter and less damped. In principle, this means that new footbridge structures tend to be easier to excite than older ones and there is a higher potential for vibration serviceability problems to occur. This has already been experienced by many new structures in the last decade - the new London Millennium Bridge (Dallard et al., 2001c) being a particularly high-profile example. For slender and lightly damped bridges, their dynamic response due to near-resonant excitation governs their vibration performance. When doing response calculations in design, simulation of this type of near-resonant dynamic response is very sensitive to even small variations in modal properties, such as damping ratio, natural frequency and modal mass. These are key input parameters in the analysis. Therefore, knowing modal properties of a footbridge, together with its mode shapes, as precisely as possible has become very important. This is important not only for the design of new structures with similar layouts, but also for the rectification of existing lively footbridges, as well as for seismic analysis and general research into vibration serviceability. However, despite the huge importance of modal properties in the assessment of vibration performance of footbridges, their reliability when predicted via finite element (FE) modelling is still rather uncertain. The main reason for this is the general lack of information on modal properties of as-built footbridge structures and their correlation with FE modelling based on design data and best engineering judgement.

Developing a numerical model of a civil engineering structure that has sufficiently reliable dynamic properties is a complex issue. It requires a rather wide range of skills and expertise in areas as diverse as FE modelling, modal testing of full-scale structures and FE model correlation, tuning and updating with regard to experimentally obtained modal properties. This methodology is nowadays used routinely in the mechanical and aerospace engineering disciplines, where prototyping is part of a normal design process of structures subjected to dynamic loading.

Unfortunately, prototyping is not common in civil structural engineering design. Therefore, all this cannot be done easily during the design (of, say, a footbridge) bearing in mind that the modal testing can be conducted only on an already built structure, which is a unique 'prototype' never to be built again. Thus, it may appear that the whole idea of getting reliable structural modal properties by FE modelling, modal testing, and FE model correlation and updating is pointless in the case of civil engineering structures after they are built. However, this is not the case as exercises like this are the only reliable way to gauge our ability to predict vibration behaviour of future civil engineering structures. The whole process of FE modelling, modal testing, and FE model correlation and updating adds to the currently very limited body of knowledge on vibration performance of as-built structures with significant potential to use this knowledge in future designs.

Therefore, the aim of this chapter is to demonstrate the complete combined analytical and

experimental process required to obtain as reliable as possible estimates of modal properties of a steel box girder footbridge. For this purpose, every phase of the process and its purpose will be first explained briefly, with particular attention paid to the automatic FE model updating procedure, which is a new technology still not used commonly in civil engineering.

However, in current civil structural engineering design practice, it has become common to develop an FE model of the structure and use it for calculation of its static and/or dynamic responses. To obtain a good model it is necessary to reduce the mathematical modelling errors to an acceptable level. Therefore, the assumptions on which the model is based should be evaluated carefully. Nevertheless, even with most careful and detailed numerical modelling based on design data available and best engineering judgement, differences regularly occur between the modal properties of an as-built structure and their counterparts predicted numerically. This is typically due to inevitable uncertainties linked with modelling of, in the case of footbridges, boundary conditions, material properties, and effects of non-structural elements, such as handrails and asphalt.

The errors in the natural frequencies for footbridges predicted by very reasonable FE model in the design can be as large as 37% (Deger et al., 1996). Not surprisingly, it is now widely accepted that modal testing is much more reliable way for estimating dynamic properties of as-built structures than FE modelling (Mottershead & Friswell, 1993; Modak et al., 2002).

Once the modal dynamic properties of a footbridge (mainly natural frequencies and mode shapes) are identified experimentally and the level of error introduced by the initially developed FE models is identified, then drawbacks in the FE modelling can be found and the initial FE model can be corrected. This procedure is called FE model updating, and can be considered as an attempt to use the best features from both the experimental and analytical model (Modak et al., 2002). The former gives more reliable modal properties of the structure, including modal damping which cannot be obtained analytically, while the latter retains very detailed representation of the structure.

In this chapter, first presented is a background review regarding the FE model updating technology. This is followed by examples of implementation of the procedure in civil structural engineering, especially in bridge engineering. After this, a lively steel box girder footbridge is briefly described and the initial FE model is presented. After the presentation of experimentally identified modal properties obtained in Chapter 3, the manual tuning necessary to prepare the FE model for an automatic updating is given. Then, a sensitivity-based automatic model updating is conducted and results are discussed.

4.2 Background Review

In this section general information about FE model updating techniques is given first, followed by their implementation in civil structural engineering.

4.2.1 Finite Element Model Updating

The FE model updating procedure typically minimises the differences between FE and experimentally estimated modal properties. This is done by changing some uncertain FE modelling parameters which have the potential to influence modal properties. The resulting FE model can then be used in further analyses.

The updating process typically consists of manual tuning and then automatic (or formal) model updating using some specialised software. The manual tuning involves manual changes of the model geometry and modelling parameters by trial and error, guided by engineering judgement. The aim of this is to bring the numerical model closer to the experimental one. Often, in this process an analyst is able to improve the initial structural idealisation typically related to boundary conditions and non structural elements. This process usually includes only a small number of key parameters manageable manually. The aim of automatic updating is to improve further the correlation between the numerical and experimental modal properties by taking into account a larger number of uncertain parameters.

The term 'parameter' is used here for all input values which define the numerical model. Moreover, all measured modal properties which are targeted in the updating process will be called 'target responses' hereafter.

It is important to emphasise here that not all FE models of a structure can be updated. To have a successful automatic updating of an FE model, it is necessary to prepare the initial FE model for it. To do this, firstly it would be necessary to minimise discretisation errors and to use modelling strategies which can represent truly all important aspects of structural behaviour and geometry (Brownjohn et al., 2001; Chen & Ewins, 2001). This means that careful attention should be paid to model geometry and various other details. This is important because the automatic model updating procedure cannot easily correct large errors in the geometry of the initial modelling. It can only rectify the errors caused by uncertainties of modelling parameters in a geometrically well defined model. Also, when preparing the FE model for the automatic updating, the differences between analytical and experimental modal responses (usually natural frequencies and mode shapes) should be as small as practicable. If they are too large, the automatic updating procedure can have numerical difficulties and/or produce physically unrealistic parameter changes during the updating process. These are reasons to recommend the manual tuning (by trial and error and engineering judgement) of the initial FE model first. The tuned model should therefore feature meaningful starting parameters for the formal updating (Pavic et al., 1998; Brownjohn & Xia, 2000).

Formal FE model updating is now a mature technology. It is widely used in the mechanical and aerospace engineering disciplines to update analytical models of structural prototypes. A large number of updating procedures exist (Mottershead & Friswell, 1993; Friswell & Mottershead, 1995) and their detailed discussion is beyond the scope of this work. Here, only the principles on which model updating is based are reviewed briefly.

4.2.2 Basic Theory Used in FE Model Updating

The main idea in formal FE model updating of minimising the differences between the analytical and experimental models is, in essence, an optimisation problem. This problem can be solved in many different ways. In general, there are two groups of updating methods: direct methods and iterative (or parametric) methods. The former are based on updating of stiffness and mass matrices directly, in a way that often has no physical meaning. The latter, on the other hand, concentrates on the direct updating of physical parameters which indirectly update the stiffness and mass matrices in which these parameters feature (Modak et al., 2002; Kim & Park, 2004). Iterative methods are slower than their direct counterparts. However, their main advantage is that changes in the updated model can be interpreted physically. Also, iterative methods can be implemented easily using existing FE codes (Wu & Li, 2004). These are the main reasons why iterative methods are widely accepted and now used almost exclusively in the updating exercises. This link between the iterative updating and the physical world is very important in civil structural engineering and is the main reason why only this type of updating is considered in this chapter. Numerous examples of implementation of direct methods, mainly in mechanical engineering and control theory, can be found elsewhere (Minas & Inman, 1990; Friswell & Mottershead, 1995; Cha & Tuck-Lee, 2000).

The iterative methods are mainly sensitivity based. This requires the sensitivity matrix [S] to be calculated in every iteration. The sensitivity matrix is a rectangular matrix of order $m \times n$, where m and n are the number of target responses and parameters, respectively (DDS, 2004). Its element S_{ij} can be defined as:

$$S_{ij} = \frac{\delta R_i}{\delta P_j}, \tag{4.1}$$

and it represents the sensitivity of the target response R_i $(i = 1, 2, ..., m)$ to a certain change in parameter P_j $(j = 1, 2, ..., n)$. Operator δ presents the variation of the variable. Elements of the sensitivity matrix can be calculated numerically using, for example, the forward finite difference approach (DDS, 2004):

$$S_{ij} = \frac{R_i(P_j + \Delta P_j) - R_i(P_j)}{(P_j + \Delta P_j) - P_j} \tag{4.2}$$

where $R_i(P_j)$ is the value of the i^{th} response at the current state of the parameter P_j, while $R_i(P_j + \Delta P_j)$ is the value of the same i^{th} response when the parameter P_j is increased by value ΔP_j.

Obviously, for calculation of the sensitivities, the relevant target responses and structural parameters should be selected. The target responses should be chosen between those measured. The responses which are mainly considered in civil engineering applications are natural frequencies, mode shapes and frequency response functions (FRFs), or some combination of these. The choice depends on the measured data available, their quality, and (non)existence

of close modes (Mottershead & Friswell, 1993). As a rule, only high quality measured modal properties should be used as target responses. As natural frequencies are normally measured quite accurately, they are almost always selected. If close modes are present, FRFs might be a better choice for target responses.

Selection of updating parameters is probably the most important step on which the success of the model updating depends. It is recommended to choose uncertain parameters only, and between them to choose those to which the selected target responses are most sensitive. Also, the number of parameters should be kept to an absolute minimum. All this is to avoid numerical problems due to ill-conditioning (Kim & Park, 2004).

Once relevant (measured) target responses and structural parameters for updating have been selected, the sensitivity matrix can be calculated. Since in the iterative model updating process the updating parameters change at every step, the sensitivity matrix has to be re-calculated in each iteration. Let us denote, for a given iteration, the starting parameter and response vectors as $\{\mathbf{P}_0\}$ and $\{\mathbf{R}_0\}$, respectively. The vector of updated parameters in the current iteration is $\{\mathbf{P}_u\}$, while the target response vector obtained experimentally is $\{\mathbf{R}_e\}$. The targeted experimental response vector $\{\mathbf{R}_e\}$ can be approximated via vectors $\{\mathbf{R}_0\}$, $\{\mathbf{P}_u\}$ and $\{\mathbf{P}_0\}$ using the linear term in a Taylor's expansion series:

$$\{\mathbf{R}_e\} \approx \{\mathbf{R}_0\} + [\mathbf{S}]\left(\{\mathbf{P}_u\} - \{\mathbf{P}_0\}\right). \tag{4.3}$$

The iterative process is required here because the relationship between target responses and parameters that is mainly non-linear is approximated by the linear term. This means that updating parameters need to be changed by a small amount in each iterative step until the required minimum difference between the calculated and experimentally measured responses is achieved. Therefore, the finally updated parameters cannot be calculated in a single step (Collins et al., 1974).

The task of updating aimed at finding parameter values $\{\mathbf{P}_u\}$ in the current iteration can be solved in different ways such as using a pseudo-inverse (least squares) method, weighted least squares or Bayesian method. This depends on whether weighting coefficients for parameters and/or target responses are used as is the case in last two methods (Wu & Li, 2004). The purpose of these weighting coefficients is to give different significance to numerical parameters and measured target responses depending on the confidence in these data. For example, weighting coefficients for responses take into account the confidence in the measured values, which is typically higher for natural frequencies than for mode shapes. Weighting coefficients for input parameters take into account the degree of uncertainty in them. The more uncertain a parameter is, the lower is the confidence in it, which means that the weighting value is lower too.

If a Bayesian method is chosen, which is often the case in the commercially available model updating software, then the aim of the updating procedure is not to simply minimise the difference between numerical and measured target responses. Instead, an error function which

includes differences, not only between the target experimental and numerical responses, but also between updating parameters in two successive iterations as well as parameters and target responses' weights, is defined. In this way the aim of the updating procedure is to minimise response differences $\{\Delta\mathbf{R}\}$ and simultaneously to ensure convergence of the process via minimisation of parameter differences $\{\Delta\mathbf{P}\}$ in two successive iterations. Therefore, this error function is, in general, defined as a function of input parameters and target responses, as well as the weighting factors. The error function used for the case study presented in this chapter is defined as (DDS, 2004):

$$E(\{\Delta\mathbf{R}\},\{\Delta\mathbf{P}\},[\mathbf{C}_R],[\mathbf{C}_P]) = \{\Delta\mathbf{R}\}^T\cdot[\mathbf{C}_R]\cdot\{\Delta\mathbf{R}\}+\{\Delta\mathbf{P}\}^T\cdot[\mathbf{C}_P]\cdot\{\Delta\mathbf{P}\} \tag{4.4}$$

where $\{\Delta\mathbf{R}\} = \{\mathbf{R}_e\} - \{\mathbf{R}_0\}$ is the vector which represents the errors in target responses while $\{\Delta\mathbf{P}\} = \{\mathbf{P}_u\} - \{\mathbf{P}_0\}$ is the vector of parameter changes. $[\mathbf{C}_R]$ and $[\mathbf{C}_P]$ are diagonal matrices of weighting coefficients for target responses and parameters, respectively, and both should be defined by the analyst based on their experience. Higher values of these coefficients indicate greater confidence. From Equation 4.4 it can be seen that the greater the confidence, the finer tuning of the corresponding quantities is needed to make the error sufficiently small. On the other hand, the parameters and target responses in which the confidence is small will not contribute significantly to the error value and therefore will have a less strong influence on the final results.

Using the linear relationship between the target responses and parameters given in Equation 4.3, estimating the confidence into the parameters and target responses and expressing parameter differences $\{\Delta\mathbf{P}\}$ in the current iteration as:

$$\{\Delta\mathbf{P}\} = \{\mathbf{P}_u\} - \{\mathbf{P}_0\} = [\mathbf{G}](\{\mathbf{R}_e\} - \{\mathbf{R}_0\}) \tag{4.5}$$

one can find matrix $[\mathbf{G}]$ in the way to minimise the error function (Collins et al., 1974; Hongxing et al., 2000). It can be proven that matrix $[\mathbf{G}]$ in the case when there are more responses than parameters ($m > n$) is (DDS, 2004):

$$[\mathbf{G}] = \left([\mathbf{C}_P] + [\mathbf{S}]^T[\mathbf{C}_R][\mathbf{S}]\right)^{-1}[\mathbf{S}]^T[\mathbf{C}_R]. \tag{4.6}$$

Otherwise, when there are more parameters than responses ($n > m$) matrix $[\mathbf{G}]$ is:

$$[\mathbf{G}] = [\mathbf{C}_P]^{-1}[\mathbf{S}]^T\left([\mathbf{C}_R]^{-1} + [\mathbf{S}][\mathbf{C}_P]^{-1}[\mathbf{S}]^T\right)^{-1}. \tag{4.7}$$

Bearing all this in mind, the updating procedure can be summarised as follows:

1. Calculate the sensitivity matrix $[\mathbf{S}]$ for the given state of parameters $\{\mathbf{P}_0\}$ and responses $\{\mathbf{R}_0\}$.

2. Choose the weighting factors for parameters and target responses.

3. Calculate matrix [**G**] using either Equation 4.6 or 4.7.

4. Calculate the updated parameter vector $\{\mathbf{P}_u\}$ via a re-arranged Equation 4.5:

$$\{\mathbf{P}_u\} = \{\mathbf{P}_0\} + [\mathbf{G}]\left(\{\mathbf{R}_e\} - \{\mathbf{R}_0\}\right). \tag{4.8}$$

5. Calculate a new response vector which corresponds to updated parameters $\{\mathbf{P}_u\}$ via modal analysis. This response vector and the vector of updated parameters then become the starting vectors $\{\mathbf{R}_0\}$ and $\{\mathbf{P}_0\}$ for the next iteration.

The procedure then goes back to step 1 to calculate a new sensitivity matrix (which changes whenever the model is updated between two iterations). Steps 1 to 5 are repeated until a satisfactory convergence of numerical responses to the experimental data is achieved (that is until the error function is minimised to a prespecified tolerance).

An updating process which produces good correlation between experimental and analytical responses can be regarded as successful only if finally obtained parameters are physically viable. If not, then either a different error function or different parameter selection, or both, should be considered (Kim & Park, 2004). Also, some changes in the weighting matrices should be considered, having in mind that these coefficients can be difficult to assume correctly first time round (Collins et al., 1974). Therefore, it is expected that some kind of additional trial and error approach is used before a satisfactory set of updated parameters is obtained.

Generally, the updating which targets larger number of measured responses at a time is preferable because it puts more constraints to the optimisation process. Successful updating in this case becomes more difficult but once it is achieved it gives more confidence in the results than the same procedure using only a few responses. This becomes clear if a simple example is considered with only one target response, say a natural frequency. There is an infinite number of ways to achieve good correlation for this response by changing either only one parameter at a time or some combination of them. In this way it is not possible to decide which parameter change is most realistic. Therefore, targeting more responses at a time decreases the number of combinations for parameter changes. Finally, to ensure that parameter changes are physically possible, some additional constraints in the form of physically acceptable limits for updating parameters can also be introduced. This makes sure that if the parameter reaches its limit in a particular iteration, it will stay constant through all subsequent iterations until the end of the updating process.

Finally, the success of the updating process is usually judged through a comparison of natural frequencies, overlaying mode shapes and calculation of the Modal Assurance Criterion (MAC) and the Coordinate Modal Assurance Criterion (COMAC). However, if the measured responses are not particularly reliable (say from noisy data), then convergence of the iterative procedure can become a problem. It seems that higher modes are more difficult to update in this situation (Brownjohn & Xia, 2000). Also, if a measurement grid is not dense enough to

prevent spatial aliasing, the MAC values can suggest correlation between modes which are otherwise linearly independent (Modak et al., 2005).

4.2.3 Applications in Civil Structural Engineering

Over the last decade there have been several attempts to transfer the updating technology from the mechanical and aerospace engineering to civil structural engineering. The whole procedure is more difficult to implement in civil engineering because of the larger size of the structures leading to poorer quality of experimental data gathered in open-space noisy environments. Also, the inherent non-linear amplitude dependent behaviour, the presence of numerous non-structural elements and difficult to define boundary conditions mean that the structural modelling parameters are not so controllable as is often the case in the mechanical and aerospace disciplines. However, some successful examples of updating in civil engineering do exist and are presented here.

In principle, papers dealing with the complete process of experimental modal testing and analytical/numerical modelling and updating of civil engineering structures are rare. However, there are many good papers devoted to modal testing of civil engineering structures (Abdel-Ghaffar, 1978; Buckland et al., 1979; Rainer & Pernica, 1979; Brownjohn et al., 1992; Brownjohn, 1997; Chang et al., 2001). As the modal testing technology has developed and been accepted as a way for reliable estimation of dynamic properties, more researchers have started to pay attention to the correlation between the initial FE model and experimental results from real-life as-built structures. In this process, the structural parameters which influenced the analytical results most and managed to shift them towards the experimental ones were identified in general. In the case of footbridges these are: stiffness of supports and non structural elements (decks, asphalt surfacing and handrails) as well as material properties, such as dynamic modulus of elasticity for concrete (Gardner-Morse & Huston, 1993; Brownjohn et al., 1994; Pimentel, 1997).

The logical step forward was then to try the automatic updating procedure by using specialist software developed for this purpose. The procedure was successfully implemented on different types of structure, such as a 48-storey building (Lord et al., 2004), a high rise tower (Wu & Li, 2004), road and/or rail bridges (Brownjohn & Xia, 2000; Zhang et al., 2001; Jaishi & Ren, 2005) and two footbridges (Pavic et al., 1998). Also, model updating has been attempted as a tool for damage identification (Brownjohn et al., 2001; Xia & Brownjohn, 2003; Teughels & De Roeck, 2004).

Reviewed papers suggest that the automatic updating of full-scale road and railway bridges might have difficulties in achieving a high level of correlation with experimental results. For example, when updating a 750 m long road and railway bridge, Zhang et al. (2001) got a maximum frequency error in the updated model of about 10%. A similar result was obtained by Brownjohn & Xia (2000) for a curved road bridge spanning 100 m. Maximum frequency difference for a 90 m long road bridge of 6.2% was obtained by Jaishi & Ren

(2005). On the other hand, the automatic updating conducted by Pavic et al. (1998) for two footbridges spanning 34 m and 20 m produced maximum frequency difference of only 2.0% and 1.1%, respectively. It, therefore, seems that it is easier to update smaller bridges, such as pedestrian ones. This is not surprising considering that larger structures tend to have many more features which are important for their dynamic behaviour (e.g. connections, supports, etc.) but are difficult to model in detail in the FE model. Also, experimental data on larger structures tend to be of poorer quality compared with their smaller counterparts. Moreover, it is worth noting that, for example, Zhang et al. (2001) conducted updating which targeted as many as 17 measured natural frequencies, which put a lot of constraints to the optimisation procedure, whilst in the case of the footbridge where the maximum frequency error was 1.1% the updating was done according to natural frequencies and mode shapes for three measured modes only (Pavic et al., 1998). Regarding MAC values, in most cases, they were higher than 0.80, which is a very good mode shape agreement for civil structural engineering applications of updating.

4.3 Description of Test Footbridge Structure

The investigated footbridge spans 104 m over the Morača River in Podgorica, capital of Montenegro. It is a still box girder bridge described earlier in Chapter 3 (Figures 3.1 and 3.2). As explained in Chapter 3, the footbridge experienced strong vibrations in the vertical direction under pedestrian walking excitation immediately after its construction. This was due to the fact that the footbridge fundamental natural frequency for the vertical mode was in the region of the normal walking frequencies, which is 1.3-2.5 Hz (Matsumoto et al., 1978). In order to supress its liveliness, the footbridge was strengthened by a concrete slab cast over the bottom steel flange in the regions around the columns as well as over the top flange of the box girder in the central part of the main span (Figure 3.2). At the same time, additional steel plates were added to the box columns, as learned during attempts to correlate significant differences in frequencies of horizontal modes present when comparing the design FE and experimental models (Chapter 3). However, all this added not only stiffness but also some mass to the dynamic system. Consequently the fundamental natural frequency did not change very much and the footbridge still remains very lively.

4.4 Initial FE Modelling, Modal Testing and Model Tuning

This section describes briefly the development of the initial FE model for the footbridge investigated as well as its modal testing. Then, the manual model tuning is discussed.

4.4.1 Initial Finite Element Modelling

To minimise discretisation and modelling errors a very detailed initial 3D FE model was developed using the ANSYS FE code (SAS, 1994). This initial FE model differs from the design FE model described previously in Chapter 3 only in the fact that the late information about additional steel plates used to strengthen the columns in the rectification phase is now taken into account. In the absence of more precise data, it was assumed that two different plates used for strengthening of columns were as thick as the types of plates used in the initial design, that is 2 and 3 cm. Therefore, the initial model for the analysis in this chapter is actually 'Model 2' from Chapter 3. Features of the model are described in Chapter 3 and will not be repeated here.

Seven lowest modes of vibration from the initial FE model are presented in Figure 4.1. As before, labels H and V stand for the horizontal and vertical modes, respectively. Similarly, S and A stand for the symmetric and anti-symmetric modes, respectively.

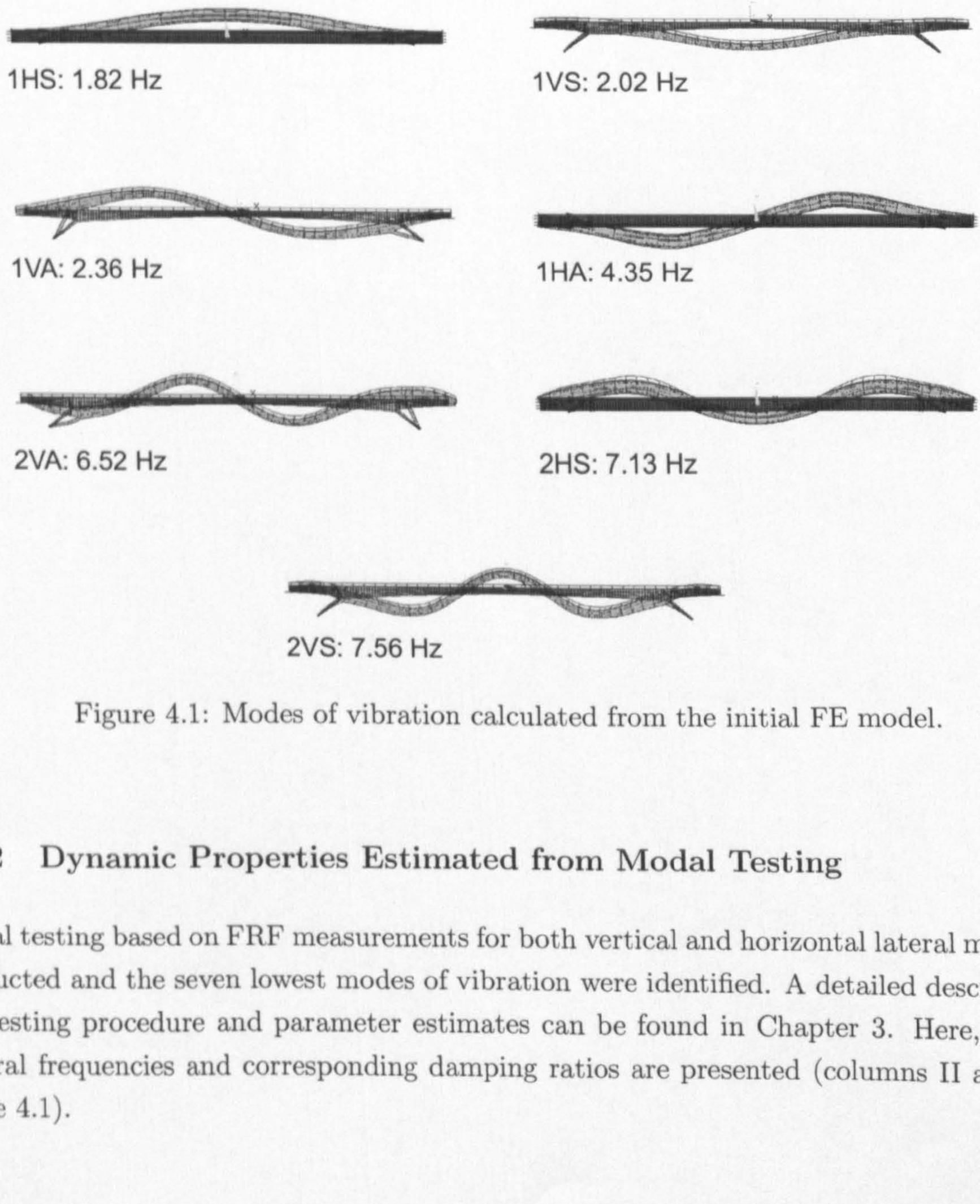

Figure 4.1: Modes of vibration calculated from the initial FE model.

4.4.2 Dynamic Properties Estimated from Modal Testing

Modal testing based on FRF measurements for both vertical and horizontal lateral modes was conducted and the seven lowest modes of vibration were identified. A detailed description of the testing procedure and parameter estimates can be found in Chapter 3. Here, only the natural frequencies and corresponding damping ratios are presented (columns II and III in Table 4.1).

Table 4.1: Correlation between experimental and initial FE model.

I	II	III	IV	V	VI	VII
Exp. mode	**Modal testing**		**FE mode**	**Initial FEM**	**Frequency error**	**MAC**
#	f [Hz]	ζ [%]	#	f [Hz]	$(fv - fII)/fII$ [%]	[%]
1	1.83 (1HS)	0.26	1	1.82 (1HS)	-0.6	99.5
2	2.04 (1VS)	0.22	2	2.02 (1VS)	-1.0	99.7
3	3.36 (1VA)	1.86	3	2.36 (1VA)	-29.8	97.8
4	4.54 (1HA)	0.98	4	4.35 (1HA)	-4.2	98.6
5	7.35 (2HS)	2.68	6	7.13 (2HS)	-3.0	80.7
6	7.56 (2VA)	0.76	5	6.52 (2VA)	-13.8	86.6
7	7.98 (2VS)	0.60	7	7.56 (2VS)	-5.3	97.9

4.4.3 FE Model Tuning

All seven modes identified experimentally had their counterparts in the initial FE model (Table 4.1, column V). However, the sequence of 2VA and 2HS FE modes was reversed compared to their experimental counterparts (Table 4.1: columns I and IV). Also, natural frequencies of all experimental modes were underestimated, with the frequency error being exceptionally high (29.8%) for mode 1VA (Table 4.1: column VI). Another mode with quite large error of 13.8% was also vertical and anti-symmetric one (2VA). On the other hand, all mode shapes were well correlated, with the minimum MAC being 0.81. Something was clearly wrong with the prediction of anti-symmetric modes in the initial FE model. A parametric study revealed that introducing the horizontal springs in the longitudinal direction at girder ends instead of free edges could improve significantly the correlation between measured and analytical vertical modes, in particular the anti-symmetric ones, as mentioned in Chapter 3. The stiffness of these springs (modelled as COMBIN14 element in ANSYS) was varied by trial and error until the best correlation with measured frequencies was obtained. A stiffness value of 10^8 N/m per metre width of the bridge deck produced the smallest difference between the measured and FE-calculated natural frequencies for the first four vertical modes of vibration (Figure 4.2). This value was adopted in the manually tuned FE model developed prior to automatic updating. Also, in this way the sequence of mode appearance became the same as in the experimental model, and frequency error was decreased significantly with the maximum value being 4.0% for mode 1HA (Table 4.2). The MAC values were improved only slightly.

The data given in Tables 4.1 and 4.2 are also presented graphically in Figure 4.3. The ratio between analytical and measured natural frequencies for the seven modes of vibration is given for the initial FE model and the manually tuned model. Having in mind that the information about column strengthening was not present in the original design data available, and that this information was found some time after the first FE model had been developed, it is also interesting to show the frequency error which would have resulted from not introducing this information (and horizontal springs) into the modelling. The frequency ratios in this model, labelled as 'design model' in Figure 4.3, are also shown. It can be seen that strengthening

the columns influenced the frequencies of horizontal modes strongly ('initial FE model' in Figure 4.3), while the added springs then improved correlation with vertical modes ('manually tuned model' in Figure 4.3).

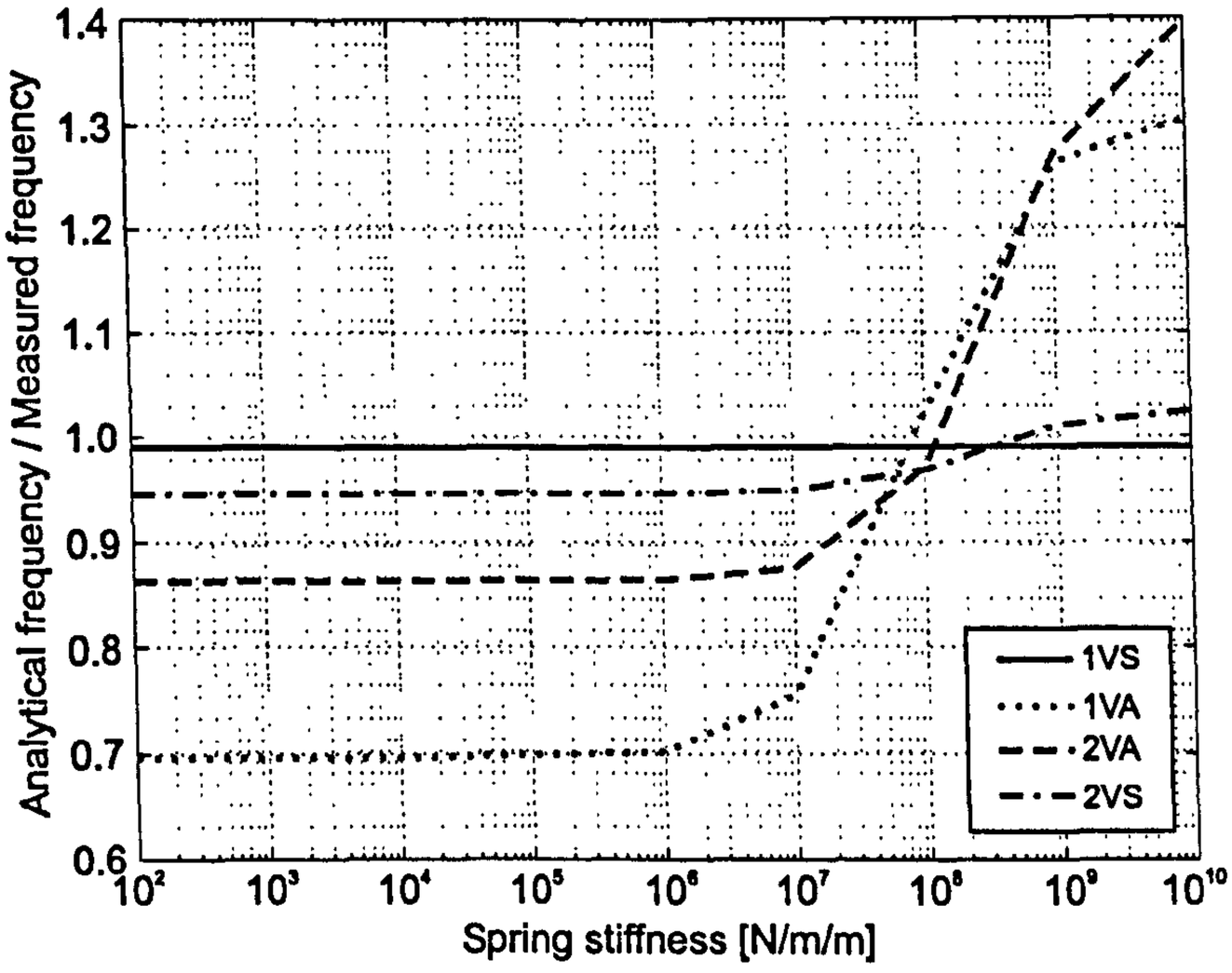

Figure 4.2: Choice of appropriate stiffness for spring supports at the ends of the box girder.

Table 4.2: Correlation between experimental and manually tuned FE model.

I	II	III	IV	V
Exp. mode	**Exp. model**	**Tuned model**	**Frequency error**	**MAC**
#	f [Hz]	f [Hz]	$(f_{III} - f_{II})/f_{II}$ [%]	[%]
1	1.83 (1HS)	1.82 (1HS)	-0.6	99.5
2	2.04 (1VS)	2.02 (1VS)	-1.0	99.7
3	3.36 (1VA)	3.47 (1VA)	3.3	99.9
4	4.54 (1HA)	4.36 (1HA)	-4.0	98.7
5	7.35 (2HS)	7.15 (2HS)	-2.7	81.1
6	7.56 (2VA)	7.34 (2VA)	-2.9	88.9
7	7.98 (2VS)	7.74 (2VS)	-3.0	98.0

Having reduced the maximum frequency error in the manually tuned model to 4.0% and matching the sequence of experimental and FE modes facilitated the successful and physically meaningful automatic updating by the updating software (DDS, 2004). Also, it can be concluded that very detailed FE modelling and some manual tuning led to a very good correlation between experimental and analytical model. However, it would be interesting to see if/how the automatic updating could improve these results, having in mind that this starting model for automatic updating was much closer to the experimental results than most of the automatically updated models reported in the reviewed literature.

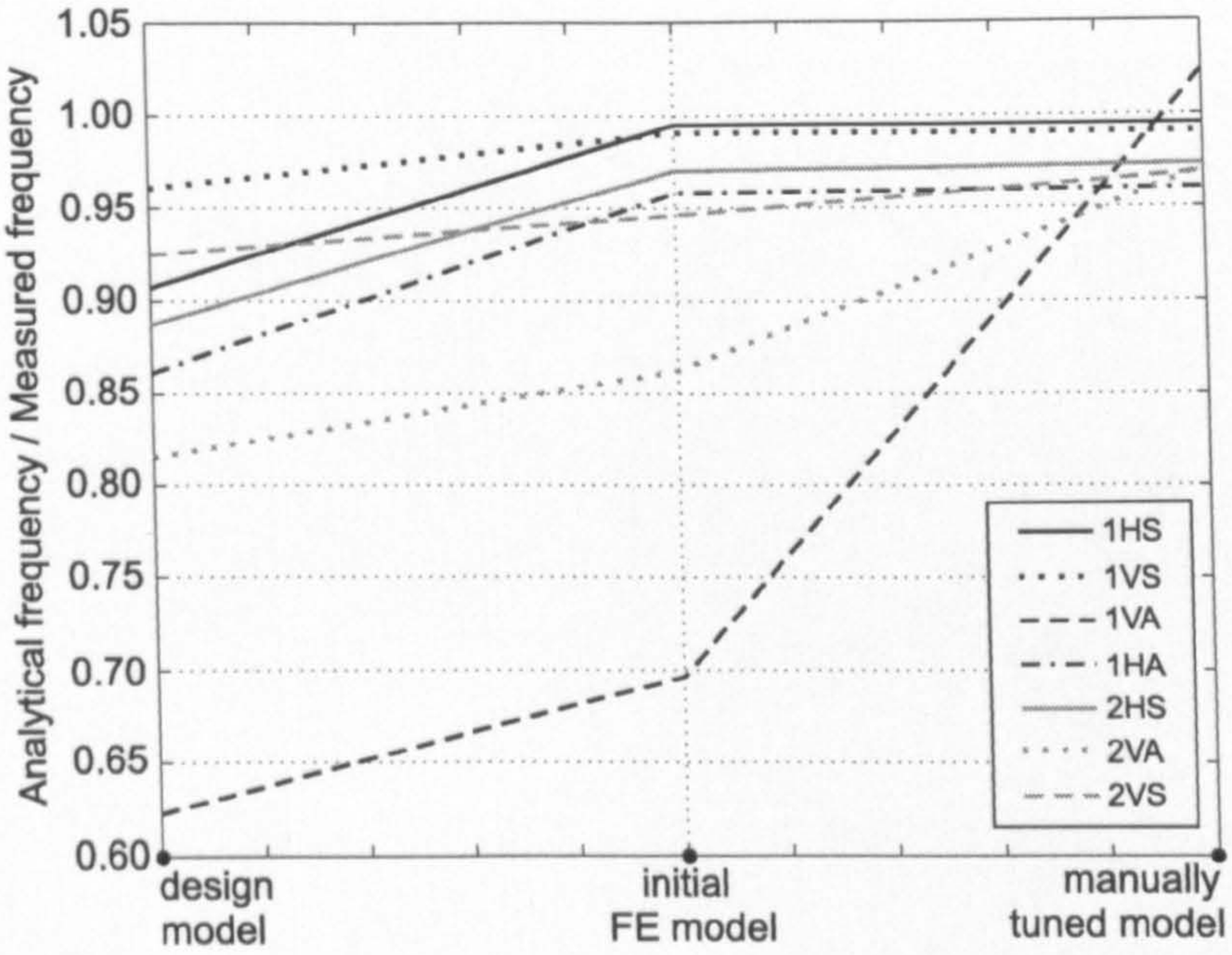

Figure 4.3: Manual frequency tuning of different FE models.

4.5 Automatic Model Updating

The updating procedure was conducted with the aim to improve further the analytical model so that it could be used in vibration response analysis. The procedure is based on the theoretical principles outlined in Section 4.2.2.

4.5.1 Target Response Selection

Having in mind the good quality of the experimental data, all seven measured modes of vibration were targeted in the updating process. Both measured natural frequencies and MAC values were taken into account. Therefore, in total 14 target responses were selected for updating. To take into account the lower reliability of identified mode shapes in comparison with measured natural frequencies, the confidence factor for MAC values was taken to be ten times lower than that for natural frequencies. This was chosen based on previous experience (Pavic et al., 1998). These confidence factors feature in $[\mathbf{C}_R]$ matrix that is a part of the error function (Equation 4.4).

4.5.2 Parameter Selection

As previously mentioned, the main criteria for parameter selection are their uncertainty and sensitivity. Therefore, parameters related to the geometry that was not precisely described in the design data available were selected as uncertain. These parameters are shown in Figure 4.4. For simplicity, only half of the bridge is presented in the figure having in mind its symmetry with respect to the YZ plane. It can be seen that all parameters that characterise

the deck were selected. This is because of uncertain contribution of the asphalt and composite slab to the stiffness of the bridge deck. Besides this, only approximate data about asphalt and concrete thicknesses were available. The same applies to the composite slabs in the column-girder connections (Figure 3.2). Also, the fact that the bridge is more than 30 years old may contribute to the deterioration of its components (such as the asphalt layer). Because of the unavailability of precise data related to column strengthening, the thicknesses of the column steel plates as well as their dynamic modulus were also selected for updating. The density of water pipe material was selected to take into account the uncertainty about the amount of water in the pipes. Finally, the stiffnesses of the horizontal-longitudinal support springs at the girder ends were also taken into account. In total, 25 parameters were selected, with their sequence number given in parentheses in Figure 4.4.

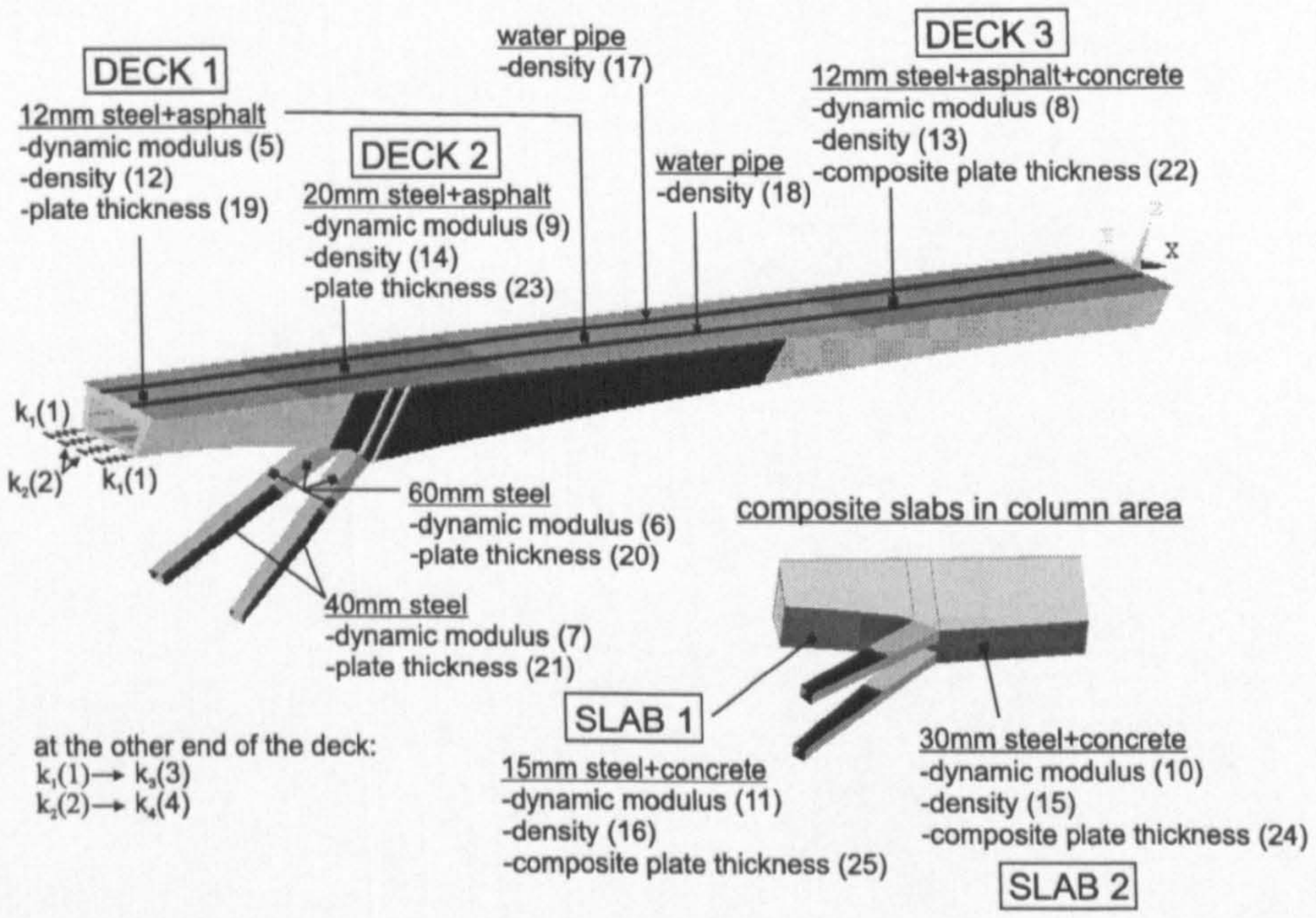

Figure 4.4: Uncertain parameters in the manually tuned FE model.

After the parameter selection, a sensitivity analysis was conducted. To be able to compare the sensitivity values of different target responses to changes in different parameters, the normalised sensitivity, that is the dimensionless number $S_{n,ij}$, defined as

$$S_{n,ij} = \frac{\Delta R_i / \Delta P_j}{R_i / P_j} = \frac{\Delta R_i}{\Delta P_j} \cdot \frac{P_j}{R_i} \tag{4.9}$$

was calculated for each combination of target responses and parameters. This was done by using the forward finite difference approach (DDS, 2004) with an assumed parameter change of +1% for all updating parameters.

The plot of sums of normalised sensitivities corresponding to all responses and for all parameters is shown in Figure 4.5. It was found that target responses were much less sensitive to three parameters (numbered as 11, 16 and 25 in Figures 4.4 and 4.5) defining a composite

slab in the column connection areas in comparison with other parameters. Because of this, these three parameters were excluded from the updating process. All other parameters entered the updating process with their starting values given in Table 4.3 (column IV). Also, physically meaningful upper and lower limits for these parameters were estimated and are given in columns V and VI.

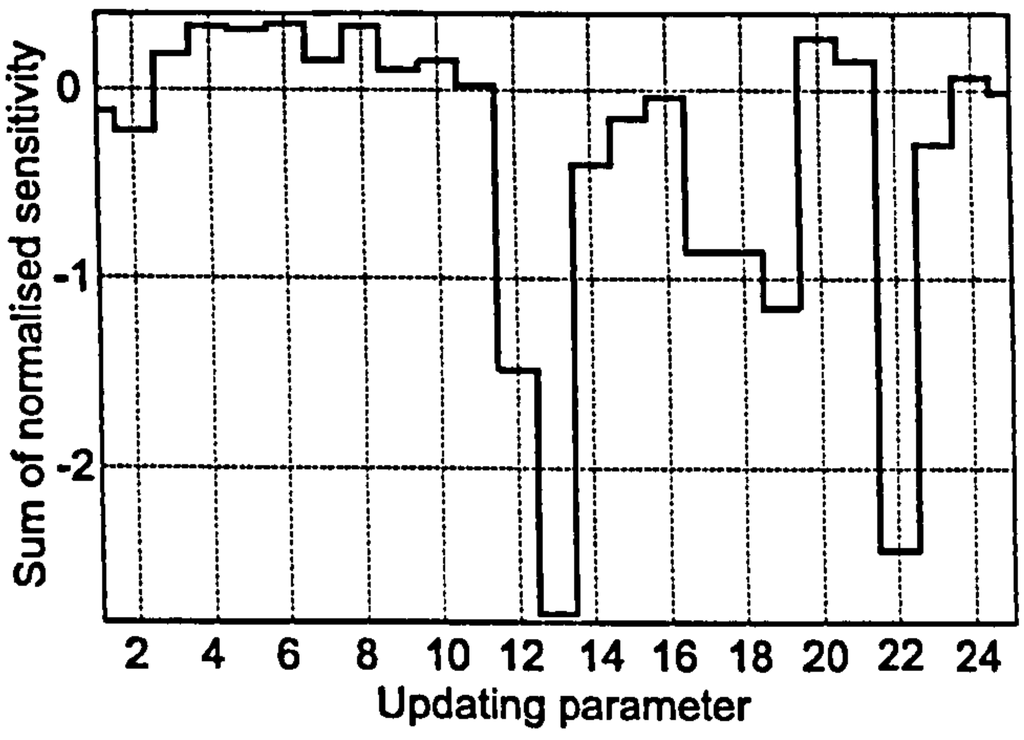

Figure 4.5: Plot of sum of normalised sensitivity of 14 selected target responses to 25 uncertain parameters.

4.5.3 Formal Updating and its Results

The updating procedure was conducted using the FEMtools updating software (DDS, 2004) based on the Bayesian algorithm presented in Section 4.2.2. The aim was to minimise the error function of the kind defined in Equation 4.4, where both natural frequencies and MAC values for mode shapes were selected as target responses. A constraint to the updating procedure was the introduction of the upper and the lower allowable limits for parameter values. The parameter changes per iteration were not limited. For all parameters the same confidence value featuring the matrix $[C_P]$ was chosen.

The updating process converged after five iterations. For every mode of vibration the error in calculated natural frequencies compared with their measured counterparts was defined as an absolute value of the relative difference between numerical f_a and experimental f_e natural frequency:

$$\text{frequency error} = \left| \frac{f_a - f_e}{f_e} \right|. \tag{4.10}$$

The average value of this error across all seven modes for each iteration is presented in Figure 4.6.

Table 4.3: The value of starting and updated parameters (E, ρ and h stand for dynamic modulus of elasticity, density and thickness of appropriate elements in FE model, respectively).

I	II	III	IV	V	VI	VII	VIII
Parame--ter # (Fig. 4.4)	**Type**	**Structu--ral part**	**Starting value**	**Allowed decrease [%]**	**Allowed increase [%]**	**Updated parame--ter value**	**Parame--ter change [%]**
1	k_1	spring support	36.1 [MN/m/m]	no limit	no limit	25.9 [MN/m/m]	-28.6
2	k_2	spring support	72.1 [MN/m/m]	no limit	no limit	41.4 [MN/m/m]	-42.6
3	k_3	spring support	36.1 [MN/m/m]	no limit	no limit	30.5 [MN/m/m]	-16.0
4	k_4	spring support	72.1 [MN/m/m]	no limit	no limit	55.0 [MN/m/m]	-23.7
5	E	deck 1	210 [GPa]	-10	+10	230 [GPa]	9.5
6	E	column plate	210 [GPa]	-35	+35	283 [GPa]	35.0
7	E	column plate	210 [GPa]	-35	+35	228 [GPa]	8.6
8	E	deck 3	210 [GPa]	-35	+35	141 [GPa]	-32.9
9	E	deck 2	210 [GPa]	-10	+10	189 [GPa]	-10.0
10	E	slab 2	210 [GPa]	-35	+35	253 [GPa]	20.5
12	ρ	deck 1	17475 [kg/m^3]	-20	+20	15987 [kg/m^3]	-8.5
13	ρ	deck 3	6712 [kg/m^3]	-20	+20	7450 [kg/m^3]	11.0
14	ρ	deck 2	13625 [kg/m^3]	-20	+20	10900 [kg/m^3]	-20.0
15	ρ	slab 2	4977 [kg/m^3]	-10	+10	4480 [kg/m^3]	-10.0
17	ρ	water pipe	4858 [kg/m^3]	-50	+50	4479 [kg/m^3]	-7.8
18	ρ	water pipe	4858 [kg/m^3]	-50	+50	4475 [kg/m^3]	-7.9
19	h	deck 1	12 mm	0	+30	13.5 mm	12.5
20	h	column plate	60 mm	-50	+50	63.9 mm	6.5
21	h	column plate	40 mm	-50	+50	42.0 mm	5.0
22	h	deck 3	67 mm	-30	+30	51.2 mm	-23.6
23	h	deck 2	20 mm	0	+20	20.0 mm	0.0
24	h	slab 2	110 mm	-20	+20	102.7 mm	-6.6

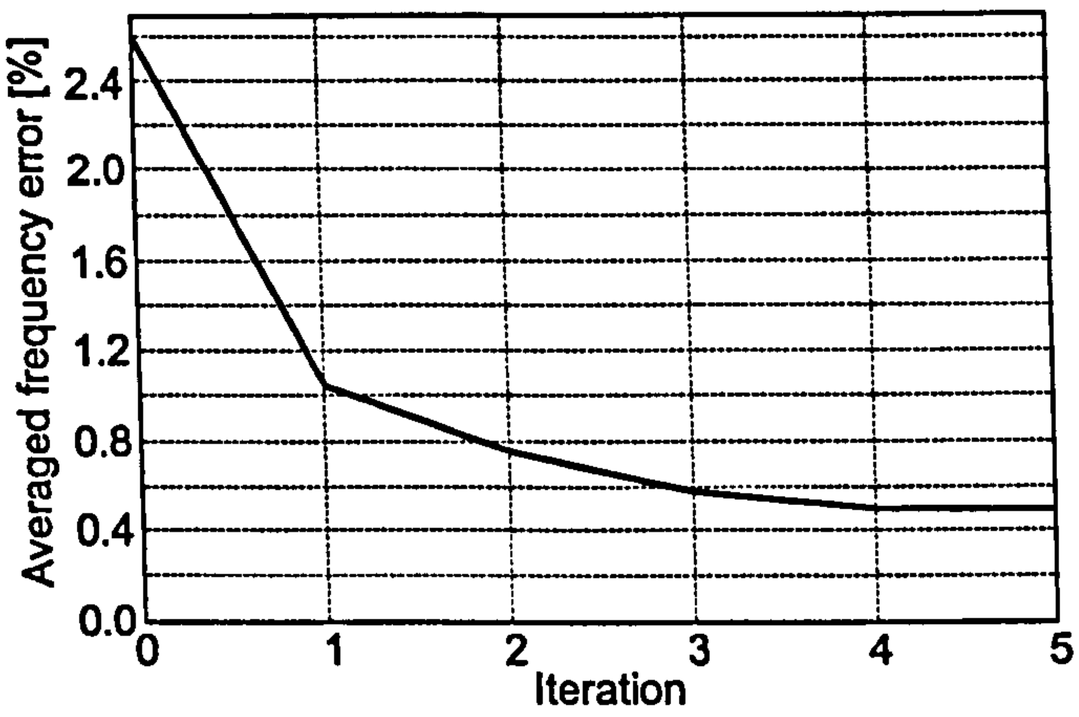

Figure 4.6: Convergence of the iterative process presented via averaged frequency error.

The frequencies and MAC values obtained as a result of the updating process are presented in Table 4.4. It can be seen that previous maximum frequency difference of 4.0% decreased to 1.2%. Minimum MAC value increased from 0.81 to 0.85, with all other values being well above 0.90. The complete MAC matrix is shown in Figure 4.7. The agreement between mode shapes in updated FE model and the experimental data was very good, which can be seen in Figure 4.8.

The final parameter values are presented in Table 4.3 (column VII). The absolute maximum parameter change was 42.6% for the stiffness of a support spring. Only four parameters, amongst 22 selected, reached their allowable limits. The fact that most parameters did not go to their limiting values is a sign of a good parameter choice.

However, when changes in the parameter values through iterations were checked it was found that very large changes occurred in the first iteration. Maximum change was for parameter 2 (k_2) which was -23%. This could be important because of the fact that the Taylor's series given in Equation 4.3 was limited to its linear term only. However, the relationship between responses and parameters is, in fact, non-linear, and having very large changes in parameters in a single iteration can violate the main principles on which the updating procedure was based. Because of this, the updating process was repeated with parameter changes in every iteration limited to 1% - the value which was used to calculate the sensitivity matrix in each iteration. Limiting the maximum parameter change per iteration makes sure that parameter will take new value in the vicinity of the previous value, enabling a more reasonable linear approximation used in Equation 4.3. Nevertheless, the new updating setup produced almost the same level of agreement between experimental and numerical target responses as those presented previously. This time, results were obtained after 50 iterations (lasting 10 times longer than previously used five iterations). The agreement of results gave some confidence in their reliability.

Table 4.4: Correlation between experimental and updated FE model.

I	II	III	IV	V
Exp. mode	**Exp. model**	**Updated model**	**Frequency error**	**MAC**
#	f [Hz]	f [Hz]	$(f_{III} - f_{II})/f_{II}$ [%]	[%]
1	1.83 (1HS)	1.84 (1HS)	0.6	99.9
2	2.04 (1VS)	2.05 (1VS)	0.5	99.8
3	3.36 (1VA)	3.38 (1VA)	0.6	99.9
4	4.54 (1HA)	4.50 (1HA)	-0.9	99.3
5	7.35 (2HS)	7.34 (2HS)	-0.1	84.7
6	7.56 (2VA)	7.47 (2VA)	-1.2	93.8
7	7.98 (2VS)	7.98 (2VS)	0.0	98.9

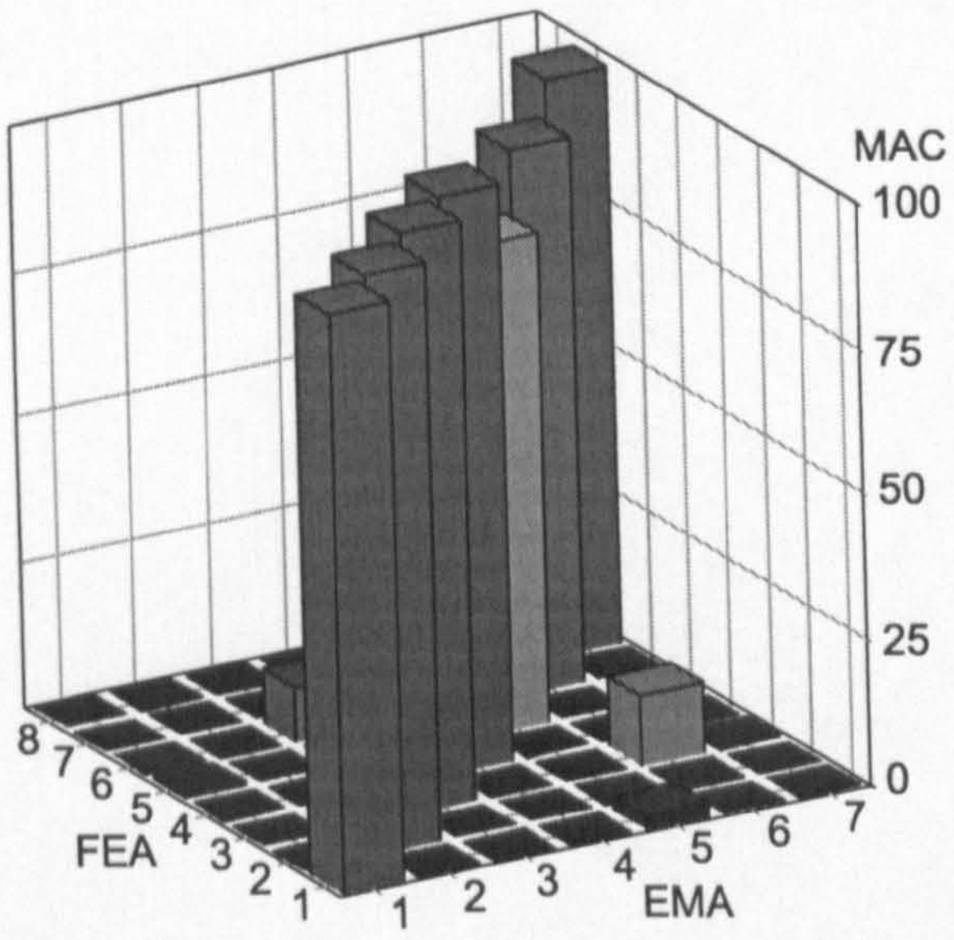

Figure 4.7: MAC matrix after updating. FEA and EMA stand for FE model and experimental model, respectively.

Finally, it should be said that an attempt to update the initial FE model (not featuring horizontal springs) under the condition of maximum parameter changes per iteration of 1% led to much worse frequency and MAC correlation (after 140 iterations) although the limits for parameters were free. At the same time, changes in some parameters were physically impossible. For example, the thickness of the column plates was about 25 cm which meant that all columns are completely cast in steel, which is obviously wrong. Moreover, the column stiffness was additionally increased via increase in dynamic modulus by a factor of 2. Obviously, the non existence of the horizontal-longitudinal support springs in the initial FE model required changes in the column parameters which were too large in order to try to correlate vertical modes. Therefore, the manual model tuning conducted before the formal updating proved to be crucial for the success of the formal updating procedure.

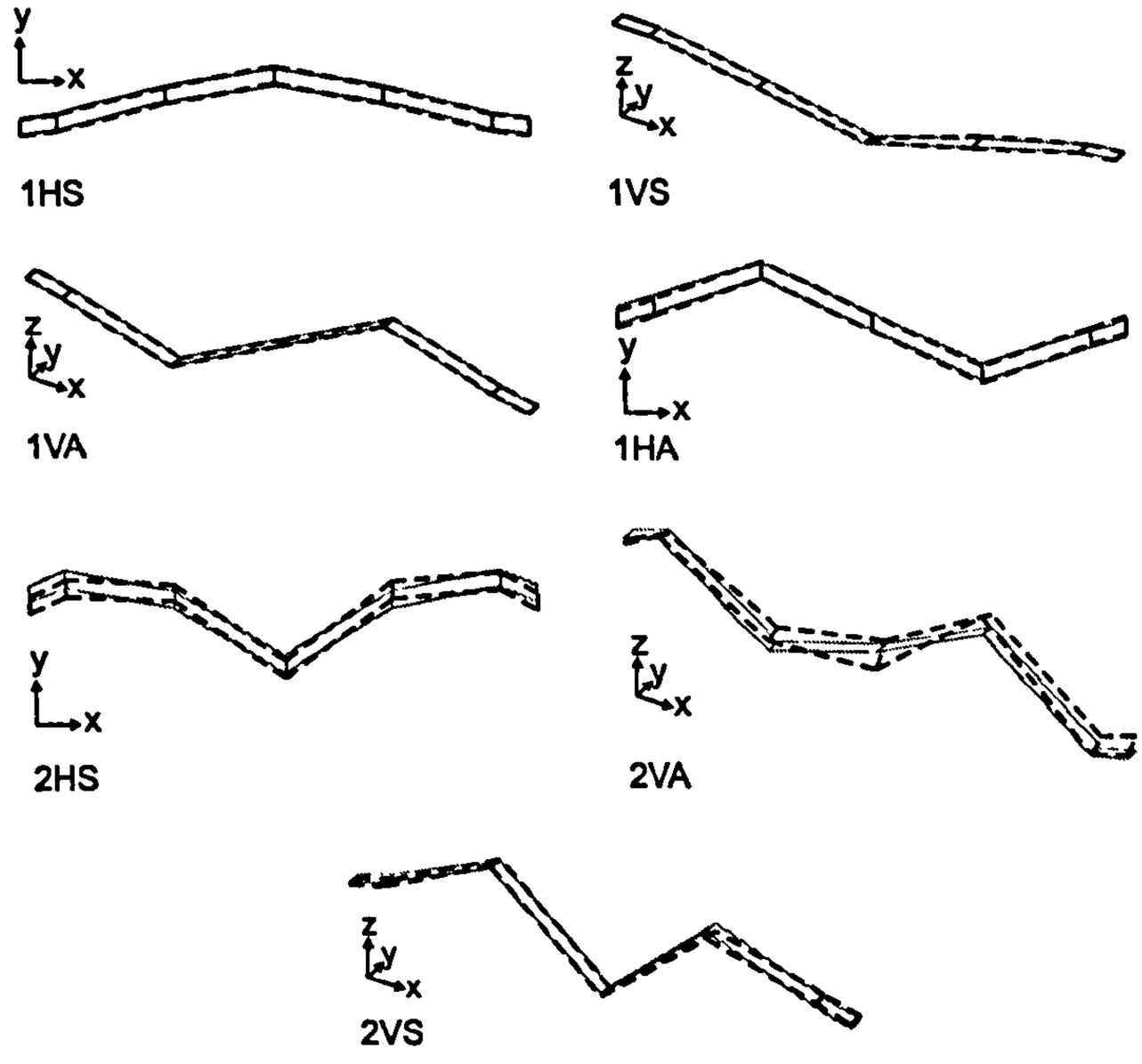

Figure 4.8: Overlaying of mode shapes obtained experimentally (black-dashed line) and numerically in the final FE model (grey line).

4.6 Discussion

Although a very detailed initial FE model of the Podgorica footbridge was developed based on design data available and best engineering judgement, the discrepancies in the natural frequencies of the first seven modes were quite large between the experimental and numerical results. Particularly poor correlation was obtained for anti-symmetric modes and an error as high as 30% occurred for mode 1VA.

This initial FE model could not be updated in a physically meaningful way by using a sensitivity-based procedure implemented in the FEMtools updating software. This confirmed conclusions found in papers by Pavic et al. (1998) and Brownjohn & Xia (2000) that the initial FE model usually cannot be updated successfully when large differences between their modal properties and their experimental counterparts exist. This is because these large differences violate the key assumption used in updating that the relationship between response errors and parameter changes in Equation 4.3 can be expressed using the first term in the Taylor's series only.

Therefore, the manual tuning which would reconcile as much as practicable the difference between the initial FE model and its experimental counterpart was required before implementing the automatic updating. For the bridge investigated, it was found that flexible supports in the longitudinal direction should be introduced instead of free edges at girder ends to improve the correlation between the measured and FE-calculated modes. It seems

that the expansion joints at both ends of the bridge deck got jammed due to lack of maintenance and therefore provided a restraint to the bridge movement in the longitudinal direction. Such movement was much more pronounced in the anti-symmetric modes. Also, it might be that the end supports deteriorated and obstructed free movement of the box girder ends.

A simple manual tuning by trial and error guided by engineering judgement was necessary to prepare the FE model for the automatic updating and proved to be crucial for its successful implementation. Of 25 parameters which were considered as uncertain, three were excluded from the updating process because the target responses were not sensitive to them. This is a usual procedure which should help to prevent problems with ill conditioning during updating. After this, the updating procedure was successfully conducted improving correlation of natural frequencies and MAC values between the final FE and the experimental models. Having said this, it would be interesting here to analyse physical meaning of the parameter changes presented in Table 4.3.

Water pipes: For both pipes the density approximately decreased for 7.8%. This is an equivalent to the situation when water fills 43% of the pipes volume, a little bit less than the initially assumed 50%.

Deck 1: The stiffness of deck 1 tended to increase through both dynamic modulus of elasticity and thickness of shell elements. This means that the asphalt layer contributed to the overall stiffness of the deck which was neglected when developing the manually tuned FE model. The overall mass of the deck remained approximately the same.

Deck 2: In this area the shell stiffness tended to decrease as well as the overall mass. Having in mind the asphalt contribution to the stiffness in the deck 1 area, it would be expected that the same happened here but it did not. However, the result obtained for deck 2 probably means that the designed increase in the steel plate thickness from 12 mm in the area of deck 1 to 20 mm in the area of deck 2 was actually not carried out. It was impossible to confirm this information within the scope of this work.

Deck 3: Changes in dynamic modulus of elasticity, shell thickness and its density suggested that the total mass and stiffness of this composite slab are smaller than assumed. This means that the composite slab is composed of 1.2 cm of steel and 7.2 cm of concrete, instead of 1.2 cm of steel and 10.0 cm of concrete, as initially assumed. The 33% decrease in dynamic modulus of elasticity also suggests that the concrete was probably cracked over time and there was possibly certain level of slippage between the steel and concrete layers.

Slab 2: The mass of this composite slab decreased, meaning that the concrete layer is 9.4 cm thick instead of the previously used 13.0 cm. However, the dynamic modulus of elasticity increased by 20%. This, together with the increase of the same parameter for column plates suggests that the whole area of connection between the box girder and columns is very stiff. The exact source of this stiffness is difficult to identify having in mind that there are no precise data about the geometry of columns as well as of the concrete layer in the composite slab. The final plate thicknesses in columns almost stayed unchanged at 6 and 4 cm, which was in

agreement with the rule from the national bridge design code in Montenegro. According to this code the plates used for stiffening of a structure can have the thickness which is, as a maximum, the same as the thickness of the original plates.

Longitudinal spring supports: The stiffnesses of these springs were free to increase and decrease. It is interesting here that springs at the right side of the bridge were on average about 25% stiffer than those on the left side. This parameter change probably happened due to an attempt of the numerical procedure to accommodate slight violation of the anti-symmetry in the measured mode 2VA (Figure 4.8).

Finally, having in mind that the first vertical mode of vibration is responsible for the footbridge liveliness, the modal parameters related to this mode important for further vibration analysis of the bridge were possible to be identified accurately by combining the FE and experimental results. These are: natural frequency of 2.04 Hz (from testing) and modal mass (from the fully updated FE model) of 58,000 kg. This mass was about 10% higher than that obtained from modal testing in Chapter 3, being 53,188 kg. The damping ratio estimated from FRF-based testing was 0.22%. However, when assessing vibration performance of the footbridge under human-induced load, it is recommended to use the value of 0.26% identified by analysing the footbridge response that typically occurs due to human-induced walking excitation (Figure 3.15 in Chapter 3).

4.7 Conclusions

When developing an FE model of the footbridge structure based on the design data available and best engineering judgement where necessary, there is no guarantee that this initial model can reasonably well estimate the modal properties (natural frequencies and mode shapes) of the bridge even when it is very detailed. First seven modes of vibration of the Podgorica footbridge were identified via modal testing. A comparison with their estimates from the initial FE model revealed errors in the natural frequencies, particularly large for two vertical anti-symmetric modes.

An attempt to formally update this design model by changing its input parameters failed to produce physically meaningless changes in some parameters. This was due to large differences in the initial and experimental models which cannot be supported by the iterative updating procedure used.

Because of this, a manual tuning of the initial FE model was required with the aim to reconcile these differences. Adding flexible supports to the free edges in the bridge longitudinal direction at the girder ends improved considerably the correlation between the numerical and the experimental models. Only then was it possible to automatically update the numerical model via the FEMtools software.

This formal updating further improved the frequency correlation and increased MAC values by changing the values of 22 uncertain and sensitive structural parameters. The fact that

all parameter changes were within their physically acceptable limits was very important for judging the updated parameters as meaningful, and therefore the whole of the updating process as successful. The parameter changes suggested that the composite slabs in the bridge were less stiff than assumed. Also, it seemed that the asphalt layer contributed to the deck stiffness.

Preface to Chapter 5

Estimation of modal properties of the Podgorica footbridge described in Chapters 3 and 4 provided a reliable modal model of the bridge that could be used in further dynamic analysis. This model, together with two similar models for two other lively footbridges investigated by the Vibration Engineering Section in the past, became available as a tool for investigating human-structure dynamic interaction during a footbridge crossing. This investigation is presented in Chapter 5. The primary motivation for it was to investigate possible differences between walking on a rigid and a perceptibly moving surface. The work was conducted by looking at vibration development during the crossing of the structure and by studying in detail the parameters that influence the vibrations.

Therefore, Chapter 5 gives insight into the human-structure dynamic interaction that occurs in the seldom investigated vertical direction while crossing lively footbridges. It makes use of this interaction to define a possible limiting vertical vibration level for walking people.

Chapter 5

Human-Structure Dynamic Interaction during Footbridge Crossing

This chapter, in an amended form, has been published under the following reference:

Živanović, S., Pavic, A. and Reynolds, P. (2005) Human-Structure Dynamic Interaction in Footbridges, Proceedings of the Institution of Civil Engineers - Bridge Engineering, 158 (4), 165-177.

Abstract

Dynamic force induced in the vertical direction by a single person walking across a footbridge structure is usually modelled as a harmonic force having frequency that matches one of the footbridge natural frequencies. A comparison between modal responses generated by this harmonic force and a walking force measured on a treadmill confirmed that using the harmonic force is justifiable in the case of walking across a structure that does not vibrate perceptibly, especially in case when walking frequency is controlled with help of a metronome. It is further shown that using this harmonic force for predicting the response of a perceptibly vibrating footbridge can significantly overestimate the real footbridge response and therefore its degree of liveliness. This is because of the inability of pedestrians to keep pacing steadily when perceiving strong vibrations. A methodology for systematic comparison of the measured and simulated responses is proposed with the aim of identifying vibration levels which disturb normal walking. On two footbridges investigated this level was $0.33\,\mathrm{m/s^2}$ and $0.37\,\mathrm{m/s^2}$, in both cases being lower than the levels allowed by the current British footbridge design code. Finally, the observed effect of losing steady walking step can be expressed via either increased damping or modified harmonic dynamic force over time periods when test subjects lose their steps. The average increase in the damping over the analysed time periods of imperfect walking was up to 10 times higher than the damping of an empty footbridge.

5.1 Introduction

Footbridge structures are becoming increasingly slender due to aesthetic design requirements and a tendency to utilise fully the carrying capacity of structural materials which are constantly improving. As a consequence, it is the vibration serviceability of these structures under human-induced load that is becoming their governing design criterion. In the UK, BS 5400 (BSI, 1978) and BD 37/01 (HA, 2001) recognise a dynamic load induced by a single person walking across the bridge at a frequency that matches a footbridge natural frequency as a critical design case when dealing with vibrations in the vertical direction. Furthermore, since the widely publicised problem of excessive lateral sway vibrations under crowd load occurred on the London Millennium Bridge (Dallard et al., 2001a), an additional check related to the level of lateral vibrations is expected to be conducted (HA, 2001). However, a methodology to perform this check has not yet been codified. To deal with this problem, BD 37/01 indicates a threshold natural frequency of a sway mode of 1.5 Hz, above which lateral vibration problems are unlikely to occur.

The majority of the current design procedures for calculating footbridge vibration response (in the vertical direction) induced by a single walking person model the corresponding excitation force as a sinusoidal force moving across the bridge with a constant speed (Rainer et. al., 1988; Grundmann et al., 1993). The modal force induced in this way is equivalent to the same sinusoidal force weighted by a mode shape. The frequency of the sinusoidal force is either the walking frequency, being in the range 1.5-2.4 Hz (Matsumoto et al., 1978), or an integer multiple if one of the higher harmonics of the walking force (assumed to be periodic) is analysed. The serviceability checks are usually conducted for cases when the frequency of one or more of the first three harmonics (Young, 2001) coincides with one of the natural frequencies of the footbridge. The amplitude of the sinusoidal force is expressed as a fraction of the pedestrian's weight, via the so called dynamic loading factor (DLF). The value of DLF depends on the walking harmonic considered as well as on its frequency and in addition, it varies between different pedestrians (Rainer et al., 1988; Kerr, 1998). This variability of DLFs implies that a value of DLF used in modelling should, in principle, be taken as a stochastic variable.

There is a lot of work which concentrates on measuring the DLFs for different walking frequencies and harmonics (Rainer et al., 1988; Kerr, 1998). Generally speaking, DLFs have been obtained by measuring the dynamic force induced by different test subjects by walking on a rigid (i.e. not perceptibly vibrating) surface. Based usually on the average DLF obtained experimentally for a certain walking frequency, the harmonic force representing walking is typically defined and used to simulate the response on a particular footbridge. This response can then be compared with a measured response. Often, significant differences between the two responses are noticed and they are attributed to inappropriate values of DLFs used in simulations (Pimentel, 1997). However, there are not many works investigating the nature of and causes for the observed differences.

This study investigated the nature and possible causes of differences between the simulated and measured responses and the way these differences can be taken into account in a design model. This research is based on the response measurements due to single person walking excitation and its numerical modelling for three footbridges of different structural systems. Since these footbridges have fundamental natural frequencies in the range of the first walking harmonic, only this harmonic is investigated. All three footbridges are briefly described and their modal properties required in the response simulations are presented.

Aberfeldy footbridge is a light glass-reinforced plastic, cable-stayed footbridge, with a total length of 113 m. Its total mass is about 20,000 kg. An investigated mode of vibration was the fundamental vertical mode at a frequency of 1.52 Hz. Podgorica footbridge is a heavy (260,000 kg) steel box girder footbridge spanning 104 m having the first vertical natural frequency of 2.04 Hz, as obtained in Chapters 3 and 4. Hope footbridge is a catenary-shaped stressed-ribbon structure spanning 34 m. Its mass is about 30,000 kg and the first mode of vibration is at 2.44 Hz. Vertical vibration of all three footbridges can be felt during walking. The footbridges are presented in Figure 5.1 together with modal properties (mode shape, natural frequency, damping ratio and modal mass) of relevant mode of vibration. The modal properties of vibration modes were obtained by combination of modal testing for all three footbridges and their FE modelling and model updating. The three bridges have natural frequencies covering well the full range of walking frequencies (1.5-2.4 Hz). All three footbridges are lightly damped, which is a common feature in footbridges.

A more detailed description of the three footbridges and the modal testing conducted can be found in publications by Pavic et al. (2000) for Aberfeldy footbridge and Pavic and Reynolds (2002) for Hope footbridge, while Podgorica footbridge, as already mentioned, is described in detail in Chapters 3 and 4.

This chapter concentrates on the interaction phenomenon between a single pedestrian and footbridges which are perceptibly lively in the vertical direction. It first compares the measured and simulated resonant response time histories on as-built footbridges. Then, walking forces measured on a treadmill (Brownjohn et al., 2004b) are introduced into the simulations. After this, the differences between the simulated and measured responses on as-built footbridges are explained and their possible causes identified. This is done for walking with both controlled and not controlled (by a metronome) pacing rates. Finally, a way forward in terms of a possible modelling strategy for predicting vibration response on footbridges which vibrate perceptibly is suggested.

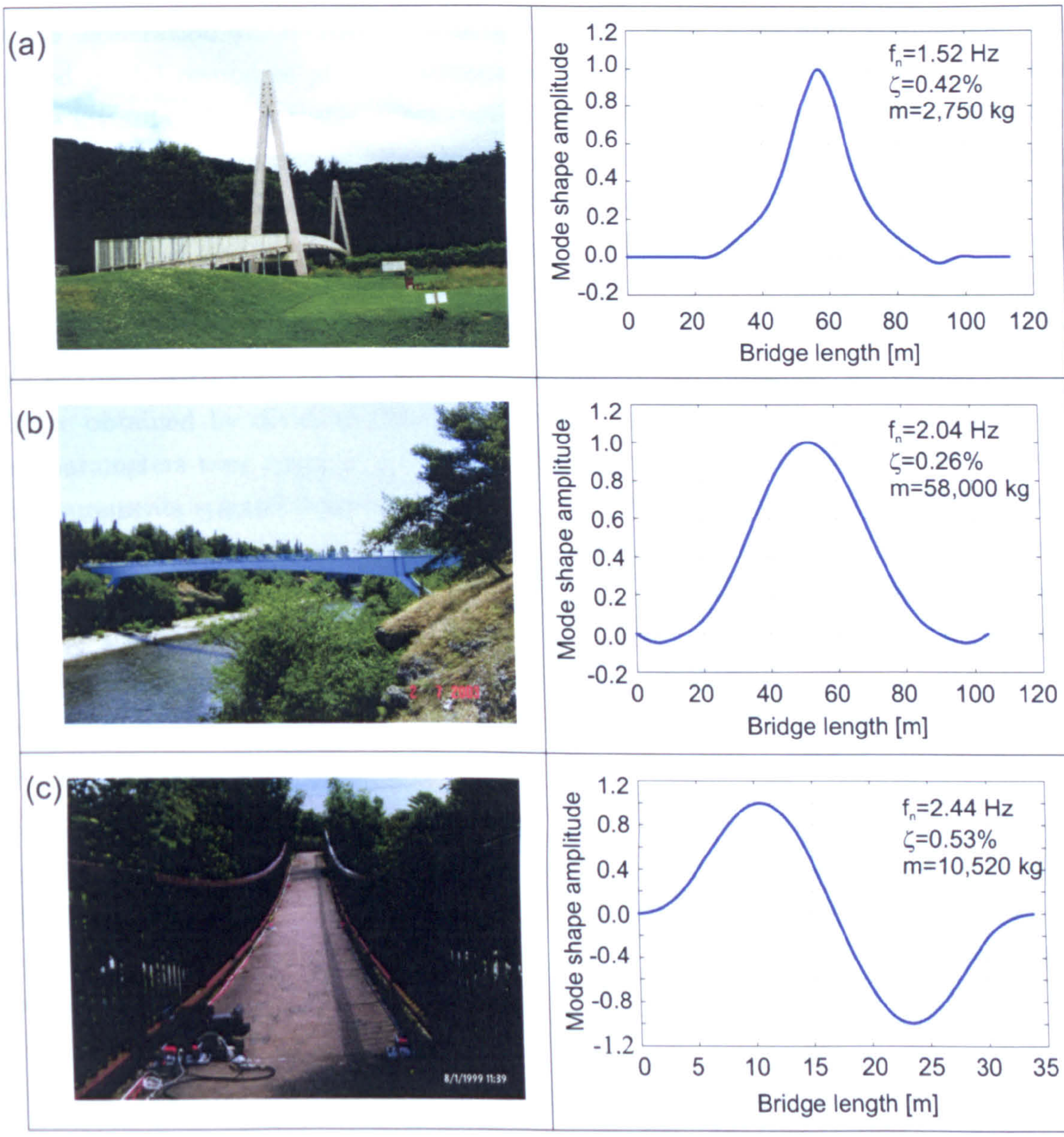

Figure 5.1: Photograph and the vibration mode investigated for: (a) Aberfeldy footbridge, (b) Podgorica footbridge and (c) Hope footbridge.

5.2 Measured and Simulated Responses

To generate the maximum responses for all three footbridges, test subjects were asked to walk with a pace matching the footbridge natural frequency, which was established prior to pedestrian tests. To help achieve this, a metronome set to a beat equivalent to the natural frequency was used. The footbridge response was recorded at the midspan point for the first two footbridges and at a quarter-span point for the third one considering that it had an anti-symmetric first vertical mode, which is common in catenary structures. As the measurement point in the last case was not exactly placed at the maximum mode shape amplitude, the

recorded acceleration was increased by an appropriate scale factor to be comparable with the simulated modal responses at the antinode of the excited mode of vibration. In addition, the time instants when a test subject entered and left the bridge in a single crossing were monitored by a video camera and/or by a sound recording system with whistle signs given at the entry and exit times. In this way, and assuming a constant walking speed, it was possible to match the pedestrian location on the bridge with the acceleration response at that location. Therefore, the level of vibrations felt while walking at every point in time during the crossing could be identified. Moreover, in this way the crossing time was known which enabled calculation of pedestrian velocity. Consequently, the pedestrian step length could be obtained by dividing the constant velocity with the step/metronome frequency. These parameters were required for the response simulations to be carried out. In addition, all measurements started from an ambient level of footbridge vibrations. This was done to make sure that the investigated effects of a single person walking are not superimposed with vibrations generated by some previous crossings made by the same or other pedestrians. All measured acceleration time histories were dominantly influenced by only the mode shape investigated, indicating predominantly single degree of freedom (SDOF) behaviour. They were filtered to obtain modal acceleration. Typical modal responses for all three footbridges are shown in Figure 5.2 (black lines).

For all three cases, the pedestrian dynamic load was then defined as a sinusoid having frequency f_n and amplitude $DLF \cdot W$, where W is the weight of the test subject. Then the modal force $F(t,x)$ is calculated by weighting the sinusoid by the mode shape $\Phi_n(x)$, to take into account the pedestrian location on the bridge during a crossing. Therefore, the modal force induced by walking can be written as (Smith, 1988):

$$F(t,x) = \Phi_n(x)(DLF \cdot W \cdot \sin(2\pi f_n t)) \tag{5.1}$$

where t is the time while x is the pedestrian location on the bridge. These two variables (t and x) are interdependent since the pedestrian location on the bridge x at any time instant t during a crossing can be obtained via multiplication of the pedestrian speed v_p by this time instant (assuming that $t = 0\,\mathrm{s}$ is a time instant when the pedestrian enters the bridge). Since the DLF value in Equation 5.1 directly influences the level of force amplitude, it was chosen carefully using the methodology explained in Section 5.4.

Considering the footbridge as a SDOF system with known modal properties (natural frequency f_n, damping ratio ζ and modal mass m given in Figure 5.1), the well-known modal equation of motion:

$$a(t) + 2\zeta(2\pi f_n)v(t) + (2\pi f_n)^2 d(t) = \frac{F(t,x)}{m} \tag{5.2}$$

could be solved numerically. In this equation $a(t)$, $v(t)$ and $d(t)$ are modal acceleration, velocity and displacement, respectively. The modal acceleration responses obtained for all three

footbridges are shown in Figure 5.2 (grey lines). It can be seen that the level of footbridge modal response is the highest for the first footbridge, followed by the third and the second ones. Moreover, with the exception of the second structure (in which the measurements and simulations, i.e. black and grey lines, match), the simulated responses overestimated the corresponding measured responses. In the case of the first footbridge, the measured peak acceleration response was overestimated by a highly significant 76% while for the third structure the simulated peak response was 28% higher than that measured. It should be emphasised that these differences exist (and can be quite significant, as in the case of the first bridge) even though the tests had been conducted in a strictly controlled manner and simulations were done with as precise input parameters as possible. This behaviour was noted for many other test subjects repeating the same test. Therefore, an investigation of the causes of these differences was carried out.

The modal force used in the simulation of the response of the Hope footbridge (presented as grey line in Figure 5.2c) was obtained by multiplication of the sinusoidal force by absolute value of the amplitude of the anti-symmetric mode shape shown in Figure 5.1c instead by the amplitude itself. This has a specific meaning and will be explained in Section 5.4.

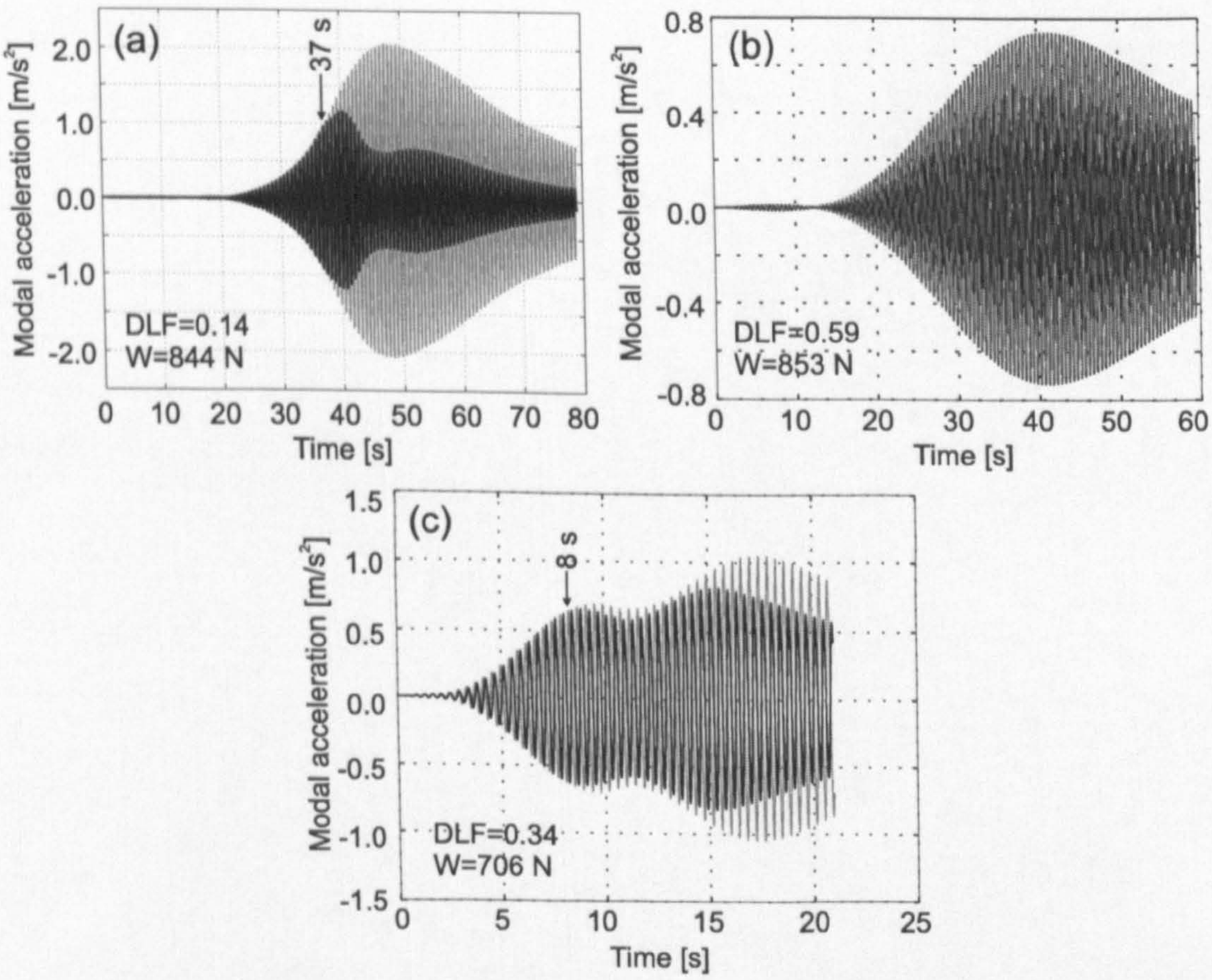

Figure 5.2: Measured (black line) and simulated (grey line) resonant modal responses on (a) Aberfeldy footbridge, (b) Podgorica footbridge and (c) Hope footbridge, for walking with a metronome. Note that the black and grey lines match in case (b).

5.3 Response Simulations to Measured Walking Forces

In the research related to vertical forces induced by walking, Brownjohn et al. (2004b) measured these forces on an instrumented treadmill at the National Institute of Education in Singapore. Eight test subjects walked on a treadmill, set to a constant speed, for about one minute or longer. The treadmill speed ranged between 2.5 km/h and 8.0 km/h. A typical walking force time history (after subtraction of the test subject's weight) is shown in Figure 5.3a. Figure 5.3b presents 10 s of the same walking force extracted between 30 s and 40 s of the record to give further insight into the shape of the forcing function. The spectral content of the walking force measured during 86 s is presented in Figure 5.3c. The spectrum is obtained by transforming a full number of cycles of the force time history to the frequency domain to avoid the signal leakage. It can be seen in Figure 5.3c that in the frequency domain there is a spread of energy in the measured force around its main harmonics, in this case at 1.52 Hz and its integer multiple frequencies. This phenomenon indicates that the walking force is not a periodic but a narrow-band random process, which has been investigated in some previous works (Eriksson, 1994; Brownjohn et al., 2004b). It can safely be assumed here that this spread of energy would be smaller if the walking frequency was controlled by a metronome instead of controlling the walking/treadmill speed. This is because the use of a sound prompt for pacing reduces the level of randomness in the walking forcing function.

The force presented in Figure 5.3a was band-pass filtered around its first harmonic with a filter width of $0.5 \cdot 1.52$ Hz=0.76 Hz. The filtered force is shown in Figure 5.4. It is noticeable that this force has a slightly variable amplitude - again, an indication of a narrow-band process.

As already said, this study aims to explain differences between measured and simulated responses starting with walking controlled by metronome first. For this purpose the measured force time histories with the least energy spreading were chosen for resonant response simulation on the as-built footbridges. Furthermore, the footbridge with the longest crossing time is most preferable in this analysis. The long crossing time is important here because it is more probable that general trends in the footbridge dynamic response will be better developed and easier to notice than in the case of shorter crossing times. This applies to footbridges with damping ratios of the same order, which is the case for the three footbridges considered. The crossing time T_c for every bridge could be calculated as:

$$T_c = \frac{L}{v_p} = \frac{L}{f_n \cdot l_s} \tag{5.3}$$

where L is the footbridge length, while v_p, f_n and l_s are the pedestrian velocity (equal to the treadmill velocity in this analysis), step frequency and step length, respectively. Typical crossing times under forces measured on the constant velocity treadmill would be around 110 s for Aberfeldy footbridge, 60 s for Podgorica footbridge and only about 20 s for Hope footbridge. Therefore, the crossing time was longest for Aberfeldy footbridge. From Equa-

tion 5.3 it is clear that this is not only because this footbridge was the longest but also because of the slowest walking (resonant) frequency (1.52 Hz) for this bridge.

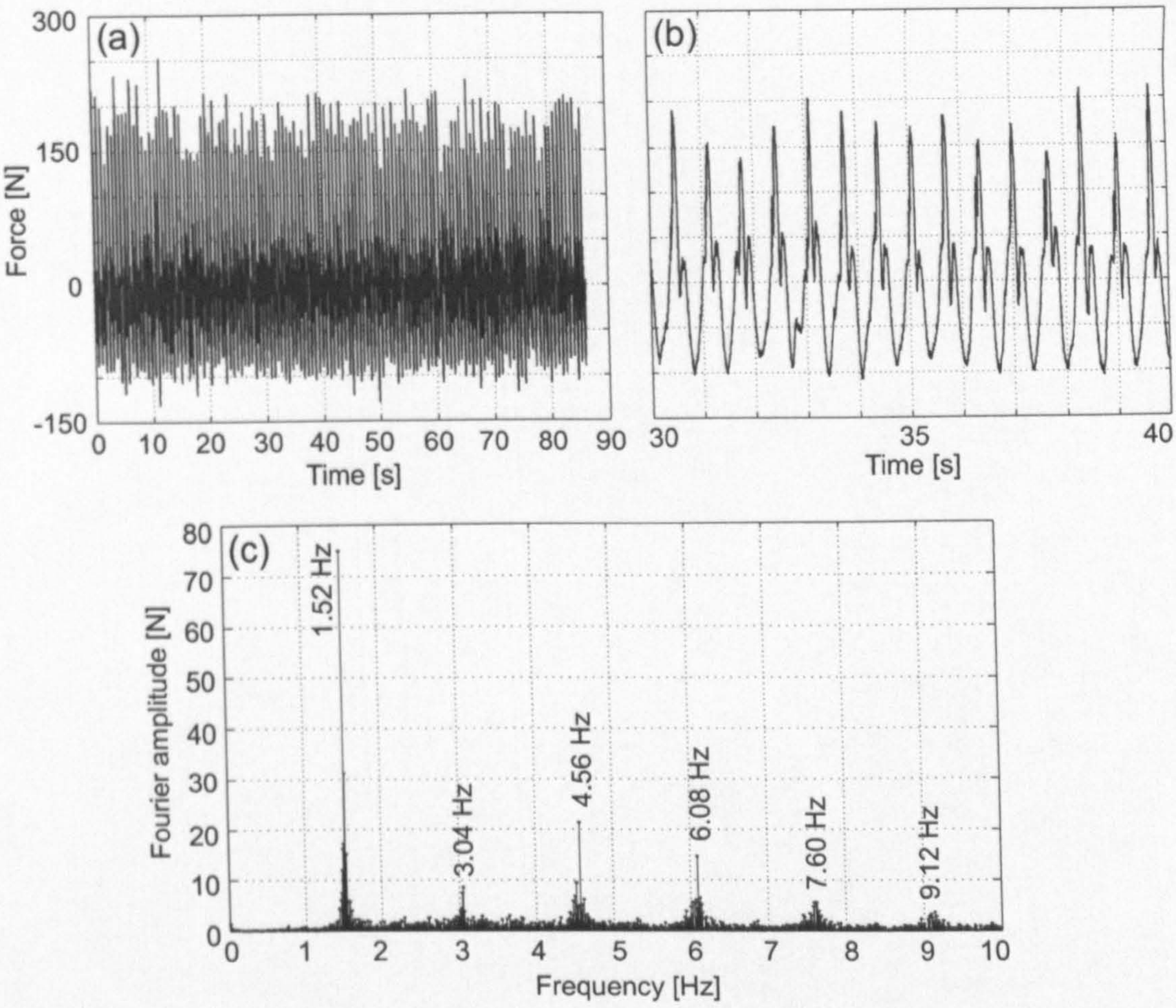

Figure 5.3: (a) Measured walking force time history. (b) Force detail between 30 and 40 s. (c) Fourier spectrum of the measured force.

The procedure for calculating the expected footbridge modal acceleration response under a measured force was as follows. First the time length of the measured force is compared with the crossing time. If it was longer, the measured force was shortened to the crossing time length. If the force duration was shorter than the crossing time, the force record was extended by repeating the same force record as long as it was required to reach the crossing time. This force was then slightly shortened to consist of an integer number of steps, to avoid signal leakage when numerically transforming the signal to the frequency domain. The force was then filtered, modulated by the mode shape, and used for SDOF response simulation. The result of this simulation will hereafter be referred to as Simulation 1. Next, the filtered force was approximated using a harmonic force having frequency of 1.52 Hz. The amplitude of this harmonic force was obtained as the average of all amplitudes in the filtered force. The first five cycles were excluded from averaging since they have low amplitudes as a result of the filtering process. The response to this harmonic force is called Simulation 2.

The two simulated responses under a test subject walking at a speed of 3.4 km/h (0.94 m/s) are shown in Figure 5.5. The agreement between the two responses is quite good. This means that, theoretically, it is possible to approximate the first harmonic of the walking force by a sinusoid without losing significant accuracy of analysis.

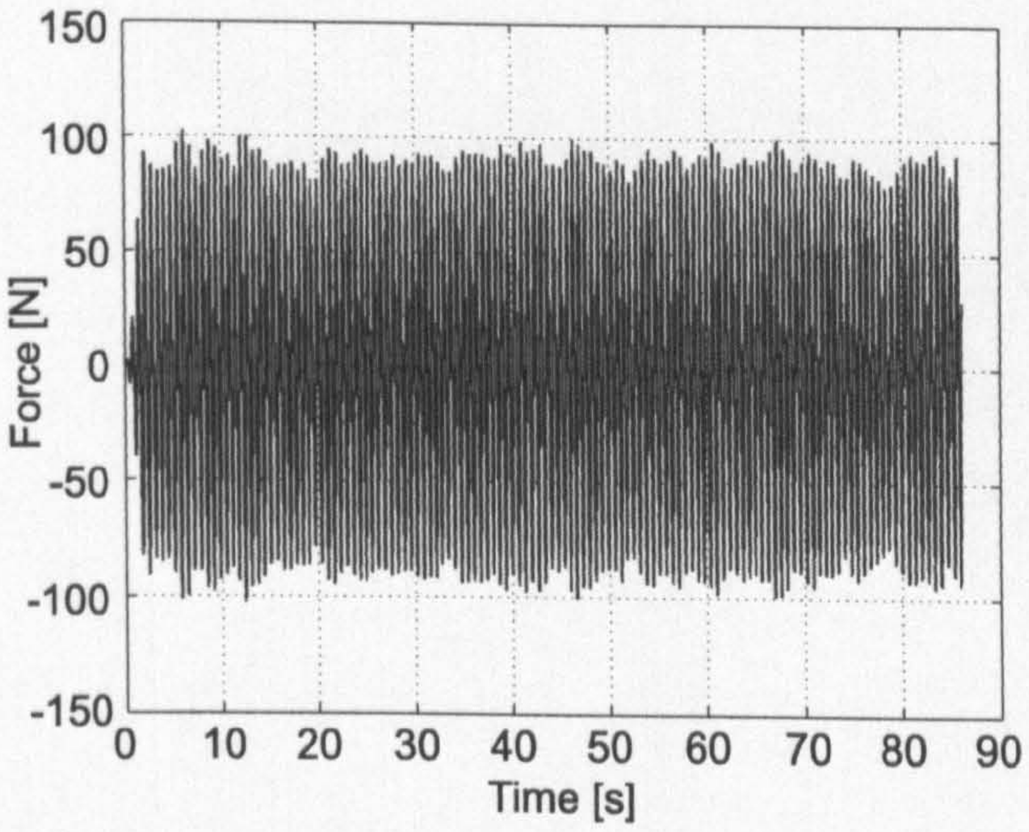

Figure 5.4: Measured force after filtering at the frequency of the first walking harmonic.

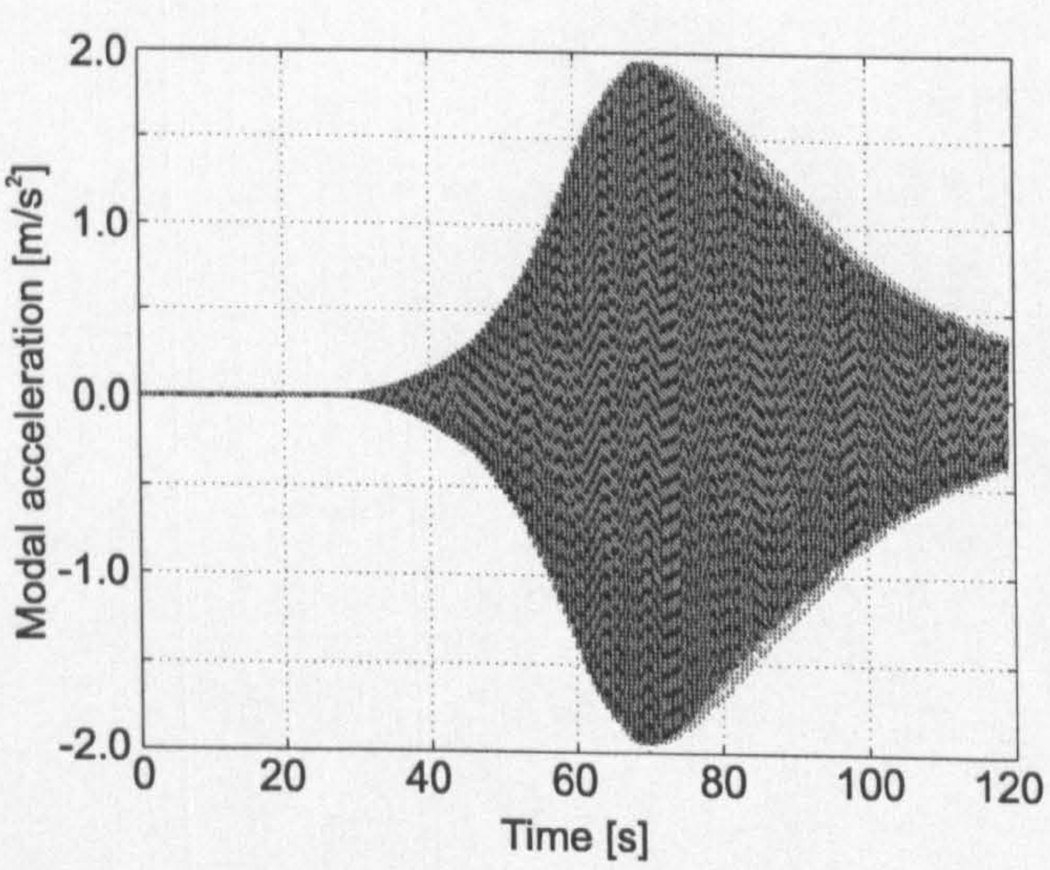

Figure 5.5: Modal response simulations to the first walking harmonic of a measured narrow-band force (black line) and a harmonic force (grey line).

To research this further, all measured walking forces with a first harmonic in the frequency range between $0.95f_n$ and $1.05f_n$, where f_n is the footbridge natural frequency, were considered. For Aberfeldy footbridge with natural frequency of 1.52 Hz this range was between 1.44 Hz and 1.60 Hz. In total, nine measured walking force time histories had a first harmonic in this frequency range. The two response simulations were carried out for all nine forces, but with a slight change in the SDOF natural frequency to match the dominant walking frequency. This was done to preserve resonance in all simulations. A comparison between Simulations 1 and 2 revealed that the agreement between them was not always as good as that shown in Figure 5.5. This is because some test subjects often changed their walking

frequency slightly and therefore introduced larger spreading of energy around the main harmonics in comparison with that given in Figure 5.3c. However, in four of nine tests test subjects walked very steadily. As a result, the peak response due to sine force was only up to 5% higher than that due to the measured force. On the other hand, in the remaining five tests test subjects had problems with keeping constant walking frequency. This resulted in 20-26% higher peak response in Simulation 2 in comparison with Simulation 1.

An important conclusion can be drawn here. Namely, despite the fact that all walking forces analysed were measured without controlling pacing frequency by a metronome, some test subjects were still clearly able to walk in a stable manner producing negligible energy spreading around their forcing harmonics. As a consequence, modal responses due to the filtered measured force and its approximation by a sinusoid were almost the same. This suggests that walking with a metronome would produce a force which can be replaced by a sinusoid even more accurately. However, this conclusion is related to walking on a rigid (i.e. not perceptibly vibrating) surface.

5.4 Nature of Differences between Measured and Simulated Responses

Based on the analysis in Section 5.3 it can be stated that a harmonic force is a good approximation of the walking force when walking on a rigid surface with a metronome. However, this was not always the case when comparing the measured and simulated responses due to walking on the investigated as-built footbridges (Figure 5.2). There are at least two possible explanations for observed differences in the responses. Either some inappropriate parameters were used in the simulations while getting numerical responses, or there were differences between human walking on a rigid and on a perceptibly moving surface.

As for the first explanation, it can be said that all parameters used in the simulations such as structural modal properties, pedestrian weight, walking frequency, walking speed and crossing time were all quite reliable, well established and controlled. This applies under a reasonable assumption that these parameters remain constant during the crossing analysed. The only remaining parameter was the DLF. This parameter was found in a systematic way. Specifically, since all test subjects started their footbridge crossings from an ambient level of vibrations, it is reasonable to assume that they did not perceive these low-level vibrations in the initial part of the crossing. Therefore these vibrations could not disrupt test subjects' walking patterns. Consequently, it can be said that at least in the initial part of the footbridge crossing, walking of the test subjects can be considered as walking across a rigid surface. Based on this, the DLF for each case was determined by trial and error. Namely, the DLF was changed iteratively until a good amplitude agreement between the simulated and measured responses was achieved. This agreement was in fact excellent as visible in the initial part of responses for all three simulations presented in Figure 5.2. The DLFs obtained

in this way are given in the same figure. It should be noticed that they are all within the range of values measured (on a rigid surface) by Kerr (1998) for given walking frequencies.

An additional methodology can be used for identifying the DLFs. It is based on constructing the envelopes of maximum modal forces per cycle for several different DLF values (black lines in Figure 5.6). These envelopes can then be compared with that identified from the measured modal acceleration time history following the procedure proposed by Dallard et al. (2001a) for the Millennium Bridge. The envelopes corresponding to the measured data are shown for all three footbridges in Figure 5.6 by grey-dashed lines. The value of DLF for which the initial part of the modal force envelope best fits that given by Dallard et al. is the one which is realistic for a footbridge crossing analysed. The range of the DLF for Aberfeldy footbridge is clearly around 0.12, for Podgorica footbridge it is 0.59, while for Hope footbridge it is between 0.28 and 0.42. The precise values of DLF for Aberfeldy and Hope bridges can be obtained by linear interpolation and they are equal to the value determined previously in Figure 5.2. It was reassuring to see such a good agreement indicating the robustness of the assumed DLFs for the three footbridges.

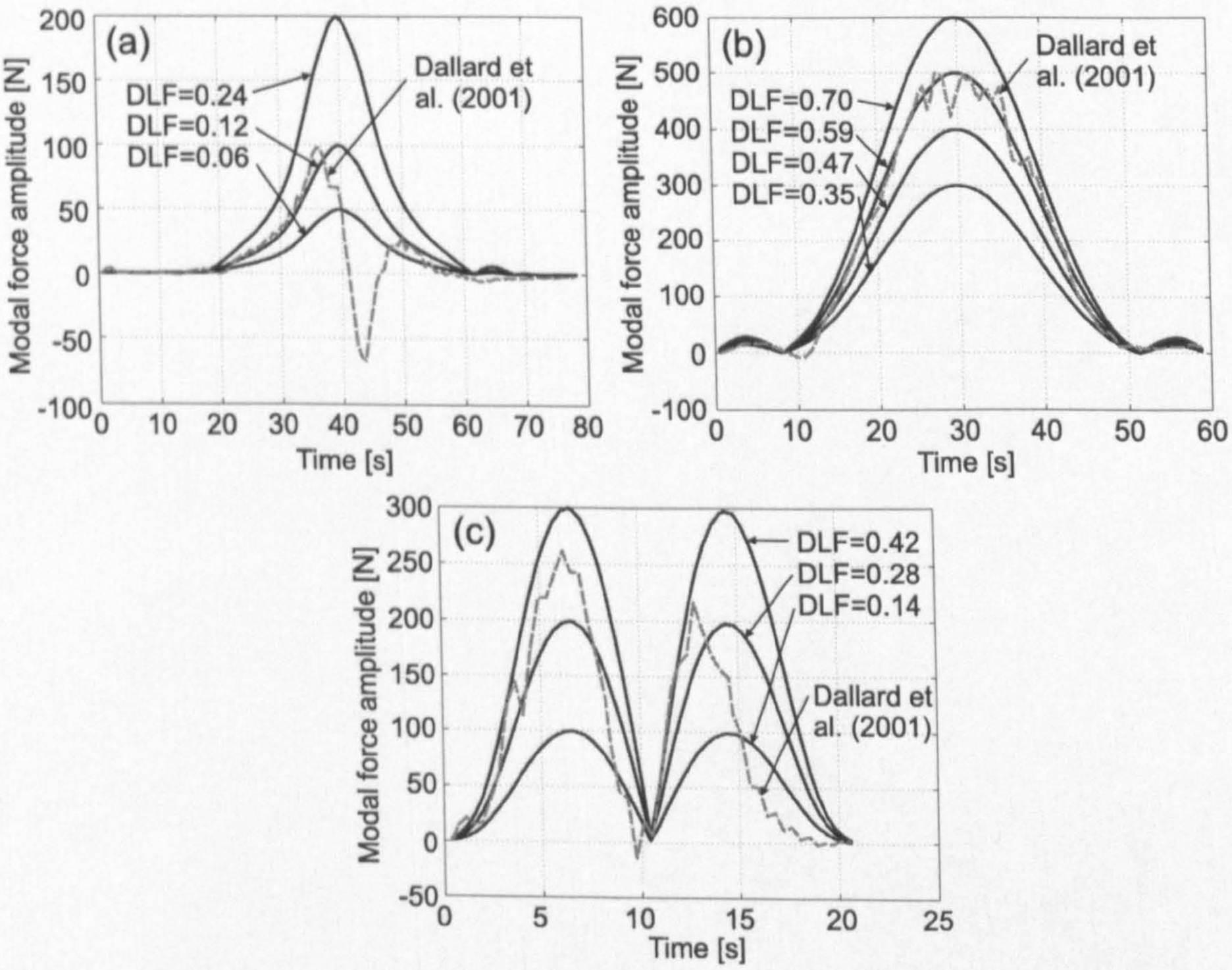

Figure 5.6: Estimation of the DLF by comparing initial part of envelopes of different modal forces with that derived by Dallard et al. (2001a) for (a) Aberfeldy footbridge, (b) Podgorica footbridge and (c) Hope footbridge.

Therefore, the logical way to explain the differences in the responses in Figure 5.2 is to conclude that the some test subjects were influenced by increasing vibrations which they felt during their footbridge crossing. Even with a help of a metronome, they could not keep the step after they started feeling stronger levels of vibrations. The point when the simulated and measured responses start to differ can be denoted as the point when the test subjects lost their step under the influence of the perceived vibrations. This occurred on Aberfeldy footbridge at $t = 37\,\mathrm{s}$, and at $t = 8\,\mathrm{s}$ on Hope footbridge, while it did not occur at all for Podgorica footbridge during a complete crossing (Figure 5.2). After the step was lost on Aberfeldy and Hope bridges, the walking frequency did not match the footbridge natural frequency precisely. As a result, a decrease in the footbridge response in comparison with the simulated one occurred. This is often interpreted in the literature as a decrease of the DLF on as-built footbridges, in comparison with the DLF measured on the rigid surface (Pimentel et al., 2001).

An additional argument that supports the existence of the interaction between a pedestrian and the footbridge can be given for case of Hope footbridge. This bridge has an anti-symmetric mode of vibration (Figrure 5.1c). If the modal force was modelled in a usual way, i.e. by multiplication of a sinusoidal force by the mode shape, then this force would have changed its phase at the middle of the bridge where the node of the mode shape is. As a result, the footbridge response would be reduced to zero after certain amount of time, as presented in Figure 5.7. The fact that this did not happen in actual measurements (one example is shown as black line in Figure 5.2c) proves a pedestrian's inability to keep the steady pacing after passing the nodal point of the mode shape. This probably happens because the required change in the phase of the walking force for 180^0 requires that the pedestrian walks (relatively to the structural movement) in an opposite way to that done before crossing the nodal point. Since this would cause the discomfort (when the footbridge vibrates perceptibly) the pedestrian adjusts their step to the structural movement in order to maintain the same relative movement between the bridge and themselves as it was before the passing the nodal point of the mode shape. This seemingly develops stronger vibrations than in the case when phase of the walking force has been changed by 180^o (compare the vibration levels presented as black lines in Figures 5.2c and 5.7 after $t = 15\,\mathrm{s}$). This pedestrian interaction with the bridge after crossing the nodal point was the reason to model the human-induced modal force for simulations across Hope bridge as the sinusoidal force multiplied by an absolute value of the mode shape amplitude. This was done since it produced more realistic vibration response of the footbridge. Since the most important consideration in this chapter is related to the time instant when a pedestrian loses their step, and this occurs at $t = 8\,\mathrm{s}$ (i.e. before reaching the nodal point of the mode shape) regardless of the way of modelling the modal force, the human-structure interaction after crossing the nodal point is not analysed in more detail here.

By multiplying the maximum measured vibration level per vibration cycle over time for every crossing with the mode shape amplitude which corresponds to the location of the test

subject at the given time instant, vibration perception curves as a function of time can be constructed. These curves present the level of vibrations felt by the test subject during the footbridge crossings. They are shown in Figure 5.8. It can be seen that in the case of Aberfeldy footbridge, the test subject lost his step when feeling vibrations of $0.82\,m/s^2$. This was in agreement with the fact that the test subject on Podgorica footbridge, who felt a maximum acceleration level of $0.56\,m/s^2$ during the complete crossing, did not lose his step at all. Finally, the test subject crossing Hope footbridge lost his step when perceiving vibrations of $0.51\,m/s^2$. His walking frequency of 2.44 Hz was very fast, which made it more difficult to keep step when perceiving strong vibrations.

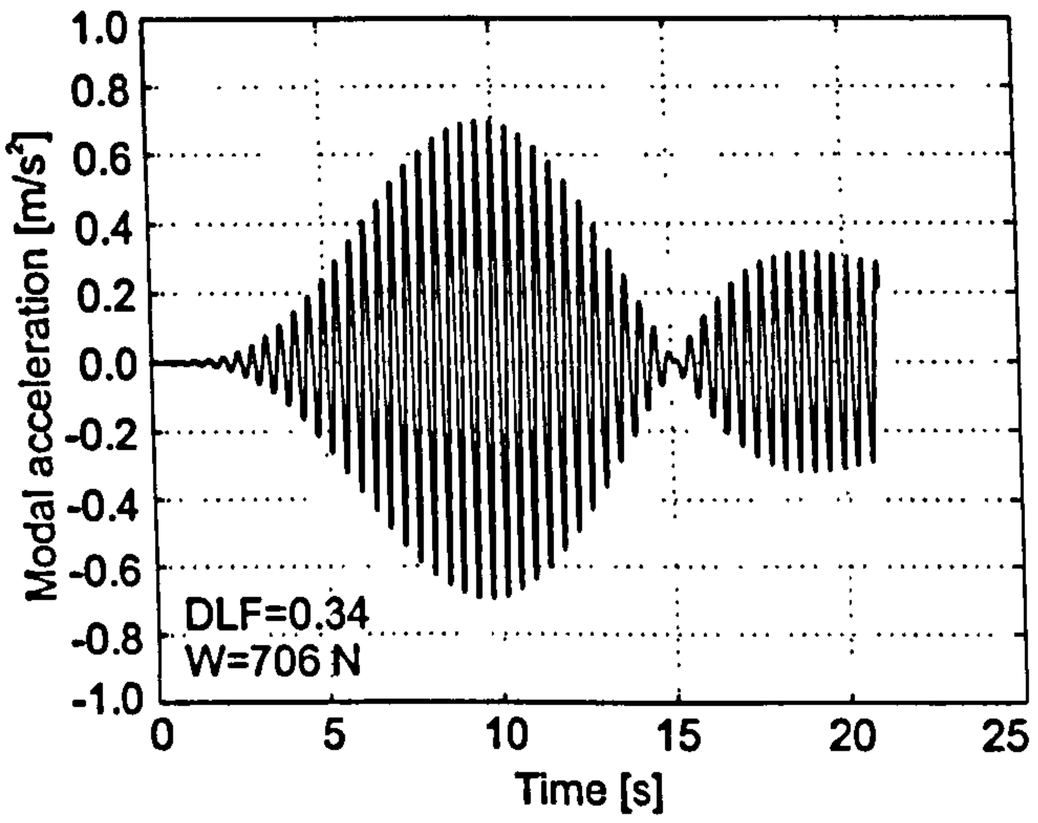

Figure 5.7: Simulation of the modal response due to the modal force that changes its phase at the nodal point of the mode shape.

It should be noticed here that the maximum level of perceived vibrations is not necessarily the same as the measured peak acceleration. For example, the maximum perceived level on Podgorica footbridge of $0.56\,m/s^2$ (Figure 5.8b) was lower than the peak acceleration of $0.73\,m/s^2$ (Figure 5.2b). This is because the peak acceleration was recorded at the midspan point about 12 s after the test subject passed this point.

The observed differences in the vibration level when the step was lost (Aberfeldy and Hope footbridge) are expected since the vibration perception depends on vibration frequency and test subject's sensitivity to vibrations (Griffin, 1996). Although the findings found here cannot be generalised due to small number of test subjects and test structures investigated, it is interesting that the jerk value, defined as the first derivative of acceleration (Griffin, 1996), was the same for the two cases when the step was lost (Aberfeldy and Hope footbridge). This value was exactly $7.8\,m/s^3$. The same jerk value for Podgorica footbridge required an acceleration level of $0.61\,m/s^2$, the value that was higher than $0.56\,m/s^2$ - the maximum that the test subject experienced during the crossing (Figure 5.8b).

As the crossing time for Aberfeldy footbridge was long enough, the Fourier spectra for the first 37 s (i.e. until the step was lost) and the next 37 s (i.e. between 37 s and 74 s) of the

measured modal response were calculated. They are presented in Figure 5.9 (grey vertical lines). In the first 37 s the dominant response frequency was at 1.52 Hz (Figure 5.9a). The second spectrum has two peaks - at 1.46 Hz and 1.52 Hz (Figure 5.9b) indicating that the walking frequency dropped to 1.46 Hz. Therefore, the average walking frequency did not match the natural frequency between 37 s and 74 s of the crossing which is in agreement with the finding that the test subject lost step after 37 s. Furthermore, as the walking frequency was slightly changed this caused a variation of the response amplitude known as the 'beating' effect (Figure 5.2a).

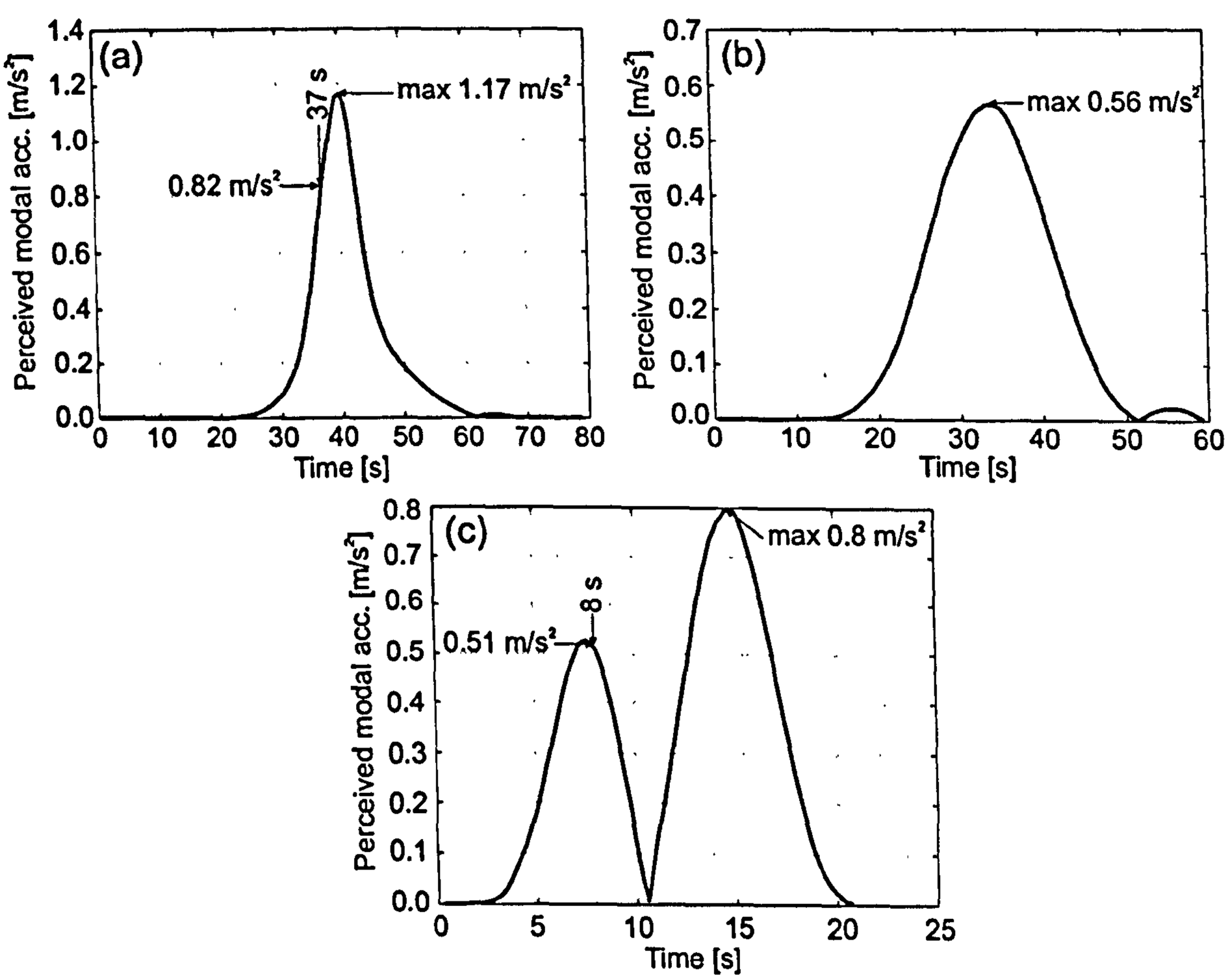

Figure 5.8: Vibration perception curves during crossing of the (a) Aberfeldy footbridge, (b) Podgorica footbridge and (c) Hope footbridge.

5.5 Walking Without Metronome

Since walking with a metronome is not a natural situation on as-built footbridges, it is interesting to see what happens if the same test subject walks without a metronome but close to or at the resonant frequency. This condition is difficult to fulfil during tests, since many tests should be conducted until a test subject manages to walk at the resonant frequency. However, the two test subjects who conducted tests with a metronome shown in Figures 5.2a and 5.2b had success in matching the resonant frequency when walking freely. Regarding

Hope footbridge none of the seven test subjects who took part in the testing programme matched the frequency of 2.44 Hz during free walking, which is expected bearing in mind that this is an unnaturally fast walking frequency.

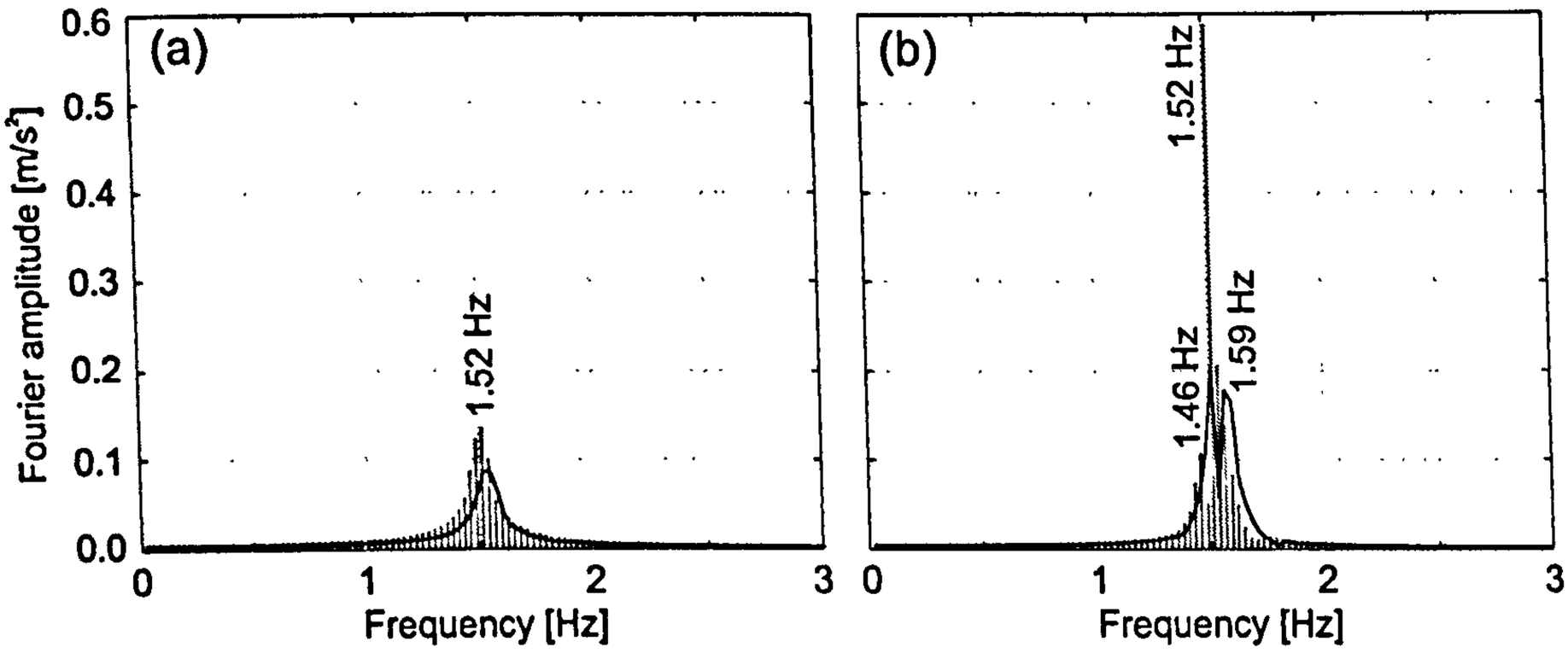

Figure 5.9: The spectrum of measured acceleration response (grey vertical lines) on Aberfeldy footbridge for: (a) the first 37 s of the response, (b) the response between 37 and 74 s, when walking with a metronome. Black line is related to the crossing without a metronome (Section 5.5).

The recorded resonant modal responses from the first two footbridges are presented in Figures 5.10a and 5.10b (black lines). These responses were obtained only by giving a simple instruction to the test subject to walk slowly, in case of Aberfeldy footbridge, and fast, in case of Podgorica footbridge. The corresponding simulated responses are presented as grey lines. It can be seen that both test subjects generated lower vibration levels than when walking with a metronome (Figures 5.2a and 5.2b: black line). The perception curves during the two uncontrolled crossings are also presented in Figures 5.10c and 5.10d.

In these tests both test subjects generated responses that followed the simulated modal response (grey line in Figures 5.10a and 5.10b) closely in the initial 35 s for Aberfeldy footbridge and 26 s for Podgorica footbridge. After these time instants the differences between measured and simulated responses arose, being greater than when walking with help of a metronome. Namely, simulated peak response for Aberfeldy footbridge was now 3.47 times higher than that measured, whereas for Podgorica footbridge this ratio was 1.30. These differences now probably originate not only from losing step due to perception of footbridge vibrations but also from natural variations of the step frequency seen for some test subjects walking on the treadmill without a metronome. However, assuming that the test subject lost their step when the simulated and measured responses start to differ, the vibration level perceived by the test subject at that moment can be adopted as the level of vibration which disturbs their normal walking. Therefore, the disturbing level of vibrations obtained in this way might be conservative, that is on the safe side.

Having this in mind, it can be concluded that for a test subject walking across Aberfeldy footbridge, the disturbing vibration level dropped from $0.82\,\mathrm{m/s^2}$ when walking with a metronome (Figure 5.8a), to $0.33\,\mathrm{m/s^2}$ when walking without it (Figure 5.10c). Also, it can be noticed again that the Fourier spectrum in the first 35 s has only one peak (black line in Figure 5.9a) whereas the two peaks at 1.52 Hz and 1.59 Hz are present in the response measured between 35 s and 70 s (black line in Figure 5.9b). On the other hand, the test subject on Podgorica footbridge did not have problems with keeping step at as high vibration level as $0.56\,\mathrm{m/s^2}$ when walking at metronome beat (Figure 5.8b), but lost his step at vibration level of $0.37\,\mathrm{m/s^2}$ when walking freely (Figure 5.10d). Corresponding jerk values for these two disturbing vibration levels (i.e. $0.33\,\mathrm{m/s^2}$ and $0.37\,\mathrm{m/s^2}$) on the two footbridges are $3.2\,\mathrm{m/s^3}$ and $4.7\,\mathrm{m/s^3}$, respectively.

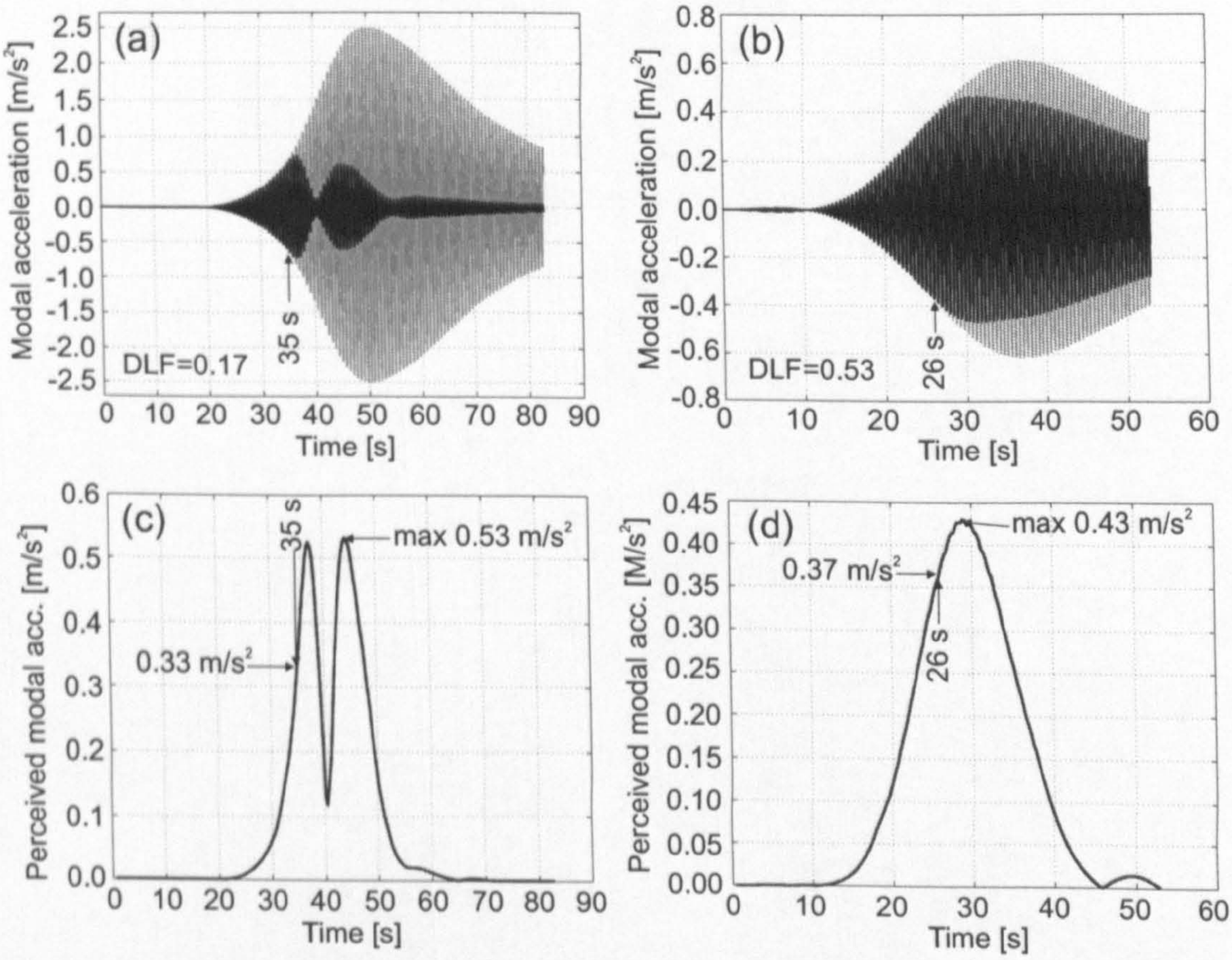

Figure 5.10: (a) Simulated (grey line) and measured (black line) modal responses on Aberfeldy footbridge. (b) Simulated (grey line) and measured (black line) modal responses on Podgorica footbridge. (c) Vibration perception curve during slow walking on Aberfeldy footbridge. (d) Vibration perception curve during fast walking on Podgorica footbridge.

The disturbing vibration levels, at which a test subject loses their step, obtained in this way for more test subjects can help establish the (un)acceptable level of vibrations for pedestrians, an area currently not well researched. The allowable vibration levels defined by BS 5400 (BSI, 1978) are $0.62\,\mathrm{m/s^2}$ for Aberfeldy footbridge, $0.71\,\mathrm{m/s^2}$ for Podgorica footbridge and $0.78\,\mathrm{m/s^2}$ for Hope footbridge, while those defined by ISO 10137 (ISO, 1992) are $0.70\,\mathrm{m/s^2}$, $0.60\,\mathrm{m/s^2}$ and $0.54\,\mathrm{m/s^2}$, respectively. The analysis conducted in this study suggests that

disturbing vibration levels might be lower than those defined by the BS 5400 and ISO 10137. This is in agreement with results obtained from interviewing 300 randomly chosen pedestrians who were asked to rate the vibration level perceived during their crossing of Podgorica footbridge (Appendix A). Additionally, Kasperski (2005) reported similar conclusions regarding applicability of codified vibration perception scales on people walking across as-built footbridges. However, more research in this area is needed to establish if the vibration level which disturbs the normal walking, calculated by the methodology suggested in this study, is at the same time the level which annoys pedestrians.

The behaviour of losing step under increased levels of vibration seemingly prevents the developing of high level of vertical vibrations for single person walking at resonant frequency. However, in case of similar behaviour of a pedestrian walking at a near-resonant frequency, it is quite possible that losing step at high level of vibrations perceived will lead to adjusting step to resonant frequency (as long as the pedestrian is capable of keeping this resonant walking frequency) and developing stronger vibration than initially anticipated. This is a phenomenon called lock-in (Bachmann, 2002) and might be relevant when considering normal pedestrian traffic in which all sorts of walking frequencies are possible (Matsumoto et al., 1978).

It is also worth noting that DLF values used in the simulations for walking with and without a metronome were different for the same test subject walking at the same pacing frequency. This just means that this value is not only an inter-subject variable but also intra-subject variable. Inter-subject variability means that different test subjects will generate different DLFs even when walking with the same pacing rate, while the intra-subject variability means that the same test subject can generate different DLFs in two tests conducted under the same conditions (Griffin, 1996).

5.6 Modelling of Human-Footbridge Interaction

The effect of losing step when strong vibrations are perceived reduces the actual vibration response to below the expected level assuming perfect resonance (Figure 5.10). This situation may be modelled by the damping increase in the resonating structure, after a certain vibration level is achieved. Therefore, it would be interesting to present the human-structure interaction in terms of the damping change over time. This additional damping ratio $\zeta_p(t)$ can be introduced in the SDOF equation of motion written in its modal form as follows:

$$a(t) + 2(\zeta + \zeta_p(t))2\pi f_n \cdot v(t) + (2\pi f_n)^2 d(t) = \frac{F(x,t)}{m}. \tag{5.4}$$

All variables used in this equation were defined previously.

To get $\zeta_p(t)$ the following procedure was used. First the total damping ratio $\zeta + \zeta_p(t)$ was kept as the value for the empty bridge (i.e. $\zeta_p(t) = 0$) until the time instant when the step was

lost. After the time instant when simulated and measured responses started to differ, say at time t_1, the total damping ratio $\zeta + \zeta_p(t)$ was changed iteratively. This was done until good agreement between measured and simulated responses was achieved for a time slot after the time instant t_1. Once the good agreement was obtained, the new time instant $t_2 > t_1$ when the two responses start to differ was spotted. Then new value for the total damping ratio was chosen. The procedure was repeated until good agreement between the two responses was achieved for the complete response time history. During this procedure, the harmonic dynamic force was kept constant.

The procedure was conducted for both walking with a metronome and without it for Aberfeldy footbridge, walking without a metronome for Podgorica footbridge and walking with a metronome on Hope footbridge; namely for all response time histories presented in Figures 5.2 and 5.10 for which the simulated and measured responses differed.

The change of total damping ratio $\zeta + \zeta_p(t)$ over time is shown in Figure 5.11. Furthermore, additional damping ratio $\zeta_p(t)$ is presented in the same figure to illustrate the degree of added damping due to imperfect human walking. It can be seen that some damping changes were quite significant and long lasting, especially for walking without a metronome on Aberfeldy footbridge (Figure 5.11b). To illustrate these changes more clearly the added damping was averaged over the time periods when it was significant, say greater than 50% of the damping of the empty bridge. This value is also given in Figure 5.11. In this way we can say, for example, that the average additional damping was about 3.9 times higher for Aberfeldy footbridge when test subject walked without a metronome (Figure 5.11b), in comparison with walking with a metronome (Figure 5.11a). In both cases this significant damping increase lasted more than 20 s. For other two footbridges (Figures 5.11c and 5.11d) the additional damping was of the same order as the damping of the empty bridge.

The physical interpretation of this damping increase should be intuitive to anybody who has walked over a vertically bouncing footbridge. Namely, often the pedestrian can feel up and down vibrations of the footbridge which are opposite to the movement of the pedestrian's foot. What the pedestrians feel in this situation is that the bridge deck 'hits' their feet. Since this can be also considered as the pedestrian's opposition to the footbridge movement then it can be said that the pedestrians act similarly to active dampers.

Alternatively, this dampening effect of the walking person can be described as a change in the modal force, while the structural damping stays the same as that for the empty structure. Namely, if the additional damping force from Equation 5.4 is transferred to the right side of the equation then this right side of the new equation:

$$a(t) + 2\zeta \cdot 2\pi f_n \cdot v(t) + (2\pi f_n)^2 d(t) = \underbrace{\frac{F(x,t)}{m}}_{F_h} - \underbrace{2\zeta_p(t) \cdot 2\pi f_n \cdot v(t)}_{F_d}, \tag{5.5}$$

can be interpreted as the modal force which takes into account the human-structure interaction. This force consists of the two terms (F_h and F_d) that are, at resonance, in phase

with each other as well as with velocity. This resulting force is shown in the first column of Figure 5.12 (black line) in comparison with the initially assumed harmonic force multiplied by the mode shape (grey line). It can be seen that the effect of the human-structure interaction can be generally interpreted as a modification of the initially assumed harmonic force F_h when perceiving high level vibrations. This modification is actually an attenuation of the initially assumed harmonic force F_h as long as the amplitude of the dampening force in absolute sense $|F_d|$ is smaller than the amplitude of the harmonic force $|F_h|$. In this case the amplitude of the resulting force on the right hand side of Equation 5.5 $F_h - F_d$ is still in phase with the footbridge velocity. However, when the amplitude of the dampening force $|F_d|$ becomes greater than that for the harmonic force $|F_h|$ then the resulting force $F_h - F_d$ acts out of phase with the velocity. Additionally, if the dampening effect of the pedestrian is extremly strong and $|F_d| > 2|F_h|$ then the resulting force $F_h - F_d$ is not only out of phase with velocity but also greater in amplitude sense than the initial force $|F_h|$. This effect is noticeable in Figure 5.12b around 39^{th} second of pedestrian's crossing.

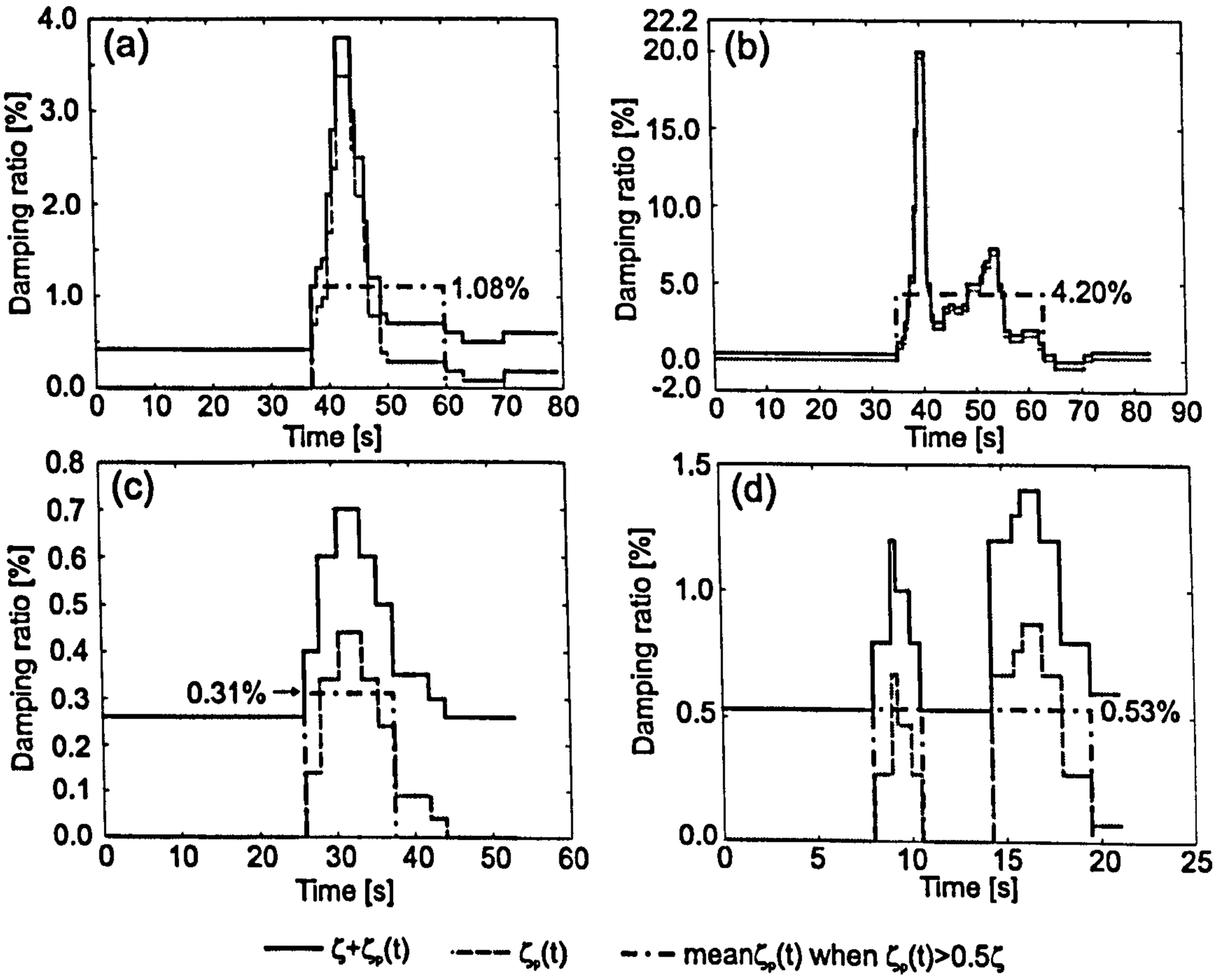

Figure 5.11: Dampening effect of a single pedestrian walking on (a) Aberfeldy footbridge with a metronome beat, (b) Aberfeldy footbridge without a metronome, (c) Podgorica footbridge without a metronome, (d) Hope footbridge with a metronome.

The peak values of this force per vibration cycle are presented in the second column of Figure 5.12 (black line) and compared with the same kind of force obtained following the previously mentioned procedure developed by Dallard et al. (2001a) for lateral sway forces

on the Millennium Bridge. A good agreement between the two modal forces can be noticed. However, it also can be seen that the modal force evaluated by Dallard et al. (2001a) for Aberfeldy footbridge (Figures 5.12a and 5.12b) becomes negative over some time periods, mainly at 41-46 s in Figure 5.12a and 37-41 s as well as 48-55 s in Figure 5.12b. This has a specific meaning. Namely, in the model with constant structural damping, the modal force must act out of phase with velocity to produce good agreement with measured response over time intervals observed. Normally, this force is in phase with velocity over all other time intervals, as explained before. Therefore, the pedestrian opposition to the structural movement is strongest over these time periods. In the previous model when human-structure interaction is modelled via damping change while keeping the dynamic force constant, it is expected that the strongest damping increase will be seen over the time periods observed. It can be seen in Figures 5.11a and 5.11b that this is the case.

Therefore, when analysing the vibrations in the vertical direction the effect of human-structure dynamic interaction while walking can be looked at as either the damping increase or the harmonic force modification. This approach is basically the same as the approach used by Dallard et al. (2001a) for explaining excessive vibrations on the London Millennium Bridge. A difference is that the approach of Dallard et al. (2001a) was applied for crowd-induced vibrations in the lateral direction. Furthermore, another difference is that crowd loading increased lateral vibrations on the Millennium Bridge and therefore had then the effect of decreasing apparent damping. In contrast, vibrations induced by a single pedestrian in the vertical direction are being reduced, meaning that a single person walking has a dampening effect similar to an active damper.

However, the suggestions for treating the human-structure dynamic interaction during a footbridge crossing as either the damping increase or the harmonic force modification are simplifications of the real situation. Namely, it seems that a pedestrian changes the frequency and probably amplitude and phase of the walking force when perceiving the high level of vibrations. Therefore, the resonant condition is not fulfilled in this situation and consequently the walking force does not stay in phase with the velocity of the structure, as assumed in this study. Clearly, a complex phenomenon, such as the human-structure interaction is, deserves further research and refined modelling.

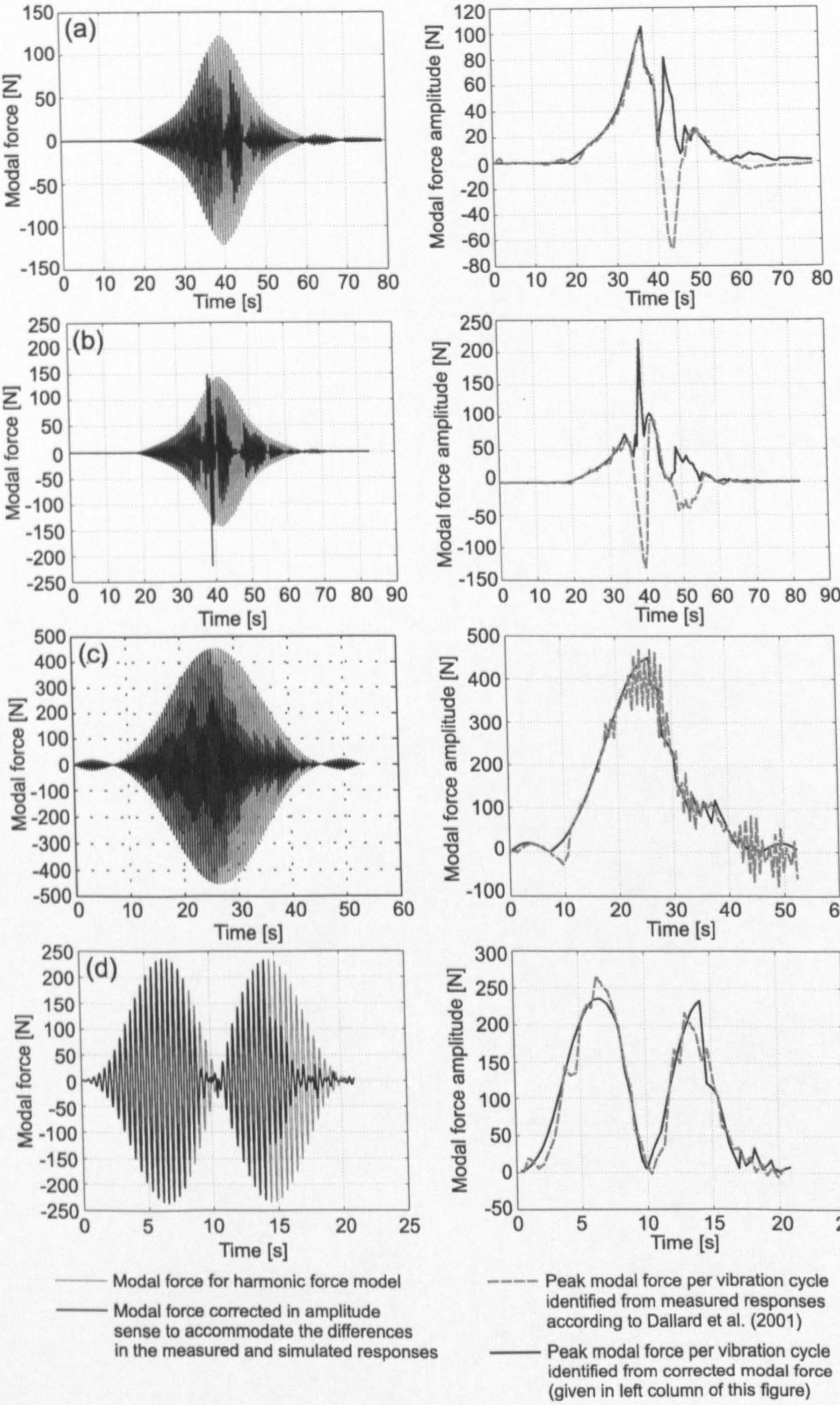

Figure 5.12: Modal forces and peak modal forces per cycle on (a) Aberfeldy footbridge (walking with a metronome), (b) Aberfeldy footbridge (walking without a metronome), (c) Podgorica footbridge (walking without a metronome) and (d) Hope footbridge (walking with a metronome).

5.7 Conclusions

In this chapter the interaction between a single pedestrian and footbridge structure in the vertical direction during walking across the footbridge at or near a natural footbridge frequency has been analysed. It was found that modelling of the first harmonic of the human-induced modal force as a sinusoidal force modulated by the mode shape is appropriate when walking across an imperceptibly moving surface, especially in case when walking frequency is controlled with the help of a metronome. However, this approach can significantly overestimate the footbridge vibration response if the footbridge develops perceptible vibrations during a single person's crossing.

By comparing measured and simulated responses on three lively footbridges, it was found that differences in responses can be significant when walking with or without a metronome. It has been argued that these differences originate in the inability of the pedestrian to keep in a steady step when feeling strong vibrations. This applies to the case of walking with the help of a metronome. Moreover, these differences become larger when walking without the metronome. The increased differences originate not only in the fact that it is easier to lose a steady step when step frequency is not controlled, but also in natural variability of the walking frequency (i.e. not perfectly periodic walking force) caused by the fact that humans are not perfect machines.

The time instant when differences in the simulated and measured responses start to occur was adopted as the one when a pedestrian loses steady step during their walking. The corresponding vibration level felt by the pedestrian at this time instant can then be calculated and is called the disturbing vibration level. This value was $0.33\,\mathrm{m/s^2}$ and $0.37\,\mathrm{m/s^2}$ for walking naturally (i.e. without controlling the step frequency) across two footbridges. Therefore, the acceleration level of around $0.35\,\mathrm{m/s^2}$ could be considered as a provisional limiting vibration level. This is about 50% lower than values defined by the British footbridge design code indicating that the code limit may not be appropriate to apply. However, this vibration level was obtained in a limiting testing programme and should be researched further.

The methodology for determining disturbing vibration levels in an objective way (and not a subjective way usually used in literature) presented in this chapter can be used as a systematic approach for creating a vibration perception database of a walking person. This should be based on response measurements on more footbridges and with more test subjects. To the best of the author's knowledge, a database of this kind does not currently exist in the available literature.

The effect of losing steady step during walking while perceiving strong vibrations was modelled via footbridge damping increase. Not surprisingly this effect was more emphasised when walking at the resonant frequency without a metronome. Alternatively, the phenomenon of the human-structure interaction could be modelled by a modification of the human-induced modal force. One of these two methodologies can be used for predicting responses on footbridges with perceptible vibration levels once a wider database from different footbridges is

formed.

However, what actually happens on the footbridge is that the pedestrian loses their steady walking frequency when perceiving a certain level of vibrations. Therefore, some future study might attempt to model this phenomenon directly (via say change in walking frequency, force amplitude, and so on) rather then to express it via either damping increase, while keeping constant harmonic excitation force, or harmonic force modification while keeping the damping constant.

Preface to Chapter 6

Chapter 6 describes a framework for a probability-based procedure for estimating vibration response of footbridges due to a single person walking. It was assumed that only the first harmonic of the walking force is relevant for estimating the response that occurs only in a single mode. The same assumptions are made in the current British code provision (BSI, 1978).

This procedure makes use of the vibration level indicated in Chapter 5 as the provisional limiting value (being approximately $0.35\,\mathrm{m/s^2}$) for serviceability assessment of two footbridges for which data were available. This value is supported by subjective evaluation of vibration response of Podgorica footbridge obtained by interviewing 300 randomly chosen pedestrians. The work on interviewing pedestrians is not part of the main body of this thesis since it is a part of an investigation of multi-person traffic that is beyond the scope of this thesis. For this reason this work, published as a paper presented at EURODYN 2005 conference in Paris, is shown separately in Appendix A.

Chapter 6

Probability-Based Estimation of Vibration Response of Footbridges

This chapter, in an amended form, has been submitted for publication under the following reference:

Živanović, S., Pavic, A. and Reynolds, P. Novel Probability-Based Framework for Prediction of Vibration Response to Single Person Walking across Footbridge, ASCE Journal of Structural Engineering.

Abstract

Due to their slenderness, many modern footbridges may vibrate significantly under pedestrian traffic. Consequently, the vibration serviceability of these structures under human-induced loading is becoming their governing design criterion. Most current design codes consider the dynamic force induced by a single pedestrian as the relevant loading scenario when predicting footbridge vibration response in the vertical direction. This excitation is modelled as a deterministic harmonic force having frequency that matches a footbridge natural frequency and amplitude defined as a certain percentage of the pedestrian's weight. However, walking is not a deterministic phenomenon since the force induced by human walking is a narrow band random process, rather than a periodic force representable by a Fourier series. In addition, all human beings are different and therefore generate different dynamic forces, both in terms of their amplitude and frequency. A way to deal with this randomness and include these uncertainties, which influence force modelling and response prediction, is to represent them by probability density functions. A formulation of these probability density functions and their implementation into a procedure for vibration response prediction underpins a novel probabilistic approach presented in this chapter. Instead of a single response value obtained using currently available design guidelines throughout the world, this new analytical framework yields a probability that a certain level of vibration response will not be exceeded for single person walking. It is shown that this approach is appropriate for describing the physics of walking more realistically. Moreover, this approach leads to a lower probability of liveliness of footbridges having natural frequencies away from mean pacing rates, which is what has been observed in practice. With regard to this, it is also shown that the deterministic approach usually significantly overestimates the actual observed response of full-scale footbridges. Finally, there are strong indications that the single person loading scenario may not be representative when predicting responses of footbridges conveying multi-person traffic.

6.1 Introduction

Due to their slenderness, many new footbridges are susceptible to vibration serviceability problems under human-induced load. Since the infamous problem with excessive lateral vibrations of the London Millennium Bridge in 2000 (Dallard et al., 2001a), the research community worldwide has been attracted by this new challenge to study lateral vibration response of footbridges, especially under crowd load (Dallard et al., 2001a; 2001c; Newland, 2004; Strogatz et al., 2005). In the meantime, the design approach to check for vibration serviceability of footbridges in the vertical direction has remained where it was in the 1970s when it was originally developed. For this check, the design codes (BSI, 1978; OHBDC, 1983) currently require calculation of the response to a single person walking across a footbridge at a frequency that matches one of footbridge natural frequencies. The human-induced walking force is modelled as a sinusoidal, and therefore deterministic, force moving across the bridge at a constant speed and having predefined amplitude. The reason for choosing this resonant force model is that it is considered as the worst-case scenario.

The main shortcomings of this deterministic model are:

- It does not take into account inter-subject variability, i.e. that different people generate different forces during walking (Kerr, 1998).
- It neglects intra-subject variability, i.e. that a pedestrian can never repeat two exactly the same steps (Brownjohn et al., 2004b).
- It assumes that the resonant condition is achieved under a single person walking on an as-built footbridge. However, it is very often difficult to match the footbridge natural frequency during walking, especially when that natural frequency requires either too slow or too fast pacing for an average pedestrian.
- It does not take into account the fact that pedestrians adapt their behaviour to the footbridge vibration felt, that is they interact with the structure. As demonstrated in Chapter 5, due to human-structure interaction, people cannot easily keep a steady step when perceiving a high level of vibrations. On two lively footbridges investigated, this level was apparently around $0.35\,\mathrm{m/s^2}$. After perceiving such a level of acceleration, pedestrians responded to footbridge vibration by slightly changing their walking frequency in an attempt to avoid discomfort.

As a consequence of these shortcomings, the harmonic force model often significantly overestimates the experimentally measured footbridge response, even that measured at resonance when a pedestrian deliberately walks at a pacing rate to match a footbridge natural frequency (Pimentel, 1997).

To overcome these shortcomings, and take into account both inter- and intra-subject variability when simulating forces during walking, a probabilistic framework for force modelling and

response prediction is required. In such an approach, the factors that describe the two types of variability can be defined via their probability density functions and therefore introduced into calculation via their probability of occurrence. The factors which require probabilistic treatment are briefly reviewed, as follows:

1. **Walking (step) frequency** differs between different people and can be described via a normal distribution (Matsumoto et al., 1978). The normal walking frequency is usually in the range between 1.5 and 2.5 Hz.

2. People walk with different **speeds** (Pachi & Ji, 2005), even when walking with the same frequency.

3. **Magnitude of the dynamic force** induced by different people is also an inter-subject variable (Rainer et al., 1988; Kerr, 1998) and depends on walking frequency.

4. A pedestrian cannot make two steps in the exactly same way. For example, the walking frequency and force amplitude vary slightly in each step, which is an indicator of **the intra-subject variability** in the force induced. This is a consequence of the fact that the human-induced force is in fact a narrow band random phenomenon, rather than a periodic force (Brownjohn et al., 2004b; Sahnaci & Kasperski, 2005).

It should be mentioned that Ebrahimpour et al. (1996) have been working on a probability approach for modelling of a walking force. They observed the importance of inter- and intra-subject variability in modelling but without introducing it into a comprehensive force model that can be used for structural response prediction in practice.

The aim of this study therefore is to propose a novel probability-based framework for predicting vibration response due to a single person walking. This is considered to be a prudent way forward to update the current single person walking model featuring in many codes of practice. For this purpose, the probability distributions for the four parameters mentioned are proposed based on the data currently available. These proposals are building blocks of an analytical framework which is open for further improvement. This can be done when more data related to a specific variable become available leading to more reliable probability distributions. Also, these distributions should be critically evaluated when taken into calculation since they might be different for footbridges located in different countries, environments and having different purpose. For example, it seems that people in Japan generally walk with faster step frequency than people in Montenegro, as will be demonstrated in Section 6.2.2. This is probably a consequence of the way of life in these two countries as well as the fact that Montenegrians are, on average, taller than Japanese.

After defining the main modelling assumptions, a probability based analytical procedure for modal response calculation is explained and applied to two footbridges with known modal properties. Based on this, the probability of exceeding a certain level of vibration is obtained. Then, the same kind of analysis was conducted using computationally more demanding Monte

Carlo simulations. In this way the proposed analytical approach was verified. Finally, the results were compared with those from a deterministic procedure and checked against some available real-life measurements considered to be relevant to this investigation.

6.2 Modelling Assumptions

This section aims at analysing the parameters important for the probabilistic modelling of the walking force and calculating the corresponding vibration response. Probability distributions of these parameters (walking frequency and amplitude, number of steps needed to cross the bridge and imperfections in human walking) are defined. They are based either on data available in literature or the data gathered previously during work on this thesis (Appendix A). This information should enable statistical prediction of footbridge vibration response to a force induced by a single walker. However, some additional uncertain parameters could not be included into the model developed because of unavailability of the experimental data. These parameters are discussed at the end of this section (Subsection 6.2.6).

Based on experience from full scale lively footbridges where the first harmonic of the walking force is often responsible for generating strong structural vibrations, it was decided to consider only this harmonic in this study. However, the general procedure suggested in the study can be extended easily to footbridges where higher harmonics are relevant by taking into account an appropriate distribution for amplitude of the harmonic considered.

6.2.1 Footbridge as SDOF System

Footbridges are structures that often have well separated frequencies of different modes of vibration. In this case, the footbridge can be modelled as an SDOF system with known modal properties (natural frequency, modal mass and damping ratio). Furthermore, among the structural vibration modes, often only one mode, with a shape that can be approximated by a half-sine shape, is responsible for the footbridge liveliness (Bachmann et al., 1995a). This assumption of having a half-sine mode shape is used in this study. For some bridges this might seem to be too restrictive. However, the methodology presented here can be extended for other mode shapes provided that the analysis of the kind presented in Section 6.2.5 is conducted beforehand. Here, the aim is to present the framework for the methodology itself rather than to cover all possible footbridge structural layouts.

6.2.2 Walking (Step) Frequency

Matsumoto et al. (1978) identified a normal distribution of human walking frequencies with a mean value of 2.00 Hz and standard deviation of 0.173 Hz. This was identified using a sample of 505 people. However, recently a more extensive work has been conducted by the author of this thesis on Podgorica footbridge in Montenegro where the step frequency was

estimated by analysing video records of 1,976 people crossing over the footbridge. Detailed description of this work can be found in Appendix A. Here, it will only be mentioned that it was confirmed that the distribution of human walking frequencies follows a normal distribution, but with mean value of 1.87 Hz and standard deviation of 0.186 Hz (Figure 6.1a). As already mentioned, it is likely that the distribution parameters differ between different countries (say, between Japan and Montenegro), different footbridge locations, etc. In this study, the distribution identified on the footbridge in Montenegro is used since it has been established by video monitoring of one of the two footbridges investigated in this study. Also, this distribution has a mean value that is closer to that found by some other European researchers in recent years: 1.9 Hz measured by Kerr & Bishop (2001) and 1.8 Hz measured by Pachi & Ji (2005), as well as by Sahnaci & Kasperski (2005).

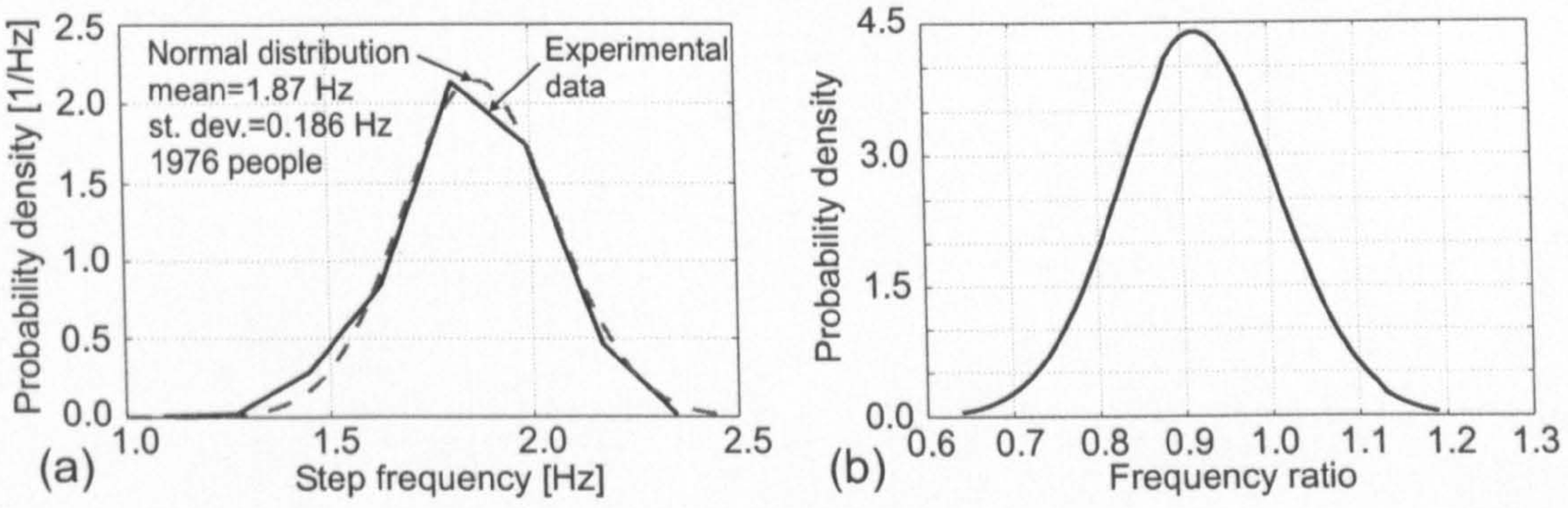

Figure 6.1: (a) Normal distribution of walking frequencies. (b) Normal distribution when the frequency axis is normalised to a footbridge natural frequency in the vertical direction (2.04 Hz in this example).

To incorporate the probability density function shown in Figure 6.1a into the calculation of footbridge response, it is convenient to transform the horizontal axis into a frequency ratio between the step frequency and the natural frequency of a particular footbridge. An example for Podgorica footbridge having a natural frequency of 2.04 Hz is presented in Figure 6.1b. It can be seen that the frequency ratio ranges between 0.64 and 1.19 for this particular bridge. During this transformation the vertical axis is multiplied by 2.04 Hz to preserve the area defined by the probability density function being dimensionless number equal to 1 (Montgomery & Runger, 1999).

6.2.3 Number of Steps

It is known that there is a variability between people in their walking speeds (Bertram & Ruina, 2001). It is expected that even people who walk with the same step frequency f_s will have different walking speeds v_p due to different step length l_s when crossing a footbridge. The relationship between these walking parameters is given by the formula $v_p = f_s l_s$. When the walking speed v_p is known and assuming that it is constant, crossing time T_c needed to cross a bridge can be calculated as $T_c = \frac{L}{v_p}$, where L is the footbridge length. The crossing

time calculated defines the duration of the dynamic force induced by a pedestrian.

From biomechanics research, it is also known that walking speed is dependent on the walking frequency (Bertram & Ruina, 2001). Rare experimental data about walking speed when crossing footbridges, such as those presented by Pachi & Ji (2005), show that the mean velocity μ_v can be linearly related to the walking frequency f_s according to the formula $\mu_v = 0.71 f_s$ (black line in Figure 6.2a), where 0.71 is the average step length expressed in metres. However, it would also be interesting to know distribution of walking velocities at a certain frequency. Observing data in Figure 6.2a it can be seen that most points are concentrated in the area $\mu_v \pm 0.2\mu_v$. These upper and lower limits (i.e. $0.8\mu_v$ and $1.2\mu_v$) are represented in Figure 6.2a by grey lines. Based on a visual inspection, it is estimated that they accommodate approximately 95% of all data points. Assuming that the walking velocity is normally distributed at each walking frequency and knowing that 95% of points that follow a normal distribution are located in the area $\mu \pm 2\sigma$, where μ is the mean value and σ is the standard deviation (Montgomery & Runger, 1999), it can be concluded that the standard deviation for walking speed σ_v in this case can be calculated from the equation $2\sigma_v = 0.2\mu_v$, that is $\sigma_v = 0.1\mu_v = 0.071 f_s$. This assumption of normal distribution of walking speeds with the standard deviation being $0.071 f_s$ for a particular walking frequency is confirmed experimentally for walking frequency between 1.75 and 1.85 Hz (Figure 6.2b). This is based on the data extracted from Figure 6.2a and obtained through personal communication (Ji, 2005). The calculated linear dependence of the standard deviation σ_v to the walking frequency f_s ($\sigma_v = 0.071 f_s$) takes into account that the walking velocity of different people is more scattered with increased step frequency, as can be noticed in Figure 6.2a.

It is convenient here to calculate the number of steps N required to cross the bridge as follows:

$$N = T_c f_s = \frac{L}{v_p} f_s. \tag{6.1}$$

According to normal distribution theory (Montgomeri & Runger, 1999), almost all points (99.7%) of a normally distributed variable, in this case the walking velocity, lie in the interval $\mu_v \pm 3\sigma_v = 0.71 f_s \pm 0.213 f_s$ i.e. between $0.497 f_s$ and $0.923 f_s$. Taking these extreme values for velocities back to Equation 6.1 it can be seen that number of steps needed to cross the bridge (at any walking frequency) lies in the range:

$$\frac{L}{0.923 f_s} f_s \leq N \leq \frac{L}{0.497 f_s} f_s, \tag{6.2}$$

that is

$$\frac{L}{0.923} \leq N \leq \frac{L}{0.497}, \tag{6.3}$$

and depends only on the footbridge length L in metres, which is a quite interesting observation from this exercise. This actually means that the step length is normally distributed between

0.497 m and 0.923 m (with the mean value of 0.71 m and the standard deviation of 0.071 m) regardless of walking frequency.

The probability density function for walking velocities at any walking frequency can be translated to a probability density function for a number of steps by transforming the horizontal walking speed axis (Figure 6.2b) into an axis describing the number of steps via Equation 6.1 and preserving the area of the function being equal to 1. For a footbridge with span length of 78 m this probability density function is presented in Figure 6.2c where it can be seen that the number of steps required to cross the footbridge ranges from 85 to 155 steps and is the same function for each walking frequency.

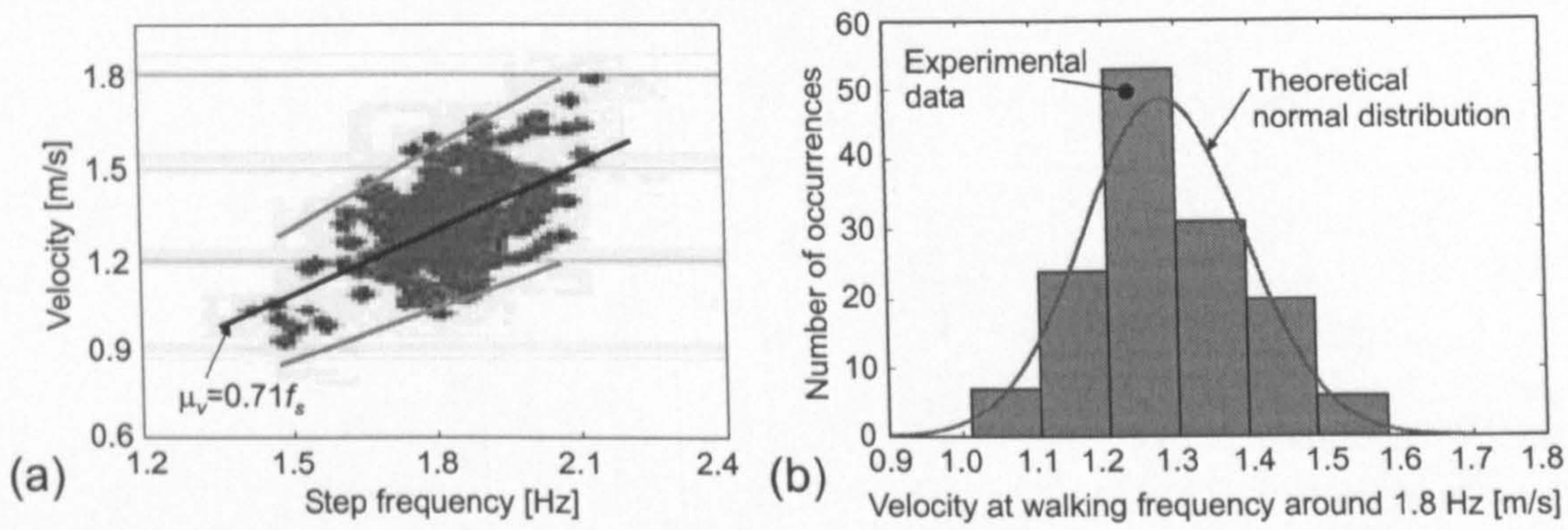

Figure 6.2: (a) Walking speed as a function of step frequency (after Pachi and Ji, 2005). (b) Normal distribution of walking speed when walking with step frequency around 1.8 Hz. (c) Probability density function (independent on step frequency) for number of steps required to pass a 78 m long bridge.

6.2.4 Force Amplitude

When modelling the force generated by human walking as a harmonic force, one usually defines the amplitude of this force as a portion of the pedestrian's weight, that is as a product of a dimensionless coefficient called dynamic loading factor (DLF) and the pedestrian's weight W. The most extensive research into DLFs was conducted by Kerr (1998). He analysed about 1,000 force records produced by 40 test subjects and presented DLFs for different force harmonics as a function of the walking frequency. DLFs for the first harmonic as ob-

tained by Kerr are shown in Figure 6.3a. The dependence of the mean value of DLF μ_{DLF} on the step frequency f_s is given by:

$$\mu_{DLF} = -0.2649 f_s^3 + 1.3206 f_s^2 - 1.7597 f_s + 0.7613. \tag{6.4}$$

Kerr (1998) also found that in the walking frequency range 1.5-2.2 Hz, 95% of DLFs lie in the area $\mu_{DLF} \pm 0.32\mu_{DLF}$. Under an assumption that DLFs are normally distributed around their mean value (for a certain walking frequency), the standard deviation can be defined as $\sigma_{DLF} = 0.16\mu_{DLF}$.

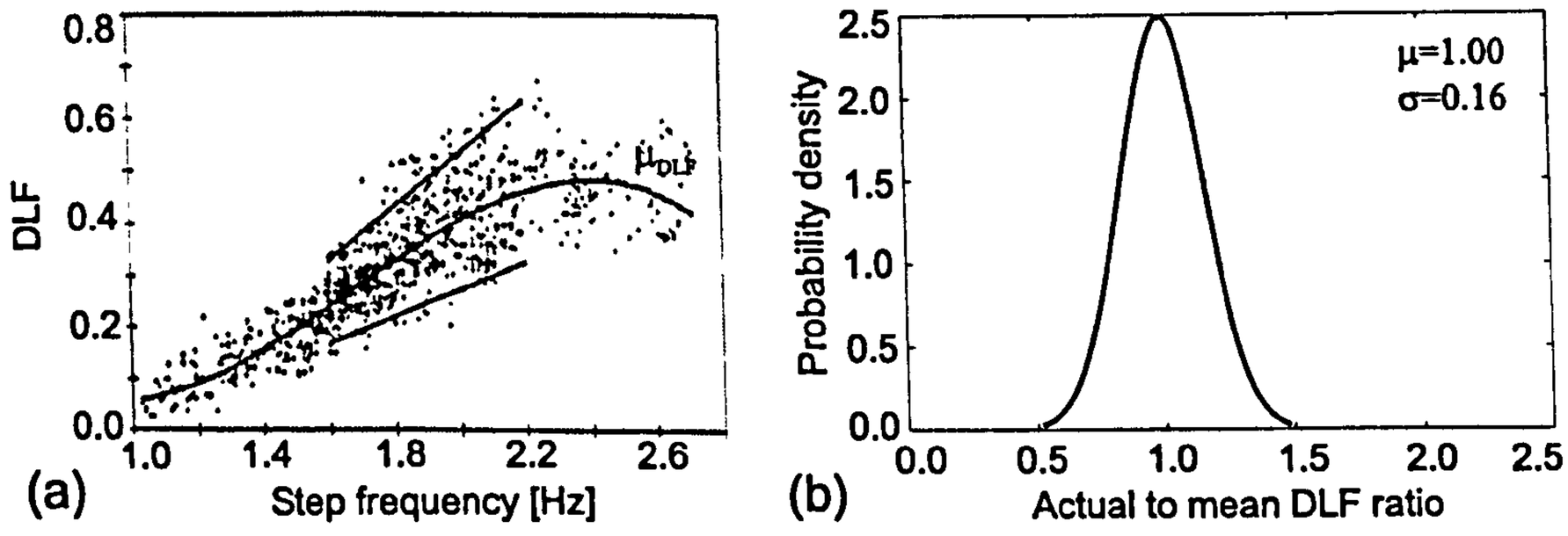

Figure 6.3: (a) DLF for first harmonic of the walking force (after Kerr, 1998). (b) Distribution of actual to mean DLF ratio for the first walking harmonic of the force induced by walking.

The described probability density function for a DLF can be normalised to the value of the mean DLF. Since the modal response of a linear SDOF footbridge model is directly proportional to the DLF then, for example, 1.2 times increase in the DLF will generate 1.2 times higher modal response. By this analogy it can be concluded that the probability of the ratio between the actual modal acceleration response and the response calculated under assumption of the mean value of DLF is the same as the probability of the ratio between the actual DLF and the mean DLF. This enables use of only the mean DLF when calculating structural modal response. In a later stage of the analysis, the probability that this 'mean' response is different from the one calculated can be estimated. As before, the area under the probability density curve for this distribution has to be equal to 1. This probability density function is presented in Figure 6.3b. It should be noticed that this function does not depend on the walking frequency.

6.2.5 Intra-Subject Variability in Force

Until now, the analysis has been concentrated on defining probability distributions related to parameters (such as step frequency, walking velocity and force amplitude) that describe differences in walking forces induced by different people. This was done under the assumption that a human-induced walking force can be modelled as a sinusoidal force. Under this

force the modal acceleration response $a_{sin}(t)$ can be calculated, taking into account the half-sine mode shape. This procedure is partly justifiable since there are human induced forces (measured on a treadmill) that can be approximated by a sinusoidal force when considering the first harmonic of walking (Brownjohn et al., 2004b). It has also been confirmed on full-scale footbridges that these forces can indeed induce a response that is almost the same as that induced by a corresponding sinusoidal force, as explained in Chapter 5 and shown in Figure 5.2b.

On the other hand, in the same way that some people are able to walk steadily and induce an almost perfect sinusoidal force to the footbridge, there are many more people who cannot do this. Namely, due to intra-subject variability the force induced in every step is usually different in terms of its frequency and amplitude (Brownjohn et al., 2004b; Sahnaci & Kasperski, 2005). As a result, it is not realistic to model the force exclusively as a harmonic force. Instead, the fact that this force is a narrow band random process (Newland, 1993) should be taken into account. Although this variation of the force in successive steps for the first harmonic does not have significant influence on the structural response when the footbridge is excited in the resonance (Brownjohn et al., 2004; Chapter 5), it deserves studying and quantification. The whole procedure can later be repeated for higher harmonics of the walking force, if required.

One way to consider the force variation, and at the same time to keep simplicity of the response calculation corresponding to harmonic force excitation, is to define the probability that the modal response to an actual (measured) walking force $a_c(t)$ will be different from that generated by a sine force $a_{sin}(t)$. Examples of such responses are shown in Figure 6.4 as black and grey lines, respectively. The corresponding peak responses in Figure 6.4 are denoted as A_c and A_{sin}.

Figure 6.4a presents the two modal responses when a pedestrian walks at a step frequency that matches a footbridge natural frequency, while in Figure 6.4b they walk at a step frequency equal to 80% of the natural frequency. In the latter case the beating response, noticed in some real-life measurements when walking with out-of-resonance frequency, is present in the response to measured walking time history (Figure 6.4b: black-dashed line), while it is almost non-existent in the case of simulation due to the sinusoidal force (Figure 6.4b: grey line).

The ratio between the two peak modal responses will be called the correction coefficient c:

$$c = \frac{A_c}{A_{sin}} \tag{6.5}$$

and it is this factor that will be used for introducing the intra-subject variability into calculation of the actual peak modal response.

To define the probability density function for the correction coefficient, 95 walking forces measured by Brownjohn et al. (2004b) on a treadmill were analysed. These walking forces were produced by nine test subjects who were asked to walk for at least 60 s on a treadmill set

to a constant speed. The speed range was between 2.5 km/h and 8.0 km/h in different tests. Therefore, the walking speed was set to a constant value during each test, while the walking frequency was freely chosen by the test subjects so that they could walk in a comfortable manner.

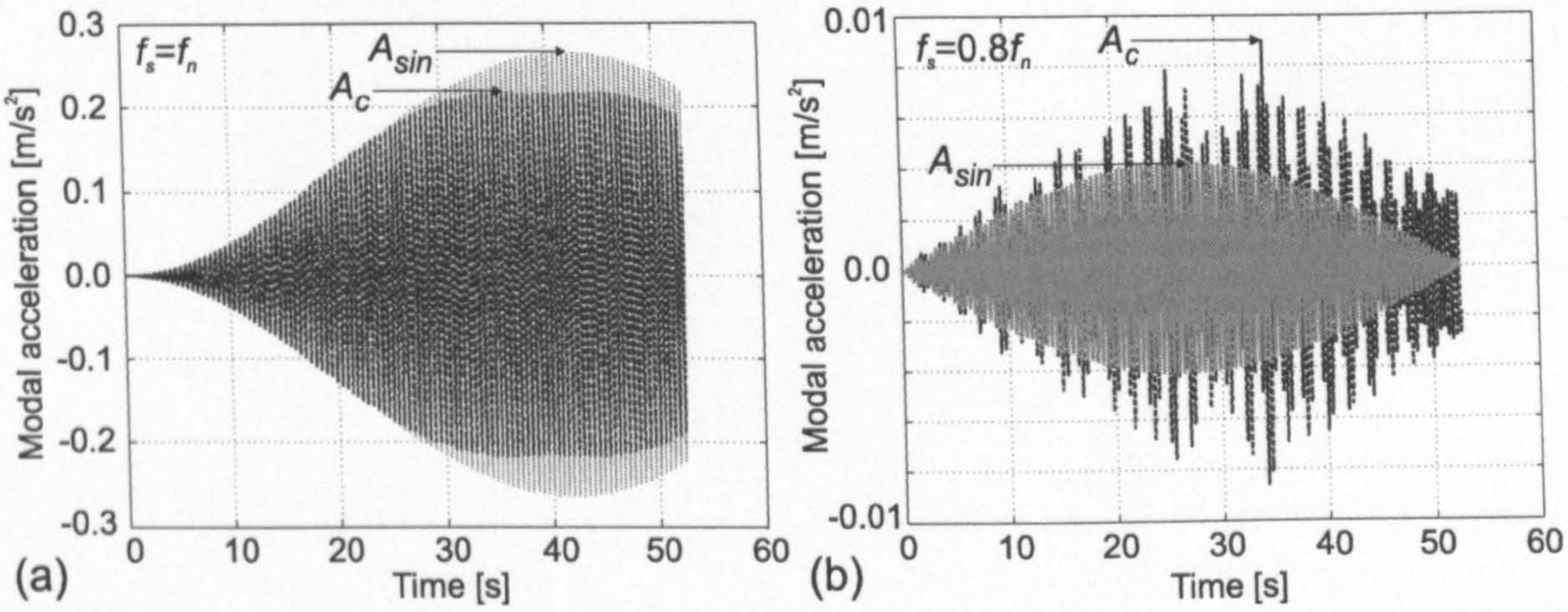

Figure 6.4: Comparison of modal responses due to measured force (black-dashed line) and corresponding sine force (grey line) when walking at a step frequency equal to (a) a footbridge natural frequency and (b) 80% of the natural frequency.

The measured walking forces were band-pass filtered around the walking frequency so that only force components pertinent to the first harmonic remained. Then, the filtered force was multiplied by the half sine mode shape to get the modal force. Finally, peak modal acceleration response of the SDOF model to this force was calculated. The natural frequency of the footbridge was assumed to be in the range between $f_s/1.20$ and $f_s/0.80$, where f_s is the average walking frequency, while modal damping ratio ζ ranged between 0.1% and 2.0%. For all these combinations of different natural frequencies and dampings, the different number of steps needed to cross the bridge was also considered (50-250). The peak modal acceleration response obtained in this way A_c was divided by the peak modal acceleration response A_{sin} due to a corresponding sinusoidal force to calculate the correction coefficient c. The amplitude of the sinusoidal force was defined as the average amplitude of the filtered force measured on the treadmill. As a result of this analysis, the correction coefficient depending on the ratio between walking and footbridge natural frequency, damping ratio of the footbridge as well as different number of steps was found. It was noticed that the distribution of the correction coefficient was quite independent from the number of steps. An example illustrating this is shown in Figure 6.5. It can be seen that for any number of steps the correction coefficient is distributed in similar way and between approximately the same limiting values (which are different for different footbridge damping and walking to natural frequency ratio) for both walking at the step frequency that matches the footbridge natural frequency (Figure 6.5a) and that differs from the natural frequency (Figure 6.5b). This was the reason to eliminate the number of steps as a variable in this analysis of intra-subject variability, keeping only the frequency ratio and modal damping as factors relevant for describing coefficient c.

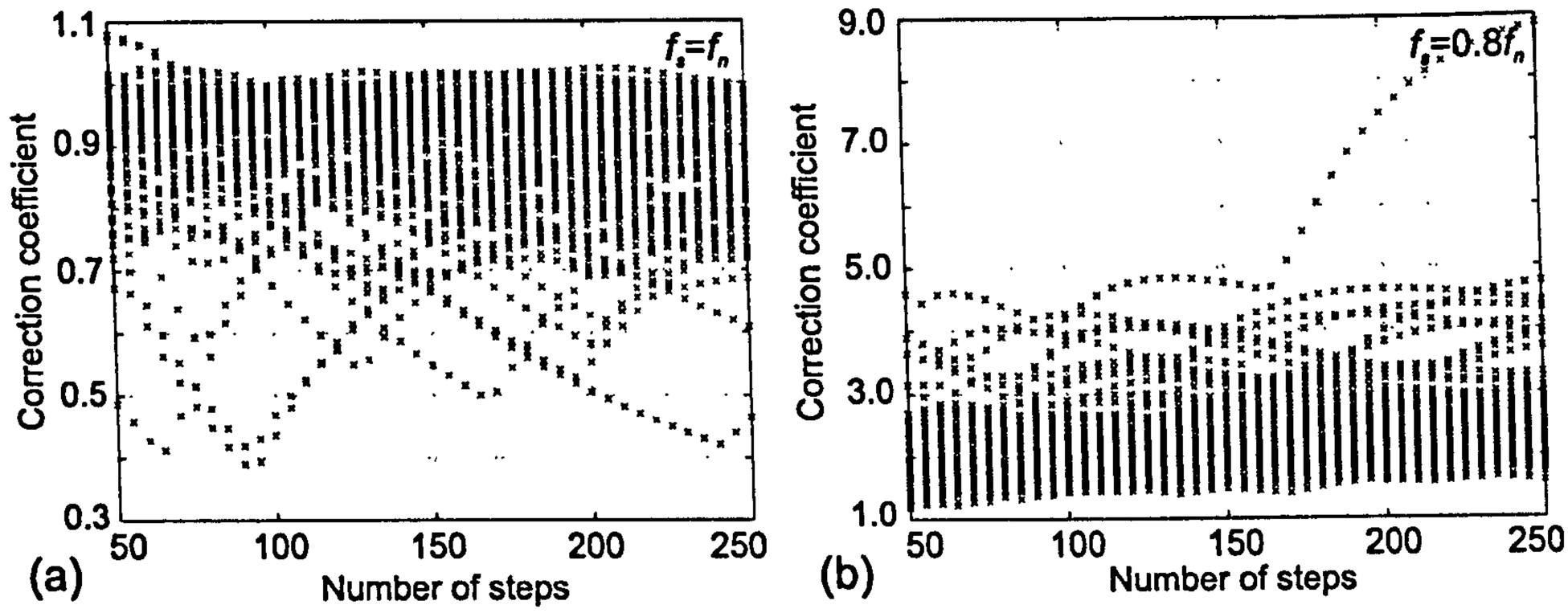

Figure 6.5: Correction coefficient calculated for different number of steps required to cross a footbridge when walking at a step frequency equal to (a) a footbridge natural frequency and (b) 80% of the natural frequency. The damping ratio for the footbridge considered is 0.4%.

A general observation from the results obtained is that the peak modal acceleration due to measured walking force is attenuated when walking in the way to match the footbridge natural frequency in comparison with that produced by the corresponding sinusoidal force, i.e. the correction coefficient is less than 1 (Figure 6.4a). An example of the distribution of the coefficient that illustrates this is given in Figure 6.6a. This is a consequence of inability of the test subject to walk at the constant frequency all the time. It should, however, be noticed that some test subjects produced almost perfect sine force leading to the correction coefficient equal to 1. In few cases, the correction coefficient was even greater than 1. This was a consequence of having several heavy footfalls (i.e. footfalls in which the force amplitude was higher than the average one) occurring when vibrations have already been well developed. On the other hand, the correction coefficient is mainly greater than 1 when the step frequency is different from the natural frequency (Figure 6.6b). The reason for this are again imperfections in human walking frequency from one step to another, but this time its slight change leads to being closer to the resonant frequency from time to time, causing an actual acceleration response higher than the one generated by a sine force. Moreover, the beating is quite pronounced in the response to the measured force (Figure 6.4b).

Since the distribution of the correction coefficient could not be presented by a single function for different combinations of modal damping and walking to natural frequency ratio, different distributions having different sets of parameters were considered. Among them, it was found that a gamma distribution best described the probability distribution of the correction coefficient. The quality of the approximation can be seen in Figure 6.6 where two sets of results are approximated by a gamma distribution presented as black line. The gamma distribution could describe a trend that with increasing damping ratio the scatter of the calculated correction coefficient decreases, with the most probable correction coefficient approaching 1.0. An example for $f_s = 1.15f_n$ is shown in Figure 6.7a. Also, the gamma distribution can represent the fact that for non resonant walking, the increase in the walking to natural frequency ratio

leads to smaller scatter in the correction coefficient, with its peak approaching the value equal to 1. An example for a bridge with a damping ratio of $\zeta = 0.4\%$ is presented in Figure 6.7b.

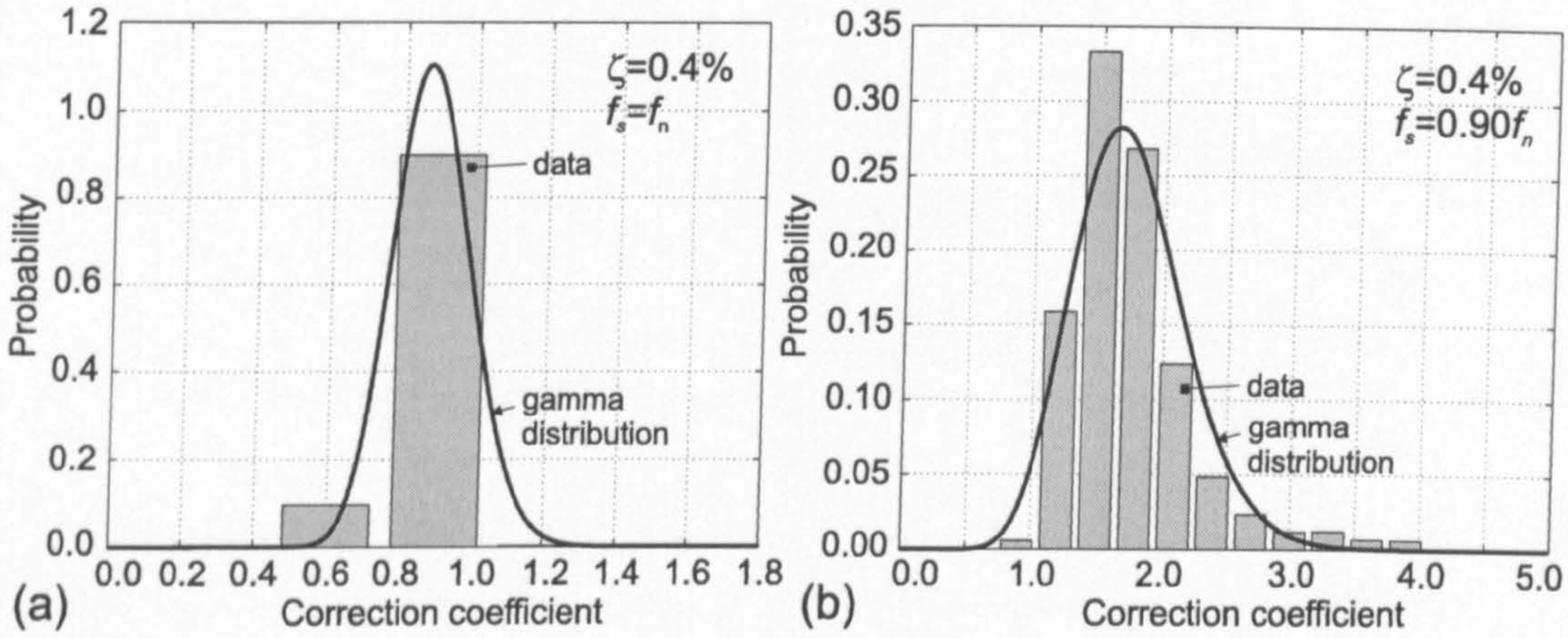

Figure 6.6: (a) Attenuation factor for the modal acceleration response to measured force in comparison with the one due to sine force when walking at step frequency that matches the natural frequency of a footbridge. (b) Amplification factor for the modal acceleration response to measured force in comparison with the one due to sine force when walking at a step frequency equal to 90% of the natural frequency.

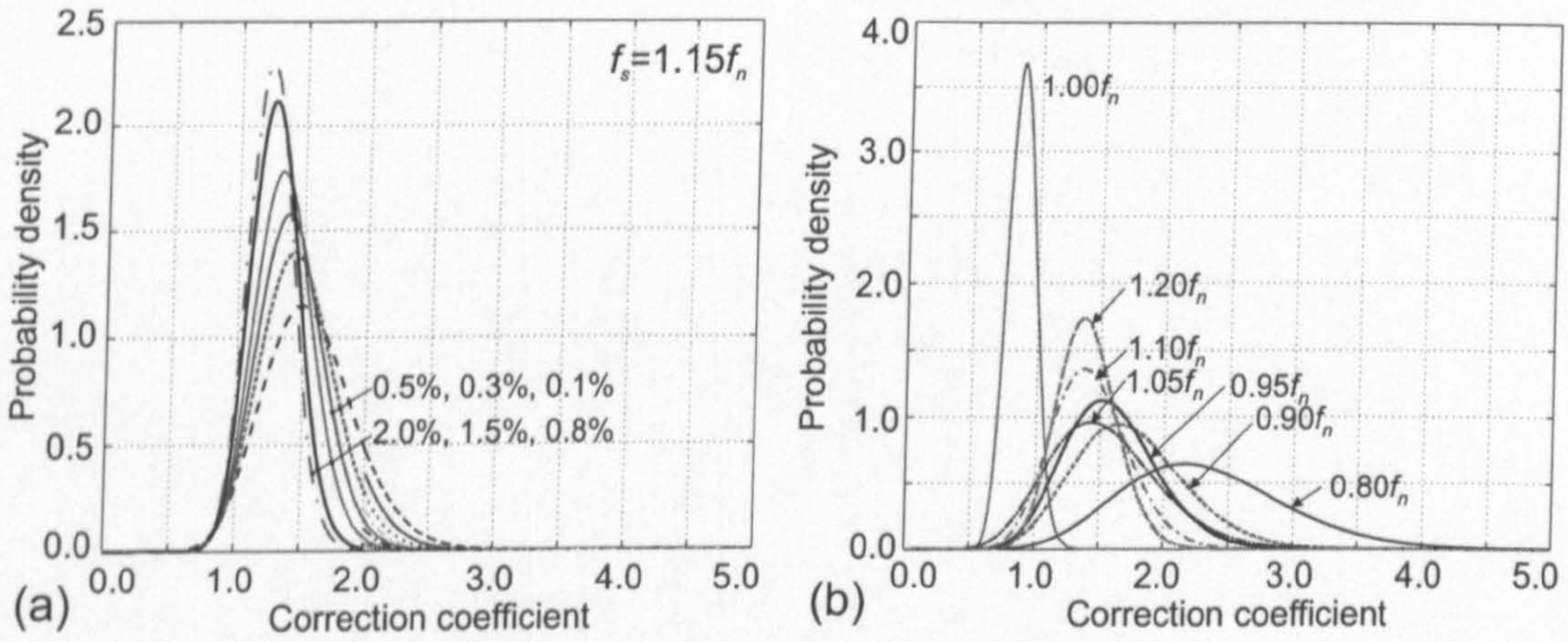

Figure 6.7: (a) Gamma distributions for the correction coefficient for footbridges with different damping. (b) Gamma distributions for the correction coefficient when walking at different frequencies on a bridge with damping ratio equal to 0.4%.

The probability density function $f(x)$ for the gamma distribution is defined by the following formula (Montgomery & Runger, 1999):

$$f(x) = \frac{x^{a-1}e^{-\frac{x}{b}}}{b^a \int_0^\infty x^{a-1}e^{-x}\mathrm{d}x} \tag{6.6}$$

where x is the random variable (i.e. correction coefficient c), while a and b are parameters that describe the distribution. According to the definition of the gamma distribution, x, a

and b have to be positive numbers.

Parameters a and b define the shape of the distribution function. They were identified for footbridges with different damping ratios and different walking to natural frequency ratios, and are presented in Figure 6.8. The precise values of these parameters can be found in Appendix B. Based on the two graphs in Figure 6.8, the two parameters can be found by linear interpolation for a footbridge with a particular damping ratio.

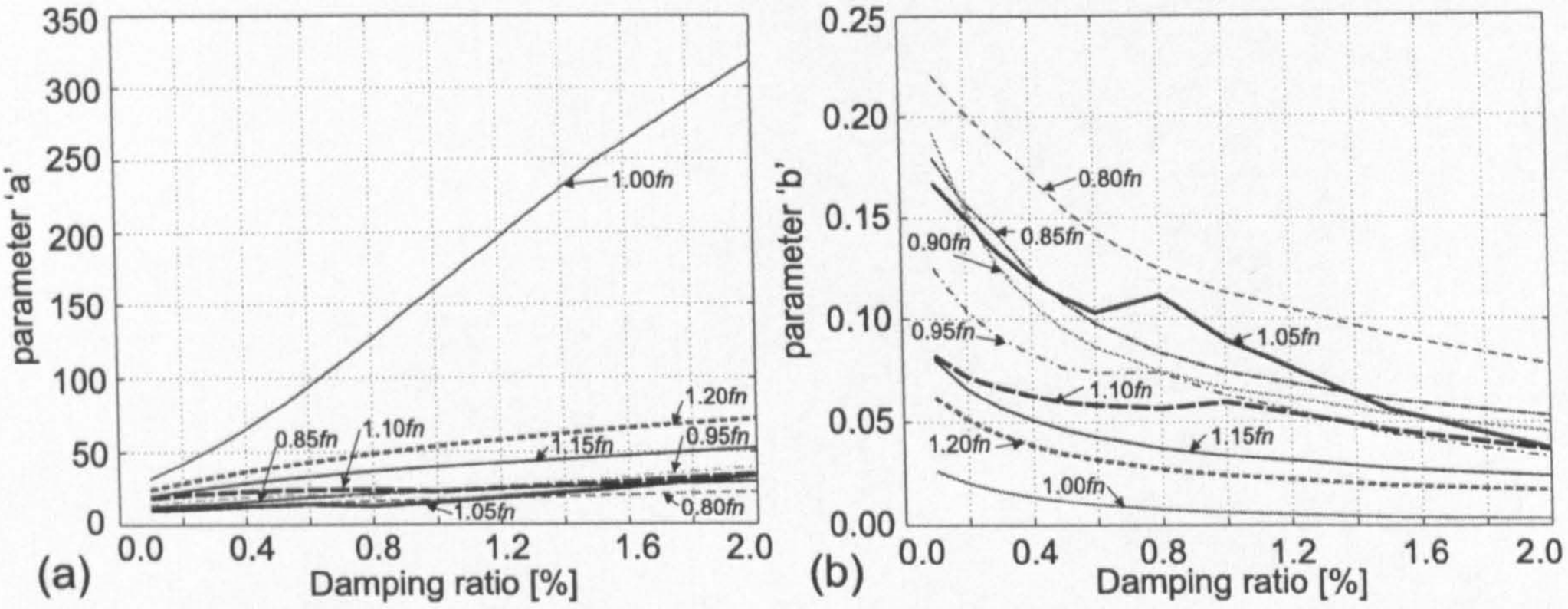

Figure 6.8: (a) Parameter 'a' and (b) parameter 'b' for gamma distribution depending on structural damping and ratio between the walking and natural frequency.

6.2.6 Other Uncertain Parameters

The research reported in this chapter aims at modelling the uncertainties in parameters describing the walking force via their probability treatment. These parameters are the forcing frequency and amplitude, number of steps required to cross the bridge, and imperfections in human walking, as already mentioned. An additional parameter that influences the force modelling but is not considered in this thesis is pedestrian's weight W. There are indications that increasing the pedestrian's weight leads to increased DLFs (Galbraith & Barton, 1970). However, there is no quantification of this dependence known to the author. Also, it is difficult to find a precise description of the probability distribution of the weight (i.e. its type and parameters describing it) at the same place, although some (incomplete) information is available (DH, 2005). These were the reasons to omit this distribution from the analysis and use an average weight of 750 N (DH, 2005) in the formulation of the force model. When more data describing the distribution of the weight and its relationship with the DLFs are collected, they might be combined with the probability distribution of DLFs (Figure 6.3b) to a single probability distribution defining the amplitude of the walking force ($DLF \cdot W$).

Apart from variabilities in parameters that describe the dynamic force induced by pedestrians, there is another group of uncertain parameters when designing a new footbridge. This group is related to the dynamic properties of the structure to be built. These include modal mass, damping ratio and natural frequency. However, the research in this thesis is concentrated

on dealing with uncertainties in the force description and their influence on the structural vibration response while the uncertainties in structural dynamic properties are beyond the scope of this work. However, they certainly deserve to be researched in future.

Finally, the inter-subject variability in the limiting (disturbing) vibration level for walking person is not included into the analysis conducted in this thesis. This is because most of published research deals with a standing person as a receiver of vibrations and more research is required for establishing vibration acceleration limits for walking people. Therefore, instead of treating the vibration limit for a walking pedestrian in a probabilistic sense, a single (and only provisional) vibration limit of $0.35\,\mathrm{m/s^2}$ is used in this work. This value is obtained based on the methodology explained in Chapter 5. However, when probability distribution of vibration limit for different walkers becomes available, then it can simply be combined (see Chapter 8) with probability distribution of the acceleration response (that is an outcome of the methodology presented in this chapter, as will be shown in Section 6.3) in order to estimate percentage of pedestrians that might complain of footbridge vibrations caused by their own walking.

6.3 Statistical Prediction of Footbridge Response to Single Person Walking

This section describes a methodology for statistical description of footbridge response to a single person crossing. Statistical distributions for different parameters defined in the previous section are used for this purpose. The procedure is explained step by step and applied to Podgorica footbridge in Montenegro where the first walking harmonic was relevant and the mode shape could be approximated by a half sine function. After this, the procedure is repeated for Aberfeldy footbridge.

Podgorica footbridge is described in detail in Chapters 3 and 4. Here, only the most important characteristics of the bridge that are required in the analysis will be summarised briefly. The bridge is a steel box girder shown in Figure 6.9a. Its length is 104 m, with 78 m between inclined columns. The footbridge responds to normal walking excitation dominantly in the first vibration mode with frequency at 2.04 Hz. The mode shape and modal properties of this mode (natural frequency f_n, damping ratio ζ and modal mass m), as estimated from modal testing and finite element model updating described in Chapters 3 and 4, are shown in Figure 6.9b.

6.3.1 Peak Modal Response to Sinusoidal Excitation

The first step in the analysis is to calculate the peak modal response of an SDOF system to sinusoidal excitation. Under the assumption of the bridge having a half-sine mode shape, the equation of motion in its modal form can be written as (Inman, 2001):

$$a(t) + 2\zeta(2\pi f_n)v(t) + (2\pi f_n)^2 d(t) = \frac{1}{m}\underbrace{DLF \cdot W \sin(2\pi f_s t)}_{F_{sin}(t)} \cdot \underbrace{\sin\left(\frac{\pi f_s}{N}t\right)}_{\phi(t)}, \qquad (6.7)$$

where $a(t)$, $v(t)$ and $d(t)$ are modal acceleration, velocity and displacement of the footbridge structure, respectively, while ζ, m and f_n are modal damping, mass and natural frequency, respectively. The right hand side of the equation represents the modal force acting on the SDOF system obtained by multiplication of the sinusoidal force $F_{sin}(t)$ by the half-sine mode shape $\phi(t)$. The frequency of the force $F_{sin}(t)$ is f_s while its amplitude is defined as a product of the mean DLF dependent on f_s (defined in Equation 6.4) and an assumed average pedestrian weight $W = 750\,\text{N}$ (DH, 2005). The mode shape $\phi(t)$ was initially a space function dependent on pedestrian position on the bridge x and footbridge length L. However, by assuming a constant pedestrian velocity v_p, the mode shape defined along the bridge length can be transformed into a time-varying function:

$$\sin\frac{\pi x}{L} = \sin\frac{\pi v_p t}{L} = \sin\left(\frac{\pi}{L}\frac{L f_s}{N}t\right) = \sin\left(\frac{\pi f_s}{N}t\right) \qquad (6.8)$$

where N is the number of steps required to cross the bridge.

Equation 6.7 has an analytical closed-form solution (see `PHASE 5` in Appendix B). For the Podgorica footbridge the solution was found for different combinations of step to natural frequency ratios (0.64-1.19 as shown in Figure 6.1b) and number of steps needed to cross the bridge (85-155 as shown in Figure 6.2c). The resulting peak modal acceleration shown in Figure 6.10 gives a range of possible peak modal acceleration responses A_{sin} under sinusoidal force excitation.

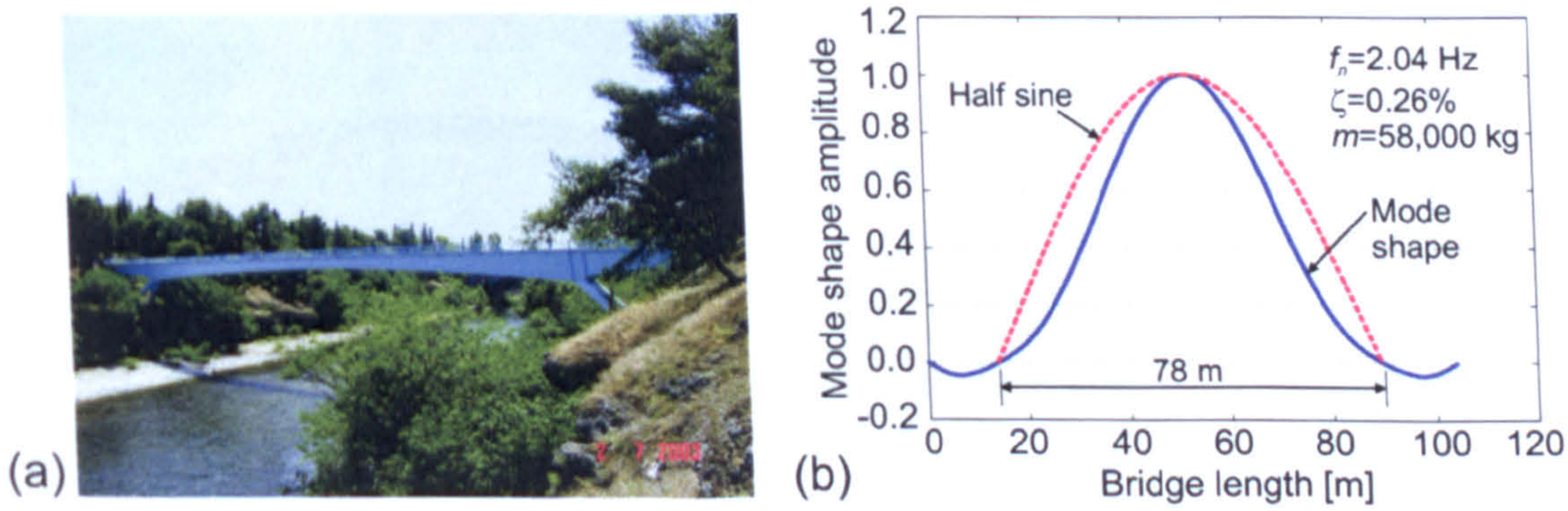

Figure 6.9: Podgorica footbridge - (a) photograph and (b) modal properties of the fundamental mode of vibration.

6.3.2 Joint Probability for Walking Parameters

As explained previously, the walking frequency is a normally distributed variable, with the probability density function presented in Figure 6.1. It has also been explained that the

probability density function for number of steps needed to cross the bridge can be obtained from the probability distribution of walking velocities. This probability density function is shown in Figure 6.2c and depends on the footbridge length only. For Podgorica footbridge this length is 78 m, since the mode shape can be considered as being close to a sinusoidal shape on the main span while its amplitude can be neglected on the relatively short side spans because of their low magnitude (Figure 6.9b). Since the walking frequency and number of steps are independent variables, the joint probability of walking at a particular frequency f_s and making a particular number of steps N during a footbridge crossing can be calculated by multiplication of the probability density functions from Figures 6.1b and 6.2c (Montgomery & Runger, 1999). The resulting joint probability density function is shown in Figure 6.11.

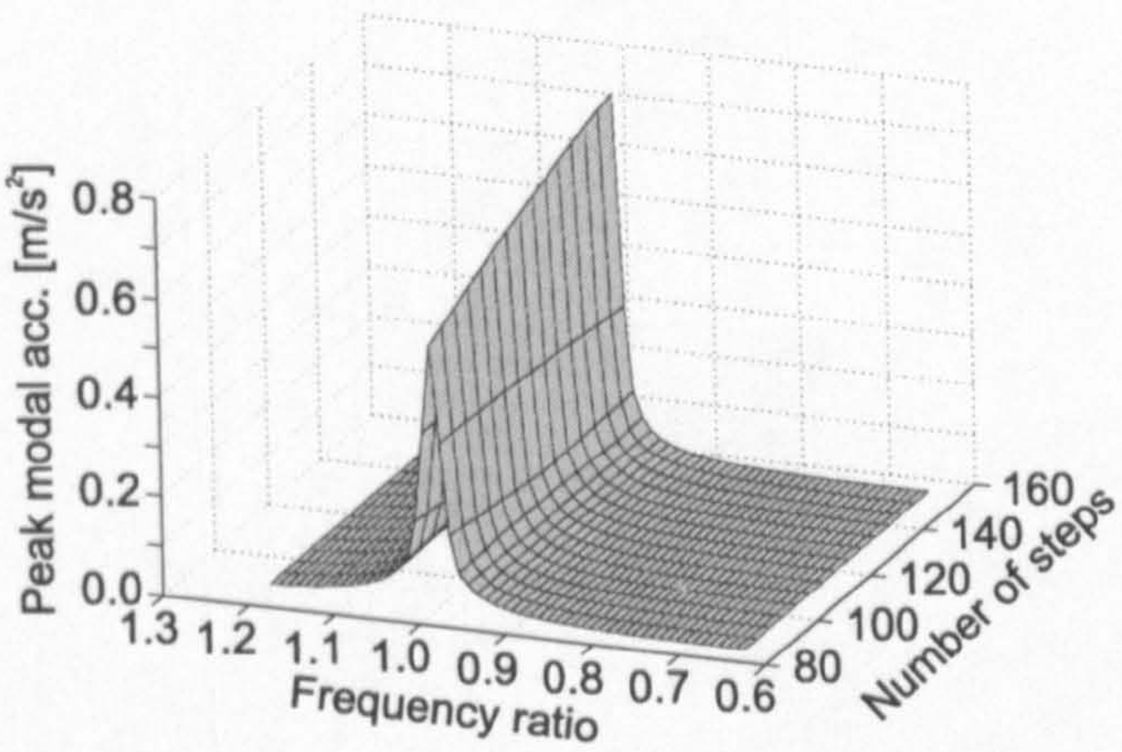

Figure 6.10: Peak modal acceleration response due to sinusoidal walking force.

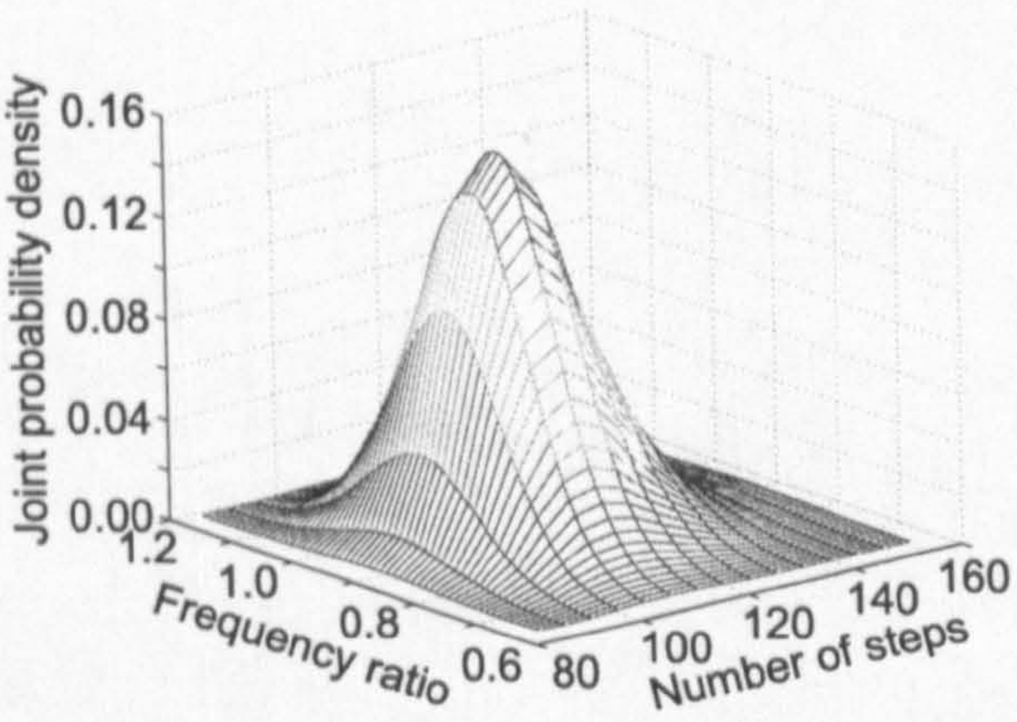

Figure 6.11: Joint probability density function $p(f_s/f_n, N)$ for different combinations of step to natural frequency ratio and number of steps during the crossing of the Podgorica footbridge.

6.3.3 Modification of Peak Modal Response A_{sin} due to Intra-Subject Variability

For every pair of frequency ratio f_s/f_n and number of steps N, it is possible to find the peak modal acceleration A_{sin} due to a sine force (Figure 6.10) as well as a point in the probability density function $p(f_s/f_n, N)$ that has exactly this combination of f_s/f_n and N (Figure 6.11). After this, the fact that the peak acceleration level A_c could be higher or lower than that in Figure 6.10 due to intra-subject variability can be introduced. For this purpose the peak acceleration A_{sin} from Figure 6.10 for each point $(f_s/f_n, N)$ is multiplied by a range of correction coefficients c from the appropriate gamma distribution defined in Section 6.2.5:

$$A_c = cA_{sin}. \tag{6.9}$$

In this way a range of possible peak acceleration values A_c for each acceleration A_{sin} from Figure 6.10 has been obtained. It should be noted here that the gamma distribution of the correction coefficient chosen for this calculation depends on the walking to natural frequency ratio (f_s/f_n). At the same time the probability density function of the three variables $p(f_s/f_n, N, c)$ corresponding to each combination of $f_s/f_n, N$ and c used for calculation of A_c can be obtained by multiplication of every point in the joint probability density function $p(f_s/f_n, N)$ (Figure 6.11) with a gamma probability density function p_c (dependent on f_s/f_n ratio) of the kind presented in Figure 6.7:

$$p(f_s/f_n, N, c) = p(f_s/f_n, N)p_c. \tag{6.10}$$

For further calculation it would be convenient to present peak acceleration A_c (calculated according to Equation 6.9) as a function of x, where x is a variable that contains all possible combinations of discrete random variables f_s/f_n, N and c. This function is given in Figure 6.12a as an arbitrary discrete function. At the same time an arbitrary function that presents a discrete probability density function calculated according to Equation 6.10 is shown in Figure 6.12b. The functions mentioned here are discrete functions because computer calculation of A_c and $p(f_s/f_n, N, c)$ (Equations 6.9 and 6.10) require discretisation of the variables included in the analysis $(f_s/f_n, N, c)$.

Probability $P_{x=x_i}$ of having variable $x = x_i$ can then be calculated approximately as the black area in Figure 6.12b:

$$P_{x=x_i} = p(x_i)\Delta x = p_i \Delta x, \tag{6.11}$$

where Δx is the discrete step for variable x.

The obtained value $P_{x=x_i}$ is actually a probability that variables f_s/f_n, N and c (contained in variable x) are equal to $(f_s/f_n)_i$, N_i and c_i, respectively. This probability is at the same time a probability of having a peak acceleration response A_{c_i} that corresponds to the choice

of the three variables. This probability will be denoted as P_{c_i} hereafter. Probability P_{c_i} that $f_s/f_n = (f_s/f_n)_i$, $N = N_i$ and $c = c_i$ therefore can be presented as follows:

$$P_{c_i} = p\left(f_s/f_n = (f_s/f_n)_i, N = N_i, c = c_i\right) \Delta(f_s/f_n) \Delta N \Delta c, \tag{6.12}$$

where $\Delta(f_s/f_n)$, ΔN and Δc are discrete steps chosen for discrete representation of variables f_s/f_n, N and c, respectively.

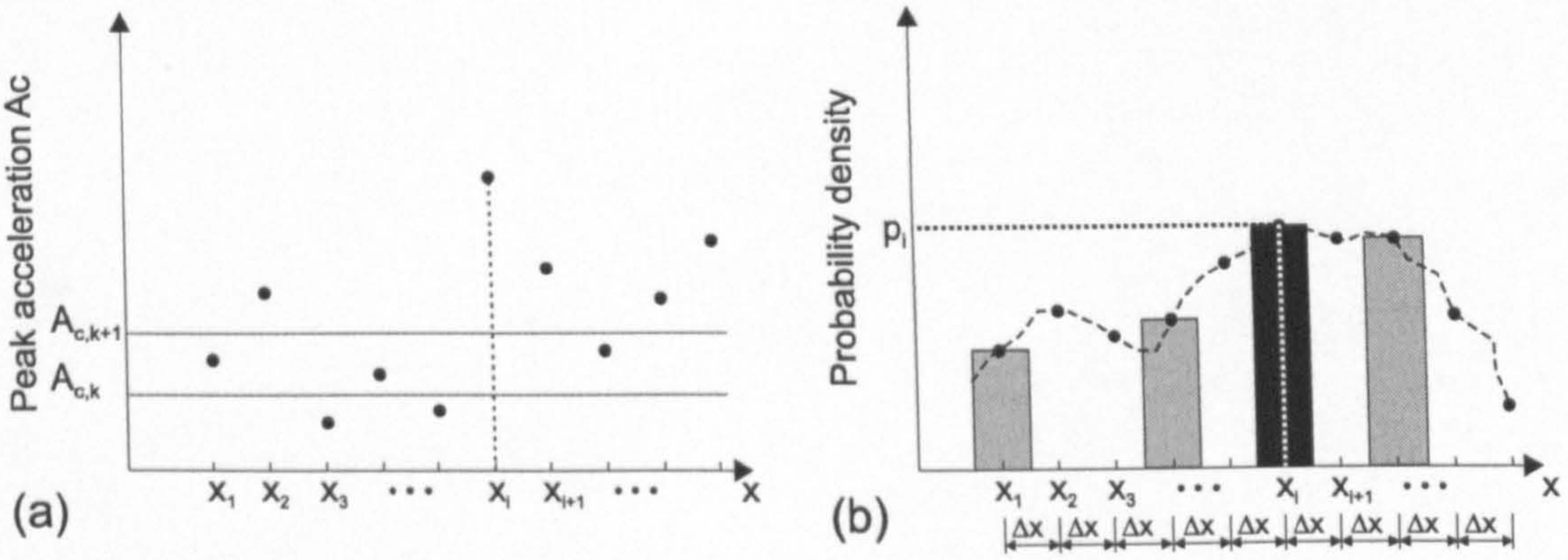

Figure 6.12: (a) Graphical representation of (a) peak acceleration A_c as a discrete function of variable x, (b) probability density function as a discrete function of x.

Once a probability for each combination of variables f_s/f_n, N and c (and therefore a corresponding peak acceleration A_c) is found, the probability that the peak acceleration response A_c is within a certain interval, such as $A_{c,k} < A_c \leq A_{c,k+1}$ can be found. There are three points in this acceleration range in Figure 6.12a. They define the three grey areas in Figure 6.12b. Adding them together the peak acceleration in the interval considered can be calculated as follows:

$$P_{A_{c,k}:A_{c,k+1}} = \sum_{A_{c,k} < A_c \leq A_{c,k+1}} P_c(A_c). \tag{6.13}$$

This probability calculated for the Podgorica footbridge is shown in Figure 6.13b. For a comparison purpose the probability of having certain peak acceleration response without taking into account the intra-subject variability is shown in Figure 6.13a. It can be seen that probability of extremely low accelerations (below $0.05\,\mathrm{m/s^2}$) as well as of extremely high accelerations (around $0.6\,\mathrm{m/s^2}$) decreases after taking into account the intra-subject variability. In the former case it is because walking with the step frequency away from the footbridge natural frequency (small acceleration levels) is likely to produce higher accelerations than the corresponding sine walking force (as also demonstrated in Figures 6.4b and 6.6b), while in latter case the walking at the footbridge natural frequency (high acceleration levels) is likely to produce a lower acceleration response than that induced by a sine force (as shown in Figures 6.4a and 6.6a).

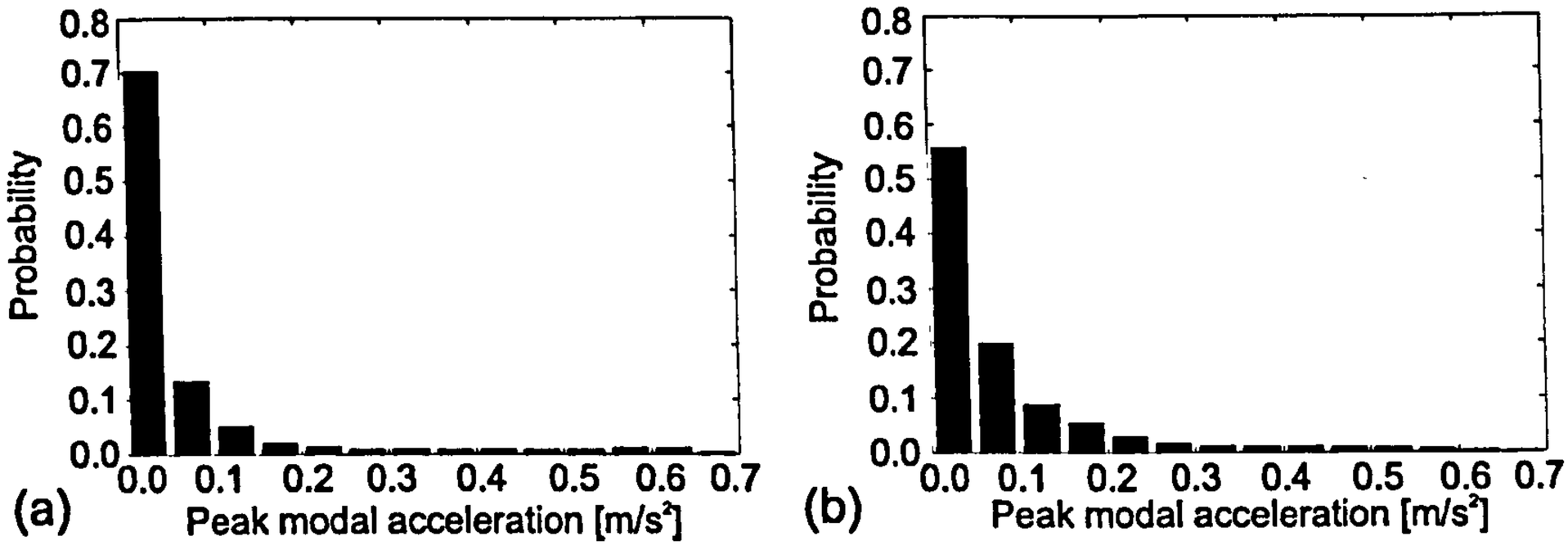

Figure 6.13: Podgorica footbridge - (a) Probability of certain acceleration level (a) before and (b) after taking into account imperfections in human walking.

6.3.4 Influence of DLF Variability on Peak Modal Response

As the final step in the analysis, the influence of probability of DLF being different from the mean value used in previous calculation should be taken into account. This can be done by multiplying the probability density function that corresponds to the probability of certain acceleration response shown in Figure 6.13b by the probability density related to DLF variation (Figure 6.3b). After this, the probability that the vibration level is within a certain range can be obtained as presented in Figure 6.14a. In the case of Podgorica footbridge, this function is almost the same as the one shown in Figure 6.13b before taking into account the probability density for DLFs. This is a consequence only of choosing an acceleration step as large as $0.05\,\mathrm{m/s^2}$ for data presentation.

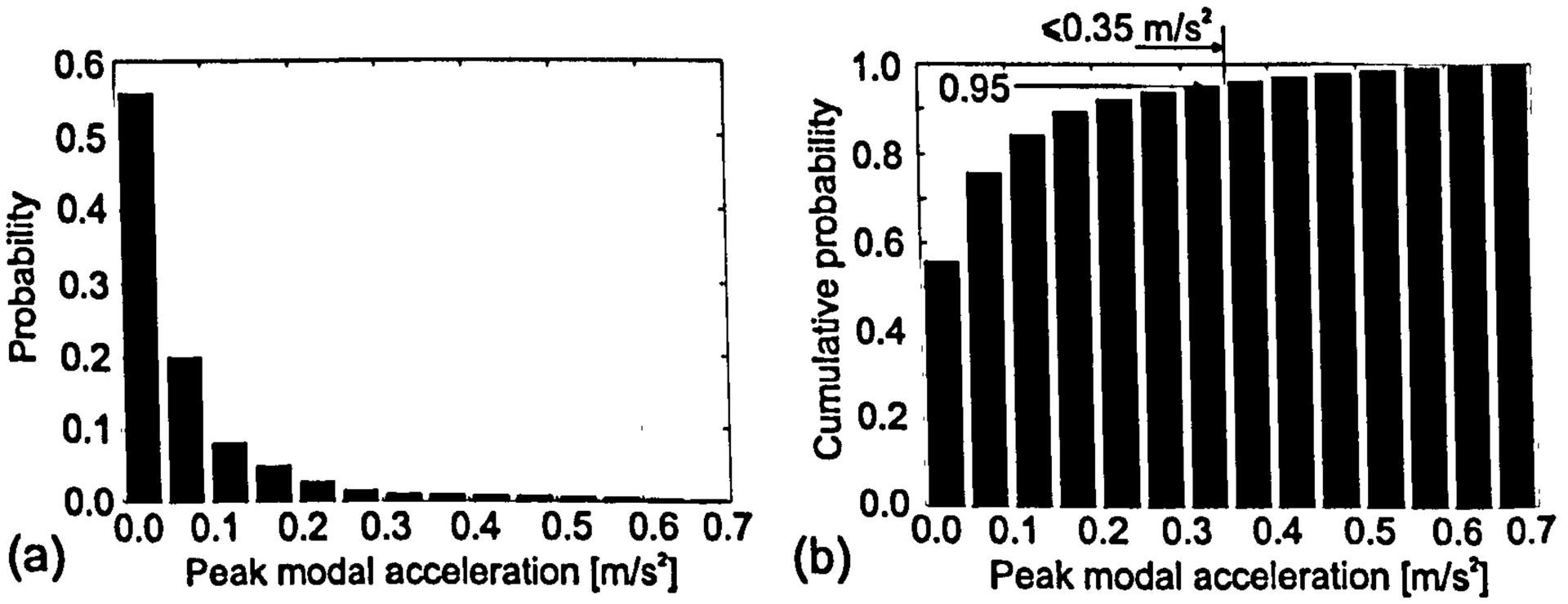

Figure 6.14: Podgorica footbridge - (a) Final probability of a peak modal acceleration level due to single person crossing the bridge. (b) Cumulative probability that the acceleration level is smaller than or equal to the acceleration level considered (shown on the horizontal axis).

A more interesting cumulative probability that the acceleration level is either smaller than or equal to a certain level is presented in Figure 6.14b. Having this distribution, the information

about the level of vibration that is not acceptable for pedestrians would be very useful in order to judge acceptability of the bridge in case of a single pedestrian traffic. If a peak acceleration of $0.35\,\mathrm{m/s^2}$ - a value obtained from the analysis in Chapter 5 - is considered as an unacceptably high vibration level, then it can be expected that this level of vibration is exceeded once in every 20 crossings by a single person (5% exceedance probability). In other words, it can be expected that every 20^{th} person crossing the footbridge is disturbed by its vibration.

A MATLAB script written for implementing the described analytical procedure for obtaining the cumulative distributions for the Podgorica footbridge is presented in Appendix B.

6.3.5 Aberfeldy Footbridge

The procedure applied to Podgorica footbridge is repeated for a light cable-stayed footbridge made of glass reinforced plastic (Aberfeldy footbridge). The total length of this footbridge is 113 m and its total mass is only about 20,000 kg. The footbridge is shown in Figure 6.15a, and the properties of its first mode of vibration, as measured during modal testing, are given in Figure 6.15b.

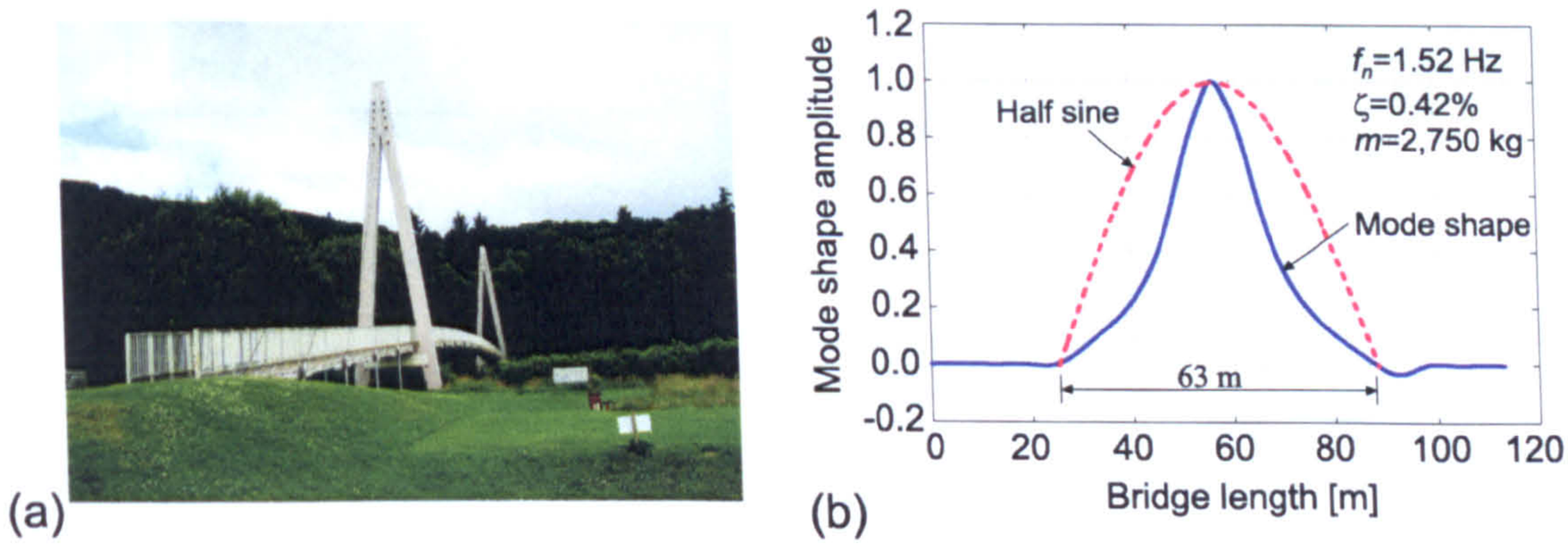

Figure 6.15: Aberfeldy footbridge - (a) photograph and (b) modal properties of the fundamental mode of vibration.

Aberfeldy footbridge is a very light structure that is prone to significant vibrations generated by human walking. Following exactly the same procedure as for Podgorica footbridge, the probability of acceleration level (due to fundamental mode excitation) being within a certain range is calculated and shown in Figure 6.16a. The cumulative distribution of this probability is presented in Figure 6.16b. It can be seen that only 46% of people would cross the bridge without being disturbed, when the disturbance limit is set to the previously mentioned $0.35\,\mathrm{m/s^2}$. In other words, approximately every second person crossing the footbridge would be disturbed by the movement of the bridge due to excitation of first vertical mode at 1.52 Hz.

However, the footbridge is considered in practice as being lively almost all the time. This is likely to be a consequence of the fact that its second vertical mode of vibration is at 1.86 Hz, therefore almost the same as the mean pacing rate shown in Figure 6.1a. The second

mode is anti-symmetric (Figure 6.17a) and can easily be excited by normal walking. A large percentage of people (Figure 6.1) can be expected to walk with pacing rate equal or near to 1.86 Hz. In other words, mode 2 is more likely to be excited than mode 1. The same analytical procedure as for the first mode is applied for the second mode, taking into account only a 31.5 m long part of the bridge length on which the mode shape can be approximated by a half-sine function. As before, the modal mass, damping and mode shape were obtained from full-scale tests on the bridge and are shown in Figure 6.17a. The cumulative probability obtained is shown in Figure 6.17b. It shows that 82% of people will generate vibrations higher than the assumed 0.35 m/s^2 threshold of acceptability. Since both vertical modes of vibration will respond to pedestrian walking across the footbridge, it is not surprising that it was observed during full scale tests that almost all pedestrians perceived strong vibrations caused by their own walking.

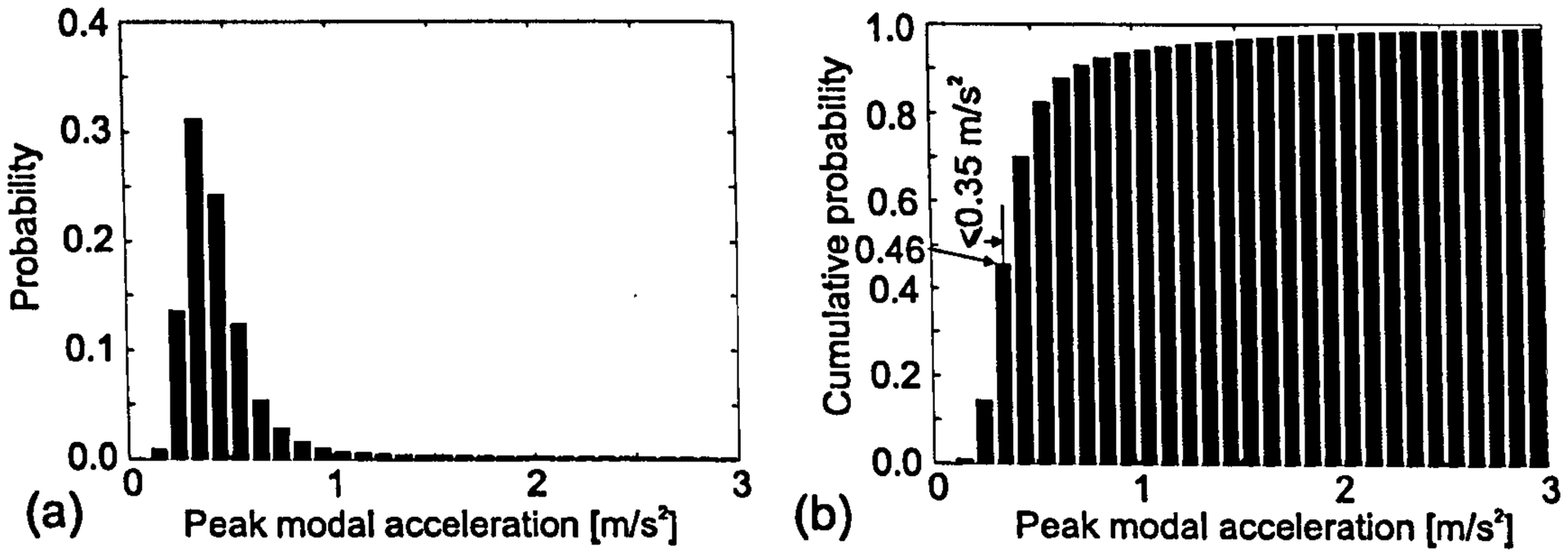

Figure 6.16: Aberfeldy footbridge - (a) Probability of certain acceleration level. (b) Cumulative probability that the acceleration level is smaller than or equal to the acceleration level shown on the horizontal axis.

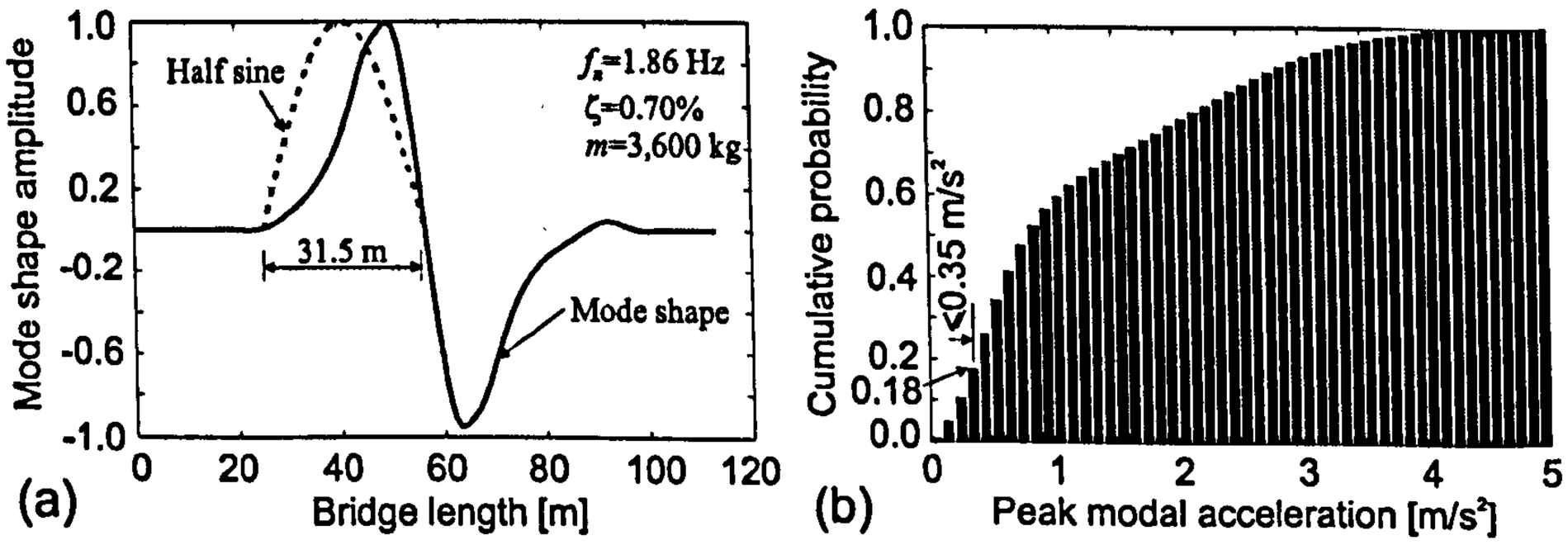

Figure 6.17: Aberfeldy footbridge - (a) Modal properties for mode at 1.86 Hz. (b) Cumulative probability that the acceleration level is smaller than or equal to the acceleration level shown on the horizontal axis.

The result of the analytical study for Aberfeldy footbridge is partly verified by the response measurements to single person excitation. Seven test subjects were asked to cross the bridge with their 'fast', 'normal' and 'slow' pacing rate. For each pacing rate two tests were con-

ducted. Therefore, in total 42 crossings of the bridge were analysed, and peak modal acceleration was extracted from each of them. In this limited testing programme, the footbridge response was measured at the midspan point only, which is a nodal point for the second mode. Therefore, only the response in the first mode was recorded.

Figure 6.18 shows the probability of different levels of peak modal acceleration measured. It can be seen that the observed probability distribution is similar to the one calculated (Figure 6.16a) verifying to some extent the analytical framework used. The fact that probability of the peak acceleration to be higher than $0.4\,m/s^2$ is slightly lower in the measured than in the calculated sample is likely to be a consequence of the human-structure interaction taking place on such a lively bridge during response measurements.

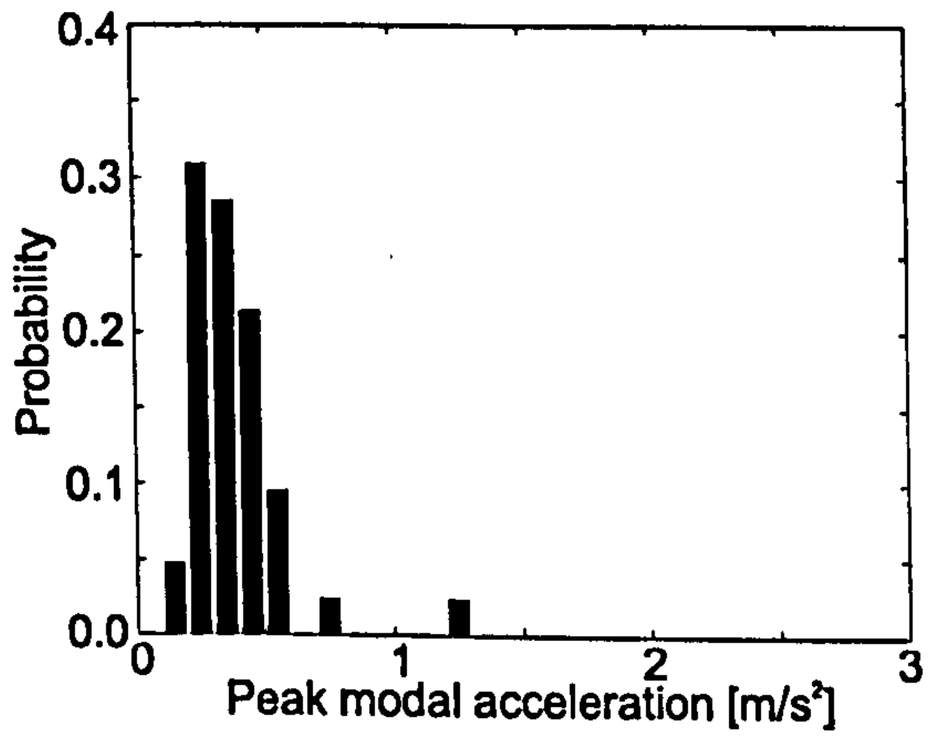

Figure 6.18: Probability of measured peak modal acceleration on Aberfeldy footbridge.

6.4 Monte Carlo Simulations

To check results obtained using the presented analytical probabilistic approach, 2,000 Monte Carlo (MC) simulations were conducted for both footbridges. Besides modal properties of footbridges, input parameters were also force properties. Firstly, 2,000 normally distributed walking frequencies were generated. Then, 2,000 possibilities for the number of steps required to cross the bridge were generated independently from the walking frequency. The amplitude of the force was obtained using the mean value of DLF for the given step frequency (Equation 6.4) and assuming a pedestrian weight of 750 N.

The response of the footbridge to the generated modal forces was calculated. After this, each response was multiplied by a factor which takes into account the variability of DLFs - again a value generated as normal distribution (Figure 6.3b) and independent from the step frequency. Finally, depending on the frequency of walking, gamma distributions (Section 6.2.5) that take into account imperfections in the human induced force (i.e. differences between subsequent steps made by the same person during walking) were generated. In this way a deviation of the real modal acceleration from the one calculated in the previous step was obtained. As a result, a cumulative distribution of peak modal acceleration response was calculated

for both footbridges. These distributions are shown in Figures 6.19a, b and c. They are very similar to those given in Figures 6.14b, 6.16b and 6.17b, respectively. In this way the previously described analytical probabilistic approach was verified. Since the analytical procedure required about 40 times less computational time than the MC method for these two footbridges, it is recommended to use it rather than MC simulations that are computationally quite demanding.

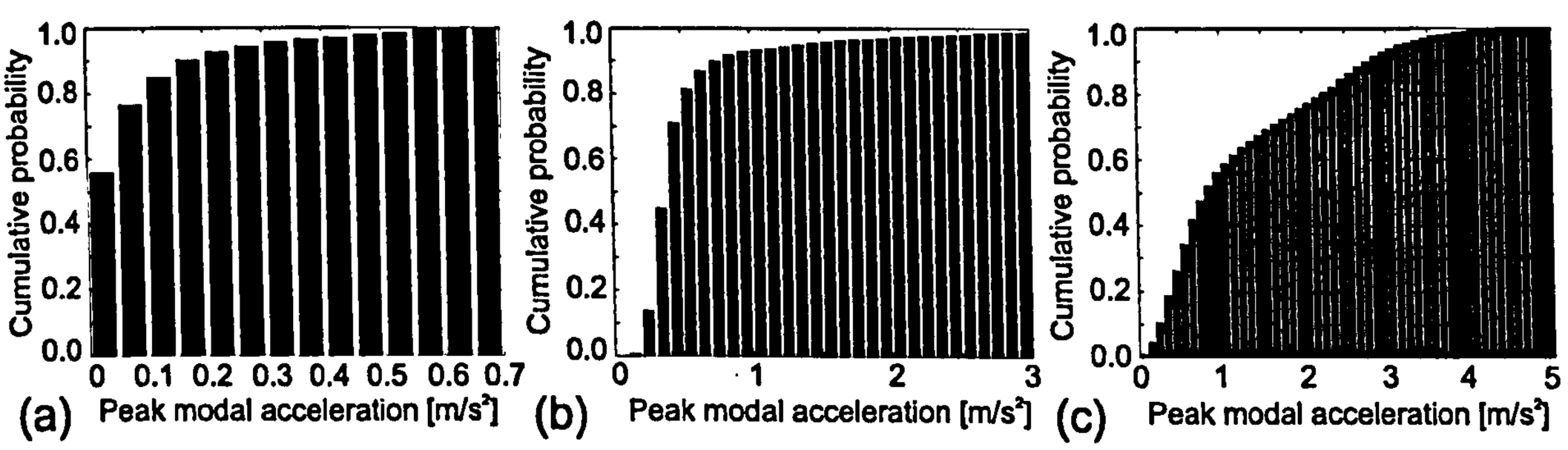

Figure 6.19: Cumulative probability as a result of MC simulations for: (a) Podgorica footbridge, (b) Aberfeldy footbridge (mode 1) and (c) Aberfeldy footbridge (Mode 2).

6.5 Discussion

In the case of the two footbridges investigated, a probabilistic approach was able to estimate the probability that people will be disturbed by footbridge vibrations. When the allowable vibration limit is set to $0.35\,m/s^2$, as many as 95% of people would not feel strong vibrations whilst crossings Podgorica footbridge. This is quite a satisfactory percentage and shows that single pedestrian traffic would not produce significant disturbance for a person crossing the bridge. However, the bridge is subjectively considered as lively during normal multi-pedestrian traffic when peak acceleration regularly reaches $0.4\,m/s^2$ and occasionally goes up to $0.6\,m/s^2$ (Appendix A). This is consistent with the $0.35\,m/s^2$ threshold. It also means that the single pedestrian loading scenario may not be sufficient when designing heavily trafficked footbridges regularly conveying groups of pedestrians. Moreover, it indicates the need for a similar probability-based multi-pedestrian (as opposed to single pedestrian) loading model which currently does not exist.

On the other hand, for Aberfeldy footbridge, more than 50% of people would be disturbed by footbridge vibrations if only the first mode responds to their excitation. In case it is only the second mode that responds, this percentage goes above 80%. Since the footbridge normally responds in both vibration modes at the same time, it is quite likely that it will be perceived as lively at any time even for a single pedestrian traffic case investigated here. This is what was observed during in-situ monitoring of Aberfeldy footbridge. This conclusion also points out the need to extend the analytical framework not only to multi-person, but also to multi-mode response.

It is interesting to compare results of the single pedestrian study conducted here with those from the classical deterministic approach. Probably the most often used implementation of this approach is that given in the British Standard BS 5400 (BSI, 1978), which also features in the Canadian design guideline (OHBDC, 1983). It is well known (Pimentel, 1997) that some parameters used in this code are well out-of-date (such as a single DLF value for all walking frequencies). This is a reason to make use of more realistic (average) modelling parameters for presenting the results of the deterministic approach in this study. The walking force therefore is modelled as a resonant sine force with parameters given in Table 6.1. Following the BS 5400 procedure, the peak modal response is calculated and shown in the last row of the table. It is equal to $0.52\,\mathrm{m/s^2}$ for Podgorica footbridge, and $3.12\,\mathrm{m/s^2}$ and $2.70\,\mathrm{m/s^2}$ for Aberfeldy footbridge, for modes 1 and 2, respectively.

Table 6.1: Parameters for response simulations under a single pedestrian on two footbridges.

Footbridge	**Podgorica**	**Aberfeldy (1^{st} mode)**	**Aberfeldy (2^{nd} mode)**
Weight [N]	750	750	750
Step frequency [Hz]	2.04	1.52	1.86
DLF	0.42	0.21	0.35
Walking speed [m/s]	1.45	1.08	1.32
Peak modal response [$\mathrm{m/s^2}$]	0.52	3.12	2.70

Based on the cumulative probabilities previously calculated (Figures 6.14b, 6.16b and 6.17b), it can be concluded that the probability of exceeding the calculated accelerations of $0.52\,\mathrm{m/s^2}$, $3.12\,\mathrm{m/s^2}$ and $2.70\,\mathrm{m/s^2}$ under a single person excitation is very small. Therefore, the single person model based on resonant excitation is quite conservative. There are schools of thought that the single person resonant approach is designed to cater for some more complicated (for calculation) loading scenarios, such as normal multi-person pedestrian traffic. In case of Podgorica footbridge the estimate of $0.52\,\mathrm{m/s^2}$ is quite good for the in-situ observed peak vibration level under multi-person pedestrian traffic, being between 0.4 and $0.6\,\mathrm{m/s^2}$ (Appendix A). However, this seems to occur simply by chance and a generalisation of this approach to all footbridges can significantly both under- and over-estimate the response depending on the particular footbridge investigated. Because of this, the aim should be to consider all possible (but reasonable) loading scenarios for a particular bridge, depending on their realistic probability of occurrence. In this way the vibration serviceability design would be based on basic physical principles and actual vibration performance, as appropriate for serviceability checks. Also, it would not be at risk of replacing a complicated problem with a simpler but non representative one.

Finally, it should be mentioned that acceleration limits allowed by BS 5400 (BSI, 1978) are $0.71\,\mathrm{m/s^2}$ for Podgorica footbridge and $0.62\,\mathrm{m/s^2}$ for Aberfeldy footbridge. It is interesting that the first footbridge is considered as being lively by many people crossing it although $0.71\,\mathrm{m/s^2}$ is almost never achieved in normal usage (Appendix A). On the other hand, experience from Aberfeldy footbridge is that it is considered as being lively even under a single

person excitation. This is interesting as the probability that acceleration level being higher than $0.62\,\mathrm{m/s^2}$ under single person walking is only about 12% for this footbridge responding in first mode (Figure 6.16b) and about 60% for the footbridge responding in the second mode (Figure 6.17b). It is likely that these considerations indicate serious possible deficiency in the BS 5400 limit for peak acceleration a_{lim} given by the well-known empirical formula $a_{lim} = 0.5\sqrt{f_0}$, where f_0 is the fundamental natural frequency in the vertical direction. This formula is, in fact, a compromise between two sets of rather different and old data gathered by Leonard (1966) and Smith (1969) in the 1960s and seems to set the allowable vibration limit to a higher level than what is observed in practice.

6.6 Conclusions

A novel probability based framework for predicting vibration response to single person excitation is presented in this chapter. A single person force is modelled as a harmonic force with its amplitude, frequency and duration described via probability density functions. These factors represent inter-subject variability between people in the force induced by their walking. In addition, intra-subject variability in terms of force induced is taken into account as a probability density function representing (in)ability of people to produce sinusoidal force. The aim here was to consider as many parameters relevant to the study of a single person as possible. When including the four probability distributions into the calculation, the cumulative probability that the response will not exceed a certain peak acceleration under a single person walking can be calculated. This can be used as key design information when making decision about vibration serviceability of the footbridge. In this way shortcomings of having only one response value, as defined in currently used deterministic force modelling, are avoided. Results presented in this study have been partially verified on two full scale footbridges.

The probability procedure developed in this chapter can be used when designing footbridges that are not very busy and where a single person loading scenario is reasonable. Having good mathematical representation of a single person provided in this study is a necessary prerequisite for developing a similar probability-based model for multi-person excitation of footbridges in future.

Preface to Chapter 7

The probability-based procedure from Chapter 6 was extended in Chapter 7 to deal with footbridges that respond in several vibration modes to a single person excitation. Because of this multi-mode response, it was necessary to model the walking force in such a way that all relevant harmonics could be taken into account.

Chapter 7

Prediction of Multi Mode Vibration Response of Footbridges

This chapter, in a slightly amended form, has been submitted for publication under the following reference:

Živanović, S., Pavic, A. and Reynolds, P. Probability Based Prediction of Multi Mode Vibration Response to Walking Excitation, Engineering Structures.

Abstract

In vibration serviceability checks of footbridges, a force induced by a single person walking is usually modelled as a harmonic force having frequency that matches one of the footbridge natural frequencies. This approach assumes that, among the infinite number of harmonics a walking force is composed of, only a single harmonic is important for a vibration serviceability check. Another usual assumption is that the footbridge can be modelled as an SDOF system, implying that only vibration in a single mode is of interest. In addition, due to the deterministic nature of this approach, it cannot take into account inter- and intra-subject variabilities in the walking force that are now well documented in the literature. To account for these variabilities, a novel probabilistic approach to carry out a vibration serviceability check is developed in this chapter. Factors such as probability distribution of walking frequencies, step lengths and amplitude of walking force for its five lowest harmonics and subharmonics are taken into account. Using walking force time histories measured on a treadmill, the frequency content of the force was investigated, resulting in the formulation of a multi-harmonic force model. This model can be used to estimate multi-mode response in footbridges. This was verified successfully on an as-built catenary footbridge structure. Although only vibration response of footbridges was analysed in this chapter, the force model proposed has potential to be implemented in estimation of vibration for low frequency floors as well, where multi-mode response occurs more frequently. The model is easily programmable and as such could present a powerful tool for estimating efficiently the probability of various levels of vibration response due to a single person walking. Therefore, the proposed probability-based methodology has the potential to revolutionise the philosophy of the current codes of practice dealing with vibration serviceability of structures under human-induced excitation.

7.1 Introduction

Vibration serviceability checks for slender footbridges that are potentially lively in the vertical direction are usually based on the assumption that an average single pedestrian is crossing the bridge with a step frequency matching one of the structural natural frequencies. In these analyses, it is assumed that the human-induced walking force is a sinusoidal force and that a footbridge structure responds in a single vibration mode (BSI, 1978; OHBDC, 1983; Bachmann & Amman, 1987; CSA, 2000; HA, 2001; BSI, 2004). This practice can significantly overestimate the footbridge vibration response (Pimentel, 1997). This occurs due to neglecting inter- and intra-subject variability in the walking force induced (Ebrahimpour et al., 1996; Kerr, 1998; Brownjohn et al., 2004b; Sahnaci & Kasperski, 2005). The former term implies that different pedestrians generate different dynamic forces, and the latter means that even a single pedestrian induces a walking force that differs with each step. Therefore, the walking force is not a sinusoidal force as assumed in the mathematical model used widely for vibration serviceability check of footbridges. Rather, it is a considerably more complex narrow band random process, as demonstrated by Brownjohn et al. (2004b).

Variability in the walking force can be taken into account via probability-based modelling described in Chapter 6. In this approach, variables that characterise the human-induced force can be described via their probability density functions. These can be defined for the parameters characterising both inter-subject variability (such as the walking frequency, step length and force amplitude) and intra-subject variability (that is the inability of people to repeat the same force in each step). As a logical consequence of this probabilistic approach, the estimate of the vibration response can be expressed as a probability that a certain level of vibration, considered to be a limiting value for vibration serviceability check, will not be exceeded. Rather than ending up with a single number and a binary pass or fail outcome, the novelty of the proposed approach is that a range of possible vibration responses and the probability of their occurrence is produced. An assessment of these is a much more logical way of judging vibration serviceability.

The previously defined probability based model (Chapter 6) was developed for the case when a single force harmonic and the corresponding single mode response were sufficient for the vibration serviceability check. However, there are footbridge and other structures, even with very simple configurations, such as catenary footbridges (as will be shown in this study), that respond to pedestrian-induced excitation in several vibration modes simultaneously, with more than one of them being important. These modes often can be excited by energy around different force harmonics. Therefore, it is necessary to take into account all relevant harmonics of the walking force. By doing this, and knowing modal properties of the relevant vibration modes, the multi-mode response of the structure can be found via the mode superposition principle (Clough & Penzien, 1993).

This chapter aims to formulate a multi-harmonic force model for calculation of the multi-mode structural response to a single person walking across a footbridge. This will be done

using a probability-based framework developed in the previous chapter. Therefore, a single harmonic force model will be extended to a multi-harmonic force model. This new model will contain not only the main harmonics usually dealt with in literature, but also subharmonics that appear between main harmonics in the force spectrum (Sahnaci & Kasperski, 2005).

As in Chapter 6, the probability distribution of weight for human population, variability in the structural dynamic properties (which are difficult to predict in the design stage) and the probability distribution for limiting vibration level are not taken into account in the modelling. The reasons for this have been explained in Chapter 6.

In the first part of this chapter, the appearance of the subharmonics in the force spectrum is explained. After this, probability density functions describing inter-subject variability in the walking force are defined. Then, the intra-subject variability, that is the imperfections in human induced force, is analysed to formulate a time domain force model. This force model is then experimentally verified leading to the main conclusions presented at the end of the chapter.

7.2 Subharmonics in Walking Force

Human-induced walking force is not periodic, but rather it is a narrow band random process (Brownjohn et al., 2004b). This means that there is a leaking of energy around main harmonics in force spectrum. To illustrate this, 80 steps of a dynamic part of the walking force, measured on an instrumented treadmill (Brownjohn et al., 2004b) and shown in Figure 7.1a, are analysed. The average number of steps per second made by a test subject during this measurement was 1.96 steps/s, that is the walking frequency f_s was 1.96 Hz. The force presented was transformed into the frequency domain. Fourier amplitudes and phases are shown in Figures 7.1b and 7.1c, respectively. The aforementioned leaking of energy around the main harmonics can clearly be seen in Figure 7.1b. Here, the main harmonics are those present at frequencies equal to the average walking frequency (1.96 Hz) and its integer multiples. However, it can be seen that there are also some subharmonics appearing at frequencies between the main harmonics. This phenomenon has recently been reported in detail by Sahnaci & Kasperski (2005). The explanation for this lies in the fact that the fundamental period of the force time history is equal to the time required to make two successive steps, rather than one, as has been widely accepted in the literature. In this way, the fundamental period is actually approximately two times higher than when analysing one step only and consequently the fundamental frequency of the walking force is approximately two times lower than that for a single step. The reason for this is that walking process for two legs can be described by slightly different parameters (walking frequency/period and step length) meaning that one leg is 'stronger' than another (Sahnaci & Kasperski, 2005). An illustration of this are differences in the periods for the two feet that are presented in Figure 7.1d. Crosses represent the period for the left foot while circles represent period for the the right foot. It can be seen that time required for the left foot to make one step is consistently longer than that for the

right foot.

Based on this anlaysis, it would be more appropriate to call the harmonic appearing at a frequency of $0.5f_s$ (Figure 7.1b) as the fundamental harmonic. However, for the sake of consistency with the literature published in the last 40 years and bearing in mind the narrow-band nature of the walking force, the terminology used is as follows. The energy around peaks that appear at frequencies that are integer multiples of the average step frequency will be called 'harmonics' (or 'main harmonics') of the walking force, while the energy corresponding to peaks between these will be called 'subharmonics'.

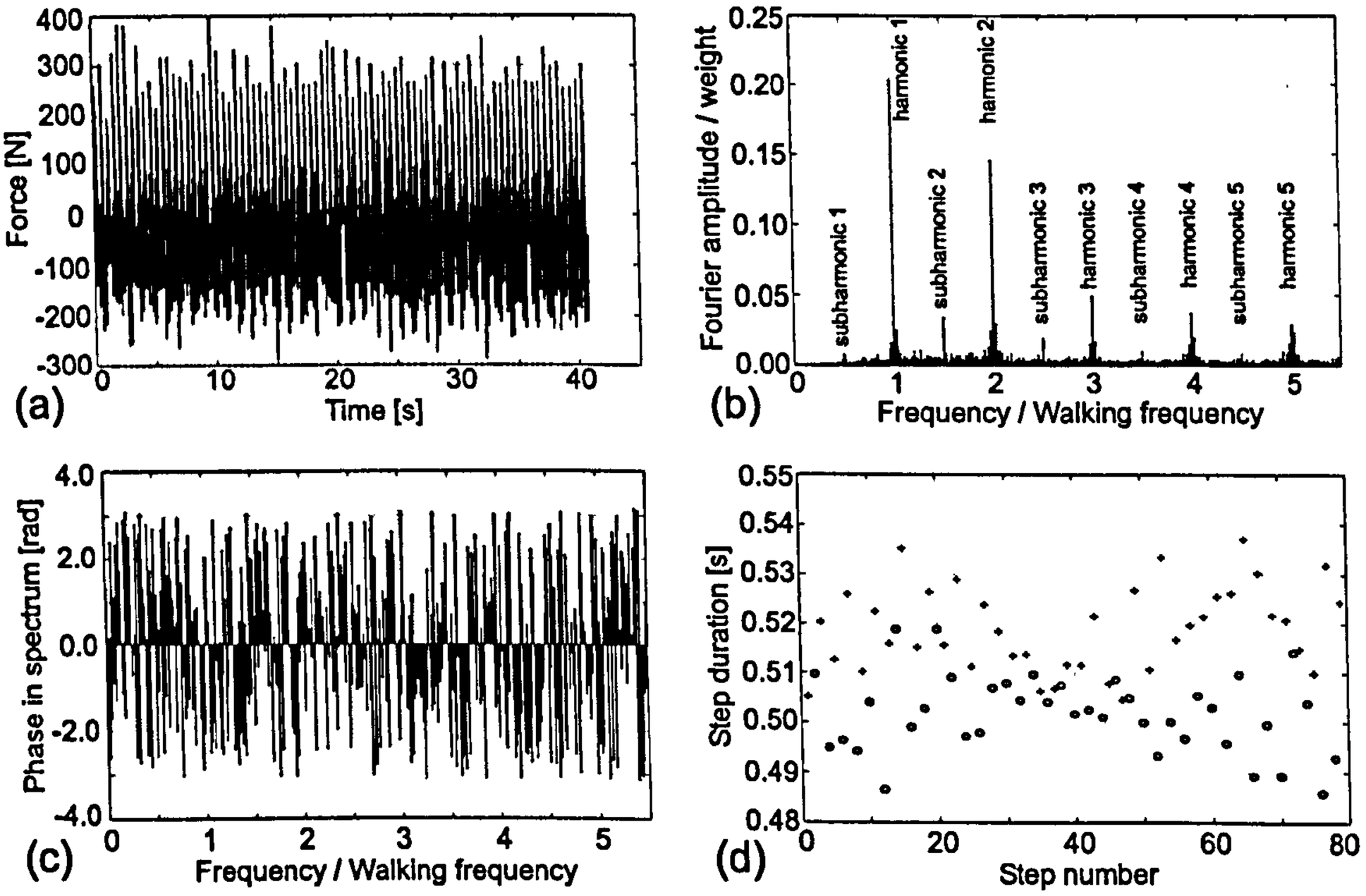

Figure 7.1: (a) Dynamic part of a force induced by walking. (b) Amplitude of force Fourier spectrum. (c) Phase of force Fourier spectrum. (d) Period of each step.

7.3 Inter-Subject Variability during Walking

Parameters that describe variability in walking forces induced by different pedestrians are walking frequency, step length and magnitude of the walking force. These parameters are described in this section.

7.3.1 Walking Frequency and Step Length

Walking frequency f_s and step length l_s can be considered as two independent modelling parameters as explained in Chapter 6. It is necessary to have information about them when doing force modelling. f_s in fact defines the forcing fundamental frequency and together with

l_s is required for the calculation of time T_c required for footbridge crossing. This time can be obtained from:

$$T_c = \frac{L}{f_s l_s}, \tag{7.1}$$

where L is the length of the footbridge. T_c basically defines the duration of the walking force. Therefore, it is useful to know probability distributions of f_s and l_s. These were described earlier in Chapter 6 as normal distributions. They are shown in Figures 7.2a and 7.2b, respectively. The mean values of walking frequency and step length in Figure 7.2 are denoted as μ_{fs} and μ_{ls}, respectively, while their standard deviations are denoted as σ_{fs} and σ_{ls}, respectively. Letters μ and σ will be used throughout the chapter to describe the mean value and standard deviation of a variable whose name will be given as their subscript.

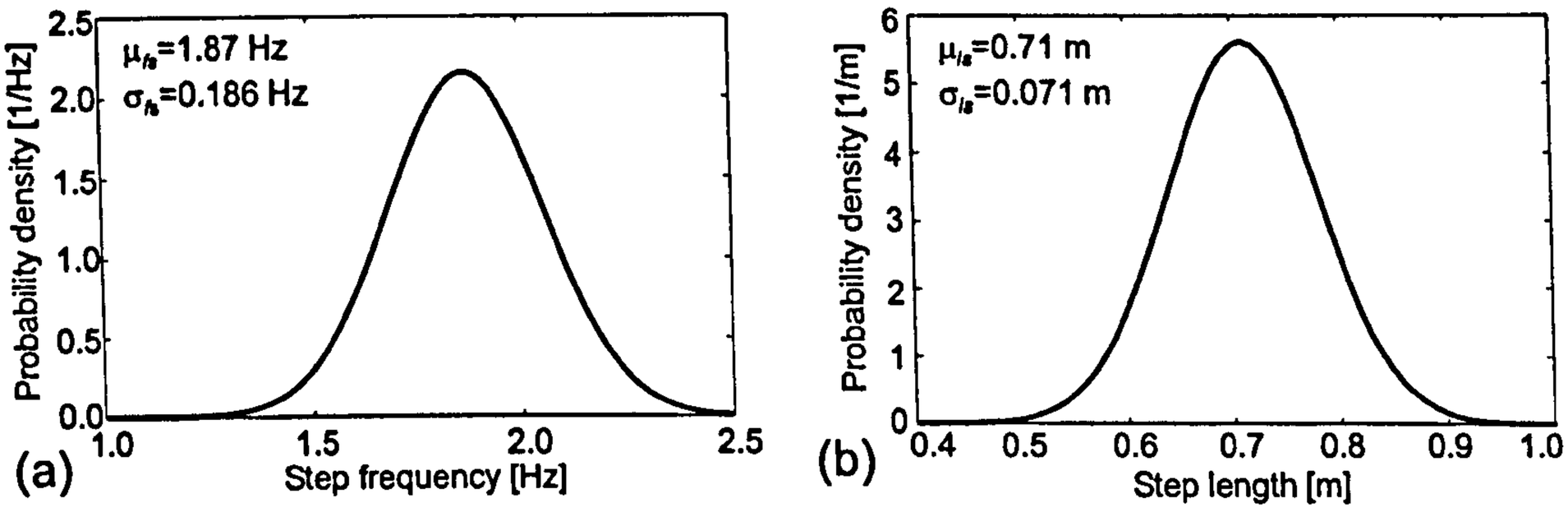

Figure 7.2: Probability density functions for: (a) walking frequency and (b) step length.

7.3.2 Force Magnitude

The third parameter required for force description is the magnitude of the walking force. Since this force is composed of harmonics and subharmonics (Figure 7.1b), it is necessary to define the amplitude of each of them. This is not a straightforward task because of energy spreading around main harmonics and subharmonics. However, for each of them a sinusoidal force can be defined in such a way that its power is equal to the power of the (sub)harmonic analysed taking into account its neighbouring frequency lines, say those in the range of $\pm 0.25 f_s$ around the (sub)harmonic. The amplitude of this sinusoid, divided by test subject's weight, is the value widely accepted for characterisation of the strength of each (sub)harmonic. This value is called the dynamic loading factor (DLF).

7.3.2.1 DLFs for Main Harmonics

Different people generate different values of DLFs, even when walking at the same frequency (Rainer et al., 1988; Kerr, 1998). For the first harmonic, Kerr (1998) found that the mean value of its DLF is dependent on the walking frequency f_s, as follows:

$$\mu_{DLF1} = -0.2649 f_s^3 + 1.3206 f_s^2 - 1.7597 f_s + 0.7613. \tag{7.2}$$

Distribution of DLF_1 around its mean value, for a particular walking frequency, can be obtained via multiplication of the mean value by a normally distributed factor MF shown in Figure 7.3a by solid line.

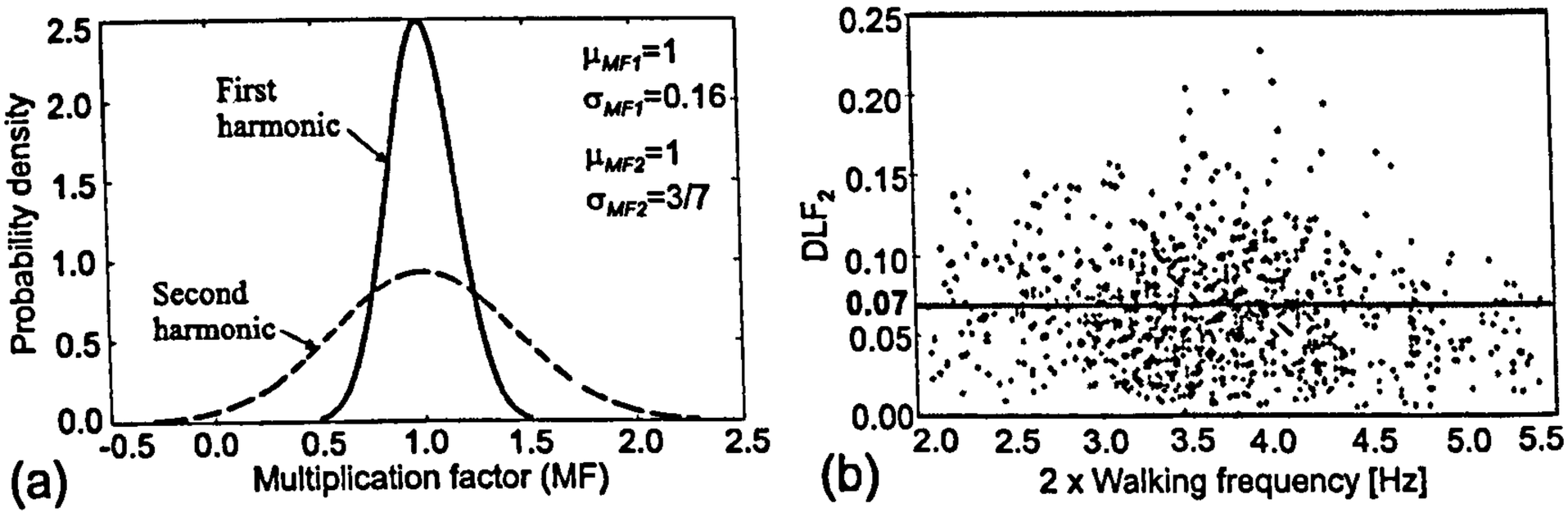

Figure 7.3: (a) Probability density function for multiplication factor for DLF_1 (solid line) and DLF_2 (dashed line). (b) DLF_2 measured by Kerr (1998).

For complete description of the walking force, the probability distributions of DLFs for higher harmonics are also required. This study deals with the first five harmonics of the walking force, since it is believed that harmonics higher than the fifth are not capable of inducing perceptible vibrations in footbridges.

Kerr (1998) reported a mean value for DLF_2 equal to 0.07 (Figure 7.3b) regardless of the walking frequency. Under an assumption of normal distribution of DLF_2 for each walking frequency and assuming that DLF_2 is independent from DLF_1, a normal distribution of a multiplication factor for getting DLF_2 from its mean value can be presented based on Kerr's data (dashed line in Figure 7.3a). It should be noted that, due to large standard deviation, some negative values of DLF_2 tend to appear in Figure 7.3a. These do not have physical meaning and as such should be removed from the calculation procedure by replacing them with zero values. It can be seen that the scattering of DLF_2 is much higher in comparison with that for the first harmonic.

Based on Kerr's research (Kerr, 1998), the normal distribution for third and forth harmonic can be defined in similar way as it was done for the second harmonic. By analysing 95 force time histories measured by Brownjohn et al. (2004b), the data related to the fifth harmonic have also been collected. The mean values and standard deviations describing the normal distributions of the second, third, fourth and fifth harmonics are listed in Table 7.1. Similarly to DLF_2, all negative values of DLFs that appear in the probability distributions due to large scatter should be replaced by zero values.

Table 7.1: Parameters describing normal distribution of DLFs for higher harmonics.

Harmonic #	Mean	Standard deviation
2	0.07	0.030
3	0.05	0.020
4	0.05	0.020
5	0.03	0.015

7.3.2.2 DLFs for Subharmonics

This section aims to define DLFs for the first five subharmonics in the walking force. These data are missing from the literature available. Because of this, the 95 time histories measured by Brownjohn et al. (2004b) for nine test subjects walking on a treadmill were transformed into the frequency domain. Then the power for each subharmonic was calculated in the frequency range $(i-0.5)f_s \pm 0.25f_s$, where i is the subharmonic considered ($i = 1, 2, 3, 4, 5$). After this, the amplitude of a sinusoidal force having the same power was calculated and divided by the weight of the test subject to get the DLF. However, since force time histories for only nine test subjects taking part in 95 measurements with different walking speeds were available, it is not prudent to construct probability density functions for these subharmonics as there were insufficient data points around each walking frequency. Instead, it is possible to establish a relationship between DLFs for subharmonic and, say, first walking harmonic DLF_1. These relationships are presented in Figure 7.4, based on DLFs obtained for 95 force time histories. Also, a linear fit in the least square sense is presented for each graph in the figure. Therefore, for modelling purpose only the relative relationship between subharmonics and the first harmonic is adopted. In this way the magnitude of the DLF for subharmonics can be obtained only after the magnitude of DLF_1 is known.

7.4 Intra-Subject Variability during Walking

Due to the inability of human beings to walk in the same way when making every single step, the walking force is not a perfectly periodic process. Imperfections in the human walking force can be described via slight changes of the walking frequency (that is reciprocal value of the period presented in Figure 7.1d), amplitude (Figure 7.1a) and phase lag in each step. These changes can be taken into account via investigation of the force in the frequency domain that is inherently part of the force modelling described in the next section.

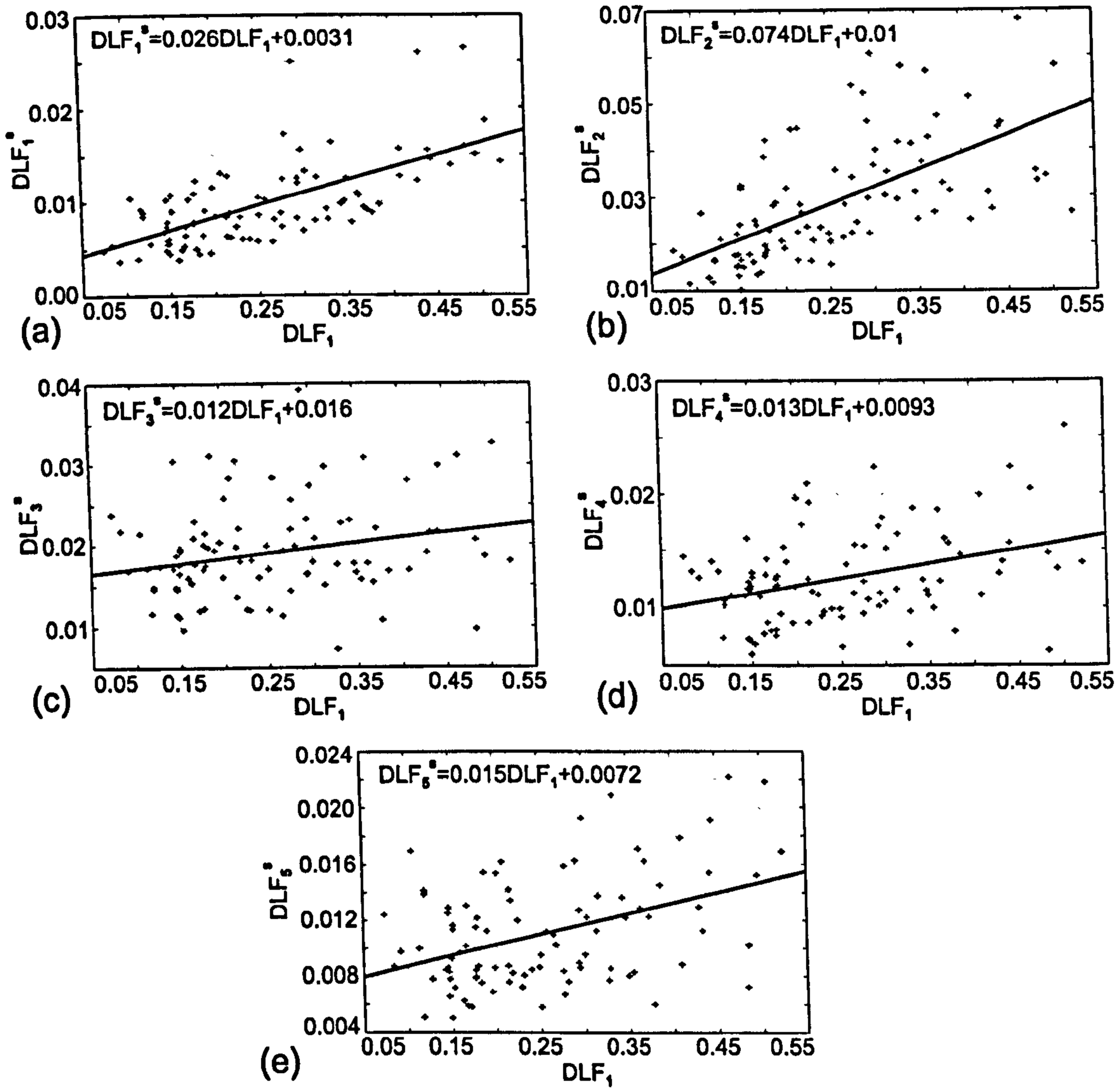

Figure 7.4: DLFs for subharmonics as functions of DLF_1.

7.5 Force Modelling

In this section, frequency content of the measured walking forces is analysed first, followed by description of the force model adopted. Then a procedure for model usage is briefly summarised.

7.5.1 Force Description in the Frequency Domain

The force induced by walking can be presented in the frequency domain via its amplitudes and phases characterising each frequency line in the force spectrum (Figures 7.1b and 7.1c). Since a decision to cover the frequency range of walking force related to the first five harmonics and subharmonics was made, a force model covering the frequency range $0.25f_s$-$5.25f_s$ will be formulated.

To formulate this force model, 95 time histories measured on a treadmill set to a constant speed in each test (Brownjohn et al., 2004b) were analysed. The Fourier spectrum of exactly 80 steps for each time history was found. Amplitudes of this spectrum in the range $\pm 0.25 f_s$ around each (sub)harmonic were divided with the corresponding DLF for this (sub)harmonic. In this way the normalised amplitude spectra were obtained. They were overlayed for each (sub)harmonic, and are presented as grey lines in Figure 7.5. After this, the mean functions for all spectra were found and fitted in the least square sense. The normalised amplitudes $\overline{DLF_i}(\bar{f}_j)$ for i^{th} harmonic are fitted by a function available as a built-in function in MATLAB (MathWorks, 2006):

$$\overline{DLF_i}(\bar{f}_j) = a_{i,1} e^{-\left(\frac{\bar{f}_j - b_{i,1}}{c_{i,1}}\right)^2} + a_{i,2} e^{-\left(\frac{\bar{f}_j - b_{i,2}}{c_{i,2}}\right)^2} + a_{i,3} e^{-\left(\frac{\bar{f}_j - b_{i,3}}{c_{i,3}}\right)^2}, \tag{7.3}$$

where $a_{i,k}, b_{i,k}$ and $c_{i,k}$ $(k = 1,2,3)$ are nine fitting parameters for i^{th} harmonic. $\bar{f}_j$ is the frequency ratio between the current frequency line and the step frequency f_s, and it belongs to the interval $[i - 0.25, i + 0.25)$ with step $\frac{1}{80}$, including its left limit. Therefore, for the first harmonic variable $\bar{f}_j$ is in the range 0.75-1.25, for the second harmonic 1.75-2.25, for third 2.75-3.25, forth 3.75-4.25 and fifth 4.75-5.25. In this way, the spectrum width of $0.5 f_s$ around each harmonic is taken into account when defining the normalised DLF for that harmonic. Since every time history analysed contained 80 steps, this was the reason to have spacing between frequency lines equal to $\frac{f_s}{80}$. When spectrum width of $0.5 f_s$ used for each harmonic is divided by the frequency spacing, it follows that each harmonic is described by 40 lines. The nine parameters for each of the first five harmonics are listed in Table 7.2.

For fitting the normalised amplitudes for subharmonics $\overline{DLF_i^s}(\bar{f}_j^s)$ a chosen function has the following form:

$$\overline{DLF_i^s}(\bar{f}_j^s) = a_{i,1}^s e^{-\left(\frac{\bar{f}_j^s - b_{i,1}^s}{c_{i,1}^s}\right)^2} + a_{i,2}^s e^{-\left(\frac{\bar{f}_j^s - b_{i,2}^s}{c_{i,2}^s}\right)^2}, \tag{7.4}$$

where $a_{i,k}^s, b_{i,k}^s$ and $c_{i,k}^s$ $(k = 1,2)$ are six fitting parameters for i^{th} subharmonic. $\bar{f}_j^s$ is the frequency ratio between the current frequency line and step frequency f_s, and it belongs to the interval $[i - 0.75, i - 0.25)$ including its left limit. So, for first subharmonic this variable is in the range 0.25-0.75, for the second subharmonic it is 1.25-1.75, and so on. As in the case of the main harmonics, 40 lines are used for the description of a subharmonic. The six parameters for each of the five subharmonics are listed in Table 7.3.

The functions in Equations 7.3 and 7.4 used to fit the mean functions for the harmonics and subharmonics are shown as black lines in Figure 7.5. It can be seen that the fit for subharmonics is quite similar for all of them in terms of normalised amplitude and shape of the fitting function. In the case of main harmonics, it is evident that the higher ones are weaker in amplitude and broader in frequency content than the lower ones. This indicates higher degree of randomness for higher harmonics.

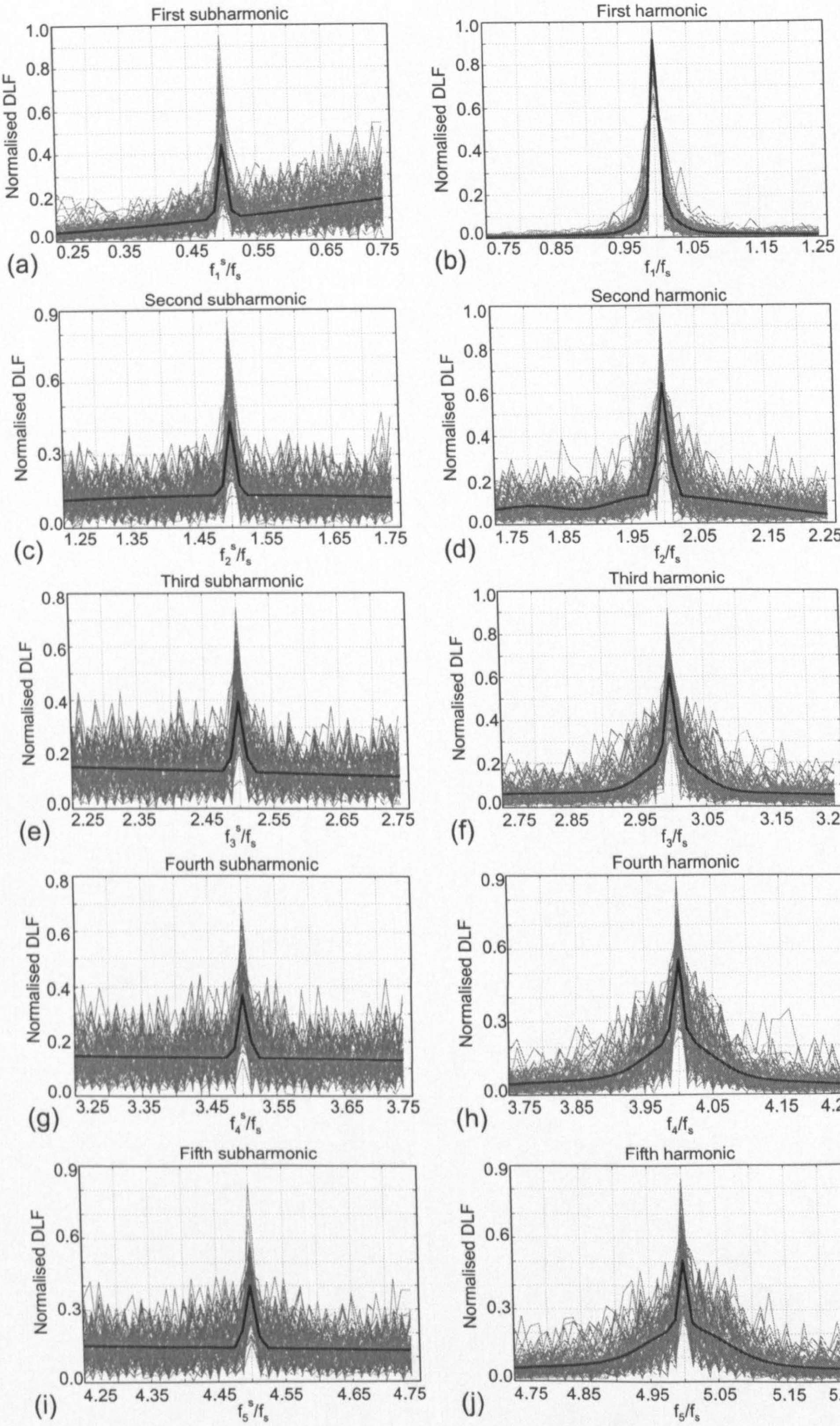

Figure 7.5: Normalised DLFs for first five subharmonics (left column) and harmonics (right column).

Table 7.2: Fitting parameters for five harmonics.

i	1	2	3	4	5
$a_{i,1}$	0.785200	0.513000	0.390800	0.325500	0.280600
$b_{i,1}$	0.999900	2.000000	3.000000	4.000000	4.999000
$c_{1,1}$	0.008314	0.011050	0.009560	0.008797	0.007939
$a_{i,2}$	0.020600	0.133000	0.156700	0.164700	0.158400
$b_{i,2}$	1.034000	1.957000	3.000000	4.001000	5.004000
$c_{i,2}$	0.252400	0.263200	0.055250	0.066410	0.078250
$a_{i,3}$	0.107400	-0.049840	0.068660	0.068880	0.072890
$b_{i,3}$	1.001000	1.882000	2.957000	3.991000	4.987000
$c_{i,3}$	0.036530	0.058070	0.560700	0.375000	0.450100

Table 7.3: Fitting parameters for five subharmonics.

i	1	2	3	4	5
$a^s_{i,1}$	0.340600	0.302400	0.262700	0.234400	0.264500
$b^s_{i,1}$	0.498800	1.500000	2.500000	3.501000	4.499000
$c^s_{i,1}$	0.008337	0.008735	0.009748	0.009898	0.010190
$a^s_{i,2}$	0.280300	0.134500	0.245600	0.235500	0.238900
$b^s_{i,2}$	1.133000	1.532000	0.231200	-1.576000	1.153000
$c^s_{i,2}$	0.638800	0.723300	2.932000	7.050000	4.561000

Having a model representing amplitudes in the spectrum of the walking force, additional information about phase for each frequency line is required for accurate force representation in the time domain. For this purpose, the phase spectra of measured forces were examined. It was noticed that the phases for all 400 frequency lines in the range $0.25f_s - 5.25f_s$ are approximately uniformly distributed in the interval $[-\pi, +\pi]$ for any force time history analysed. An example of this distribution for phase diagram presented in Figure 7.1c is shown by a histogram in Figure 7.6. Any interdependence between phase changes around the main harmonics (where the amplitudes are the highest and most important) as well as between different harmonics could not be noticed. This was the reason to adopt a uniformly distributed random phase in the force model.

It should be said here that the modelling presented in this section is an extension of a model formulated by Brownjohn et al. (2004b), as:

- subharmonics are now included into the force model,
- phase information is taken into account, and
- complete frequency content of the force spectrum, up to the frequency of 5.25 f_s, is now included into the model without any discontinuities.

With all frequency lines considered and phase information added, the reconstruction of the force in the time domain is possible. This, in turn, makes it possible to weight the human-

induced force by mode shape in order to take into account that the force moves across the footbridge and has limited duration. This weighted (modal) force can then be used to calculate structural modal response in a particular mode of vibration. This kind of analysis is not possible if only the magnitude of the walking force is defined in the frequency domain, such as in the force model formulated by Brownjohn et al. (2004b).

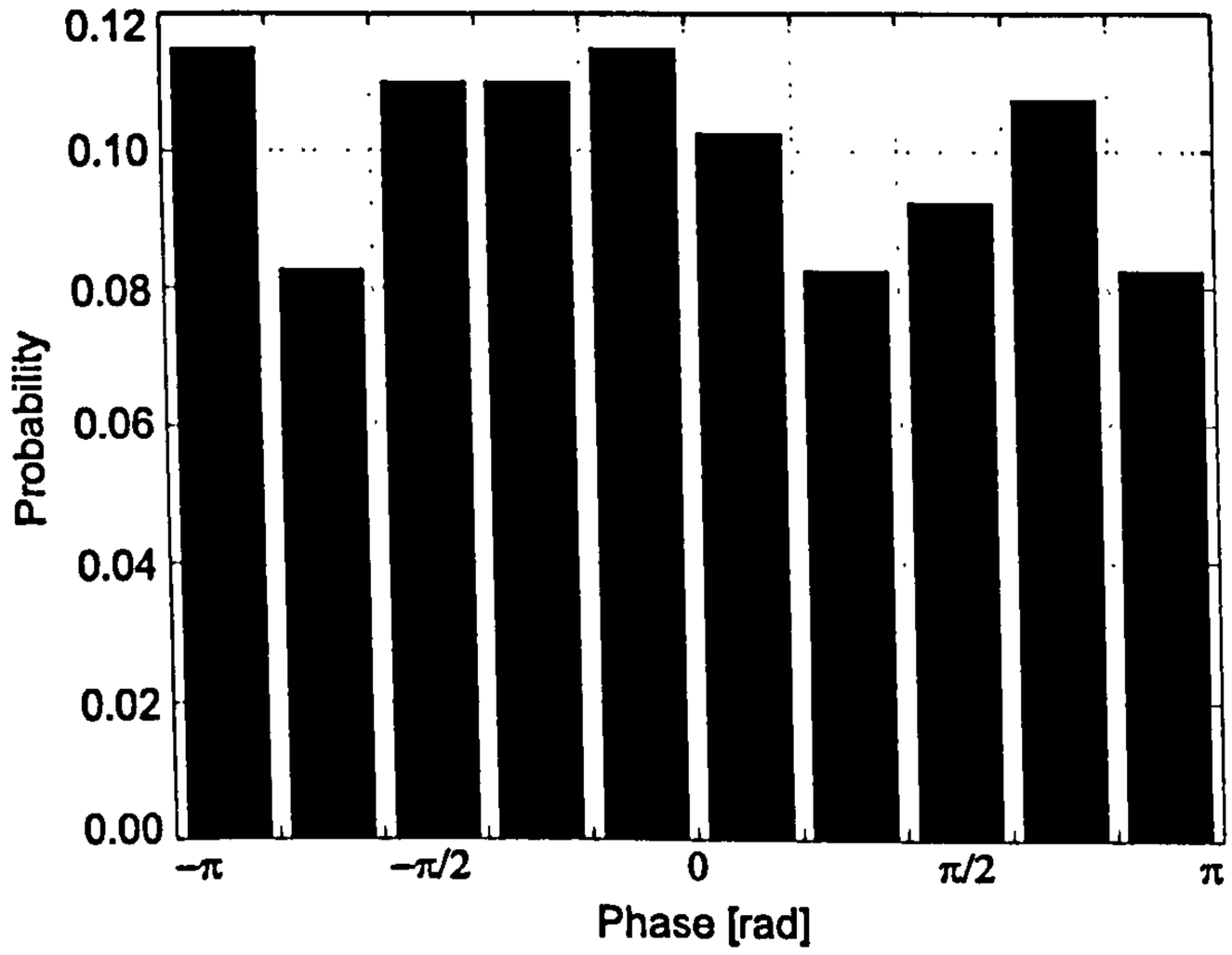

Figure 7.6: Distribution of phases for 400 lines in force spectrum.

7.5.2 Time Domain Force Model

For i^{th} harmonic, occurring at frequency if_s, the force can be reconstructed in the time domain via following formula:

$$F_i(t) = W \cdot DLF_i \sum_{\bar{f}_j = i-0.25}^{i+0.25} \overline{DLF}_i(\bar{f}_j) \cos\left(2\pi \bar{f}_j f_s t + \theta(\bar{f}_j)\right), \tag{7.5}$$

while for i^{th} subharmonic it would be

$$F_i^s(t) = W \cdot DLF_i^s \sum_{\bar{f}_j^s = i-0.75}^{i-0.25} \overline{DLF}_i^s(\bar{f}_j^s) \cos\left(2\pi \bar{f}_j^s f_s t + \theta(\bar{f}_j^s)\right). \tag{7.6}$$

Here, i is the (sub)harmonic considered, $\bar{f}_j f_s$ is a frequency of the current line in the spectrum within the energy range of the harmonic analysed while $\theta(\bar{f}_j)$ is phase assigned to the same line. This assignment is based on a uniform distribution of phases in the interval $[-\pi, +\pi]$. DLF_i is the DLF for the harmonic analysed, $\overline{DLF}_i(\bar{f}_j)$ is the normalised amplitude for the same harmonic for each line, while $W = 750\,\mathrm{N}$ is the average weight of a pedestrian. Variables containing superscript s are related to subharmonics. Finally, the total force can be obtained as:

$$F(t) = \sum_{i=1}^{5} F_i(t) + \sum_{i=1}^{5} F_i^s(t). \tag{7.7}$$

To demonstrate the quality of the force model presented, an attempt to model the force shown in Figure 7.1a has been made. The fundamental frequency of this force as well as its DLFs are already known. The frequency is 1.96 Hz while DLFs for all harmonics and subharmonics are obtained based on procedure explained in Section 7.3.2. These values were used as input values for defining normalised amplitudes in the frequency domain for the force analysed. The force spectrum obtained in this way is presented in Figure 7.7a. The peaks in this spectrum are a bit attenuated in comparison with the real spectrum (Figure 7.1b) due to using an average spectrum of walking forces defined by Equations 7.3 and 7.4 and Figure 7.5. After obtaining the spectrum of amplitudes, uniformly distributed random phases were generated for all 400 lines in the spectrum and the force was reconstructed in the time domain (Figure 7.7b). It can be noticed that force model (Figure 7.7b) differs from that in Figure 7.1a. The two forces could visually be, in general, both more similar and more different from each other than obtained here, depending on the randomly generated phase values for each case. Since the probability-based response calculation will be based on a large sample of generated forces, it can be assumed that the phase influence on the results in such a sample is not significant. It should be noticed that the energy of the force is not influenced by the phase values.

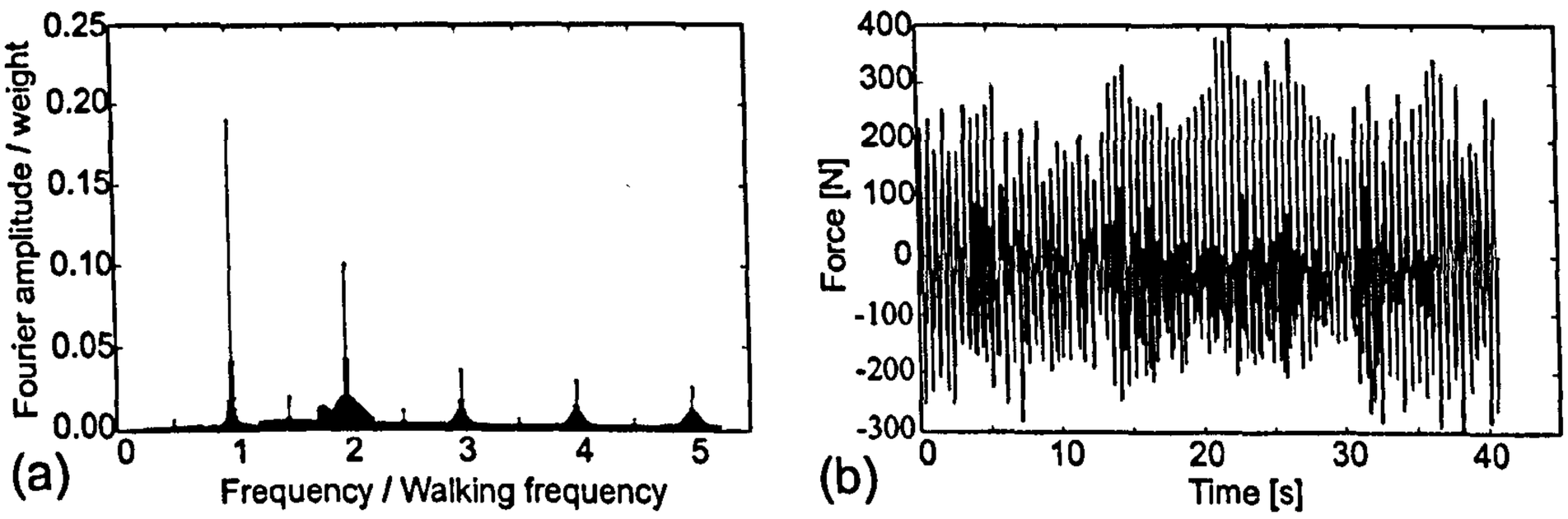

Figure 7.7: (a) Force spectrum for force shown in Figure 7.1a according to the force model adopted. (b) Force reconstructed in the time domain.

7.5.3 Procedure for Response Simulations

This section reviews briefly the key steps required for estimation of a modal response of a footbridge when using the force model formulated. This is based on Monte Carlo simulations. To simplify explanation, it is assumed that simulations for 2,000 individual pedestrians walking on their own across a bridge will be conducted. It is further assumed that only a single mode is relevant for the calculation, and that its modal properties are known. In the case that more than one mode is relevant, the modal responses obtained for individual vibration modes should be summed according to the mode superposition principle. The procedure for a single mode response can be described as follows:

1. Generate the walking frequency and step length for each of 2,000 pedestrians (Fig-

ures 7.2a and 7.2b).

2. Calculate μ_{DLF1} for each walking frequency (Equation 7.2).

3. Calculate crossing time for each person via Equation 7.1.

4. Generate multiplication factors for each DLF_1 (Figure 7.3a) and multiply them by μ_{DLF1} one by one to get 2,000 DLFs for the first harmonic.

5. Generate 2,000 DLFs for higher harmonics (Table 7.1).

6. Generate 2,000 DLFs for each subharmonic depending on DLF_1 values (Figure 7.4).

7. Generate functions for normalised DLFs for harmonics and subharmonics by using functions defined in Equations 7.3 and 7.4.

8. For each pedestrian do the following:

   - Generate 400 random phase values for each frequency line in the 400-line force spectrum.
   - Reconstruct force in the time domain by using Equations 7.5, 7.6 and 7.7. The force should be reconstructed for time equal to the crossing time for the person analysed.
   - Calculate the modal force by multiplying individual forces $F(t)$ by the mode shape.
   - Calculate footbridge modal response to each of 2,000 modal forces.
   - Calculate peak and/or RMS value of the response and save it.

9. Find probability that a certain footbridge vibration level will be less than or equal to a prescribed acceleration value.

7.6 Verification of the Force Model

Verification of the force model was conducted by analysing the response of two structures to walking excitation. The first 'structure' is an imaginary 3DOF bridge while the second one is the Hope footbridge near Sheffield in the UK.

7.6.1 Imaginary Footbridge

The imaginary 3DOF footbridge is a lightly damped 'structure' that responds to dynamic excitation in three vibration modes. It is assumed that all three vibration modes have maximum displacement at the same point. This allows simple summation of the responses in individual modes in order to get total response of the structure. The modal properties of the vibration modes were chosen to be:

- Modal mass equal to 10,000 kg in each vibration mode.
- Natural frequencies equal to 1.9 Hz, 3.8 Hz and 5.7 Hz, for the first, second and third mode respectively.
- Modal damping equal to 0.3% for all modes.

The natural frequencies of vibration modes were chosen to correspond with the dominant walking frequency and its integer multiples. Therefore, it is expected that all three modes of vibration will be excited since their frequencies are matched by the dominant frequencies for the first three harmonics. Since the three harmonics will all generate structural responses that cannot be neglected, it is expected that phase difference between different harmonics will play an important role in the estimation of the total vibration response.

The structural response was calculated in two ways. Firstly, 95 responses to 95 measured forces, lasting 60 s each, were calculated. Then, 95 forces were generated using the force model described in Section 7.5.2. The walking frequencies and DLFs for all harmonics and subharmonics for these 95 forces were manually adjusted to be the same as those for measured forces. The responses obtained in this way were then compared with those obtained from measured force time histories. Before presenting the results, it should be said that all simulations were conducted under an assumption of the force being stationary i.e. acting at the point of maximum modal response in each mode. This does not reduce the value of this comparison.

Obtained results can be sumarised as follows:

- Cumulative distribution of RMS value for the response in each vibration mode individually under the measured forces, was almost the same as that under the simulated forces (Figure 7.8).
- Cumulative distribution of RMS values for the sum of responses in any two modes was almost the same for cases of measured and simulated forces. For comparison, only the sum of responses in the second and third mode is presented in Figures 7.9a and 7.9b.
- Cumulative distribution of RMS values for the total response of all three modes to measured forces was almost the same as the one to simulated forces (Figures 7.9c and 7.9d).

Based on this example, it seems that taking phases in the force model as random variables does not change the vibration response significantly (comparing it with the response to measured forces).

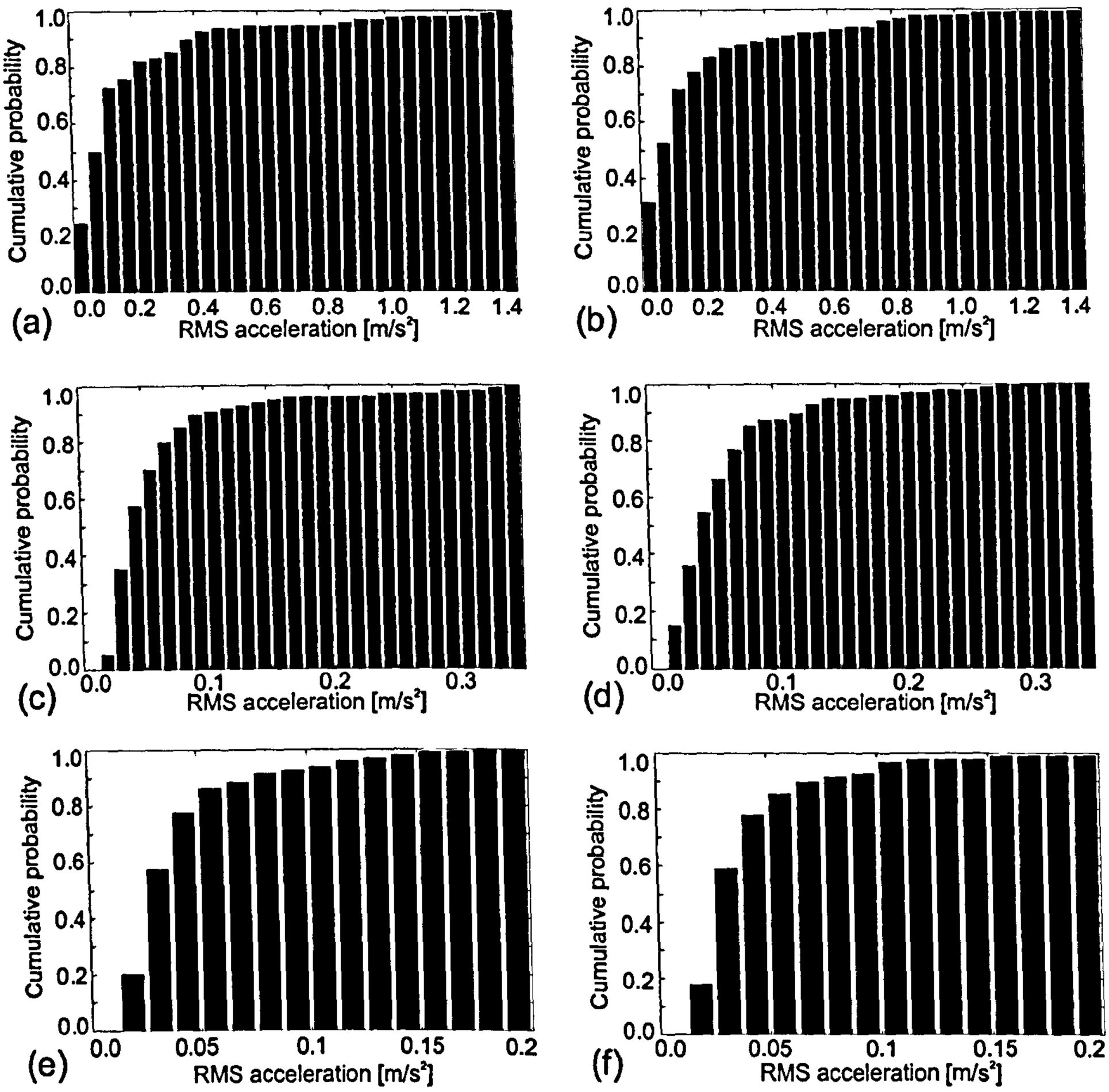

Figure 7.8: Cumulative probability that the acceleration level is smaller than or equal to the acceleration level shown on the horizontal axis for the response in (a) Mode 1 due to measured forces, (b) Mode 1 due to simulated forces, (c) Mode 2 due to measured forces, (d) Mode 2 due to simulated forces, (e) Mode 3 due to measured forces and (f) Mode 3 due to simulated forces.

7.6.2 Hope Footbridge

Hope footbridge is a 30,000 kg catenary structure near Sheffield spanning 34 m (Figure 7.10a). The footbridge is quite short and simple structure. It has five well separated vertical modes of vibration in the frequency range up to 10 Hz. Their mode shapes are presented in Figure 7.10b, while their natural frequencies, modal damping ratios and modal masses, as identified by Pavic & Reynolds (2002), are listed in Table 7.4. Note that the first mode is anti-symmetric, which is a consequence of the curvature of the undeformed shape of the bridge deck.

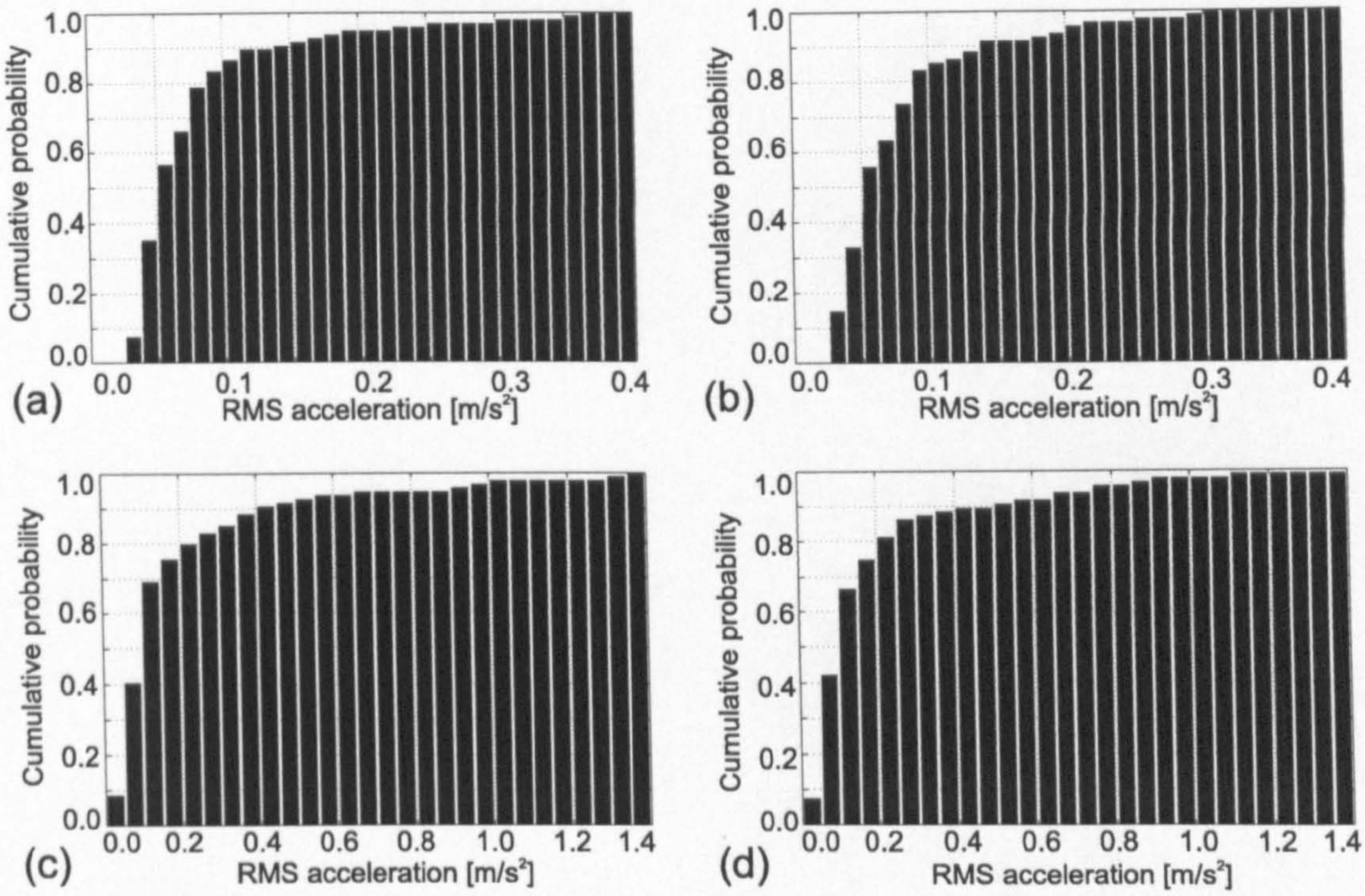

Figure 7.9: Cumulative probability of acceleration response in Modes 2 and 3 due to (a) measured forces and (b) simulated forces. Cumulative probability of total response to (c) measured forces and (d) simulated forces.

Table 7.4: Modal properties of the catenary footbridge.

Mode	**1**	**2**	**3**	**4**	**5**
Natural frequency [Hz]	2.44	3.66	4.86	6.66	9.50
Modal damping ratio [%]	0.53	0.65	0.96	0.73	0.77
Modal mass [kg]	10,520	5,880	8,690	10,767	10,319

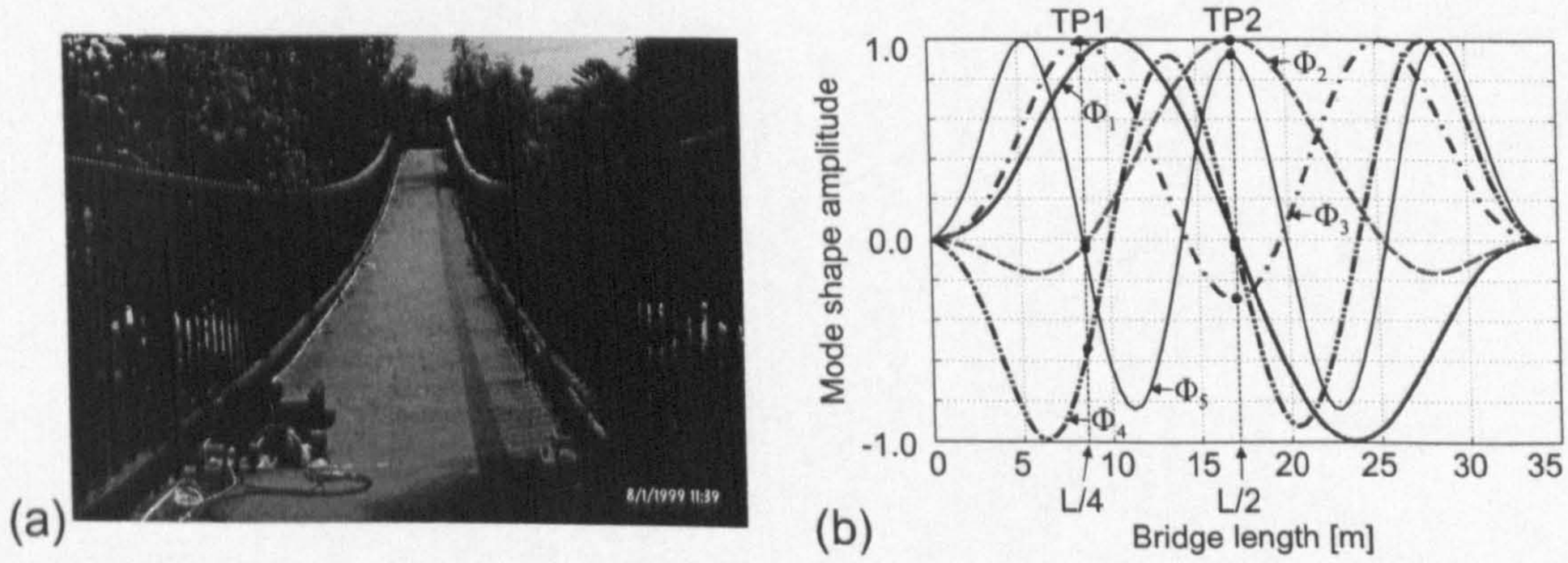

Figure 7.10: (a) Catenary footbridge. (b) Mode shapes for five vertical vibration modes.

7.6.2.1 Response Measurements

Acceleration response of this footbridge to a single person excitation was measured at a quarter-span (hereafter referred to as test point 1) and at the midspan point (test point 2) (Athanasiadou, 2001). Seven test subjects were asked to cross the bridge with a pacing rate they personally considered to be normal. The exercise was repeated twice for each test subject so that in total 14 responses were recorded. By using a video camera, the crossing time was also recorded for every crossing. Typical acceleration time histories measured at test point 1 (TP1) and test point 2 (TP2) are shown in Figures 7.11a and 7.11b, respectively. Their Fourier spectra are presented in Figures 7.11c and 7.11d. It can be seen that at the quarter-span point (TP1) several modes respond significantly to walking excitation. These are Φ_1, Φ_3 and Φ_4, i.e. all modes that have nonzero amplitude at TP1 (Figure 7.10b). Also, at the midspan point (TP2), the response is mainly a combination of the second and the fifth mode (Figure 7.10b). Based on these measurements it is evident that the contribution of several vibration modes should be taken into account when estimating vibration response to human-induced force. The measured accelerations are low-pass filtered (up to 10 Hz) in order to contain only the frequency content related to the first five vertical modes analysed. Results are summarised in Figures 7.12 and 7.13. They are shown as solid lines on probability histograms presented in Figures 7.12a and 7.12b for TP1, and Figures 7.12c and 7.12d for TP2. Cumulative probabilities are also presented as solid lines in Figures 7.13a and 7.13b for TP1, and Figures 7.13c and 7.13d for TP2.

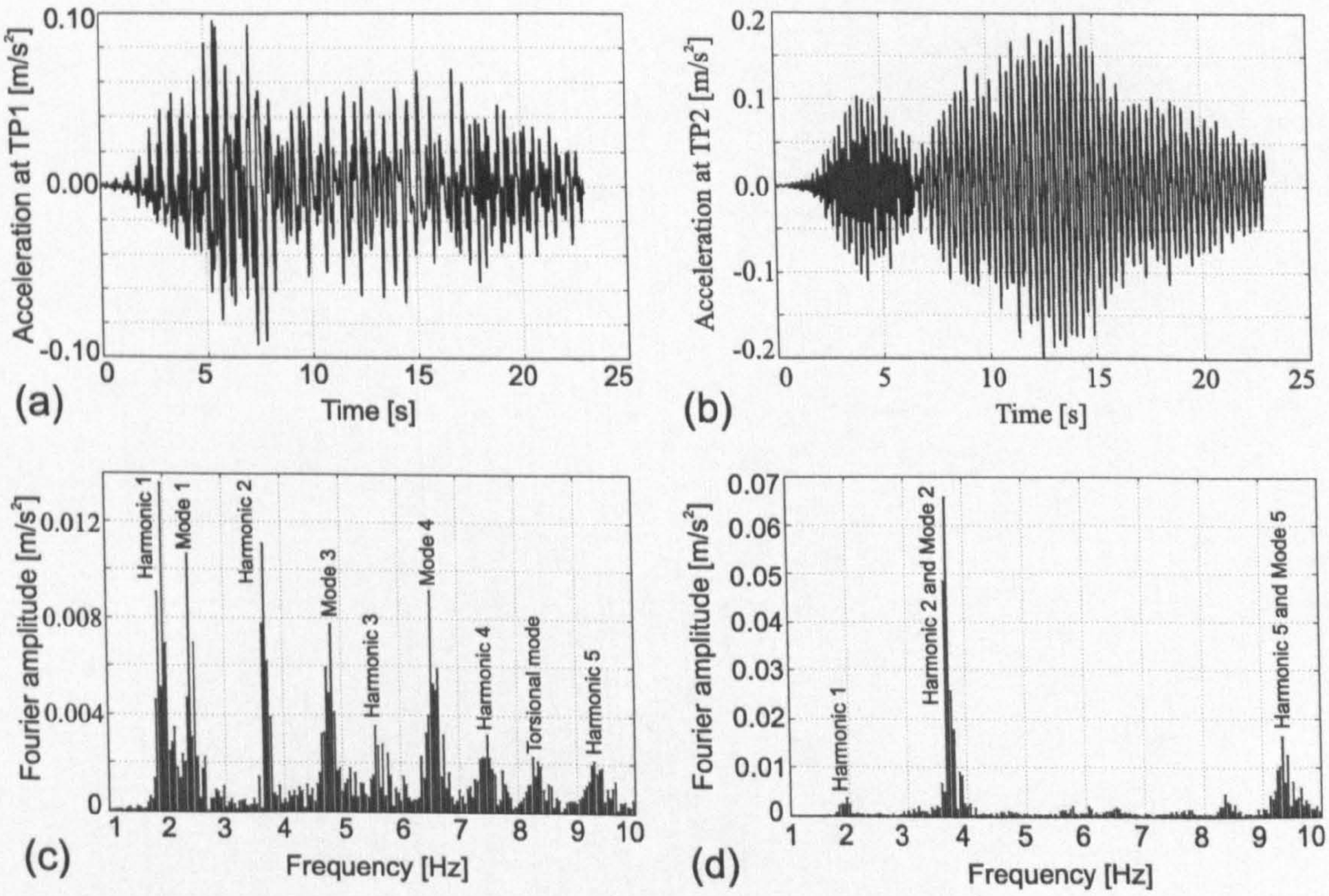

Figure 7.11: Measured time history at (a) TP1 and (b) TP2. Fourier spectrum of signal at (c) TP1 and (d) TP2.

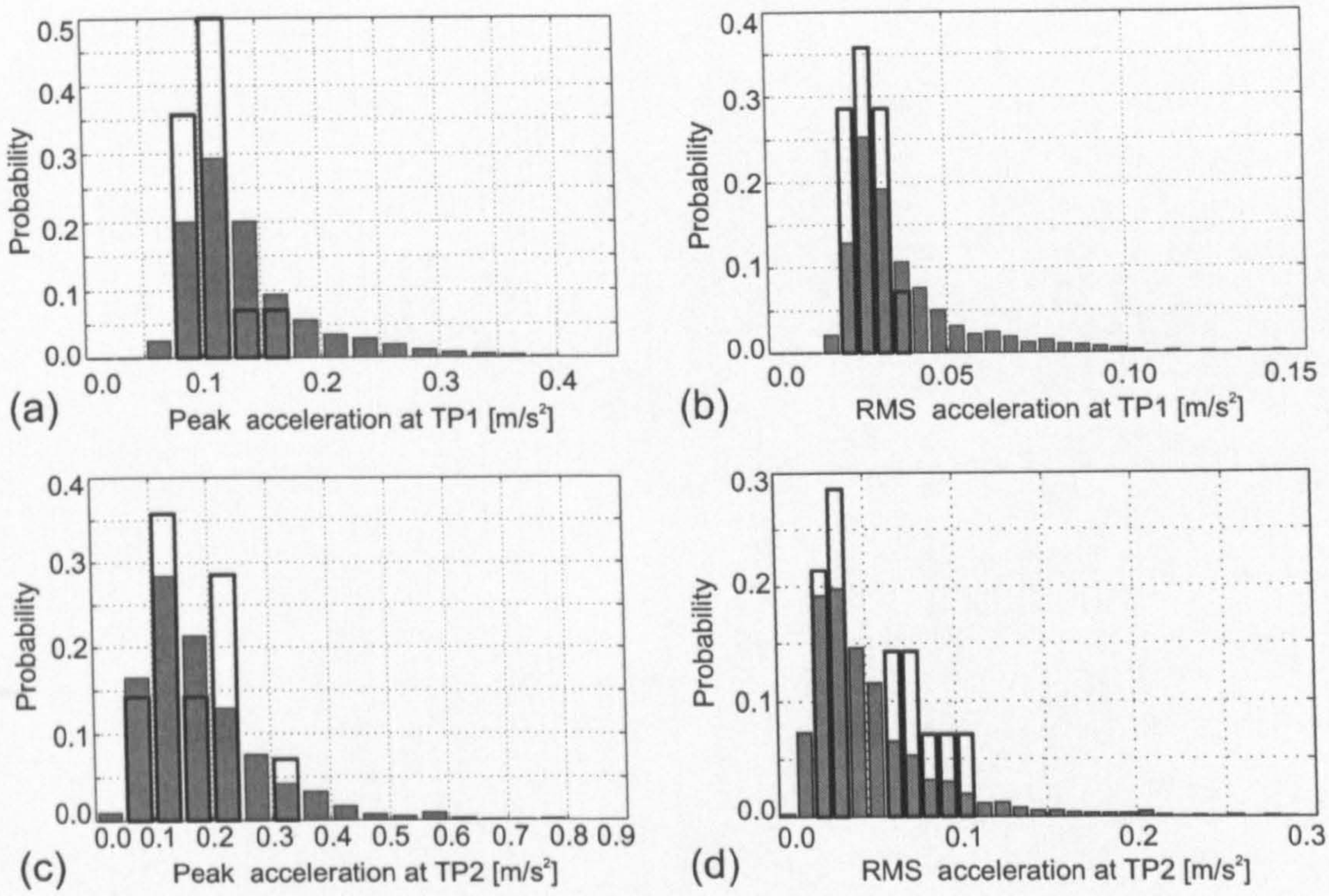

Figure 7.12: Probability of certain acceleration level for (a) peak acceleration at TP1, (b) RMS acceleration at TP1, (c) peak acceleration at TP2, and (d) RMS acceleration at TP2. Measured data are presented as solid lines while calculated responses are shown as grey.

7.6.2.2 Multi-Mode Response Simulations

The response of the bridge was calculated for 2,000 different force time histories generated according to the procedure described in Section 7.5.3. The modal responses at TP1 and TP2 were obtained for individual vibration modes and then summed after multiplication of each modal response by the mode shape amplitude at the point considered. In this way the total physical responses were obtained at both test points. A MATLAB-based program developed and used for this calculation is presented in Appendix C.

The probability and the corresponding cumulative distribution for peak and RMS values of total acceleration responses in these two points are shown as grey in Figures 7.12 and 7.13, respectively. Comparing them with the probability distribution of measured accelerations (solid lines in Figures 7.12 and 7.13), it can be seen that probability of having higher level of peak responses generally exists for the calculated responses only (Figures 7.12a and 7.12c). This is an estimate that is on the safe side and is a consequence of the fact that the probability of having forces with greater amplitudes and with frequencies of their harmonics closer to some of natural frequencies is much greater in simulations than in the measured sample of only seven pedestrians making 14 crossings in total. An additional reason not to have high level responses in the measured data is that some pedestrians lost their steady step due to human-structure interaction when perceiving a vibration level that they personally considered

as disturbing, as explained in Chapter 5.

The differences in the measured and calculated responses can also be a consequence of the fact that the modelling of the pedestrian-induced walking force is very difficult when the pedestrian walks over nodal points of the mode shape of a lively footbridge, which the Hope bridge is. The problem with this modelling has already been mentioned in Chapter 5 and it is a part of a complex human-structure dynamic interaction phenomenon. Further research into the phenomenon is required with the aim of improving the force modelling.

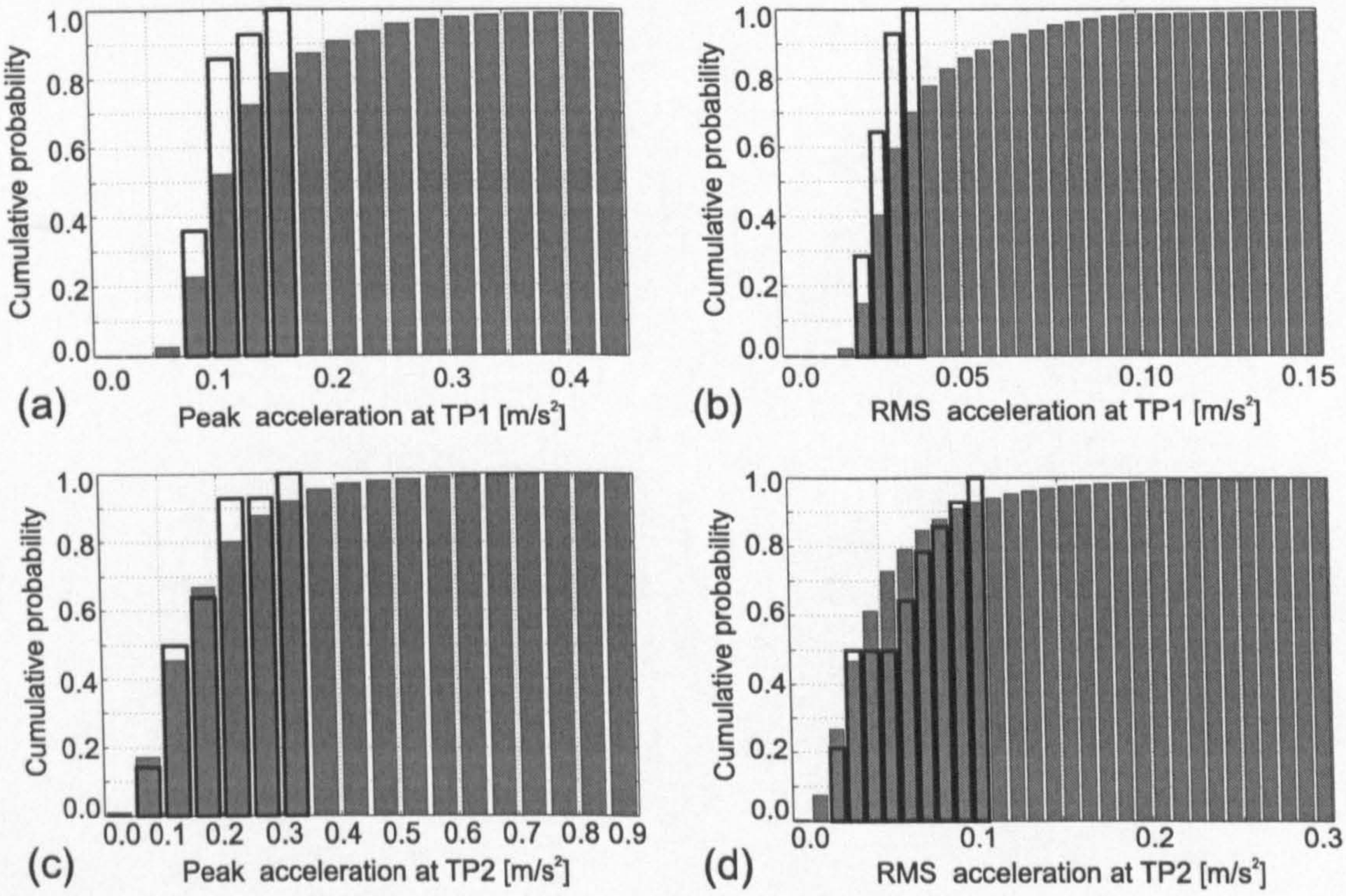

Figure 7.13: Cumulative probabilities of acceleration being less than or equal to the acceleration level shown on the horizontal axes. These are presented for measured (solid lines) and simulated (grey) (a) peak acceleration at TP1, (b) RMS acceleration at TP1, (c) peak acceleration at TP2, and (d) RMS acceleration at TP2.

Finally, the model is much more accurate in prediction of vibration response of footbridges to single person excitation than BS 5400 (BSI, 1978) currently used in the UK. To illustrate this, a deterministic 'single-harmonic - single-mode' response defined in BS was applied on the first two modes individually. In both cases, the amplitude of the dynamic force is taken to be 180 N, i.e. 25.7% of the test subject weight, being 700 N. It was assumed, based on the recommendations in BS 5400 (BSI, 1978), that the pedestrian walking at a step frequency that matches the natural frequency of the first mode at 2.44 Hz crosses the bridge with a quite fast, and also quite improbable, walking speed of 2.2 m/s, while the one walking at the step frequency that matches the second mode at 3.66 Hz moves with an even less probable speed of 3.3 m/s. The peak acceleration responses calculated in this way were 0.42 m/s^2 and 0.72 m/s^2 for the first two modes respectively. Comparing these results with those presented in Figures 7.13a and 7.13c, it can be concluded that the values estimated by BS 5400 are

highly unlikely to occur on the bridge analysed. This is despite the fact that the BS takes into consideration only a single vibration mode.

7.7 Conclusions

This chapter describes the modelling of the human-induced walking force for a single pedestrian. A probability based model is proposed that takes into account inter- and intra-subject variability in the walking force. The model takes into account all of the frequency content of walking force up to the fifth harmonic. In this way, a general multi-harmonic force model is formulated that allows for calculation of multi-mode response of a structure.

This model is an extension of a probability based 'single-harmonic - single-mode' response calculation model developed in Chapter 6. The inter-subject variability is modelled via probability distributions of walking frequencies, force amplitudes and step lengths. The intra-subject variability is modelled via frequency domain representation of both amplitudes and phases in the spectrum of the walking force. As such, this modelling of intra-subject variability is an extension of the model formulated by Brownjohn et al. (2004b).

Based on case studies of one imaginary 3DOF footbridge simulation model and one real-life as-built footbridge, the proposed model was successfully verified. It was shown that it predicts the multi-mode response of footbridges with sufficient accuracy. The new challenge in the next stage of research is the verification of the model on slender low frequency floors, where multi-mode response occurs more frequently as well as an implementation of the model for multi person traffic.

The model defined is easily programmable and as such could present a powerful tool for estimating efficiently the probability of footbridge vibration response due to single person walking. The novel methodology has the potential to revolutionise the current codes of practice dealing with vibration serviceability assessment due to dynamic excitation caused by human-walking. At the same time, however, further research into modelling of the force phase spectrum as well as the human-structure interaction phenomenon, with the aim of improving prediction of the multi-mode response of footbridges, are recommended.

Chapter 8

Discussion

This chapter discusses findings described in the previous chapters as well as their possible application for the vibration serviceability assessment of footbridges. The discussion will be presented separately for the three issues (vibration source, path and receiver) characterising the vibration serviceability check according to ISO (1992) guidelines. However, before this, a discussion regarding human-structure dynamic interaction during walking will be presented.

8.1 Human-Structure Interaction

The phenomenon of human-structure dynamic interaction during footbridge crossing, as discussed in the literature review (Chapter 2), tends to occur more often nowadays than in the past because of the increased slenderness of footbridge structures. The interaction can be manifested in two different ways: via changes in structural modal properties caused by human presence and via synchronisation of movement between pedestrians themselves as well as between the pedestrians and the perceptibly moving structure. Since only a single person loading scenario was investigated in this thesis, it was interesting to consider possible interaction between a single person and the vibrating footbridge. This topic was interesting since it was evident that existing design models, based on the analysis of walking forces measured on a rigid surface, usually overestimate structural response under a single person walking across lively footbridges. Therefore, the logical question was if these models can be used on footbridges that vibrate perceptibly.

This question was systematically investigated in Chapter 5 by comparing the measured and simulated responses to three single pedestrians crossing three as-built footbridges. Parameters describing the human-induced force and structural modal properties used in the analysis were either strictly controlled or estimated in a reliable way, and they were assumed to remain constant in the analysis. Based on this, it was possible to conclude that differences that almost inevitably occur between measured and simulated responses originate in the inability of people to keep a perfectly steady step during a footbridge crossing when perceiving vibrations. This

inability introduces variations in the frequency (and probably in the amplitude and phase) of the walking force that are greater than when walking on a rigid surface. Therefore, the degree of randomness in parameters describing the walking force is higher when the human-structure interaction is taken into account. This implies that the walking force should be modelled differently when vibrations are and are not strong enough to be disturbing for the walker. These perceptible vibrations most often occur when a pedestrian walks at or close to a footbridge natural frequency. Being disturbed by the perceptible vibrations the pedestrian may change their pacing frequency slightly shifting it away from resonance. As a consequence, the vibration response may be attenuated. This suggests that pedestrians might in fact act as active dampers, as long as vibration in the vertical direction is concerned. Some indications about this beneficial effect of walking people on dampening vertical vibrations already exist in published literature (Willford, 2002; Brownjohn et al., 2004a). Therefore, human-structure dynamic interaction can be understood as increase of modal damping of the structure. But, equally well, it can be simulated as an attenuation of the resonant force induced when walking across a perceptibly moving surface in comparison with that induced when walking on a rigid surface. This force attenuation is in agreement with observations from experiments related to jumping and walking on flexible surfaces made by other researchers in the past but not studied in detail (Ohlsson, 1982; Pimentel, 1997; Yao et al., 2002).

Logically, this dampening effect is quite useful in the sense of preventing the development of the vertical lock-in of the kind that can happen in the lateral direction (Dallard et al., 2001a). Therefore, human-structure dynamic interaction in the vertical direction seems to have beneficial effect on the structure. However, the question that remains is if the high-level vibrations that trigger human-structure interaction should be allowed in first place. This is important in today's world where the comfort of users of every product, including footbridges, is a major concern. If the answer to this question is yes, then there is a need to model the walking force in two different ways for two cases when the human-structure interaction does and does not take place, as explained previously. On the other hand, if the answer is negative, then the force model can be based on forces measured on rigid surfaces. In both cases, some limiting vibration level must be established, as a necessary ingredient in the vibration serviceability check.

8.2 Force Induced by Walking

Modelling of walking forces is quite a complex task, bearing in mind the natural diversity between human beings regarding magnitude of the walking force induced, walking frequency and step length, as well as variability in parameters characterising each step in an individual force time history. When the fact that there is some interaction between a pedestrian and perceptibly moving structure is included into the analysis then the modelling becomes even more complicated. When all these facts are taken into account, then it comes as no surprise that most current design codes (BSI, 1978; AASHTO, 1997; CSA, 2000) often fail to predict

vibration levels induced by a single pedestrian, usually overestimating it significantly. This happens because all these codes are based on the assumption that an average single pedestrian crosses the bridge at a footbridge natural frequency. Therefore, the attempt to model the human population via an average superbly coordinated person is a major drawback of current design guidelines. Another drawback is that the human-induced load is based on information about forces measured on rigid surfaces, even when checking vibration response on potentially lively structures where human-structure interaction, in the form explained previously, is quite likely to occur. For such structures, it is logical that the current codes will overestimate the actual footbridge vibration response, as shown in Chapter 5.

Force modelling as presented in Chapters 6 and 7 of this thesis, was mainly concerned with the first drawback in the existing force models. In this sense, the inter- and intra-subject variabilities in the walking forces were taken into account to develop a probability-based model for prediction of vibrations due to a single person walking. As an output of this force modelling, a probability that a certain vibration level will not be exceeded could be obtained. In this way, a range of possible acceleration levels induced by an individual walker was calculated, which is a much more logical way of assessing the pedestrian influence on the structural vibration response than via a single vibration level dictated by an average person. The results obtained from the implementation of such walking force models were supported by observations on three real-life footbridges, as discussed earlier in Chapters 6 and 7.

The analytical force model developed in Chapter 6 includes the first harmonic of the walking force only, and assumes that the footbridge will respond in a single vibration mode having a half-sine mode shape. This approach was motivated by the fact that these assumptions are quite realistic for large number of as-built footbridges, which is the reason why BS 5400 uses them too. However, since there are some bridges where higher harmonics of walking force are relevant and/or which respond in several vibration modes, the probabilistic force model described in Chapter 6 was extended for these additional cases in Chapter 7. This was done also because a more general model of the kind described in Chapter 7 has potential to be used for vibration serviceability assessment of other pedestrian structures exposed to walking force. However, it should be noted that the model from Chapter 7 is based on Monte Carlo simulations, which means that it requires a statistically reliable number of pedestrians to be taken into calculations. This might be a time consuming task only for the reason that the vibration response to each pedestrian from the sample has to be found via numerical integration of the equation(s) of motion. In this work, the not particularly efficient Newmark method of numerical integration has been used and programmed in MATLAB (Appendix C). Therefore, it might be worth considering some other more efficient numerical methods. On the other hand, the force method described in Chapter 6 is purely analytical, and consequently is quite time efficient.

Finally, the fact remains that the human-structure interaction was not directly included in the force models developed in this thesis. This was based on the assumption that relatively high-level vibrations that trigger human-structure interaction in footbridges should not ac-

tually be allowed to occur in the first place when designing new footbridges. Instead, the backbone of the design models developed in this thesis is that they are capable of predicting a percentage of pedestrians that will generate high-level vibrations (that trigger the human-structure interaction) and therefore be disturbed by them. If this percentage is too high to be acceptable for a particular footbridge, then the design of the footbridge should be modified.

The design models presented in this thesis deal with a single person excitation and uncertainties in the corresponding walking force. A natural way forward in the modelling would be to extend the probability-based methodology used to multi-person traffic. Also, it would be useful to include the probability distribution for some additional uncertain parameters, not considered in this thesis, into the modelling. These are: the weight of pedestrians, vibration limit for different pedestrians and structural modal properties that are difficult to predict in the design stage.

8.3 Footbridge as Vibration Path

Identification of reliable modal properties of structures is a necessary requirement when doing vibration serviceability assessment of any structure. It is known, and it has been demonstrated in this thesis, that these properties are difficult to estimate at the design stage, even with the help of a very detailed finite element model. This especially applies to the modal damping values since they can be estimated only based on either prior experience in dealing with similar structures or based on vibration testing of the structure itself (that is not possible at the design stage because the structure does not exist).

Estimation of modal properties of a footbridge based on modal testing and finite element modelling and updating is presented in Chapters 3 and 4 of this thesis. This work was motivated by the fact that verification of the force model, which development was the primary task within the scope of the work on this project, is possible only if reliable dynamic properties of the considered structures are provided for this purpose. Therefore, it was important to reduce, if not eliminate, any possible errors in the vibration serviceability check originating from inaccurate modal properties. In this way the real picture about reliability of the force models proposed can be obtained.

However, it is worth saying that the modal identification exercise presented in Chapters 3 and 4 is usually expected to be conducted when rectifying footbridges that are lively in normal usage. Therefore, the whole exercise was highly useful and it is worth repeating the two interesting outcomes here.

First, when doing FRF-based modal testing with chirp excitation, a sufficient accuracy when estimating modal properties can be achieved even in case when signal averaging is not employed. The necessary prerequisite for it is that the signal to noise ratio is high. It goes without saying that avoiding averaging can significantly reduce the time required for testing, which is always limited when testing structures in operation. Another result is that boundary

conditions of a structure should be modelled with caution when doing finite element modelling. In most cases these boundary conditions are not straightforward. In such situations it is highly recommended to conduct a parametric study that can suggest a possible range for natural frequencies. These results should then be used when estimating a range of possible vibration responses to different types of dynamic loading.

8.4 Pedestrian as Receiver

The problem of establishing a vibration limit that can be allowed to be perceived by a walking pedestrian is inherently linked with investigation of the human-structure dynamic interaction during footbridge crossing. As explained previously, the work in this thesis was based on the assumption that vibrations that trigger human-structure interaction should not be allowed. Instead, the existence of human-structure interaction during walking should be used to establish an allowable vibration limit for footbridge vibrations, in the way proposed in Chapter 5, and probably depending on footbridge natural frequency. Bearing in mind inter- and intra-subject variability in vibration perception (Griffin, 1996), these scales should preferably be defined in a probabilistic sense. Currently, in the design codes worldwide the acceleration levels allowed are defined in form of a single value for each vibration frequency. If the structural vibration response is higher than that value, the structure is considered as not performing satisfactorily. While this binary pass or fail criterion is appropriate when dealing with the ultimate limit states where the structural integrity is in question, it might not be appropriate for vibration serviceability checks. This is because a single response value might not be a good indicator of (un)acceptability of vibrations for most users. The reason for this is that people's reaction to vibrations vary significantly between different individuals (Griffin, 1996).

In this thesis a peak modal acceleration of around $0.35\,\mathrm{m/s^2}$ was found to be an indicative limiting vibration value for two pedestrians crossing two footbridges of different modal properties. This limit is significantly lower that those defined by BSI (1978) and ISO 10137 (1992), and is supported by recent research reported by Kasperski (2005). Clearly, more research on other footbridges and with more test subjects involved is required for reliable definition (in a probabilistic sense) of vibration scales for walking (moving) human receivers.

Once these scales are defined the cumulative probability distribution function for unacceptable vibration limit can be combined with the probability function for acceleration level generated by a single person. This probability function of acceleration level is an outcome of the design model developed in this thesis. As a result of the combination, a percentage of people that will be disturbed by vibrations generated by their own walking may be calculated.

An example illustrating the calculation procedure is shown in Figure 8.1. For this purpose a possible probability function in form of a histogram for acceleration level generated by a single person crossing a footbridge is shown in Figure 8.1a. The function is expressed as a number

of people (out of 100) that generate certain vibration response shown on the horizontal axis. Figure 8.1b presents an assumed arbitrary cumulative probability function of unacceptable vibration level. This function is chosen arbitrarily since the research related to vibration limit for walking people is scarce, as explained previously. Number of people disturbed by high-level vibrations can then be calculated as follows:

$$10 \cdot 0 + 15 \cdot 0.4 + 35 \cdot 0.5 + 25 \cdot 0.7 + 10 \cdot 0.8 + 5 \cdot 0.9 + 0 \cdot 1.0 = 53.5. \tag{8.1}$$

The calculation is based on the assumption that, for example, among 35 people generating the peak vibration level between $0.2\,\mathrm{m/s^2}$ and $0.3\,\mathrm{m/s^2}$ all groups of people with different perception levels are present. Since 50% of people in human population would consider vibration level being less than or belonging to the range $0.2-0.3\,\mathrm{m/s^2}$ as unacceptable (based on Figure 8.1b) then 35 people had to be multiplied by 0.5 to get a number of people annoyed by vibrations in this particular group (of 35 people). Therefore about 54% of people (out of 100), as obtained in Equation 8.1, would perceive strong vibrations (from personal point of view) during crossing over the footbridge for which the probability function of acceleration is given in Figure 8.1a.

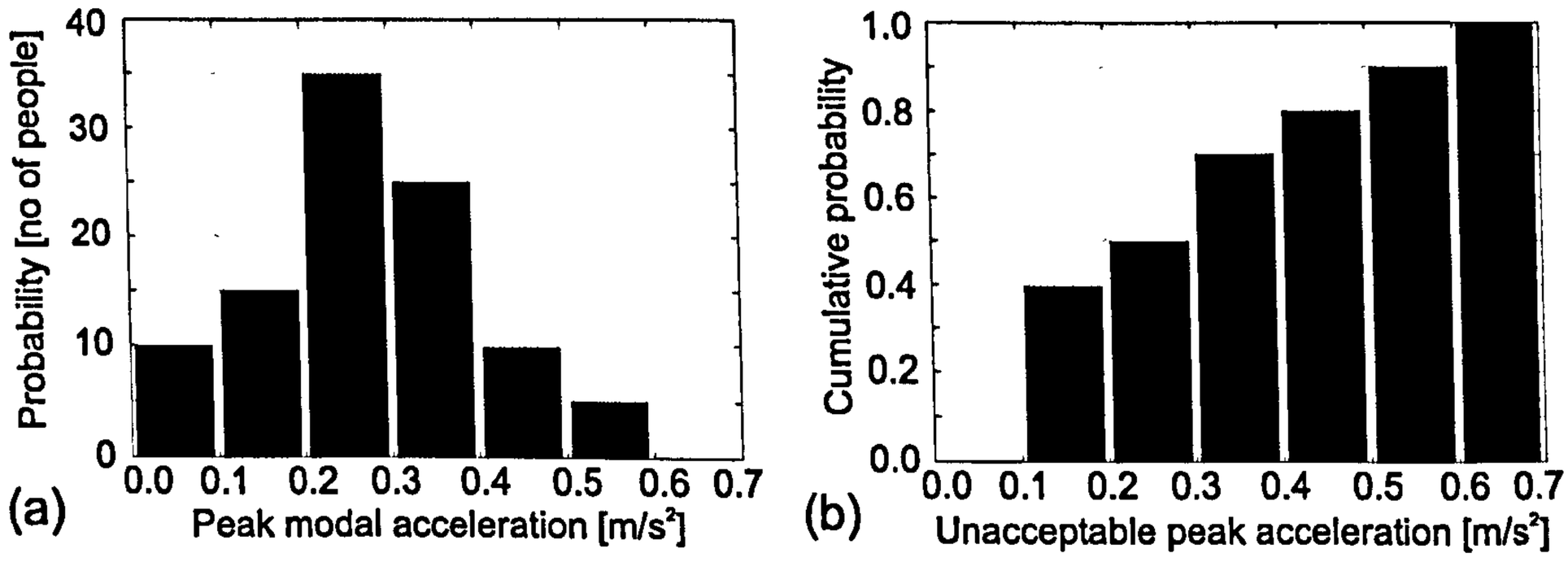

Figure 8.1: (a) Probability of certain peak acceleration level. (b) Cumulative probability of unacceptable peak vibration level being less than or equal to the vibration level shown on the horizontal axis.

Chapter 9

Conclusions and Recommendations for Future Work

In this chapter, the main conclusions related to the work presented in this thesis are summarised and then some recommendations for future work are suggested.

9.1 Conclusions

1. Existence of well known inter- and intra-subject variabilities in the force induced during walking can be described via probability distributions for the following factors: walking frequency, step length, force amplitude and imperfections (i.e. step by step differences) in human walking. All these distributions have been proposed in Chapter 6 based on literature search and own data. They are given in a form that can be used in design.

2. Due to undoubtable inter- and intra-subject variabilities of walking forces, the estimation of the vibration response of footbridges to a single person crossing should not be expressed via a single number. The binary pass or fail criteria, as is currently the case in design codes worldwide, appears not to be a particularly prudent approach to footbridge vibration serviceability. Instead, a probability based procedure that takes into account the aforementioned variabilities in the walking force is developed in this thesis. This yields a probability that a certain vibration response due to a single person walking will not be exceeded. An analytical probability-based design procedure for obtaining this probability function, when the first force harmonic and a single mode response are sufficient for the vibration serviceability check, is developed in Chapter 6. The model was verified on two as-built footbridges.

3. In the case when a footbridge responds to forced vibration in more than one vibration mode, then usually more than one force harmonic is responsible for such a multi-mode response. For footbridges belonging to this category, a probability-based design

procedure for calculation of the response is developed in Chapter 7 based on Monte Carlo simulations. This model was verified using data from a real-life footbridge.

4. Design procedures developed in Chapters 6 and 7 can be used for updating the current single person walking model featuring in many codes of practice.

5. There are indications that the single pedestrian loading scenario may not be sufficient when designing heavily trafficked footbridges that regularly convey groups of pedestrians. Therefore, in addition to the single person force models, a multi-pedestrian loading model should be developed.

6. A pedestrian walking across a perceptibly moving footbridge having relatively low damping ratio of about 0.5% or less tends to lose their steady step and unconsciously change their walking frequency. Since these strong vibrations usually occur when a pedestrian generates a walking force that excites a footbridge resonant frequency, then - due to low damping - by changing the walking frequency and/or phase even slightly, the pedestrian prevents further development of the resonant structural response and may act as an active damper. It was found that this phenomenon is a consequence of human-structure dynamic interaction that occurs due to the inability of people to keep a steady step under strong vibrations. This can mathematically be described either as an increase of the structural damping or through the attenuation of the walking force induced by the same pedestrian when walking across a rigid surface.

7. The vibration level felt by a pedestrian at a time instant when they start losing their step can be determined in an objective way, as described in Chapter 5. This vibration level can be adopted as the disturbing (i.e. maximum allowed) vibration level for a walking person. For two footbridges investigated, a provisional value for this level was found to be around $0.35\,\mathrm{m/s^2}$. This is about 50% lower than values defined by the British footbridge design code indicating that the code limit might not be appropriate to apply. This is also about 40% lower than the ISO 10137 (1992) limit. This vibration limit for a walking person that apparently seems to be lower than those recommended in the current design codes is supported by recent findings reported by Kasperski (2005). The provisional vibration limit of $0.35\,\mathrm{m/s^2}$ agrees well with subjective evaluations of vibrations by 300 interviewed pedestrians on an as-built lively box-girder footbridge (Appendix A).

8. Finally, two outcomes of the testing and finite element model updating exercises described in Chapters 3 and 4, are worth mentioning. Namely, it is possible, in situation when the signal to noise ratio is quite high, to conduct good quality FRF-based modal testing even without performing signal averaging. Another result is that boundary conditions of a structure should be modelled with extreme caution when doing finite element modelling.

9.2 Recommendations for Future Work

1. A probability distribution of pedestrian's weight should be added to the force model developed. To do this the data describing this probability distribution should be collected and its possible dependence on the force amplitude should be defined.

2. Sensitivity of the structural response to different input probability distributions should be parametrically studied in order to investigate the impact of the errors in probability distributions on results.

3. Since probabilistic force models developed in this thesis are formulated for the case of a single pedestrian crossing the bridge, further work is required for extending them to multi-person pedestrian traffic, again following a probabilistic approach to pedestrian arrival times and their behaviour on the bridge (moving and standing). In case of having high-level response to multi-person traffic, some human-structure dynamic interaction can be expected. Therefore, a modification of the force induced by each pedestrian perceiving strong vibration would be required in this situation. Modelling of this modification is expected to be the most complicated aspect of estimating the response to multi-person traffic.

4. Having in mind that the multi-harmonic force model developed in this thesis is capable of predicting the multi-mode response of a structure and knowing the frequency range on which the model is defined, it would be prudent to check its applicability on slender structures, such as long-span low frequency floors, that tend to respond to walking excitation in several vibration modes.

5. A similar probability-based methodology for estimation of vibration response can be developed for estimating vibration response of staircases, where walking forces are different in comparison with those induced into a flat surface, as well as for other types of human-induced excitation (jumping, running, bouncing, and so on).

6. A method for generating the walking force in the time domain to closely resemble the measured force should be developed.

7. More reliable data regarding some probability distributions required in the force modelling (such as probability distributions for DLFs for harmonics and subharmonics) are worth acquiring. This especially applies to defining the probability distributions for the DLFs at an individual walking frequency. Moreover, further research investigating interdependence between DLFs for different (sub)harmonics is required.

8. Distribution of step lengths at each walking frequency also require further experimental investigation.

9. It would be interesting to develop a force model that takes into account human-structure dynamic interaction during walking. Namely initial (intra-subject) variability in the parameters describing the walking force appears to be increased due to the interaction

when perceiving high-level vibrations. A possible way to model this could be via increasing degree of randomness in the parameters compared with those for walking across rigid surfaces. This model, as already mentioned, would be very useful for modelling of the multi-person traffic.

10. Although a procedure for establishing the vibration perception limit for a walking pedestrian in an objective way has been suggested in this thesis, together with a provisional limiting acceleration value of $0.35\,m/s^2$, more data should be collected for drawing final conclusions. The future tests should involve more people to account for inter-subject variability in vibration perception. Preferably, the tests should be conducted on footbridges of different size and with different modal properties (especially natural frequencies) since vibration perception may be different for different response frequencies. Ideally, these vibration limits for a moving person should be defined in a probabilistic sense and then combined with probability distribution of vibration response to predict a percentage of people that would sense high-level vibrations, as explained in Section 8.4.

11. Further investigation of human-structure dynamic interaction when a pedestrian crosses a nodal point of the mode shape is required.

12. Since structural modal properties are difficult to predict during the design process there is a need to include their uncertainties in a probability-based design model.

13. Based on biomechanics research, it seems possible to reconstruct human-induced forces from the recorded motion of the human body. Therefore, it would be interesting to monitor motion and behaviour of people on real-life pedestrian structures. Once a wide database of this kind is available, different loading scenarios can be extracted from it and statistically described. Then, reconstruction of forces characterising these loading scenarios and their influence on dynamic response would be feasible, regardless of the exact type of human activity (walking, running, standing, bouncing, etc.). In this way information about the influence of the human-structure interaction on human gait and consequently on forces generated can be obtained. Moreover, the way in which pedestrians walking in groups and/or crowds influence each other's movement can be studied. Finally, a method for determining dynamic forces from groups/crowds of pedestrians could be established, using only video data of groups/crowds walking.

References

AASHTO (1997) *Guide Specifications for Design of Pedestrian Bridges.* American Association of State, Highway and Transportation Officials, August.

Abdel-Ghaffar, A. M. (1978) Vibration Studies and Tests of a Suspension Bridge. *Earthquake Engineering and Structural Dynamics*, 6 (5), 473-496.

Allen, D. E. (1990) Floor Vibrations from Aerobics. *Canadian Journal of Civil Engineering*, 17 (5), 771-779.

Allen, D. E. and Murray, T. M. (1993) Design Criterion for Vibrations due to Walking. *Engineering Journal*, 30 (4), 117-129.

Andriacchi, T. P., Ogle, J. A. and Galante, J. O. (1977) Walking Speed as a Basis for Normal and Abnormal Gait Measurements. *Journal of Biomechanics*, 10, 261-268.

Athanasiadou, A. (2001) Determination of Vertical Lock-In Levels for Pedestrians Crossing a Footbridge. MSc thesis, University of Sheffield, Sheffield, UK.

Bachmann, H. and Ammann, W. (1987) *Vibration in Structures - Induced by Man and Machines.* Structural Engineering Documents 3e, International Association of Bridge and Structural Engineering (IABSE), Zürich.

Bachmann, H. (1988) Practical Cases of Structures with Man-Induced Vibrations. In: *Symposium/Workshop on Serviceability of Buildings*, 419-434, Ottawa, Canada, 16-18 May.

Bachmann, H. (1992a) Case Studies of Structures with Man-Induced Vibrations. *ASCE Journal of Structural Engineering*, 118 (3), 631-647.

Bachmann, H. (1992b) Vibration Upgrading of Gymnasia, Dance Halls and Footbridges. *Structural Engineering International*, 2 (2), 118-124.

Bachmann, H., Pretlove, A. J. and Rainer, H. (1995a) Vibrations Induced by People. In: *Vibration Problems in Structures: Practical Guidelines*, Birkhäuser Verlag, Basel.

Bachmann, H., Pretlove, A. J. and Rainer, H. (1995b) Dynamic Forces from Rhythmical Human Body Motions. Appendix G in: *Vibration Problems in Structures: Practical Guidelines*, Birkhäuser Verlag, Basel.

Bachmann, H. (2002) "Lively" Footbridges - a Real Challenge. In: *Proceedings of the In-*

ternational Conference on the Design and Dynamic Behaviour of Footbridges, 18-30, Paris, France, 20-22 November.

Bachmann, H. and Weber, B. (1995) Tuned Vibration Absorbers for "Lively" Structures. *Structural Engineering International*, 5 (1), 31-36.

Barker, C. (2002) Some Observations on the Nature of the Mechanism That Drives the Self-Excited Lateral Response of Footbridges. In: *Proceedings of the International Conference on the Design and Dynamic Behaviour of Footbridges*, Paris, France, 20-22 November.

Bertram, J. E. A. and Ruina, A. (2001) Multiple Walking Speed-Frequency Relations are Predicted by Constrained Optimization. *Journal of Theoretical Biology*, 209 (4), 445-453.

Biliszczuk, J., Berger, K., Machelski, C., Wegrzyniak, M., Onysyk, J. and Prabucki, P. (2002) Examples of New Built Footbridges in Poland. In: *Proceedings of the International Conference on the Design and Dynamic Behaviour of Footbridges*, Paris, France, 20-22 November.

Bishop, N. W. M., Willford, M. and Pumphrey, R. (1993) Multi-Person Excitation of Modern Slender Staircases. In: *Proceedings of the International Conference on Engineering for Crowd Safety*, London, UK, 17-18 March.

Blanchard, J., Davies, B. L. and Smith, J. W. (1977) Design Criteria and Analysis for Dynamic Loading of Footbridges. In: *Proceedings of the DOE and DOT TRRL Symposium on Dynamic Behaviour of Bridges*, 90-106, Crowthorne, UK, 19 May.

Block, C. and Schlaich, M. (2002) Dynamic Behaviour of a Multi-Span Stress-Ribbon Bridge. In: *Proceedings of the International Conference on the Design and Dynamic Behaviour of Footbridges*, Paris, France, 20-22 November.

Borges, J. F., Marecos, J., Pereira, J. and Castanheta, M. (1968) The Observation of the Tagus River Suspension Bridge. *Proc. 37/1/2203*, 563-578, Laboratoria Nacional de Engenharia Civil, Lisbon.

Breukelmann, B., Gamble, S., Kottelenberg, J. and Haskett, T., (2002) Footbridge Damping Systems: A Case Study. In: *Proceedings of the International Conference on the Design and Dynamic Behaviour of Footbridges*, Paris, France, 20-22 November.

Briseghella, B., Meneghini, G. and Siviero, E. (2002) Consideration on The Vibration Problem in Recently Built Footbridges and The Adoptable Solution to Smoothen Their Effects. In: *Proceedings of the International Conference on the Design and Dynamic Behaviour of Footbridges*, Paris, France, 20-22 November.

Brown, C. W. (1977) An Engineer's Approach to Dynamic Aspects of Bridge Design. In: *Proceedings of the DOE and DOT TRRL Symposium on Dynamic Behaviour of Bridges*, 107-113, Crowthorne, UK, 19 May.

Brownjohn, J. W. (1988) *Assessment of Structural Integrity by Dynamic Measurements*. PhD Thesis, University of Bristol, Bristol, UK.

Brownjohn, J. M. W., Dumanoglu, A. A., Severn, R. T. and Taylor, C. A. (1987) Ambient Vibration Measurements of the Humber Suspension Bridge and Comparison with Calculated Characteristics. In: *Proceedings of The Institution of Civil Engineers*, 83, 561-600.

Brownjohn, J. M. W., Dumanoglu, A. A. and Severn, R. T. (1992) Ambient Vibration Survey of the Fatih Sultan Mehmet (Second Bosporus) Suspension Bridge. *Earthquake Engineering and Structural Dynamics*, 21, 907-924.

Brownjohn, J. M. W., Dumanoglu, A. A. and Taylor, C. A. (1994) Dynamic Investigation of a Suspension Footbridge. *Engineering Structures*, 16 (6), 395-406.

Brownjohn, J. M. W. (1997) Vibration Characteristics of a Suspension Footbridge. *Journal of Sound and Vibration*, 202 (1), 29-46.

Brownjohn, J. M. W. and Xia, P.-Q. (2000) Dynamic Assessment of Curved Cable-Stayed Bridge by Model Updating. *ASCE Journal of Structural Engineering*, 126 (2), 252-260.

Brownjohn, J. M. W., Xia, P.-Q., Hao, H. and Xia, Y. (2001) Civil Structure Condition Assessment by FE Model Updating: Methodology and Case Studies. *Finite Elements in Analysis and Design*, 37 (10), 761-775.

Brownjohn, J. M. W., Fok, P., Roche, M and Omenzetter, P. (2004a) Long Span Steel Pedestrian Bridge at Singapoore Changi Airport - part 2: Crowd Loading Tests and Vibration Mitigation Measures. *The Structural Engineer*, 82 (16), 28-34.

Brownjohn, J. M. W., Pavic, A. and Omenzetter, P. (2004b) A Spectral Density Approach for Modelling Continuous Vertical Forces on Pedestrian Structures due to Walking. *Canadian Journal of Civil Engineering*, 31 (1), 65-77.

BSI (1978) *Steel, Concrete and Composite Bridges, Part 2: Specification for Loads; Appendix C: Vibration Serviceability Requirements for Foot and Cycle Track Bridges.* BS 5400, British Standards Institution, London, UK.

BSI (2004) *Mechanical Vibration - Evaluation of Measurement Results from Dynamic Tests and Investigations on Bridges.* BS ISO 18649: 2004, British Standards Institution, London, UK.

Buckland, P. G., Hooley, R., Morgenstern, B. D., Rainer, J. H. and Van Selst (1979) Suspension Bridge Vibrations: Computed and Measured. *ASCE Journal of Structural Division*, 105 (ST5), 859-874.

Caetano, E. and Cunha, A. (2002) Dynamic Tests on a "Lively" Footbridge. In: *Proceedings of the International Conference on the Design and Dynamic Behaviour of Footbridges*, Paris, France, 20-22 November.

Cantieni, R., Eggermont, P. and Tilly, G. P. (1986) Bridges. In: *Dynamic Behaviour of Concrete Structures*, Report of the RILEM 65 MDB Committee. Edited by G. P. Tilly, Elsevier, Amsterdam.

Cantieni, R. (1996) Updating of Analytical Models of Existing Large Scale Structures Based on Modal Testing. In: *Proceedings of the US-Europe Workshop on Bridge Engineering* 153-177, Barcelona, Spain, 15-17 July.

Cantieni, R. and Pietrzko, S. (1993) Modal Testing of a Wooden Footbridge Using Random Excitation. In: *Proceedings of the* 11^{th} *International Modal Analysis Conference*, 1230-1236, Florida, USA, 1-4 February.

CDLB (1958) Deflection Limitations of Bridges. Progress Report of the Committee on Deflection Limitations of Bridges of the Structural Division. *ASCE Journal of the Structural Division*, 84 (ST3), Proc. Paper 1633.

CEB (1993) *CEB-FIP Model Code 1990, Design Code.* Comité Euro-Internatinal du Béton, Thomas Telford Services, London.

Cha, P. D. and Tuck-Lee, J. P. (2000) Updating Structural System Parameters Using Frequency Response Data. *ASCE Journal of Engineering Mechanics*, 126 (12), 1240-1246.

Chang, C. C., Chang, T. Y. P. and Zhang, Q. W. (2001) Ambient vibration of long-span cable-stayed bridge. *ASCE Journal of Bridge Engineering*, 6 (1), 46-53.

Chasteau, V. A. L. (1973) The Use of Tuned Vibration Absorbers to reduce Wind Excited Oscillations of a Steel Footbridge. *The Civil Engineer in South Africa*, 15 (6), 147-154.

Chen, P. W. and Robertson, L. E. (1972) Human Perception Thresholds of Horizontal Motion. *ASCE Journal of Structural Division*, 98 (ST8), 1681-1695.

Chen, G. and Ewins, D. J. (2001) Verification of FE models for Model Updating. In: *Proceedings of the* 19^{th} *International Modal Analysis Conference*, Vol. 1, 385-391, Kissimmee, Florida, USA, 5-8 February.

Clough, R. W. and Penzien, J. (1993) *Dynamics of Structures.* McGraw-Hill, New York.

Collette, F. S. (2002) Tuned Mass Dampers for a Suspended Structure of Footbridges and Meeting Boxes. In: *Proceedings of the International Conference on the Design and Dynamic Behaviour of Footbridges*, Paris, France, 20-22 November.

Collins, J. D., Hart, G. C., Hasselman, T. K. and Kennedy, B. (1974) Statistical identification of structures. *American Institute of Aeronautics and Astronautics Journal*, 12 (2), 185-190.

Cross, R. (1999) Standing, Walking, Running and Jumping on a Force Plate. *American Journal of Physics*, 67 (4), 304-309.

CSA (2000) *Canadian Highway Bridge Design Code CAN/CSA-S6-00.* Canadian Standards Association.

Dallard, P., Fitzpatrick, A. J., Flint, A., Le Bourva, S., Low, A., Ridsdill-Smith, R. M. and Willford, M. (2001a) The London Millennium Footbridge. *Structural Engineer*, 79 (22), 17-33.

Dallard, P., Fitzpatrick, T., Flint, A., Low, A., and Ridsdill-Smith, R. (2001b) The Millen-

nium Bridge, London: Problems and Solutions. *The Structural Engineer*, 79 (8), 15-17.

Dallard, P., Fitzpatrick, T., Flint, A., Low, A., Ridsdill-Smith, R., Willford, M. and Roche, M. (2001c) London Millennium Bridge: Pedestrian-Induced Lateral Vibration. *ASCE Journal of Bridge Engineering*, 6 (6), 412-417.

DDS (2004) *FEMtools Theoretical Manual, Version 3.0.03.* Dynamic Design Solutions, Leuven, Belgium.

Deger, Y., Felber, A., Cantieni, R. and Smet, C. A. M. (1996) Dynamic Modelling and Testing of a Cable Stayed Pedestrian Bridge. In: *Proceedings of the* 14^{th} *International Modal Analysis Conference*, Vol. 1, 211-217, Dearborne, Michigan, USA.

Den Hartog, J. P. (1985) *Mechanical Vibrations.* Dover Publications, Inc., New York.

Dieckmann, D. (1958) A Study of the Influence of Vibration on Man. *Ergonomics*, 4 (1), 347-355.

Dinmore, G. (2002) Dynamic Wave Behaviour Through Dense Media of Varied Dynamic Stiffness. In: *Proceedings of the International Conference on the Design and Dynamic Behaviour of Footbridges*, Paris, France, 20-22 November.

Djuranović, N. (2002). Vibration Testing of Footbridges. *Roads and Bridges*, 48 (5-6), 131-140. (in Serbian).

DH (2005) Department of Health, UK, webpage:
http://www.dh.gov.uk/PublicationsAndStatistics/PublishedSurvey/HealthSurveyForEngland/HealthSurveyResults.

DTA (1995) *DTA handbook: Volume 3.* Dynamic Testing Agency, London.

Ebrahimpour, A. (1987) *Modeling Spectator Induced Dynamic Loads.* PhD thesis, University of Idaho, Moscow, Idaho, USA.

Ebrahimpour, A. and Sack, R. L. (1989) Modeling Dynamic Occupant Loads. *ASCE Journal of Structural Engineering*, 115 (6), 1476-1496.

Ebrahimpour, A., Sack. R. L. and Van Kleek, P. D. (1989) Computing Crowd Loads Using a Nonlinear Equation of Motion. In: *Proceedings of the Fourth International Conference on Civil and Structural Engineering Computing*, Edited by B. H. Topping, Vol. 2, 47-52, Civil-Comp Press, London.

Ebrahimpour, A. and Sack, R. L. (1992) Design Live Loads for Coherent Crowd Harmonic Movements. *ASCE Journal of Structural Engineering*, 118 (4), 1121-1136.

Ebrahimpour, A., Sack, R. L., Patten, W. N. and Hamam, A. (1994) Experimental Measurements of Dynamic Loads Imposed by Moving Crowds. In: *Proceedings of Structures Congress XII*, Atlanta, Georgia, USA, April.

Ebrahimpour, A. and Fitts, L. L. (1996) Measuring Coherency of Human-Induced Rhythmic Loads Using Force Plates. *ASCE Journal of Structural Engineering*, 122 (7), 829-831.

Ebrahimpour, A., Hamam, A., Sack, R. L. and Patten, W. N. (1996) Measuring and Modeling Dynamic Loads Imposed by Moving Crowds. *ASCE Journal of Structural Engineering*, 122 (12), 1468-1474.

Ellis, B. R. and Ji, T. (1994) Floor vibration induced by dance-type loads: Verification. *The Structural Engineer*, 72 (3), 45-50.

Ellis, B. R. and Ji, T. (1997) Human-Structure Interaction in Vertical Vibrations. *Structures and Buildings*, 122 (1), 1-9.

Ellis, B. R. (2000) On the Response of Long-Span Floors to Walking Loads Generated by Individuals and Crowds. *The Structural Engineer*, 78 (10), 17-25.

Ellis, B. R. and Ji, T. (2002) On the Loads Produced by Crowds Jumping on Floors. In: *Proceedings of the Fourth International Conference on Structural Dynamics - EURODYN*, 2, 1203-1208, Munich, Germany, 2-5 September.

Ellis, B. R. (2003) The Influence of Crowd Size on Floor Vibrations Induced by Walking. *The Structural Engineer*, 81 (6), 20-27.

ENV (1997) Eurocode 5, *Design of Timber Structures -Part 2: Bridges, ENV 1995-2: 1997.* European Committee for Standardization, Brussels, Belgium.

Eriksson, P. E. (1994) *Vibration of Low-Frequency Floors - Dynamic Forces and Response Prediction.* PhD thesis, Unit for Dynamics in Design, Chalmers University of Technology, Göteborg, Sweden.

Eyre, R. (1976) *Dynamic Tests on the Cleddau Bridge at Milford Haven.* TRRL Supplementary Report No. 200UC, Transport and Road Research Laboratory, Department of the Environment, Crowthrone, UK.

Eyre, R. and Tilly, G. P. (1977) Damping Measurements on Steel and Composite Bridges. In: *Proceedings of the DOE and DOT TRRL Symposium on Dynamic Behaviour of Bridges*, 22-39, Crowthorne, UK, 19 May.

Eyre, R. and Cullington, D. W. (1985) *Experience with Vibration Absorbers on Footbridges.* TRRL Research Report No. 18, Transport and Road Research Laboratory, Crowthrone, UK.

Eyre, J. (2002) Aesthetics of Footbridge Design. In: *Proceedings of the International Conference on the Design and Dynamic Behaviour of Footbridges*, 96-103, Paris, France, 20-22 November.

Ewins, D. J. (2000) *Modal Testing: Theory, Practice and Application.* Research Studies Press, Baldock.

Fillod, R., Lallement, G., Piranda, J. and Raynaud, J. L. (1985) Global Method of Modal Identification. In: *Proceedings of the Third International Modal Analysis Conference*, 1145-1151, Orlando, USA, 28-31 January.

Fitzpatrick, T. and Ridsdill-Smith, R. R. (2001) Stabilising the London Millennium Bridge.

Ingenia, The Royal Academy of Engineering, No.9, 18-22.

Fitzpatrick, T., Dallard, P., Le Bourva, S., Low, A., Ridsdill-Smith, R. and Willford, M. (2001) *Linking London: The Millennium Bridge.* Report No. L12.32, The Royal Academy of Engineering, London, UK, June.

Firth, I. (2002) New Materials for Modern Footbridges. In: *Proceedings of the International Conference on the Design and Dynamic Behaviour of Footbridges*, 174-186, Paris, France, 20-22 November.

Fletcher, M. S. and Parker, J. S. (2003) Dynamics of the Hungerford Millennium Footbridges, UK. *Bridge Engineering*, 156 (BE2), 57-62.

Friswell, M. I. and Mottershead, J. E. (1995) *Finite Element Model Updating in Structural Dynamics.* Kluwer Academic Publishers, Dordrecht.

Fujino, Y., Sun, L., Pacheco, B. M. and Chaiseri, P. (1992) Tuned Liquid Damper (TLD) for Suppressing Horizontal Motion of Structure. *ASCE Journal of Engineering Mechanics*, 118 (10), 2017-2030.

Fujino, Y., Pacheco, B. M., Nakamura, S. and Warnitchai, P. (1993) Synchronization of Human Walking Observed During Lateral Vibration of a Congested Pedestrian Bridge. *Earthquake Engineering and Structural Dynamics*, 22, 741-758.

Fujino, Y. and Sun, L. M. (1993) Vibration Control by Multiple Tuned Liquid dampers (MTLDs). *ASCE Journal of Structural Engineering*, 119 (12), 3482-3502.

Galbraith, F. W. and Barton, M. V. (1970) Ground Loading from Footsteps. *The Journal of The Acoustical Society of America*, 48 (5), 1288-1292.

Gardner-Morse, M. G. (1990) *Modal Analysis of a Cable-Stayed Pedestrian Bridge.* MSc Thesis, The Faculty of the Graduate College, The University of Vermont, USA.

Gardner-Morse, M. G. and Huston, D. R. (1993) Modal Identification of Cable-Stayed Pedestrian Bridge. *ASCE Journal of Structural Engineering*, 119 (11), 3384-3404.

Gaukroger, D. R., Skingle, C. W. and Heron, K. H. (1973) Numerical Analysis of Vector Response Loci. *Journal of Sound and Vibration*, 29 (3), 341-353.

Goldman, D. E. (1948) A Review of Subjective Responses to Vibratory Motion of the Human Body in the Frequency Range 1 to 70 Cycles per Second. *Naval Medical Research Institute*, Report NM-004-001, Washington, USA.

Griffin, M. J. (1996) *Handbook of Human Vibration.* Academic Press, London.

Grundmann, H. and Schneider, M. (1991) Stochastic Representation of Footbridge Vibrations Taking Into Account Feedback Effects. In: *Proceedings of the European Conference on Structural Dynamics - EURODYN '90*, Bochum, Edited by W.B. Krätzig et al., Balkema, Rotterdam.

Grundmann, H., Kreuzinger, H. and Schneider, M. (1993) Dynamic Calculations of Foot-

bridges (in German). *Bauingenieur*, 68, 215-225.

HA (2001) *Design Manual for Roads and Bridges. Volume 1, Section 3: Loads for Highway Bridges (BD37/01).* Highways Agency, London, UK.

Hamm, P. (2002) Vibrations of Wooden Footbridges Induced by Pedestrians and a Mechanical Shaker. In: *Proceedings of the International Conference on the Design and Dynamic Behaviour of Footbridges*, Paris, France, 20-22 November.

Hansen, S. O. and Sørensen, J. D. (2002) Dynamic Loads due to Synchronized Movements of People. In:*Proceedings of the Fourth International Conference on Structural Dynamics - EURODYN*, Munich, Germany, September, 2-5.

Harper, F. C., Warlow, W. J. and Clarke, B. L. (1961) The Forces Applied to the Floor by the Foot in Walking. *National Building Studies*, Research Paper 32, Department of Scientific and Industrial Research, Building Research Station, London, UK.

Harper, F.C. (1962) The Mechanics of Walking. *Research Applied in Industry*, 15 (1), 23-28.

Hartley, M. J., Pavic, A. and Waldron, P. (1999) Investigation of Pedestrian Walking Loads on a Cable Stayed Footbridge Using Modal Testing and FE Model Updating. In: *Proceedings of the* 17^{th} *International Modal Analysis Conference- IMAC*, Vol. 1, 1076-1082, Florida, USA, 8-11 February.

Hatanaka, A. and Kwon, Y. (2002) Retrofit of Footbridge for Pedestrian Induced Vibration Using Compact Tuned Mass Damper. In: *Proceedings of the International Conference on the Design and Dynamic Behaviour of Footbridges*, Paris, France, 20-22 November.

HD (2002) *Structures Design Manual for Highway and Railways.* Highway Department, Government of the Hong Kong Special Administrative Region, Hong Kong.

Hongxing, H., Sol, H. and De Wilde, W. P. (2000) On a Statistical Optimisation Method Used in Finite Element Model Updating. *Journal of Sound and Vibration*, 231 (4), 1071-1078.

Hudson, D. E. (1977) Dynamic Tests of Full-Scale Structures. *ASCE Journal of Engineering Mechanics*, 103 (EM6), 1141-1157.

Hunt, J. B., *Dynamic Vibration Absorbers.* Mechanical Engineering Publications, London.

Huston, D. R., Gardner-Morse, M. and Beliveau, J. G. (1988) Impact Testing Modal Identification of a Cable-Stayed Pedestrian Bridge, In: *Bridge Research, Progress Symposium Proceedings*, 89-92, Iowa State University, USA.

IC (2000) *ICATS, MODENT, MODESH, MODAQ, MESHGEN. Users guide.* Imperial College Analysis and Testing Software, London, UK.

Inman, D. J. (2001) *Engineering Vibration.* Prentice Hall, Upper Saddle River, New Jersey.

Irwin, A. W. (1978) Human Response to Dynamic Motion of Structures. *The Structural Engineer*, 56A (9), 237-244.

ISO (1989) *Evaluation of Human Exposure to Whole-Body Vibration - Part 2: Continuous and Shock-Induced Vibration in Buildings (1 to* $80Hz$*).* ISO 2631-2. International Standardization Organization, Geneva, Switzerland.

ISO (1992) *Bases for Design of Structures - Serviceability of Buildings Against Vibrations.* ISO 10137. International Standardization Organization, Geneva, Switzerland.

ISO (2005) *Bases for Design of Structures - Serviceability of Buildings and Walkways against Vibration.* Draft of the standard ISO/CD 10137.2, International Organization for Standardization.

Iso, M. and Masubuchi, F. (2002) The Progress of Structural Design of Footbridges in Japan. In: *Proceedings of the International Conference on the Design and Dynamic Behaviour of Footbridges*, Paris, France, 20-22 November.

Jacklin, H. M. (1936) Human Reactions to Vibration. *Journal of Society of Automotive Engineers*, 39 (4), 401-407.

Jaishi, B. and Ren, W.-X. (2005) Structural Finite Element Model Updating Using Ambient Vibration Test Results. *ASCE Journal of Structural Engineering*, 131 (4), 617-628.

Ji, T. (2000) On the Combination of Structural Dynamics and Biodynamics Methods in the Study of Human-Structure Interaction. *The* 35^{th} *UK Group Meeting on Human Response to Vibration, ISVR*, Vol. 1, 183-194, Institute of Sound and Vibration Research, University of Southampton, England, 13-15 September.

Ji, T. (2005) Personal correspondence.

Jones, R. T. and Pretlove, A. J. (1979) Vibration Absorbers and Bridges. *The Highway Engineer*, 2-9 January.

Jones, R. T., Pretlove, A. J. and Eyre, R. (1981) Two Case Studies in the Use of Tuned Vibration Absorbers on Footbridges. *The Structural Engineer*, 59B (2), 27-32.

Kajikawa, Y. and Kobori, T. (1977) Probabilistic Approaches to the Ergonomical Serviceability of Pedestrian-Bridges. *Transactions of JSCE*, 9, 86-87.

Kasperski, M. (2005) The Response of Pedestrians to Lively Footbridges. In: Proceedings of The Sixth European Conference on Structural Dynamics, Vol. 1, pp. 539-544, Paris, France, 4-7 September.

Kerr, S. C. (1998) *Human Induced Loading on Staircases.* PhD Thesis, Mechanical Engineering Department, University College London, UK.

Kerr, S. C. and Bishop, N. W. M. (2001) Human Induced Loading on Flexible Staircases. *Engineering Structures*, 23, 37-45.

Khalifa, M. A., Hodhod, O. A. and Zaki, M. A. (1996) Analysis and Design Methodology for an FRP Cable-Stayed Pedestrian Bridge. *Composites: Part B*, 27B, 307-317.

Kim, G.-H. and Park, Y.-S. (2004) An Improved Updating Parameter Selection Method and

Finite Element Model Update Using Multiobjective Optimisation Technique. *Mechanical Systems and Signal Processing*, 18 (1), 59-78.

Kobori, T. and Kajikawa, Y. (1974) Ergonomic Evaluation Methods for Bridge Vibrations. *Transactions of JSCE*, 6, 40-41.

Leonard, D. R. (1966) Human Tolerance Levels for Bridge Vibrations. *TRRL Report No. 34*, Transport and Road Research Laboratory, Crowthorne, UK.

Leonard, D. R. (1974) Dynamic Tests on Highway Bridges - Test Procedures and Equipment. *TRRL Laboratory Report 654*, Structures Department, Crowthorne, UK.

Leonard, D. R. and Eyre, R. (1975) Damping and Frequency Measurements on Eight Box Girder Bridges. *TRRL Report LR682*, Department of The Environment, Crowthorne, UK.

Lenzen, K. H. (1966) Vibration of Steel Joist-Concrete Slab Floors. *American Institute of Steel Construction Engineering Journal*, 3, 133-136.

Lippert, S. (1947) Human Response to Vertical Vibration. *Journal of Society of Automotive Engineers*, 55 (5), 32-34.

Lintermann, C. (1986) *Impact Testing and Finite Element Presentation of a Cable-Stayed Pedestrian Bridge.* MSc thesis, The Faculty of the Graduate College, The University of Vermont, USA.

Lord, J.-F., Ventura, C. E. and Dascotte, E. (2004) Automated Model Updating Using Ambient Vibration Data from a 48-Storey Building in Vancouver. In: *Proceedings of the 22nd International Modal Analysis Conference*, Dearborn, Detroit, USA, 26-29 January.

Maia, N. M. M., Silva, J. M. M., He, J., Lieven, N. A. J., Lin, R. M., Skingle, G. W., To, W.-M., Urgueira, A. P. V. (1997) *Theoretical and Experimental Modal Analysis.* Research Studies Press, Wiley, Taunton, England.

Masani, K., Kouzaki, M. and Fukunaga, T. (2002) Variability of Ground Reaction Forces During Treadmill Walking. *Journal of Applied Physiology*, 92 (5), 1885-1890.

Mason, A. F. and Duncan, M. A. G. (1962) Composite Steel and Concrete Bridge Construction in Southern Rhodesia. *Journal of the Institution of Civil Engineers*, 21 (4), Paper No. 6513, 785-810.

MathWorks (2006) MATLAB: The Language of Technical Computing.

Matsumoto, Y., Sato, S., Nishioka, T. and Shiojiri, H. (1972) A Study on Design of Pedestrian Over-Bridges. *Transaction of JSCE*, 4, 50-51.

Matsumoto, Y., Nishioka, T., Shiojiri, H. and Matsuzaki, K. (1978) Dynamic Design of Footbridges. *IABSE Proceedings*, No. P-17/78, 1-15.

McRobie, A. and Morgenthal, G. (2002) Risk Management for Pedestrian-Induced Dynamics of Footbridges. In: *Proceedings of the International Conference on the Design and Dynamic Behaviour of Footbridges*, Paris, France, 20-22 November.

McRobie, A., Morgenthal, G., Lasenby, J. and Ringer, M. (2003) Section Model Tests on Human-Structure Lock-In. *Bridge Engineering*, 156 (BE2), 71-79.

Minas, C. and Inman, D. J. (1990) Matching Finite Element Models to Modal Data. *Transactions of the ASME: Journal of Vibration and Acoustics*, 112 (1), 84-92.

Mimram, M. (2002) Towards Reasoned, Open-Minded Footbridge Design. In: *Proceedings of the International Conference on the Design and Dynamic Behaviour of Footbridges*, 8-17, Paris, France, 20-22 November.

Miyamori, Y., Obata, T., Hayashikawa, T. and Sato, K. (2001) Study on Identification of Human Walking Model Based on Dynamic Response Characteristics of Pedestrian Bridges. In: *Proceedings of the Eighth East Asia-Pacific Conference on Structural Engineering & Construction (EASEC-8)*, Singapore, 5-7 December.

Modak, S. V., Kundra, T. K. and Nakra, B. C. (2002) Comparative Study of Model Updating Methods Using Experimental Data. *Computers and Structures*, 80 (5-6), 437-447.

Modak, S. V., Kundra and T. K., Nakra, B. C. (2005) Studies in Dynamic Design Using Updated Models. *Journal of Sound and Vibration*, 281 (3-5), 943-964.

Montgomery, D. C. and Runger, G. C. (1999) *Applied Statistics and Probability for Engineers.* John Wiley & Sons, New York.

Mouring, S. E. (1993) *Dynamic Response of Floor Systems to Building Occupant Activities.* PhD Thesis, The Johns Hopkins University, Baltimore, Maryland, USA.

Mouring, S. E. and Ellingwood, B. R. (1994) Guidelines to Minimize Floor Vibrations from Building Occupants. *ASCE Journal of Structural Engineering*, 120 (2), 507-526.

Moutinho, C., Caetano, E., Cunha, A. and Adao Da Fonseca, A. (2002) Dynamic Behaviour of a Long Span Stainless Steel Arch Footbridge. In: *Proceedings of the International Conference on the Design and Dynamic Behaviour of Footbridges*, Paris, France, 20-22 November.

Nakamura, S. and Fujino, Y. (2002) Lateral Vibration on a Pedestrian Cable-Stayed Bridge. *Structural Engineering International*, 12 (4), 295-300.

Nakamura, S. (2003) Field Measurements of Lateral Vibration on a Pedestrian Suspension Bridge. *The Structural Engineer*, 81 (22), 22-26.

Nakata, S., Tamuru, Y. and Otsuki, T. (1993) Habitability Under Horizontal Vibration of Low Rise Buildings. In: *International Colloquium on Structural Serviceability of Buildings*, Göteborg, Sweden, 8-11 June.

Newland, D. E. (1993) *An Introduction to Random Vibrations and Spectral Analysis.* Longman Group, Harlow.

Newland, D. E. (2004) Pedestrian excitation of bridges. *Journal of Mechanical Engineering Science*, 218 (5), 477-492.

Obata, T., Hayashikawa, T. and Sato, K. (1995) Experimental and Analytical Study of

Human Vibration Sensibility on Pedestrian Bridges. In: *Proceedings of the Fifth East Asia-Pacific Conference on Structural Engineering and Construction Building for the* 21^{st} *Century*, Vol. 2, 1225-1230, Griffith University, Gold Coast, Australia.

Obata, T., Hayashikawa, T. and Sato, K. (1999) Study on Dynamic Response Characteristics and Identification of Walking Force on Pedestrian Bridges. In: *Proceedings of the Seventh East Asia-Pacific Conference on Structural Engineering and Construction (EASEC-7)*, Japan, August 27-29.

Occhiuzzi, A., Spizzuoco, M. and Serino, G. (2002) Semi-Active MR Dampers in TMD's for Vibration Control of Footbridges, Part 1: Numerical Modelling and Control Algorithm. In: *Proceedings of the International Conference on the Design and Dynamic Behaviour of Footbridges.* Paris, France, 20-22 November.

Ohlsson, S. V. (1982) *Floor Vibration and Human Discomfort*, PhD Thesis, Chalmers University of Technology, Göteborg, Sweden.

OHBDC (1983) *Ontario Highway Bridge Design Code.* Highway Engineering Division, Ministry of Transportation and Communication, Ontario, Canada.

Ormondroyd, J. and Den Hartog, J. P. (1928) The Theory of the Dynamic Vibration Absorber. *Journal of Applied Mechanics*, APM-50-7, 9-22.

Pachi, A. and Ji, T. (2005) Frequency and velocity of people walking. *The Structural Engineer*, 83 (3), 46-40.

Parker, J. S., Hardwick, G., Carroll, M, Nicholls, N. P. and Sandercock, D. (2003) Hungerford Bridge Millennium Project - London. *Proceedings of ICE: Civil Engineering*, 156 (2), 70-77.

Pavic, A., Hartley, M. J. and Waldron, P. (1998) Updating of The Analytical Models of Two Footbridges Based on Modal Testing of Full-Scale Structures. In: *Proceedings of the International Conference on Noise and Vibration Engineering (ISMA 23)*, 1111-1118, Leuven, Belgium, 16-18 September.

Pavic, A. (1999) *Vibration Serviceability of Long-Span Cast In-Situ Concrete Floors.* PhD thesis, Department of Civil and Structural Engineering, University of Sheffield, Sheffield, UK.

Pavic, A., Reynolds, P., Cooper, P. and Harvey, W. J. (2000) *Report: Dynamic Testing and Analysis of Aberfeldy Footbridge.* Department of Civil and Structural Engineering, University of Sheffield, Sheffield, UK.

Pavic, A. and Reynolds (2002) Modal Testing of a 34m Catenary Footbridge. In: *Proceedings of the* 20^{th} *International Modal Analysis Conference (IMAC)*, Vol. 2, 1113-1118, Los Angeles, California, USA, 4-7 February.

Pavic, A., Armitage, A., Reynolds, P. and Wright, J. (2002a) Methodology for Modal Testing of the Millennium Bridge, London. *Structures and Buildings*, 152 (2), 111-121.

Pavic, A, Reynolds, P., Willford, M. and Wright, J. (2002b) Key Results of Modal Testing

of the Millennium Bridge, London. In: *Proceedings of the International Conference on the Design and Dynamic Behaviour of Footbridges*, 225-233, Paris, France, 20-22 November.

Pavic, A., Yu, C. H., Brownjohn, J. and Reynolds, P. (2002c) Verification of the Existence of Human-Induced Horizontal Forces due to Vertical Jumping. In: *Proceedings of IMAC XX*, 1, 120-126, Los Angeles, California, 4-7 February.

Pavic, A., Živanović, S., Reynolds, P., Vujović, P. and Pizzimenti, D. (2004) Dynamic Testing and Analysis of a Footbridge under Walking-Induced Excitation in Podgorica, Montenegro. *SEMC 2004: The Second International Conference on Structural Engineering, Mechanics and Computation*, Cape Town, South Africa, 5-7 July.

Pavic, A. and Willford, M. (2005) Vibration Serviceability of Post-Tensioned Concrete Floors. *Appendix G in Post-Tensioned Concrete Floors Design Handbook. Technical Report 43.* Concrete Society, Slough, UK.

Pedrazzi, G. and Beltrami, C. (2002) Design of Long Span Timber Footbridge. In: *Proceedings of the International Conference on the Design and Dynamic Behaviour of Footbridges*, Paris, France, 20-22 November.

Peeters, B. (2000) *System Identification and Damage Detection in Civil Engineering.* PhD Thesis, Katholieke Universiteit Leuven, Heverlee, Belgium.

Pernica, G. (1990) Dynamic Load Factors for Pedestrian Movements and Rhythmic Exercises. *Canadian Acoustics*, 18 (2), 3-18.

Pimentel, R. L. (1997) *Vibrational Performance of Pedestrian Bridges Due to Human-Induced Loads.* PhD Thesis, University of Sheffield, Sheffield, UK.

Pimentel, R. L. and Waldron, P. (1996) Validation of the Numerical Analysis of a Pedestrian Bridge for Vibration Serviceability Applications, In: *Proceedings of the International Conference on Identification in Engineering Systems*, 648-657.

Pimentel, R. and Waldron, P. (1997) Validation of the pedestrian load model through the testing of a composite footbridge. In: *Proceedings of the* 15^{th} *IMAC Conference*, 1, 286-292, Orlando, USA, 3-6 February.

Pimentel, R. and Fernandes, H. (2002) A Simplified Formulation for Vibration Serviceability of Footbridges. In: *Proceedings of the International Conference on the Design and Dynamic Behaviour of Footbridges*, Paris, France, 20-22 November.

Pimentel, R., Pavic, A. and Waldron, P. (1999) Vibration Performance of Footbridges Established via Modal Testing. *IABSE Symposium: Structures for the Future - The Search for Quality*, 602-609, Rio de Janeiro, Brazil, 25-27 August.

Pimentel, R. L., Pavic, A. and Waldron, P. (2001) Evaluation of Design Requirements for Footbridges Excited by Vertical Forces from Walking. *Canadian Journal of Civil Engineering*, 28 (5), 769-777.

Poovarodom, N., Kanchanosot, S. and Warnitchai, P. (2001) Control of Man-Induced Vibrations on a Pedestrian Bridge by Nonlinear Multiple Tuned Mass Dampers. In: *The Eighth East Asia-Pacific Conference on Structural Engineering and Construction*, paper No. 1344, Singapore, 5-7 December.

Poovarodom, N., Mekanannapha, C. and Nawakijphaitoon, S. (2002) Vibration Problem Identification of Steel Pedestrian Bridges and Control Measures. In: *Proceedings of the Third World Conference on Structural Control*, Como, Italy, 7-12 April.

Poovarodom, N., Kanchanosot, S. and Warnitchai, P. (2003) Application of Non-Linear Multiple Tuned Mass Dampers to Suppress Man-Induced Vibrations of a Pedestrian Bridge, *Earhquake Engineering and Structural Dynamics*, 32 (7), 1117-1131.

Postlethwaite, F. (1944) Human Susceptibility to Vibration. *Engineering*, 157, No. 4072, 61-63.

Pretlove, A. J. and Rainer, J. H. (1995) Human Response to Vibrations. Appendix I in: *Vibration Problems in Structures: Practical Guidelines*, Birkhäuser Verlag, Basel.

Przemieniecki, J. S. (1968) *Theory of Matrix Structural Analysis.* Dover Publications, New York.

Rana, R. and Soong, T. T. (1998) Parametric Study and Simplified Design of Tuned Mass Dampers. *Engineering Structures*, 20 (3), 193-204.

Rainer, J. H. (1979) Dynamic Testing of Civil Engineering Structures. In: *Proceedings of the Third Canadian Conference on Earthquake Engineering*, 551-574.

Rainer, J. H. and Pernica, G. (1979) Dynamic Testing of a Modern Concrete Bridge. *Canadian Journal of Civil Engineering*, 6 (3), 447-455.

Rainer, J. H., Pernica, G. and Allen, D. E. (1988) Dynamic Loading and Response of Footbridges. *Canadian Journal of Civil Engineering*, 15 (1), 66-71.

Rainer, J. H. and Van Selst, A. (1976) Dynamic Properties of Lions' Gate Suspension Bridge. In: *ASCE/EMD Specialty Conference on Dynamic Response of Structures*, 243-252, UCLA, California, USA, 30-31 March.

Richardson, M. H. and Formenti, D. L. (1982) Parameter Estimation from Frequency Response Measurements using Rational Fraction Polynomials. In: *Proceedings of the First International Modal Analysis Conference*, 167-181, Orlando, USA, 8-10 November.

Sachse, R. (2002) *The Influence of Human Occupants on the Dynamic Properties of Slender Structures.* PhD Thesis, University of Sheffield, Sheffield, UK.

Sachse, R., Pavic, A. and Reynolds, P. (2002) The Influence of a Group of Humans on Modal Properties of a Structure. In: *Proceedings of the Fourth International Conference on Structural Dynamics (EURODYN)*, Vol. 2, 1241-1246, Munich, Germany, 2-5 September.

Sahnaci, C. and Kasperski, M. (2005) Random Loads Induced by Walking. In: *Proceedings of*

The Sixth European Conference on Structural Dynamics (EURODYN 2005), Vol. 1, 441-446, Paris, France, 4-7 September.

Salawu O. S. and Williams, C. (1995) Review of Full-Scale Dynamic Testing of Bridge Structures. *Engineering Structures*, 17 (2), 113-121.

SAS (1994) *ANSYS User's Manual, release 5.0.* Swanson Analysis System, Houston.

Saul, W. E., Tuan, C. Y-B., McDonald, B. (1985) Loads due to Human Movements. In: *Proceedings of the Structural Safety Studies*, edited by Yao, J. T. P., 107-119.

Schlaich, M. (2002) Planning Conditions for Footbridges. In: *Proceedings of the International Conference on the Design and Dynamic Behaviour of Footbridges*, 40-52, Paris, France, 20-22 November.

Seiler, C., Fisher, O. and Huber, P. (2002) Semi-Active MR Dampers in TMD's for Vibration Control of Footbridges, Part 2: Numerical Analysis and Practical Realisation. In: *Proceedings of the International Conference on the Design and Dynamic Behaviour of Footbridges*, Paris, France, 20-22 November.

Selberg, A. (1950) Dampening Effect in Suspension Bridges. *IABSE Publications*, 10, 183-198.

Severn, R. T., Brownjohn, J. M. W., Dumanoglu, A. A. and Taylor, C. A. (1988) A Review of Dynamic Testing Methods for Civil Engineering Structures. *University of Bristol and SECED Conference: Civil Engineering Dynamics*, 1-23, Bristol, UK, 24-25 March.

SIA (1989) *Action on Structures.* Swiss Society of Engineers and Architects, SIA Standard 160, Zürich.

Simiu, E. and Scanlan, R. H. (1996) *Wind Effects on Structures: Fundamentals and Applications to Design.* Wiley, New York.

Skorecki, J. (1966) The Design and Construction of a New Apparatus for Measuring the Vertical Forces Exerted in Walking: a Gait Machine. *Journal of Strain Analysis*, 1 (5), 429-438.

Smith, J. W. (1969) *The Vibration of Highway Bridges and the Effects on Human Comfort.* PhD Thesis, University of Bristol, Bristol, UK.

Smith, J. W. (1988) *Vibrations in Structures, Applications in Civil Engineering Design.* Chapman and Hall, London.

Stevenson, R. (1821) Description of Bridges of Suspension. *Edinburgh Philosophical Journal*, 5 (10), 237-256.

Stoyanoff, S., Hunter, M. and Byuers, D. D. (2002) Human-Induced Vibrations on Footbridges. In: *Proceedings of the International Conference on the Design and Dynamic Behaviour of Footbridges*, Paris, France, 20-22 November.

Strasky, J. (2002) New Structural Concepts for Footbridges. In: *Proceedings of the Inter-*

national Conference on the Design and Dynamic Behaviour of Footbridges, 147-155, Paris, France, 20-22 November.

Strogatz, S. H., Abrams, D. M., McRobie, A., Eckhardt, B. and Ott, E. (2005) Crowd synchrony on the Millennium Bridge. *Nature*, 438, 43-44.

SVS (2004) *ARTeMIS Extractor Pro, Release 3.43.* Structural Vibration Solutions, Denmark.

Takenouchi, K. and Ito, M. (2002) Function and Development of Pedestrian Bridges in Japan. In: *Proceedings of the International Conference on the Design and Dynamic Behaviour of Footbridges*, Paris, France, 20-22 November.

Teughels, A. and De Roeck, G. (2004) Structural Damage Identification of the Highway Bridge Z24 by FE Model Updating. *Journal of Sound and Vibration*, 278 (3), 589-610.

Taylor, D. (2002) Damper Retrofit of the Millennium Footbridge - A Case Study in Biodynamic Design. In: *Proceedings of the* 73^{rd} *Shock and Vibration Symposium*, Newport, USA, 18-22 November.

Tilden, C. J. (1913) Kinetic Effects of Crowds. In: *Proceedings of ASCE*, 39 (3), 325-340.

Tilly, G. P. (1977) Damping of Highway Bridges: A Review. In: *Proceedings of the DOE and DOT TRRL Symposium on Dynamic Behaviour of Bridges*, 1-9, Crowthorne, UK, 19 May.

Tilly, G. P., Cullington, D. W. and Eyre, R. (1984) Dynamic Behaviour of Footbridges. *IABSE Surveys S-26/84*, IABSE Periodica, No. 2/84, 13-24.

Tuan, C. Y. and Saul, W. E. (1985) Loads due to Spectator Movements. *ASCE Journal of Structural Engineering*, 111 (2), 418-434.

Ventura, C. E., Kharrazi, M. H. K., Turek, M. and Horyna, T. (2002) Dynamic Analysis of a Pedestrian Walkway, University of British Columbia, Canada. *Proceedings of the International Modal Analysis Conference (IMAC XX)*, Vol. 1, 114-119, Los Angeles, California, USA, February.

Walley, F. (1959) St James's Park Bridge., *Proceedings of The Institution of Civil Engineers*, 12, No. 6257, 217-222.

Warburton, G. B. (1982) Optimum Absorber Parameters for Various Combinations of Response and Excitation Parameters. *Earthquake Engineering and Structural Dynamics*, 10, 381-401.

Weber, B. (2002) Damping of Vibrating Footbridges, In: *Proceedings of the International Conference on the Design and Dynamic Behaviour of Footbridges*, 196-207, Paris, France, 20-22 November.

Wheeler, J. E. (1980) Pedestrian - Induced Vibrations in Footbridges. In: *Proceedings of the* 10^{th} *Australian Road Research Board (ARRB) Conference*, 10 (3), 21-35, Sydney, Australia, 27-29 August.

Wheeler, J. E. (1982) Prediction and Control of Pedestrian Induced Vibration in Footbridges.

ASCE Journal of the Structural Division, 108 (ST9), 2045-2065.

Willford, M. (2001) An Investigation Into Crowd-Induced Vertical Dynamic Loads Using Available Measurements, *The Structural Engineer*, 79 (12), 21-25.

Willford, M. (2002) Dynamic Actions and Reactions of Pedestrians. In: *Proceedings of the International Conference on the Design and Dynamic Behaviour of Footbridges*, 66-73, Paris, France, 20-22 November.

Williams, C., Rafiq, M. Y. and Carter, A. (1999) Human Structure Interaction: The Development of an Analytical Model of the Human Body. *International Conference: Vibration, Noise and Structural Dynamics '99*, 32-39, Venice, Italy, 28-30 April.

Wolmuth, B. and Surtees, J. (2003) Crowd-Related Failure of Bridges. *Civil Engineering*, 156 (3), 116-123.

Wood, R. H. (1948) Some Notes on Vibrations in Structures. *The Journal of Royal Institute of British Architects*, third series, 55 (12), 553-555.

Wörner, S. and Schlaich, M. (2002) Covered Footbridges. In: *Proceedings of the International Conference on the Design and Dynamic Behaviour of Footbridges*, Paris, France, 20-22 November.

Wright, D. T. and Green, R. (1959) *Human Sensitivity to Vibration.* Report No. 7, Queen's University, Kingston, Ontario, Canada, February.

Wright, D. T. and Green, R. (1963) *Highway Bridge Vibrations, Part II: Ontario Test Programme.* Report No. 5, Queen's University, Kingston, Ontario, Canada, September.

Wu, J. R. and Li, Q. S. (2004) Finite Element Model Updating for a High-Rise Structure Based on Ambient Vibration Measurements. *Engineering Structures*, 26 (7), 979-990.

Wyatt, T. A. (1977) Mechanisms of Damping. In: *Proceedings of the DOE and DOT TRRL Symposium on Dynamic Behaviour of Bridges*, 10-19, Crowthorne, UK, 19 May.

Xia, P.-Q. and Brownjohn, J. M. W. (2003) Residual Stiffness Assessment of Structurally Failed Reinforced Concrete Structure by Dynamic Testing and Finite Element Model Updating. *Experimental Mechanics*, 43 (4), 372-378.

Xu, K. and Igusa, T. (1992) Dynamic Characteristics of Multiple Substructures with Closely Spaced Frequencies. *Earthquake Engineering and Structural Dynamics*, 21 (12), 1059-1070.

Yao, S., Wright, J., Pavic, A. and Reynolds, P. (2002) Forces Generated When Bouncing or Jumping on a Flexible Structure. In: *Proceedings of the International Conference on Noise and Vibration*, 2, 563-572, Leuven, Belgium, 16-18 September.

Yao, S., Wright, J., Pavic, A., Reynolds, P. and Sachse, R. (2003) The Effect of People Jumping on a Flexible Structure. In: *Proceedings of IMAC XXI*, Kissimmee, Florida, 3-6 February.

Yoneda, M. (2002) A Simplified Method to Evaluate Pedestrian-Induced Maximum Response

of Cable-Supported Pedestrian Bridges, In: *Proceedings of the International Conference on the Design and Dynamic Behaviour of Footbridges*, Paris, France, 20-22 November.

Yoshida, J., Abe, M., Fujino, Y. and Higashiuwatoko, K. (2002) Image Analysis of Human Induced Lateral Vibration of a Pedestrian Bridge. In: *Proceedings of the International Conference on the Design and Dynamic Behaviour of Footbridges*, Paris, France, 20-22 November.

Young, P. (2001) Improved Floor Vibration Prediction Methodologies. *ARUP Vibration Seminar*, 4 October, London, UK.

Zhang, Q. W., Chang, T. Y. P. and Chang, C. C. (2001) Finite Element Model Updating for the Kap Shui Mun Cable-Stayed Bridge. *ASCE Journal of Bridge Engineering*, 6 (4), 285-293.

Zheng, X. and Brownjohn, J. M. W. (2001) Modelling and Simulation of Human-Floor System Under Vertical Vibration. In: *Proceedings of SPIE, Smart Structures and Materials*, 4327, 513-520, Newport Beach, California, USA, 5-8 March.

Conference Papers Produced During Work on the Thesis

Pavic, A., Živanović, S., Reynolds, P., Vujović, P. and Pizzimenti, D. (2004) Dynamic Testing and Analysis of a Footbridge under Walking-Induced Excitation in Podgorica, Montenegro. *SEMC 2004: The Second International Conference on Structural Engineering, Mechanics and Computation*, Cape Town, South Africa, 5-7 July.

Živanović, S., Pavic, A., Reynolds, P. and Vujović, P. (2005) Dynamic Analysis of Lively Footbridge under Everyday Pedestrian Traffic. In: *Proceedings of the Sixth European Conference on Structural Dynamics (EURODYN)*, Vol. 1, pp. 453-459, Paris, France, 4-7 September.

Živanović, S., Pavic, A. and Reynolds, P. (2005) Modal Testing and Finite Element Modelling and Updating of Lively Footbridge. In: *Proceedings of the International Conference on Experimental Vibration Analysis for Civil Engineering Structures (EVACES 2005)*, pp. 537-544, Bordeaux, France, 26-28 October.

Journal Papers Produced During Work on the Thesis

Pavic, A., Živanović, S. and Reynolds, P. (2005) Errors in Numerical Solution of Equation of Motion of Lightly Damped SDOF System near Resonance. *International Journal of Structural Stability and Dynamics*, 5 (1), 135-142.

Živanović, S., Pavic, A. and Reynolds, P. (2005) Vibration Serviceability of Footbridges under Human-Induced Excitation: A Literature Review. *Journal of Sound and Vibration*, 279 (1-2), 1-74.

Živanović, S., Pavic, A. and Reynolds, P. (2005) Human-Structure Dynamic Interaction in

Footbridges. *Proceedings of the Institution of Civil Engineers: Bridge Engineering*, 158 (4), 165-177.

Živanović, S., Pavic, A. and Reynolds, P. (2006) Modal Testing and Finite Element Model Tuning of a Lively Footbridge Structure. *Engineering Structures*, 28 (6), 857-868.

Živanović, S., Pavic, A. and Reynolds, P. Finite Element Modelling and Updating of a Lively Footbridge: The Complete Process. Provisionally accepted for publication in *Journal of Sound and Vibration*, Academic Press, ISSN 0022-460X.

Živanović, S., Pavic, A. and Reynolds, P. Novel Probability-Based Framework for Prediction of Vibration Response to Single Person Walking across Footbridge. Submitted for review to *ASCE Journal of Structural Engineering*, American Society of Civil Engineers, ISSN 0733-9445.

Živanović, S., Pavic, A. and Reynolds, P. Probability Based Prediction of Multi Mode Vibration Response to Walking Excitation. Submitted for review to *Engineering Structures*, Elsevier, ISSN 0141-0296.

Appendix A

Dynamic Analysis of Podgorica Footbridge under Pedestrian Traffic

This appendix was presented as a paper at EURODYN 2005 conference under reference:

Živanović, S., Pavic, A., Reynolds, P. and Vujović, P. (2005) Dynamic Analysis of Lively Footbridge under Everyday Pedestrian Traffic. In: Proceedings of The Sixth European Conference on Structural Dynamics, Vol. 1, pp. 453-459, Paris, France, 4-7 September.

Abstract

A footbridge known to be lively under vertical pedestrian excitation was tested and the lowest modes of vibration were identified. It was established that the first vertical mode had the natural frequency of 2.05 Hz and a very low damping ratio of only 0.28%. These were the main factors which influenced most of 300 randomly interviewed pedestrians to rate the footbridge as lively. A detailed finite element model was developed and formally updated using a sensitivity based model updating approach to match the measured natural frequencies. By monitoring pedestrian traffic, pedestrian arrival time distribution and frequency distribution of their steps were identified. Using these data and modal properties of the updated finite element model, the vibration response of the bridge to everyday pedestrian traffic was simulated using a stochastic approach (Monte Carlo simulations) and compared with the measured acceleration.

A.1 Introduction

This paper presents a combined experimental and analytical case study which aims to investigate the vibration performance of a full-scale footbridge structure known to be lively under normal pedestrian traffic.

The paper describes first the test structure and key results of a limited dynamic testing programme. Then, numerical modelling of the structure is described together with the assumptions made to update the numerical model to match the measured natural frequencies. Furthermore, results of monitoring of pedestrian traffic and the corresponding structural dynamic response are described. Statistical distributions for pedestrian arrivals on the bridge as well as for their step frequencies are identified. Based on these data and the updated finite element model, the response of the bridge to normal pedestrian traffic, consisting mainly of groups of people rather than individuals, is simulated and compared with the measurements. Finally, results of subjective rating of vibrations as experienced by pedestrians on this footbridge are presented.

A.2 Structural Description

The investigated footbridge spans 104 m over the Morača River in Podgorica, capital of Montenegro (Figure A.1).

Figure A.1: Photograph of the Podgorica footbridge.

The structural system of the Podgorica footbridge is a steel box girder with inclined supports. The main span between inclined columns is 78 m while two side spans are 13 m each. Along its whole length the box girder is stiffened by longitudinal and transverse stiffeners, as shown in Figure A.2. The connection between the inclined columns and box girder is enhanced by vertical stiffeners visible in Figure A.1 as well as by a concrete slab cast over the bottom steel flange forming a composite slab structure (Figure A.2). The aim of this enhancement

is to strengthen this part of the box section so that it can resist large column reaction forces and compression due to negative bending moments. A similar layout of the steel-concrete composite slab exists around the midspan of the footbridge, but the concrete is cast over the top flange of the box girder (Figure A.2).

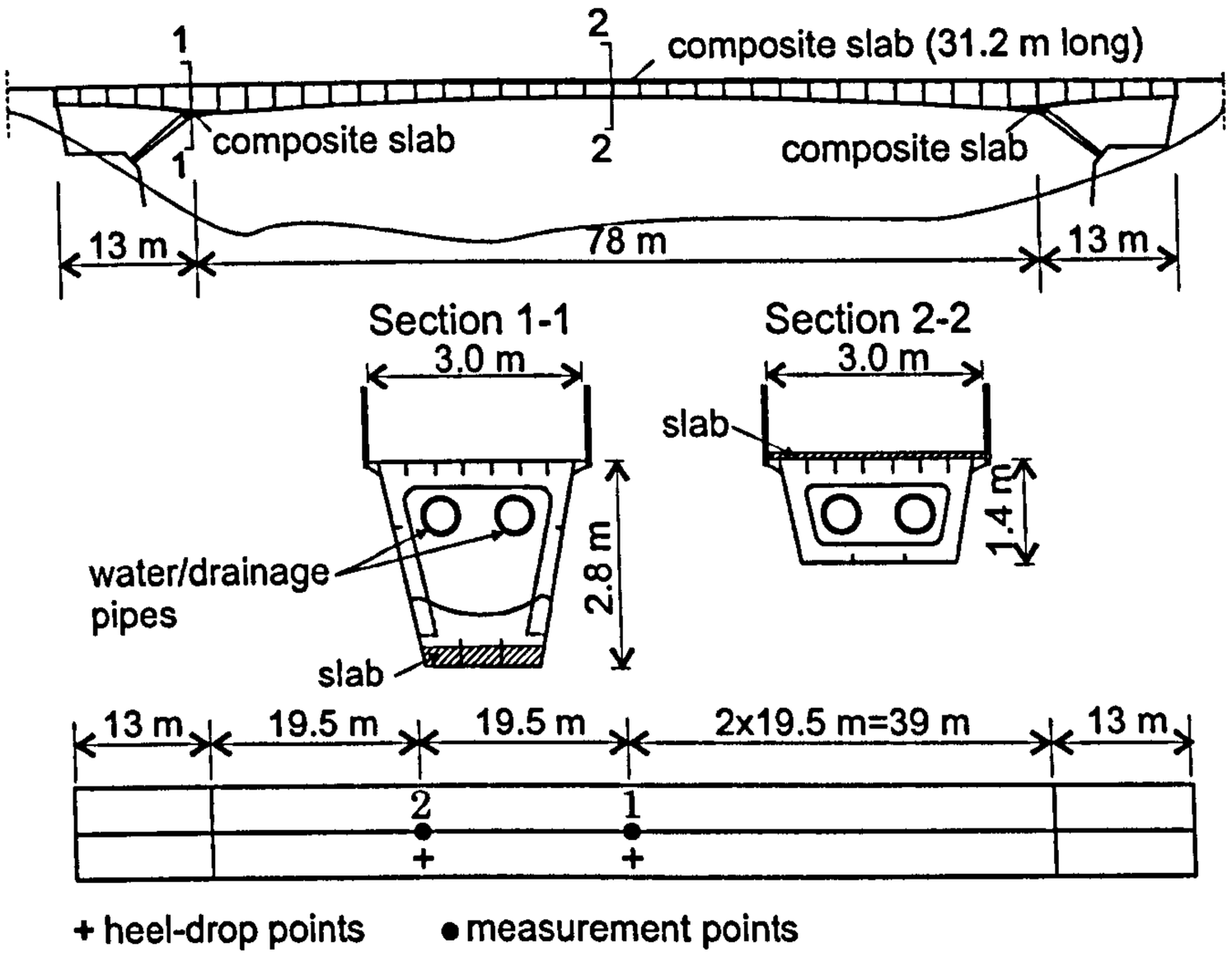

Figure A.2: General arrangement drawing (not to scale) of Podgorica footbridge and measurement points.

Since its construction, this footbridge has been very lively in the vertical direction. Sometimes, perceptible vibrations have been excited even by a single pedestrian crossing over it. The vibrations are perceptible to the person generating them and also to other pedestrians, either stationary or walking, who are present on the footbridge deck. At the first sight (Figures A.1 and A.2), this is somewhat surprising considering how massive the 260-tonne structure is.

Because of the liveliness of the footbridge, some limited testing was conducted in order to:

1. estimate the natural frequencies for the lowest modes of vibration in both the vertical and in the horizontal-lateral directions,
2. establish the as-built key dynamic properties of the footbridge structure,
3. assess the footbridge vibrations due to everyday pedestrian traffic, and
4. gather information on the perception of pedestrians of the footbridge vibrations.

A.3 Experimental Modal Identification

Due to the limitation of measurement equipment available as well as short time scales, it was decided to perform only the heel-drop testing to estimate the lowest footbridge natural frequencies.

Heel-drop testing was conducted in April 2004. Two Endevco 7754-1000 piezoelectric accelerometers were available for these tests. They were placed in the vertical direction at quarter-span (point 2) and at midspan (point 1) of the main span (Figure A.2). Then, heel-drop tests at these two points were conducted.

Fourier amplitude spectra of the two signals measured are shown in Figure A.3. The frequency resolution was 0.05 Hz. The signal measured at midspan (Ch1) due to a heel-drop at this point is presented by a solid grey solid line while the one measured at point 2 (Ch2), due to a heel-drop at point 2, is presented by a black dashed line. Bearing in mind the behaviour of a classical beam and the sequence of symmetric and anti-symmetric modes of vibration, in both signals a peak at frequency 2.05 Hz clearly indicated the natural frequency of the first vertical symmetric mode. Also, a peak at 8.00 Hz was found. These two modes seemed to have symmetric mode shapes. On the other hand, the presence of two peaks at 3.15 Hz and 7.25 Hz only at Ch2 indicated possible presence of two anti-symmetric mode shapes. While the first peak at 3.15 Hz was clearly a mode of vibration, the much weaker peak at 7.25 Hz was unexpected. Its presence indicated that the third mode seemed to be anti-symmetric which was surprising having in mind that the second mode (at 3.15 Hz) was also anti-asymmetric. The low magnitude of this peak could have been simply a consequence of just a small vibration amplitude for this mode at the position of the accelerometer.

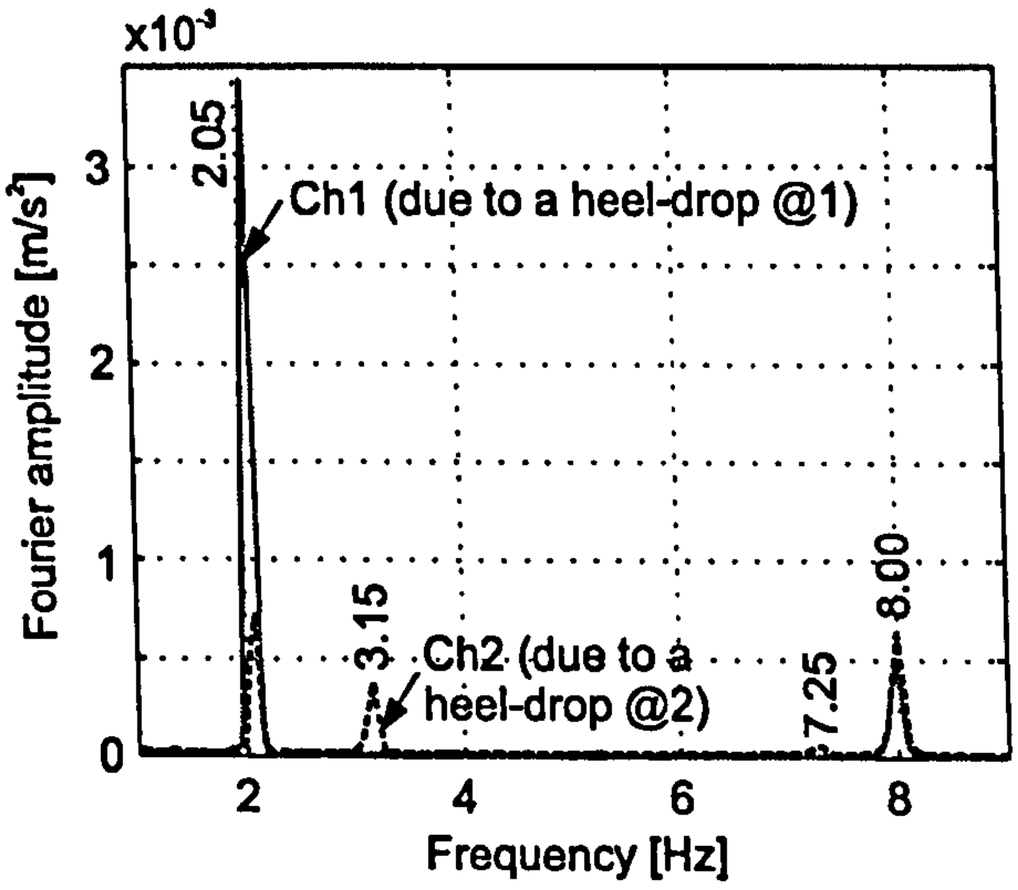

Figure A.3: Fourier spectra of vertical accelerations.

In the second part of the test it was decided to repeat heel-drop tests but this time with accelerometers rotated by 90° to measure the horizontal-lateral response. The idea was to identify modes with predominant horizontal motion. These modes could have been excited

by heel-drops if there was some vertical movement in them.

By doing this, two modes were clearly identified. The first one at 1.85 Hz was picked up by both accelerometers while the second at 4.55 Hz was present only in the spectrum of the response at the quarter point (Figure A.4). This suggested that these two modes are the first symmetric and the first anti-symmetric horizontal modes, respectively.

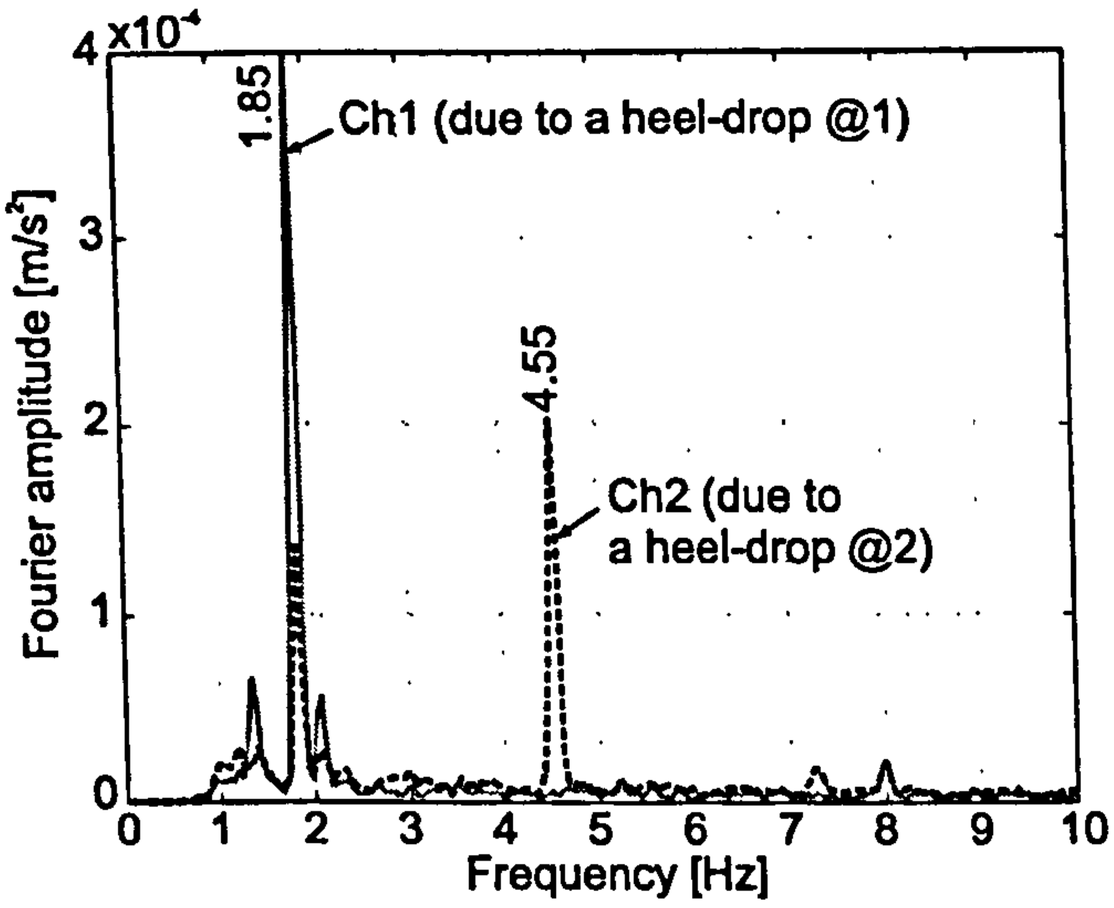

Figure A.4: Fourier spectra of horizontal accelerations.

The first vertical mode of vibration was known to be the main contributor to the footbridge liveliness (Pavic et al., 2004). The damping ratio of this mode was identified by Pavic et al. (2004) from free decay of the response after a single pedestrian near-resonant excitation was removed from the footbridge and it was only 0.28%.

A.4 Modelling and Updating

A finite element (FE) model of the bridge was developed before the testing (Pavic et al., 2004). This section describes the formal updating of the model to match the measured frequencies. In this way a more reliable FE model was developed and used for calculation of the modal mass of the relevant vibration mode needed for response analysis.

A.4.1 Initial FE Model and Manual Tuning

Firstly, a 3D finite element model was developed using the ANSYS FE code. The key modelling assumptions were as follows:

- The main steel box girder and its longitudinal and transverse stiffeners and box section columns were modelled using SHELL63 elements with isotropic properties.

- The composite steel-concrete slabs (Figure A.2) were modelled using an equivalent steel thickness and, again, SHELL63 elements.
- The handrails were modelled using BEAM4 elements (3D beams).
- Water and drainage pipes were modelled as distributed mass along the lines connecting points at which the pipes were suspended from the bridge deck. The mass was calculated taking into account that water filled a half of the pipes' volume.
- Column supports were modelled as fully fixed considering solid rock foundations.
- Supports at both ends of the main girder were modelled as pinned.

The initially developed FE model is presented in Figure A.5.

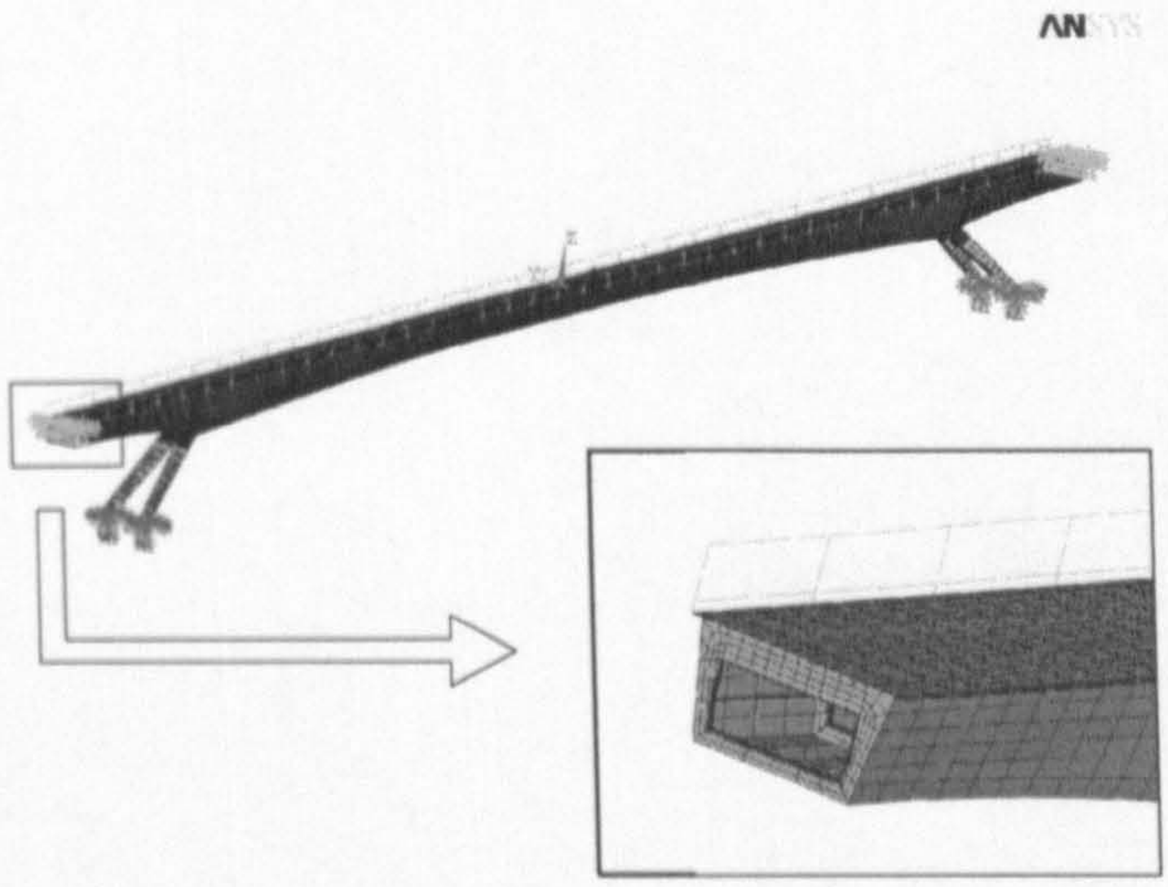

Figure A.5: Initially developed FE model. Note: in the inset, supports are removed for clarity.

The eight lowest natural frequencies in this model are shown in the second column of Table A.1. Labels H, V and T stand for horizontal, vertical and torsional modes, respectively, while S and A stand for symmetric and anti-symmetric modes, respectively.

Regarding vertical modes, it can be seen that the frequency of the first vertical anti-symmetric mode (1VA) was overestimated by more than 1 Hz (4.30 Hz calculated vs. 3.15 Hz measured). Also, mode 2VA did not appear in frequency range up to 10 Hz. Moreover, modes 1HA and 1VA changed their sequence of appearance in comparison with the corresponding experimental values. For these reasons, to obtain a reasonably accurate starting model necessary for automatic FE model updating (Brownjohn & Xia, 2000), manual tuning was conducted.

Based on experience gathered during the previous modelling and limited manual tuning of only the first vertical mode of the same bridge (Pavic et al., 2004), as well as on the reliability of the input data, a number of parameters was selected for more extensive manual tuning aimed at several modes of vibration. These were: the thickness of the composite slabs, their

Young's modulus and density, mass of the water pipes with water in them and boundary conditions at both ends of the bridge girder (flexible instead of rigid supports). It was found that by far the most important parameter, which influenced the first vertical anti-symmetric mode, was the stiffness of the support springs in the longitudinal direction. Elastic springs (COMBIN14 element) having stiffness of 10^8 N/m per metre length of the edge of the bridge deck were adopted. Frequencies obtained in this way are shown in the third column of Table A.1. It can be seen that 1VA mode became much closer to the measured frequency, and that this mode became lower than 1HA, which is what was measured. At the same time, it can be seen that frequencies of the vertical modes were much closer to the measured values, while the horizontal ones were still very different. What was interesting was that mode 2VA appeared and its frequency was lower than the frequency of mode 2VS. Therefore, two vertical anti-symmetric modes (1VA and 2VA) appeared next to each other in the vertical direction and this gave some confidence that the measured peak at 7.25 Hz (Figure A.3) really presented a vibration mode (2VA). Because of the vicinity of point 2 to the node of this mode (see mode 2VA in Figure A.6) the peak magnitude was so weak in the measurements. These facts suggested that the FE model updated in this way could be used as a starting model for automatic updating.

Table A.1: Natural frequencies [Hz] in different models.

Mode #	Initial model	Manual tuning	Automatic updating	Experimental model
1	1.58 (1HS)	1.56 (1HS)	1.60 (1HS)	1.85 (1HS)
2	1.94 (1VS)	1.94 (1VS)	2.06 (1VS)	2.05 (1VS)
3	3.74 (1HA)	3.38 (1VA)	3.12 (1VA)	3.15 (1VA)
4	4.30 (1VA)	3.65 (1HA)	3.69 (1HA)	4.55 (1HA)
5	6.62 (2HS)	6.28 (2HS)	6.22 (2HS)	-
6	7.92 (2VS)	6.92 (2VA)	6.98 (2VA)	7.25 (2VA)
7	9.44 (2HA)	7.51 (2VS)	7.85 (2VS)	8.00 (2VS)
8	9.70 (1T)	8.90 (2HA)	9.09 (2HA)	-
m_2 [kg]	66,220	66,050	61,552	-

A.4.2 Automatic Updating

Automatic updating was conducted using the FEM-tools software (DDS, 2004) with the aim to match analytical and experimental natural frequencies. The main rationale for this updating was to obtain the modal mass and mode shape of the first vertical mode of vibration, needed for the response analysis.

The parameters selected for the updating were of the same kind as those chosen for manual tuning:

- stiffness of the support springs in the longitudinal direction,
- the density of the deck elements,

- the 'density' of the pipes with water in them,
- thickness of the deck layers, and
- Young's modulus for some steel and composite SHELL63 elements. This was selected only for the elements which modulus had strong influence on the vertical modes, as demonstrated in the sensitivity analysis (not presented here due to limited space).

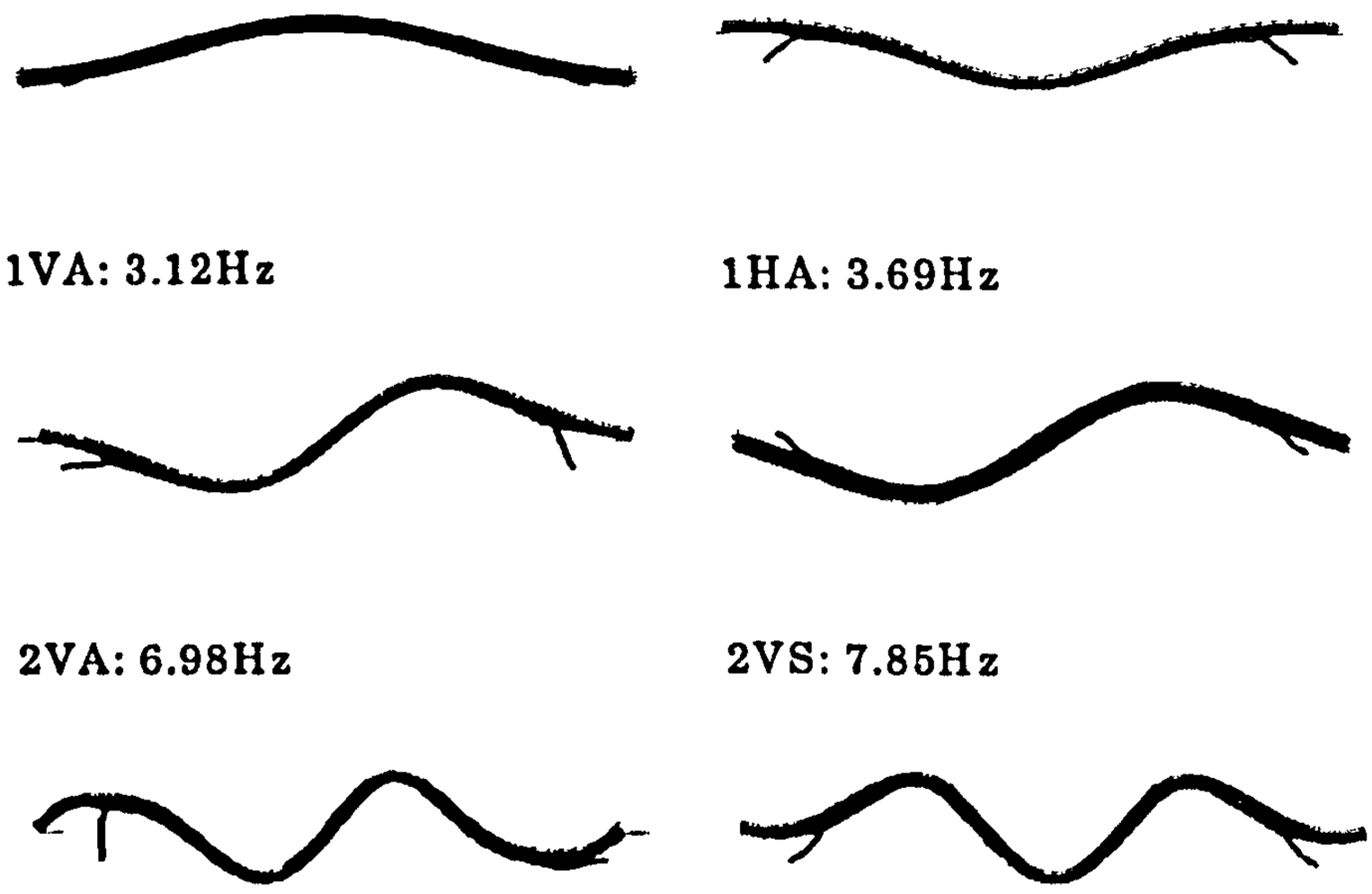

Figure A.6: Vibration modes from the updated model.

In this way, in total 23 parameters were selected for updating. The main results are presented in Table A.2.

Table A.2: Starting and updated uncertain parameters.

Parameter	Initial value	Updated value
Support stiffness [N/m/m]	1.00×10^8	0.55×10^8
Asphalt thickness [cm]	5.5	8.0
Composite slab thickness (on the top flange) [cm]	6.7	4.8
Composite slab thickness (on the top of columns) [cm]	11.0	11.6
Percentage of water in pipes [%]	50	32

Natural frequencies of the FE model updated in this way are shown in the fourth column of Table A.1. The modal mass was found to be approximately 62,000 kg. This is the value adopted for further dynamic analysis. The six horizontal and vertical modes are shown in Figure A.6.

It can be noticed that the updating process almost did not affect the horizontal modes. In an additional analysis it was shown that frequencies of the two measured horizontal modes were very sensitive to the change of the stiffness of the inclined columns. Namely, it seemed that these two columns were much stiffer than it was taken into account in the starting model. The reason could be that during enhancement of the top parts on the columns the columns themselves were also reinforced. More detailed analysis of this issue was not possible having in mind the data available. It should be emphasised that vertical mode 1VS at 2.05 Hz was not sensitive to the small increase of the stiffness of the inclined columns (which was affecting horizontal modes). This is because its modal displacements at column points were already close to zero. Therefore, the modal mass of this mode was not dependent on this uncertain parameter.

A.5 Pedestrian Monitoring Tests

The vertical response of the footbridge under normal pedestrian traffic was monitored during three time slots, each lasting 45 minutes. The acceleration was measured at the midspan point, next to the railing. About 2,000 pedestrians crossed the bridge during this time. Their crossings were recorded by two video cameras on both ends of the bridge. Immediately after crossing, 300 randomly selected pedestrians were asked to characterise vibrations felt during their crossings.

A.5.1 General Observations

A typical measured acceleration time history during 45 minute slot is presented in Figure A.7 (upper). Its spectrum in Figure A.7 (lower) reveals that the first vertical mode dominates the response. Its frequency dropped from 2.05 Hz to 2.00 Hz probably due to increased modal mass caused by the presence of pedestrians.

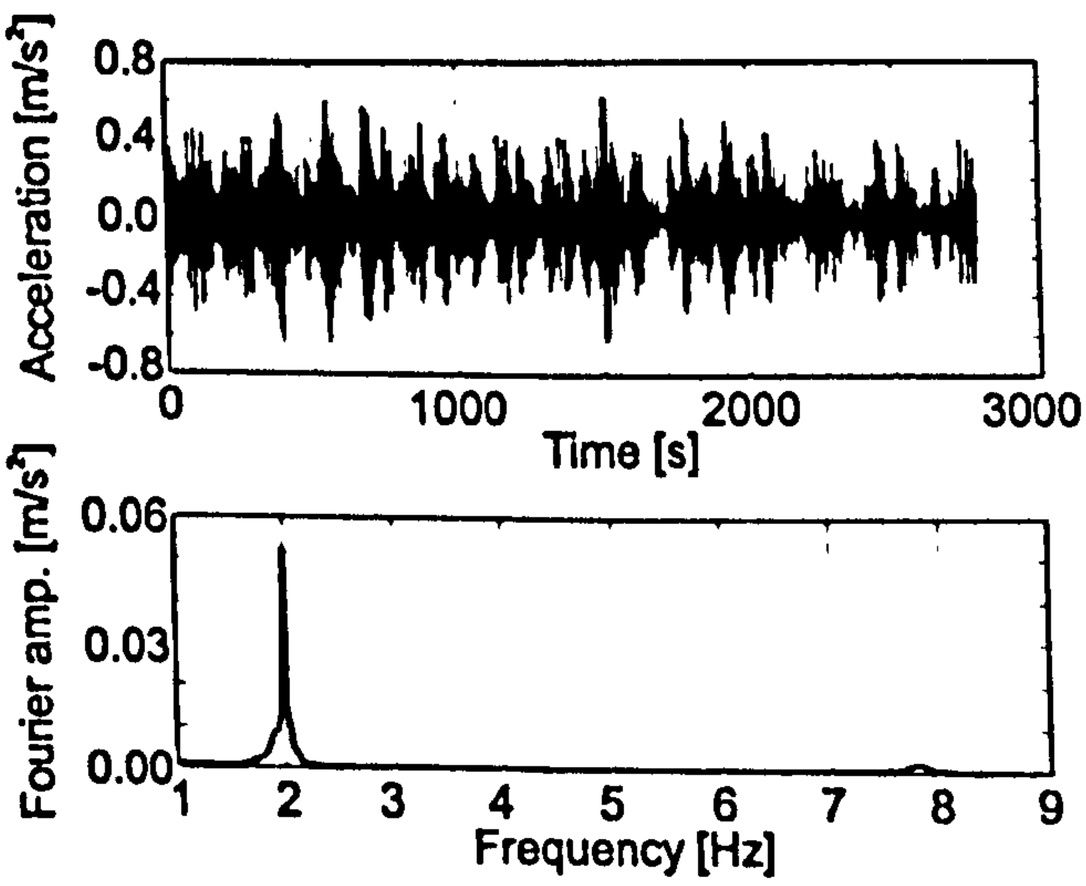

Figure A.7: Measured acceleration (upper) and its spectrum (lower). Sampling rate 0.025 s.

Using the video records, the time needed for each analysed pedestrian to make 20 steps was estimated. This was done for 1976 pedestrians. Then the 20 steps were divided by the time estimated to get the average step frequency. The mean step frequency across all subjects was 1.87 Hz. This was close to 1.9 Hz reported by Kerr & Bishop (2001) in their experiments and slightly lower than 2.0 Hz suggested by Matsumoto et al. (1978). The obtained distribution of step frequencies can be considered as normal distribution with mean value of 1.87 Hz and standard deviation of 0.186 Hz (Figure A.8). Based on video records of crossings of the bridge, it could be said that only people who were in a hurry achieved a step frequency of 2.0 Hz or more. Also, it was noticed that people walking in groups and/or in a crowd tended to adjust their walking velocity, rather than step frequency, to each other. This means that they were prone to walk at different frequencies (but with same speeds), especially if their height differed significantly.

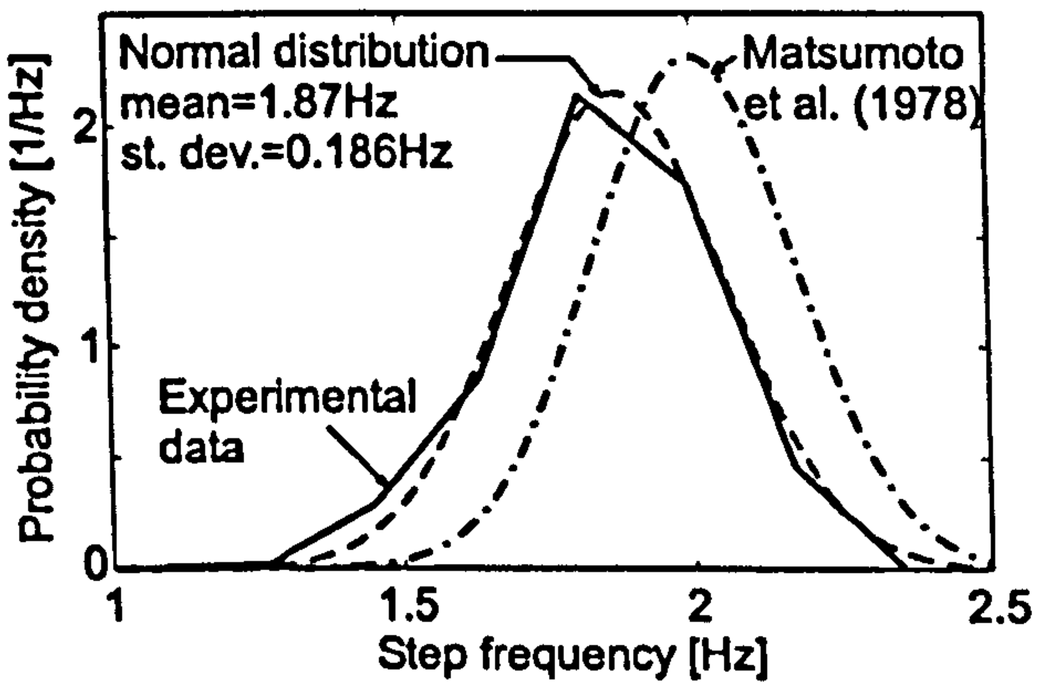

Figure A.8: Distribution of step frequencies.

Further analysis confirmed that the arrival times of pedestrians at the bridge can be approximated by the Poisson distribution, as claimed by Matsumoto et al. (1978).

A.5.2 Vibration Perception

300 randomly selected pedestrians were asked, immediately after they crossed the footbridge, to answer a questionnaire about their perception of the vertical vibrations. As many as 220 among them answered they had felt footbridge vibrations during the crossing. These pedestrians were asked to rate the vibrations according to the following three categories:

- acceptable,
- unpleasant and
- unacceptable.

More than a half of 220 test subjects who felt vibrations (56% exactly) rated vibrations as either unpleasant or unacceptable (Figure A.9: upper).

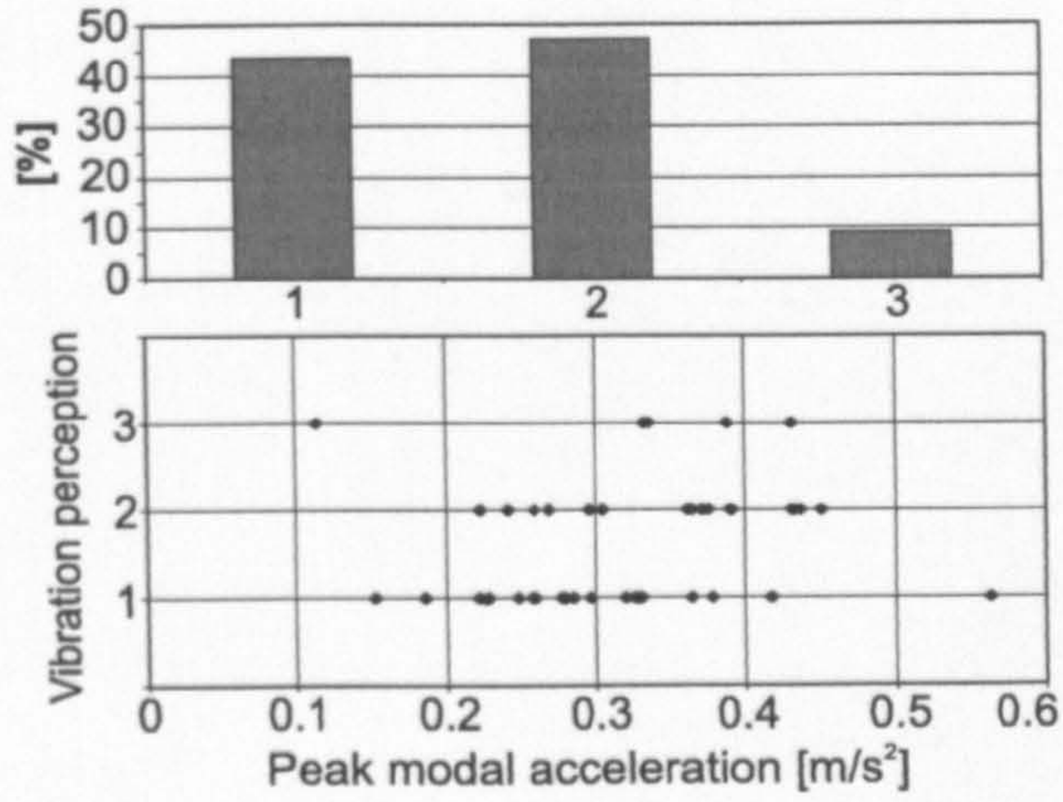

Figure A.9: Rating of vibrations (upper) and vibration perception as a function of modal peak acceleration (lower): 1-acceptable, 2-unpleasant, 3-unacceptable.

For 41 pedestrians it was possible to identify the level of modal peak acceleration they felt during the crossing. This level is shown in Figure A.9: lower as a function of the rating of vibrations. Boundaries between the three categories of vibrations cannot be clearly identified, although a general trend of increasing the modal peak acceleration with decreasing the degree of its acceptability is noticeable. It is interesting that a large number of pedestrians found peak accelerations between 0.2 and 0.5 $\mathrm{m/s^2}$ unpleasant. Also, for some people modal peak acceleration levels between 0.3 and 0.45 $\mathrm{m/s^2}$ were unacceptable, although they were still well bellow the acceleration level allowed by BS 5400 (BSI, 1978), which is equal to 0.7 $\mathrm{m/s^2}$ for this particular bridge. In this situation, defining probability functions of acceptability of vibrations for different acceleration levels could be the way forward instead of using the apparently unreliable and unsafe single acceleration value defined in BS 5400.

It is worth noting that there is anecdotal evidence that some people in Podgorica avoid crossing this footbridge altogether because of its liveliness. These people are, obviously, not included in this statistical study of vibration rating.

A.5.3 Dynamic Response: Measured vs. Simulated

Acceleration response of the bridge was simulated taking into account all data gathered during tests. Each pedestrian force F_1 was modelled as a sinusoidal force modulated by the mode shape of the first vertical mode of vibration $\phi(x)$ (Smith, 1988):

$$F_1(x,t) = DLF \cdot W \cdot \sin(2\pi f_s t + \varphi)\phi(x). \tag{A.1}$$

DLF is the dynamic loading factor dependent on the step frequency and calculated according to Young's (2001) model while $W = 700\,\mathrm{N}$ is assumed average pedestrian weight. Step frequency f_s is taken according to the identified normal distribution, while the time t during which the pedestrian was crossing the bridge was based on the Poisson distribution of pedes-

trian arrivals and an assumed step length of 0.75 m. The force phase shift φ was generated by MATLAB program for all pedestrians as a random number in the interval $[0, 2\pi]$ (uniform distribution). The mode shape $\phi(x)$ along the bridge axis was obtained from the fully updated FE model of the footbridge.

The bridge was modelled as a single degree of freedom system with the dynamic properties of the first vertical mode of vibration: the natural frequency of 2 Hz, modal mass of 62,000 kg and damping ratio of 0.28%.

The modal responses as simulated and measured are shown in Figure A.10.

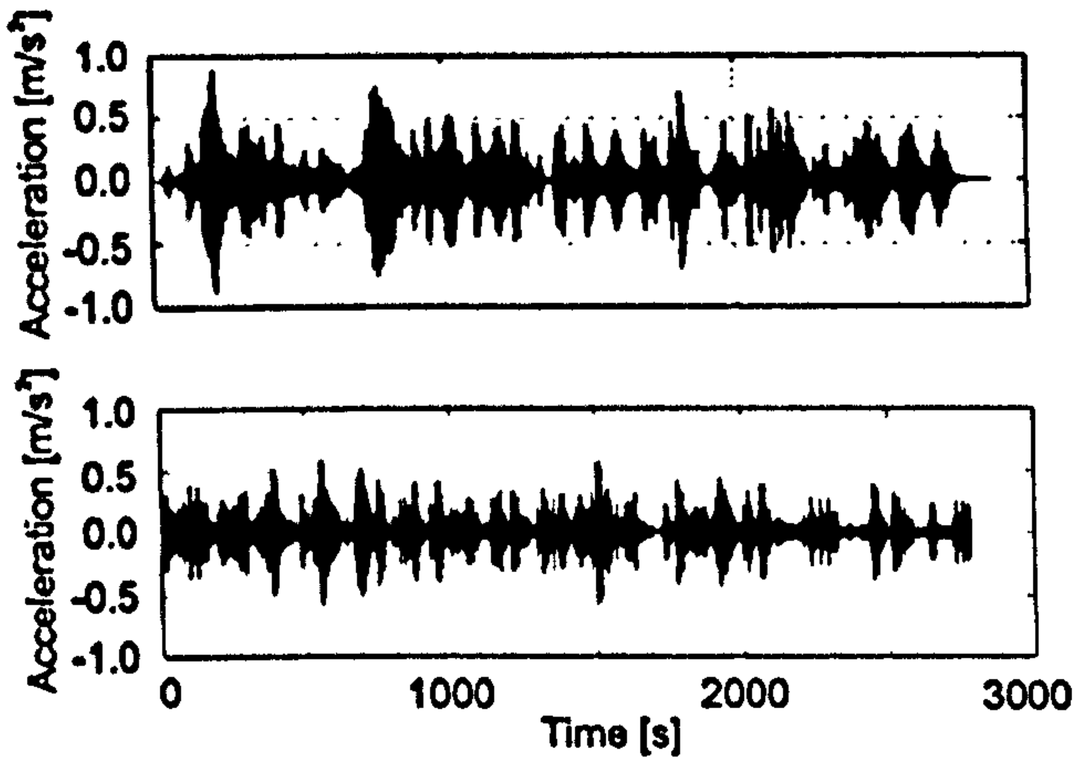

Figure A.10: Modal acceleration: simulated (upper) and measured (lower).

It can be said that the simulated responses were up to 45% higher than the measured one (in a sense of RMS of the whole signal). This can be considered as a very good first estimate. The reason for difference could be that walking on a flexible surface would decrease the force in comparison with that measured on a rigid surface. Also, the possibility that some people damp out vibrations by walking opposite to footbridge movement might have an influence. It is interesting that the difference in two responses in terms of RMS values can be minimised if structural damping is increased to 0.6%. These issues are the subject of further research.

A.6 Conclusions

A limited heel-drop testing programme of a footbridge known to be lively under vertical pedestrian excitation identified the first four vertical and two horizontal modes of vibration. The natural frequency of the fundamental vertical mode was in the range of normal walking frequencies. This was, coupled with the very low damping ratio of only 0.28%, the main reason for the liveliness of the footbridge.

A detailed initial 3D finite element model based on best engineering judgment failed to predict all six measured modes of vibration. Decreasing the stiffness of the girder edge supports in the longitudinal direction improved the model significantly and fairly well predicted the vertical modes of vibration.

Traffic on the bridge was monitored for 135 minutes. It was found that the distribution of step frequencies followed the normal distribution with mean value of 1.87 Hz which was slightly lower than what was found in the literature. Also it was concluded that pedestrian arrival on the bridge followed a Poisson distribution.

Most of 300 randomly interviewed pedestrians felt vibrations of the bridge during their crossing. It is interesting that for a number of pedestrians, vertical vibrations between 0.2 and 0.45 m/s^2 were either unpleasant or unacceptable. This despite the fact that these vibrations were well below the acceleration limit of 0.7 m/s^2 given by BS 5400.

Finally, Monte Carlo simulations of the bridge response due to normal pedestrian traffic estimated reasonably well the measured response due to up to 40 people on the bridge at the same time. The simulations were based on the distributions of step frequencies and pedestrian arrival on the bridge as identified during the monitoring tests. Some improvements of this predictive mathematical model have been suggested including the increase of damping due to walking pedestrians.

Appendix B

MATLAB script FHSM.m

MATLAB script FHSM.m is a program developed for probability-based estimation of vibration response to walking excitation under a single pedestrian. The theory behind the procedure has been explained in Chapter 6.

```
% ------------------------------------------------------------
% FHSM.m - First Harmonic Single Mode
% ------------------------------------------------------------
% Created by S. Zivanovic on 16 July 2005
% ------------------------------------------------------------------------
% Program for probability-based estimation of vibration response of footbridges
% First Harmonic of the walking force is considered only
% Footbridge responds in a Single Mode of vibration
% ------------------------------------------------------------------------
% ------------------------------------------------------------------------
% INPUT: Footbridge modal properties:   m    =   modal mass [kg]
%                                       fn   =   natural frequency [Hz]
%                                       ceta =   damping ratio
%       L = length on which mode shape is close to half-sine [m]
%       W = 750 N (average pedestrian weight)
% ------------------------------------------------------------------------
% OUTPUT: Probability of certain acceleration level
%         Cumulative probability of certain acceleration level
% ------------------------------------------------------------------------
% ------------------------------------------------------------------------
% PHASE 1: Normal distribution of step frequencies fs
%          Taken according to Zivanovic et al. (2005), EURODYN, Paris
% mean  =   1.87Hz
% std   =   0.186Hz
% ------------------------------------------------------------------------
% PHASE 2: Define DLF=f(fs). Mean value as given by Kerr's PhD (1998) (page 86)
% DLF   =   -0.2649*fs^3 + 1.3206*fs^2 - 1.7597*fs + 0.7613
% DLF   =   Dynamic Loading Factor
% fs    =   Step Frequency
% ------------------------------------------------------------------------
% PHASE 3: Define probability distribution for number of steps needed to cross the bridge
% Based on Pachi & Ji (2005): walking velocity at each frequency is defined as normally distributed
% mean  =   0.71*fs [m/s]
% std   =   0.10*mean [m/s]
% L     =   bridge length [m] (on which mode shape is close to a half-sine)
```

```
% N     =   L/v * fs          (number of walking cycles)
% ------------------------------------------------------------------------
% PHASE 4: Walking frequency ratio distribution is independent from number of steps distribution
%          Present their joint probability density
%          Joint distribution = (pd for fs/fn) * (pd for number of steps)
% ------------------------------------------------------------------------
% PHASE 5: Peak modal acceleration taking into account half-sine mode shape (Inman, 2001)
% ------------------------------------------------------------------------
% PHASE 6: Probability that certain level of acceleration will occur is calculated.
%          DLF variability and imperfections in walking are not taken into account.
% ------------------------------------------------------------------------
% PHASE 7: Probability that certain level of acceleration will occur is calculated.
%          Imperfections in walking are taken into account.
% ------------------------------------------------------------------------
% PHASE 8: Final probability that certain level of acceleration will occur is calculated.
%          DLF variability is taken into account.
% ------------------------------------------------------------------------

clear all

% INPUT
% --------------------
m=58000;
fn=2.04;
omegan=2*pi*fn;
k=m*omegan^2;
ceta=0.0026;
c=2*ceta*sqrt(k*m);
L=78;
W=750;
% ------------------------------------------------------------------------
% Choice of some calculation parameters
df=0.01;            % resolution for frequency fs [Hz]
a_step=1/20;        % resolution for response (acceleration) [m/s2]
dN=5;               % resolution for number of steps
dt=0.005;           % resolution for response time history [s]
% ------------------------------------------------------------------------

% PHASE 1
% ========================================================================
fs=1.31:df:2.43;    % range of step frequencies (99% points of a normally distributed sample)
mean_fs=1.87; std_fs=0.186;
pd_fs=1/(sqrt(2*pi)*std_fs) * exp(-(fs-mean_fs).^2/2/std_fs^2);     % probability density (pdf)

ratio_f=fs/fn;
pd_fratio=pd_fs*fn;                                                 % pdf for fs/fn
% ------------------------------------------------------------------------

% PHASE 2
% ========================================================================
DLF=-0.2649*fs.^3 + 1.3206*fs.^2 - 1.7597*fs + 0.7613;
% ------------------------------------------------------------------------

% PHASE 3
% ========================================================================
mean_vel=0.71*2;
std_vel=0.10*mean_vel;
vel=0.994:0.001:1.846;                                  % range of mean_vel +- 3*std_vel (for fs=2Hz)
pd_vel=1/(sqrt(2*pi)*std_vel) * exp(-(vel-mean_vel).^2/2/std_vel^2);  % pdf for velocity for fs=2Hz
```

```
Ns=L*2./vel;                                          % range of Number of steps for any fs
N=round(min(Ns)/dN)*dN:dN:round(max(Ns)/dN)*dN;       % range for Ns with step dN for any fs

for i=1:length(N)
    qq=abs(Ns-N(i));
    pp=find(qq==min(qq));
    pd_N(i)=pd_vel(pp);
end
pd_N=pd_N/(trapz(pd_N)*dN);                           % pdf for Ns for any fs
% ------------------------------------------------------------------------------------------

% PHASE 4
% ==========================================================================================
for i=1:length(ratio_f)
    for j=1:length(N)
        pd2(i,j)=pd_fratio(i)*pd_N(j);
    end
end

figure(1)
mesh(N,ratio_f,pd2)
grid on
title('Chapter 6 - Figure 11')
xlabel('Number of cycles')
ylabel('Frequency ratio')
zlabel('Joint probability density')
% ------------------------------------------------------------------------------------------

% PHASE 5
% ==========================================================================================
omegan=2*pi*fn; omegas=2*pi*fs;

for i=1:length(fs)
    for j=1:length(N)
        v=fs(i)*L/N(j);
        t=0:dt:(L/v);

        A=DLF(i)*W;

        f0=-A/2/m;  alfa=omegas(i)+pi*v/L;
        PP=omegan^2-alfa^2; omegad=omegan*(sqrt(1-ceta^2));
        RR=2*ceta*omegan*alfa;

        a1_t=ceta^2*omegan^2*exp(-ceta*omegan*t) .* (-f0*PP/(PP^2+RR^2)*cos(omegad*t) - ceta*omegan/omegad * ...
            f0*PP/(PP^2+RR^2)*sin(omegad*t) - RR*alfa*f0/omegad/(PP^2+RR^2)*sin(omegad*t))-...
            2*ceta*omegan*exp(-ceta*omegan*t) .* ( f0*omegad*PP/(PP^2+RR^2)*sin(omegad*t) - ceta*omegan*...
            f0*PP/(PP^2+RR^2)*cos(omegad*t) - RR*alfa*f0/(PP^2+RR^2)*cos(omegad*t) )+...
            exp(-ceta*omegan*t) .* ( f0*omegad^2*PP/(PP^2+RR^2)*cos(omegad*t) + ceta*omegan*omegad*...
            f0*PP/(PP^2+RR^2)*sin(omegad*t) + RR*alfa*omegad*f0/(PP^2+RR^2)*sin(omegad*t) );
        a1_ss=-f0/(PP^2+RR^2)*(PP*alfa^2*cos(alfa*t)+RR*alfa^2*sin(alfa*t));

        f0=A/2/m;  alfa=omegas(i)-pi*v/L;
        PP=omegan^2-alfa^2; omegad=omegan*(sqrt(1-ceta^2));
        RR=2*ceta*omegan*alfa;

        a2_t=ceta^2*omegan^2*exp(-ceta*omegan*t) .* (-f0*PP/(PP^2+RR^2)*cos(omegad*t) - ceta*omegan/omegad *...
            f0*PP/(PP^2+RR^2)*sin(omegad*t) - RR*alfa*f0/omegad/(PP^2+RR^2)*sin(omegad*t))-...
            2*ceta*omegan*exp(-ceta*omegan*t) .* ( f0*omegad*PP/(PP^2+RR^2)*sin(omegad*t) - ceta*omegan*...
            f0*PP/(PP^2+RR^2)*cos(omegad*t) - RR*alfa*f0/(PP^2+RR^2)*cos(omegad*t) )+...
```

```
        exp(-ceta*omegan*t) .* ( f0*omegad^2*PP/(PP^2+RR^2)*cos(omegad*t) + ceta*omegan*omegad*...
        f0*PP/(PP^2+RR^2)*sin(omegad*t) + RR*alfa*omegad*f0/(PP^2+RR^2)*sin(omegad*t) );
    a2_ss=-f0/(PP^2+RR^2)*(PP*alfa^2*cos(alfa*t)+RR*alfa^2*sin(alfa*t));

    a_modal=a1_t+a1_ss+a2_t+a2_ss;        % modal acceleration

    mAcc(i,j)=max(a_modal);     % peak modal acceleration
  end
end

figure(2)
mesh(N,ratio_f,mAcc)
grid on
title('Chapter 6: Figure 10')
xlabel('Number of steps')
ylabel('Frequency ratio')
zlabel('Peak modal acceleration [m/s^2]')

% PHASE 6
% ================================================================================
d_acc=0:a_step:(max(max(mAcc))+a_step);

for i=1:(length(d_acc)-1)
    qq=find(mAcc>d_acc(i) & mAcc<=d_acc(i+1));
    Macc(i)=d_acc(i+1);

    p_acc(i)=sum(pd2(qq))*dN*df/fn;
end

figure(3)
bar(Macc-a_step/2,p_acc)
grid on
title('Chapter 6: Figure 12a')
xlabel('Peak modal acceleration [m/s^2]')
ylabel('Probability')

% PHASE 7
% ================================================================================
% Read a and b coefficients from MAT files. ceta_all is the vector of all damping ratios considered
% Coefficients are listed in Tables B.1 and B.2 of this appendix
load a_gamma; load b_gamma;

zeta=ceta*100; pp=1; i=1; while pp==1
    if zeta>=ceta_all(i) & zeta<ceta_all(i+1)
        a_0_80=(a(1,i+1)-a(1,i))*(zeta-ceta_all(i))/(ceta_all(i+1)-ceta_all(i))+a(1,i);
        a_0_85=(a(2,i+1)-a(2,i))*(zeta-ceta_all(i))/(ceta_all(i+1)-ceta_all(i))+a(2,i);
        a_0_90=(a(3,i+1)-a(3,i))*(zeta-ceta_all(i))/(ceta_all(i+1)-ceta_all(i))+a(3,i);
        a_0_95=(a(4,i+1)-a(4,i))*(zeta-ceta_all(i))/(ceta_all(i+1)-ceta_all(i))+a(4,i);
        a_1_00=(a(5,i+1)-a(5,i))*(zeta-ceta_all(i))/(ceta_all(i+1)-ceta_all(i))+a(5,i);
        a_1_05=(a(6,i+1)-a(6,i))*(zeta-ceta_all(i))/(ceta_all(i+1)-ceta_all(i))+a(6,i);
        a_1_10=(a(7,i+1)-a(7,i))*(zeta-ceta_all(i))/(ceta_all(i+1)-ceta_all(i))+a(7,i);
        a_1_15=(a(8,i+1)-a(8,i))*(zeta-ceta_all(i))/(ceta_all(i+1)-ceta_all(i))+a(8,i);
        a_1_20=(a(9,i+1)-a(9,i))*(zeta-ceta_all(i))/(ceta_all(i+1)-ceta_all(i))+a(9,i);

        b_0_80=(b(1,i+1)-b(1,i))*(zeta-ceta_all(i))/(ceta_all(i+1)-ceta_all(i))+b(1,i);
        b_0_85=(b(2,i+1)-b(2,i))*(zeta-ceta_all(i))/(ceta_all(i+1)-ceta_all(i))+b(2,i);
        b_0_90=(b(3,i+1)-b(3,i))*(zeta-ceta_all(i))/(ceta_all(i+1)-ceta_all(i))+b(3,i);
        b_0_95=(b(4,i+1)-b(4,i))*(zeta-ceta_all(i))/(ceta_all(i+1)-ceta_all(i))+b(4,i);
        b_1_00=(b(5,i+1)-b(5,i))*(zeta-ceta_all(i))/(ceta_all(i+1)-ceta_all(i))+b(5,i);
```

```
        b_1_05=(b(6,i+1)-b(6,i))*(zeta-ceta_all(i))/(ceta_all(i+1)-ceta_all(i))+b(6,i);
        b_1_10=(b(7,i+1)-b(7,i))*(zeta-ceta_all(i))/(ceta_all(i+1)-ceta_all(i))+b(7,i);
        b_1_15=(b(8,i+1)-b(8,i))*(zeta-ceta_all(i))/(ceta_all(i+1)-ceta_all(i))+b(8,i);
        b_1_20=(b(9,i+1)-b(9,i))*(zeta-ceta_all(i))/(ceta_all(i+1)-ceta_all(i))+b(9,i);

        pp=2;
    end
    i=i+1;
end

step_rat=0.1;
ratio=0:step_rat:6;     % range of frequency ratio on which gamma pdf will be generated
% Gamma distributions for different step/natural frequency ratios
g_1=ratio.^(a_0_80-1).*exp(-ratio/b_0_80)/b_0_80^a_0_80/gamma(a_0_80);
g_2=ratio.^(a_0_85-1).*exp(-ratio/b_0_85)/b_0_85^a_0_85/gamma(a_0_85);
g_3=ratio.^(a_0_90-1).*exp(-ratio/b_0_90)/b_0_90^a_0_90/gamma(a_0_90);
g_4=ratio.^(a_0_95-1).*exp(-ratio/b_0_95)/b_0_95^a_0_95/gamma(a_0_95);
g_5=ratio.^(a_1_00-1).*exp(-ratio/b_1_00)/b_1_00^a_1_00/gamma(a_1_00);
g_6=ratio.^(a_1_05-1).*exp(-ratio/b_1_05)/b_1_05^a_1_05/gamma(a_1_05);
g_7=ratio.^(a_1_10-1).*exp(-ratio/b_1_10)/b_1_10^a_1_10/gamma(a_1_10);
g_8=ratio.^(a_1_15-1).*exp(-ratio/b_1_15)/b_1_15^a_1_15/gamma(a_1_15);
g_9=ratio.^(a_1_20-1).*exp(-ratio/b_1_20)/b_1_20^a_1_20/gamma(a_1_20);

pp=1; for i=1:length(ratio_f)
    if ratio_f(i)<=0.83
        g=g_1;
    end
    if ratio_f(i)>0.83 & ratio_f(i)<=0.88
        g=g_2;
end
if ratio_f(i)>0.88 & ratio_f(i)<=0.93
    g=g_3;
end
if ratio_f(i)>0.93 & ratio_f(i)<=0.98
    g=g_4;
end
if ratio_f(i)>0.98 & ratio_f(i)<=1.02
    g=g_5;
end
if ratio_f(i)>1.02 & ratio_f(i)<=1.07
    g=g_6;
end
if ratio_f(i)>1.07 & ratio_f(i)<=1.12
    g=g_7;
end
if ratio_f(i)>1.12 & ratio_f(i)<=1.17
    g=g_8;
end
if ratio_f(i)>1.17
    g=g_9;
end

for j=1:length(N)
    for ii=1:length(g)
        AA(pp)=ratio(ii)*mAcc(i,j);
        pd3(pp)=g(ii)*pd2(i,j);
        pp=pp+1;
    end
end
```

```
end

d_AA=0:a_step:(max(AA)+a_step);

for i=1:(length(d_AA)-1)
    qq=find(AA>d_AA(i) & AA<=d_AA(i+1));
    Macc1(i)=d_AA(i+1);

    p_AA(i)=sum(pd3(qq))*dN*df/fn*step_rat;
end

figure(4)
bar(Macc1-a_step/2,p_AA)
grid on
title('Chapter 6: Figure 12b (walking imperfections included)')
xlabel('Peak modal acceleration [m/s^2]')
ylabel('Probability')

% pdf for acceleration AA
pd_AA=p_AA/a_step;

% PHASE 8
% ========================================================================================
step_dlf=0.01;

% dlf ratio distribution (Kerr, 1998)
dlf=0.52:step_dlf:1.48;
mean_dlf=1;
std_dlf=0.16;
rat_dlf=(0.52+step_dlf/2):step_dlf:(1.48-step_dlf/2);

pd_dlf=1/(sqrt(2*pi)*std_dlf) * exp(-(rat_dlf-mean_dlf).^2/2/std_dlf^2);

for i=1:length(Macc1)
    for j=1:length(rat_dlf)
        pd_AAA(i,j)=pd_AA(i)*pd_dlf(j);
        AAA(i,j)=(Macc1(i)-a_step/2)*rat_dlf(j);
    end
end

pd_AAA=pd_AAA(:); AAA=AAA(:);

d_AAA=0:a_step:(max(AAA)+a_step);

for i=1:(length(d_AAA)-1)
    qq=find(AAA>d_AAA(i) & AAA<=d_AAA(i+1));
    Macc2(i)=d_AAA(i+1);

    p_AAA(i)=sum(pd_AAA(qq))*a_step*step_dlf;
end

figure(5)
bar(Macc2-a_step/2,p_AAA)
grid on
title('Chapter 6: Figure 13a')
xlabel('Peak modal acceleration [m/s^2]')
ylabel('Probability')

pp=0; for i=1:length(Macc2)
```

```
    p3(i)=pp+p_AAA(i);
    pp=p3(i);
end

figure(6)
bar(Macc2-a_step/2,p3);
grid on title('Chapter 6: Figure 13b')
xlabel('Peak modal acceleration [m/s^2]')
ylabel('Cumulative probability')

% end of program
```

Table B.1: Parameter a.

f_e/f_n	Damping ratio [%]									
	0.1	0.2	0.3	0.4	0.5	0.6	0.8	1.0	1.5	2.0
0.80	12.227	12.622	13.001	13.587	14.454	15.166	16.470	17.353	19.560	22.013
0.85	12.646	13.735	14.510	16.177	17.706	19.067	21.345	23.200	26.629	29.289
0.90	10.353	12.251	14.350	16.197	17.846	19.273	21.543	23.444	27.443	31.284
0.95	13.967	16.214	17.874	19.251	20.478	20.701	20.170	22.874	30.449	39.159
1.00	31.431	41.659	52.926	65.341	78.930	93.821	126.460	161.180	247.620	318.600
1.05	10.061	10.886	11.934	12.934	13.744	14.415	13.112	15.665	23.409	33.318
1.10	18.589	20.680	21.812	22.868	23.721	24.045	24.268	22.713	28.083	34.101
1.15	19.687	23.154	26.071	28.565	30.816	32.872	36.517	39.651	46.277	52.192
1.20	24.319	28.624	32.605	36.314	39.736	42.967	48.834	53.939	64.153	71.769

Table B.2: Parameter b.

f_e/f_n	Damping ratio [%]									
	0.1	0.2	0.3	0.4	0.5	0.6	0.8	1.0	1.5	2.0
0.80	0.2202	0.2019	0.1870	0.1715	0.1550	0.1429	0.1246	0.1133	0.0928	0.0777
0.85	0.1795	0.1567	0.1422	0.1226	0.1084	0.0979	0.0836	0.0743	0.0609	0.0530
0.90	0.1922	0.1541	0.1260	0.1080	0.0954	0.0863	0.0745	0.0665	0.0539	0.0455
0.95	0.1250	0.1038	0.0915	0.0829	0.0762	0.0741	0.0740	0.0632	0.0447	0.0332
1.00	0.0261	0.0203	0.0163	0.0135	0.0113	0.0097	0.0073	0.0059	0.0039	0.0031
1.05	0.1673	0.1500	0.1330	0.1197	0.1103	0.1032	0.1114	0.0900	0.0563	0.0376
1.10	0.0820	0.0719	0.0668	0.0627	0.0596	0.0581	0.0565	0.0596	0.0464	0.0371
1.15	0.0801	0.0659	0.0570	0.0509	0.0463	0.0427	0.0375	0.0338	0.0279	0.0241
1.20	0.0618	0.0510	0.0438	0.0386	0.0348	0.0317	0.0273	0.0243	0.0198	0.0173

Appendix C

MATLAB script MHMM.m

MATLAB script MHMM.m is a program developed for probability-based estimation of multi-mode vibration response to walking excitation under a single pedestrian. The theory behind the procedure has been explained in Chapter 7.

```
% ------------------------------------------------------------
% MHMM.m - Multi Harmonic Multi Mode
% ------------------------------------------------------------
% Created by S. Zivanovic on 6 January 2006
% ------------------------------------------------------------------------
% Program for probability-based estimation of vibration response of footbridges
% First five harmonics of the walking force are considered
% Footbridge responds in several vibration modes (natural frequencies <=10Hz)
% ------------------------------------------------------------------------
% ------------------------------------------------------------------------
% INPUT: Footbridge modal properties: mi    = modal mass for i-th mode [kg]
%                                     fni   = natural frequency for i-th mode [Hz]
%                                     cetai = damping ratio for i-th mode
%        Mode shape for each mode
%        W = 750 N (average pedestrian weight)
%        NoP - number of people to enter a simulation
% ------------------------------------------------------------------------
% OUTPUT: Probability of certain acceleration level
%         Cumulative probability of certain acceleration level
% ------------------------------------------------------------------------
% ------------------------------------------------------------------------

clear all

% ---------------
% INPUT MODAL DATA
% ---------------
dt=0.001;

m1=10520;   m2=5880;    m3=8690;    m5=10767;   m7=10319;
fn1=2.44;   fn2=3.66;   fn3=4.86;   fn5=6.66;   fn7=9.50;

k1=(2*pi*fn1)^2*m1;
k2=(2*pi*fn2)^2*m2;
k3=(2*pi*fn3)^2*m3;
```

```
k5=(2*pi*fn5)^2*m5;
k7=(2*pi*fn7)^2*m7;

ceta1=0.0053; ceta2=0.0065; ceta3=0.0096; ceta5=0.0073; ceta7=0.0077;

c1=2*ceta1*sqrt(k1*m1);
c2=2*ceta2*sqrt(k2*m2);
c3=2*ceta3*sqrt(k3*m3);
c5=2*ceta5*sqrt(k5*m5);
c7=2*ceta7*sqrt(k7*m7);

load ModeShape_Hope1; % .MAT file containing length L and mode shape amplitude fi
L1=L; FI1=fi;

load ModeShape_Hope2; L2=L; FI2=fi;
load ModeShape_Hope3; L3=L; FI3=fi;
load ModeShape_Hope5; L5=L; FI5=fi;
load ModeShape_Hope7; L7=L; FI7=fi;

NoP=2000;
W=750;

% STATISTICAL DISTRIBUTIONS
% -------------------------

% normal distribution of step frequencies (mean=1.87Hz, std=0.186Hz)
fs=1.87+0.186*randn(NoP,1);                          % generates NoP step frequencies
DLFmean=-0.2649*fs.^3+1.3206*fs.^2-1.7597*fs+0.7613;  % mean DLF1

DLF_rat=1+0.16*randn(NoP,1);     % distribution of MF1
DLF=DLFmean.*DLF_rat;            % generate NoP values for DLF1

DLF2=0.07+0.03*randn(NoP,1);     % distribution of DLF2
wd2=find(DLF2<0);
DLF2(wd2)=0;                     % removal of negative DLFs

DLF3=0.05+0.02*randn(NoP,1);     % distribution of DLF3
wd3=find(DLF3<0);
DLF3(wd3)=0;
DLF4=0.05+0.02*randn(NoP,1);     % distribution of DLF4
wd4=find(DLF4<0);
DLF4(wd4)=0;

DLF5=0.03+0.015*randn(NoP,1);    % distribution of DLF5
wd5=find(DLF5<0);
DLF5(wd5)=0;

% DLFs for first five subharmonics
DLF05=0.026*DLF+0.0031;
DLF15=0.074*DLF+0.01;
DLF25=0.012*DLF+0.016;
DLF35=0.013*DLF+0.0093;
DLF45=0.015*DLF+0.0072;

mean_ls=0.71;
std_ls=0.071;
ls=mean_ls+std_ls*randn(NoP,1); % distribution for step length
NoC=max(L1)./ls;                % transferring step length to number of steps
Crossing=NoC./fs;               % crossing time for NoP pedestrians
```

```
% Fitted force model (40 amplitudes in the spectrum for each harmonic)
f05=0.25:1/80:(0.75-1/80);
f1=0.75:1/80:(1.25-1/80);
f15=1.25:1/80:(1.75-1/80);
f2=1.75:1/80:(2.25-1/80);
f25=2.25:1/80:(2.75-1/80);
f3=2.75:1/80:(3.25-1/80);
f35=3.25:1/80:(3.75-1/80);
f4=3.75:1/80:(4.25-1/80);
f45=4.25:1/80:(4.75-1/80);
f5=4.75:1/80:(5.25-1/80);

H1=0.7852*exp(-((f1-0.9999)/0.008314).^2) + 0.0206*exp(-((f1-1.034)/0.2524).^2) + ...
   0.1074*exp(-((f1-1.001)/0.03653).^2);
H2=0.5130*exp(-((f2-2.0000)/0.011050).^2) + 0.1330*exp(-((f2-1.957)/0.2632).^2) - ...
   0.04984*exp(-((f2-1.882)/0.05807).^2);
H3=0.3908*exp(-((f3-3.0000)/0.009560).^2) + 0.1567*exp(-((f3-3.000)/0.05525).^2) + ...
   0.06866*exp(-((f3-2.957)/0.5607).^2);
H4=0.3255*exp(-((f4-4.0000)/0.008797).^2) + 0.1647*exp(-((f4-4.001)/0.06641).^2) + ...
   0.06888*exp(-((f4-3.991)/0.375).^2);
H5=0.2806*exp(-((f5-4.9990)/0.007939).^2) + 0.1584*exp(-((f5-5.004)/0.07825).^2) + ...
   0.07289*exp(-((f5-4.987)/0.4501).^2);

H05=0.3406*exp(-((f05-0.4998)/0.008337).^2) + 0.2803*exp(-((f05-1.133)/0.6388).^2);
H15=0.3024*exp(-((f15-1.5000)/0.008735).^2) + 0.1345*exp(-((f15-1.532)/0.7233).^2);
H25=0.2627*exp(-((f25-2.5000)/0.009748).^2) + 0.2456*exp(-((f25-0.2312)/2.932).^2);
H35=0.2344*exp(-((f35-3.5010)/0.009898).^2) + 0.2355*exp(-((f35+1.576)/7.05).^2);
H45=0.2645*exp(-((f45-4.4990)/0.010190).^2) + 0.2389*exp(-((f45-1.153)/4.561).^2);

% Uniformly distributed random phase for each line in spectrum
Pha1=-pi+2*pi*rand(NoP*40,1);
Pha2=-pi+2*pi*rand(NoP*40,1);
Pha3=-pi+2*pi*rand(NoP*40,1);
Pha4=-pi+2*pi*rand(NoP*40,1);
Pha5=-pi+2*pi*rand(NoP*40,1);

Pha05=-pi+2*pi*rand(NoP*40,1);
Pha15=-pi+2*pi*rand(NoP*40,1);
Pha25=-pi+2*pi*rand(NoP*40,1);
Pha35=-pi+2*pi*rand(NoP*40,1);
Pha45=-pi+2*pi*rand(NoP*40,1);

for i=1:NoP

    t=0:dt:Crossing(i);

    F=0;
    for ii=1:40
        F=F+W*( DLF(i)*H1(ii)*cos(2*pi*f1(ii)*fs(i)*t+Pha1((i-1)*40+ii)) + ...
          DLF2(i)*H2(ii)*cos(2*pi*f2(ii)*fs(i)*t+Pha2((i-1)*40+ii)) + ...
          DLF3(i)*H3(ii)*cos(2*pi*f3(ii)*fs(i)*t+Pha3((i-1)*40+ii)) + ...
          DLF4(i)*H4(ii)*cos(2*pi*f4(ii)*fs(i)*t+Pha4((i-1)*40+ii)) + ...
          DLF5(i)*H5(ii)*cos(2*pi*f5(ii)*fs(i)*t+Pha5((i-1)*40+ii))   )   ;
        F=F+W*( DLF05(i)*H05(ii)*cos(2*pi*f05(ii)*fs(i)*t+Pha05((i-1)*40+ii)) + ...
          DLF15(i)*H15(ii)*cos(2*pi*f15(ii)*fs(i)*t+Pha15((i-1)*40+ii)) + ...
          DLF25(i)*H25(ii)*cos(2*pi*f25(ii)*fs(i)*t+Pha25((i-1)*40+ii)) + ...
          DLF35(i)*H35(ii)*cos(2*pi*f35(ii)*fs(i)*t+Pha35((i-1)*40+ii)) + ...
          DLF45(i)*H45(ii)*cos(2*pi*f45(ii)*fs(i)*t+Pha45((i-1)*40+ii))  )   ;
```

```
end

vv(i)=max(L1)/Crossing(i);
xp=vv(i)*t;
[fi1]=Lin_interpolation(L1,FI1,xp);      % Lin_iterpolation.m is a subroutine
[fi2]=Lin_interpolation(L2,FI2,xp);      % for linear interpolation of mode shape
[fi3]=Lin_interpolation(L3,FI3,xp);      % listed after this program
[fi5]=Lin_interpolation(L5,FI5,xp);
[fi7]=Lin_interpolation(L7,FI7,xp);

% modal forces for each mode of vibration
mF1=F.*fi1; mF2=F.*fi2; mF3=F.*fi3; mF5=F.*fi5; mF7=F.*fi7;

% modal response in each vibration mode
[d1,v1,a1]=Newmark(k1,m1,c1,mF1,dt);     % Newmark.m is a subroutine
[d2,v2,a2]=Newmark(k2,m2,c2,mF2,dt);     % for numerical integration of
[d3,v3,a3]=Newmark(k3,m3,c3,mF3,dt);     % equation of motion listed
[d5,v5,a5]=Newmark(k5,m5,c5,mF5,dt);     % at the end of this appendix
[d7,v7,a7]=Newmark(k7,m7,c7,mF7,dt);

% peak response for each vibration mode
max_a1(i)=max(abs(a1)); max_a2(i)=max(abs(a2));
max_a3(i)=max(abs(a3)); max_a5(i)=max(abs(a5)); max_a7(i)=max(abs(a7));

% rms response for each vibration mode
rms_a1(i)=sqrt(mean(a1.^2)); rms_a2(i)=sqrt(mean(a2.^2));
rms_a3(i)=sqrt(mean(a3.^2)); rms_a5(i)=sqrt(mean(a5.^2)); rms_a7(i)=sqrt(mean(a7.^2));

% mode superposition
    c14=a1*0.894-a2*0.033+0.988*a3-0.594*a5-0.011*a7;      % at a quarter-span point (8.5m)
    c12=a2-0.290*a3-0.019*a5+0.921*a7;                     % at the midspan point

    max_c14(i)=max(abs(c14)); max_c12(i)=max(abs(c12));
    rms_c14(i)=sqrt(mean(c14.^2)); rms_c12(i)=sqrt(mean(c12.^2));
end

% calculation of cumulative distributions for response at the quarter-span point
% the same set of commands can be used to present response at the midspan point
a_step=1/40;        % acceleration resolution for histogram of maximum response
a_stepr=1/200;      % acceleration resolution for histogram of rms response

% peak modal acceleration
d_a=0:a_step:(max(max_c14)+a_step);

p_a=[];
for i=1:(length(d_a)-1)
    qq=sum(max_c14>d_a(i) & max_c14<=d_a(i+1));
    p_a(i)=qq/NoP;
end

Macc=d_a(2:length(d_a))-a_step/2;

figure(1)
pp=0; pc=[];
for i=1:length(Macc)
    pc(i)=pp+p_a(i);
    pp=pc(i);
end
bar(Macc,pc);
```

```
grid on
title('Chapter 7: Figure 7.12a')
xlabel('Peak modal acceleration [m/s^2]')
ylabel('Cumulative probability')

% rms modal acceleration
d_ar=0:a_stepr:(max(rms_c14)+a_stepr);

p_ar=[];
for i=1:(length(d_ar)-1)
    qqr=sum(rms_c14>d_ar(i) & rms_c14<=d_ar(i+1));
    p_ar(i)=qqr/NoP;
end

Maccr=d_ar(2:length(d_ar))-a_stepr/2;

figure(2)
pp=0; pcr=[];
for i=1:length(Maccr)
    pcr(i)=pp+p_ar(i);
    pp=pcr(i);
end
bar(Maccr,pcr);
grid on
title('Chapter 7: Figure 7.12b')
xlabel('RMS modal acceleration [m/s^2]')
ylabel('Cumulative probability')

% end of program

% ------------------------------------------------------------------------
% ------------------------------------------------------------------------
% Subroutine for linear interpolation of an arbitrary discrete function

% INPUT: vector x - independent variable
%        vector y - function value (at each x)
%        vector xp - variable x for which the function y should be interpolated

% OUTPUT: vector yp - value of y in xp

function[yp]=Lin_interpolation(x,y,xp);

epsilon =0.00001;

le_xp=length(xp);

for i=1:le_xp
    k=1;
    while x(k) < xp(i)-epsilon
        k=k+1;
    end

    if xp(i) == x(k)
        yp(i) = y(k);
    else
        yp(i) = y(k-1) + (y(k)-y(k-1)) / (x(k)-x(k-1)) * (xp(i)-x(k-1));
    end
end
```

```
% end of subroutine

% ------------------------------------------------------------------------------
% ------------------------------------------------------------------------------
% Subroutine for numerical integration of dynamic equation of motion

% INPUTS:  k - modal stiffness [N/m],
%          m - modal mass [kg],
%          c - modal damping [N/(m/s)],
%          mF - modal force [N],
%          dt - time step for numerical integration [s] (=time step in the force vector)

% OUTPUTS: x - modal displacement [m],
%          v - modal velocity [m/s],
%          a - modal acceleration [m/s/s]

function [d,v,a]=Newmark(k,m,c,mF,dt)

% initial displacement & velocity
d0=0;
v0=0;
a0=(mF(1)-k*d0-c*v0)/m;

d(1)=d0;
v(1)=v0;
a(1)=a0;

kk=k+4/(dt^2)*m+2/dt*c;

for i=2:(length(mF));
    qq(i)=mF(i)+m*(4/(dt^2)*d(i-1)+4/dt*v(i-1)+a(i-1))+c*(2/dt*d(i-1)+v(i-1));
    d(i)=qq(i)/kk;
    v(i)=2/dt*d(i)-2/dt*d(i-1)-v(i-1);
    a(i)=4/(dt^2)*d(i)-4/(dt^2)*d(i-1)-4/dt*v(i-1)-a(i-1);
end

% end of subroutine
```